

5-1-2010

An Investigation of the Storage Stability of Auger and Entrained Flow Reactor Produced Bio-oils

Javeed Mohammad

Follow this and additional works at: <https://scholarsjunction.msstate.edu/td>

Recommended Citation

Mohammad, Javeed, "An Investigation of the Storage Stability of Auger and Entrained Flow Reactor Produced Bio-oils" (2010). *Theses and Dissertations*. 600.
<https://scholarsjunction.msstate.edu/td/600>

This Dissertation - Open Access is brought to you for free and open access by the Theses and Dissertations at Scholars Junction. It has been accepted for inclusion in Theses and Dissertations by an authorized administrator of Scholars Junction. For more information, please contact scholcomm@msstate.libanswers.com.

AN INVESTIGATION OF THE STORAGE STABILITY OF AUGER AND
ENTRAINED FLOW REACTOR PRODUCED BIO-OILS

By

Javeed Mohammad

A Dissertation
Submitted to the Faculty of
Mississippi State University
in Partial Fulfillment of the Requirements
for the Degree of Doctor of Philosophy
in Chemical Engineering
in the Department of Chemical Engineering

Mississippi State, Mississippi

May 2010

Copyright by
Javeed Mohammad
2010

AN INVESTIGATION OF THE STORAGE STABILITY OF AUGER AND
ENTRAINED FLOW REACTOR PRODUCED BIO-OILS

By

Javeed Mohammad

Approved:

Ray M. Bricka
Associate Professor of Dave C. Swalm
School of Chemical Engineering
(Director of Dissertation)

Mark G. White
Professor and Director of Dave C.
Swalm School of Chemical Engineering
(Committee Member)

Hossein D. Toghiani
Associate Professor of Dave C. Swalm
School of Chemical Engineering
(Committee Member)

Rafael Hernandez
Associate Professor and Graduate
Coordinator of Dave C. Swalm
School of Chemical Engineering
(Committee Member)

Janice L. DuBien
Associate Professor of the Department
of Mathematics and Statistics
(Committee Member)

Sarah A. Rajala
Dean and Professor of the Bagley
College of Engineering

Name: Javeed Mohammad

Date of Degree: May 01, 2010

Institution: Mississippi State University

Major Field: Chemical Engineering

Major Professor: Dr. Ray M. Bricka

Title of Study: AN INVESTIGATION OF THE STORAGE STABILITY OF AUGER
AND ENTRAINED FLOW REACTOR PRODUCED BIO-OILS

Pages in Study: 441

Candidate for Degree of Doctor of Philosophy

This project is primarily focused on improving the storage stability of bio-oils or pyrolysis oils by varying feedstock, reactor, and storage conditions. Pyrolysis oil is a complex medley of oxygenated chemicals (aliphatic and aromatic) that are well known to undergo unstable polymeric reactions (auto-catalyzed) if suitable additives are not utilized. These reactions can be severely detrimental to the long-term storage stability of pyrolysis oils. Hence, a detailed investigation was conducted in four phases namely: 1) pyrolysis oil production 2) additive prescreening 3) concentration optimization and 4) stability testing. During the first phase a lab-scale semi-continuous auger reactor is utilized to produce 16 pyrolysis oils. The reactor variables include pyrolysis temperature and vapor residence time. The feed stocks include pine wood, pine bark, oak wood, and oak bark. During the second phase a range of chemical additives (26) are prescreened to obtain three best performing additives. Anisole, glycerol, and methanol are consequently utilized to perform concentration optimization studies during the third phase. Viscosity,

water content, and pH of pyrolysis oils are timely measured to assess the accelerated storage stability of pyrolysis oils during the phases 2-3. During the fourth phase, pyrolysis oils produced from three different reactor systems (lab-scale auger, large-scale auger, and entrained flow) were tested for their storage stability. Viscosity, water content, pH, density, and acid value are timely measured to assess the ambient and accelerated storage stability of pyrolysis oils during phase 4. Extrinsic variables such as light and filtration are utilized during the experimental testing of phase 4. The rheological data (Newtonian/non-Newtonian) enhanced the understanding of pyrolysis oil storage stability both qualitatively and quantitatively. The stability performance of a chemical additive is very much dependent on the concentration and its organic functional group. Consequently, alcohols fared above all the other functional groups in stabilizing the pyrolysis oils. Glycerol is observed to have special blending and homogenizing properties compared to all other additives. Feedstock seems to be the single most important factor affecting storage stability of pyrolysis oils. Consequently, pine wood resulted in the most stable pyrolysis oil whereas pine bark resulted in the least stable pyrolysis oil.

Key words: lignocellulosic pyrolysis, auger, fluidized/entrained flow, bio-oil, storage stability, rheology, Karl Fisher, additive prescreening, concentration optimization, modeling.

DEDICATION

Foremost, I want to remember ‘The Almighty Creator’ who also created me and blessed me with countless bounties in this life. The firm belief in Him inspired me to see through all the hurdles during this project.

I would like to thank all of my dearest family members, friends, and colleagues for their moral support. Together they made my career ambitions possible. I would like to dedicate this work to my mom who recently underwent three life-threatening surgeries in a row. She is and will be the most beloved person to me in my life.

This task sans support of my beloved ‘mom, dad, and brother’ was bound to be a non-reality. I would like to pay them utmost tribute for their constant patience and encouragement during my unstable times as a graduate researcher.

Believe it or not; the first teacher who taught me the English grammar is none other than my dad Mehboob. I would like to thank my beloved brother Ahmed for instilling engineering interest during my early boyish days. I revere and love them both forever and ever.

Finally, the moral support that I received from all of my friends and colleagues during the graduate school education is truly unparalleled. They are Devkant, Jaricus, Amy, Heather, Prashant, Dr.Amit Gujar, Dr.Farag Gaber, Dr.Sami Wuhaibi, Dr.Hassan Barbary, Dr.Emad Giar, Dr.Ejaz Ashraf, and Dr.Delwar Hossain.

ACKNOWLEDGMENTS

Foremost, I would like to thank Dr.Mark Bricka (Major Advisor), Dr.Hossein Toghiani, Dr.Janice DuBien, Dr.Rafael Hernandez, and Dr.Mark White from the bottom of my heart for graciously serving in my committee.

I am greatly indebted to Dr.Bricka in multitude ways that have led to my professional and personal growth at Mississippi State University (MSU). His knowledge, experience, guidance, and support during the critical and non-critical times of this project helped me tremendously to retain my focus in perspective. I well and truly look forward to continuing my research in his footsteps.

I can not possibly thank all of my committee members enough for their academic coaching during the group and non-group meetings. In my professional life I hope to fully utilize the teaching and research skills that my favorite professors ‘Dr.Toghiani and Dr.DuBien’ imparted during the classes. I think it will be impossible for me to forget the first course ‘Advance Chemical Engineering Thermodynamics’ that I took with Dr.Toghiani apart from all of his vivacious lectures at MSU. As far as the advanced statistics classes that I took with Dr.DuBien go; they were clearly the best among all the classes that I ever took at the statistics and the math department.

I acknowledge that my critical thinking during this project is mostly attributed to one person and that is none other than Dr.Hernandez. Many a times his questions during my presentations puzzled me as a young graduate researcher. But those questions only motivated me further to improve my research skills.

The vast impetus provided by Dr.White during this project will be applied forever in my professional career. I would like to extend special appreciation to Dr.White for his moral and professional support during the most difficult times of this project. In short, I feel truly honored to have him as a most experienced committee member.

I would like to specially thank Dr.Philip Steele, Dr.Charles Pittman Jr., and Dr.Priscilla Hill for their advice, critical input, and encouragement during this project. I would like to specially acknowledge Mr.Philip Badger at Renewable Oil International (ROI) and Dr.Richard Bain at national renewable energy laboratory (NREL) for sharing the critical information of auger and entrained flow reactors. I am greatly thankful to Brian Mitchell for his enduring assistance during the auger reactor operation and troubleshooting process.

There have been numerous upturns and downturns in this project just like many others. It is these turns that made my graduate school experience a memorable one. I want to thank my fellow undergraduate students (Alex Taylor, Chad Alderman, and John Guyton) immensely for assisting me during the busiest times of this project. I am positive that their hard working ethics will not go unnoticed in their professional career.

Last but never the least; I would like to thank Ms.Sherre Denson, Ms.Tina Gilliland, Mr.Mike Hillhouse, Ms.Sandra Shumaker, and Ms.Ellen Weeks for their invaluable contribution during this project. I would like to humbly thank Respected Dave

C. Swalm (posthumously) for providing us an opportunity to ‘study and work’ at the state-of-the-art chemical engineering ‘classrooms and laboratories’.

Finally, in a jiffy note, I would like to thank United States Department of Agriculture (USDA) for funding this project. Needless to say; this project would have been just a dream without their essential fiscal support.

TABLE OF CONTENTS

DEDICATION	ii
ACKNOWLEDGMENT.....	iii
LIST OF TABLES	xi
LIST OF FIGURES	xvii
LIST OF MAJOR SYMBOLS USED	xlii
CHAPTER	
I. INTRODUCTION	1
Introduction.....	1
Pyrolysis Background.....	3
Pyrolysis Technologies	5
Pyrolysis Oil Applications	6
Pyrolysis Oil Stability.....	7
Pyrolysis Oil Properties	8
Research Objectives.....	11
II. LITERATURE REVIEW	15
Energy Demand and Supply	15
Wood Chemistry	17
Thermo-chemical Conversion (Pyrolysis)	19
Reactors and Operating Conditions	24
Rheology	29
Introduction.....	29
Classification of Liquids.....	29
Viscosity Measurement.....	32
Moduli or Oscillatory Testing.....	33
Pyrolysis Oil.....	34
Pyrolysis Oil vs. Conventional Fuel	34

Engineering Challenges	35
Quality Upgrading	36
Chemical Composition and Analysis.....	40
Elemental Composition and Analysis.....	42
Storage, Testing, and Commercialization.....	43
Stability Testing Methods.....	45
Background.....	45
Distillate Fuel.....	46
Motor Oil	49
Aviation Fuel	50
Cooking Oil.....	52
Bio-diesel.....	53
Pyrolysis Oil.....	54
Pyrolysis Oil Stability.....	57
Catalytic Effects.....	57
Compositional Changes	57
Chemical Reactions	59
Esterification Rxn	61
Transesterification Rxn.....	61
Homopolymerization Rxn.....	61
Hydration Rxn.....	61
Hemiacetal Formation Rxn.....	61
Acetalization Rxn.....	61
Resin Formation Rxn	62
Dimerization Rxn.....	62
Alcohol Addition Rxn.....	62
Gas Forming Rxn.....	62
Esterification of Aldehydes and Ketones.....	63
Hemiacetal and Acetal Formation from Aldehydes and Ketones.....	64
Acetal Formation from Monosaccharides.....	64
Physico-chemical Stability.....	65
Flow Stability.....	65
Phase Stability.....	67
Structural Stability	70
 III. MATERIALS AND METHODS.....	 95
Project Overview	95
Introduction.....	98
MSU Pyrolysis Oil Production (Phase I).....	99
Feedstock Preparation.....	99
MSU Auger Reactor	100
System Description.....	100
Reactor Operation.....	100
Off-Gas Analysis-MSU Auger Reactor	102

ROI [®] Auger Reactor	103
NREL Entrained Flow Reactor/Fluidized Bed	103
System Description	103
Reactor Operation	104
Preliminary Testing (Trial Runs)	106
Pyrolysis Oil Filtration	109
Additive Prescreening Studies (Phase II)	111
Concentration Optimization Studies (Phase III)	114
Stability Testing (Phase IV)	114
Karl Fisher Theory, Instrumentation, and Operation	117
Theory: Karl Fisher Reaction (Mettler Toledo, 1999)	117
Presence of Alcohol (Base: Pyridine-Py)	118
Absence of Alcohol (Base: Pyridine-Py)	118
Karl Fisher Reaction (Base: Imidazole)	118
Instrumentation: DL31 Karl Fisher Unit	119
Operation: DL31 Karl Fisher Unit	120
Rheometer Theory, Instrumentation, and Operation	122
Theory: Liquid Classification, Viscosity Measurement, and Moduli Testing	122
Instrumentation: AR1000-N Rheometer	122
Operation: AR1000-N Rheometer	123
Experimental Testing (Phases II-IV)	125
Karl Fisher (%Water)	125
Viscosity and Moduli	126
Density	128
pH	128
Total Acid Value	129
 IV. RESULTS AND DISCUSSION	 162
Pyrolysis Oil Production (Phase I)	162
Introduction	162
Fractionation of Pyrolysis Oil	162
Auger Reactor Yields	165
Influence of Reactor Conditions	167
Reactor Off-Gas Analysis	168
Reactor Temperature Control	168
Reactor Residence Time	169
Preliminary Stability Testing (Trial Runs)	172
Introduction	172
Stability of Frequently Tested Oils (Aged)	173
Stability of Refrigerated Oils (Fresh)	175
Statistical Modeling	176
Viscosity Model (ANOVA)	176
Water Content Model (ANOVA)	177

Additive Prescreening (Phase II)	179
Introduction.....	179
Influence of Shear Rate on the Pyrolysis Oil Viscosity.....	180
Influence of Additive on the Oil Viscosity (Initial).....	182
Influence of Temperature on the Pyrolysis Oil Viscosity.....	183
Influence of Storage Time on the Pyrolysis Oil Viscosity	185
Influence of Additive on the Viscosity Increase (%).....	186
Resorcinol (RSL)-Esterification Rxns	189
Glycerol (GLY)-Esterification Rxns.....	189
Polyethylene Glycol (PEG)-Esterification Rxns	190
Ester (MEF)-Hydrolysis Rxn.....	191
Alcohols (MEH and ETH)-Esterification Rxns	191
Ketone (MEK)-Acetalization Rxns.....	191
Aryl Ether (ANS)-Electrophilic Aromatic Substitution or Acylation Rxns.....	191
Rheological Modeling (Shear Stress vs. Shear Rate)	192
Influence of Additive on the Water Content of Pyrolysis Oils.....	194
Influence of Additive on the pH of Pyrolysis Oils	196
Statistical Analysis.....	197
Viscosity Model (ANOVA).....	199
Water Content Model (ANOVA).....	202
Concentration Optimization (Phase III).....	204
Introduction.....	204
Rheological Flow Behavior of Pyrolysis Oils	205
Temperature Effects on the Oil Viscosity.....	206
Additive Concentration Effects on the Oil Viscosity	208
Moduli Studies.....	210
Additive Concentration Effects on Oil Water Content.....	216
Additive Concentration Effects on Oil pH.....	217
Statistical Analysis.....	217
Viscosity Model (ANOVA).....	218
Water Content Model (ANOVA).....	220
Final Stability Testing (Phase IV).....	221
Introduction.....	221
Stability of Wood and Bark Derived Oils (MS) as a Function of Shear Rate	222
Stability of Wood Derived Oils (RI and NR) as a Function of Storage Time.....	229
Stability of Wood Derived Oils (MS, NR, and RI) as a Function of Additive Conc.	231
Additive (wt.%) @ 25 °C.....	232
Additive (wt.%) @ 80 °C.....	232
Karl Fisher Analysis	232
Density of Pyrolysis Oils	235
pH of Pyrolysis Oils.....	236

Acid Value of Pyrolysis Oils	236
Weight Loss of Pyrolysis Oils	238
Data Quality Control.....	238
Statistical Analyses and Modeling.....	239
Pine Wood Pyrolysis Oil (MSU)	240
Oak Wood Pyrolysis Oil (MSU).....	242
Oak Bark Pyrolysis Oil (MSU).....	243
Pyrolysis Oil Application.....	247
Production.....	248
Fractionation and Distillation	248
Storage and Pumping	249
Projected Energy Costs	250
Calculations.....	251
 V. CONCLUSIONS AND RECOMMENDATIONS	 348
Conclusions.....	348
Recommendations.....	350
 BIBLIOGRAPHY	 352
 APPENDIX	
A. PYROLYSIS OIL PRODUCTION-PHASE I.....	362
B. PRELIMINARY STABILITY TESTING-TRIAL RUNS	379
C. ADDITIVE PRESCREENING-PHASE II.....	385
D. CONCENTRATION OPTIMIZATION-PHASE III.....	420
E. FINAL STABILITY TESTING-PHASE IV	431

LIST OF TABLES

TABLE	Page
1.1 Most Common Reactor Types (Bridgwater, 1999).....	13
1.2 Pyrolysis Types and Associated Reactor Conditions (Maschio et al., 1992)	14
2.1 Typical Wood Composition (Schultz and Taylor, 1989).....	72
2.2 Typical Reactor Yields of Pyrolysis Oil, Gas, and Char Fractions (Graham et al., 1994)	72
2.3 Major North American Pyrolysis Units in Design/Operation (Bridgwater and Peacocke, 2000)	73
2.4 Major Criteria for the Geometry Selection in a Rheometer (Morrison, 2001)	74
2.5 Mathematical Equations Used to Compute Viscosity of a Liquid for Different Geometries of a Rheometer (Morrison, 2001)	75
2.6 Typical Properties of Bio-Crude Compared to the Conventional Crude (Czernik and Bridgwater, 2004)	76
2.7 Typical Elemental Composition (wt.%) of Bio-Crude Compared to the Conventional Crude (Czernik and Bridgwater, 2004)	76
2.8 Hansen Solubility Parameters for Selected Solvents in Pyrolysis Oil (Barton, 1983; Diebold, 2000)	77
2.9 Classification of Chemical Compounds Present in Pyrolysis Oil Organic Fraction (Bridgwater, 1999; Oasmaa et al., 2003).....	78
2.10 Major Chemical Compounds Present in the Pyrolysis Oil (Maschio et al., 1992)	79

2.11	Elemental Composition of Oak Wood, Pine Wood, and Switch Grass Pyrolysis Oils (Elliott, 1994)	80
2.12	Viscosity of Oak Wood Pyrolysis Oils as a Function of Storage Time and Storage Temperature (Czernik et al., 1994).....	81
2.13	Water Content of Oak Wood Pyrolysis Oils as a Function of Storage Time and Storage Temperature (Czernik et al., 1994).....	81
3.1	Control Variables Used for Different Reactor Systems during Pyrolysis	131
3.2	Mississippi State University (MSU) Pyrolysis Oils Obtained (8) After Mixing Similar Oils during Preliminary Testing.....	133
3.3	Pyrolysis Oils (9) Selected for Stability Testing in Phase IV.....	134
3.4	Smallest Possible Pore Size Achieved during the Control (CTL3) Sample Filtration.....	135
3.5	Additive Selection Criteria Used in Phase II	136
3.6	Chemical Structures of Additives	139
3.7	Experimental Testing Matrix Used in Phase II.....	141
3.8	Experimental Testing Matrix Used in Phase III	142
3.9	Experimental Testing Matrix Used in Phase IV	143
3.10	Relative Standard Deviation (RSD) of the Mettler Toledo [®] DL31 Karl Fisher Unit (Mettler Toledo, 1999).....	145
4.1	Average Reactor Yields (mass %) of the 16 Mississippi State University Pyrolysis Oils.....	252
4.2	Gas Chromatographic-Mass Spectrometer (GC-MS) Analysis of Mississippi State University Pyrolysis Oils Produced at High Temperature and Slow Residence Time (Ingram et al., 2008)	253
4.3	Normalized Gas Composition (vol.%) of Mississippi State University Pine Bark-Low Temperature-Fast Residence (PB-LT-FR) Pyrolysis Oil.....	253

4.4	Variable-Level-Treatment Input for the Mean Viscosity Model of Additive Free Mississippi State University (MS) Fresh Pyrolysis Oils (16)	254
4.5	Analysis of Variance (ANOVA) Model Obtained for the Mean Viscosity of Additive Free Mississippi State University (MS) Fresh Pyrolysis Oils (16)	254
4.6	Least Significant Difference (LSD) Output of Feedstock Based on the Mean Viscosity (V) of Additive Free Mississippi State University (MS) Fresh Pyrolysis Oils (16)	255
4.7	Least Significant Difference (LSD) Output of Pyrolysis Temperature (PT) Based on the Mean Viscosity (V) of Additive Free Mississippi State University (MS) Fresh Pyrolysis Oils (16).....	255
4.8	Least Significant Difference (LSD) Output of Residence Time (RT) Based on the Mean Viscosity (V) of Additive Free Mississippi State University (MS) Fresh Pyrolysis Oils (16)	256
4.9	Least Significant Difference (LSD) Output of Viscosity Temperature (VT) Based on the Mean Viscosity (V) of Additive Free Mississippi State University (MS) Fresh Pyrolysis Oils (16).....	256
4.10	Least Significant Difference (LSD) Output of Shear Rate (SR) Based on the Mean Viscosity (V) of Additive Free Mississippi State University (MS) Fresh Pyrolysis Oils (16).....	257
4.11	Variable-Level-Treatment Input for the Mean Water Content Model of Additive Free Mississippi State University (MS) Fresh Pyrolysis Oils (16)	257
4.12	Analysis of Variance (ANOVA) Model Obtained for the Mean Water Content of Additive Free Mississippi State University (MS) Fresh Pyrolysis Oils (16)	258
4.13	Least Significant Difference (LSD) Output of Feedstock Based on the Mean Water Content (WC) of Additive Free Mississippi State University (MS) Fresh Pyrolysis Oils (16).....	258
4.14	Least Significant Difference (LSD) Output of Pyrolysis Temperature (PT) Based on the Mean Water Content (WC) of Additive Free Mississippi State University (MS) Fresh Pyrolysis Oils (16).....	259

4.15	Least Significant Difference (LSD) Output of Residence Time (RT) Based on the Mean Water Content (WC) of Additive Free Mississippi State University (MS) Fresh Pyrolysis Oils (16).....	259
4.16	Mathematical Models Obtained for Viscosity of Pine Wood Pyrolysis Oils as a Function of Temperature.....	260
4.17	Chemical Classification of Additives Selected for Prescreening Studies.....	260
4.18	Rheological Models Obtained for Shear Stress of Pine Wood Pyrolysis Oils as a Function of Shear Rate.....	261
4.19	Chemical Classification of Additives Used for Statistical Analysis of Variance (ANOVA).....	261
4.20	Variable-Level-Treatment Input for the Mean Viscosity Model of Pine Wood Pyrolysis Oils (High Temperature).....	262
4.21	Analysis of Variance (ANOVA) Model Obtained for the Mean Viscosity Increase (%) of Pine Wood Pyrolysis Oils (High Temperature).....	262
4.22	Least Significant Difference (LSD) Output of Additive Group (BLK) Based on the Mean Viscosity Increase (%) of Pine Wood Pyrolysis Oils (High Temperature).....	263
4.23	Least Significant Difference (LSD) Output of Shear Rate (s^{-1}) Based on the Mean Viscosity Increase (%) of Pine Wood Pyrolysis Oils (High Temperature).....	264
4.24	Least Significant Difference (LSD) Output of Temperature ($^{\circ}C$) Based on the Mean Viscosity Increase (%) of Pine Wood Pyrolysis Oils (High Temperature).....	264
4.25	Least Significant Difference (LSD) Output of Control and Additives Based on the Mean Viscosity Increase (%) of Pine Wood Pyrolysis Oils (High Temperature).....	265
4.26	Variable-Level-Treatment Input for the Mean Water Content Model of Pine Wood Pyrolysis Oils (High Temperature).....	266
4.27	Analysis of Variance (ANOVA) Model Obtained for the Mean Water Content (wt.%) of Pine Wood Pyrolysis Oils (High Temperature).....	266

4.28	Least Significant Difference (LSD) Output of Additive Group (BLK) Based on the Mean Water Content (wt.%) of Pine Wood Pyrolysis Oils (High Temperature).....	267
4.29	Least Significant Difference (LSD) Output of Storage Time (hr) Based on the Mean Water Content (wt.%) of Pine Wood Pyrolysis Oils (High Temperature)	268
4.30	Least Significant Difference (LSD) Output of Control and Additives Based on the Mean Water Content (wt.%) of Pine Wood Pyrolysis Oils (High Temperature).....	269
4.31	Variable-Level-Treatment Input for the Mean Viscosity Model of Pine Wood Pyrolysis Oils (Low Temperature).....	270
4.32	Analysis of Variance (ANOVA) Model Obtained for the Mean Viscosity Difference (cP) of Pine Wood Pyrolysis Oils (Low Temperature).....	270
4.33	Least Significant Difference (LSD) Output of Additive Based on the Mean Viscosity Difference (cP) or VD of Pine Wood Pyrolysis Oils (Low Temperature)	271
4.34	Least Significant Difference (LSD) Output of Additive Concentration (wt.%) Based on the Mean Viscosity Difference (cP) or VD of Pine Wood Pyrolysis Oils (Low Temperature).....	271
4.35	Least Significant Difference (LSD) Output of Measurement Temperature (⁰ C) Based on the Mean Viscosity Difference (cP) or VD of Pine Wood Pyrolysis Oils (Low Temperature)	271
4.36	Least Significant Difference (LSD) Output of Shear Rate (s ⁻¹) Based on the Mean Viscosity Difference (cP) or VD of Pine Wood Pyrolysis Oils (Low Temperature).....	272
4.37	Variable-Level-Treatment Input for the Mean Water Content Model of Pine Wood Pyrolysis Oils (Low Temperature).....	272
4.38	Analysis of Variance (ANOVA) Model Obtained for the Mean Water Content Difference (wt.%) of Pine Wood Pyrolysis Oils (Low Temperature).....	273
4.39	Least Significant Difference (LSD) Output of Additive Based on the Mean Water Content Difference (wt.%) or WCD of Pine Wood Pyrolysis Oils (Low Temperature).....	273

4.40	Least Significant Difference (LSD) Output of Storage Time (hr) Based on the Mean Water Content Difference (wt.%) or WCD of Pine Wood Pyrolysis Oils (Low Temperature).....	274
4.41	Least Significant Difference (LSD) Output of Additive Concentration (wt.%) Based on the Mean Water Content Difference (wt.%) or WCD of Pine Wood Pyrolysis Oils (Low Temperature).....	274
4.42	General Linear Model (GLM) Selected during the Statistical Analyses	274
4.43	General Linear Model (GLM) Parameters and their Estimates Obtained for Additive Blended Mississippi State University Pyrolysis Oils Stored at 25 and 80 °C	275
4.44	General Linear Model (GLM) Equations Obtained for Additive Blended Mississippi State University Pyrolysis Oils Stored at 25 and 80 °C.....	275
D.1	Anisole Input Data of the Analysis of Variance (ANOVA) Viscosity Model	422
D.2	Glycerol Input Data of the Analysis of Variance (ANOVA) Viscosity Model	423
D.3	Methanol Input Data of the Analysis of Variance (ANOVA) Viscosity Model	424
D.4	Anisole Input Data of the Analysis of Variance (ANOVA) Water Content Model	425
D.5	Glycerol Input Data of the Analysis of Variance (ANOVA) Water Content Model	426
D.6	Methanol Input Data of the Analysis of Variance (ANOVA) Water Content Model	427

LIST OF FIGURES

FIGURE	Page
1.1 Methanol Pricing History in the Past Decade.....	14
2.1 Projected Energy Usage (Quadrillion BTU) in the United States from 2006 to 2030 Based on the Consumption from 1980 to 2006	82
2.2 Chemical Structure of Cellulose	82
2.3 Primary Chemical Components of Hemicellulose.....	82
2.4 Chemical Structure of Softwood Lignin (Brady, 2002).....	83
2.5 Main Chemical Components of Lignin.....	83
2.6 A Simplistic Flow Chart of Pyrolysis	83
2.7 Lumped 3-Step Kinetic Model of Wood Pyrolysis (Shafizadeh, 1982).....	84
2.8 Pyrolysis Pathways of Cellulose to Anhydrosugars (Shafizadeh, 1982).....	84
2.9 Degradation Pathways of Levoglucosan to Volatile Products (Shafizadeh, 1982)	85
2.10 Dehydration of Cellulose and Glucose Derivatives to Levoglucosenone (Shafizadeh, 1982)	86
2.11 A Simplistic Flow Chart of Bubbling Fluidized Bed Pyrolysis (Meier and Faix, 1999)	87
2.12 A Simplistic Flow Chart of Circulating Fluidized Bed Pyrolysis (Meier and Faix, 1999)	87
2.13 A Simplistic Flow Chart of Ablative Reactor Pyrolysis (Meier and Faix, 1999)	87

2.14	A Simplistic Flow Chart of Rotating Cone Reactor Pyrolysis (Meier and Faix, 1999)	88
2.15	A Simplistic Flow Chart of Vortex Reactor Pyrolysis (Meier and Faix, 1999)	88
2.16	A Simplistic Flow Chart of Vacuum Reactor Pyrolysis (Meier and Faix, 1999)	88
2.17	Rheological Classification of Liquids.....	89
2.18	Typical Viscosity versus Shear Rate Profile of a Pseudoplastic Fluid (Rosen, 1982).....	89
2.19	A Pictorial View of the Capillary Geometry Used in a Rheometer/Viscometer (Morrison, 2001).....	90
2.20	A Pictorial View of the Parallel Plate Geometry Used in a Rheometer/Viscometer (Morrison, 2001).....	91
2.21	A Pictorial View of the Cone-Plate Geometry Used in a Rheometer/Viscometer (Morrison, 2001).....	92
2.22	A Pictorial View of the Couette Geometry (Cup and Bob) Used in a Rheometer/Viscometer (Morrison, 2001).....	93
2.23	Stress or Strain as a Function of Time for a Viscoelastic Material (Young and Lovell, 1991).....	94
3.1	Study Flow Chart	146
3.2	Feed Stocks Utilized for Pyrolysis Oil Production.....	148
3.3	A Rough Schematic of the Mississippi State University (MSU) Small-Scale Auger Reactor System.....	149
3.4	Gas Analysis Setup Used with the Mississippi State University (MSU) Small-Scale Auger Reactor System.....	150
3.5	Gas Sampling and Analysis Train of Pyrolysis Conducted at Mississippi State University (MSU)	151
3.6	A Pictorial View of the Renewable Oil International (ROI [®]) Large-Scale Auger Reactor System (Obtained with Permission).....	152

3.7	A Pictorial View of the National Renewable Energy Laboratory (NREL) Entrained Flow Reactor (Obtained with Permission)	153
3.8	Process Flow Diagram (PFD) of the National Renewable Energy Laboratory (NREL) Entrained Flow Reactor (Obtained with Permission)	154
3.9	Mixing Equipment Used for Mississippi State University (MSU) Pyrolysis Oils	155
3.10	Nylon (6/6) Filter Mediums Used for Pyrolysis Oil Filtration	155
3.11	Millipore [®] Vacuum Filtration Apparatus Used for Pyrolysis Oil Filtration.....	156
3.12	Fisher Scientific Vortex Mixer Utilized for Mixing Additives	156
3.13	Ventilated Hood Used for Ambient (~25 °C) Stability Testing in Phase IV	157
3.14	Gravity Convection Oven Used for Accelerated (80±2 °C) Stability Testing in Phases II-IV	157
3.15	A Pictorial View of the Mettler Toledo [®] Volumetric Karl Fisher Apparatus (Model: DL31) Used in this Study	158
3.16	Reaction Vessel Used in DL31 Karl Fisher Apparatus	158
3.17	A Pictorial View of the TA Instruments [®] Rheometer Apparatus (Model: AR1000-N) Used in this Study.....	159
3.18	Top and Side Views of the Disk-Plate or Parallel Plate Geometry Used in AR1000-N Rheometer	159
3.19	A Typical Profile of Viscosity versus Shear Rate (SR) of a Fluid Exhibiting both Newtonian (SR< 1 s ⁻¹) and Pseudoplastic (SR>1 s ⁻¹) Behavior as Generated by AR1000-N Rheometer.....	160
3.20	A Typical Profile of Modulus (G'-Storage and Loss-G'') versus Angular Frequency of a Polymer as Generated by AR1000-N Rheometer	160
3.21	Kimax [®] Volumetric Flask (Capacity=1 ml) Used for Density Measurements	161

3.22	A Pictorial View of the Acid Value Testing Apparatus Used in this Study	161
4.1	Daily Reactor Yields of Oak Wood-High Temperature-Slow Residence (OW-HT-SR) Pyrolysis Oil	276
4.2	Average Yields of Four Fractions (Water-ARF, Oil-ORF, Char, and Unaccounted Mass-UM) Obtained from Auger Reactor	277
4.3	Tarry Pyrolyzate Collected from the Mississippi State University Auger Reactor Condensers	277
4.4	Influence of Pyrolysis Temperature on the Average Reactor Yields of Mississippi State University-Oak Wood-Slow Residence (MS-OW-SR) Pyrolysis Oils	278
4.5	Influence of Residence Time on the Average Reactor Yields of Mississippi State University-Oak Wood-Low Temperature (MS-OW-LT) Pyrolysis Oils	278
4.6	Tarry Mass Collected During Gas Analysis of Mississippi State University Pine Bark-Low Temperature-Fast Residence (PB-LT-FR) Pyrolysis Oil	279
4.7	Temperature Variation of the Ceramic Band Heaters (1-5) Observed as a Function of Reactor Length	279
4.8	Zonal (B-F) Temperature Profile Obtained as a Function of Run Time.....	280
4.9	Approximate Distances of Gas and Vapor Collection Ports from the Feed Entrance of Mississippi State University (MSU) Small-Scale Auger Reactor	280
4.10	Viscosity (cP) as a Function of Aging Time (days) of Oak Wood (OW) Pyrolysis Oils of Mississippi State University	281
4.11	Water Content (wt.%) as a Function of Aging Time (days) of Oak Wood (OW) Pyrolysis Oils of Mississippi State University	281
4.12	Acidity (pH) as a Function of Aging Time (days) of Oak Wood (OW) Pyrolysis Oils of Mississippi State University	282
4.13	Density (g/ml) as a Function of Aging Time (days) of Oak Wood (OW) Pyrolysis Oils of Mississippi State University	282

4.14	Viscosity (cP) as a Function of Shear Rate (s^{-1}) and Residence Time (SR-Slow and Fast-FR) of Pine Wood (PW) High Temperature (HT) Pyrolysis Oils of Mississippi State University.....	283
4.15	Viscosity (cP) as a Function of Shear Rate (s^{-1}) and Residence Time (SR-Slow and Fast-FR) of Oak Wood (OW) Low Temperature (LT) Pyrolysis Oils of Mississippi State University.....	283
4.16	Viscosity (cP) as a Function of Shear Rate (s^{-1}) and Pyrolysis Temperature (LT-Low and High-HT) of Pine Wood (PW) Slow Residence (SR) Pyrolysis Oils of Mississippi State University.....	284
4.17	Viscosity (cP) as a Function of Shear Rate (s^{-1}) and Pyrolysis Temperature (LT-Low and High-HT) of Oak Wood (OW) Fast Residence (FR) Pyrolysis Oils of Mississippi State University.....	284
4.18	Viscosity (cP) of Pine Wood Pyrolysis Oil Control (0 wt.%) Measured as a Function of Shear Rate (s^{-1}) and Storage Time (hr).....	285
4.19	Viscosity (cP) of Anisole Blended Pine Wood Pyrolysis Oil (10 wt.%) Measured as a Function of Shear Rate (s^{-1}) and Storage Time (hr).....	285
4.20	Viscosity (cP) of Glycerol Blended Pine Wood Pyrolysis Oil (10 wt.%) Measured as a Function of Shear Rate (s^{-1}) and Storage Time (hr).....	286
4.21	Viscosity (cP) of Methanol Blended Pine Wood Pyrolysis Oil (10 wt.%) Measured as a Function of Shear Rate (s^{-1}) and Storage Time (hr).....	286
4.22	Percentage Increase in Viscosity (0 hr vs. 192 hr) of Pine Wood Pyrolysis Oil Control (0 wt.%) Obtained as a Function of Shear Rate (s^{-1}).....	287
4.23	Percentage Increase in Viscosity (0 hr vs. 192 hr) of Anisole Blended Pine Wood Pyrolysis Oil (10 wt.%) Obtained as a Function of Shear Rate (s^{-1}).....	287
4.24	Percentage Increase in Viscosity (0 hr vs. 192 hr) of Glycerol Blended Pine Wood Pyrolysis Oil (10 wt.%) Obtained as a Function of Shear Rate (s^{-1}).....	288
4.25	Percentage Increase in Viscosity (0 hr vs. 192 hr) of Methanol Blended Pine Wood Pyrolysis Oil (10 wt.%) Obtained as a Function of Shear Rate (s^{-1}).....	288
4.26	Viscosity of Glycerol Measured as a Function of Shear Rate (s^{-1}).....	289

4.27	Viscosity (cP) of Pine Wood Pyrolysis Oil Control (0 wt.%) Measured as a Function of Temperature ($^{\circ}\text{C}$) and Storage Time (hr)	289
4.28	Viscosity (cP) of Anisole Blended Pine Wood Pyrolysis Oil (10 wt.%) Measured as a Function of Temperature ($^{\circ}\text{C}$) and Storage Time (hr)	290
4.29	Viscosity (cP) of Glycerol Blended Pine Wood Pyrolysis Oil (10 wt.%) Measured as a Function of Temperature ($^{\circ}\text{C}$) and Storage Time (hr)	290
4.30	Viscosity (cP) of Methanol Blended Pine Wood Pyrolysis Oil (10 wt.%) Measured as a Function of Temperature ($^{\circ}\text{C}$) and Storage Time (hr)	291
4.31	Viscosity (cP) of Pine Wood Pyrolysis Oil Control (CTL-0 wt.%) Measured as a Function of Storage Time (hr) and Temperature ($^{\circ}\text{C}$)	291
4.32	Viscosity (cP) of Anisole (ANS) Blended Pine Wood Pyrolysis Oil (10 wt.%) Measured as a Function of Storage Time (hr) and Temperature ($^{\circ}\text{C}$)	292
4.33	Viscosity (cP) of Glycerol (GLY) Blended Pine Wood Pyrolysis Oil (10 wt.%) Measured as a Function of Storage Time (hr) and Temperature ($^{\circ}\text{C}$)	292
4.34	Viscosity (cP) of Methanol (MEH) Blended Pine Wood Pyrolysis Oil (10 wt.%) Measured as a Function of Storage Time (hr) and Temperature ($^{\circ}\text{C}$)	293
4.35	Viscosity (cP) of 2-Furaldehyde (2FL) Blended Pine Wood Pyrolysis Oil (10 wt.%) Measured as a Function of Storage Time (hr) and Temperature ($^{\circ}\text{C}$)	293
4.36	Percentage Increase in Viscosity of Control (0 wt.%) and Additive Blended (10 wt.%) Pine Wood Pyrolysis Oils Obtained at a Shear Rate of 100 s^{-1} and a Temperature of $25\text{ }^{\circ}\text{C}$	294
4.37	Viscosity (cP) of Alcohol Blended Pine Wood Pyrolysis Oils Measured as a Function of Storage Time (hr) [Shear Rate = 100 s^{-1}]	294
4.38	Shear Stress versus Shear Rate Profiles of Control, Anisole, Glycerol, and Methanol Blended Pine Wood Pyrolysis Oils at a Storage Time of 0 hr and Measurement Temperature of $25\text{ }^{\circ}\text{C}$	295

4.39	Shear Stress versus Shear Rate Profiles of Control, Anisole, Glycerol, and Methanol Blended Pine Wood Pyrolysis Oils at a Storage Time of 192 hr and Measurement Temperature of 25 °C	295
4.40	Increase in Water Content (%) of Control (0 wt.%) and Additive Blended (10 wt.%) Pine Wood Pyrolysis Oils Measured at Storage Times of 0 and 192 hr	296
4.41	Water Content (wt.%) of Alcohol Blended (10 wt.%) Pine Wood Pyrolysis Oils Measured as a Function of Storage Time (hr)	296
4.42	Typical Behavior of the Water Content (wt.%) of Additive Blended (10 wt.%) Pine Wood Pyrolysis Oils Measured as a Function of Storage Time (hr)	297
4.43	The pH of Control (0 wt.%) and Additive Blended (10 wt.%) Pine Wood Pyrolysis Oils Measured at Initial Storage Time (0 hr)	297
4.44	The pH of Alcohol Blended (10 wt.%) Pine Wood Pyrolysis Oils Measured as a Function of Storage Time (hr)	298
4.45	Viscosity Measured at 25 °C and 0 hr as a Function of Shear Rate for Control (0 wt.%) and Additive Blended (10 wt.%) Pyrolysis Oils	298
4.46	Viscosity Measured at 25 °C and 192 hr as a Function of Shear Rate for Control (0 wt.%) and Additive Blended (10 wt.%) Pyrolysis Oils	299
4.47	Viscosity Measured at 25 °C and 192 hr as a Function of Shear Rate for Glycerol Blended (0-20 wt.%) Pyrolysis Oils	299
4.48	Shear Stress Measured at 25 °C as a Function of Shear Rate and Storage Time for Control (0 wt.%) Pyrolysis Oil	300
4.49	Shear Stress Measured at 25 °C as a Function of Shear Rate and Storage Time for Glycerol Blended (5 wt.%) Pyrolysis Oil	300
4.50	Shear Stress Measured at 25 °C as a Function of Shear Rate and Storage Time for Glycerol Blended (10 wt.%) Pyrolysis Oil	301
4.51	Shear Stress Measured at 25 °C as a Function of Shear Rate and Storage Time for Glycerol Blended (15 wt.%) Pyrolysis Oil	301
4.52	Shear Stress Measured at 25 °C as a Function of Shear Rate and Storage Time for Glycerol Blended (20 wt.%) Pyrolysis Oil	302

4.53	Viscosity (cP) Measured at 25 ⁰ C as a Function of Shear Rate (SR=s ⁻¹) and Storage Time (hr) for Control (0 wt.%) Pyrolysis Oil	302
4.54	Viscosity (cP) Measured at 50 ⁰ C as a Function of Shear Rate (SR=s ⁻¹) and Storage Time (hr) for Control (0 wt.%) Pyrolysis Oil	303
4.55	Viscosity (cP) Measured at 80 ⁰ C as a Function of Shear Rate (SR=s ⁻¹) and Storage Time (hr) for Control (0 wt.%) Pyrolysis Oil	303
4.56	Viscosity (cP) Measured at 25 ⁰ C as a Function of Shear Rate (SR=s ⁻¹) and Storage Time (hr) for Glycerol (10 wt.%) Blended Pyrolysis Oil.....	304
4.57	Viscosity (cP) Measured at 50 ⁰ C as a Function of Shear Rate (SR=s ⁻¹) and Storage Time (hr) for Glycerol (10 wt.%) Blended Pyrolysis Oil.....	304
4.58	Viscosity (cP) Measured at 80 ⁰ C as a Function of Shear Rate (SR=s ⁻¹) and Storage Time (hr) for Glycerol (10 wt.%) Blended Pyrolysis Oil.....	305
4.59	Viscosity (cP) Measured at 25 ⁰ C as a Function of Shear Rate (SR=s ⁻¹) and Storage Time (hr) for Anisole (5 wt.%) Blended Pyrolysis Oil.....	305
4.60	Viscosity (cP) Measured at 25 ⁰ C as a Function of Shear Rate (SR=s ⁻¹) and Storage Time (hr) for Anisole (10 wt.%) Blended Pyrolysis Oil.....	306
4.61	Viscosity (cP) Measured at 25 ⁰ C as a Function of Shear Rate (SR=s ⁻¹) and Storage Time (hr) for Anisole (15 wt.%) Blended Pyrolysis Oil.....	306
4.62	Viscosity (cP) Measured at 25 ⁰ C as a Function of Shear Rate (SR=s ⁻¹) and Storage Time (hr) for Glycerol (5 wt.%) Blended Pyrolysis Oil.....	307
4.63	Viscosity (cP) Measured at 25 ⁰ C as a Function of Shear Rate (SR=s ⁻¹) and Storage Time (hr) for Glycerol (15 wt.%) Blended Pyrolysis Oil.....	307
4.64	Viscosity (cP) Measured at 25 ⁰ C as a Function of Shear Rate (SR=s ⁻¹) and Storage Time (hr) for Glycerol (20 wt.%) Blended Pyrolysis Oil.....	308

4.65	Viscosity (cP) Measured at 25 °C as a Function of Shear Rate (SR=s ⁻¹) and Storage Time (hr) for Methanol (5 wt.%) Blended Pyrolysis Oil.....	308
4.66	Viscosity (cP) Measured at 25 °C as a Function of Shear Rate (SR=s ⁻¹) and Storage Time (hr) for Methanol (10 wt.%) Blended Pyrolysis Oil.....	309
4.67	Viscosity (cP) Measured at 25 °C as a Function of Shear Rate (SR=s ⁻¹) and Storage Time (hr) for Methanol (15 wt.%) Blended Pyrolysis Oil.....	309
4.68	Viscosity Increase (%) of Pine Wood Pyrolysis Oils Obtained at 25 °C and 100 s ⁻¹ as a Function of Additive Concentration (0-20 wt.%)	310
4.69	Storage Modulus (25 °C) of Anisole Blended Pyrolysis Oil (15 wt.%) Measured as a Function of Frequency and Storage Time.....	310
4.70	Loss Modulus (25 °C) of Anisole Blended Pyrolysis Oil (15 wt.%) Measured as a Function of Frequency and Storage Time.....	311
4.71	Storage Modulus (25 °C) of Glycerol Blended Pyrolysis Oil (15 wt.%) Measured as a Function of Frequency and Storage Time.....	311
4.72	Loss Modulus (25 °C) of Glycerol Blended Pyrolysis Oil (15 wt.%) Measured as a Function of Frequency and Storage Time.....	312
4.73	Storage Modulus (25 °C) of Methanol Blended Pyrolysis Oil (15 wt.%) Measured as a Function of Frequency and Storage Time.....	312
4.74	Loss Modulus (25 °C) of Methanol Blended Pyrolysis Oil (15 wt.%) Measured as a Function of Frequency and Storage Time.....	313
4.75	Storage Modulus of Control (0 wt.%) and Additive Blended Pyrolysis Oils (15 wt.%) Measured at 192 hr and 25 °C	313
4.76	Loss Modulus of Control (0 wt.%) and Additive Blended Pyrolysis Oils (15 wt.%) Measured at 192 hr and 25 °C.....	314
4.77	Storage Modulus of Anisole Blended Pyrolysis Oil Measured as a Function of Concentration (0-20 wt.%) and Frequency at 192 hr and 25 °C	314
4.78	Loss Modulus of Anisole Blended Pyrolysis Oil Measured as a Function of Concentration (0-20 wt.%) and Frequency at 192 hr and 25 °C.....	315

4.79	Storage Modulus of Glycerol Blended Pyrolysis Oil Measured as a Function of Concentration (0-20 wt.%) and Frequency at 192 hr and 25 °C	315
4.80	Loss Modulus of Glycerol Blended Pyrolysis Oil Measured as a Function of Concentration (0-20 wt.%) and Frequency at 192 hr and 25 °C	316
4.81	Storage Modulus of Methanol Blended Pyrolysis Oil Measured as a Function of Concentration (0-20 wt.%) and Frequency at 192 hr and 25 °C	316
4.82	Loss Modulus of Methanol Blended Pyrolysis Oil Measured as a Function of Concentration (0-20 wt.%) and Frequency at 192 hr and 25 °C	317
4.83	Storage Modulus of Anisole Blended Pyrolysis Oil Measured as a Function of Concentration (0-20 wt.%) and Strain at 192 hr and 25 °C	317
4.84	Loss Modulus of Anisole Blended Pyrolysis Oil Measured as a Function of Concentration (0-20 wt.%) and Strain at 192 hr and 25 °C	318
4.85	Storage Modulus of Control (0 wt.%) and Additive Blended (5 wt.%) Pyrolysis Oil Measured as a Function of Strain at 192 hr and 25 °C.....	318
4.86	Loss Modulus of Control (0 wt.%) and Additive Blended (5 wt.%) Pyrolysis Oil Measured as a Function of Strain at 192 hr and 25 °C.....	319
4.87	Microscopic Images (200X and 40X) Obtained for the Fresh (0 hr) Pine Bark Pyrolysis Oil at 25 °C.....	319
4.88	Microscopic Images (200X) Obtained for the Aged (192 hr) Pine Bark Pyrolysis Oil at 25 °C.....	320
4.89	Water Content (wt.%) of Anisole Blended Pyrolysis Oil as a Function of Concentration (0-20 wt.%) and Storage Time	321
4.90	pH of Anisole Blended Pyrolysis Oil as a Function of Concentration (0-20 wt.%) and Storage Time.....	321
4.91	Viscosity (cP) of Pine Wood Pyrolysis Oil Control (0 wt.%) Measured at 96 hr as a Function of Shear Rate (s ⁻¹) and Temperature (°C).....	322

4.92	Viscosity (cP) of Anisole Blended (10 wt.%) Pine Wood Pyrolysis Oil Measured at 96 hr as a Function of Shear Rate (s^{-1}) and Temperature ($^{\circ}C$)	322
4.93	Viscosity (cP) of Mississippi State University (MS) Pine Wood Oil Control (CTL2) as a Function of Shear Rate (s^{-1}) and Storage Time (Month-M).....	323
4.94	Viscosity (cP) of Mississippi State University (MS) Pine Wood Oil Control (CTL2) as a Function of Shear Rate (s^{-1}) and Storage Time (Hour-H).....	323
4.95	Viscosity (cP) as a Function of Shear Rate (s^{-1}) of Mississippi State University (MS) Fresh (0 hr) Oak Wood Oil Controls (CTL's 1-3).....	324
4.96	Viscosity (cP) as a Function of Shear Rate (s^{-1}) of Mississippi State University (MS) Oak Wood Oil Controls (CTL's 1-3) Aged to 192 hours.....	324
4.97	Viscosity (cP) as a Function of Shear Rate (s^{-1}) of Additive Blended (5 wt.%) Mississippi State University (MS) Fresh (0 hr) Oak Wood Oils	325
4.98	Viscosity (cP) as a Function of Shear Rate (s^{-1}) of Additive Blended (5 wt.%) Mississippi State University (MS) Oak Wood Oils Aged to 192 hours.....	325
4.99	Viscosity (cP) as a Function of Shear Rate (s^{-1}) of Additive Blended (10 wt.%) Mississippi State University (MS) Fresh (0 hr) Oak Wood Oils	326
4.100	Viscosity (cP) as a Function of Shear Rate (s^{-1}) of Additive Blended (10 wt.%) Mississippi State University (MS) Oak Wood Oils Aged to 192 hours.....	326
4.101	Viscosity (cP) of Mississippi State University (MS) Oak Bark Oil Control (CTL2) as a Function of Shear Rate (s^{-1}) and Storage Time (Month-M).....	327
4.102	Viscosity (cP) of Mississippi State University (MS) Oak Bark Oil Control (CTL2) as a Function of Shear Rate (s^{-1}) and Storage Time (Hour-H).....	327

4.103 Viscosity (cP) as a Function of Shear Rate (s^{-1}) of Mississippi State University (MS) Fresh (0 hr) Pine Bark Oil Controls (CTL's 1-3)	328
4.104 Viscosity (cP) as a Function of Shear Rate (s^{-1}) of Mississippi State University (MS) Pine Bark Oil Controls (CTL's 1-3) Aged to 180 days	328
4.105 Viscosity (cP) as a Function of Shear Rate (s^{-1}) of Additive Blended (5 wt.%) Mississippi State University (MS) Fresh (0 hr) Pine Bark Oil.....	329
4.106 Viscosity (cP) as a Function of Shear Rate (s^{-1}) of Additive Blended (10 wt.%) Mississippi State University (MS) Fresh (0 hr) Pine Bark Oil.....	329
4.107 Viscosity (cP) as a Function of Shear Rate (s^{-1}) of Additive Blended (5 wt.%) Mississippi State University (MS) Pine Bark Oil Aged to 180 days	330
4.108 Viscosity (cP) as a Function of Shear Rate (s^{-1}) of Additive Blended (10 wt.%) Mississippi State University (MS) Pine Bark Oil Aged to 180 days	330
4.109 Rheometer Spindle Revealing the Sheared Pine Bark Pyrolysis Oil.....	331
4.110 Viscosity (cP) as a Function of Storage Time (days) of Renewable Oil International (RI) Low Temperature Pine Wood Pyrolysis Oils (Controls and Additive Blended).....	332
4.111 Viscosity (cP) as a Function of Storage Time (hours) of Renewable Oil International (RI) Low Temperature Pine Wood Pyrolysis Oils (Controls and Additive Blended).....	332
4.112 Viscosity (cP) as a Function of Storage Time (days) of National Renewable Energy Laboratory (NR) Low Temperature Oak Wood Pyrolysis Oils (Controls and Additive Blended).....	333
4.113 Viscosity (cP) as a Function of Storage Time (hours) of National Renewable Energy Laboratory (NR) Low Temperature Oak Wood Pyrolysis Oils (Controls and Additive Blended).....	333
4.114 Viscosity Increase (%) as a Function of Methanol Concentration (wt.%) of Mississippi State University (MS) and National Renewable Energy Laboratory (NR) Low Temperature Oak Wood Pyrolysis Oils	334

4.115 Viscosity Increase (%) as a Function of Storage Temperature of Renewable Oil International (RI) Low Temperature Pine Wood Pyrolysis Oils (Controls and Additive Blended)	334
4.116 Water Content (wt.%) as a Function of Storage Time (days) of National Renewable Energy Laboratory (NR) Low Temperature Oak Wood Pyrolysis Oils (Controls and Additive Blended).....	335
4.117 Water Content (wt.%) as a Function of Storage Time (hours) of National Renewable Energy Laboratory (NR) Low Temperature Oak Wood Pyrolysis Oils (Controls and Additive Blended).....	335
4.118 Water Content (wt.%) as a Function of Storage Time (days) of Mississippi State University (MS) Low Temperature Oak Bark Pyrolysis Oils (Controls and Additive Blended)	336
4.119 Water Content (wt.%) as a Function of Storage Time (hours) of Mississippi State University (MS) Low Temperature Oak Bark Pyrolysis Oils (Controls and Additive Blended)	336
4.120 Water Content Increase (%) as a Function of Storage Temperature of Mississippi State University (MS) Low Temperature Oak Bark Pyrolysis Oils (Controls and Additive Blended)	337
4.121 Water Content Increase (%) as a Function of Methanol Concentration (wt.%) of Mississippi State University (MS) and Renewable Oil International (RI) Low Temperature Pine Wood Pyrolysis Oils	337
4.122 Density (g/ml) as a Function of Storage Time (days) of National Renewable Energy Laboratory (NR) Low Temperature Oak Wood Pyrolysis Oils (Controls and Additive Blended).....	338
4.123 Density (g/ml) as a Function of Storage Time (hours) of National Renewable Energy Laboratory (NR) Low Temperature Oak Wood Pyrolysis Oils (Controls and Additive Blended).....	338
4.124 pH as a Function of Storage Time (days) of National Renewable Energy Laboratory (NR) Low Temperature Oak Wood Pyrolysis Oils (Controls and Additive Blended)	339
4.125 pH as a Function of Storage Time (hours) of National Renewable Energy Laboratory (NR) Low Temperature Oak Wood Pyrolysis Oils (Controls and Additive Blended)	339

4.126 Breakthrough Curves of pH as a Function of Storage Time (Month-M) and Titrant Volume (ml) for National Renewable Energy Laboratory (NR) High Temperature Pine Wood Pyrolysis Oil Control (CTL1).....	340
4.127 Breakthrough Curves of pH as a Function of Storage Time (Month-M) and Titrant Volume (ml) for National Renewable Energy Laboratory (NR) High Temperature Anisole Blended (10 wt.%) Pine Wood Pyrolysis Oil.....	340
4.128 Breakthrough Curves of pH as a Function of Storage Time (Month-M) and Titrant Volume (ml) for National Renewable Energy Laboratory (NR) High Temperature Oak Wood Pyrolysis Oil Control (CTL1).....	341
4.129 Breakthrough Curves of pH as a Function of Storage Time (Month-M) and Titrant Volume (ml) for National Renewable Energy Laboratory (NR) High Temperature Anisole Blended (10 wt.%) Oak Wood Pyrolysis Oil.....	341
4.130 Acid Value (mg KOH/g Oil) as a Function of Storage Time for National Renewable Energy Laboratory (NR) High Temperature Pine Wood (PW) and Oak Wood (OW) Pyrolysis Oils (Control-CTL1 and Anisole-10 wt.%)	342
4.131 Sample Weight as a Function of Storage Time (days) of National Renewable Energy Laboratory (NR) Low Temperature Oak Wood Pyrolysis Oils (Control and Additive Blended)	342
4.132 Sample Weight as a Function of Storage Time (hours) of National Renewable Energy Laboratory (NR) Low Temperature Oak Wood Pyrolysis Oils (Control and Additive Blended)	343
4.133 Surface Response Plots Obtained for the Normalized Viscosity (cP) of Mississippi State University (MS) Pine Wood Pyrolysis Oil as a Function of Storage Time (month) and Methanol Concentration (wt.%).....	344
4.134 Contour Plots Obtained for the Normalized Viscosity (cP) of Mississippi State University (MS) Pine Wood Pyrolysis Oil as a Function of Storage Time (month) and Methanol Concentration (wt.%)	344
4.135 Surface Response Plots Obtained for the Normalized Viscosity (cP) of Mississippi State University (MS) Oak Wood Pyrolysis Oil as a Function of Storage Time (month) and Shear Rate (s ⁻¹).....	345

4.136	Contour Plots Obtained for the Normalized Viscosity (cP) of Mississippi State University (MS) Oak Wood Pyrolysis Oil as a Function of Storage Time (month) and Shear Rate (s^{-1})	345
4.137	Surface Response Plots Obtained for the Normalized Viscosity (cP) of Mississippi State University (MS) Oak Bark Pyrolysis Oil as a Function of Shear Rate (s^{-1}) and Anisole Concentration (wt.%)	346
4.138	Contour Plots Obtained for the Normalized Viscosity (cP) of Mississippi State University (MS) Oak Bark Pyrolysis Oil as a Function of Shear Rate (s^{-1}) and Anisole Concentration (wt.%).....	346
4.139	Ball and Spoke Models Obtained for the Hydrogen Bonding of Anisole with a) Guaiacol and b) Syringol as Predicted by Spartan Wave Function [©]	347
4.140	Cost of Glycerol Addition to Pine Wood Pyrolysis Oil as a Function of its Concentration (wt.%).....	347
A.1	Reactor Yields of Mississippi State-Pine Wood-Low Temperature-Fast Residence (MS-PW-LT-FR) Bio-Oil.....	364
A.2	Reactor Yields of Mississippi State-Pine Wood-High Temperature-Fast Residence (MS-PW-HT-FR) Bio-Oil	364
A.3	Reactor Yields of Mississippi State-Pine Wood-Low Temperature-Slow Residence (MS-PW-LT-SR) Bio-Oil.....	365
A.4	Reactor Yields of Mississippi State-Pine Wood-High Temperature-Slow Residence (MS-PW-HT-SR) Bio-Oil	365
A.5	Reactor Yields of Mississippi State-Oak Wood-Low Temperature-Fast Residence (MS-OW-LT-FR) Bio-Oil.....	366
A.6	Reactor Yields of Mississippi State-Oak Wood-High Temperature-Fast Residence (MS-OW-HT-FR) Bio-Oil.....	366
A.7	Reactor Yields of Mississippi State-Oak Wood-Low Temperature-Slow Residence (MS-OW-LT-SR) Bio-Oil	367
A.8	Reactor Yields of Mississippi State-Pine Bark-Low Temperature-Fast Residence (MS-PB-LT-FR) Bio-Oil.....	367
A.9	Reactor Yields of Mississippi State-Pine Bark-High Temperature-Fast Residence (MS-PB-HT-FR) Bio-Oil	368

A.10	Reactor Yields of Mississippi State-Pine Bark-Low Temperature-Slow Residence (MS-PB-LT-SR) Bio-Oil.....	368
A.11	Reactor Yields of Mississippi State-Pine Bark-High Temperature-Slow Residence (MS-PB-HT-SR) Bio-Oil	369
A.12	Reactor Yields of Mississippi State-Oak Bark-Low Temperature-Fast Residence (MS-OB-LT-FR) Bio-Oil	369
A.13	Reactor Yields of Mississippi State-Oak Bark-High Temperature-Fast Residence (MS-OB-HT-FR) Bio-Oil.....	370
A.14	Reactor Yields of Mississippi State-Oak Bark-Low Temperature-Slow Residence (MS-OB-LT-SR) Bio-Oil	370
A.15	Reactor Yields of Mississippi State-Oak Bark-High Temperature-Slow Residence (MS-OB-HT-SR) Bio-Oil.....	371
A.16	Average Reactor Yields of Mississippi State-Pine Wood-Slow Residence (MS-PW-SR) Bio-Oils	371
A.17	Average Reactor Yields of Mississippi State-Pine Wood-Fast Residence (MS-PW-FR) Bio-Oils.....	372
A.18	Average Reactor Yields of Mississippi State-Pine Wood-Low Temperature (MS-PW-LT) Bio-Oils	372
A.19	Average Reactor Yields of Mississippi State-Pine Wood-High Temperature (MS-PW-HT) Bio-Oils.....	373
A.20	Average Reactor Yields of Mississippi State-Oak Wood-Fast Residence (MS-OW-FR) Bio-Oils	373
A.21	Average Reactor Yields of Mississippi State-Oak Wood-High Temperature (MS-OW-HT) Bio-Oils	374
A.22	Average Reactor Yields of Mississippi State-Pine Bark-Slow Residence (MS-PB-SR) Bio-Oils.....	374
A.23	Average Reactor Yields of Mississippi State-Pine Bark-Fast Residence (MS-PB-FR) Bio-Oils.....	375
A.24	Average Reactor Yields of Mississippi State-Pine Bark-Low Temperature (MS-PB-LT) Bio-Oils	375

A.25	Average Reactor Yields of Mississippi State-Pine Bark-High Temperature (MS-PB-HT) Bio-Oils	376
A.26	Average Reactor Yields of Mississippi State-Oak Bark-Slow Residence (MS-OB-SR) Bio-Oils	376
A.27	Average Reactor Yields of Mississippi State-Oak Bark-Fast Residence (MS-OB-FR) Bio-Oils	377
A.28	Average Reactor Yields of Mississippi State-Oak Bark-Low Temperature (MS-OB-LT) Bio-Oils.....	377
A.29	Average Reactor Yields of Mississippi State-Oak Bark-High Temperature (MS-OB-HT) Bio-Oils	378
B.1	Viscosity (cP) as a Function of Aging Time (days) of Pine Wood (PW) Pyrolysis Oils [Temperature (LT-Low and High-HT) and Time (SR-Slow and Fast-FR)] of Mississippi State University	381
B.2	Density (g/ml) as a Function of Aging Time (days) of Pine Wood (PW) Pyrolysis Oils [Temperature (LT-Low and High-HT) and Time (SR-Slow and Fast-FR)] of Mississippi State University	381
B.3	Acidity (pH) as a Function of Aging Time (days) of Pine Wood (PW) Pyrolysis Oils [Temperature (LT-Low and High-HT) and Time (SR-Slow and Fast-FR)] of Mississippi State University	382
B.4	Water Content (wt.%) as a Function of Aging Time (days) of Pine Wood (PW) Pyrolysis Oils [Temperature (LT-Low and High-HT) and Time (SR-Slow and Fast-FR)] of Mississippi State University	382
B.5	Viscosity (cP) as a Function of Shear Rate (s^{-1}) and Residence Time (SR-Slow and Fast-FR) of Pine Wood (PW) Low Temperature (LT) Oils of Mississippi State University.....	383
B.6	Viscosity (cP) as a Function of Shear Rate (s^{-1}) and Residence Time (SR-Slow and Fast-FR) of Oak Wood (OW) High Temperature (HT) Oils of Mississippi State University	383
B.7	Viscosity (cP) as a Function of Shear Rate (s^{-1}) and Pyrolysis Temperature (LT-Low and High-HT) of Pine Wood (PW) Fast Residence (FR) Oils of Mississippi State University	384

B.8	Viscosity (cP) as a Function of Shear Rate (s^{-1}) and Pyrolysis Temperature (LT-Low and High-HT) of Oak Wood (OW) Slow Residence (SR) Oils of Mississippi State University	384
C.1	Viscosity (cP) of Methyl Tertiary Butyl Ether Blended Pyrolysis Oil (10 wt.%) Measured as a Function of Shear Rate (s^{-1}) and Storage Time (hr).....	387
C.2	Viscosity (cP) of Methyl Ethyl Ketone Blended Pyrolysis Oil (10 wt.%) Measured as a Function of Shear Rate (s^{-1}) and Storage Time (hr).....	387
C.3	Viscosity (cP) of Ethanol Blended Pyrolysis Oil (10 wt.%) Measured as a Function of Shear Rate (s^{-1}) and Storage Time (hr).....	388
C.4	Viscosity (cP) of Decahydronaphthalene Blended Pyrolysis Oil (10 wt.%) Measured as a Function of Shear Rate (s^{-1}) and Storage Time (hr).....	388
C.5	Viscosity (cP) of Acetone Blended Pyrolysis Oil (10 wt.%) Measured as a Function of Shear Rate (s^{-1}) and Storage Time (hr).....	389
C.6	Viscosity (cP) of Xylene Blended Pyrolysis Oil (10 wt.%) Measured as a Function of Shear Rate (s^{-1}) and Storage Time (hr).....	389
C.7	Viscosity (cP) of Tetrahydronaphthalene Blended Pyrolysis Oil (10 wt.%) Measured as a Function of Shear Rate (s^{-1}) and Storage Time (hr).....	390
C.8	Viscosity (cP) of Methyl Formate Blended Pyrolysis Oil (10 wt.%) Measured as a Function of Shear Rate (s^{-1}) and Storage Time (hr).....	390
C.9	Viscosity (cP) of Isopropyl Ether Blended Pyrolysis Oil (10 wt.%) Measured as a Function of Shear Rate (s^{-1}) and Storage Time (hr).....	391
C.10	Viscosity (cP) of Ethyl Ether Blended Pyrolysis Oil (10 wt.%) Measured as a Function of Shear Rate (s^{-1}) and Storage Time (hr).....	391
C.11	Viscosity (cP) of Cyclopentanone Blended Pyrolysis Oil (10 wt.%) Measured as a Function of Shear Rate (s^{-1}) and Storage Time (hr).....	392
C.12	Viscosity (cP) of Acetaldehyde Blended Pyrolysis Oil (10 wt.%) Measured as a Function of Shear Rate (s^{-1}) and Storage Time (hr).....	392
C.13	Viscosity (cP) of t-Butanol Blended Pyrolysis Oil (10 wt.%) Measured as a Function of Shear Rate (s^{-1}) and Storage Time (hr).....	393

C.14	Viscosity (cP) of Tetrahydrofuran Blended Pyrolysis Oil (10 wt.%) Measured as a Function of Shear Rate (s^{-1}) and Storage Time (hr).....	393
C.15	Viscosity (cP) of Methyl Acetate Blended Pyrolysis Oil (10 wt.%) Measured as a Function of Shear Rate (s^{-1}) and Storage Time (hr).....	394
C.16	Viscosity (cP) of Ethyl Acetate Blended Pyrolysis Oil (10 wt.%) Measured as a Function of Shear Rate (s^{-1}) and Storage Time (hr).....	394
C.17	Viscosity (cP) of Cyclohexane Blended Pyrolysis Oil (10 wt.%) Measured as a Function of Shear Rate (s^{-1}) and Storage Time (hr).....	395
C.18	Viscosity (cP) of 2-Propanol Blended Pyrolysis Oil (10 wt.%) Measured as a Function of Shear Rate (s^{-1}) and Storage Time (hr).....	395
C.19	Viscosity (cP) of Resorcinol Blended Pyrolysis Oil (10 wt.%) Measured as a Function of Shear Rate (s^{-1}) and Storage Time (hr).....	396
C.20	Viscosity (cP) of Polyethylene Glycol Blended Pyrolysis Oil (10 wt.%) Measured as a Function of Shear Rate (s^{-1}) and Storage Time (hr).....	396
C.21	Viscosity (cP) of Furfuryl Alcohol Blended Pyrolysis Oil (10 wt.%) Measured as a Function of Shear Rate (s^{-1}) and Storage Time (hr).....	397
C.22	Viscosity (cP) of Dimethyl Ether Blended Pyrolysis Oil (10 wt.%) Measured as a Function of Shear Rate (s^{-1}) and Storage Time (hr).....	397
C.23	Viscosity (cP) of 2-Furaldehyde Blended Pyrolysis Oil (10 wt.%) Measured as a Function of Shear Rate (s^{-1}) and Storage Time (hr).....	398
C.24	Percentage Increase in Viscosity (0 hr vs. 192 hr) of Methyl Tertiary Butyl Ether Blended Pyrolysis Oil (10 wt.%) Obtained as a Function of Shear Rate (s^{-1})	398
C.25	Percentage Increase in Viscosity (0 hr vs. 192 hr) of Methyl Ethyl Ketone Blended Pyrolysis Oil (10 wt.%) Obtained as a Function of Shear Rate (s^{-1})	399
C.26	Percentage Increase in Viscosity (0 hr vs. 192 hr) of Ethanol Blended Pyrolysis Oil (10 wt.%) Obtained as a Function of Shear Rate (s^{-1}).....	399
C.27	Percentage Increase in Viscosity (0 hr vs. 192 hr) of Decahydronaphthalene Blended Pyrolysis Oil (10 wt.%) Obtained as a Function of Shear Rate (s^{-1}).....	400

C.28	Percentage Increase in Viscosity (0 hr vs. 192 hr) of Acetone Blended Pyrolysis Oil (10 wt.%) Obtained as a Function of Shear Rate (s^{-1}).....	400
C.29	Percentage Increase in Viscosity (0 hr vs. 192 hr) of Xylene Blended Pyrolysis Oil (10 wt.%) Obtained as a Function of Shear Rate (s^{-1}).....	401
C.30	Percentage Increase in Viscosity (0 hr vs. 192 hr) of Tetrahydronaphthalene Blended Pyrolysis Oil (10 wt.%) Obtained as a Function of Shear Rate (s^{-1}).....	401
C.31	Percentage Increase in Viscosity (0 hr vs. 192 hr) of Methyl Formate Blended Pyrolysis Oil (10 wt.%) Obtained as a Function of Shear Rate (s^{-1}).....	402
C.32	Percentage Increase in Viscosity (0 hr vs. 192 hr) of Isopropyl Ether Blended Pyrolysis Oil (10 wt.%) Obtained as a Function of Shear Rate (s^{-1}).....	402
C.33	Percentage Increase in Viscosity (0 hr vs. 192 hr) of Ethyl Ether Blended Pyrolysis Oil (10 wt.%) Obtained as a Function of Shear Rate (s^{-1}).....	403
C.34	Percentage Increase in Viscosity (0 hr vs. 192 hr) of Cyclopentanone Blended Pyrolysis Oil (10 wt.%) Obtained as a Function of Shear Rate (s^{-1}).....	403
C.35	Percentage Increase in Viscosity (0 hr vs. 192 hr) of Acetaldehyde Blended Pyrolysis Oil (10 wt.%) Obtained as a Function of Shear Rate (s^{-1}).....	404
C.36	Percentage Increase in Viscosity (0 hr vs. 192 hr) of t-Butanol Blended Pyrolysis Oil (10 wt.%) Obtained as a Function of Shear Rate (s^{-1}).....	404
C.37	Percentage Increase in Viscosity (0 hr vs. 192 hr) of Tetrahydrofuran Blended Pyrolysis Oil (10 wt.%) Obtained as a Function of Shear Rate (s^{-1}).....	405
C.38	Percentage Increase in Viscosity (0 hr vs. 192 hr) of Methyl Acetate Blended Pyrolysis Oil (10 wt.%) Obtained as a Function of Shear Rate (s^{-1}).....	405

C.39	Percentage Increase in Viscosity (0 hr vs. 192 hr) of Ethyl Acetate Blended Pyrolysis Oil (10 wt.%) Obtained as a Function of Shear Rate (s^{-1}).....	406
C.40	Percentage Increase in Viscosity (0 hr vs. 192 hr) of Cyclohexane Blended Pyrolysis Oil (10 wt.%) Obtained as a Function of Shear Rate (s^{-1}).....	406
C.41	Percentage Increase in Viscosity (0 hr vs. 192 hr) of 2-Propanol Blended Pyrolysis Oil (10 wt.%) Obtained as a Function of Shear Rate (s^{-1}).....	407
C.42	Percentage Increase in Viscosity (0 hr vs. 192 hr) of Polyethylene Glycol Blended Pyrolysis Oil (10 wt.%) Obtained as a Function of Shear Rate (s^{-1}).....	407
C.43	Percentage Increase in Viscosity (0 hr vs. 192 hr) of Dimethyl Ether Blended Pyrolysis Oil (10 wt.%) Obtained as a Function of Shear Rate (s^{-1}).....	408
C.44	Percentage Increase in Viscosity (0 hr vs. 192 hr) of 2-Furaldehyde Blended Pyrolysis Oil (10 wt.%) Obtained as a Function of Shear Rate (s^{-1}).....	408
C.45	Viscosity (cP) of Methyl Tertiary Butyl Ether Blended Pyrolysis Oil (10 wt.%) Measured as a Function of Storage Time (hr) and Temperature ($^{\circ}C$).....	409
C.46	Viscosity (cP) of Methyl Ethyl Ketone Blended Pyrolysis Oil (10 wt.%) Measured as a Function of Storage Time (hr) and Temperature ($^{\circ}C$).....	409
C.47	Viscosity (cP) of Ethanol Blended Pyrolysis Oil (10 wt.%) Measured as a Function of Storage Time (hr) and Temperature ($^{\circ}C$).....	410
C.48	Viscosity (cP) of Decahydronaphthalene Blended Pyrolysis Oil (10 wt.%) Measured as a Function of Storage Time (hr) and Temperature ($^{\circ}C$).....	410
C.49	Viscosity (cP) of Acetone Blended Pyrolysis Oil (10 wt.%) Measured as a Function of Storage Time (hr) and Temperature ($^{\circ}C$).....	411
C.50	Viscosity (cP) of Xylene Blended Pyrolysis Oil (10 wt.%) Measured as a Function of Storage Time (hr) and Temperature ($^{\circ}C$).....	411

C.51	Viscosity (cP) of Tetrahydronaphthalene Blended Pyrolysis Oil (10 wt.%) Measured as a Function of Storage Time (hr) and Temperature ($^{\circ}\text{C}$)	412
C.52	Viscosity (cP) of Methyl Formate Blended Pyrolysis Oil (10 wt.%) Measured as a Function of Storage Time (hr) and Temperature ($^{\circ}\text{C}$)	412
C.53	Viscosity (cP) of Isopropyl Ether Blended Pyrolysis Oil (10 wt.%) Measured as a Function of Storage Time (hr) and Temperature ($^{\circ}\text{C}$)	413
C.54	Viscosity (cP) of Ethyl Ether Blended Pyrolysis Oil (10 wt.%) Measured as a Function of Storage Time (hr) and Temperature ($^{\circ}\text{C}$)	413
C.55	Viscosity (cP) of Cyclopentanone Blended Pyrolysis Oil (10 wt.%) Measured as a Function of Storage Time (hr) and Temperature ($^{\circ}\text{C}$)	414
C.56	Viscosity (cP) of Acetaldehyde Blended Pyrolysis Oil (10 wt.%) Measured as a Function of Storage Time (hr) and Temperature ($^{\circ}\text{C}$)	414
C.57	Viscosity (cP) of t-Butanol Blended Pyrolysis Oil (10 wt.%) Measured as a Function of Storage Time (hr) and Temperature ($^{\circ}\text{C}$)	415
C.58	Viscosity (cP) of Tetrahydrofuran Blended Pyrolysis Oil (10 wt.%) Measured as a Function of Storage Time (hr) and Temperature ($^{\circ}\text{C}$)	415
C.59	Viscosity (cP) of Methyl Acetate Blended Pyrolysis Oil (10 wt.%) Measured as a Function of Storage Time (hr) and Temperature ($^{\circ}\text{C}$)	416
C.60	Viscosity (cP) of Ethyl Acetate Blended Pyrolysis Oil (10 wt.%) Measured as a Function of Storage Time (hr) and Temperature ($^{\circ}\text{C}$)	416
C.61	Viscosity (cP) of Cyclohexane Blended Pyrolysis Oil (10 wt.%) Measured as a Function of Storage Time (hr) and Temperature ($^{\circ}\text{C}$)	417
C.62	Viscosity (cP) of 2-Propanol Blended Pyrolysis Oil (10 wt.%) Measured as a Function of Storage Time (hr) and Temperature ($^{\circ}\text{C}$)	417

C.63	Viscosity (cP) of Resorcinol Blended Pyrolysis Oil (10 wt.%) Measured as a Function of Storage Time (hr) and Temperature ($^{\circ}\text{C}$)	418
C.64	Viscosity (cP) of Polyethylene Glycol Blended Pyrolysis Oil (10 wt.%) Measured as a Function of Storage Time (hr) and Temperature ($^{\circ}\text{C}$)	418
C.65	Viscosity (cP) of Furfuryl Alcohol Blended Pyrolysis Oil (10 wt.%) Measured as a Function of Storage Time (hr) and Temperature ($^{\circ}\text{C}$)	419
C.66	Viscosity (cP) of Dimethyl Ether Blended Pyrolysis Oil (10 wt.%) Measured as a Function of Storage Time (hr) and Temperature ($^{\circ}\text{C}$)	419
D.1	Viscosity Decrease (cP) of Anisole Blended (wt.%) Pyrolysis Oil Obtained as a Function of Measurement Temperature ($^{\circ}\text{C}$)	428
D.2	Viscosity Decrease (cP) of Glycerol Blended (wt.%) Pyrolysis Oil Obtained as a Function of Measurement Temperature ($^{\circ}\text{C}$)	428
D.3	Viscosity Decrease (cP) of Methanol Blended (wt.%) Pyrolysis Oil Obtained as a Function of Measurement Temperature ($^{\circ}\text{C}$)	429
D.4	Mean Water Content Increase (wt.%) of Anisole Blended (wt.%) Pyrolysis Oil Obtained as a Function of Storage Time (hr).....	429
D.5	Mean Water Content Increase (wt.%) of Glycerol Blended (wt.%) Pyrolysis Oil Obtained as a Function of Storage Time (hr).....	430
D.6	Mean Water Content Increase (wt.%) of Methanol Blended (wt.%) Pyrolysis Oil Obtained as a Function of Storage Time (hr).....	430
E.1	Viscosity (cP) of Renewable Oil International (ROI) Pine Wood Oil Control (CTL2) as a Function of Shear Rate (s^{-1}) and Storage Time (month).....	433
E.2	Viscosity (cP) of National Renewable Energy Laboratory (NREL) Low Temperature Pine Wood Oil Control (CTL2) as a Function of Shear Rate (s^{-1}) and Storage Time (month)	433
E.3	Viscosity (cP) of Mississippi State University (MSU) Oak Wood Oil Control (CTL2) as a Function of Shear Rate (s^{-1}) and Storage Time (month)	434

E.4	Viscosity (cP) of Mississippi State University (MSU) Pine Bark Oil Control (CTL2) as a Function of Shear Rate (s^{-1}) and Storage Time (month)	434
E.5	Viscosity (cP) as a Function of Shear Rate (s^{-1}) of Mississippi State University (MSU) Fresh Oak Bark Oil Controls (CTL's 1-3).....	435
E.6	Viscosity (cP) as a Function of Shear Rate (s^{-1}) of Mississippi State University (MSU) Oak Bark Oil Controls (CTL's 1-3) Aged to 180 days	435
E.7	Viscosity (cP) as a Function of Shear Rate (s^{-1}) of Additive Blended (5 wt.%) Mississippi State University (MSU) Fresh Oak Bark Oil.....	436
E.8	Viscosity (cP) as a Function of Shear Rate (s^{-1}) of Additive Blended (5 wt.%) Mississippi State University (MSU) Oak Bark Oil Aged to 180 days	436
E.9	Viscosity (cP) as a Function of Shear Rate (s^{-1}) of Additive Blended (10 wt.%) Mississippi State University (MSU) Fresh Oak Bark Oil.....	437
E.10	Viscosity (cP) as a Function of Shear Rate (s^{-1}) of Additive Blended (10 wt.%) Mississippi State University (MSU) Oak Bark Oil Aged to 180 days	437
E.11	Viscosity (cP) as a Function of Shear Rate (s^{-1}) of Mississippi State University (MSU) Fresh Pine Wood Oil Controls (CTL's 1-3)	438
E.12	Viscosity (cP) as a Function of Shear Rate (s^{-1}) of Mississippi State University (MSU) Pine Wood Oil Controls (CTL's 1-3) Aged to 192 hours	438
E.13	Viscosity (cP) of Mississippi State University (MSU) Oak Wood Oil Control (CTL2) as a Function of Shear Rate (s^{-1}) and Storage Time (hour).....	439
E.14	Viscosity (cP) of Mississippi State University (MSU) Pine Bark Oil Control (CTL2) as a Function of Shear Rate (s^{-1}) and Storage Time (hour).....	439
E.15	Viscosity (cP) as a Function of Shear Rate (s^{-1}) of Additive Blended (5 wt.%) Mississippi State University (MSU) Fresh Pine Wood Oil.....	440

E.16	Viscosity (cP) as a Function of Shear Rate (s^{-1}) of Additive Blended (5 wt.%) Mississippi State University (MSU) Pine Wood Oil Aged to 192 hours.....	440
E.17	Viscosity (cP) as a Function of Shear Rate (s^{-1}) of Additive Blended (10 wt.%) Mississippi State University (MSU) Fresh Pine Wood Oil.....	441
E.18	Viscosity (cP) as a Function of Shear Rate (s^{-1}) of Additive Blended (10 wt.%) Mississippi State University (MSU) Pine Wood Oil Aged to 192 hours.....	441

LIST OF MAJOR SYMBOLS USED

μ	Fluid Viscosity
η_0	Zero Rate Viscosity
η_∞	Infinite Rate Viscosity
ρ	Fluid Density
ω	Angular Frequency
δ	Solubility Parameter
$\dot{\gamma}$	Shear Rate
τ	Shear Stress
α	Statistical Significance Level
G^*	Complex Modulus
G'	Storage Modulus
G''	Loss Modulus
I	Electron Inductive Effect
k	Reaction Rate Constant
K	Limiting Viscosity (Chapter IV)
P	Fluid Pressure
Q	Fluid Flow Rate
T	Instrument Torque

M	Solution Molarity
M_w	Weight Average Molecular Weight
M_n	Number Average Molecular Weight
N	Number of Observations
n	Number of Repeat Units in a Polymer (Chapter II)
n	Viscosity Rate Index (Chapter IV: Phase II)
pH	Negative Logarithm of Hydrogen Ion Concentration
R^2	Regression Coefficient
t	Statistical Test Parameter
W	Sample Weight
X	Reactor Length (Chapter IV: Phase I)
X	Microscope Magnification (Chapter IV: Phase III)

CHAPTER I

INTRODUCTION

Introduction

The increasing consumption of the depleting fossil fuels and their environmental impact has propelled several researchers towards developing alternative and renewable fuels. One such alternative and renewable fuel is pyrolysis oil also known as bio-oil. Pyrolysis oil currently has a tremendous potential to be utilized as a substitute for heavy fuel oil (ASTM No. 4) meeting the 21st century energy demand at least partially. Pyrolysis oil in its crude form is difficult to use as an engine fuel. However, with certain quality upgrading techniques including catalytic hydrodeoxygenation, hot gas filtration, and solvent addition; pyrolysis oil can be used as a potential carbon neutral light fuel oil (ASTM No. 2). Being a novel liquid fuel in the today's market, both chemical and physical properties of the pyrolysis oil need to be studied extensively before its engine application.

Due to the rapid condensation process that is employed during the pyrolysis, complex pyrolysis oil vapor can undergo secondary reactions in the form of cracking and polymerization. During the condensation process many char fines are collected in the pyrolysis oil that is difficult to remove from the pyrolysis oil even after cold filtration. The char fines act as autocatalytic sites for the polymerization reactions to continue until; the pyrolysis oil becomes completely polymerized and phase-separated. Pyrolysis oil

even when stored at room temperature is known to undergo polymerization reactions in the form of condensation and polycondensation that decrease its stability with aging. Consequently, pyrolysis oil viscosity and water content increase as a function of time depending much upon the feedstocks used to produce the oil and its storage conditions. As such, American Society for Testing and Materials (ASTM), Deutsches Institut für Normung (DIN), and other standard testing methods for pyrolysis oil are still in the early stages of development. Therefore, most researchers have resorted to the indirect assessment of pyrolysis oil stability by monitoring its' key physico-chemical properties as a function of storage time (Czernik et al., 1994; Diebold, 2000; Perez et al., 2006; and others).

Pyrolysis oils are prone to polymerization with time and consequently destabilize if proper additives (solvents) are not utilized. Solvent addition has been reported to be the most practical approach for pyrolysis oil quality upgrading (Oasmaa and Czernik, 1999). The addition of solvents to the pyrolysis oils decreases the most essential fuel property (viscosity) with aging. Furthermore, solvents are capable of reducing oil acidity and improving heating value. Extensive testing of the pyrolysis oils is indicated as a must for the better understanding of their chemical and physical properties. The degree or extent of polymerization in the pyrolysis oils can be best measured by its viscosity (Diebold and Czernik, 1997). The resulting information can benefit in the successful commercialization of pyrolysis oils. At present, only limited research is reported on the use of solvents to improve the pyrolysis oil stability. Among the results reported most researchers used methanol as a low-cost solvent. However, its price is projected to increase significantly over the coming years as shown in Figure 1.1. Therefore, the development of a database

of solvents that are effective in the oil stabilization might be useful for both pyrolysis oil producers and end-users.

Pyrolysis Background

Development and utilization of alternative fuel is a direct consequence of increasing energy consumption, rising fuel costs, stricter environmental regulations, and depletion of conventional fuels (Zabaniotou, 1999; Gullu et al., 2001; Huber et al., 2006). One such alternative energy technology is pyrolysis, which utilizes thermo-chemical conversion or thermolysis (thermal degradation) reaction in the absence of oxygen to produce thermal breakdown products (Demirbas, 2002). The use of pyrolysis for the production of liquid fuels started as early as 1980's in the United States. Historically, the use of pyrolysis existed for many centuries primarily for the production of charcoal and coke (Farag et al., 2002). The main advantage of pyrolysis is its feedstock adaptability that can also be its limitation due to the wide variation in oil properties. Hence, the pyrolysis process improvements are absolutely essential.

Lignocellulosic biomass generally refers to the mixture of cellulose, hemicellulose, and lignin polymers. The structural components of wood are cellulose, hemi-cellulose, lignin and a small quantity of extraneous compounds (ash and extractives). Generally, depending on the type of wood (soft or hard) these components differ in their percentage composition (Schultz and Taylor, 1989; McGinnis and Shafizadeh, 1991). Thermal breakdown products of the lignocellulosic biomass constitute a mixture of organic and aqueous rich fractions of pyrolysis oil, char, and off-gas. Pyrolysis oil fractions prior to condensation are known to result from the thermal

fragmentation and defragmentation of polymeric constituents (cellulose, hemicellulose, and lignin) of biomass during the pyrolysis reaction (Bridgwater and Peacocke, 2000).

Pyrolysis oil is a medley of oxygenated hydrocarbons (OHCs) and over 300 chemicals have been identified comprising the pyrolysis oil and more are continuously being identified. However, these compounds are present in negligible quantities in the pyrolysis oil. The resulting oxygenated hydrocarbon fuel (pyrolysis oil) is known to recover 80% of the energy content (maximum yield) from the feedstocks on a dry basis assuming that the char and gas are utilized in the pyrolysis process for heat generation. Pyrolysis oil has been reported to have almost half the high heating value (HHV) of hydrocarbon fuels (petroleum 42-44 MJ/kg) because of its high oxygen and water content. Solid byproduct bio-char/char and non-condensable gases (H_2 , CO, CO_2 , CH_4 , C_2H_4 , and C_2H_6) are also produced from the pyrolysis process. Char being rich in carbon has the potential to be used as a fuel or an adsorbent commercially. Char can also be used as a slow release fertilizer as it is known to contain alkali (Li, Na, and K) and alkaline (Ca, Mg, and Ba) earth metals. The non-condensable gases could be recycled for heat recovery during the pyrolysis process. The organic vapor resulting from pyrolysis could very well be a complex mixture of aerosols, mist, particulate matter and non-condensable gases. Consequently, material balance closures are difficult to obtain during the pyrolysis process (Bridgwater and Peacocke, 2000; Mohan et al., 2006; Mohan et al., 2007; Huber et al., 2006).

Pyrolysis, if operated correctly can produce negligible waste, which makes it a very appealing technology. Common reactor types currently available in the market are shown in Table 1.1 (Bridgwater, 1999). Fluid and circulating beds are frequently used

because of their operational flexibility and ease in scale-up (Bridgwater and Peacocke, 2000). Pyrolysis processes and their associated reactor conditions are presented in Table 1.2. Conventional pyrolysis is traditionally used for making char where as fast and flash pyrolyses are currently targeted for making liquid fuels (Maschio et al., 1992).

Pyrolysis Technologies

The most commonly utilized process these days to produce pyrolysis oil is fast pyrolysis, which utilizes high heat transfer rate followed by rapid quenching (condensation) of the thermal breakdown products of the biomass. Typical fast pyrolysis treatment conditions include small particle size (~2-6 mm), short residence time (0.03-1.5 s), and lower temperature (435-520 °C) in comparison with gasification process (>700 °C). By selectively varying ‘pyrolysis temperature and vapor residence time’ the yields of the pyrolysis oil can be maximized. Further pyrolysis oil recovery efficiencies have been reported to vary as a direct function of process conditions and feed stock types utilized (Bridgwater, 1999).

Many reactor technologies currently exist in the market: circulating fluid bed, ablative reactor, rotating cone, transported bed, and vacuum moving bed to name a few. However, fluidized bed and circulating bed reactor systems are more commonly used and these are reported to produce significantly higher pyrolysis oil yields than most other reactor systems currently available. Minimal time lag during the heat transfer seems to be primarily responsible for higher yields of pyrolysis oil as produced from fluidized bed and circulating bed pyrolysis. Typically, high pyrolysis temperature and fast (or low)

residence time in combination seems to produce the highest yields of pyrolysis oil and lowest yields of char (Bridgwater and Peacocke, 2000).

An auger reactor has been utilized in this research to study biomass pyrolysis. Very few studies were available in the literature pertaining to the use of auger reactors when this research was undertaken. Pyrolysis oil yields as high as 80% are reported in the literature using different reactor systems. However, pyrolysis oil yields of most reactor systems seem to range from 65-75% (Bridgwater and Peacocke, 2000). In the past, different pyrolysis reactor technologies have been utilized to produce pyrolysis oil from forest thinning, sawdust, animal husbandry waste, sewage sludge, black liquor, and other biomass wastes resulting from natural disasters. Consequently, successful production of pyrolysis oil from diverse feedstocks makes pyrolysis technology is a very attractive fuel option (Mohan et al., 2006; Doshi et al., 2005; Johnson and Maclean, 1993).

Pyrolysis Oil Applications

Pyrolysis oil offers several advantages over hydrocarbon fuels to the producers and consumers (Luo et al., 2004; Johnson and Maclean, 1993) namely:

1. Potential alternative to the petroleum-derived fuels
2. Reduces the rate of depletion of fossil fuels from nature
3. Lowers greenhouse gas (GHG) emissions compared to fossil fuels
4. Increased fuel energy density compared to the raw biomass
5. Completely renewable and
6. Extraction and recovery of specialty chemicals for other than fuel applications

One such specialty application includes the utilization of phenolic rich fraction for replacing United State-Environmental Protection Agency (US-EPA) regulated chromated copper arsenate (CCA) wood preservative. Currently, the Forest Products Department at Mississippi State University is working in this area of research. Results indicated that phenolic fractions of the wood and bark derived pyrolysis oils when used in 10% concentration had a greater fungicidal inhibition effect than the whole pyrolysis oils (Mohan et al., 2008). Traditionally, pyrolysis oil also known as ‘liquid-smoke’ has been used as a food flavoring chemical. Pyrolysis oil is currently produced by DynaMotive, Ensyn, Red Arrow Products, Renewable Oil International, VTT and other companies for testing heavy equipment and machinery (Ex: boilers, turbines, diesel engines etc.). Dynamotive in collaboration with Orenda Corporation has been able to lower NO_x and SO_x emissions significantly by the use of pyrolysis oil in comparison with traditional hydrocarbon/diesel fuel (DynaMotive, 2001). Contrary to the petroleum based fuels and their byproducts; numerous applications of pyrolysis oil can be envisioned in the form of resin chemicals, agri-chemicals, emission control agents, and many other specialty byproducts (Bridgwater and Peacocke, 2000). Ensyn is currently involved in the research and development of specialty chemicals as derived from the pyrolysis oil.

Pyrolysis Oil Stability

Several ‘engineering and chemistry’ problems associated with the pyrolysis oil production, storage, and transportation have motivated ‘engineers and scientists’ to develop better technologies in increasing the long-term stability (≥ 1 yr) of pyrolysis oil. Pyrolysis oils when stored for long time periods are known to undergo several

polymerization reactions altering their chemical and physical stability (Diebold, 2000). Consequently, during storage the stability of pyrolysis oils decreases significantly with time if proper additives are not utilized. The measurement of viscosity and water content as a function of time has been a decisive factor in establishing the storage stability trends in pyrolysis oils. Previously, long-term stability of pyrolysis oil has been conducted at both accelerated and ambient temperatures by selectively varying the storage time periods on the order of few days to several months. Ambient and accelerated storage temperatures utilized in the previous studies are reported at 25, 37, 40, 50, 60, 80 and 90 °C (Czernik et al., 1994; Boucher et al., 2000; Oasmaa and Kuoppala, 2003; Chaala et al., 2004; and others). Recently methanol, ethanol, acetone, ethyl acetate, methyl isobutyl ketone and a few other additives were utilized to stabilize the pyrolysis oil. Methanol in 10% concentration level is reported to be effective in stabilizing the pyrolysis oils produced from poplar wood, pine wood, oak wood and other wooden feed stocks (Diebold and Czernik, 1997). However, recent increase in the methanol prices has motivated us to perform extensive studies by utilizing different chemical additives. The average price of methanol for a period of 12 months for the past 8 years has been shown in Figure 1.1. Over the past four years methanol prices have almost doubled.

Pyrolysis Oil Properties

Higher density of pyrolysis oil compared to the green biomass increases the cost-efficiency of fuel handling and transportation significantly (Mohan et al., 2006). Density of pyrolysis oils is reported to range from 1.1 to 1.3 g/ml (Oasmaa and Czernik, 1999) which is roughly 2-3 times that of the dry wood depending on the feed source. At 20 °C,

the kinematic viscosity of the pyrolysis oil from forest residues has been reported to be 80 centi Poise (cP) for fresh pyrolysis oil and 120 cP for 6 month old pyrolysis oil (Oasmaa and Kuoppala, 2003). Dynamic viscosity of fresh oak wood pyrolysis oil has been reported to be 152 cP at 37 °C and 144 cP at 90 °C. However, dynamic viscosity of oak wood pyrolysis oil has been reported to be 258 cP at 37 °C stored for a period of 84 days and 309 cP at 90 °C stored for a period of 15 hours (Czernik et al., 1994). Most cases studied reveal that pyrolysis oil viscosity was not only specific to the feedstock and reaction parameters but also to the measurement conditions. Dynamic viscosity of the pyrolysis oils was measured in the past using rotational viscometers from Brookfield (Czernik, 1994; Diebold and Czernik, 1997, Doshi et al., 2005, Perez et al., 2006), falling ball viscometer from Haake (Radovanovic, 2000), and Bohlin Rheometer (Boucher et al., 2000) and various other methods. Kinematic viscosity of the pyrolysis oils was measured in the past (ASTM D 445) using Cannon-Fenske and Ubbelohde capillary viscometers (Boucher et al., 2000; Oasmaa and Kuoppala, 2003; Scholze, 2002; Das et al., 2004; and others). The use of capillary viscometers is a function of both efflux time, instrument constant, and temperature of the bath. Due to the high opacity and viscosity of pyrolysis oils the use of capillary viscometers presents a significant challenge especially at room temperatures. Hence, dynamic viscosity as a function of shear rate has been studied in this research utilizing a rotational rheometer. A few papers have reported the dynamic or kinematic viscosity of pyrolysis oils at 25 °C. Depending upon the pyrolysis oil type, whether it is Newtonian or non-Newtonian, the shear rate or shear stress becomes important during viscosity measurements. Consequently, if the pyrolysis oil is non-Newtonian then its' viscosity is primarily a function of the shearing factor.

The water content of various pyrolysis oils has been reported to range from 15 to 30%. The pH of pyrolysis oils has been reported to range from 2.00 to 3.70 (Oasmaa and Czernik, 1999). Low pH of the pyrolysis oil makes it very corrosive for long-term storage, transportation, and engine related applications. However, corrosive impact of pyrolysis oil could be minimized by the proper selection of materials like stainless steel, and polyethylene and also by utilizing alcoholic additives (Czernik, 1994). Methanol has been used as an additive to stabilize and lower the viscosity of softwood bark pyrolysis oil obtained from vacuum pyrolysis (Boucher et al. 2000). Water produced during the pyrolysis reaction aids in lowering the viscosity of pyrolysis oil by existing as a well dispersed polar phase in the fresh pyrolysis oil. Density and viscosity are the two fundamental physical properties of pyrolysis oil that would dictate the design of pumps and piping for flow equipment, injectors, nozzles and other engine related equipment. Hence, the proper assessment of physico-chemical properties of the pyrolysis oils is essential to study their long-term storage and thermal stability.

Polymerization and phase separation are commonly reported to occur in pyrolysis oils that become unstable during storage. Once the pyrolysis oil becomes unstable (significantly polymerized and phase-separated) the measurement of its chemical and physical properties becomes difficult. Consequently, consistency in the test results cannot be obtained easily. Several polymerization reactions could occur simultaneously increasing the viscosity and water content of pyrolysis oils. Pyrolysis oil being a very complex mixture of chemicals, kinetic studies of the multiple reactions responsible for instability is beyond the scope of this study. During accelerated stability testing the unstable polymeric reactions take place more severely giving rise to significant

increments in viscosity and water content of pyrolysis oils. By measuring these two properties as a function of storage time the stability of pyrolysis oils can be monitored. As a general trend once the water content exceeds 30-35% the pyrolysis oils are known to become highly unstable and phase-separated. By utilizing proper additives, drastic increases in both the viscosity and water concentration of pyrolysis oils could be minimized during their potential long-term storage (Oasmaa and Kuoppala, 2003; Chaala et al., 2004).

Research Objectives

The primary objective of this research is to investigate the storage stability of wood and bark derived pyrolysis oils that are produced from different reactor systems. These systems included small-scale auger, large-scale auger, and pilot-scale entrained flow reactors. While there are several secondary objectives of this research the most important among them are listed below.

1. To investigate the effects of feedstock composition and reactor operating conditions on pyrolysis oil yields using a small-scale auger reactor
2. To investigate the use of chemical additives to increase the shelf-life stability of freshly produced pyrolysis oils
3. To determine if the rheological, pH, water content, and acid value properties can be used as a measure of pyrolysis oil stability
4. To determine if the chemical additives with different functional groups are successful in stabilizing pyrolysis oils
5. To identify the most effective chemical additives and their optimal concentrations
6. To identify the most stable pyrolysis oils and their associated feedstock, production, and storage conditions

7. To add to the existing body of knowledge regarding the rheological properties of pyrolysis oils
8. To investigate the photo-oxidative effects of light on the pyrolysis oil storage stability
9. To broadly understand the effects of particulate matter on the storage stability of pyrolysis oils
10. To investigate the feedstock, storage temperature, storage time, and additive concentration effects on the storage stability of pyrolysis oils

Table 1.1

Most Common Reactor Types (Bridgwater, 1999)

Reactor Type	Heat Transfer Mode (Predominant)	Advantages	Disadvantages
Ablative	Conduction	Compact Design Accepts Large Size Feed Stock Heat Transfer Gas Not Required	Heat Supply Problematical Very High Mechanical Char Abrasion From Biomass
Circulating Fluid Bed	Conduction	High Heat Transfer Rate Maximum Particle Size of 6mm	Solids Recycle Required High Char Abrasion From Biomass Possible Liquids Cracking by Hot Solids Greater Reactor Wear Possible Complex System
Fluid Bed	Conduction	High Heat Transfer Rate Limited Char Abrasion Very Good Solids Mixing Simple Reactor Configuration	Particle Size Limit (<2 mm)
Entrained Flow	Convection	Not Available	Low Heat Transfer Rate Particle Size Limit (<2 mm) Limited Gas/Solid Mixing

Table 1.2

Pyrolysis Types and Associated Reactor Conditions (Maschio et al., 1992)

Reactor Condition	Very Slow or Conventional	Fast	Flash
Operating Temperature ($^{\circ}\text{C}$)	300-700	600-1000	800-1000
Heating Rate ($^{\circ}\text{C/s}$)	0.1-1	10-200	≥ 1000
Solid Residence Time (s)	600-6000	0.5-5	< 0.5
Particle Size (mm)	5-50	< 1	Negligible (Dust)

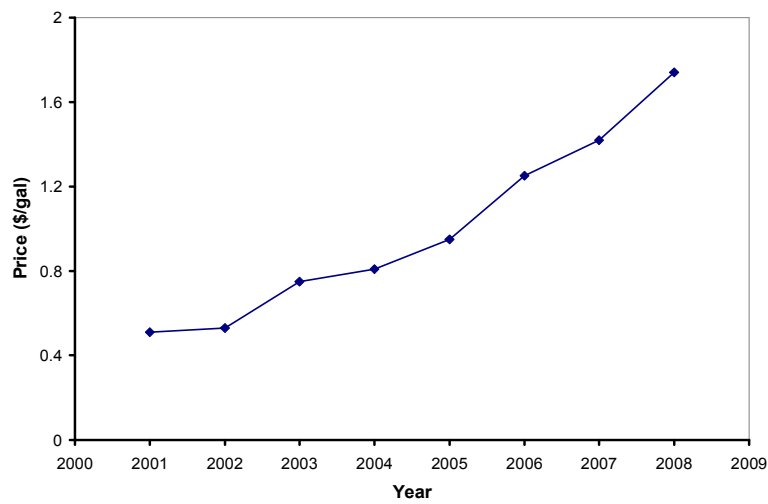


Figure 1.1 Methanol Pricing History in the Past Decade

(Source: http://www.methanex.com/products/documents/MxAvgPrice_Sept292008_000.pdf)

CHAPTER II

LITERATURE REVIEW

Energy Demand and Supply

During the 21st century global energy demand has skyrocketed largely because of the rapid population growth and hectic industrialization. The extinction of fossil fuels is near if this trend continues to occur (Demirbas, 2002). Major forms of energy as consumed by the United States (U.S) in the recent past and the years to come have been provided in Figure 2.1. The industrial consumption of biomass is projected to increase significantly in the coming years. Biomass has the potential to meet 14% of the current energy demand worldwide (Demirbas, 2002; Sensoz, 2003). The United States has a tremendous potential to grow energy crops by more than 450 million tonnes per year. Along with that the U.S generates large quantities of biomass waste weighing at least 170 million tonnes per year. The waste biomass comprises of forestry residues, agricultural residues, yard waste, construction and demolition wood. Valuable energy products in the form of bio-crude oil and charcoal could be obtained from these huge quantities of biomass with a recovery efficiency of greater than 85% (Johnson and Maclean, 1993). With the ever increasing demand for energy mainly in the form of fossil fuels like coal and petroleum; thermochemical conversion technologies (pyrolysis and gasification) for the successful utilization of biomass are becoming essential. Pyrolysis and gasification

have a great potential to provide the future energy supply to the globe in a self-sustainable, renewable, and environmentally benign fashion (Luo et al., 2004).

Major efforts are underway in the Zhejiang province of China to utilize fast pyrolysis for the production of liquid fuels. As this province is rich in forestry and other forms of biomass while deficient in fossil fuels, biomass pyrolysis is expected to meet the growing energy demand in the region. The use of bio-fuels in power generation using diesel engines and boilers is one possible potential energy application. Preliminary testing of pyrolysis oil produced from a small-scale fluidized bed reactor at low pyrolysis temperature resulted in low quality pyrolysis oil because of higher ash content. Among the four feedstocks tested (*F.mandshurica*, *C.lanceolata*, *P.indicus*, and Rice Straw) the highest yields of pyrolysis oil (55.7%) and water (24.6%) were obtained for *P.indicus* at 500 °C. Reactor optimization and pyrolysis oil upgrading were eventually considered for the large-scale production and utilization of bio-fuels (Luo et al., 2004). The use of agricultural waste, olive pits, olive wood, cotton plantation residues, fruit waste, and other forms of waste biomass as feed stocks has been suggested for pyrolysis from one of the first pyrolysis oil pilot plants built and located in Greece (Zabaniotou, 1999). Drying of feed stocks ensures that lower energy is spent during pyrolysis along with lower water content in the pyrolysis oil. The available moisture content of dried biomass has been reported to range from 5 to 10% (Diebold et al., 1995). The use of bark during pyrolysis presents significant challenges owing to its complex chemical structures. Furthermore the use of bark in industrial applications is also limited. Hence, minimal work pertaining to bark pyrolysis is available in the literature (Sensoz, 2003).

Wood Chemistry

Wood is composed of cellulose (40-45%), hemicellulose (20-30%), lignin (20-40%), and extractives (<10%). Extractives are regarded as non-structural wood components that are soluble in neutral organic solvents or water. Extractives comprise of terpenoids, steroids, resin acids, fats, waxes, ash, and phenolic constituents in the form of stilbenes, flavanoids, lignans, and tannins. Wood primarily exists in softwood and hardwood forms. Generally, softwoods are reported to have a higher content of lignin than the other components. Contrarily, hardwoods are reported to have a higher content of cellulose, hemicellulose, and extractives than lignin. The general chemical composition of softwood and hardwood has been provided in Table 2.1 (Demirbas, 2006; Sjoström, 1993; Schultz and Taylor, 1989).

Bark is known to have a complicated cellular type structure as compared to wood. Typically, bark has been known to possess higher content of extractives and minerals than wood. Otherwise, many of the primary constituents that are present in the wood are also present in the bark (Sjoström, 1993). Softwood bark derived pyrolysis oils were reported to have higher content of lignin and extractives compared to the hardwood bark derived pyrolysis oils (Ba et al., 2004).

Cellulose is a straight chain polymer derived from the dehydration of glucose ($C_6H_{12}O_6$) molecules. The repeat unit 'n' as shown in Figure 2.2 is termed as cellobiose and is approximately 30000. The exact molecular weight and polydispersity of cellulose are unknown. Cellulose has also been described as a homopolysaccharide composed of β -D-glucopyranose units linked together by (1 \rightarrow 4) glycosidic bonds. Because of the linear nature of cellulose molecules they have a strong tendency to form both intra and inter

molecular hydrogen bonding. Cellulose contains both amorphous and crystalline regions alternating with each other in the form of micro fibrils. Because of the fibrous nature and strong hydrogen bonding cellulose is found to be insoluble in majority of the solvents (Sjostrom, 1993; Brady, 2002).

Hemicellulose is described as a branched chain polymer comprised of both five and six sugar carbons. Individual sugar molecules polymerize to form hemicellulose. The degree of polymerization (or number of repeat units) of hemicellulose is predicted to be close to 200. Consequently, molecular weight of a hemicellulose molecule is much lower than a cellulose molecule. The chemical structures of main components present in hemicellulose are shown in Figure 2.3. They are glucose, galactose, manose, xylose, arabinose, and glucuronic acid. Hemicelluloses support the cell walls and are known to range from 20 to 30% based on the dry weight of wood. Hemicellulose is also considered as a heterogeneous polysaccharide, which can be easily hydrolyzed by acids to the monomeric components. Monomeric components include D-glucose, D-mannose, D-galactose, D-xylose, L-arabinose, L-rhamnose, D-glucuronic acid, and D-galacturonic acid (Sjostrom, 1993; Brady, 2002).

Lignin is a macromolecular polymer as shown in Figure 2.4. It is also referred to as a glue or binding agent in wood. The basic chemical unit of lignin is phenyl propane. The phenyl propane units in lignin are joined by ether (C-O-C) and carbon-to-carbon (C-C) linkages. C-O-C linkages are higher in number than the C-C linkages. Lignin is also known to contain methoxyl, phenolic, hydroxyl, and terminal aldehyde groups in the side chain with limited solubility in most solvents. The weight average molecular weight of softwood lignin has been reported to be in the order of 20000. The polydispersity index

(M_w/M_n) or the ratio of weight average molecular weight (M_w) to number average molecular weight (M_n) of lignin has been reported to be higher than that of cellulose. The chemical structures of main components present in lignin are shown in Figure 2.5 (Sjostrom, 1993; Brady, 2002). They are p-coumaryl alcohol, coniferyl alcohol, and sinapyl alcohol. Further, it has been reported that softwood lignin contains guaiacyl units but hardwood lignin contains both guaiacyl and syringyl units. Guaiacyl or 2-methoxy phenol is a phenolic group with one methoxy group for example coniferyl alcohol. Syringyl or 1,3-Dimethoxy-2-hydroxybenzene is a phenolic group with two methoxy groups for example sinapyl alcohol (Shafizadeh, 1982).

Thermo-chemical Conversion (Pyrolysis)

Pyrolysis can be defined as the degradation of macromolecular materials with heat in the absence of oxygen (Meier and Faix, 1999). Pyrolysis has been quoted as an emerging thermo-chemical technology with a great potential for a fuel oil substitute in the form of pyrolysis oil (Oasmaa and Czernik, 1999). Evidence suggests that pyrolysis was initiated in North America and Europe as early as 1970 (Scott et al., 1999). However, not until 1980 pyrolysis was recognized to be a cost feasible alternative to the expensive hydrocracking technology (Meier and Faix, 1999).

Pyrolysis of biomass can lead to both primary and secondary reactions during the vapor releasing process. Primary reactions lead to the gas evolution from the biomass solid surface, which is quickly quenched during the condensation process. High vapor condensation efficiency at a fast rate is essential. Otherwise secondary reactions will occur resulting in lower pyrolysis oil yields due to the release of non condensable gases

and water vapor. Secondary reactions usually lead to the formation of higher molecular weight compounds like tar. Tarry compounds plug the condenser lines and hence increase the shut down frequency of the reactor (Meier and Faix, 1999).

Pyrolysis is a thermo-chemical conversion process resulting in three fractions as shown in Figure 2.6. A wide variety of biomass feed stocks can be utilized namely wood, bark, bagasse, animal waste, forestry residues, saw dust, sewage sludge, and others for the pyrolysis oil production (Demirbas, 2002). However, feedstock adaptability of pyrolysis process does not always result in a consistent fuel oil quality. Rather the quality of pyrolysis oil is strongly dependant upon the type of feedstock utilized and the oil production conditions. Fraction I (pyrolysis oil) as shown in Figure 2.6 is usually the predominant fraction if fast pyrolysis is conducted. Otherwise fraction II (char) is the predominant fraction when slow pyrolysis is conducted. A significant fraction in the form of non-condensables (III) has been reported in many pyrolysis processes slow or fast. This is due to the secondary reactions that occur during the mass transport process catalyzed by char fines and other forms of particulate matter (Johnson and Maclean, 1993).

Pyrolysis oil recovery efficiencies are not very high because of heat transfer limitations during the vapor condensation process. Since the pyrolysis vapor is a complex stream of organic vapor, water droplets, mist, particulates, and aerosols the condensation efficiencies are typically not very high. The rapid quenching of complex pyrolysis vapor is essential to offset process equipment blockage and liquid fractionation (Bridgwater, 1999). Evidence suggests that fraction III (non-condensables) can be burned to generate process heat preventing adverse effects on the environment. Prior studies indicate that a

furnace was used to burn the non-condensable gases during ablative fast pyrolysis. During this process non-condensable gases were mixed with natural gas/char to supply heat to the vortex reactor tube (Johnson and Maclean, 1993).

As mentioned previously pyrolysis has been divided into three types' namely conventional/slow pyrolysis, fast pyrolysis, and flash pyrolysis. These types of pyrolysis are performed by selectively varying the reactor conditions namely operating temperature, heating rate, particle size, and solid residence time. Traditionally, conventional pyrolysis with low to medium heating rates has been used for making charcoal targeted for adsorbent and solid fuel applications. Ash content of the fast pyrolysis char has been reported to be higher than that of conventional pyrolysis char making it less valuable. Ash content obtained during fast pyrolysis is higher than the conventional pyrolysis probably because of higher reactor temperature and smaller particle size requirements. Currently, fast pyrolysis has been the major type geared towards producing bio-fuels ultimately providing an alternative to the dwindling fossil fuel reserves. Flash pyrolysis is performed using very small sized biomass particles along with shortest possible residence times. High heating rates are utilized during flash pyrolysis (Maschio et al., 1992; Huber et al., 2006).

Pyrolysis presents great benefits in the form of bio-char and high energy density oil. Bio-char has been used as a fuel, controlled release biodegradable fertilizer, and also in producing activated carbon for environmental applications. Pyrolysis units are relatively inexpensive, easy to construct, and can be easily located near a biomass source. However, the reactor conditions have to be tuned properly with the type of feedstock utilized to increase the pyrolysis oil productivity (Sensoz, 2003; Czernik and Bridgwater,

2004). Generally, high oil yields were reported at low pyrolysis temperature and fast residence time. Contrarily, high non-condensable gas yields were observed at high pyrolysis temperature and slow residence time. The thermal breakdown of biomass constituents has been reported to occur in the following temperature ($^{\circ}\text{C}$) range (Demirbas, 2002; Demirbas, 2000; Demirbas and Küçük, 1993):

1. Cellulose: 196.9-256.9 $^{\circ}\text{C}$
2. Hemicellulose: 236.9-346.9 $^{\circ}\text{C}$
3. Lignin: 276.9-496.9 $^{\circ}\text{C}$

Primary and secondary reactions occur during the pyrolysis process as mentioned earlier. Secondary reactions alter the chemistry of bio-formation products by increasing the volatile content from sugars and carbohydrates of the biomass utilized. Shafizadeh [1982] has proposed a lumped 3-step kinetic model as shown in Figure 2.7 by eliminating the constraints of secondary char catalyzed reactions. This model has been experimentally verified under vacuum conditions at a lower temperature range of 260-340 $^{\circ}\text{C}$. Vacuum was employed as it was easier to remove the products after formation with less time for secondary cracking reactions. All the rate constants (K_1 , K_2 , and K_3) of the Shafizadeh model are strongly dependent upon the temperature of pyrolysis. The rate (\mathbf{r}) equations of all the components (5) taking part in the kinetic model are provided below.

$$r_W = d[W]/dt = -k_1[W] = -k_1C_w \quad (2-1)$$

$$r_{W^*} = d[W^*]/dt = k_1[W] - (k_2 + k_3)[W^*] = k_1C_w - (k_2 + k_3)C_{w^*} \quad (2-2)$$

$$r_V = d[V]/dt = k_2[W^*] = k_2C_{w^*} \quad (2-3)$$

$$r_C = d[C]/dt = k_3[W^*] = k_3C_{w^*} \quad (2-4)$$

$$r_G = d[G]/dt = k_3[W^*] = k_3C_{w^*} \quad (2-5)$$

The step 1 of Shafizadeh kinetic model is the conversion of a wood component (W) to an active wood component (W^*) from the initiation reactions. Then the active wood component (Ex: cellulose) would decompose by two competing first-order reactions (step 2 and step 3). The formation of volatiles (V) from the step 2 takes place in the form of transglycosylation reactions yielding anhydrosugars. The pathway for the formation of anhydrosugars has been shown in Figure 2.8. Another set of reactions that occur during volatile formation is the degradation of a tarry pyrolyzate levoglucosan (1, 6-anhydro- β -D-glucopyranose) occurring during the pyrolysis. The degradation pathway of levoglucosan has been shown in Figure 2.9. The formation of the volatile products is considered to be highly endothermic or energy consuming reaction. The formation of char (C) and gases (G) takes place as shown in the step 3 of Figure 2.7. The formation of char can be thermodynamically classified as an exothermic or energy releasing reaction. At a lower pyrolysis temperature (<300 °C) the formation of char, water, CO, and CO₂ is favored. At a higher pyrolysis temperature (300-500 °C) the formation of tar, anhydrosugars, oligosaccharides, and pyran and furan dehydration compounds are

avored. At a much higher pyrolysis temperature ($>500\text{ }^{\circ}\text{C}$), low-molecular weight gaseous or volatile products are formed. Major reactions occurring during the product formation are fission, dehydration, disproportionation, decarboxylation, and decarbonylation. Dehydration pathways of the major wood component cellulose have been shown in Figure 2.10.

Reactors and Operating Conditions

During the pyrolysis process heat transfer to the biomass particles can be achieved in three ways. They are: 1) external/indirect heating 2) internal/direct heating using a heat transfer medium and 3) energy supplied by partial combustion (Maschio et al., 1992; Zaror and Pyle, 1982). Currently, pyrolysis systems with direct heating are more common in the market. Pyrolysis systems in general have been known to operate in any of the batch, continuous, and semi-continuous modes. Most large-scale pyrolysis systems are operated in a continuous mode to reduce the operating costs (Zaror and Pyle, 1982). The use of a very small particle size is expected to provide higher pyrolysis yields because of increased heat transfer rates and mass transfer efficiencies. However, size reduction significantly increases the overall cost of feedstock preparation. Higher holocellulosic content (sum of cellulose and hemicellulose) in the feed stocks is beneficial in increasing the yields of oils during fast pyrolysis (Scott et al., 1999). Typical reactor yields (normalized) obtained during fast pyrolysis for different kinds of biomass have been shown in Table 2.2 (Graham et al., 1994). The major pyrolysis reactor units with different operating capacities located in the North American region are shown in Table 2.3.

Pyrolysis oil yields as high as 75% have been reported in the literature using bubbling fluidized bed, circulating fluidized bed, ablative, rotating cone, vortex, vacuum, and few others. The general process overview of some of these reactors has been shown in Figures 2.11-2.16. The most common and widely used reactors have been bubbling fluidized and circulating fluidized beds mainly because they provide a higher tolerance for the feed size (2-6 mm). Size reduction is an expensive step during the feed stock preparation. In each of the above reactor systems an electrostatic separator is preferably installed after the condensation unit to separate condensables and non-condensables from a complex stream of aerosol, mist, particulates, organics, and water vapor (Meier and Faix, 1999).

Bubbling fluidized bed or fluidized bed was developed by the University of Waterloo, Canada as shown in Figure 2.11. The process was named as Waterloo Flash Pyrolysis Process (WFPP). Throughputs for this process vary from 100 g/h to 250 kg/h. Different liquid fractions are collected from the condensation process while the non-condensable gases are recycled to the reactor. The heat captured during the gas burning is used to dry the feedstocks (Meier and Faix, 1999). Shallow bed depth and high gas flow rate are usually employed to achieve short residence times in the bubbling fluidized bed pyrolysis. But there can be some processing problems (transverse temperature and concentration gradients) associated with the low bed height to diameter ratio. To counter this problem special design methods are employed. In spite of such technical challenges the thermal efficiency is still observed to range from 60 to 70% for most fluidized bed systems. Char attrition is unlikely to occur during fluidized bed pyrolysis but vapor cracking can occur because of the catalytic effects of char (Scott et al., 1999).

Rapid thermal process (RTP) developed by Ensyn, Canada is based on the principle of circulating fluidized bed as shown in Figure 2.12. Feed rates as high as 650 kg/hr have been reported using this reactor. Presently RTP technology is used for making flavoring and other chemicals (Meier and Faix, 1999). Heat transfer rates are not very high because circulating beds are highly dependent upon gas-convective transfer. Char attrition can be observed in this process along with some carryover into pyrolysis oil. Hence, an additional step might be needed to remove the char from the pyrolysis oil (Scott et al., 1999).

Ablative pyrolysis process as shown in Figure 2.13 was developed by Aston University, United Kingdom. According to this process the biomass particles are pressed against the heated surface of a rotating blade. Consequently, the resulting friction separates the liquid film that is formed in layers from the biomass particle. Ablative pyrolysis has been indicated to provide high heat and mass transfer rates. Industrially this technology sounds very promising with few exceptions (Meier and Faix, 1999). Ablative pyrolysis can be performed using cone or plate type reactor geometry by largely relying on heat conduction. The unreacted solids need to be recycled to achieve a better degree of conversion in this process. The disadvantages of ablative pyrolysis system are char attrition, mechanical complexity, and operational heat loss (Scott et al., 1999).

Rotating cone reactor was developed at Twente University, Netherlands. Sand or a catalytically active material is used in this reactor to increase heat transfer efficiency to the biomass particles. Small sized biomass particles are used during the rotating cone pyrolysis, which can be a disadvantage to this system. Otherwise the throughput capacity of this system is indicated to be very high. There are two beds in this reactor system

along with a small riser system in the inside bed as shown in Figure 2.14. Pyrolysis of the biomass particles takes place in the inside bed during multiple passes while moving spirally from downward direction to the upward direction. The outside bed containing both sand and char is also known as the combustion chamber. Char particles are utilized in the process to provide the necessary heat to the cone reactor (Meier and Faix, 1999).

Vortex reactor system developed at National Renewable Energy Laboratory (NREL, USA) was utilized to conduct oak wood pyrolysis. The principle of heat transfer in this system is same as that of ablative pyrolysis. Small biomass particles are fed through a preheated (625 °C) vortex reactor system in a radial direction at a very high speed of 1200 m/s (Meier and Faix, 1999). Carrier gas nitrogen was used to feed the biomass particles at a very high temperature of 700 °C. The reactor itself was maintained at 625 °C (Czernik et al., 1994). The particles thus fed into the reactor continue to move in a helical pathway along the walls of the reactor. During the movement biomass particles conduct heat from the reactor wall inside and become pyrolyzed. Biomass that is not pyrolyzed will be recycled back to the reactor as shown in Figure 2.15. A cyclone is used to collect the char from the reactor (Meier and Faix, 1999). The recycling of unreacted solid biomass particles through a hot loop increased pyrolysis efficiency. High heat transfer rates coupled with short residence times seem to be responsible for increasing the overall reactor yields. Excessive cracking of the vapor seems to significantly affect the overall yields of pyrolysis oil. Incomplete reactor mass balance closures were also reported due to inefficient condensation (Czernik et al., 1994).

Pro-cycling vacuum pyrolysis process was developed by Pyrovac Incorporated. Accordingly, pyrolysis is conducted in a vacuum chamber, which utilizes a special

agitation system as shown in Figure 2.16. Biomass is heated through contact with hot plates and the heating medium used is molten salt. The main advantage of vacuum pyrolysis is the rapid removal of the volatiles from the reactor. The main challenge for this system though is its design especially the vacuum locks for inlets and outlets (Meier and Faix, 1999).

Among other small-scale reactor systems fixed bed and auger type are under investigation currently. Slow pyrolysis was conducted using a fixed bed reactor by varying heating rate and pyrolysis temperature. The use of bark derived from Turkish red pine produced low yields of pyrolysis oil and high yields of char. Char yields decreased as the pyrolysis temperature was increased. However, oil yields were observed to increase as the pyrolysis temperature was increased from 300 to 450 °C. This trend reversed as the pyrolysis temperature was further increased from 450 to 500 °C. A maximum yield (33.25%) of the bark-derived pyrolysis oil was reported to occur at a heating rate of 7 °C/min and a pyrolysis temperature of 450 °C (Sensoz, 2003). At Mississippi State University a semi-continuous auger reactor system first of its kind has been used for wood and bark pyrolysis. More details of this system are provided in Chapter III of this document. Literature pertaining to the use of auger reactor has been limited in the past. However, recently its use in biomass pyrolysis has been studied by few other researchers (Perez et al., 2007, and Ingram et al., 2008).

Rheology

Introduction

Rheology is defined as the branch of science dealing with the flow and deformation of materials (Colo et al., 2004). A wide range of materials can be examined using this tool namely low-viscosity fluids, semisolids, gelly substances, and solid-like materials. The resulting rheological information can be utilized in the design of flow processes (production and quality control), prediction of storage stability, understanding and controlling texture of the materials. Semisolid materials have been termed as the most difficult materials to characterize as these materials possess both liquid like and solid like properties. Pharmaceutical and cosmetic industries are some that rely heavily on the rheological flow properties (to determine shelf-lives) of formulations, pastes, creams, and other materials.

Classification of Liquids

Dynamic viscosity (μ) of a liquid can be defined as a measure of its internal resistance when the liquid is subjected to certain flow conditions. Shear stress and shear rate are the most common variables that are applied to the liquid to measure its dynamic viscosity. Generally, all liquids are classified as either Newtonian or non-Newtonian. The liquid which obeys the Newton's law of viscosity is termed Newtonian and the one that does not obey the law is termed as non-Newtonian. Newton's law of viscosity has been provided in Equation 6. It is derived from the original mathematical Equation 7, which represents the flow behavior of liquids as depicted in Figure 2.17. When the slope of the shear stress versus shear rate curve becomes unity with a zero intercept ($A=0$) the

mathematical Equation 7 reduces to Newton's law of viscosity (Equation 6). For all other cases, when the slopes and intercepts are not 1 and 0 respectively, Equation 7 changes based on the values of intercept A, power n, and coefficient B. A liquid which obeys power law as shown in Equation 8 is considered as a power law or Ostwald-de Waele liquid. Accordingly, if $n < 1$ the liquid is considered a pseudoplastic liquid. For this liquid viscosity decreases with the rate of shear. Contrarily, If $n > 1$ the liquid is considered as a dilatant liquid. For this liquid viscosity increases with the rate of shear. Among the non-Newtonian liquids, time-dependent and time-independent liquids exist as well. Here the liquid is subjected to a constant shear rate while the viscosity is measured as a function of time. The liquid is classified as a thixotropic liquid if the viscosity decreases as a function of time. However, the liquid is classified as a rheopectic liquid if the viscosity increases as a function of time. The liquid that has certain yield stress value before it begins to flow is termed as a plastic or a Bingham plastic. Ideal liquid is assumed to have zero viscosity but it does not exist practically. However, it is considered for theoretical purposes only.

$$\tau = -\mu(du/dy) \quad (2-6)$$

$$\tau = -\mu(du/dy)^n \pm \tau_0 \quad (2-7)$$

$$\tau = -\mu(du/dy)^n \quad (2-8)$$

Where,

$$\tau = \text{Shear stress} = \text{dyne/cm}^2$$

$$\tau_0 = \text{Yield Stress} = \text{dyne/cm}^2$$

$$\mu = \text{Viscosity} = \text{cP}$$

$$du/dy = \text{Velocity gradient or shear rate } (\dot{\gamma}) = \text{s}^{-1}$$

$$n = \text{Power law exponent}$$

(Source: Transport Phenomena, Bird et al., 1994)

All fluids namely liquids, gels, colloids, emulsions, and suspensions are generally classified as either Newtonian or non-Newtonian. If the viscosity of a fluid is independent of shear rate then it is considered to be Newtonian otherwise it is considered as non-Newtonian. In practice Newtonian fluids can be pumped at any shear rate whereas non-Newtonian fluids need to be pumped at a shear rate which corresponds to the infinite rate viscosity. Infinite rate corresponds to the state of a fluid in which all its molecules, structural alignments, networks, and chains are aligned in an organized fashion (or complete flow situation) as opposed to the completely randomized state (or initial flow situation). Pyrolysis oil has been reported to behave as a Bingham plastic with a minimal yield stress (Perez et al., 2006). Typically, the non-Newtonian fluids (shear thinning or pseudoplastic) exhibit three regimes of flow as depicted in Figure 2.18. Most research papers have reported viscosity of the pyrolysis oils as a function of single shear rate instead of multiple shear rates. If the pyrolysis oil is Newtonian then the viscosity value for any given shear rate is sufficient. Otherwise viscosity as a function of multiple shear rates or a range is necessary to understand the complete flow behavior of pyrolysis oils. Limited work has been conducted to investigate the rheological properties of pyrolysis oil which is the focus of this study.

First phase of flow as shown in regime 1 is ideally Newtonian but only for a very small range of shear rates that typically a rheometer can produce. During regime 1 the random molecular chains and structural networks present in the fluid start to align with each other. After regime 1 is completed the onset of regime 2 initiates which is the pseudoplastic or shear thinning region but it does not depict a complete flow situation. Regime 2 is usually a broader shear rate region when compared to regime 1 or regime 3.

After the complete rearrangement of molecular chains and random networks during regime 2 the onset of regime 3 begins. Regime 3 is also Newtonian but it indicates the complete flow of a fluid. Regime 3 is initiated once the applied shear rate is high enough such that all the molecular chains, structural alignments, and networks have changed from a random state (regime 1) to the structured flow. Viscosity corresponding to the regime 3 is often referred to as infinite rate viscosity (η_{∞}). Likewise viscosity corresponding to the shear rate in regime 1 is often referred to as zero rate viscosity (η_0). For practical purposes one would assume that the complete flow situation is desired especially when the pyrolysis oil is non-Newtonian. Hence, the shear rate for pumping (SR_p) corresponding to the infinite rate viscosity should be utilized in most engineering design calculations.

Viscosity Measurement

Viscosity as a function of shear rate/shear stress is widely used to understand the flow behavior of liquids. Information such as yield stress, pseudoplastic or dilatant behavior, thixotropic or rheopectic behavior, and steady state flow characteristics are essential in characterizing the liquid properties. Viscosity of a liquid could be measured by either a viscometer or a rheometer and for a viscometer the measurement values are dependent upon the combination of spindle geometry and shear rate. In the case of a rheometer complete analysis of the liquid flow properties independent of the shear rate can be achieved. Practically, two types of rheometers are available for the viscosity measurement. They are capillary and rotational rheometers. Capillary type geometry is presented in Figure 2.19. In the case of a rotational rheometer, the measurement geometry

can be changed to any of the parallel plate, cone-plate, and Couette type geometries. These three geometries are shown in Figures 2.20-2.22. Generally, the use of a rheometer provides sophistication and precision to the analysis of fluid flow properties without replacing the geometry for each test condition desired. That said, the use or selection of a rheometer is dependent mainly upon the sample viscosity (how thick or how thin), sample size constraints, torque measurement capabilities, desired shear rate range, and sample loading issues. Some of the rationales in the selection of measurement geometry are provided in Table 2.4 (Morrison, 2001). Parallel plate seems to provide the much-needed convenience of using a small sample size (< 1g) for varying viscous samples (low, medium, and thick). Mathematical equations used for the calculation of liquid viscosities (steady-state conditions) for each type of geometry are provided in Table 2.5 (Morrison, 2001). By the careful selection of geometry, shear rate range, and measurement temperature problems such as sample volatility and slipping can be avoided.

Moduli or Oscillatory Testing

Moduli or dynamic oscillatory testing is known to provide a better understanding of the material microstructure and its visco-elastic behavior. Experimentally, the fluid is subjected to a sinusoidal shear stress (or strain) smaller than the critical value. Then the amplitude of the resulting strain (or stress) and the phase angle between the imposed stress and the output strain are measured as depicted in Figure 2.23. Consequently, the deformation of the material can be expressed as a complex mathematical function ($G^*=G'+iG''$) of two components where real part G' is storage modulus and the

imaginary part G'' is loss modulus. Storage modulus or elastic component represents the elastic energy stored per unit volume. Loss modulus or viscous component represents the energy dissipated per unit deformation rate per unit volume (Colo et al., 2004). During the oscillatory experiments linear visco-elastic range of different materials is determined by the strain sweep test [storage modulus (y) vs. % strain (x)]. Linear visco-elastic range of different materials is dependent upon the critical strain or the minimum energy needed to disrupt the structure. Hence, materials with larger visco-elastic range would be considered more stable materials. In a frequency sweep test [storage modulus (y) versus angular frequency (x)] particle size distribution and concentration is known to affect the storage modulus. Hence, a material whose storage modulus is strongly dependent on angular frequency indicates weaker storage stability.

Pyrolysis Oil

Pyrolysis Oil vs. Conventional Fuel

Pyrolysis oil or bio-oil can be defined as a complex mixture of oxygenated aliphatic and aromatic compounds (Meier and Faix, 1999). Bio-oil term seems to be a misnomer as it is commonly misunderstood as oil. Bio-oil has many synonyms in the form of pyrolysis liquid, pyrolysis oil, bio-crude oil, wood oil, wood liquid, wood distillate, pyroligneous acid, pyroligenous tar, liquid wood, and liquid smoke (Mohan et al., 2006). Pyrolysis oil compared to petroleum derived oil is largely composed of oxygenated compounds with negligible quantities of hydrocarbons. Petroleum derived oil on the contrary is predominantly a hydrocarbon based liquid fuel (Sensoz, 2003). Aqueous-rich and organic-rich fractions are usually produced from the condensation

process during biomass pyrolysis. Aqueous rich fraction is termed as an acid phase where as the organic rich fraction is termed as a tar phase. Acid phase is reported to contain mainly acetic acid, methanol, and acetone. Tar phase however is reported to be a mixture of phenolic, carbonyl, and other compounds (Zaror and Pyle, 1982). Yield numbers for pyrolysis oil product generally included both the aqueous-rich and organic-rich fractions.

The viscosity of pyrolysis oils at 40 °C has been reported to range from 35-1000 cP. Such a wide variation is indicative of the fact that pyrolysis oil viscosity is a strong function of feedstock and process conditions. High heating value (HHV) of pyrolysis oil has been reported to be 16-19 MJ/kg, which is almost half of the HHV of heavy fuel oil. Lower HHV and lower stability of pyrolysis oil as compared to the conventional fuels is due to the fact that pyrolysis oil is highly oxygenated along with a high water content of 15-30% (Czernik and Bridgwater, 2004). Typical properties and elemental composition of pyrolysis oils as compared to the conventional fuels are shown in Tables 2.6-2.7 (Czernik and Bridgwater, 2004).

Engineering Challenges

Among many pyrolysis oil challenges that we face today most significant of them are summarized below (Czernik and Bridgwater, 2004).

1. High acidity or low pH causes corrosion of storage and engine equipment
2. High viscosity limits the combustion applications
3. Feedstock variability affects the oil composition
4. Stability decreases with time unless proper additives are used
5. Upgrading is necessary to improve overall oil quality

6. High concentration of oxygenated compounds cause strong odor
7. Marketability concerns exist because of all the above challenges

Quality Upgrading

Pyrolysis oil upgrading to transport fuels could be conducted by a variety of different techniques. Such techniques could include catalytic hydrodeoxygenation, hot vapor filtration, and stabilization by adding suitable solvents. Catalytic hydrodeoxygenation involves two steps that are hydrotreating and catalytic vapor cracking. By using a combination of high temperature, high hydrogen pressure, and suitable catalysts the oxygen present in the pyrolysis oil can be removed as water. This process provides additional benefit of lowering pyrolysis oil viscosity by cracking the large sized polyaromatic molecules. However, the above steps can significantly increase the overall pyrolysis oil production costs (Oasmaa and Czernik, 1999; Czernik and Bridgwater, 2004; Elliott and Baker, 1987). Viscosity and ash content of the pyrolysis oil are generally high for the raw pyrolysis oils. By successfully upgrading the pyrolysis oils most of the previously stated challenges could be addressed. Removal of high molecular weight compounds is essential to increase the fuel atomization efficiencies. Otherwise they adversely plug the fuel injectors, spray nozzles, and other engine equipment (Czernik et al., 1994).

During the pyrolysis process alkali metals are trapped in the sub-micron char particles that are almost impossible to remove from the pyrolysis oil. The sub-micron char particles along with the alkali metals lower significantly the combustion efficiencies of the oil. An effort was made to upgrade the pyrolysis oil quality for its successful

utilization as a fuel in turbines, diesel engines, and boilers. Hence, hot gas filtration was performed during pyrolysis. Consequently, lower ash content and alkali metals (<10 ppm) were seen in the switch grass derived pyrolysis oil. Contrarily, cold filtration was ineffective in removing the alkali metals from the pyrolysis oil. Although leaching of metals was not observed during the pyrolysis oil storage, the agglomeration of sub-micron char particles can significantly affect the storage stability of pyrolysis oil (Agblevor and Besler, 1996). Proper control of pyrolysis reaction and vapor cracking conditions increased the pyrolysis oil yields with less ash and alkali content. Thus, pyrolysis oil produced from poplar wood can be modified to meet the ASTM No. 4 fuel oil standard. Study indicates that higher ash, alkali, and char content have a significant effect on increasing the viscosity of poplar wood pyrolysis oil when stored at accelerated test conditions. Hot gas filtration has a great potential to reduce the char and alkali metal content at the expense of lower pyrolysis oil yields. Improvement in the storage stability and properties of pyrolysis oils has been observed by performing hot-gas filtration. Consequently, medium to light fuel oil was produced with low sulfur content as opposed to a heavy fuel oil substitute. Ceramic filters made by 3M were used to conduct hot gas filtration (Diebold et al., 1995).

Addition of solvents has been postulated to positively affect the stability of pyrolysis oils in three ways. They are: 1) physical dilution 2) reaction rate control and 3) inhibit network polymerization and repolymerization. Phase separation in pyrolysis oils can be minimized by the addition of solvents like methanol, ethanol, ethylene glycol, and acetone. These solvents help maintain the homogeneity of pyrolysis oil by dispersing the aqueous rich and organic rich phases. Further, they are known to regulate the untoward

viscosity increase in pyrolysis oils during their storage (Oasmaa and Czernik, 1999). Addition of solvents has been predicted to chain terminate or even reverse the higher order polymerization reactions, physically dilute the high molecular weight compounds, and produce a change in the oil microstructure. Chain termination reactions could prevent the monomers from becoming polymers. Rather the monomers present in the pyrolysis oil could be chain terminated as dimers and oligomers. Consequently, the viscosity of the pyrolysis oil may be significantly reduced by the addition of low molecular weight solvents especially methanol (5-10%). Among the additives utilized (10% ethanol, 10% acetone, 10% methanol, 10% ethyl acetate, 5% methanol + 5% acetone, 5% methanol + 5% methyl isobutyl ketone); methanol (10%) is reported to provide the least viscosity increase as a function of aging time (Diebold and Czernik, 1997). Addition of solvents methanol, ethanol, and butanol have been reported to increase the stability and decrease the odor of pyrolysis oil derived from sewage sludge. Esters formed from the alcohols have been reported to mask the pungent odor of pyrolysis oil by their fruity smell. Ethanol was concluded as the best choice of solvents by Doshi et al. [2005].

Hansen solubility parameters of potential solvents for pyrolysis oil are shown in Table 2.8 (Barton, 1983; Diebold, 2000). The components listed in Table 2.8 are most commonly found in the pyrolysis oil. By considering the principle 'like dissolves like' solvents with higher solubility parameters among each group of additives (alcohols, aldehydes, esters, ethers, ketones, and phenolics) were chosen in this study. Co-solvency of a component in pyrolysis oil is affected by its molecular weight, relative polarity, and hydrogen bonding interactions. Low molecular weight compounds are predicted to be generally more soluble than the high molecular weight compounds. Compounds that

possess polar and non-polar groups in their structure for example n-butanol seem to favor the mutual solubility especially since pyrolysis oil is known to have both the groups. The ability of a compound like alcohol or a carboxylic acid is that it would favorably increase the heat of vaporization and hence the solubility parameter by forming hydrogen bonding with pyrolysis oil. Accordingly, total solubility parameter of a solvent (δ_t) in pyrolysis oil is an additive function of its dispersivity (δ_d), polarity (δ_p), and hydrogen bonding (δ_h) as shown in Equation 9. These parameters are determined usually by using thermodynamic modeling techniques as well as empirically from the literature. Generally, higher the solubility parameters greater the solubility power of a given compound in the pyrolysis oil.

$$\delta_t^2 = \delta_d^2 + \delta_p^2 + \delta_h^2 \quad (2-9)$$

Apart from the techniques discussed previously, few researchers have found other ways of improving overall quality of the pyrolysis oil. Removal of low molecular compounds that cause unpleasant odor and a flash point decrease is predicted to improve the stability of pyrolysis oil. Low molecular weight or light compounds causing unpleasant odor were reported to be mainly acids, aldehydes, and ketones. Light compounds and excess water from the pyrolysis oil were eventually replaced by methanol using concentration method. Accordingly, the light compounds were removed using a rotavapor operated at low temperature and low vacuum. Concentration method was employed for improving overall pyrolysis oil quality that resulted in high quality pyrolysis oil with out unpleasant odor. Also, the pyrolysis oil heating value was increased by lowering its water content and viscosity (Oasmaa et al., 2005; Sipila and Oasmaa, 1999). Attempts were made to separate the aqueous and non-aqueous phases of pyrolysis

oil using high-speed centrifugation but to no avail (Elliott, 1994). However, high amounts of char removal from the pyrolysis oil can be achieved by the use of high-speed centrifugation. Char recovery efficiencies of 29% and 36% were reported for oak wood and pine wood respectively.

Chemical Composition and Analysis

Pyrolysis oil being a very complex assortment of chemical compounds analysis of each of them presents a major analytical challenge. Hence, hyphenated multiple analytical tools are needed to identify all the compounds present in pyrolysis oil. In spite of this difficulty researchers (Oasmaa et al., 2003; Bridgwater et al., 1999) have provided a broader classification of major organic groups that are known to exist in the pyrolysis oil. The composition range of pyrolysis oil chemicals as derived from organic fraction of bark free wood has been shown in Table 2.9. Water (~25%) has been reported to be the single largest group present in the pyrolysis oil. The other major compounds reported elsewhere in pyrolysis oil are hydroxyacetaldehydes, hydroxyketones, sugars, carboxylic acids, and phenolics. The chemical composition of pyrolysis oil is expected to vary much depending on the type of feedstock utilized. Aqueous phase of the pyrolysis oil consists mostly water, acids (formic and acetic), and a small concentration of low molecular weight compounds. Low molecular weight compounds constitute aldehydes, ketones, alcohols, ethers, and few others (Boucher et al., 2000).

High-pressure liquefaction and fast pyrolysis are considered to be major thermo-chemical conversion technologies for the production of fuels and value-added chemicals. Both these technologies are beneficial in recovering a wide variety of chemical

byproducts. Chemicals that are usually present in the pyrolysis oils produced from high-pressure liquefaction are ‘volatile organic acids, alcohols, aldehydes, ethers, esters, ketones, furans, phenols, hydrocarbons, and non-volatile components’. Some of the chemicals that are usually present in the pyrolysis oils produced from fast pyrolysis are ‘cyclopentanone, methoxyphenol, acetic acid, methanol, acetone, furfural, phenol, formic acid, levoglucosan, guaiacol, and their alkylated phenol derivatives’ (Demirbas, 2006; Elliott and Schiefelbein, 1989).

Gas chromatography (GC) has been used to identify approximately 120 compounds from the pyrolysis oil. During pyrolysis biomass components cellulose, hemicellulose, and lignin are known to undergo complex thermal degradation reactions. Biomass components ‘cellulose and hemicellulose’ are described to undergo cyclization and dehydration reactions followed by transglycosylation. Both low molecular and high molecular weight compounds are formed during the holocellulosic (sum of cellulose and hemicellulose) decomposition. Some of the compounds that are known to form during these reactions are hydroxyacetaldehyde, acetic acid, hydroxypropanone, [3-hydroxypropanol], [5-hydroxy-2,3-dihydroxy-(4H)-pyran-4-one], [5-hydroxymethyl-2-furaldehyde], [2-hydroxymethyl-5-hydroxy-2,3-dihydro-(4H)-pyran-4-one], [1,5-anhydro- β -D-xylofuranose], and levoglucosan. Contrarily, lignin is expected to undergo dehydration reaction only and hence many side chain unsaturated compounds like styrene-derivatives, eugenol, iso-eugenol, p-hydroxy-cinnamicalcohols are formed (Meier and Faix, 1999). Gas chromatography mass spectroscopic (GC MS) analysis of the organic rich fractions (predominantly pyrolysis oil) and aqueous rich fraction (predominantly water) obtained from different forms of biomass has been

provided in Table 2.10. Most of the compounds are present in both the fractions but their concentration levels differed significantly. The different biomasses included in the study were wood, hazel nutshells, olive husks, corncobs, wheat straw, and Lucerne pressed cake (Maschio et al., 1992). It should be noted that except for methanol and acetic acid most of the chemical compounds are less than 1 wt.% in the aqueous rich fraction.

Elemental Composition and Analysis

Elemental composition of carbon, oxygen, and hydrogen contents in the pyrolysis oil are expected to range as 54-58%, 35-40%, and 5.5-7.7% by weight respectively. Nitrogen and ash content are reported to be <0.2 wt.% (Czernik and Bridgwater, 2004). Many of the inorganic elements present in the pyrolysis oils are known to cause problems during their combustion in engines. Elemental analysis was performed for the pyrolysis oils derived from hardwood (oak), softwood (pine) and herbaceous biomass (switch grass). The elemental composition of the three pyrolysis oils has been provided in Table 2.11. The trace elemental analysis was performed by either atomic absorption (AA) or inductively coupled plasma atomic emission spectroscopy (ICP-AES). Acid digestion was used for AA, while alkali fusion followed by dissolution was utilized for ICP-AES. The poorest quality of oils was reported for the pyrolysis oil derived from switch grass. The oils were produced using flash pyrolysis with a residence time of <1s and a pyrolysis temperature of 520 °C (Elliott, 1994). Biomass ash from switch grass derived pyrolysis oil has been reported (Agblevor and Besler, 1996) to contain mainly potassium (K), calcium (Ca), sodium (Na), silicon (Si), and phosphorous (P). Previous studies have reported that the metals found in the char had a catalytic effect on the biomass

decomposition (DeGroot and Shafizadeh, 1984; Radlein et al., 1992; Pan and Richards, 1989; Evans et al., 1991). Highest concentrations of K (319 ± 55 ppm) and Ca (95 ± 23 ppm) were found in the unfiltered switch grass derived pyrolysis oil. Thus, K metal and Ca metalloid seem to have a higher potential to catalyze biomass decomposition and char forming reactions during pyrolysis (Aglevor and Besler, 1996).

Storage, Testing, and Commercialization

Pyrolysis oils are reported to have a corrosive effect on ordinary steel and aluminum but they are non-corrosive for stainless steel and polymers. Hence, pyrolysis oils could be stored in tanks made of stainless steel (304/316) or plastic either at room temperature or refrigerated conditions (Czernik, 1994). Studies suggest that the influence of copper and stainless steel on the phase separation of softwood bark and hardwood derived pyrolysis oils is not significant (Perez et al., 2006). During lab-scale testing the pyrolysis oils were stored in glass vials with plastic seals as reported by Diebold and Czernik [1997].

Accurate testing of pH is difficult for pyrolysis oils as the electrodes are prone to fouling. However, rapid measurements of pH are possible using electrodes provided frequent calibrations are performed during measurements. Karl Fisher testing has been recommended for measuring water content of pyrolysis liquids. Method calibrations with water standards are suggested during Karl Fisher analysis. It has been verified that side reactions occurring due to aldehydes, ketones, acids, and other compounds in pyrolysis oil were insignificant during the titration performed (Czernik et al., 1994). Preliminary norms and standards for measuring viscosity, water content, solids, pH, and other

properties of the pyrolysis liquids have been proposed during the round Robin test (Oasmaa and Meier, 2005). Kinematic viscosity measurements of the homogeneous and Newtonian pyrolysis liquids have been recommended at a temperature of 40 °C. A temperature of 40 °C was recommended because of smaller measurement error and lower standard deviation. However, the Newtonian behavior of extractive rich pyrolysis oils needs to be verified using a closed-cup rotaviscotester. During the lab-scale testing oil samples with weight losses of >0.1 wt.% should be excluded as part of the quality control measures.

At present large-scale commercialization and utilization of pyrolysis oil as a fuel is under evaluation. A promising sign though for the pyrolysis oil is that it has been tested in engines, turbines, and boilers successively with considerably lower emissions (Czernik and Bridgwater, 2004). To achieve success on large-scale pyrolysis oil should be homogeneous, low in solid content (char and ash), viscosity, and acidity while it is high in heating value and flash point (Oasmaa and Czernik, 1999; Oasmaa et al., 2005; Oasmaa and Kuoppala, 2003; Oasmaa, 2003; Peacocke et al., 2003; Meier and Faix, 1999). Canadian companies 'DynaMotive and Ensyn' are playing a key role in the pyrolysis oil commercialization by supplying large quantities of oil that are needed during the testing and developmental phase (Scott et al., 1999). The future of pyrolysis oil as an alternative renewable fuel in today's fuel market looks very bright because the supply of fossil fuels is shrinking and the demand for energy is blooming.

Stability Testing Methods

Background

Broadly speaking stability of fuels can be classified in three types' namely thermal stability, oxidative stability and storage stability. 1) Thermal stability of a fuel can be assessed to determine its performance in a simulated environment. Here the objective is to study the thermal behavior of the fuel prior to its utilization in the engine. 2) Oxidative stability of a fuel can be assessed to determine gum or deposit formation due to the chemical changes occurring during accelerated storage. 3) Storage stability of a fuel can be assessed to determine the shelf-life of a fuel during its long-term storage. For some fuels oxidative stability also meant storage stability as observed in the literature. During the current research however storage stability is of primary concern. Storage stability of a fuel has been defined by the American Society for Testing and Materials (ASTM) D 6985 method as 'the resistance of a fuel to the formation of degradation products when stored at ambient temperatures'. Long-term storage of the fuel means that it can be stored safely for at least a year after being received by the user. A brief summary of the ASTM methods used in determining the storage stability of different fuels is provided as follows. Most of these methods do not seem to be applicable in the case of pyrolysis oils because of the filtration challenges, high viscosity, and large volatile compound concentration associated with them. Hence, testing methods involving the use of rancimat 743, oxygen bomb, and oxygen overpressure cell do not seem to be applicable as the oxidation level of pyrolysis oil is already affected. Methods using scanning or light reflectance techniques may not work for pyrolysis oil directly because

of its high opacity unless diluted significantly. Such dilution techniques may have the potential to alter the chemistry of pyrolysis oil altogether and hence they must be used with caution. Also pyrolysis oil is not soluble in hydrocarbon solvents as some of the traditional test methods may require during dilution.

Distillate Fuel

Storage stability of a petroleum derived distillate fuels (Grade No.'s 1-3) is measured using the ASTM D 4625 method. Accordingly, 400 ml of filtered fuel samples are stored in borosilicate glass containers at 43 °C for a period of 0, 4, 8, 12, 18, and 24 weeks. Sample bottles with caps made of polytetrafluoroethylene (PTFE) liners are used along with a borosilicate glass bend for breathing or venting. After storing each sample for a specific time period it is cooled to room temperature and then analyzed for filterable insolubles and adherent insolubles. A 1.5 µm nominal pore size glass fiber filter with a diameter of 2.5 cm is used according to this method. Adherent solubles are determined by washing the leftover fuel in the bottles during the filtration operation. A Gooch crucible with two glass filters is used during the filtration process. The filtered crucibles are oven dried for 4 h and placed in a desiccator without desiccant. After cooling to room temperature the weights of the crucibles are recorded to the nearest 0.1mg. Isooctane is used as solvent during all washing and cleaning operations in determining filterable insolubles. Equal parts of acetone, methanol, and toluene are however mixed to determine adherent solubles. Total insolubles (filterable and adherent) in the fuel are reported as mg insolubles per 100 ml of fuel used. Sediment formation, color change, oxidation, and degradation of the fuel are mildly accelerated during this test. The overall

significance of this method is that it can be used to study the storage properties of fuels. But it does not provide the exact assessment of the fuel behavior as it will be stored in different containers at different storage conditions. Different container here refers to the storage tank with a different material of construction.

ASTM D 5304 method for storage stability has been reported to be applicable for both middle distillate fuels, grade 1D, and grade 2D diesel fuels. Middle distillate fuel is a generic term used by a refinery or supplier primarily intended for its use in diesel engine, non-aviation gas turbine engine, and other non-automotive applications like burner fuel (ASTM D 6985). According to the ASTM D 5304 method, 100 ml of the filtered fuel is placed in a borosilicate glass container. The glass container is then pressurized to 100 psig (absolute) in a vessel with oxygen. The pressurized vessel is then placed in a forced convection oven at 90 °C for 16 h. After the test is complete the total amount of fuel insolubles are determined. The practical significance of this method is that it can be used to evaluate different fuels with and without additives. Similar storage stability test method ASTM D 2274 for middle distillate fuels (No. 2) has been stated to be inapplicable for fuels which have non-petroleum derived components in them.

Dupont Petroleum Laboratories has developed a test method (F31-81) to test the stability of some distillate fuels. According to this method the sample is stored for 7-14 days at a temperature of 80 °C. The laboratories claim that this method gives better prediction of the sample behavior during actual storage conditions as opposed to the ASTM D 4625 method in which the sample is stored at 43 °C. After the sample is stored at 80 °C (2 weeks) it is filtered and the filter pad rating is evaluated using a reflection meter. The color changes of fuel sample before and after aging are also monitored during

this test. Millipore vacuum filtration apparatus is used during this test. Filtration of the fuel sample is performed using Whatman No.1 filter paper (4.7 cm) to collect residues. ASTM D 1500 colorimeter is used to determine the color changes of the sample. Pad ratings for each filter are developed based on the % reflectance obtained. This test method is applicable for distillate fuels such as heating oils, kerosene, and diesel oils. The impact of adding an additive to the fuel can be evaluated using this test method. Dupont petroleum laboratories have reported [1981] that aging of the distillate fuels stored at 80 °C for a period of 7 days is equivalent to a period of 4-8 weeks at 43 °C or a period of 4-8 months at ambient storage temperature.

Storage stability of gasoline can be measured using the ASTM D 525 method. Accordingly, the sample is oxidized in a bomb filled with oxygen at a pressure of 100 psi. The temperature of the bomb before loading the sample is 15-25 °C. After the sample is loaded the temperature of the bomb is slowly raised to 98-102 °C and pressure drop recorded as a function of time. The time required for the sample to reach the break point is considered as induction period. The resulting induction period could be used as an indication of gum forming tendency during the storage of motor gasoline.

Asphaltenes are defined (ASTM D 7061) as ‘the heteroatomic molecules with high molecular mass and high carbon/hydrogen ratio’. Asphaltenes seem to be the primary reason for causing instability in heavy fuel oils (Grade No.’s 4-6). Consequently, phase separation and accumulation of sludge deposits eventually take place in storage tanks of the unstable oils. To detect these phenomena early and also the overall stability reserve of the heavy fuel oils, Buron and others [2005] have recently developed a unique method that utilizes a turbiscan. Stability reserve has been defined as ‘the property of an

oil to maintain asphaltenes in a peptized state and prevent flocculation of the asphaltenes'. Accordingly, ASTM D 7061 method is used to determine the stability of heavy fuel oils. This method requires turbiscan a scanning device which utilizes both pulsed near infrared light source (850 nm) and a transmittance detector. The transmittance detector is located at an angle of 180⁰ away from the light source. According to this method the oil is diluted with toluene and heptane before scanning is performed. After the diluted sample is loaded in a capped long cylindrical glass vial the light is passed and the % transmittance recorded every minute. The transmittance is measured every 0.04 mm along the sample height of the vial over a total period of 15 minutes. The mathematical formula as shown in Equation 10 defines the stability reserve of the oils also named as separability number. Lower separability number means higher stability of heavy fuel oil and vice versa.

$$\text{Separability Number} = \sqrt{\frac{\sum_{i=1}^n (X_i - X_T)^2}{n-1}} \quad (2-10)$$

Where,

X_i = Average transmittance (%) for each minute

X_T = Average of X_i

n = Number of replicates (16)

Motor Oil

Based on this investigation ASTM methods for measuring motor oil storage stability do not exist. However, motor oil stability has been measured in terms of colloidal stability (Lashkhi et al., 1986). Storage stability of motor oils with different additives was evaluated based on their ash content, sludge content, and base number. Accordingly, motor oils with higher values of ash content, sludge content, and base

number were less stable than the others. Motor oil during its long-term storage in the vented tanks can accumulate water from the environment. Due to the excessive water contamination in oil tanks, layering occurs and the effect of additives is lost along with sludge accumulation at the bottom of the tank. The degree and the rate of sludge formation are known to be dependent on the water content and oxidation extent of the oil. The sludge formed during motor oil storage has been described as a mixture of 85.9-97.8% oil, 1.4-5.5% solids, and 0.5-8.6% water. The solid component of the sludge has been known to contain ash elements as high as 80%. Base number (mg KOH/g oil) of the fresh and aged oils was determined as a function of height in the tank (settler). Results clearly indicated that the base number for the aged oil increased from top to the bottom of the tank. However, for the fresh oil the base number was same across the entire height of the tank. Furthermore, it is not clear whether the hydroxy acids that are formed during the oil storage are due to the destabilization of additives or chemical oxidation processes.

Aviation Fuel

Storage stability of aviation fuels used in reciprocating, turbine, and jet engines can be determined by the method ASTM D 873. Accordingly, the fuels are stored in a glass container that is enclosed in an oxidation pressure vessel. A maximum temperature of 100 °C is used to accelerate the sample aging for 'X' hours (Ex: 16 h) as predetermined during the test. After the test is completed the glass container is analyzed for three fractions. They are soluble gum (A), insoluble gum (B), and precipitate (C). Fraction B is obtained by measuring the amount of material adhered to the sample

container which is the difference in container weights before and after the test. A mixture of toluene and acetone is used to wash the sample container. Fraction C in the sample is thus obtained as a residue by filtering the aged sample along with container washings. The filtrate obtained is then evaporated to determine the fraction A in the fuel as non-volatile residue or soluble gum. Aging characteristic in this test is reported as mg of fraction (A, B, and or C) per 100 ml of sample used. By combining the three fractions A, B, and C the total potential residue in the fuel can be determined. A major drawback of this method is that it can not be used for determining storage stability of fuels with unsaturated low boiling compounds as they could potentially cause explosions in the testing apparatus.

High temperature stability of gas turbine fuels is measured by the jet fuel thermal oxidation tester (JFTOT) as outlined in the ASTM D 3241 procedure. According to this procedure the stability of turbine fuels is measured by subjecting them to the actual conditions encountered during the turbine operation. A known quantity (450 ml) of fuel is pumped at a constant volumetric flow rate through an aluminum heater tube where heating takes place for 2.5 hours. After the heating is performed the fuel is passed through a precision stainless steel filter with 17 μm nominal porosity. The temperature used for heating is dependent upon the fuel system specifications in a gas turbine. Based on the amount of deposits built inside the heater tube and the plugging rate of the filter the oxidative stability of gas turbine fuels is assessed.

Cooking Oil

Currently, food industry is using American Oil Chemists Society (AOCS) Cd 12b-92 method to determine the shelf-life or storage stability of cooking oils or fats. Accordingly, the Oil Stability Index (OSI) of cooking oil is measured using a rancimat based on the induction time period. Induction time period can be arbitrarily defined as the time consumed by the sample to become completely oxidized from the time of loading in the cell. The oils with longer induction time periods are more stable than the oils with smaller induction time periods and vice versa. Metrohm developed Rancimat 743 is used to measure the OSI of cooking oils as shown in Equation 11.

$$\text{OSI} = \frac{[\text{Induction Time of 'FAME+Antioxidant'}]}{[\text{Induction Time of Pure FAME}]} \quad (2-11)$$

Where,

FAME=Fatty Acid Methyl Esters Present in Oil

Antioxidant: Examples of common antioxidants used in the food industry are butylated hydroxytoluene (BHT), butylated hydroxyanisole (BHA), t-butylhydroquinone (TBHQ)

Rancidity index or OSI of the oil can be determined at elevated temperatures (Ex: 60-130 °C) to advance the oxidation reactions. Accordingly, the sample is exposed to air at elevated temperature for a certain time period during which oxidation takes place. During the oxidation process the volatile acids from the sample are driven off and collected in deionized water (ASTM I). The conductivity increase of water as a function of time is monitored and plotted automatically to observe for the sharp inflection point. The time taken from the start of the test to the observation of sharp increase in conductivity of water is considered as the induction time period of the sample. The induction time period of the sample is usually in the order of several hours. Furthermore,

by plotting measurement temperature (ordinate) versus induction time (abscissa) the eventual shelf-life of the oil at room temperature can be extrapolated. Rancimat test gives a better prediction of shelf-life and the condition of the oil at the time of test as opposed to the iodine value test used to determine the unsaturation of oil.

Bio-diesel

Bio-diesel oxidation has been reported to cause the formation of corrosive acids and deposits. These acids and deposits corrode the engine equipment (Westbrook and McCormik, 2005). Hence, measuring the oxidative stability of fatty acid methyl esters (FAME's) present in the bio-diesel is critical for its evaluation as a potential bio-fuel. Oxidative stability test (DIN EN 14112) using a rancimat (Metrohm) is included as part of the European bio-diesel specifications. Bio-diesel is a relatively new fuel in the market. Hence, its storage stability needs to be investigated. The United States Department of Energy (U.S DOE) has reported that ASTM methods are currently unavailable for bio-diesel oxidative or storage stability testing. Furthermore, experiments were conducted to measure the bio-diesel viscosity, acid number, and insoluble sediments as a function of storage time (DOE, 2006). The bio-diesels used in the tests were B20 and B100 (B20 is a mixture of 20% bio-diesel and 80% diesel fuel, where as B100 is 100% bio-diesel or pure bio-diesel). Viscosity (cSt, 40 °C), acid number (mg KOH/g), and insoluble sediment (mg/100 ml) tests provided an assessment of the bio-diesel long-term storage stability. These tests were performed over a period of 16 weeks and the samples were stored at 43 °C. As per ASTM D 4625 the accelerated storage of a fuel at 43 °C for a week is equivalent to a month of storage at ambient temperature. The least stable B100

bio-diesel was projected to have a maximum storage life of eight months where as the most stable bio-diesel was projected to have a minimum storage life of one year. In either case the bio-diesels tested were well above the average fuel turn over time of 2-4 months in the commercial systems. Furthermore, the National Bio-diesel Board has recommended a storage life of 6 months for B100 based on these studies.

Pyrolysis Oil

A similar approach to determine pyrolysis oil storage stability as that of bio-diesel is possible depending upon the proximity in emulation between accelerated test conditions and the actual storage conditions. The chemical changes that occur in pyrolysis oil during the storage are much different from bio-diesel. For example, oxidative changes that occur in the bio-diesel are quite different from the pyrolysis oil as illustrated by the fact that linear long-chain unsaturated compounds are not to be found in pyrolysis oil. Mostly medium to long chain interconnected polyaromatic hydrocarbons are contained by pyrolysis oil as previously discussed. Along with them short chain aliphatic and carbohydrate compounds are also known to be present in the pyrolysis oil. Pyrolysis oil can be expected to have higher viscosity than bio-diesel making it very difficult to filter unless ample dilution of the sample is performed. By doing so the chemical composition of the pyrolysis oil might change totally.

Currently, there is not a standard testing method available to measure the stability of pyrolysis oil. Stability of pyrolysis oil however, has been studied predominantly by physico-chemical testing as revealed from the literature. Pyrolysis oils were stored at both ambient and accelerated conditions as per the test methods developed by different

researchers. Consequently, pyrolysis oil analysis was performed over periodic time intervals during its storage. The storage temperature was varied from 25 °C to as high as 90 °C mainly to accelerate the physico-chemical changes and study the long-term storage stability of pyrolysis oils. Accelerated storage times varied from few hours to few weeks while ambient storage times varied from few months to a year or two. During accelerated testing similar reactions can be expected to occur for the chosen range of temperature with the exception of rate.

Because of the complex chemistry of pyrolysis oil as discussed in the Chapter II, multiple analytical tools are needed to arrive at definitive conclusions. Hence, different researchers have resorted to gel permeation chromatograph (GPC), viscometer, rheometer, Karl Fisher titrator, gas chromatograph (GC), High Performance Liquid Chromatograph (HPLC), Fourier Transform Infrared spectroscope (FTIR), Nuclear Magnetic Resonance spectroscope (NMR), optical microscope, Small Angle Neutron Scattering (SANS) and others. Thus far, physico-chemical changes of pyrolysis oils studied over the entire storage periods included polymerization, phase separation, chemical compositional variation, structural dissolution, transition in flow behavior, and changes in visual coloration (Ba et al., 2004 I & II; Perez et al, 2006; Oasmaa and Kuoppala, 2003). Consequently, pyrolysis oil properties like viscosity, water content, and molecular weight were observed to increase significantly with storage time for the unstable pyrolysis oils. Among all the physico-chemical properties studied, viscosity stood out as the single most important property in characterizing the pyrolysis oil stability.

Viscosity of the pyrolysis oils was used as a primary quantitative measure to qualitatively describe the extent of polymerization that took place in the pyrolysis oil. Subsequently, if the viscosity of the pyrolysis oil increased drastically by many folds the oil was deemed to be less stable. In other instances, when the water content of pyrolysis oil increases due to polymerization then the oil was deemed to be less stable. Pyrolysis oil has the tendency to destabilize its network when polymerization occurs. Polymerization reactions in the form of 'condensation and polycondensation' contribute to the release of water in pyrolysis oil. Whenever the water concentration exceeds 30% pyrolysis oil phase separates and hence the oil is rendered unstable (Fratini et al., 2006; Oasmaa and Kuoppala, 2003).

As mentioned previously advanced spectroscopic tools can be used to study chemical changes that occur during the storage of pyrolysis oils. Similarly, microscopic tools can also be used to study the phase changes that would occur as result of sample heating for different storage times selected. Phase changes may constitute oil microstructure dissolution, melting of waxy particles found in extractives, agglomeration of char particles, coalescence of water droplets, and formation of micelle, colloid, and crystal type materials (Perez et al., 2006; Ba et al., 2004). Molecular weight increments of compounds present in the pyrolysis oil as a function of time were better understood by the use of GPC. The compounds studied were both low molecular mass lignin and high molecular mass lignin (Oasmaa et al., 2003). As a conclusion, chromatographic, spectroscopic, rheologic, and microscopic tools can be used exclusively or combinatorially to better understand and predict the long-term storage stability of pyrolysis oils.

Pyrolysis Oil Stability

Catalytic Effects

Pyrolysis oils have been reported to be acidic mainly due to the presence of formic, acetic, and propanoic acids (Ba et al. 2004 II; Oasmaa et al., 2005). A large concentration of such acids in the aqueous phase of pyrolysis oil seems to be responsible for the increasing number of polymerization reactions (Boucher et al., 2000 I). One possibility is to convert these free carboxylic acids to esters by the addition of alcohols to pyrolysis oils (Doshi et al. 2005). Proportionally, the availability of acids to participate during catalysis of detrimental polymerization reactions can be minimized. Particulate matter (PM) in the form of char is formed during the biomass pyrolysis reactions. Thus, PM becomes part of the pyrolysis oil and plays a catalytic role in decreasing pyrolysis oil stability (Diebold et al., 1995; Agblevor and Besler, 1996). Furthermore, acids and particulate matter have been known to collectively catalyze the chemical reactions that occur during the pyrolysis oil storage (Diebold 2000; Oasmaa and Kuoppala, 2003). However, chemical reactions that decrease the stability of pyrolysis oils by polymerization (condensation and polycondensation) are known to occur at a slow rate (Bridgwater et al., 1999). Hence, using accelerated storage methods for studying the pyrolysis oil stability are beneficial.

Compositional Changes

Chemical compositional changes have been reported to occur during the storage of pyrolysis oils as measured by GC (~40% detectable). Accordingly, certain chemical compounds of pyrolysis oil decreased in concentration while most others were unaffected

by the storage conditions utilized (Meier et al., 2002). During their study pyrolysis oils derived from beech wood were stored at room temperature (light and dark) and refrigerated conditions (dark, 8 °C) for a period of 32 weeks. Consequently, three sets of samples were analyzed each week for major chemical compounds. After the initial testing period (7 weeks) the samples were analyzed every four weeks. The chemical compounds analyzed were main components (acetic acid, hydroxypropanone, and levoglucosan), phenols, furans, pyrans and guaiacols. Cooling of the pyrolysis oil samples was observed to delay the polymerization reactions but did not prevent them from occurring. Main components present in the pyrolysis oils remained unaffected by the storage conditions. Aldehydes namely 'hydroxyacetaldehyde and 3-hydroxypropanal' were observed to remain stable under refrigerated conditions. At room temperature however these aldehydes were observed to decrease as a function of storage time and independent of light exposure. The aldehyde named 2-hydroxy-3-oxobutanal was observed to almost disappear after 32 weeks of storage time. Furthermore, cyclic aldehydes and ketones were also observed to decrease regardless of the storage conditions. However, phenolic compounds present in the pyrolysis oil have been reported to be stable and relatively unaffected by the storage conditions. (Meier et al., 2002).

Chemical groups (pyranones and guaiacols) exhibited higher reactivity due to the presence of unsaturated double bonds (Meier et al., 2002). The compounds reported from the above chemical groups were [3-hydroxy-5,6-dihydroxy-(4H)-pyran-4-one], vinyl-guaiacol, and vinyl-syringol. The unsaturated double bonds present in the side chain of vinyl and propenyl type aromatic compounds are understood to cause polymerization reactions in the pyrolysis oils. One possibility is that they might be reacting with

pyrolytic lignin leading to the formation of sludge during oil storage. Consequently, increase in viscosity and molecular weight of the pyrolysis oils can be observed. Further, compounds with most reactivity in pyrolysis oil are predicted to contain unsaturated aryl-alkenyl type bonds. By measuring the amounts of these bonds one might be able to assess the pyrolysis oil instability as reported (Meier et al., 2002).

Chemical Reactions

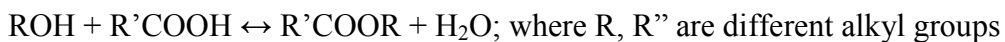
Generally, stability of pyrolysis oils is affected because of: 1) condensation of the aromatic units with formaldehyde 2) polymerization of aryl-vinyl, aryl-allyl, and aryl-crotonyl fragments of lignin and 3) interaction of carbonyl and alcohol groups to form acetal (Meier and Faix, 1999). Polyaromatic compounds with multifunctional groups and dimethoxy phenols are reported to participate in the ‘aging’ reactions with other compounds in the softwood bark pyrolysis oil leading to the formation of heavy compounds in the aged oil (Perez et al., 2006). Meier and others [2002] have explicitly stated that it is virtually impossible to obtain a clear understanding of the chemical reactions occurring in the pyrolysis oil. Because of its complex nature (>300 compounds) and multiple interfering reactions, kinetic studies of pyrolysis oil reactions are beyond the scope of any investigation. Further, there is little evidence from the literature that report on the mechanisms of reactions that occur in pyrolysis oil during its storage. Some of the possible chemical reactions that could be occurring during the pyrolysis oil storage have been schemed or proposed by few researchers and are discussed later (Diebold, 2000; Diebold and Czernik, 1997; Oasmaa et al., 2004).

Both reversible (unidirectional) and irreversible (bidirectional) reactions are predicted to occur in pyrolysis oils due to autocatalysis (Diebold, 2000). According to the LeChatalier's principle, reversible reactions result in a chemical equilibrium mixture of reactants and products. However, in an irreversible chemical reaction equilibrium cannot be attained because of the permanent change from reactants to products. Reversible chemical reactions lead to the formation of low molecular weight compounds in pyrolysis oils. The low molecular weight compounds constitute water, aliphatic esters, acetals, hemiacetals, and hydrates. Irreversible chemical reactions lead to the formation of high molecular weight compounds contributing towards a large increase in pyrolysis oil viscosity. High molecular weight compounds comprise of oligomers, resins, and polyolefins.

Significant increases in water content and viscosity can be observed for unstable pyrolysis oils because of the undesirable chemical reactions that are mostly irreversible and complex polymeric reactions (Diebold, 2000). Lower concentrations of water are beneficial in lowering the pyrolysis oil viscosity but a significant increase in water content can cause phase separation. Both types of reactions (reversible and irreversible) are not beneficial for maintaining or increasing the overall pyrolysis oil stability unless controlled. Preliminary research indicates that the addition of suitable additives at optimal concentrations can limit the undesirable chemical reactions. By adding suitable additives, the undesirable chemical reactions could be prevented from occurring at the expense of simple reversible chemical reactions like esterification, etherification, and acetalization. More experimental work is needed to support the above hypothesis as preliminary investigation conducted by Diebold and Czernik [1997] did not lead to a conclusion.

Some of the ‘reversible and irreversible’ reactions that occur in pyrolysis oils are proposed by Diebold [2000]. Some of these reversible and irreversible reactions are schemed below.

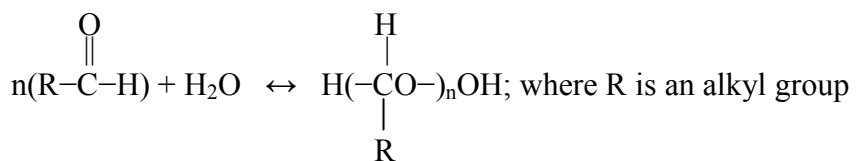
Esterification Rxn



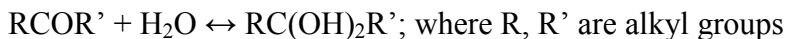
Transesterification Rxn



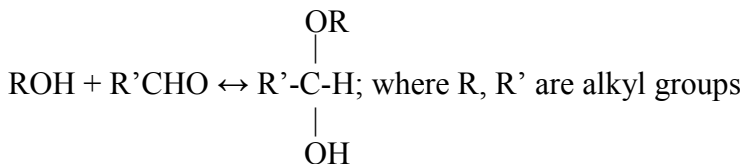
Homopolymerization Rxn



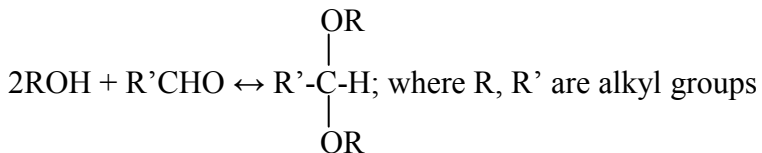
Hydration Rxn



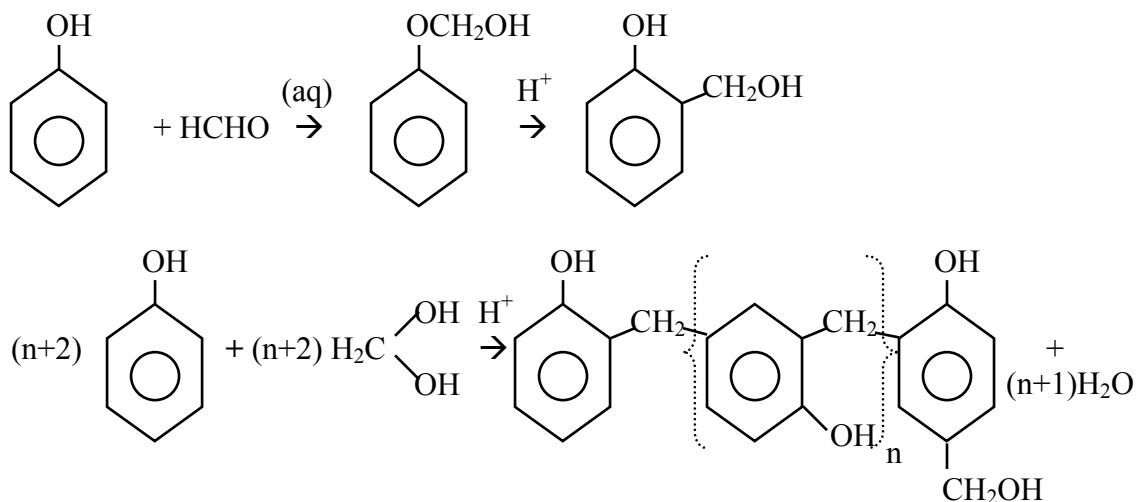
Hemiacetal Formation Rxn



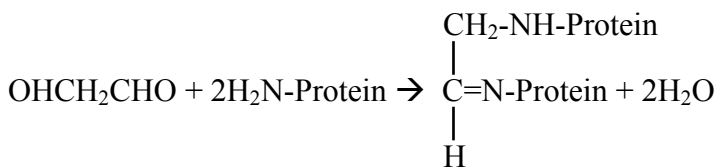
Acetalization Rxn



Resin Formation Rxn



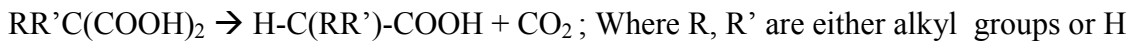
Dimerization Rxn



Alcohol Addition Rxn



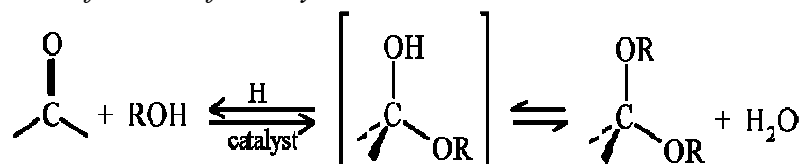
Gas Forming Rxn



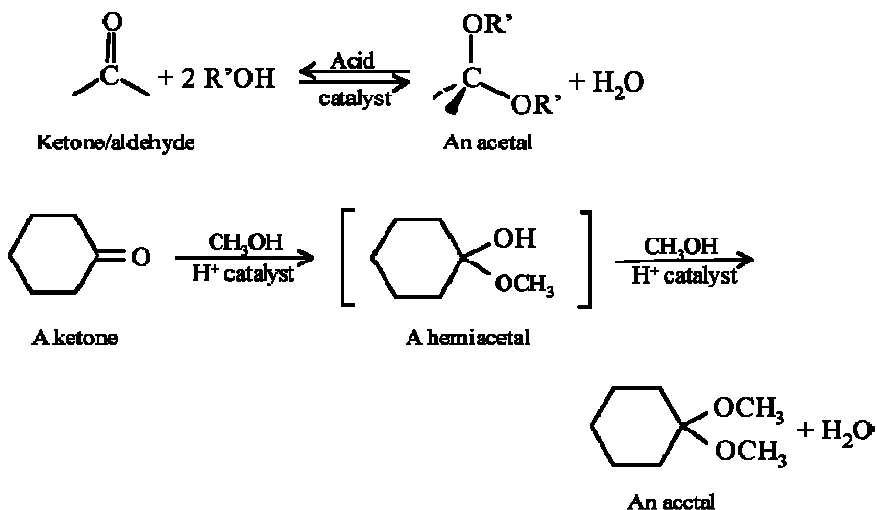
Condensation polymerization reactions in the form of esterification, etherification, and acetalization have been reported to occur in the pyrolysis oils (Czernik et al., 1994; Oasmaa et al, 2004). These reactions contribute towards slight viscosity increases in pyrolysis oils by forming low molecular weight compounds (esters, acetals, and ethers). However, the major concern is to prevent the complex polymerization reactions that lead

to the formation of high molecular weight compounds (polyesters, polyethers, polyacetals, polyketals, and polyaldehydes). These high molecular weight compounds contribute towards large viscosity increases in pyrolysis oils. Hence, through the addition of alcohols to pyrolysis oils, the formation of high molecular weight compounds can be prevented. Apart from the prevention of high molecular weight compound formation, the alcohols can physically dilute the pyrolysis oil and also produce a change in its microstructure (Diebold and Czernik, 1997; Oasmaa and Czernik, 1999; Oasmaa et al., 2004). The net result achieved by alcohol addition will be either neutral or positive by maintaining or increasing the stability of pyrolysis oils during their long-term storage. The simpler reactions such as esterification, etherification, and acetalization are projected to be beneficial for increasing the pyrolysis oil stability because they can prevent the availability of acids, aldehydes, ketones, and other compounds that take part in the complex polymerization reactions. Furthermore, addition of alcohols also seems to thermodynamically favor the simpler chemical reactions ultimately contributing to the improvement of pyrolysis oil stability. The addition of alcohols to pyrolysis oils is predicted to affect their stability positively based on the esterification and acetalization reactions schemed below (Diebold and Czernik, 1997; Diebold, 2000; Oasmaa et al., 2004).

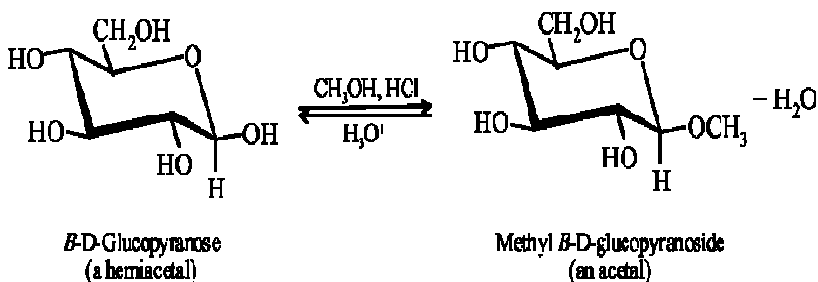
Esterification of Aldehydes and Ketones



Hemiacetal and Acetal Formation from Aldehydes and Ketones



Acetal Formation from Monosaccharides



Alcohols namely methanol, ethanol, and isopropanol improved the phase stability of pyrolysis oil by increasing the solubility of high molecular mass lignin and extractives in the pyrolysis oil. Viscosity and molecular mass increase during aging of the softwood pyrolysis oils were well controlled by alcohol addition. By the addition of 10% alcohol the aging reactions were inhibited for almost a year. Methanol was reported to be the most effective alcohol among the three alcohols tested (Oasmaa et al., 2004).

Physico-chemical Stability

The increase in high molecular mass fraction (HMM) is primarily responsible for the major physico-chemical changes that are known to occur in pyrolysis oils (Oasmaa and Kuoppala, 2003). The increase in the formation of higher molecular weight compounds was evident with the increase in storage time of the pyrolysis oil. Contrarily, lower molecular weight compounds were observed to decrease with the storage time (Czernik et al., 1994).

Both rheological and microscopic analysis revealed covalently bonded clusters in the softwood bark pyrolysis oil as the aging progressed. Contrarily, cluster formation did not occur with the pyrolysis oil derived from hardwood rich in fibers (Perez et al., 2006). Pyrolysis oil color changes were observed as visual signs of instability when stored at 9 °C. Most color changes were observed during the initial months of storage. A color change from reddish brown to dark brown was observed for the forestry residue derived pyrolysis oil (Oasmaa and Kuoppala, 2003).

Evidence suggested that hardwood pyrolysis oil did not exist as a single phase when visualized by a microscope. Both hydrophobic and hydrophilic phases were found to co-exist in the freshly produced pyrolysis oil. The hardwood pyrolysis oil has been compared with a fuel oil (Grade No.2) and surmised to possess emulsion like properties (Tzanetakis et al., 2008).

Flow Stability

Stability of the pyrolysis oil produced from forestry residues was studied by Oasmaa and Kuoppala [2003]. Viscosity of the pyrolysis oil increased steadily during the

initial months of storage at room temperature. After the first six months however the viscosity increase was drastically reduced until one year and thereby attained a plateau. Viscosity increase of the forestry residue derived pyrolysis oil stored at 80 °C for 24 hr was equivalent to the viscosity increase of the pyrolysis oil stored at room temperature for a year. Similar viscosity-storage time-storage temperature correlation was reported for the softwood bark pyrolysis oil (Chaalal et al., 2004). The viscosity (40 °C) of oak wood pyrolysis oils was observed to increase as a function of storage time for all storage temperatures. The results of viscosity are provided in Table 2.12. The viscosity increase between ‘fresh and aged’ pyrolysis oils corresponding to the storage temperatures of 37 °C (3 months), 60 °C (4 days), and 90 °C (6 hours) were all equivalent for the storage times indicated (Czernik et al., 1994). The viscosity increase (30 °C) for the pyrolysis oils stored at room temperature was rapid during the initial 65 days after which the increase was not significant. The addition of methanol (10 and 15%) to the pyrolysis oil showed that the viscosity changes were much smaller than the control oil (no additive) over a period of 260 days (Boucher et al., 2000 II).

The viscosity (measured at 40, 60, and 80 °C) of softwood bark pyrolysis oil stored at room temperature was observed to drastically increase as a function of initial storage time (2-3 months) before attaining a constant value. A minimum increase of 43.8% in viscosity (measured at 80 °C) was observed during the initial six months of storage. A maximum increase of ~100% in viscosity (measured at 40 °C) was observed during the initial six months of storage. Similar increases in viscosity (measured at 60 and 80 °C) were observed for softwood bark pyrolysis oil during the initial six months of storage. The discrepancy in ‘viscosity increase’ versus ‘measurement temperature’ is

likely explained by the phase transition that takes place when pyrolysis oil is exposed to higher temperatures (60 and 80 °C). Phase transitions are reported to occur due to the melting of polymeric constituents (≥ 40 °C) present in the pyrolysis oil (Chaala et al., 2004).

A recent study has reported that bark free hardwood pyrolysis oil derived from a mixture of apple, cherry, and oak trees is mildly pseudoplastic or mostly Newtonian with a weak elastic behavior (Tzanetakis et al., 2008). Char, wax, and the like hydrophobic phases present in the pyrolysis oil were observed to disintegrate at higher shear rates and higher measurement temperatures (Tzanetakis et al., 2008). The flow behavior of the softwood bark derived pyrolysis oils was non-Newtonian (< 50 °C) due to the presence of three dimensional rod like structures (waxy materials). At temperatures > 50 °C the flow behavior of the pyrolysis oil transitioned from non-Newtonian to Newtonian because of the disappearance of the waxy materials during the melting process (Ba et al., 2004 II).

Phase Stability

Pyrolysis feed stocks dried to moisture content of 10% or less produce water during the thermo-chemical reaction in the range of 15-25%. This range is a cumulative of the water released during the evaporation, dehydration, degradation, and polymerization reactions. The greatest benefit of this amount of thermo-chemical water is that it can retain multiple components (phenolics, carbonyls, and aliphatics) of the pyrolysis oil into a single phase. The viscosity of the pyrolysis oil is also lowered by the presence of thermo-chemical water even though it may not be beneficial during the combustion process (Scott et al., 1999). Low molecular weight compounds are known to

be soluble in the aqueous phase of pyrolysis oil when they are present in low concentrations. At saturated concentrations however these compounds form an emulsion with pyrolysis oil. Similarly, when the water concentration reaches a saturation point in the organic phase of pyrolysis oil an emulsion will result. Both hydrophilic (water attracting) and hydrophobic (water repelling) phases can co-exist at the same time in freshly produced pyrolysis oil. If any of these two phases reaches or exceeds the saturation point because of time-temperature dynamics or physico-chemical changes, pyrolysis oil ceases to exist as a homogeneous liquid (Boucher et al., 2000).

Pyrolysis oils derived from hardwood (oak), softwood (pine) and herbaceous biomass (switch grass) stored at ambient conditions for two months revealed the presence of layers on the top. However, aqueous phase separation was not evident in these pyrolysis oils. While oak wood pyrolysis oil was uniform pine wood oil was observed to have a frothy brown-black layer (10%) on the top with many fine particulates. A foamy top layer (25%) was observed for the switch grass derived pyrolysis oil. Moisture analysis of the top and bottom layers of pyrolysis oils revealed significant differences in % water compared to the whole pyrolysis oil. Water in the pyrolysis oil tends to flow upwards in the form of char-water-foam aggregates as reported (Elliott, 1994). A clear phase separation occurred in the softwood bark derived pyrolysis oil stored at 80 °C after a storage period of 96 hour. Phase separation occurred when the aqueous concentration was around 10% by mass in the pyrolysis oil. Aqueous phase concentration in the phase-separated pyrolysis oil reached a final concentration of around 20% for storage times of 168 hr and beyond. This phenomenon is not in a complete agreement with the results reported elsewhere that indicated pyrolysis oil phase separation around $\geq 30\%$ water

concentration. Rather phase separation in the pyrolysis oils seems to be affected by the network strength of the pyrolysis oil in holding the multiple phases together. Once the phase separation is initiated the pyrolysis oil degradation increases significantly. With pyrolysis oil phase separation, heavy compounds in the form of polyaromatics (naphthalenes, anthracenes, phenanthrenes, etc) settle at the bottom especially in the absence of dimethoxy phenols (Perez et al., 2006).

Water content increased drastically during the first three months of pyrolysis oil (derived from forestry residue) storage at room temperature before reaching a plateau. Phase separation of the pyrolysis oil occurred after 18 months of storage at 9 °C under darkness. This is because the water concentration in the pyrolysis oil reached 30% that is typical of many other pyrolysis oils studied. After two years of storage at 9 °C the pyrolysis oil phases were completely immiscible (Oasmaa and Kuoppala, 2003).

As stated previously phase separation occurs in pyrolysis oils as a consequence of drastic network polymerization and substantial increase in the water concentrations. If these two phenomena do not take place during the storage of pyrolysis oils then the phase-separation of the oils can be very likely prevented. Further in a study conducted by Czernik et al. [1994] phase separation was not reported to occur during the storage of oak wood pyrolysis oils. The water content of these oils showed a mild increase as a function of storage time for all storage temperatures. This was obviously due to the net increase in number of polymerization reactions but not enough to cause phase-separation of the oils. The results of water content are provided in Table 2.13. The least water content increase between 'fresh and aged' pyrolysis oils was observed at a storage temperature of 37 °C.

Structural Stability

Softwood bark derived pyrolysis oils were microscopically observed to have agglomerated particulate matter. These pyrolysis oils were observed to have both hydrophilic (bottom) and hydrophobic (upper) layers. The upper layer was observed to be rich in waxy materials in the form of fatty and resin acids while the bottom layer was rich in ash and water. Complex multi phase colloidal changes were observed in the pyrolysis oil as a function of temperature ranging 25-70 °C. Microscopic analysis indicates that the major phase changes in the pyrolysis oil occurred in the form of structure precipitation (39.2 °C), structural dissolution (43 °C), and droplet disappearance (60 °C). Multiple phases present in the pyrolysis oil were holocellulosic derived compounds, water, oil droplets, char particles, waxy materials (fatty and resin acids), and rod-like structures. Previously, waxy materials are known to form micelle-like structures or flocks in the pyrolysis oil. These flocks tend to move towards the oil-air interface, as their density is lower than the pyrolysis oil. The oil droplets were observed to coalesce because of increased molecular motion (Brownian) during the heating process. Droplet coalescence eventually caused the phase separation in pyrolysis oil. At a temperature above 60 °C the oil droplets were completely solubilized while the char particles concentrated around the dispersed phase and matrix interface. Complete dissolution of the pyrolysis oil structure occurred when the rod-like structures melted in the oil matrix (Ba et al., 2004 I, II; Chaala et al, 2004).

The present investigation comprises of both short-term and long-term stability testing of wood and bark derived pyrolysis oils that are produced from auger and entrained flow reactors. Short-term testing of pyrolysis oils is performed by aging the oils

at 80 °C to a maximum aging time of 192 hr. Long-term testing of pyrolysis oils is performed by aging the oils at 25 °C to a maximum aging time of 6 months. The actual viscosity testing of the oils is performed at three temperatures namely 25, 50, and 80 °C. Methanol is considered as a reference standard during the stability testing based on its stability performance cited in literature. Rheological and Karl Fisher analysis are the primary tools used during this pyrolysis oil stability investigation. More details on the experimental design criteria are discussed in Chapter III.

Table 2.1

Typical Wood Composition (Schultz and Taylor, 1989)

Wood Type	Wood Component (%)			
	Cellulose	Hemicellulose	Lignin	Extractives
Softwood	39-43	25-29	26-32	2-5
Hardwood	43-47	24-34	18-26	1-5

Table 2.2

Typical Reactor Yields of Pyrolysis Oil, Gas, and Char Fractions (Graham et al., 1994)

Feedstock	Temperature (°C)	Residence Time (ms)	Product Yields (% by mass)		
			Pyrolysis Oil	Gas	Char
Avicel Cellulose	505	250	90	10	0
	650	110	88	12	0
Maple	515	400	75	12	13
	520	250	78	10	12
	700	90	70	25	5
IEA Poplar	450	395	74	5	21
	500	330	76	7	17
	550	270	76	12	12
	600	270	71	20	9
	650	210	68	25	7
	700	90	70	25	5
Wheat Straw	500	200	70	11	19
	500	600	72	14	14
	550	200	75	13	12
	550	600	66	16	18
Flax Shives	515	220	64	17	19
Sorghum Bagasse	490	320	81	5	14
	535	360	78	10	12
Corrugate Cardboard	500	200	80	10	10
	580	225	81	12	7
Clarifier Sludge	547	170	79	13	8

Table 2.3

Major North American Pyrolysis Units in Design/Operation
(Bridgwater and Peacocke, 2000)

Owner	Country	Reactor Type	Pyrolysis Type	Feed Rate (kg/h)
Dynamotive	Canada	Fluidized Bed	Fast	1500
Red Arrow/Ensyn	USA	Circulating Transported Bed	Fast	1250
Red Arrow/Ensyn	USA	Circulating Transported Bed	Fast	1000
Red Arrow/Ensyn	Canada	Circulating Transported Bed	Fast	125
Red Arrow/Ensyn	Canada	Circulating Transported Bed	Fast	100
University of Laval	Canada	Vacuum Moving Bed	Fast	50
WWTC	Canada	Auger Kiln	Slow	42
Ensyn	Canada	Circulating Transported Bed	Fast	40
RTI	Canada	Fluidized Bed	Fast	20
NREL	USA	Ablative Vortex	Fast	20
Dynamotive	Canada	Fluidized Bed	Fast	20

Table 2.4

Major Criteria for the Geometry Selection in a Rheometer (Morrison, 2001)

Feature	Parallel Disk	Cone and Plate	Capillary	Couette (Cup and Bob)
<i>Stress range</i>	Good for high viscosity	Good for high viscosity	Good for high viscosities	Good for low viscosities
<i>Flow stability</i>	Edge fracture at modest rates	Edge fracture at modest rates	Melt fracture at very high rates, i.e., distorted extrudates and pressure fluctuations are observed	Taylor cells are observed at high Re due to inertia; elastic cells are observed at high De
<i>Sample size and sample loading</i>	< 1 g; easy to load	< 1 g; highly viscous materials can be difficult to load	40 g minimum; easy to load	10–20 g; highly viscous materials can be difficult to load
<i>Data handling</i>	Correction on shear rate needs to be applied; this correction is ignored in most commercial software packages	Straightforward	Multiple corrections need to be applied	Straightforward
<i>Homogeneous?</i>	No; shear rate and shear stress vary with radius	Yes (small core angles)	No; shear rate and shear stress vary with radius	Yes (narrow gap)
<i>Pressure effects</i>	None	None	High pressures in reservoir cause problems with compressibility of melt	None
<i>Shear rates</i>	Maximum shear rate is limited by edge fracture; usually cannot obtain shear-thinning data	Maximum shear rate is limited by edge fracture; usually cannot obtain shear-thinning data	Very high rates accessible	Maximum shear rate is limited by sample leaving cup due to either inertia or elastic effects; also 3-D secondary flows develop (instability)
<i>Special features</i>	Good for stiff samples, even gels; wide range of temperatures possible	Ψ_1 measurable; wide range of temperatures possible	Constant- Q or constant- ΔP modes available; wide range of temperatures possible	Narrow gap required; usually limited to modest temperatures (e.g., $0 < T < 60^\circ\text{C}$)

Table 2.5

Mathematical Equations Used to Compute Viscosity of a Liquid for Different Geometries of a Rheometer (Morrison, 2001)

Geometry	Magnitude of Shear Stress $ \tau_{21} $	Shear Rate $\dot{\gamma}$	Measured Material Function
<p><i>Capillary flow (wall conditions)</i> P_0, P_L = modified pressure at $z = 0, L$ Q = flow rate L = capillary length $R = \frac{1}{4} \left[3 + \frac{d \ln(4Q/\pi R^3)}{d \ln \tau_R} \right]$ $\tau_R = \tau_{rz} _{r=R}$</p>	$\frac{(P_0 - P_L)R}{2L}$	$\frac{4Q}{\pi R^3} R$	$\eta = \frac{\tau_R}{4Q/\pi R^3} R^{-1}$
<p><i>Parallel disk (at rim)</i> \mathcal{T} = torque on top plate Ω = angular velocity of top plate, > 0 H = gap $R = \frac{1}{4} \left[3 + \frac{d \ln(\mathcal{T}/2\pi R^3)}{d \ln \dot{\gamma}_R} \right]$ $\dot{\gamma}_R = \dot{\gamma}(R)$</p>	$\frac{2\mathcal{T}}{\pi R^3} R$	$\frac{r\Omega}{H}$	$\eta = \frac{2\mathcal{T}}{\pi R^3 \dot{\gamma}_R} R$
<p><i>Cone and plate</i> \mathcal{T} = torque on plate \mathcal{F} = thrust on plate Ω = angular velocity of cone, > 0 Θ_0 = cone angle</p>	$\frac{3\mathcal{T}}{2\pi R^3}$	$\frac{\Omega}{\Theta_0}$	$\eta = \frac{3\mathcal{T}\Theta_0}{2\pi R^3\Omega}$ $\Psi_1 = \frac{2\mathcal{F}\Theta_0^2}{\pi R^2\Omega^2}$
<p><i>Couette (bob turning)</i> \mathcal{T} = torque on inner cylinder, < 0 Ω = angular velocity of bob, > 0 R = outer radius κR = inner radius L = length of bob</p>	$\frac{-\mathcal{T}}{2\pi R^2 L \kappa^2}$	$\frac{\kappa\Omega}{1-\kappa}$	$\eta = \frac{\mathcal{T}(\kappa-1)}{2\pi R^2 L \kappa^3 \Omega}$
<p><i>Couette (cup turning)</i> \mathcal{T} = torque on inner cylinder, > 0 Ω = angular velocity of cup, > 0 R = outer radius κR = inner radius L = length of bob</p>	$\frac{\mathcal{T}}{2\pi R^2 L \kappa^2}$	$\frac{\kappa\Omega}{1-\kappa}$	$\eta = \frac{\mathcal{T}(1-\kappa)}{2\pi R^2 L \kappa^3 \Omega}$
<p>* R is radius of fixture. To calculate strain in each case, multiply shear rate by time t. Note that $\eta \equiv -\tau_{21}/\dot{\gamma}_0 = \tau_{21} /\dot{\gamma}$.</p>			

Table 2.6

Typical Properties of Bio-Crude Compared to the Conventional Crude
(Czernik and Bridgwater, 2004)

Property	Bio-Crude	Conventional Crude
Moisture (wt.%)	15-30	0.1
pH	2.5	-
Specific Gravity	1.2	0.94
HHV (MJ/kg)	16-19	40
Viscosity (cP, 50 °C)	40-100	180
Solids (wt.%)	0.2-1	1
Distillation Residue (wt.%)	≤ 50	1

Table 2.7

Typical Elemental Composition (wt.%) of Bio-Crude Compared to the
Conventional Crude (Czernik and Bridgwater, 2004)

Element	Bio-Crude	Conventional Crude
Carbon	54-58	85
Hydrogen	5.5-7.0	11
Oxygen	35-40	1
Nitrogen	0-0.2	0.3
Ash	0-0.2	0.1

Table 2.8

Hansen Solubility Parameters for Selected Solvents in Pyrolysis Oil
(Barton, 1983; Diebold, 2000)

Compound	δ_{di} (MPa ^{1/2})	δ_{pi} (MPa ^{1/2})	δ_{hi} (MPa ^{1/2})	δ_{ti} (MPa ^{1/2})
Methanol	15.1	12.3	22.3	29.6
Ethanol	15.8	8.8	19.4	26.5
Ethylene Glycol	17.0	11.0	26.0	32.9
Allyl Alcohol	16.2	10.8	16.8	25.7
1-Propanol	16.0	6.8	17.4	24.5
2-Propanol	15.8	6.1	16.4	23.5
Propanediol	16.8	9.4	23.3	30.2
Glycerol	17.4	12.1	29.3	36.1
1-Butanol	16.0	5.7	15.8	23.1
Furfuryl Alcohol	17.4	7.6	15.1	24.3
Acetaldehyde	14.7	8.0	11.3	20.3
Butanal	14.7	5.3	7.0	17.1
Furfural	18.6	14.9	5.1	24.4
Benzaldehyde	19.4	7.4	5.3	21.5
Formic Acid	14.3	11.9	16.6	24.9
Acetic Acid	14.5	8.0	13.5	21.4
1-Butanoic Acid	14.9	4.1	10.6	18.8
Benzoic Acid	18.2	7.0	9.8	21.8
Methyl Acetate	15.5	7.2	7.6	18.7
Ethyl Formate	15.5	7.2	7.6	18.7
Ethyl Acetate	15.8	5.3	7.2	18.1
Ethyl Lactate	16.0	7.6	12.5	21.6
n-Butyl Acetate	15.8	3.7	6.3	17.4
γ -Butyrolactone	19.0	16.6	7.4	26.3
Ethyl Cinnamate	18.4	8.2	4.1	20.6
Methylal	15.1	1.8	8.6	17.5
Furan	17.8	1.8	5.3	18.6
Anisole	17.8	4.1	6.8	19.5
Dibenzyl Ether	17.4	3.7	7.4	19.3
Acetone	15.5	10.4	7.0	20.0
Methyl Ethyl Ketone	16.0	9.0	5.1	19.0
Methyl Isobutyl Ketone	15.3	6.1	4.1	17.0
Phenol	18.0	5.9	14.9	24.1
Resorcinol	18.0	8.4	21.1	29.0
m-Cresol	18.0	5.1	12.9	22.7
o-Methoxy Phenol	18.0	8.2	13.3	23.8
n-Hexane	14.9	0.0	0.0	14.9
Benzene	18.4	0.0	2.0	18.6
Toluene	18.0	1.4	2.0	18.2
Styrene	18.6	1.0	4.1	19.0
Turpentine	16.4	1.4	0.4	16.5
Napthalene	19.2	2.0	5.9	20.3
Water (With Organics)	19.5	17.8	17.6	31.7
δ_d = Dispersive solubility parameter δ_p = Polar solubility parameter δ_h = Hydrogen bonding solubility parameter δ_t = Total solubility parameter				

Table 2.9

Classification of Chemical Compounds Present in Pyrolysis Oil Organic Fraction (Bridgwater, 1999; Oasmaa et al., 2003)

Compound Class	wt. %
<i>C1 Compounds:</i> Formic Acid, Methanol, Formaldehyde, and Ketones	5-10
<i>C2-C4 Compounds:</i> Linear Hydroxyl and Oxo-Substituted Aldehydes and Ketones	15-35
<i>C5-C6 Compounds:</i> Hydroxyl, Hydroxymethyl, and/or Oxo-Substituted Furans, Furanones, and Pyranones	10-20
<i>C6 Compounds:</i> Anhydrosugars Including Anhydro-oligosaccharides	6-10
Water-Soluble Carbohydrate Derived Oligomeric and Polymeric Material	5-10
Monomeric Methoxyl-Substituted Phenols	6-15
Water-Insoluble Material	15-30

Table 2.10

Major Chemical Compounds Present in the Pyrolysis Oil (Maschio et al., 1992)

Organic Rich Fraction		Aqueous Rich Fraction	
Compound	wt. %	Compound	wt. %
Methanol	0.9-1.2	Methanol	1.8-2.1
Acetic Acid	4-5	Acetic Acid	9.4-11.3
Furfural	3-4	Furfural	0.9-1
Methyl Furfural	1-2	Methyl Furfural	0.2-0.3
Guaiacol	4.5-5	Guaiacol	0.2-0.3
4-Methyl Guaiacol	4-5	4-Methyl Guaiacol	0.2-0.3
4-Ethyl Guaiacol	3-4	4-Ethyl Guaiacol	0.1-0.15
m-Cresol and p-Cresol	5-5.5	Acetone	0.5-0.75
2,4-Xylenol	1.5-2.5	2,4-Xylenol	0.1-0.15
Vanillic Alcohol	9-10	Vanillic Alcohol	0.7-1.1
Vanillic Acid	9.5-10.5	Vanillic Acid	0.9-1.5
Eugenol	2.5-3	Propionic Acid	0.6-0.75
3-Methoxy, 4-hydroxyphenyl ethylcarbinol	6-8	Phenol	0.3-0.4
Phenol	3-4	Acetaldehyde	0.1-0.2
4-Propyl Guaiacol	4-4.5	Methyl Acetate	0.3-0.4
Guaiacol Propionate	2-2.5	Ethyl Acetate	0.1-0.2
o-Cresol	3.5-4	o-Cresol	0.1-0.15
Coniferyl Alcohol	1-2	Cyclopentanone	0.3-0.4
3-Methoxy-4,5-dihydroxyphenyl Ketone	3-4	3-Methoxy-4,5-dihydroxyphenyl Ketone	<0.10
2,6-Methoxy-4-propenylphenol	1-1.5	2,6-Methoxy-4-propenylphenol	<0.10
Methyl Formate	<0.10	Methyl Formate	<0.10
Acetone	<0.10	2,5-Methyl Furan	<0.10
Acetaldehyde	<0.10	Guaiacol Propionate	<0.10
Methyl Acetate	<0.10	Other Organic Compounds (<0.05%)	4-5
2,5-Methyl Furan	<0.10	Water	74-78
Propionic Acid	<0.10		
2-Methyl-5-ethylfurfural	<0.10		
2-Hydroxy-3-methyl cyclopentanone	<0.10		
Other Organic Compounds (<0.05%)	6-7		

Table 2.11

Elemental Composition of Oak Wood, Pine Wood, and Switch Grass Pyrolysis Oils
(Elliott, 1994)

Elemental Concentration (ppm)	Oak Wood	Pine Wood	Switch Grass
Aluminum (Al)	55	41	237
Barium (Ba)	<3	<2	13
Calcium (Ca)	160	160	745
Chromium (Cr)	<17	<17	47
Iron (Fe)	86	47	243
Lithium (Li)	25	7	12
Manganese (Mn)	15	6	27
Magnesium (Mg)	<55	<45	335
Nickel (Ni)	<22	<20	52
Phosphorous (P)	<50	<50	254
Potassium (K)	55	10	165
Silicon (Si)	112	93	3130
Sodium (Na)	2	<0.1	N/A
Sulfur (S)	<60	<50	347
Titanium (Ti)	17	5	14
Zinc (Zn)	28	14	23

Table 2.12

Viscosity of Oak Wood Pyrolysis Oils as a Function of Storage Time and Storage Temperature (Czernik et al., 1994)

37 °C		60 °C		90 °C	
Time (days)	Viscosity (cP)	Time (days)	Viscosity (cP)	Time (hours)	Viscosity (cP)
0	152	0	154	0	144
7	165	1	183	1	152
17	169	2	220	2	167
28	201	3	226	4.5	210
56	252	6.7	321	8	286
84	268	9	363	15	326

Table 2.13

Water Content of Oak Wood Pyrolysis Oils as a Function of Storage Time and Storage Temperature (Czernik et al., 1994)

37 °C		60 °C		90 °C	
Time (days)	Water (%)	Time (days)	Water (%)	Time (hours)	Water (%)
0	16.1	0	16.3	0	16.2
7	16.2	1	16.3	1	16.2
17	16.6	2	16.6	2	16.6
28	16.5	3	17.1	4.5	17.3
56	16.6	6.7	17.7	8	17.5
84	16.6	9	17.7	15	17.7

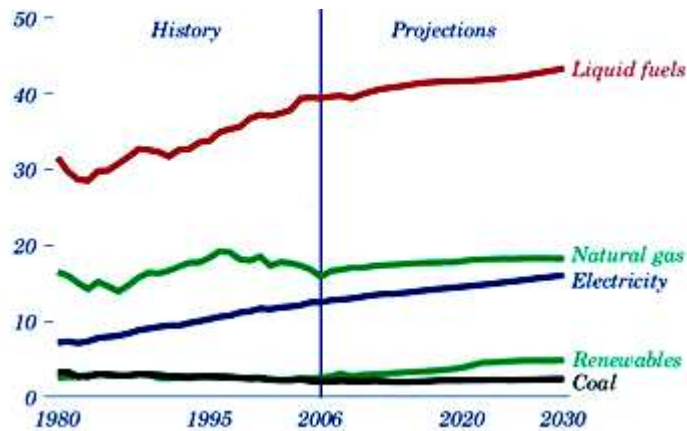


Figure 2.1 Projected Energy Usage (Quadrillion BTU) in the United States from 2006 to 2030 Based on the Consumption from 1980 to 2006

(Source: <http://www.eia.doe.gov/oiaf/aeo/demand.html>)

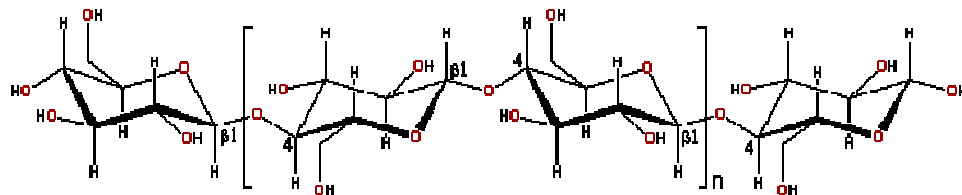


Figure 2.2 Chemical Structure of Cellulose

(Source: <http://www.chemistry.oregonstate.edu/courses/ch130/latestnews/ch130ln.htm>)

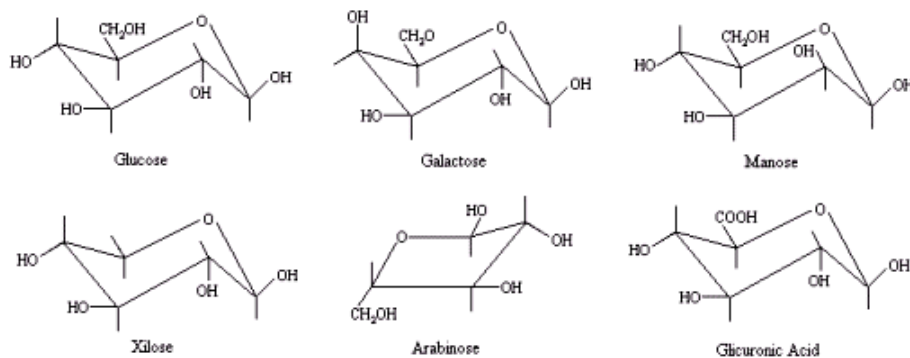


Figure 2.3 Primary Chemical Components of Hemicellulose

(Source: http://www.engin.umich.edu/dept/che/research/savage/Fernando/Fernando_main.htm)

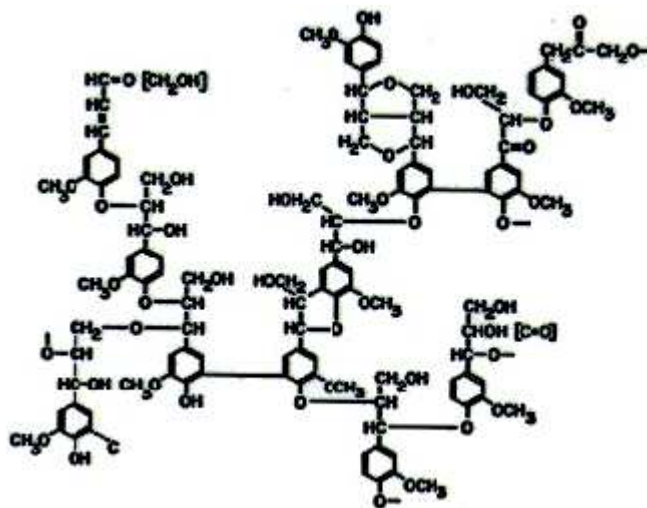


Figure 2.4 Chemical Structure of Softwood Lignin (Brady, 2002)

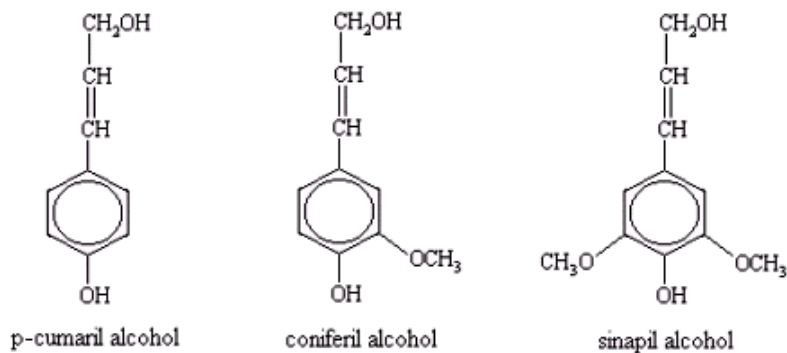


Figure 2.5 Main Chemical Components of Lignin

(Source: http://www.engin.umich.edu/dept/che/research/savage/Fernando/Fernando_main.htm)

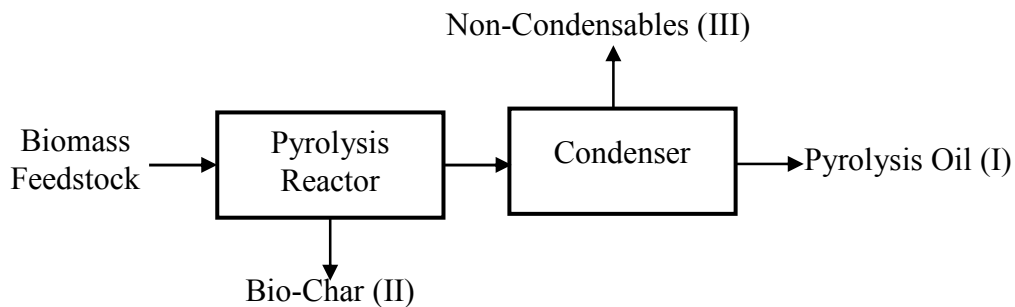


Figure 2.6 A Simplistic Flow Chart of Pyrolysis



Figure 2.7 Lumped 3-Step Kinetic Model of Wood Pyrolysis (Shafizadeh, 1982)

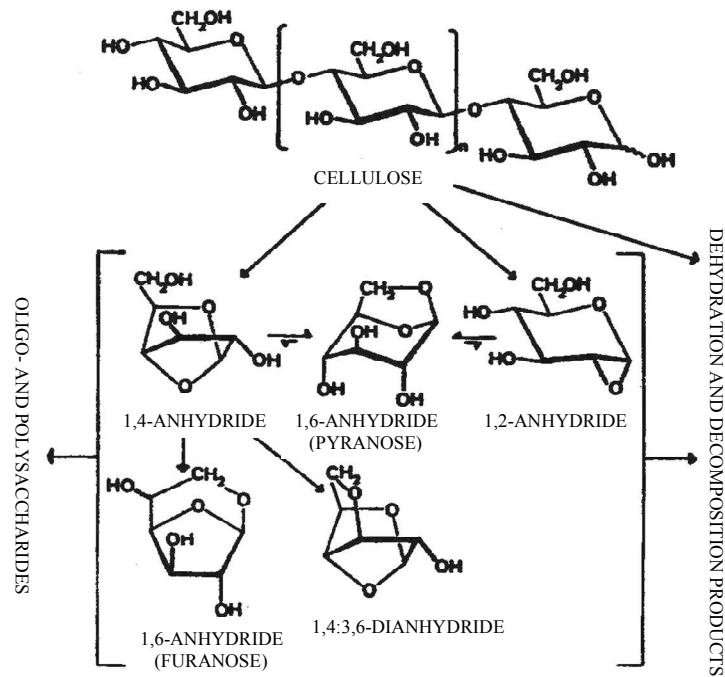


Figure 2.8 Pyrolysis Pathways of Cellulose to Anhydrosugars (Shafizadeh, 1982)

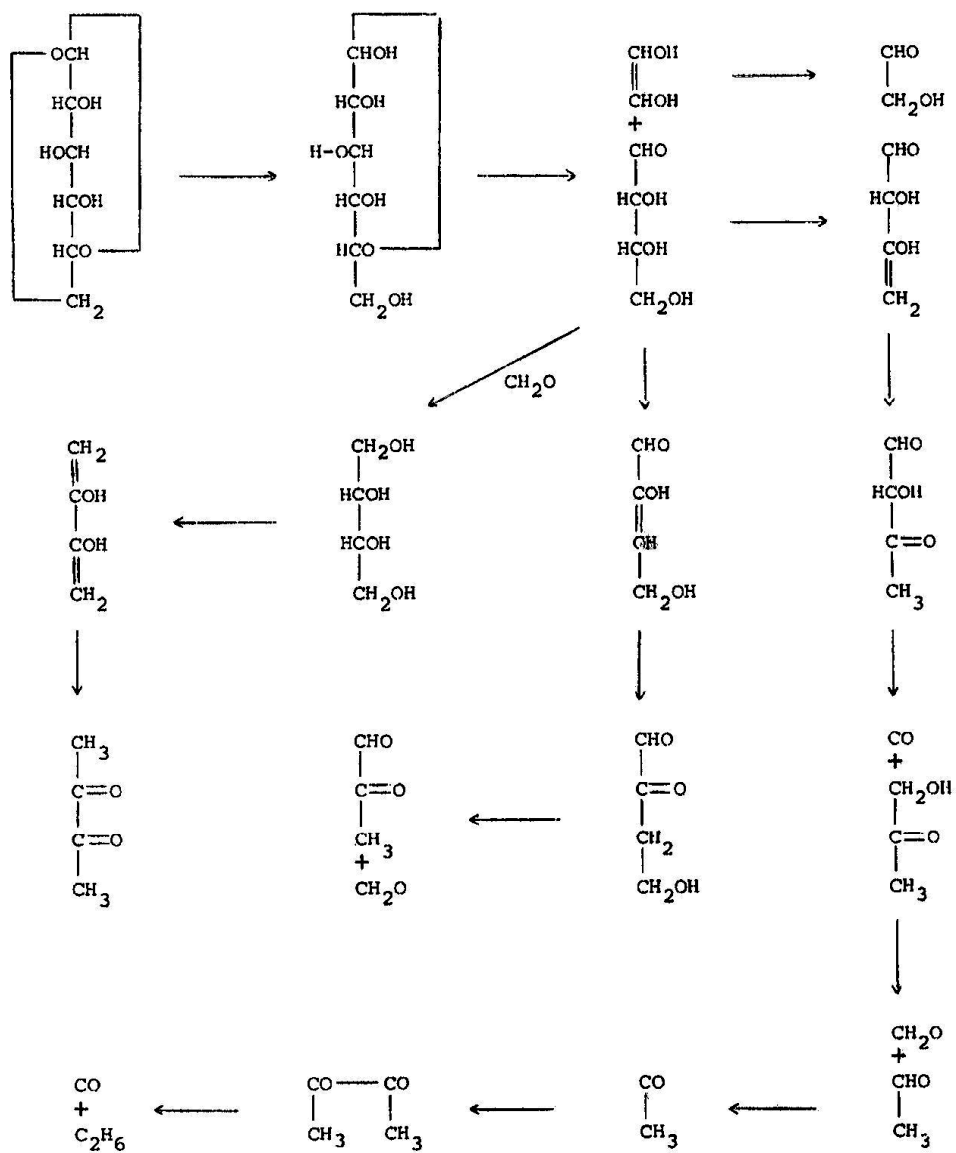


Figure 2.9 Degradation Pathways of Levoglucosan to Volatile Products (Shafizadeh, 1982)

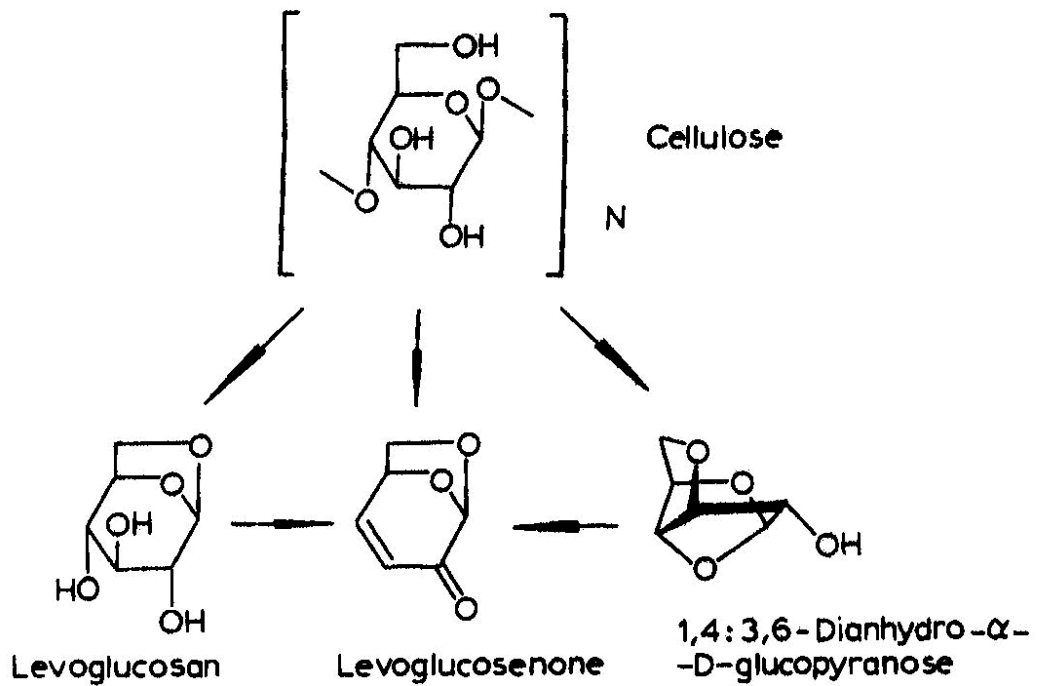


Figure 2.10 Dehydration of Cellulose and Glucose Derivatives to Levoglucosenone (Shafizadeh, 1982)

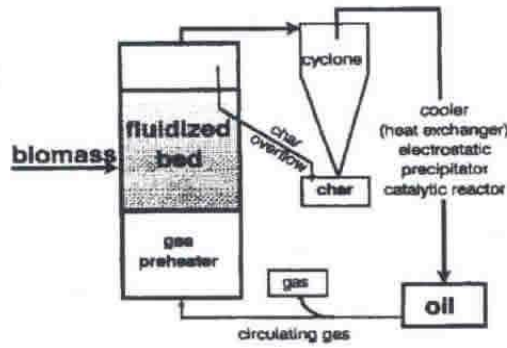


Figure 2.11 A Simplistic Flow Chart of Bubbling Fluidized Bed Pyrolysis (Meier and Faix, 1999)

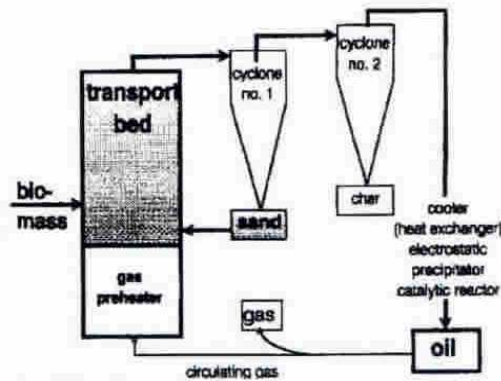


Figure 2.12 A Simplistic Flow Chart of Circulating Fluidized Bed Pyrolysis (Meier and Faix, 1999)

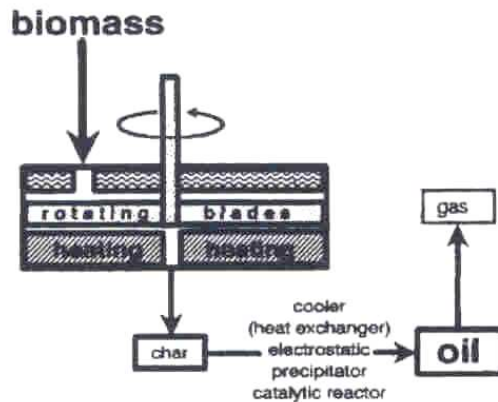


Figure 2.13 A Simplistic Flow Chart of Ablative Reactor Pyrolysis (Meier and Faix, 1999)

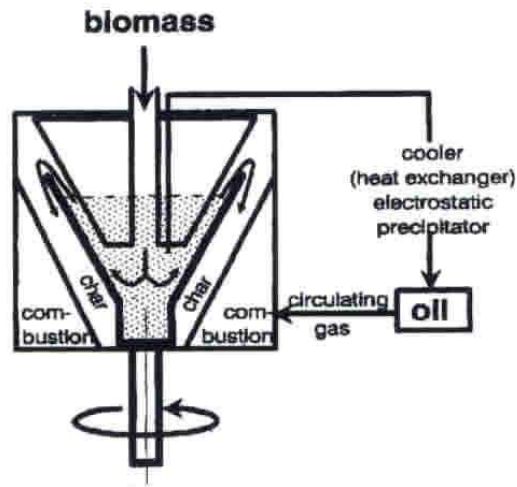


Figure 2.14 A Simplistic Flow Chart of Rotating Cone Reactor Pyrolysis (Meier and Faix, 1999)

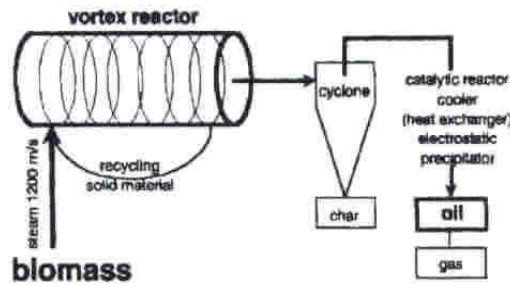


Figure 2.15 A Simplistic Flow Chart of Vortex Reactor Pyrolysis (Meier and Faix, 1999)

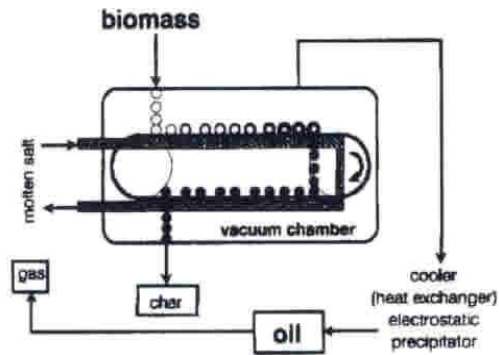


Figure 2.16 A Simplistic Flow Chart of Vacuum Reactor Pyrolysis (Meier and Faix, 1999)

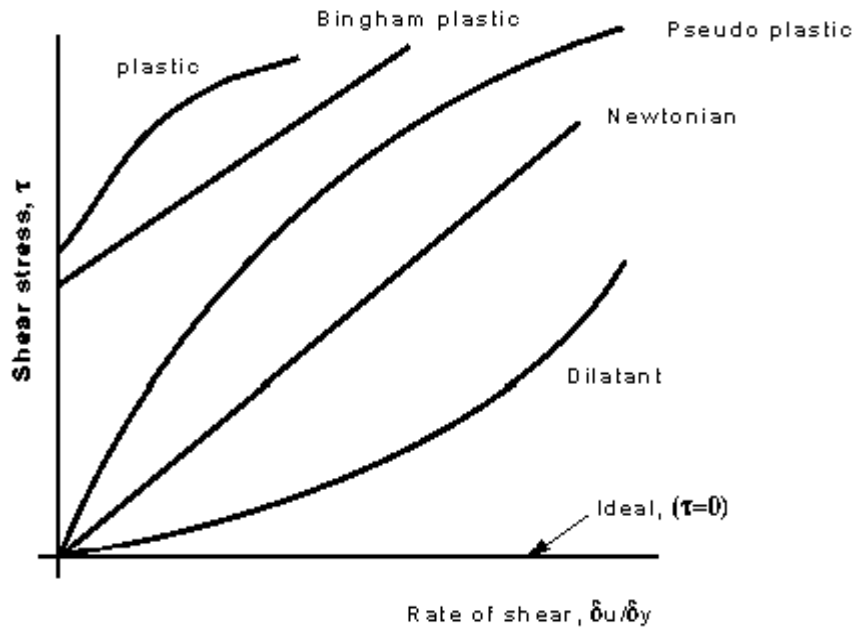


Figure 2.17 Rheological Classification of Liquids

(Source: <http://www.cartage.org.lb/en/themes/sciences/physics/Mechanics/LiquidMechanics/LiquidMechanics/NatureLiquids/NatureLiquids.htm>)

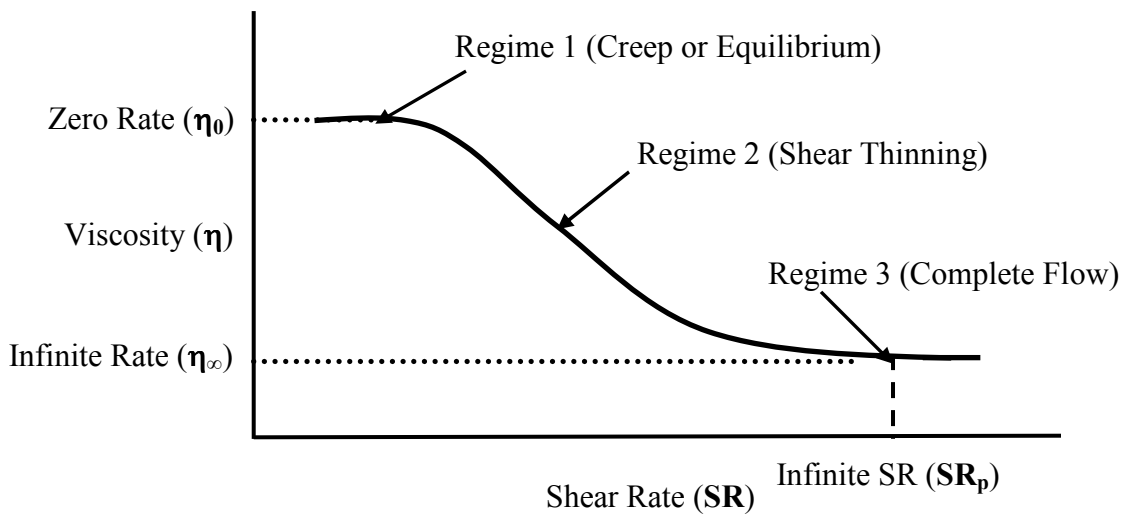


Figure 2.18 Typical Viscosity versus Shear Rate Profile of a Pseudoplastic Fluid (Rosen, 1982)

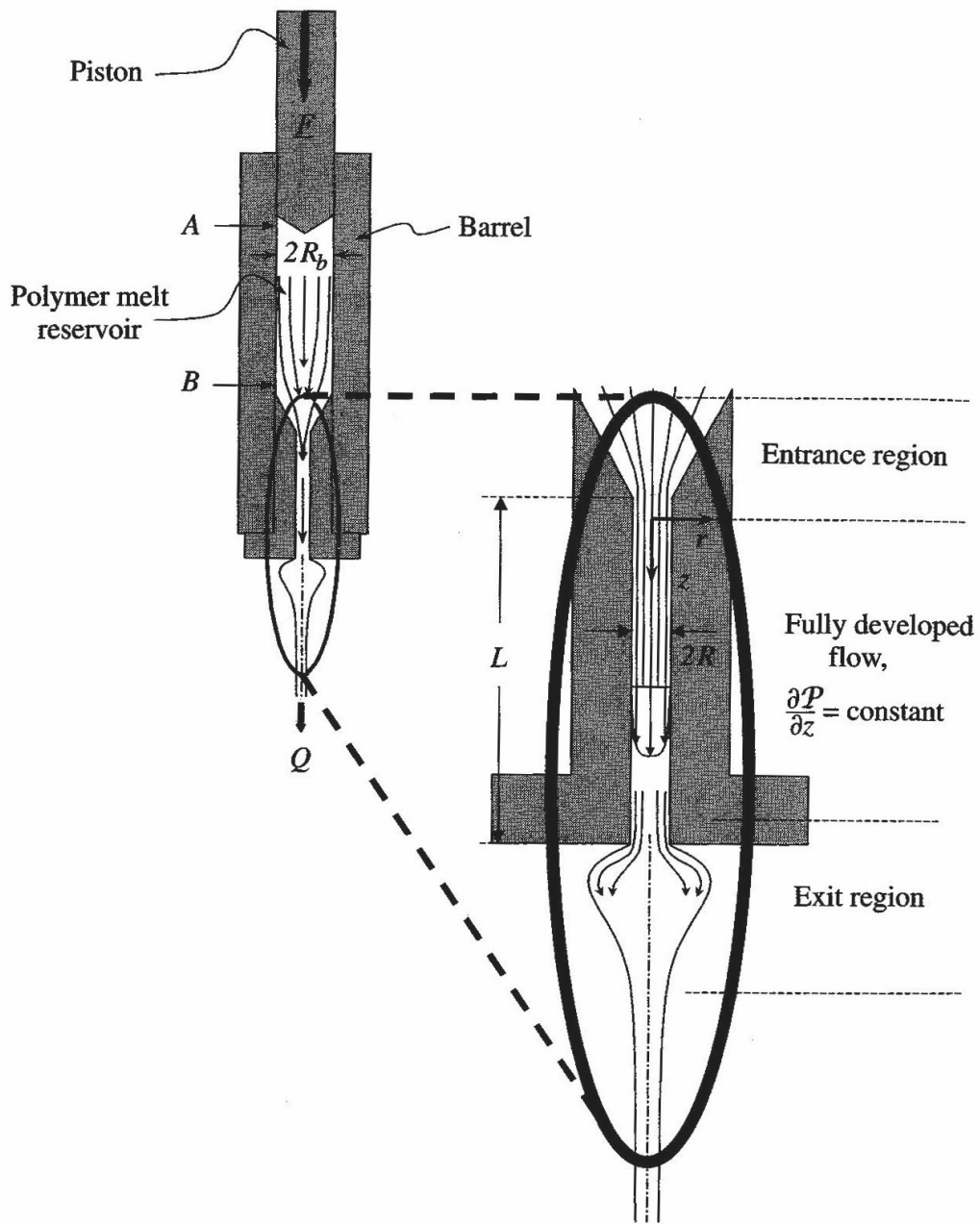


Figure 2.19 A Pictorial View of the Capillary Geometry Used in a Rheometer/Viscometer (Morrison, 2001)

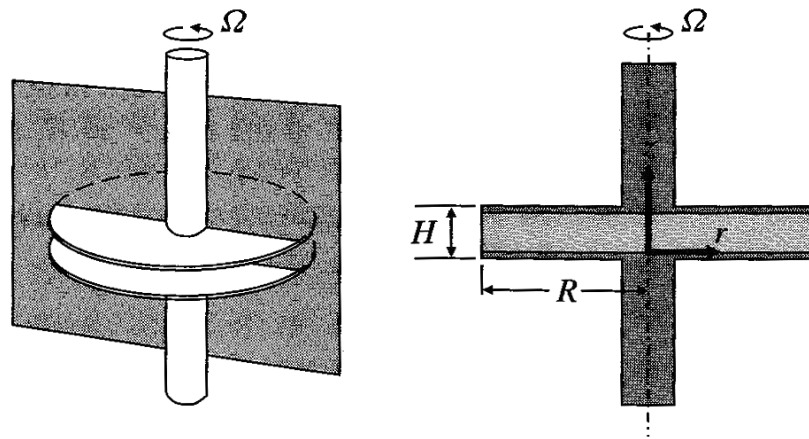


Figure 2.20 A Pictorial View of the Parallel Plate Geometry Used in a Rheometer/Viscometer (Morrison, 2001)

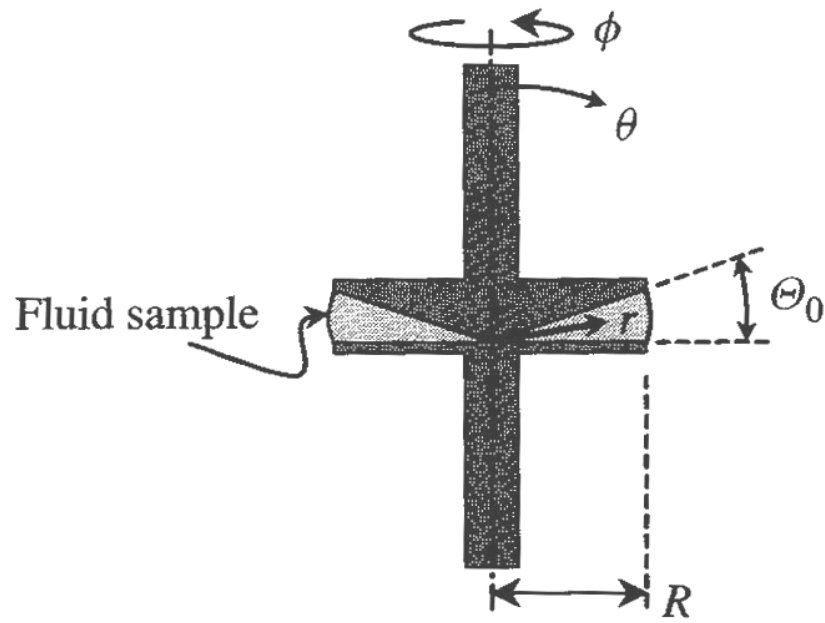


Figure 2.21 A Pictorial View of the Cone-Plate Geometry Used in a Rheometer/Viscometer (Morrison, 2001)

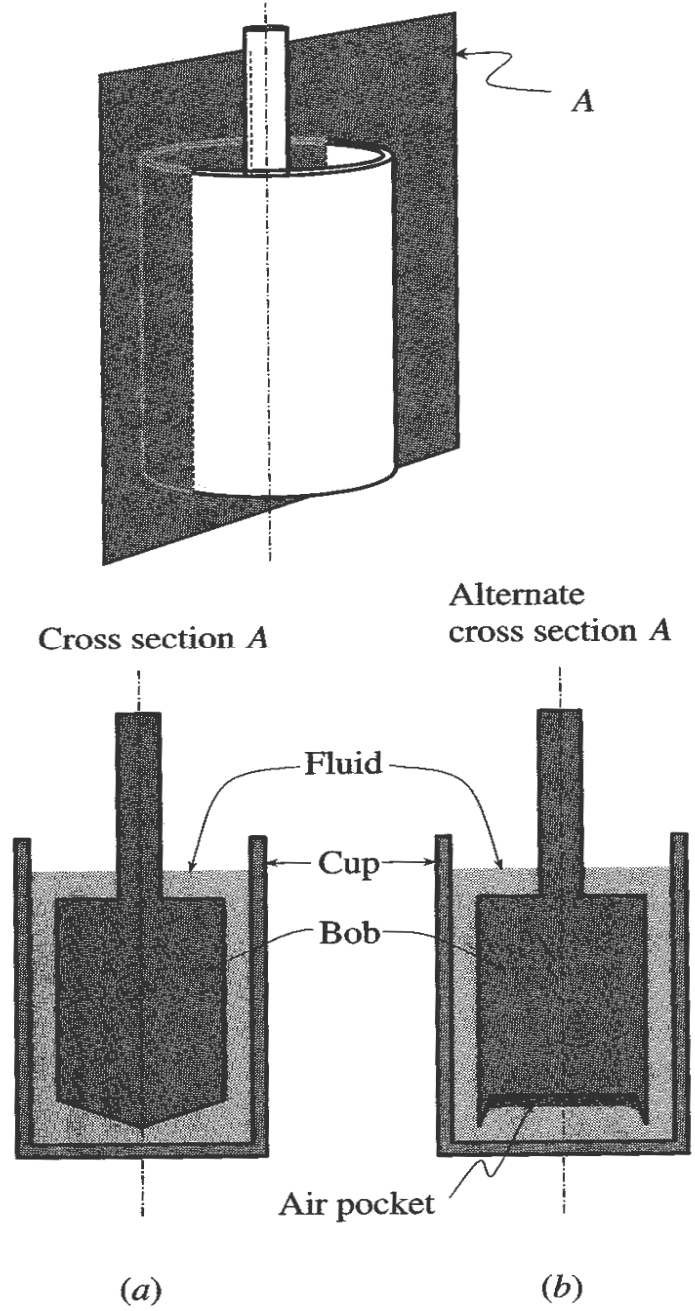


Figure 2.22 A Pictorial View of the Couette Geometry (Cup and Bob) Used in a Rheometer/Viscometer (Morrison, 2001)

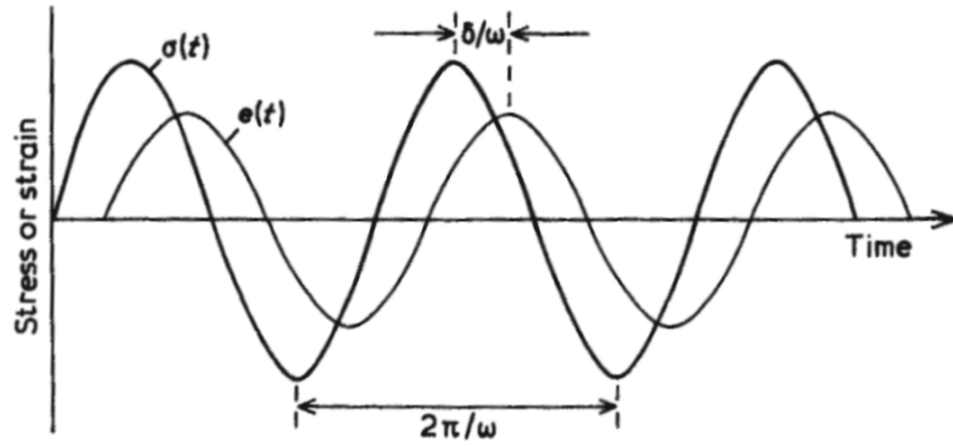


Figure 2.23 Stress or Strain as a Function of Time for a Viscoelastic Material (Young and Lovell, 1991)

CHAPTER III

MATERIALS AND METHODS

Project Overview

This project was conducted using a series of 4 phases to investigate the storage stability of pyrolysis oils. During phase 1, the auger reactor conditions [pyrolysis temperature (PT) and residence time (RT)] and feedstock (oak bark-OB, pine bark-PB, oak wood-OW, and pine wood-PW) were varied to optimize the oil yields. Prior to initiation of phase 2, trial runs were performed to study the impact of PT and RT on the oil stability and mix the oils with similar reactor conditions. During phase 2, a series of additives (26) from different chemical groups were prescreened to isolate three solvents with a highest impact on the oil storage stability. During phase 3, the concentration of three additives identified during phase 2, was optimized so as to achieve the highest oil stability. The three prescreened additives from phase 2 and the three concentrations (low, medium, and high) from phase 3 were utilized to study the oil stability in phase 4. During phase 4, the oil stability was thoroughly evaluated as a function of feedstock, pyrolysis, and storage conditions. Consequently, the pyrolysis oils produced from different reactors (auger small-scale, auger large-scale, and entrained flow) and feed stocks (PW, OW, PB, and OB) were evaluated by performing both short-term (accelerated temperature) and long-term (ambient temperature) storage stability testing.

A total of 25 pyrolysis oils were originally produced during this project using auger reactors at Mississippi State University (MSU), Renewable Oil International (ROI), and an entrained flow reactor at National Renewable Energy Laboratory (NREL). MSU produced 16 pyrolysis oils by utilizing a small-scale auger reactor where as ROI produced one pyrolysis oil by utilizing a large-scale auger reactor. NREL produced 8 pyrolysis oils by utilizing a pilot-scale entrained flow reactor system. Due to the extensive experimental testing involved during this research only 9 pyrolysis oils (4-MSU, 1-ROI, and 4-NREL) were selected to represent all the reactor systems. All the feed stocks (pine wood, pine bark, oak wood, and oak bark) were ultimately included during the selection process of 9 pyrolysis oils as shown later in Table 3.3. The other variables considered in this research were pyrolysis temperature (low and high) and vapor residence time (slow and fast). Thus, a total of 9 pyrolysis oils produced from auger reactors (2) and an entrained flow reactor were investigated for storage stability. The entire investigation was performed in 4 phases and the most stable pyrolysis oils were identified. Statistical analysis of variance (ANOVA) was utilized to judge the additive performance towards increasing pyrolysis oil stability. Specific research of the 4 phases briefly follows and is summarized in Figure 3.1.

Phase I: MSU Pyrolysis Oil Production-the purpose of phase I was to reduce the number of oils to be studied in detail (phase IV) by blending similar pyrolysis oils.

1. Produce a total of 16 pyrolysis oils using factorial treatment design feedstock (4)*pyrolysis temperature (2)*vapor residence time (2)
2. Optimize small-scale auger reactor yields utilizing ‘bark and wood’ derived from ‘red oak and southern yellow pine’
3. Utilize multi-stage condensation to fractionate the oil vapor into aqueous rich (water) and organic rich (pyrolysis oil) streams

4. Study the effects of variables ‘pyrolysis temperature and vapor residence time’ on the storage stability of wood and bark derived pyrolysis oils (16) and eliminate the insignificant variable/variables before blending
5. Blend similar pyrolysis oils by retaining the feed type (bark or wood), down select 4 oils from the 8 blended pyrolysis oils, and utilize them all in the phase IV

Phase II: Additive Prescreening-the purpose of phase II was to down select three additives from a chemical family of additives with multifunctional groups based on their stability performance.

1. Select a wide range of chemical additives with different chemical and physical properties including heat of combustion, pyrolysis oil solubility, bulk chemical costs, improvements of oil stability based on prior findings, and novelty in application
2. Utilize MSU pine wood ‘blended pyrolysis oil’ (high pyrolysis temperature-representing properties of 8 other oils studied during phase IV) from phase I to prescreen 26 additives (10% by wt.)
3. Assess the stability of control and pine wood pyrolysis oils stored at 80 °C by varying storage times (0, 12, 24, 48, 96, and 192 hr). The properties of the oils were evaluated using viscosity, water content, and pH measurements
4. Down select the top three additives (methanol or base additive included) based on their stability performance (ANOVA) during the phase II

Phase III: Additive Concentration Optimization-the purpose of phase III is to test a wide range of additive concentration (0-20% by wt.) and down select three concentrations (low, medium, and high).

1. Select a wide range of concentration for the three additives down selected in phase II and test for stability
2. Utilize MSU pine wood ‘blended pyrolysis oil’ (low pyrolysis temperature-representing properties of 8 other oils studied during phase IV) from phase I to prescreen additive concentrations of 0, 5, 10, 15, and 20%
3. Assess the stability of control and pine wood pyrolysis oils stored at 80 °C by varying storage times (0, 24, 96, and 192 hr). The properties of the oils were evaluated using viscosity, water content, moduli (storage and loss), and pH measurements
4. Down select the top three concentrations (0% or control included) based on their stability performance (ANOVA) during the phase III

Phase IV: Pyrolysis Oil Stability Testing-the purpose of phase IV is to evaluate the long-term storage stability of 9 pyrolysis oils (MSU-4, NREL-4, and ROI-1) as produced from the three reactor systems (small-scale auger reactor, pilot-scale entrained flow reactor, and large-scale auger reactor).

1. Utilize 3 additives down selected from phase II and 3 concentrations down selected from phase III to test the storage stability of 9 pyrolysis oils
2. Perform ambient testing at 25 °C for a maximum of 6 months and accelerated testing at 80 °C for a maximum of 192 hr. The properties of the oils were evaluated using viscosity, water content, pH, acid value, and density measurements
3. Correlate the monthly (0, 1, 2, 4, and 6) and hourly (0, 24, 48, 96, and 192) stability data obtained in phase IV to predict the overall shelf life of pyrolysis oils
4. Evaluate the storage stability of 9 pyrolysis oils based on the following general comparisons
 - a. Reactor Influence (Auger vs. Entrained Flow)
 - b. Pyrolysis Temperature (Low vs. High)
 - c. Residence Time (Slow vs. Fast)
 - d. Feedstock (Wood vs. Bark)
 - e. Storage Temperature (Ambient vs. Accelerated)
 - f. Additive Effect (Control-0% vs. Additive-Medium, High)
 - g. Light [Control Exposed (CTL1) vs. Control Protected (CTL2)]
 - h. Filtration [Control Non-Filtered (CTL2) vs. Control Filtered (CTL3)]

Introduction

As stated previously the main objective of this project is to investigate the stability of wood and bark derived pyrolysis oils. Pyrolysis oils are well known to undergo autocatalyzed polymeric reactions and consequently many physico-chemical, structural, and phase changes can occur during long-term storage (≥ 1 yr, ASTM D 6985). A detailed study was undertaken to utilize chemical additives with different functional groups to minimize or prevent the pyrolysis oil polymerization. During the study the pyrolysis oils were subjected to both ambient and accelerated storage conditions. The experimental work undertaken as part of this study can be divided into 4

main phases as discussed previously and has been summarized in Figure 3.1. Details of each phase are provided in the subsequent sections. Wooden feed stocks for pyrolysis oil production were originally procured in the form of pellets at Mississippi State University (MSU). However, the pellets were crushed before feeding to the small-scale auger reactor at MSU. Details will be explained in the immediate section. Large-scale auger reactor with Renewable Oil International (ROI) also utilized the crushed pellets for making pine wood pyrolysis oil. However, entrained flow reactor at National Renewable Energy Laboratory (NREL) utilized unmodified pellets to make wood pyrolysis oils.

MSU Pyrolysis Oil Production (Phase I)

Feedstock Preparation

Pine and oak wood feed stocks in the form of pellets were obtained from Fiber Resources, Pine Bluff, AK. These materials were utilized by Mississippi State University (MSU) for producing wood pyrolysis oils. However, pine bark and oak bark in the chip form as derived from local trees were utilized for producing bark pyrolysis oils. Bark pyrolysis oils were only produced from MSU auger reactor.

Dry wood pellets were manufactured from the southern yellow pine and red oak wood trees with a moisture content of 10 wt.%. The moisture content of wooden pellets was verified gravimetrically using a digital balance (SL. NO: 006247) manufactured by CSC Scientific Company Incorporated. The average diameter of the pellet before the grinding and sieving operation was 0.25". The pellets were ground using a Model 248 grinder manufactured by Bauer Brothers Corporation. The sieving operation was performed by utilizing vibratory screen (Type S) shaker manufactured from Universal

Vibrating Screen Corporation. Crushed pellet particles passing through a 4 X 4 mm² screen and retained on a 30 mesh (0.68 X 0.68 mm²) were collected. The crushed and sieved pine wood and oak wood pellets are shown in Figure 3.2.

Pine bark and oak bark chips were oven dried to a moisture content of less than 10 wt.%. Grinding and sieving operations for the bark chips were repeated as discussed above. The average size of the bark chips before grinding varied from 0.25” to 0.50” with a less uniform size distribution. The crushed and sieved pine bark and oak bark chips also are shown in Figure 3.2.

MSU Auger Reactor

System Description

The proprietary MSU reactor system is made of stainless steel with a cylindrical geometry. A rough schematic of this system is provided in Figure 3.3. This reactor is operated by a rotating auger with the distance of flight reported as 3”. The inside diameter and the length of the auger reactor have been reported to be 3” and 40” respectively (Mohan et al., 2007).

Reactor Operation

The MSU pyrolysis operation can best be described as a once-through process in a semi-continuous mode. Three fractions namely vapor, gas, and char are produced from this system during the pyrolysis of wood and bark. Here, vapor being the largest fraction, is considered as a mixture of aerosol, mist, steam, and condensable organics. However, gas being the smallest fraction, is considered as a mixture of non-condensable low

molecular weight gases such as C_XH_Y , and CO_X . The char or bio-char exits at the end of the reactor system after the biomass particles are completely pyrolyzed. The pyrolysis was performed using external band heaters through which convection and radiation are the primary heat transfer mechanisms (Ingram et al., 2008). The feed processing rate through the MSU auger reactor was approximately adjusted at 1 kg/h. The rate of feed movement was controlled using the rotating auger the speed of which was set at 12 rpm for most pyrolysis oil runs. The feed traversing time versus the pyrolysis zonal temperature along the horizontal axis of auger reactor is described elsewhere. The feed particles are heated at 110-120 °C prior to their arrival at the pyrolysis zone (8-10") as reported (Ingram et al., 2008; Mohan et al, 2007). Relatively slow pyrolysis is suspected to have occurred due to the long solid residence times (~30-50 s) of biomass particles. However, the vapor residence time is expected to occur in the order of few seconds that is characteristically slower than the fast pyrolysis (<1-2 s) as widely reported in the literature. Further, a time delay in the order of few seconds (5-10 s) is observed from the start of feeder operation to the time of vapor/gas evolution as visualized by a rise in the time-temperature profile. The pyrolysis temperatures utilized in this study are 400 and 450 °C. The vapor/gas residence times are defined qualitatively as slow and fast based upon the distance between feed port and the vapor/gas port utilized. It should be noted that different ports are used during slow and fast pyrolysis. An inert gas purge is used to minimize the oxygen intrusion into the feed lines, valves, and ports. The pyrolysis oil is fractionated using a multi-stage condenser as shown in Figure 3.3. These condensers are operated in a countercurrent flow so as to maximize the log mean temperature difference (LMTD) with water as the coolant on the shell side. The ultimate temperature of the off-

gas from the last condenser is measured to be near ambient conditions (24-25 °C) as reported (Ingram et al, 2008). All condenser cleaning operations are performed using methanol during the reactor shutdown periods. Thus, a total of 16 pyrolysis oils as shown in Table 3.1 (ID's: 1-16), are produced by varying feedstock, reactor temperature, and vapor residence time.

Off-Gas Analysis-MSU Auger Reactor

The off-gas analysis setup was not established as part of the original pyrolysis reactor setup but as an after addition. Significant weight losses were suspected in the form of condensable and non-condensable gases from the auger reactor system. Hence, off-gas analysis was performed to analyze the approximate gas composition and verify the mass losses (non-condensables) that occurred during the pyrolysis oil production. The schematic of the gas analysis setup used for MSU auger reactor has been shown in Figure 3.4. Furthermore details of the gas analysis set-up are represented in Figure 3.5. Gas analysis apparatus utilized rapid spiral tube condenser units 'C1 and C2' to quickly cool the pyrolysis slip stream to an ambient temperature. This step was followed by filtration using a 0.45 µm borosilicate glass filter (GF) for the removal of heavy particulates present in the off-gas stream. The filtered gas then passed through a series of Greensburg impingers (I-1 and I-2) stored in an ice cooled bath (IB). After the gas was cooled to approximately 0 °C it was passed through a CaSO₄ desiccant column (D), prefilter (P), and oil filter (O) before analysis. Gas analysis was performed using a NOVA[®] Model 7900P5 portable multi-gas analyzer (A). The flow rate of the gas sample analyzed was 1 L/min. The non-condensable gases analyzed were CO, CO₂, CH₄, H₂, and O₂ using the

NOVA[®] gas analyzer. Gases CO, CO₂, and CH₄ were analyzed by non-dispersive infrared (NDIR) sensor whereas O₂ was analyzed by an electrochemical sensor. Hydrogen (H₂) was analyzed by a temperature compensated thermal conductivity cell.

ROI[®] Auger Reactor

A photograph of the ROI[®] large-scale auger reactor has been shown in Figure 3.6. This reactor is mounted on an 18-foot trailer located at Florence (AL, USA) with a processing capacity of five dry ton per day of feed stocks. The only oil (ID = 25) utilized for stability testing (phase 4) as produced by the ROI[®] reactor has been shown in Table 3.1. Pyrolysis was conducted at a temperature of 400 °C with a vapor residence time of 1s.

NREL Entrained Flow Reactor/Fluidized Bed

System Description

A photograph of the NREL thermo-chemical pilot development unit (TCPDU) utilized for pelletized wood pyrolysis has been shown in Figure 3.7. The schematic of this TCPDU unit is also shown in Figure 3.8. The external feeding system consisted of a hopper (200 kg capacity), crusher, and a feeder attached with a rotary valve. The overall length of the reactor is 26 m and diameter of the reactor tubes is 3.81 cm. The product temperature can be raised to a maximum of 950 °C by independently controlling 11 electrically heated zones of this reactor. The total volume of thermal cracker is approximately 0.028 m³.

Two cyclonic separators were utilized in series with barrel diameters of 10.2 cm and 7.6 cm. Pots were utilized to collect the char obtained from these cyclones. The diameter of the pipe utilized to connect the cyclones to the scrubber system is 3.81 cm. The total volume of the piping used between cyclones and the condensers is 7.08 L. Sampling ports (heated) were utilized in this section of piping for removing process gas or vapors that can be fed to on-line analytical equipment for compositional analysis.

A conical vessel as a scrubber was utilized for mixing hot gases with dodecane [$\text{CH}_3(\text{CH}_2)_{10}\text{CH}_3$] as a cooling liquid. The diameter of the conical vessel is 25.4 cm. Another conical vessel with the same diameter in series was connected to mix hot gases with the cooling liquid. Both these vessels utilized spray nozzles to feed dodecane. The nominal size of filters utilized for filtering scrubbing liquid is 25 μm .

Product gas stream composition exiting the scrubber system can be measured using three on-line, continuous, and non-dispersive infrared (NDIR) analyzers to monitor CO , CO_2 , and CH_4 . Along with these analyzers the following instrumentation was utilized.

1. Thermal conductivity H_2 analyzer
2. Paramagnetic O_2 analyzer
3. Four channel rapid analysis gas chromatograph
4. Transportable molecular beam mass spectrometer (TMBMS)

Reactor Operation

The 8 oils (Oil ID's 17-24) as produced by the TCPDU unit are shown in Table 3.1. The TCPDU unit can be operated as a fluidized bed or in an entrained flow mode. To

achieve short residence times during wood pyrolysis entrained flow mode was utilized. Hot nitrogen gas (~ 100 °C) after passing through an eductor was utilized to feed the biomass at a rate of 5-25 kg/hr. The average biomass particle size fed to the system was 2.33 mm. During pyrolysis experiments the nominal reactor temperature was varied between 500 and 600 °C.

Char pots were emptied periodically into an intermediate vessel where the char was cooled by nitrogen gas. This vessel was operated as a lock hopper. After the char was cooled it was transferred from the vessel into a bag for further analysis or disposal.

A high flow rate of 113.6 liters/min was utilized to prevent the cooling liquid from becoming significantly hot when it gets in contact with the hot gases and vapors entering the scrubber vessels. The scrubbing liquid after filtration passed through a heat exchanger and a phase-separator. The phase-separator allowed the water soluble materials to drain from the settling tank along with the scrubbing liquid. Dodecane was recirculated as a cooling liquid to the scrubber vessels as shown in the TCPDU process flow diagram. Hydrocarbon compounds such as benzene and naphthalene were observed to accumulate over time.

Condensed steam from the reactor was pumped from the middle phase of the settling tank through a series of filters into a stripping column where light hydrocarbons were removed by nitrogen. The stripped gases and nitrogen were directed to the thermal oxidizer for destruction.

Preliminary Testing (Trial Runs)

The purpose of preliminary testing or trial runs is to reduce the 16 MSU pyrolysis oils (shown in Table 3.1) by mixing similar oils. Hence, the influence of reactor variables (pyrolysis temperature and vapor residence time) on the pyrolysis oil properties (viscosity and water content) was explored. Originally, the 16 pyrolysis oils were produced at MSU by varying feedstock type (pine wood, pine bark, oak wood, and oak bark), residence time (slow and fast), and pyrolysis temperature (low and high). After eliminating the statistically insignificant variable (residence time) the 16 MSU pyrolysis oils were then reduced to 8 by retaining the variables feedstock and pyrolysis temperature.

Statistical ANOVA was conducted to check the significance of the reactor variable/variables on the mean viscosity and the mean water content of 16 pyrolysis oils. The ANOVA models obtained for the mean viscosity and mean water content of pyrolysis oils are shown in Chapter IV (Tables 4.5, 4.12). Evidently from both these tables vapor residence time did not have a significant impact [observed significance level (α) = 0.05] on the mean viscosity and the mean water content of pyrolysis oils. Hence, as stated previously this variable was eliminated before mixing similar pyrolysis oils. Mixing of the oils with same residence time was performed using a 2L Nalgene polyethylene (PE) bottle in an end-over-end tumbler. The tumbler schematic along with bottles and marbles used during the mixing operation has been shown in Figure 3.9. A tumbling speed of 20 rpm was used with time duration of 2 hours. Empty head space in the PE bottle was avoided by using spherical glass marbles (approx. 1/2" dia.) to prevent the oxygen diffusion during the mixing process. The resultant 8 MSU pyrolysis oils obtained after mixing are shown in Table 3.2.

All the pyrolysis oils immediately after production from the MSU auger reactor were stored in a refrigerator at a temperature of 4-5 °C. Pyrolysis oils were stored at this temperature to retard the unstable polymeric reactions. The unstable polymeric reactions as discussed in Chapters I-II are known to occur immediately after their production. However, the rate of these reactions is strongly dependent on the oil storage conditions. Refrigeration of the pyrolysis oils was essential as the production phase of the 16 MSU pyrolysis oils was completed over a prolonged period of 2-3 months. Also, there was a time lag (~4 months) involved between pyrolysis oil production (phase I) and stability testing (phases II-IV). Hence, trial runs provided a preliminary assessment of the pyrolysis oil stability at prolonged-refrigerated storage conditions. Trial runs began immediately after the production of wood-derived pyrolysis oils was completed (8) and prior to the production of bark-derived pyrolysis oils (8).

Trial runs were performed to evaluate specifically the effects of reactor variables (vapor residence time and pyrolysis temperature) on the viscosity and the water content of wooden pyrolysis oils. Another purpose of preliminary testing was to study the stability of 'refrigerated pyrolysis oils' versus 'frequently tested pyrolysis oils'. Refrigerated pyrolysis oil samples were tested only at the beginning and the end of preliminary testing. However, frequently tested pyrolysis oil samples were removed periodically from the refrigerator and the oil temperature slowly raised to room temperature (natural convection) before testing. Furthermore, these pyrolysis oil samples were frequently heated and cooled (4⁰ C to 25⁰ C and back) in this study. The viscosity and the water content of all pyrolysis oil samples were tested at 25 °C during the trial

runs conducted. The trial runs were conducted over a period of 3-4 months overlapping with the bark pyrolysis oil production.

Pyrolysis oil water content measurements were performed using volumetric Karl Fisher apparatus (Mettler Toledo DL31). Pyrolysis oil viscosity measurements were performed using rotational viscometer (Brookfield LV-DV I+) and rotational rheometer (TA Instruments[®] AR 1000 N). With the Brookfield viscometer bark oil viscosity measurements were not possible due to the instrument torque limitations. Hence, in the first half of preliminary testing, viscometer was mainly used for wooden pyrolysis oils. However, in the second half of preliminary testing, TA rheometer was mainly used after its procurement and successful measurements of bark oil viscosity. Furthermore, rheometer was the only method used to determine the viscosity in the later part of pyrolysis oil stability testing (phases II-IV). The rheometer provided a better understanding of the flow behavior of pyrolysis oils over a broad range of shear rates as opposed to a viscometer whose values were dependent upon the spindle geometry and rpm used. Additionally, due to sample limitations the rheometer was conducive to the use of small sized samples (< 1 ml) thus conserving sample.

For frequently tested oils, the Brookfield[®] viscometer used S18 spindle and a small scale adapter (SSR) during the viscosity test. Further a spindle speed of 6 rpm and a sample volume of 7-10 ml were utilized. Apart from viscosity the oil water content (wt.%), pH, and density (g/ml) were also measured as a function of storage time for the frequently tested oils. For both refrigerated and frequently tested oils, the TA Instruments[®] rheometer was used to measure the viscosity as a function of shear rate (0.1 to 300 s⁻¹). A flat stainless steel spindle with 4.0 cm diameter and a sample volume of

~0.7 ml were utilized during the viscosity testing. A parallel plate gap of 2000 μm was also used during the testing to accommodate a maximum particle size of 2000 μm .

Eventually a decision was made to use 9 pyrolysis oils for the stability studies (phase IV) by choosing a) 4 MSU oils [out of 8] obtained after mixing b) 4 NREL oils and c) 1 ROI oil. The 9 oils chosen for the stability studies are shown in Table 3.3. NREL pyrolysis oils (4) with fast residence times only were selected in order to compare their performance with the MSU pyrolysis oils (4) with ‘slow and fast’ residence times combined. There is a high likelihood that the MSU oils were produced from slow to very slow residence times because of the inherent drawbacks of the reactor system. While an accurate estimate of vapor residence time was difficult to achieve the solid residence time of the MSU pyrolysis process was measured to be 30 seconds. ROI pyrolysis oil from pine wood was inevitably included in this study for evaluation because of its properties as it was produced from a large-scale auger reactor and should be comparable to the laboratory reactor.

Pyrolysis Oil Filtration

The pyrolysis oils (9) as shown in Table 3.3 were filtered through a series of nylon screens with mesh sizes of 600, 2000, and 1000 μm . Nylon 6/6 screen filters were supplied by Small Parts Incorporated[®] as shown in Figure 3.10. Gravity assisted filtration was employed to filter the 9 pyrolysis oils. Basically, the pyrolysis oils were filtered using the nylon screen placed over the top of a plastic funnel, while the oil was being collected at the bottom in a 500 ml Fisher brand Pyrex[®] glass beaker. The pyrolysis oils used in the stability studies [1 oil-phase I, 1 oil-phase II, 9 oils-phase IV] were all passed

through the 600 μm filter to ensure particles $>600 \mu\text{m}$ were removed from the oils. This assisted with the rheometer measurements (discussed in experimental testing section of this Chapter) where the gap between the parallel plates was set to 600 μm .

Three pyrolysis oil additive-free controls (ID's: CTL's 1-3) were used during phase IV of this study. While CTL1 and CTL2 pyrolysis oil samples were filtered through a minimum filter size of 600 μm , CTL3 sample was filtered using filter sizes much lower than 600 μm . The filtration test matrix for CTL3 samples has been provided in Table 3.4. The purpose of using the smallest possible filter size for the CTL3 pyrolysis oil samples was to broadly understand the effects of particulate matter removal (a higher percentage) on the pyrolysis oil stability. The smallest possible filter size for the CTL3 pyrolysis oil sample was practically achieved by the use of successive filtration (vacuum assisted) of a large sized pyrolysis oil sample. Here the smallest possible filter size achieved implies that the oil would not pass in a filter lower than this size because of the complete clogging of the pores. The smallest possible filter size for the CTL3 sample from each of the 9 pyrolysis oils has been shown in Table 3.4. Millipore[®] filtration apparatus as shown in Figure 3.11 was used to conduct vacuum filtration of CTL3 samples. Nylon screen filters used during vacuum assisted filtration were completely reusable after back washing with methanol.

Generally, moderate to low filtration efficiencies were achieved for pyrolysis oils with high viscosity accompanied with a weight loss. Removal of all the particulates present in the pyrolysis oil is difficult. However, heavy char particles are expected to be removed (as filter cake) during the filtration (both gravity assisted and vacuum assisted) while leaving the finer particular matter suspended in the filtrate. For bark-derived

pyrolysis oils, the nylon screen filters were observed to collect more particulate matter than the wood-derived pyrolysis oils. Pyrolysis oil filtration prior to additive mixing in subsequent phases (II-IV) was essential for this study as the pyrolysis oils were observed to have gross particulate matter greater than 600 micron (μm) size. Excessive particulate matter can lead to agglomeration and possibly sedimentation during pyrolysis oil storage. Consequently, it becomes difficult to maintain homogeneity and stability of pyrolysis oils if a high percentage of particles are present in them. Some of the light particulate matter is still suspended in the pyrolysis oil after filtration due to their small size. However, most of the dense particulate matter was removed during the filtration process.

Additive Prescreening Studies (Phase II)

Approximately, 30 chemical additives were utilized in the additive prescreening studies. Some of the additives butylated hydroxyanisole (BHA), polyvinyl alcohol (PVA), catechol, polystyrene, and few others did not dissolve completely in pyrolysis oils even after mixing and hence they were excluded early in this study. After preliminary investigations, a total of 26 additives were included in the screening test to evaluate the stability of pine wood pyrolysis oil. Some of the properties considered during the additive selection process are shown in *Table 3.5. The chemical structures of these additives have been provided in *Table 3.6.

 * Data was gathered from the following resources

1. Perry's chemical engineers' handbook (McGraw-Hill, 7th Edition, 1997)
2. Handbook of chemistry and physics (CRC Press, 56th Edition, 1975)
3. NIST database (<http://webbook.nist.gov/chemistry/name-ser.html>)

4. ICIS website (<http://www.icis.com/>)
5. Wikipedia (<http://en.wikipedia.org/>)
6. Sigma-Aldrich (<http://www.sigmaaldrich.com/>)
7. Chemical Vendors and Retailers as Necessary

All the chemical additives utilized were procured from either Fisher Scientific or Sigma Aldrich as indicated. All the chemicals utilized in this research had a minimum of 98% purity. Moisture content of these chemicals was less than 0.5% by weight as measured by Karl Fisher apparatus. Chemical additives were blended with pyrolysis oils using Fisher Scientific vortex mixer (Cat. No. 02-215-365) for a period of 10-15 seconds. The mixer as shown in Figure 3.12 was set at full speed during the additive blending operation. The above procedure was repeated for additive blending operations in the subsequent phases (III-IV) of this study.

The major factors considered during the additive selection process were ‘prior research findings (Diebold and Czernik, 1997; Diebold 2000; Oasmaa et al., 2004; and Doshi et al., 2005), chemical functionality (Ex: alcohol, ether, ester, etc.), molecular weight, viscosity, density, vapor pressure, boiling point, heat of combustion, pyrolysis oil solubility (Hansen parameters-discussed in Chapter II), anti-oxidation, reduction, physical dilution, odor enhancement, and bulk chemical costs’. Majority of the low molecular weight additives were selected based on their ability to prevent the complex ‘oligomerization and polymerization’ reactions by shifting the thermodynamic equilibrium towards simpler ‘monomerization and dimerization’ reactions (Diebold, 2000). Additives with low viscosity and density were selected as they can be beneficial in the physical dilution of high molecular weight compounds present in the pyrolysis oils.

Lowering viscosity and density of the pyrolysis oil would increase its dispersive properties as an engine fuel. Low vapor pressure and high boiling point of the additives is essential as the pyrolysis oils (additive blended) will be stored in large tanks at ambient storage conditions for long time periods. Any pressure build-up in the head space of the storage tanks is undesirable from the equipment and personnel safety perspective. High heat of combustion is desirable to increase the overall heating value (HHV) of the pyrolysis oil as a potential renewable fuel. High solubility or miscibility of the additive in pyrolysis oil is essential to not only ‘homogenize and stabilize’ the pyrolysis oil but also to prevent phase separation that can occur during its long-term storage. Pyrolysis oil has a pungent odor and hence the use of additives with the fruity or perfumic smell (anisole, acetaldehyde, ethyl acetate, etc) can be beneficial for increasing its overall marketability.

Pine wood pyrolysis oil produced at MSU (Oils ‘2 and 4’ combined as shown in Table 3.2) was utilized for prescreening the 26 chemical additives as shown in Table 3.5. Control pyrolysis oil (no additive) and additive blended pyrolysis oils (10% by initial wt.) were stored at an accelerated storage temperature of 80 °C in a gravity convection oven. The maximum aging period of the pyrolysis oil samples was 192 hours. During aging at specific time intervals (0, 12, 24, 48, 96, and 192 hours) the pyrolysis oil samples were tested for their water content, viscosity, and pH. The corresponding sample testing matrix has been provided in Table 3.7. A volumetric Karl Fisher unit from Mettler Toledo (Model: DL31) was utilized to test water content of all the pyrolysis oil samples. A rheometer from TA instruments[©] (Model: AR1000-N) was used to test the viscosity of pyrolysis oils. The operational details of DL31 and AR1000-N are provided in the experimental testing section of this Chapter.

Concentration Optimization Studies (Phase III)

Pine wood pyrolysis oil produced at MSU (Oils '1 and 3' combined as shown in Table 3.2) was utilized for concentration optimization studies. Anisole, glycerol, and methanol blended pyrolysis oils and control pyrolysis oil (no additive) were stored at a temperature of 80 °C in a gravity convection oven for a maximum aging period of 192 hours. During aging at specific time intervals (0, 24, 96, and 192 hours) the pyrolysis oil samples were tested for their water content, viscosity, storage modulus, loss modulus, and pH. The corresponding sample testing matrix has been provided in Table 3.8.

The additive concentrations chosen in phase III of this study were 0, 5, 10, 15, and 20% by initial oil weight. These additive concentrations were chosen similar to what is reported in the literature for pyrolysis oils produced from softwood, bark residue, and sewage sludge (Boucher et al., 2000 II; Doshi et al., 2005). An accelerated storage temperature of 80 °C and storage times of '0, 24, 96, and 192 hours' were utilized to evaluate the stability of pyrolysis oils in phase III.

Stability Testing (Phase IV)

A total of 9 pyrolysis oils produced at Mississippi State University (MSU), National Renewable Energy Laboratory (NREL), and Renewable Oil International (ROI) were utilized to conduct stability testing. The phase IV experimental test matrix has been provided in Table 3.9. The main purpose of this test matrix is to evaluate storage stability of 9 pyrolysis oils (4-MSU, 4-NREL, and 1-ROI) that were produced from 'small-scale auger reactor, large-scale auger reactor, and pilot-scale entrained flow reactor' as discussed previously. Hence, a series of experiments were conducted by varying storage

temperatures (25 °C-ambient and accelerated-80 °C) and storage times (0, 1, 2, 4, 6-monthly and hourly-0, 24, 48, 96, 192). The best additives (anisole-ANS, glycerol-GLY, and methanol-MEH) and the optimal concentrations (0, 5, and 10% by wt.) as selected from phase II and phase III respectively were utilized in the phase IV.

Three control samples (No additive: CTL1, CTL2, and CTL3) were used to evaluate the effects of light and filtration for each pyrolysis oil stored at 25 °C. The light exposed sample (CTL1 only) was used to evaluate the effects of artificial light (fluorescent bulb) on the pyrolysis oil stability. During the long-term storage of pyrolysis oils it is likely that the natural Sun light might take part in the photo-oxidation reactions. Pyrolysis oil control sample (CTL3) was filtered as per the test matrix shown in Table 3.4. Filtration (<600 µm) is expected to positively affect the pyrolysis oil (CTL3) stability. Pyrolysis oil control sample (CTL2) was protected from light during the phase IV ambient testing. Pyrolysis oil controls (CTL1 and CTL2) and all additive blended samples were filtered using a 600 µm filter to assist in the smooth operation of the AR1000-N rheometer. This applies for both ambient (25 °C) and accelerated (80 °C) testing. At a storage temperature of 80 °C and dark condition three control samples (CTL1, CTL2, and CTL3) were used to perform accelerated testing. The control (CTL1 and CTL2) and additive blended samples were subject to similar handling but differed from CTL3. Control sample CTL3 was used to evaluate the effects of filtration (<600 µm) for pyrolysis oils stored at 80 °C. The CTL3 samples were filtered as per the test matrix shown in Table 3.4. Control sample CTL2, was introduced as a backup sample for CTL1 as the control samples are generally prone to measurement error as observed during the previous phases II-III of accelerated testing.

All pyrolysis oil samples (ambient and accelerated) were stored in amber glass vials with Teflon liner caps. These screw thread amber glass vials (part # V2795A-STFE) were procured from Glass Vials Incorporated. The dimensions (O.D X H) of this Glass Packaging Institute (GPI) threaded glass vial were 27 mm X 95 mm. Ambient testing was conducted in a ventilated lab hood as shown in Figure 3.13. The temperature of the hood was measured at 25 ± 2 °C. Accelerated testing was performed in a gravity convection oven as shown in Figure 3.14. The pyrolysis oil samples were placed in a 5 cubic feet Fisher Scientific convection oven (Model: 13-247-625G) at a temperature of 80 ± 2 °C. This oven utilized a PID controller for temperature control of the pyrolysis oil samples.

During ambient testing the glass vials were tightly wrapped with aluminum foils to minimize the light exposure of samples. A Scotch[®] cellophane tape was used to tighten and increase the foil protection as necessary. A Mettler Toledo balance (Model: AL104) with 4th digit accuracy was used to record the pyrolysis oil sample weights. Pyrolysis oil sample vial weight ($W_1 = g$) was recorded before insertion in the hood/oven. Similarly, pyrolysis oil sample vial weight ($W_2 = g$) was recorded after its removal from the hood/oven. If the sample was removed from the oven it was naturally cooled to an ambient temperature before recording W_2 . The difference in weights ($W_2 - W_1 = g$) was also recorded to monitor any volatile losses during the storage of pyrolysis oil samples. The cooling time of the sample vials before recording W_2 varied from 5 to 10 minutes approximately. After this initial cooling period the glass vials were quickly quenched in a water bath to eliminate volatile losses (condensables only). This operation was only necessary for samples stored at 80 °C. The initial weight of the pyrolysis oil sample was 33-35 g. The total number of samples in the phase IV were 162 (oils*storage

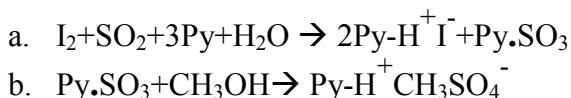
temp*additives*concentration = 9*2*3*3). Sub-sampling operations were performed at storage times as indicated in Table 3.9. The sub-sample drawn from the original sample varied from 4-6 g for all the 162 samples tested. A graduated Fisher Scientific volumetric transfer pipette (Cat. No # 13-711-9AM) with a maximum volume capacity of 5.8 ml was used to maintain consistency during sub-sampling. Significant material losses were not observed during the oil storage, cooling, and transfer operations. The total number of sub-samples in the phase IV were 1620 (oils*storage temp*additives*concentration*storage time = 9*2*3*3*10). Borosilicate glass vials (Cat. No # 03-337-26) with plastic screw caps from Fisher Scientific were used to collect the sub-samples for further testing. The dimensions (O.D X H) of this GPI threaded glass vial were 17 mm x 54 mm. After the lab-tests were performed the remnant portions of the sub-samples were stored in a refrigerator (4-5 °C) as part of the data quality analysis/quality control (QA/QC) measures. The lab tests included in the phase IV were viscosity (μ), pH, density (ρ), water content (%), and acid value (ml KOH consumed/g oil reacted). The test matrix involving the above tests has been shown in Table 3.9. Furthermore, these tests have been discussed in the experimental testing section of this chapter to follow.

Karl Fisher Theory, Instrumentation, and Operation

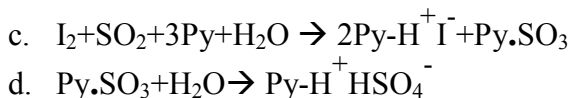
Theory: Karl Fisher Reaction (Mettler Toledo, 1999)

Karl Fisher originally proposed the use of pyridine for the analytical measurement of water content in samples. The scheme of reactions taking place in the presence and absence of alcohol is provided below.

Presence of Alcohol (Base: Pyridine-Py)

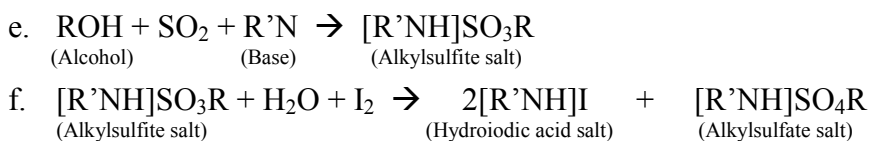


Absence of Alcohol (Base: Pyridine-Py)



After doing further research scientists 'Barenrecht E. and Verhoff J.C.' realized that the use of pyridine was not justified as it only acts as a base (replaceable) and it does not really take part in the Karl Fisher reaction. Besides pyridine is known to be pungent and also possesses toxic effects. Hence, pyridine free reagent imidazole was developed as a base in the year 1984 by researcher Scholz. Imidazole has been reported to facilitate faster and accurate titration. Consequently, the reactions that take place with the use of imidazole as a base are as follows.

Karl Fisher Reaction (Base: Imidazole)



According to the above reactions (e and f) methanol reacts with the base imidazole to form an intermediate alkylsulfite which is then oxidized to alkyl sulfate by Iodine. After all the water from the sample is consumed during the reaction (f) the presence of excess iodine is determined voltametrically by the electrode signaling the endpoint of titration.

Instrumentation: DL31 Karl Fisher Unit

DL31 Mettler-Toledo volumetric Karl Fisher unit uses a dual pin platinum probe (Model: DM143-SC) to measure the water content of pyrolysis oils by performing iodometric titration. The schematic of the Karl Fisher apparatus is shown in Figure 3.15. This unit weighs about 5 kg and consumes a small footprint [240mm (W) X 305 mm (D) X 370 mm (H)]. This Karl Fisher unit utilizes Fuzzy-logic controls to control titrant addition and endpoint detection. Conventionally, the rate of titrant addition was controlled based on the distance from the end point. However, fuzzy logic controls use both the distance from the end point and the potential change after each addition to regulate the addition rate of titrant. Consequently, fuzzy logic controls installed in DL31 provide both faster and accurate determination of end point. The DL31 apparatus has been designed to accurately ($\pm 0.3\%$) measure the moisture content of samples ranging from 1 to 99%. While the DL31 can measure the moisture content as low as 1 ppm the relative standard deviation (RSD) however increases as a function of decreasing concentration as shown in Table 3.10.

The DL31 reaction vessel is made of Pyrex[®] glass with calibration ranging from 25 to 100 ml. An integrated membrane pump was used to either pump in the solvent to the reaction vessel or pump out the reacted mixture to the waste bottle for further disposal. A conical shaped vessel as shown in Figure 3.16 was used for titration along with a small-sized (1/2") magnetic stirrer. A combination of both these factors ensures that there is enough turbulence at the point where titrant is being dispersed into the vessel solution. This turbulence is necessary to ensure fast reaction rate and consequently short titration times. To ensure proper mixing of the sample with solvent methanol the

magnetic stirrer was run at a set speed of 55%. This speed was chosen not to be very low or very high but to optimize a vortex flow at the center of the reaction mixture. The point of addition of titrant to the reaction mixture is sufficiently spaced so as to provide enough time for the iodine (from titrant) to react with water from the sample. This spacing prevents the falsified detection (by the dual pin platinum probe) of excess iodine which triggers the endpoint of titration. Measurement sensitivity of DL31 is very high and hence longer analysis time is needed when samples with high moisture content are tested. Four desiccant columns were utilized to absorb residual moisture from the titrant, solvent, reaction vessel, and waste bottle tubing lines. A mixture (1:1) of molecular sieve (zeolite) and desiccant (anhydrous CaSO_4) separated by a thin layer of glass wool was used in the desiccant columns. The pore diameter of the molecular sieve (Fluka, UOP type 3A) was 3 Å. An online balance from Mettler Toledo (AL104) with 4th digit accuracy was used to measure the weight of sample consumed during Karl Fisher titration.

Operation: DL31 Karl Fisher Unit

The Karl Fisher reagent used was Aquastar[®] one-component combititrant 5 (Prod. No.: 1.88005.2500) and the solvent used was Aquastar[®] anhydrous combimethanol (Prod. No.: 1.88005.1045). The combititrant is composed of a mixture of imidazole (1,3-diazacyclopenta-2,4-diene), iodine, sulfur dioxide, and diethylene glycol monoethyl ether. Aquastar[®] check standard[®] (Prod. No.: 1.88052.0010) of 1% (medium range) was used during DL31 calibration and sample standardization. The other available water standards from Aquastar[®] are 0.1% and 10% for measuring low and high water concentrations respectively. However, these low (0.1%) and high (10%) water standards

do not serve the purpose for measuring the pyrolysis oil water content. Furthermore, the water content of the pyrolysis oil samples is expected to vary from 10-25% as observed from the literature. A highest concentration of 30-35% when phase-separation occurs has been reported. Hence, a check standard of 1% water concentration (medium) was chosen during this study.

The operation of DL31 unit was performed in three steps namely pretitration, calibration, and sample analysis. Pretitration was essential to ensure the residual moisture in the tubing and reaction vessel due to atmospheric leaks was completely consumed. The plugs connected to the reaction vessel were tightly screwed before the pretitration was initiated. During the pretitration process the solvent or anhydrous methanol (30 ml) was allowed to react with the titrant. An initial volume of 30 ml (anhydrous methanol) in the reaction vessel ensured that the probe was properly immersed in the solvent for potential measurements. The Karl Fisher reagent was then added automatically from an inbuilt burette (piston operated; capacity=5 ml) to the solvent at a slow rate. Pretitration was continued until the residual moisture in the reaction vessel and the solvent was exhausted. After the pretitration step was completed check standard (1%) was utilized to calibrate DL31 by treating it as an unknown sample. After successful calibration DL31 was ready for sample moisture analysis.

After pretitration and calibration steps were successfully performed a known quantity of the sample ($W=mg$) was added to the solvent in the reaction vessel. The weight of the sample was manually entered using a key pad as shown in Figure 3.15. Karl Fisher reaction was completed when all the water present in the sample was consumed with I_2 as shown in reaction 3b. No further increase in the reagent consumption as a

function of time took place signaling the end point of titration. The end result was displayed in the form of percentage water. The reacted contents were emptied as soon as the solvent reached 70% of its reacting capacity. Also the solvent reacting capacity was used to determine the appropriate time for emptying the waste bottle.

Precautionary measures were taken to eliminate the non-homogeneity and multiple phase effects of pyrolysis oils during all the sampling operations. Pretitration was performed in between sample replicates to eliminate residual moisture effects. The pretitration step before sample testing ensured the reaction vessel to be completely free of remnant moisture from the previous runs. Pretitration step was usually complete when the instrument drift ($\mu\text{g}/\text{min}$) reached a single digit.

Rheometer Theory, Instrumentation, and Operation

Theory: Liquid Classification, Viscosity Measurement, and Moduli Testing

The theory of liquid classification, viscosity measurement, and moduli testing has been discussed in Chapter II. Hence, instrumentation and operation pertaining to the use of AR1000-N will only be covered in this section of Chapter III.

Instrumentation: AR1000-N Rheometer

All rheological tests were performed using AR1000-N rheometer from TA instruments[®] as shown in Figure 3.17. Although disk-plate geometry has been used in this research it will be narrated as parallel plate geometry in Chapter III for easier understanding. Parallel plate geometry as shown in Figure 3.18 was utilized with the rheometer system along with a plate gap of 600 μm . The upper plate or the spindle is

made of stainless steel and has a diameter of 4.0 cm. The fixed lower plate or disk is made of anodized aluminum with a diameter of 8.0 cm. The AR1000-N rheometer utilizes peltier plate heating system with a temperature range of -10 to 99 °C. Peltier plate system provides ‘faster and better’ temperature control during the sample ‘heating and cooling’ operations. A water bath was used to cool the Peltier plate system operated by a submersible pump.

The AR1000-N utilizes an air bearing which is fundamental to its frictionless operation. Subsequently, the smooth operation of the air bearing was ensured by maintaining a line pressure of 15 psi. Craftsman® air compressor was utilized to supply oil-free air to the rheometer. A series of water trap, oil filter, and air filter as shown in Figure 3.17 were used in the supply line to ensure moisture, oil, and particulate free air. A 6” ID spiral rubber hose and a fan were utilized to exhaust the fumes and pungent odor generated during the rheological testing (≥ 25 °C) of pyrolysis oils.

Operation: AR1000-N Rheometer

There is a series of four steps involved in the operation of AR1000-N rheometer before running any sample. They are 1) instrument calibration 2) temperature calibration 3) rotational mapping and 4) zero gapping. Instrument calibration is performed to calibrate the total system inertia as well as the geometry inertia. Instrument calibration is only necessary when the geometry is changed or when the rheometer is shut down and restarted. Temperature calibration is necessary to account for the thermal expansion of the geometry type used for a given material and its dimensions. Temperature calibration is usually performed in the same range as that of the sample test conditions. Temperature

calibration is only necessary when the geometry type and sample test conditions are changed. Rotational mapping of the rheometer is performed to eliminate sample loading, preshearing histories, and excessive torsional bearing strain. Finally, zero gapping of the plates is performed by gently lowering the spindle or top plate using the automated controls. Then the plate-gap is brought back to its set point (600 μm). After the above four steps are performed the AR1000-N is ready for sample testing.

A plate gap of 600 μm was used in the AR1000-N operation which corresponds to a sample volume of 0.67 ml (approx.). The sample was filled between the plates in a convex fashion with the liquid protruding slightly outside the perimeter of the spindle. This was necessary as AR1000-N is a stress (normal force/area) controlled rheometer. Subsequently, maximum shear rate for a parallel plate can be measured at the perimeter of the spindle (top plate) as shown in equation of Table 2.5. The range of shear rate (velocity gradient) chosen during the viscosity testing was 0.01 to 300 s^{-1} . The range of angular frequencies selected during the moduli (storage- G' and loss- G'') testing was 0.3 to 30 rad/s. Rotational mapping of the instrument was performed in between sample runs to ensure frictional losses and bearing strains were absent. Bearing friction and system inertia (with and without spindle) were calibrated frequently during the rheological testing of oil samples. Normal force of the rheometer system was constantly monitored to ensure its safe operation along with a reliable and accurate data collection. Temperature calibration in the range of 25 to 80 $^{\circ}\text{C}$ was performed to account for the thermal expansion of the spindle-plate geometry. Brookfield[®] silicone oil standards 1, 500, 5000, and 12500 cP were run frequently to calibrate the rheometer and ensure error free data.

The viscosity testing procedure itself contained 3 steps namely sample conditioning, equilibration, and steady state flow (SSF) in succession. These steps repeat themselves as the viscosities were measured at different temperatures. Whenever frequency or moduli testing was performed, an additional step was added before the steady state flow step. The viscosity of pyrolysis oil samples as a function of shear rate was measured using the SSF step. This SSF step measures the viscosity of the samples at the end of the equilibration step for each shear rate tested as a function of torque-time profile. A total of 10 data points per each order of magnitude were collected using a logarithmic scale. As stated previously, sample conditioning step was utilized at the beginning of the test to eliminate the shearing history of the pyrolysis oil samples. This was essential because of the uncontrollable variation from sampling and cooling operations. Sample equilibration steps were chosen to align the pyrolysis oil molecules in a state of equilibrium before the flow step was initiated.

Experimental Testing (Phases II-IV)

Karl Fisher (%Water)

A sample weight ranging 0.02-0.04g was utilized to measure the water content of oil samples. A mixing time of 30 seconds was employed to completely dissolve the pyrolysis oil sample in anhydrous methanol. Water content of most of the pyrolysis oil samples was measured in duplicate during the phases 2-4. Average values of these replicates are reported in Chapter IV since the variation within the replicates was not statistically significant. Frequent calibration of the volumetric Karl Fisher unit was performed using 1% Aquastar[®] check standard. Calibration was performed every time the

reaction vessel was filled with a new solvent and reacting capacity of the old solvent was exhausted. The combimethanol solvent capacity was exhausted after testing 25 pyrolysis oil samples (approx.).

Bark derived pyrolysis oils from MSU consumed longer titration times during water testing. That is possibly due to the slow release of water along with their high viscosity. Some bark-derived samples at prolonged storage times (>48 hr) needed more than two or three replicates due to the phase-separation. NREL produced pyrolysis oil samples consumed longer titration times because of significantly higher quantities of water (>40%). These samples were derived from 'oak wood and pine wood' produced at high pyrolysis temperature (450 °C). MSU produced pyrolysis oil samples consumed the least amount of time during moisture analysis. These samples were derived from 'oak wood and pine wood' produced at low pyrolysis temperature (400 °C). The consistency of test results for MSU wood pyrolysis oils was excellent because of their homogeneous nature followed by the pine wood derived ROI oil.

Viscosity and Moduli

The dynamic viscosity and moduli properties of all the pyrolysis oils were measured as single replicate using TA instruments[®] AR1000-N parallel plate rheometer. Viscosity of all the oils was measured during the phases 2-4 of this study. However, moduli properties (G' -Storage and Loss- G'') of the pyrolysis oils were studied during the phase 3 only. Moduli properties (storage and loss) of the oils provided a better understanding of the viscoelastic and structural behavior of oils as a function of additive (anisole, glycerol, and methanol) and concentration (0, 5, 10, 15, and 20 wt.%). Further,

the experimental conditions of viscosity and moduli testing are provided below. Rheological data analysis was performed using TA Advantage software supplied by TA Instruments[®]. Typical ‘viscosity vs shear rate’ and ‘moduli vs angular frequency’ profiles of a polymer are provided in Figures 3.19-3.20.

The viscosity of pyrolysis oils was measured at 25, 50, and 80 °C during phases 2-3. Angular frequency (sinusoidal) used for moduli testing during phase 3 ranged from 0.3 to 30 rad/s. Moduli properties of pyrolysis oil samples were measured at a temperature of 25 °C during phase 3. Similarly, the viscosity of pyrolysis oils was measured at 25 °C only during phase 4 or accelerated stability testing (storage temperature = 80 °C) to avoid the time lag between the samples. During phase 4 ambient stability testing (~25 °C) viscosity was measured at both 25 and 50 °C. Viscosity measurement of the least viscous NREL pyrolysis oils at shear rates ($>300 \text{ s}^{-1}$) and plate temperatures ($>50 \text{ °C}$) was difficult as these liquids tend to slip beyond the spindle diameter causing erroneous results. At higher shear rates also large centrifugal force causes the liquid to slip beyond the spindle diameter. For low viscosity liquids such as NREL pyrolysis oils a higher temperature of 80 °C can not be utilized because the surface tension of a liquid is inversely proportional to the temperature. At 80 °C it is likely that the low boiling compounds (acids, aldehydes, ketones, etc) volatilize from the oil sample during testing. NREL oils with a higher aqueous phase concentration were observed to more rapidly volatilize and dehydrate as compared to all the other oils. To avoid these problems a lighter geometry (cone and plate-6 cm diameter) made of anodized aluminum was tested apart from stainless steel spindle (parallel plate-4 cm diameter). A solvent trap was also utilized to minimize evaporation or volatilization of the low boiling compounds but to no

avail. Parallel plate geometry responded slightly better to the testing conditions ($>50\text{ }^{\circ}\text{C}$ temperature and shear rate $>300\text{s}^{-1}$) than the cone plate geometry. But the overall results were not effective (sample deformed) and hence $80\text{ }^{\circ}\text{C}$ was not considered in phase 4 of stability testing.

Density

Density of the pyrolysis oils was measured gravimetrically using 1ml long neck volumetric flask from Kimax[®] (Fisher Scientific: Cat. No. 10212J). A schematic of the volumetric flask has been shown in Figure 3.21. The accuracy of oil density measurements using the Kimax[®] flask was $\pm 0.01\text{ ml}$. During density measurements the balance was first tared (zeroed) using the empty flask with lid. Then the oil was filled up to the calibrated mark (1 ml) before recording the sample weight ($W=g$). The oil density is expressed in g/ml. Frequent cleaning of the flask with methanol was necessary during the density measurements of bark-derived pyrolysis oil samples. After cleaning with methanol ASTM type I water was also used before drying the flasks. Density of the bark derived pyrolysis oils was difficult to measure as compared to the wood derived pyrolysis oils because of higher flow resistance. Contrarily, density of the NREL pyrolysis oils was easier to measure as their water content was significantly higher compared to the ‘bark and wood’ derived oils produced by MSU and wood derived oil produced by ROI.

pH

All pH measurements of the pyrolysis oils were performed using Oakton[®] 310 series meter. Buffer standardizations (pH=4.00 and 7.00) were performed before and after testing oil samples. Generally, it was observed that the response time of the electrode

increased with an increasing viscosity of the pyrolysis oil samples. The particulate matter (carbonaceous) present in the pyrolysis oils was observed to decrease the sensitivity of the pH electrode with the increasing number of samples. Hence, the pH probes were cleaned regularly using methanol. Frequent calibrations were also performed to avoid falsified results. Consistency in the pH readings was difficult to achieve for the more viscous oils as compared to the less viscous oils.

Total Acid Value

Since most pyrolysis oils are viscous in nature the pH value may not truly reflect the total acid concentration present. Hence, acid value testing was performed to assess the total acid content of pyrolysis oils stored at ambient temperature during the phase 4. This test was performed for oil samples stored for time periods of 0, 3, and 6 months as indicated in Table 3.9. Further, acid value testing was performed for control (CTL1-light exposed) and anisole (10%) blended oils only. Anisole blended pyrolysis oil samples were chosen for testing as the water content of these oil samples dropped anomalously (>50%) after anisole addition during the initial months (1-2) of storage.

Acid value is defined as “ml of 0.01 M KOH consumed per gram of pyrolysis oil reacted”. The apparatus utilized during acid value testing has been shown in Figure 3.22. During acid value testing of oil samples, potassium hydrogen phthalate (KHP) was utilized to standardize alcoholic solution. A known quantity of KHP (CAS#877-24-7, Fisher Scientific: Cat. No. S93336) was oven dried at 110 °C for 4 hours. Afterwards, the dried KHP sample was desiccated (CaSO₄) for 2 hours. A 0.1M KHP solution was used to standardize 0.1M potassium hydroxide (KOH) solution. The KOH (CAS# 1310-58-3,

45% w/w) utilized for acid value testing had greater than 98% purity. After standardization the KOH solution (0.1M) was diluted to 0.01M for titration against a known quantity (0.3-0.4 g) of pyrolysis oil. A 50 ml glass burette was filled with 0.01M KOH before the titration was initiated. The oil sample was then slowly mixed with the ASTM type I water (75-80 ml) while titrating against 0.01M KOH. The beaker containing the water-oil mixture was placed over a Corning[®] hot plate stirrer (Model: PC-351). A ½" magnetic stirrer was utilized for mixing the oil sample in water. Titration endpoints were detected potentiometrically by carefully observing a significant increment in the voltage reading. Freshly prepared 0.01 KOH solution (≤ 2 weeks) was used to titrate against pyrolysis oil and water mixture. ASTM type I water only was used for all solution preparations, dilutions, and titrations. Fisher brand buffer solutions (4.00 and 7.00) were utilized to calibrate the pH probe before and after the acid value testing was completed.

Table 3.1

Control Variables Used for Different Reactor Systems during Pyrolysis

No.	Pyrolysis Oil ID (Venue-Feed-Temp.-Time)	Reactor Type (MS/NR/RI)			Feed Type (PW/OW/PB/OB)		Pyrolysis Temperature (LT/HT)	Residence Time (SR/FR)
		MSU Small-Scale Auger	ROI Large-Scale Auger	NREL Pilot-Scale Entrained Flow	Pine/Oak	Wood/Bark		
1	MS-PW-LT-SR	MSU Small-Scale Auger			Pine	Wood	Low	Slow
2	MS-PW-HT-SR	MSU Small-Scale Auger			Pine	Wood	High	Slow
3	MS-PW-LT-FR	MSU Small-Scale Auger			Pine	Wood	Low	Fast
4	MS-PW-HT-FR	MSU Small-Scale Auger			Pine	Wood	High	Fast
5	MS-OW-LT-SR	MSU Small-Scale Auger			Oak	Wood	Low	Slow
6	MS-OW-HT-SR	MSU Small-Scale Auger			Oak	Wood	High	Slow
7	MS-OW-LT-FR	MSU Small-Scale Auger			Oak	Wood	Low	Fast
8	MS-OW-HT-FR	MSU Small-Scale Auger			Oak	Wood	High	Fast
9	MS-PB-LT-SR	MSU Small-Scale Auger			Pine	Bark	Low	Slow
10	MS-PB-HT-SR	MSU Small-Scale Auger			Pine	Bark	High	Slow
11	MS-PB-LT-FR	MSU Small-Scale Auger			Pine	Bark	Low	Fast
12	MS-PB-HT-FR	MSU Small-Scale Auger			Pine	Bark	High	Fast
13	MS-OB-LT-SR	MSU Small-Scale Auger			Oak	Bark	Low	Slow
14	MS-OB-HT-SR	MSU Small-Scale Auger			Oak	Bark	High	Slow
15	MS-OB-LT-FR	MSU Small-Scale Auger			Oak	Bark	Low	Fast
16	MS-OB-HT-FR	MSU Small-Scale Auger			Oak	Bark	High	Fast

Table 3.1 (continued)

No.	Pyrolysis Oil ID (Venue-Feed-Temp.-Time)	Reactor Type (MS/NR/RI)		Feed Type (PW/OW/PB/OB)		Pyrolysis Temperature (LT/HT)	Residence Time (SR/FR)
		MSU Small-Scale Auger	ROI Large-Scale Auger	Pine/Oak	Wood/Bark		
17	NR-PW-LT-SR	NREL Pilot-Scale Entrained Flow		Pine	Wood	Low	Slow
18	NR-PW-HT-SR	NREL Pilot-Scale Entrained Flow		Pine	Wood	High	Slow
19	NR-PW-LT-FR	NREL Pilot-Scale Entrained Flow		Pine	Wood	Low	Fast
20	NR-PW-HT-FR	NREL Pilot-Scale Entrained Flow		Pine	Wood	High	Fast
21	NR-OW-LT-SR	NREL Pilot-Scale Entrained Flow		Oak	Wood	Low	Slow
22	NR-OW-HT-SR	NREL Pilot-Scale Entrained Flow		Oak	Wood	High	Slow
23	NR-OW-LT-FR	NREL Pilot-Scale Entrained Flow		Oak	Wood	Low	Fast
24	NR-OW-HT-FR	NREL Pilot-Scale Entrained Flow		Oak	Wood	High	Fast
25	RI-PW-LT-SR	ROI Large-Scale Auger		Pine	Wood	Low	Fast

Table 3.2

Mississippi State University (MSU) Pyrolysis Oils Obtained (8) After Mixing Similar Oils during Preliminary Testing

Oils Mixed*	Pyrolysis Oil ID (Venue-Feed-Temp-Time)	Feed Type (PW/OW/PB/OB)		Pyrolysis Temperature (LT/HT)
		Pine/Oak	Wood/Bark	Low/high
1 and 3 (1+3) ^S	MS-PW-LT-(SRFR)**	Pine	Wood	Low
2 and 4 (2+4) [#]	MS-PW-HT-(SRFR)**	Pine	Wood	High
5 and 7 (5+7)	MS-OW-LT-(SRFR)**	Oak	Wood	Low
6 and 8	MS-OW-HT-(SRFR)**	Oak	Wood	High
9 and 11 (9+11)	MS-PB-LT-(SRFR)**	Pine	Bark	Low
10 and 12	MS-PB-HT-(SRFR)**	Pine	Bark	High
13 and 15 (13+15)	MS-OB-LT-(SRFR)**	Oak	Bark	Low
14 and 16	MS-OB-HT-(SRFR)**	Oak	Bark	High
* Pyrolysis Oils were mixed as identified in Table 3.1				
** SRFR refers to combining the slow and fast residence times. This term is eliminated in Chapter IV and hence for discussion purposes these combined oils will be identified by their reactor type, feedstock, and temperature only (Ex: MS-PW-LT)				
[#] This combined oil was used for additive prescreening studies (Phase II)				
^S This combined oil was used for concentration optimization studies (Phase III)				

Table 3.3

Pyrolysis Oils (9) Selected for Stability Testing in Phase IV

Oils Selected*	Pyrolysis Oil ID (Venue-Feed-Temp.-Time)	Reactor Type (MS/NR/RI)	Feed Type (PW/OW/PB/OB)		Pyrolysis Temperature (LT/HT)	Residence Time (SRFR/FR)
			Pine/Oak	Wood/Bark		
(1+3)	MS-PW-LT-SRFR	MSU Small-Scale Auger	Pine	Wood	Low	Slow and Fast Combined
(5+7)	MS-OW-LT-SRFR	MSU Small-Scale Auger	Oak	Wood	Low	Slow and Fast Combined
(9+11)	MS-PB-LT-SRSFR	MSU Small-Scale Auger	Pine	Bark	Low	Slow and Fast Combined
(13+15)	MS-OB-LT-SRFR	MSU Small-Scale Auger	Oak	Bark	Low	Slow and Fast Combined
19	NR-PW-LT-FR	NREL Pilot-Scale Entrained Flow	Pine	Wood	Low	Fast
20	NR-PW-HT-FR	NREL Pilot-Scale Entrained Flow	Pine	Wood	High	Fast
23	NR-OW-LT-FR	NREL Pilot-Scale Entrained Flow	Oak	Wood	Low	Fast
24	NR-OW-HT-FR	NREL Pilot-Scale Entrained Flow	Oak	Wood	High	Fast
25	RI-PW-LT-SR	ROI Large-Scale Auger	Pine	Wood	Low	Fast

* Pyrolysis Oils were selected from Tables 3.1 and 3.2

Table 3.4

Smallest Possible Pore Size Achieved during the Control (CTL3) Sample Filtration

Oils Evaluated*	Pyrolysis Oil ID (Venue-Feed-Temp.-Time)	Filter Pore Size (µm)
(1+3)	(MS-PW-LT-SRFR)	53
(5+7)	(MS-OW-LT-SRFR)	20
(9+11)	(MS-PB-LT-SRFR)	210
(13+15)	(MS-OB-LT-SRFR)	210
19	(NR-PW-LT-FR)	1
20	(NR-PW-HT-FR)	1
23	(NR-OW-LT-FR)	20
24	(NR-OW-HT-FR)	20
25	(RI-PW-LT-SR)	53

* Pyrolysis Oils were selected from Tables 3.1 and 3.2

Table 3.5

Additive Selection Criteria Used in Phase II

ID	Chemical Used (IUPAC Name)	Vendor	CAS No.	Cat. No./Prod. No.
ACT	Acetone (2-Propanone)	Fisher Scientific	67-64-1	A18-500
ACH	Ethanal (Acetaldehyde)	Fisher Scientific	75-07-0	AC14951-0100
ANS	Anisole (Methoxybenzene)	<i>Sigma Aldrich</i>	100-66-3	AC15392-0010
CPE	Cyclopentanone	<i>Sigma Aldrich</i>	120-92-3	C112402
CHX	Cyclohexane	Fisher Scientific	110-82-7	C556-500
DHN	Decalin (Decalhydronaphthalene)	Fisher Scientific	91-17-8	O2126-500
ETH	Ethanol	<i>Sigma Aldrich</i>	64-17-5	S739851
EEE	Diethyl Ether (Diethoxy Ethane)	Fisher Scientific	60-29-7	E134-1
ETA	Ethyl Acetate (Ethyl Ethanoate)	<i>Sigma Aldrich</i>	141-78-6	270989
EGD	Ethylene Glycol Dimethyl Ether (1,2-Dimethoxyethane)	<i>Sigma Aldrich</i>	110-71-4	E27408
2FL	Furfural (Furan-2-carbaldehyde)	<i>Sigma Aldrich</i>	98-01-1	319910
FAL	Furfuryl Alcohol (2-furanmethanol)	Fisher Scientific	98-00-0	AC181122-500
GLY	Glycerol (Propane-1,2,3-triol)	Fisher Scientific	56-81-5	S74606
IPE	Isopropyl Ether	<i>Sigma Aldrich</i>	108-20-3	38270
MEH	Methyl Alcohol (Methanol)	Fisher Scientific	67-56-1	S75965
MTB	Methyl Tertiary Butyl Ether (2-Methoxy-2-methylpropane)	<i>Sigma Aldrich</i>	1634-04-4	306975
MEK	Methyl Ethyl Ketone	Fisher Scientific	78-93-3	M209-500
MEF	Methyl Formate	<i>Sigma Aldrich</i>	107-31-3	291056
MEA	Methyl Acetate	Fisher Scientific	79-20-9	AC18138-0010
2PL	Isopropyl Alcohol (2-Propanol)	Fisher Scientific	67-63-0	A415-4
PEG	Polyethylene Glycol [Poly(Oxyethylene)]	Fisher Scientific	25322-68-3	AAA17925-30
RSL	Resorcinol (Benzene-1,3-diol)	Fisher Scientific	108-46-3	AC13229-2500
THN	Tetralin (1,2,3,4-Tetrahydronaphthalene)	Fisher Scientific	119-64-2	AC14673-0010
TBL	Tertiary Butanol (2-Methyl-2-propanol)	Fisher Scientific	75-65-0	AC10771-0010
THF	Tetrahydro Furan (Oxacyclopentane)	Fisher Scientific	109-99-0	AC61045-0010
XYL	Xylenes-mixture of isomers	<i>Sigma Aldrich</i>	1330-20-7	214736

Table 3.5 (continued)

ID	Chemical Used	Molecular Formula	#F.W (g/mol)	##B.P.(°C)	###V.P (mm Hg)
ACT	Acetone	C ₃ H ₆ O	58.08	56.53	184 (20 °C)
ACH	Ethanal	C ₂ H ₄ O	44.05	20.20	757 (20°C)
ANS	Anisole	C ₆ H ₅ OCH ₃	108.13	154.00	10 (42.2 °C)
CPE	Cyclopentanone	C ₅ H ₈ O	84.12	131.00	11.4 (25 °C)
CHX	Cyclohexane	C ₆ H ₁₂	84.16	80.74	168.8 (37.7 °C)
DHN	Decalin	C ₁₀ H ₁₈	138.24	190.00	741 (188 °C)
ETH	Ethanol	C ₂ H ₅ OH	46.07	78.40	44.6 (20 °C)
EEE	Diethyl Ether	C ₄ H ₁₀ O	74.12	34.60	1482 (55 °C)
ETA	Ethyl Acetate	C ₄ H ₈ O ₂	88.11	77.10	73 (20 °C)
EGD	Ethylene Glycol Dimethyl Ether	C ₄ H ₁₀ O ₂	90.14	85.00	48 (20 °C)
2FL	Furfural	C ₅ H ₄ O ₂	96.08	161.70	13.5 (55 °C)
FAL	Furfuryl Alcohol	C ₅ H ₆ O ₂	98.10	170.00	5.5 (55 °C)
GLY	Glycerol	C ₃ H ₈ O ₃	92.10	290.00	<1 (20 °C)
IPE	Isopropyl Ether	(C ₃ H ₇) ₂ O	102.18	69.00	120 (20 °C)
MEH	Methyl Alcohol	CH ₄ O	32.04	64.70	410 (50 °C)
MTB	Methyl Tertiary Butyl Ether	C ₅ H ₁₂ O	88.14	55.20	209 (20 °C)
MEK	Methyl Ethyl Ketone	C ₄ H ₈ O	72.11	79.60	71 (20 °C)
MEF	Methyl Formate	HCOOCH ₃	60.05	32.00	1702 (55 °C)
MEA	Methyl Acetate	C ₃ H ₆ O ₂	74.08	56.90	165 (20 °C)
2PL	Isopropyl Alcohol	C ₃ H ₇ OH	60.10	82.00	44 (25 °C)
PEG	Polyethylene Glycol	H(OCH ₂ CH ₂) _n OH	20000.00	N/A	<0.01 (20 °C)
RSL	Resorcinol	C ₆ H ₆ O ₂	110.11	277.00	1 (21.1 °C)
THN	Tetralin	C ₁₀ H ₁₂	132.20	207.00	0.18 (20 °C)
TBL	Tertiary Butanol	C ₄ H ₁₀ O	74.12	82.40	44 (26 °C)
THF	Tetrahydro Furan	C ₄ H ₈ O	72.11	66.00	143 (20 °C)
XYL	Xylenes-racemic	C ₆ H ₄ (CH ₃) ₂	106.17	138.50	18 (37.7 °C)
# Chemical formula weight in g/mol					
## Boiling point in °C					
### Vapor pressure in mm of Hg					

Table 3.5 (continued)

ID	Chemical Used	#F.P	# ρ	Viscosity (cP)	### ΔH°_{298}	Bulk Cost (USD) [2008]	Lab Cost (USD) [2009]
ACT	Acetone	-17	0.79	0.32 @ 20°C	427.92	(0.63-0.82) \$/lb	
ACH	Ethanal	-39	0.79	0.22 @ 20°C	278.77	0.46 \$/lb	
ANS	Anisole	43	1.00	1.32 @ 20°C	905.10	1.85 \$/kg	
CPE	Cyclopentanone	26	0.95	1.29 @ 20°C	686.78		\$5419.89/200 L
CHX	Cyclohexane	-20	0.78	1.02 @ 17°C	936.87	(2.20-2.25) \$/gal	
DHN	Decalin	57	0.90	3.00 @ 20°C	1501.00		\$800.32/20 L
ETH	Ethanol	13	0.79	1.20 @ 20°C	326.68	(3.30-3.90) \$/gal	
EEE	Diethyl Ether	-45	0.71	0.22 @ 25°C	657.52		\$2335.00/200 L
ETA	Ethyl Acetate	-4	0.90	0.43 @ 25°C	536.90	(0.58-0.67) \$/lb	
EGD	Ethylene Glycol Dimethyl Ether	-2	0.87	N/A	627.06	N/A	N/A
2FL	Furfural	62	1.16	1.49 @ 25°C	559.50		\$449.11/20 L
FAL	Furfuryl Alcohol	65	1.13	4.62 @ 25°C	609.15		\$2060.00/200 L
GLY	Glycerol	160	1.26	1500 @ 25°C	397.00	(0.70-0.80) \$/lb	
IPE	Isopropyl Ether	-28	0.73	N/A	958.51	0.46 \$/lb	
MEH	Methyl Alcohol	11	0.79	0.59 @ 20°C	173.64	(1.51-2.53) \$/gal	
MTB	Methyl Tertiary Butyl Ether	-33	0.74	N/A	805.20	(2.48-3.74) \$/gal	
MEK	Methyl Ethyl Ketone	-9	0.81	0.43 @ 20°C	584.17	(0.70-0.75) \$/lb	
MEF	Methyl Formate	-27	0.98	0.36 @ 20°C	234.10	(0.55-0.65) \$/lb	
MEA	Methyl Acetate	-13	0.93	0.38 @ 20°C	381.20		\$1761.70/200 L
2PL	Isopropyl Alcohol	12	0.79	1.96 @ 25°C	474.80	(0.59-0.68) \$/lb	
PEG	Polyethylene Glycol	182 - 287	N/A	N/A	N/A		\$3080.40/200 L
RSL	Resorcinol	127	1.28	N/A	681.30	(7.50-8.50) \$/kg	
THN	Tetralin	77	0.97	N/A	1352.40		\$2710.40/200 L
TBL	Tertiary Butanol	11	0.78	3.35 @ 30°C	629.30	(0.67-0.70) \$/lb	
THF	Tetrahydro Furan	-17	0.89	0.48 @ 25°C	597.80	1.55 \$/lb	
XYL	Xylenes-racemic	24	0.86	0.69 @ 20°C	1089.73	(2.86-4.06) \$/gal	
# Flash point in °C							
## Density (g/cm ³) measured at 25°C							
### Heat of combustion in kcal/mol at 25°C							

Table 3.6

Chemical Structures of Additives

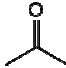

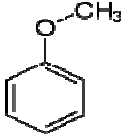
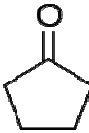
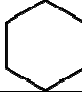
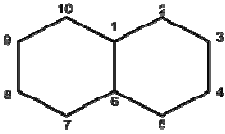

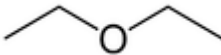
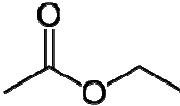

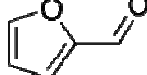
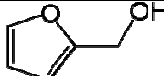
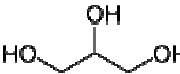
Additive (ID)	Structure
Acetone (ACT)	
Acetaldehyde (ACH)	
Anisole (ANS)	
Cyclopentanone (CPE)	
Cyclohexane (CHX)	
Decahydronaphthalene (DHN)	
Ethanol (ETH)	
Diethyl Ether (EEE)	
Ethyl Acetate (ETA)	
Ethylene Glycol Dimethyl Ether (EGD)	
2-Furaldehyde (2FL)	
Furfuryl Alcohol (FAL)	
Glycerol (GLY)	

Table 3.6 (continued)

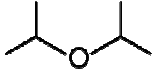
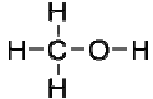
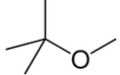
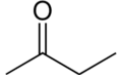
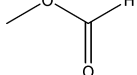
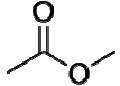
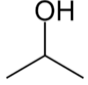
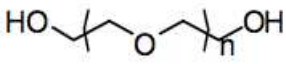
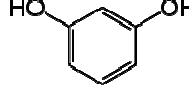
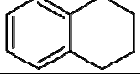
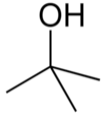
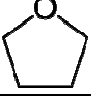
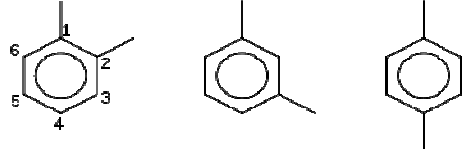
Additive (ID)	Structure
Isopropyl Ether (IPE)	
Methanol (MEH)	
Methyl Tertiary Butyl Ether (MTB)	
Methyl Ethyl Ketone (MEK)	
Methyl Formate (MEF)	
Methyl Acetate (MEA)	
2-Propanol (2PL)	
Polyethylene Glycol (PEG)	
Resorcinol (RSL)	
Tetrahydronaphthalene (THN)	
t-Butanol (TBL)	
Tetrahydrofuran (THF)	
Xylenes (XYL)	 <p data-bbox="803 1711 1339 1753"> 1,2-dimethylbenzene (xylene) <i>ortho</i>- 1,3-dimethylbenzene (xylene) <i>meta</i>- 1,4-dimethylbenzene (xylene) <i>para</i>- </p>

Table 3.7

Experimental Testing Matrix Used in Phase II

Oil Tested **TOW (g) = 33-35	Additive	Additive Conc. (wt.%)	Storage Temp. (°C)	Storage Times (hours)	Tests Conducted (Reps.)				
					pH (1)		Viscosity (1)		%H ₂ O (2)
					^SS (g)	^MT (°C)	^SS (g)	^SR (s ⁻¹)	
(MS-PW-HT-SRFR)*	CTL***	0	80	0, 12, 24, 48, 96, 192	2-3	25, 50, 80	0.03-300	0.02-0.04	
MS-PW-HT-SRFR	ACT	10	80	0, 12, 24, 48, 96, 192	2-3	25, 50, 80	0.03-300	0.02-0.04	
MS-PW-HT-SRFR	ACH	10	80	0, 12, 24, 48, 96, 192	2-3	25, 50, 80	0.03-300	0.02-0.04	
MS-PW-HT-SRFR	ANS	10	80	0, 12, 24, 48, 96, 192	2-3	25, 50, 80	0.03-300	0.02-0.04	
MS-PW-HT-SRFR	CPE	10	80	0, 12, 24, 48, 96, 192	2-3	25, 50, 80	0.03-300	0.02-0.04	
MS-PW-HT-SRFR	CHX	10	80	0, 12, 24, 48, 96, 192	2-3	25, 50, 80	0.03-300	0.02-0.04	
MS-PW-HT-SRFR	DHN	10	80	0, 12, 24, 48, 96, 192	2-3	25, 50, 80	0.03-300	0.02-0.04	
MS-PW-HT-SRFR	ETH	10	80	0, 12, 24, 48, 96, 192	2-3	25, 50, 80	0.03-300	0.02-0.04	
MS-PW-HT-SRFR	EEE	10	80	0, 12, 24, 48, 96, 192	2-3	25, 50, 80	0.03-300	0.02-0.04	
MS-PW-HT-SRFR	ETA	10	80	0, 12, 24, 48, 96, 192	2-3	25, 50, 80	0.03-300	0.02-0.04	
MS-PW-HT-SRFR	EGD	10	80	0, 12, 24, 48, 96, 192	2-3	25, 50, 80	0.03-300	0.02-0.04	
MS-PW-HT-SRFR	2FL	10	80	0, 12, 24, 48, 96, 192	2-3	25, 50, 80	0.03-300	0.02-0.04	
MS-PW-HT-SRFR	FAL	10	80	0, 12, 24, 48, 96, 192	2-3	25, 50, 80	0.03-300	0.02-0.04	
MS-PW-HT-SRFR	GLY	10	80	0, 12, 24, 48, 96, 192	2-3	25, 50, 80	0.03-300	0.02-0.04	
MS-PW-HT-SRFR	IPE	10	80	0, 12, 24, 48, 96, 192	2-3	25, 50, 80	0.03-300	0.02-0.04	
MS-PW-HT-SRFR	MEH	10	80	0, 12, 24, 48, 96, 192	2-3	25, 50, 80	0.03-300	0.02-0.04	
MS-PW-HT-SRFR	MTB	10	80	0, 12, 24, 48, 96, 192	2-3	25, 50, 80	0.03-300	0.02-0.04	
MS-PW-HT-SRFR	MEK	10	80	0, 12, 24, 48, 96, 192	2-3	25, 50, 80	0.03-300	0.02-0.04	
MS-PW-HT-SRFR	MEF	10	80	0, 12, 24, 48, 96, 192	2-3	25, 50, 80	0.03-300	0.02-0.04	
MS-PW-HT-SRFR	MEA	10	80	0, 12, 24, 48, 96, 192	2-3	25, 50, 80	0.03-300	0.02-0.04	
MS-PW-HT-SRFR	2PL	10	80	0, 12, 24, 48, 96, 192	2-3	25, 50, 80	0.03-300	0.02-0.04	
MS-PW-HT-SRFR	PEG	10	80	0, 12, 24, 48, 96, 192	2-3	25, 50, 80	0.03-300	0.02-0.04	
MS-PW-HT-SRFR	RSL	10	80	0, 12, 24, 48, 96, 192	2-3	25, 50, 80	0.03-300	0.02-0.04	
MS-PW-HT-SRFR	THN	10	80	0, 12, 24, 48, 96, 192	2-3	25, 50, 80	0.03-300	0.02-0.04	
MS-PW-HT-SRFR	TBL	10	80	0, 12, 24, 48, 96, 192	2-3	25, 50, 80	0.03-300	0.02-0.04	
MS-PW-HT-SRFR	THF	10	80	0, 12, 24, 48, 96, 192	2-3	25, 50, 80	0.03-300	0.02-0.04	
MS-PW-HT-SRFR	XYL	10	80	0, 12, 24, 48, 96, 192	2-3	25, 50, 80	0.03-300	0.02-0.04	

* Combined pyrolysis oil (2+4) as shown in Table 3.2, ** Total oil sample weight, *** Control oil sample (No additive)

^ Sub-sample size in g; \$ Viscosity measurement temperature in °C; # Spindle shear rate in s⁻¹

Table 3.8
Experimental Testing Matrix Used in Phase III

Oil Tested **TOW (g) = 33-35	Additives	Conc.'s (wt.%)	Storage Temp. (°C)	Storage Times (hours)	Tests Conducted (Reps.)			
					pH (1)	Viscosity (l)		%H ₂ O (2)
						SS (g)	MT (°C)	
(MS-PW-LT-SRFR)*	ANS	0, 5, 10, 15, 20	80	0, 24, 96, 192	2-3	25, 50, 80	0.03-300	0.02-0.04
MS-PW-LT-SRFR	GLY	0, 5, 10, 15, 20	80	0, 24, 96, 192	2-3	25, 50, 80	0.03-300	0.02-0.04
MS-PW-LT-SRFR	MEH	0, 5, 10, 15, 20	80	0, 24, 96, 192	2-3	25, 50, 80	0.03-300	0.02-0.04

* Combined pyrolysis oil (1+3) as shown in Table 3.2; ** Total oil sample weight
^ Sub-sample size in g; \$ Viscosity measurement temperature in °C; # Spindle shear rate in s⁻¹
~ Storage modulus (G' -dyne/cm²) and loss modulus (G'' -dyne/cm²) were measured at 25 °C and angular frequency (ω) of 0.3-30 rad/s
Notes: Moduli test was programmed (using a rheometer) as an additional step during the viscosity testing of the pyrolysis oil sub-samples

Table 3.9

Experimental Testing Matrix Used in Phase IV

Oils Tested* **TOW (g)	Additives	Conc.'s (wt.%)	Storage Temp. (°C)	Storage Times		Tests Conducted (Reps.)					
				25°C-Months (Vent Hood)	80°C-Hours (Dark Oven)	~AV (1)	pH (1)	***P (1)	Viscosity (1)		%H ₂ O (2)
									Months ^SS (g)	0, 3, 6 0.5-1.0	
MS-PW-LT-SRFR (1+3)	ANS, GLY, MEH	0 ¹ , 5, 10	25, 80	0, 1, 2, 4, 6 0, 24, 48, 96, 192	0, 3, 6 0.5-1.0	2-3	1-2	25 ⁺	0.01-300	0.02-0.04	
											(25, 50) ⁺⁺
MS-OW-LT-SRFR (5+7)	ANS, GLY, MEH	0, 5, 10	25, 80	0, 1, 2, 4, 6 0, 24, 48, 96, 192	0, 3, 6 0.5-1.0	2-3	1-2	25	0.01-300	0.02-0.04	
											(25, 50)
MS-PB-LT-SRFR (9+11)	ANS, GLY, MEH	0, 5, 10	25, 80	0, 1, 2, 4, 6 0, 24, 48, 96, 192	0, 3, 6 0.5-1.0	2-3	1-2	25	0.01-300	0.02-0.04	
											(25, 50)
MS-OB-LT-SRFR (13+15)	ANS, GLY, MEH	0, 5, 10	25, 80	0, 1, 2, 4, 6 0, 24, 48, 96, 192	0, 3, 6 0.5-1.0	2-3	1-2	25	0.01-300	0.02-0.04	
											(25, 50)
NR-PW-LT-FR (19)	ANS, GLY, MEH	0, 5, 10	25, 80	0, 1, 2, 4, 6 0, 24, 48, 96, 192	0, 3, 6 0.5-1.0	2-3	1-2	25	0.01-300	0.02-0.04	
											(25, 50)
NR-PW-HT-FR (20)	ANS, GLY, MEH	0, 5, 10	25, 80	0, 1, 2, 4, 6 0, 24, 48, 96, 192	0, 3, 6 0.5-1.0	2-3	1-2	25	0.01-300	0.02-0.04	
											(25, 50)
NR-OW-LT-FR (23)	ANS, GLY, MEH	0, 5, 10	25, 80	0, 1, 2, 4, 6 0, 24, 48, 96, 192	0, 3, 6 0.5-1.0	2-3	1-2	25	0.01-300	0.02-0.04	
											(25, 50)
NR-OW-HT-FR (24)	ANS, GLY, MEH	0, 5, 10	25, 80	0, 1, 2, 4, 6 0, 24, 48, 96, 192	0, 3, 6 0.5-1.0	2-3	1-2	25	0.01-300	0.02-0.04	
											(25, 50)
RI-PW-LT-SR (25)	ANS, GLY, MEH	0, 5, 10	25, 80	0, 1, 2, 4, 6 0, 24, 48, 96, 192	0, 3, 6 0.5-1.0	2-3	1-2	25	0.01-300	0.02-0.04	
											(25, 50)

Table 3.9 (continued)

<p>* Pyrolysis oils (9) as obtained from Tables 3.1 and 3.2; ** Total oil sample weight used= (33-35) g</p> <p>! During the phase 4 monthly testing (0, 1, 2, 4, 6 months), three control samples (No additive: CTL1, CTL2, CTL2) for each oil (Total = 9*3=27) were used. CTL1 samples (9) were exposed to fluorescent light while all other oil samples (72) including 'CTL2 and CTL3' were light protected using an aluminum foil. CTL2 samples (9) were treated the same way as all the additive blended oil samples (Total = 9*3*2*1=54). CTL3 samples (9) were however filtered as shown in Table 3.4 and protected from light as stated previously. During the hourly testing (0, 24, 48, 96, 192 hours) of phase 4, three control samples (No Additive: CTL1, CTL2, CTL3) from each oil (Total = 9*3 =27) were used. CTL1 and CTL2 are alike while CTL3 samples (9) were filtered as shown in Table 3.4. All the hourly oil samples (81) were stored in a dark oven at 80°C</p> <p>~ Acid value (ml KOH consumed/g of oil) tests (18*3=54) were conducted for monthly (0, 3, 6) CTL1 and ANS (10%) oil samples (9*2=18) only. Except for acid value tests all other 'monthly and hourly' tests were conducted at storage times as indicated in the 5th column of Table 3.9</p> <p>^ Sub-sample size in g; *** Density measured at room temperature; \$ Viscosity measurement temperature in °C; # Spindle shear rate in s⁻¹</p> <p>+ Viscosity tests were performed at 25°C for samples stored at 80°C; ++ Viscosity tests were performed at 25 and 50 °C for samples stored at 25°C</p>

Table 3.10

Relative Standard Deviation (RSD) of the Mettler Toledo® DL31 Karl Fisher Unit
(Mettler Toledo, 1999)

Concentration (ppm)	Relative Standard Deviation (%)
10000	< 0.5
1000	0.5-1
100	1-5
10	> 5
1	Unsuitable

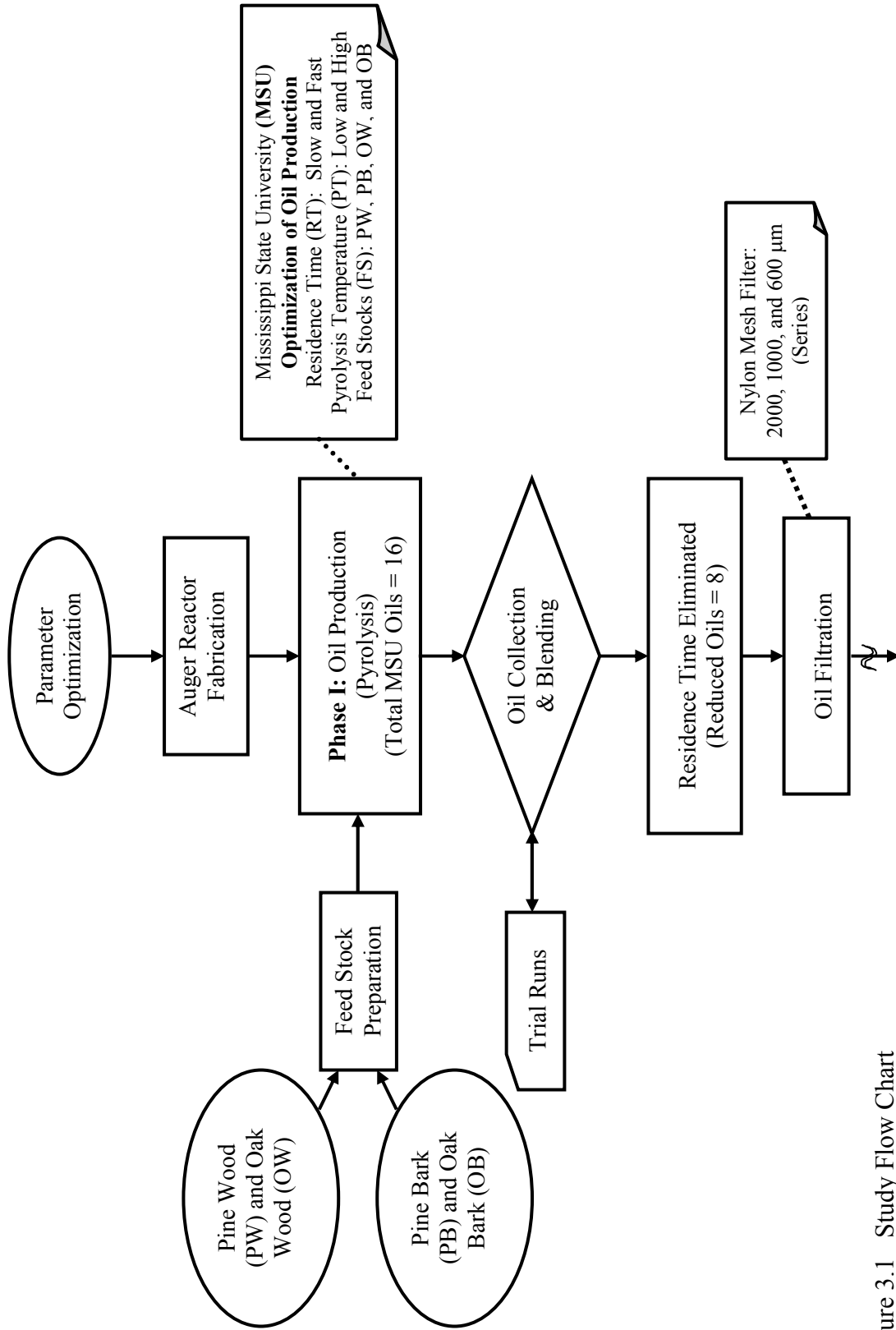


Figure 3.1 Study Flow Chart

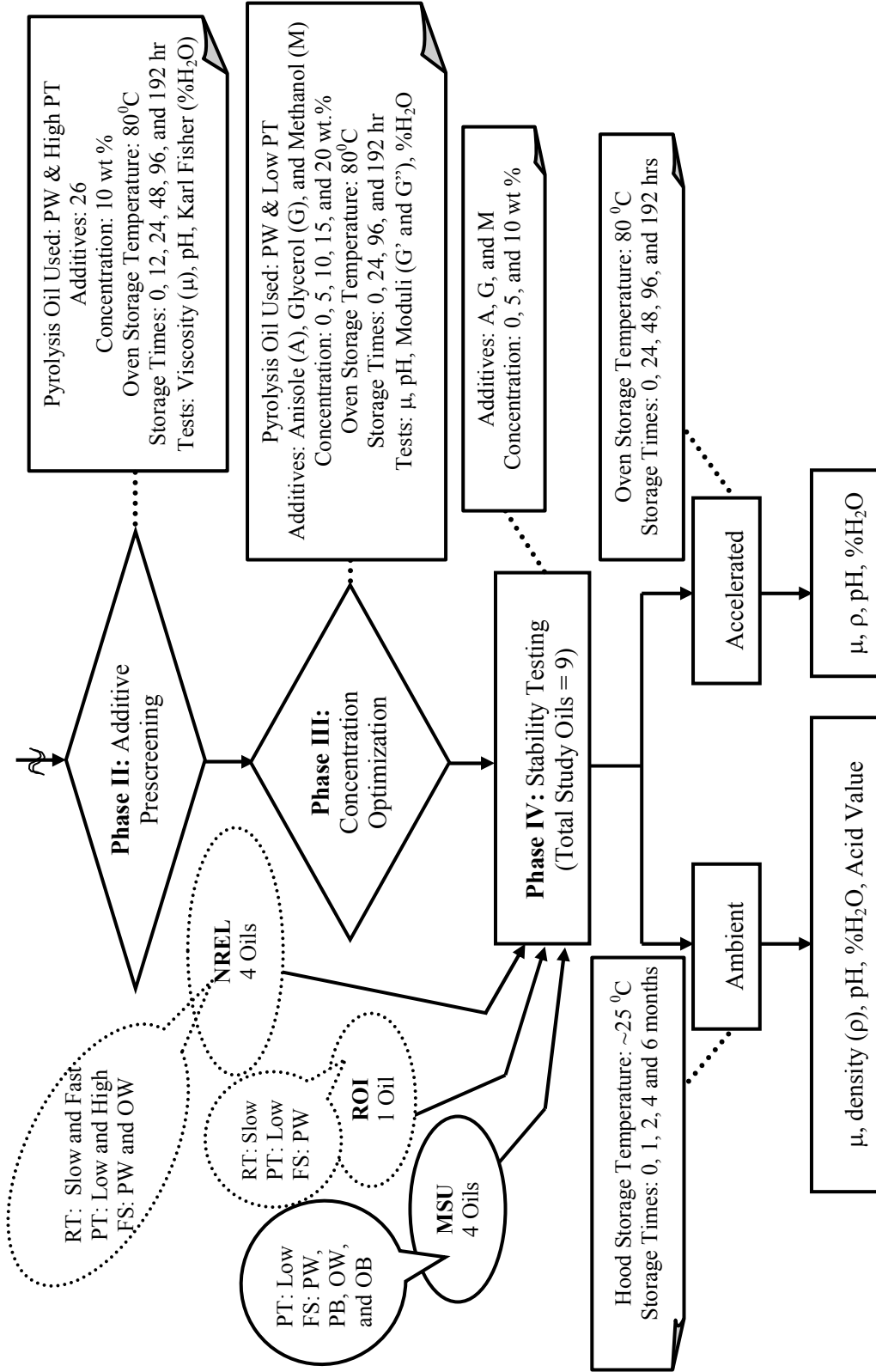


Figure 3.1 (continued)



Figure 3.2 Feed Stocks Utilized for Pyrolysis Oil Production

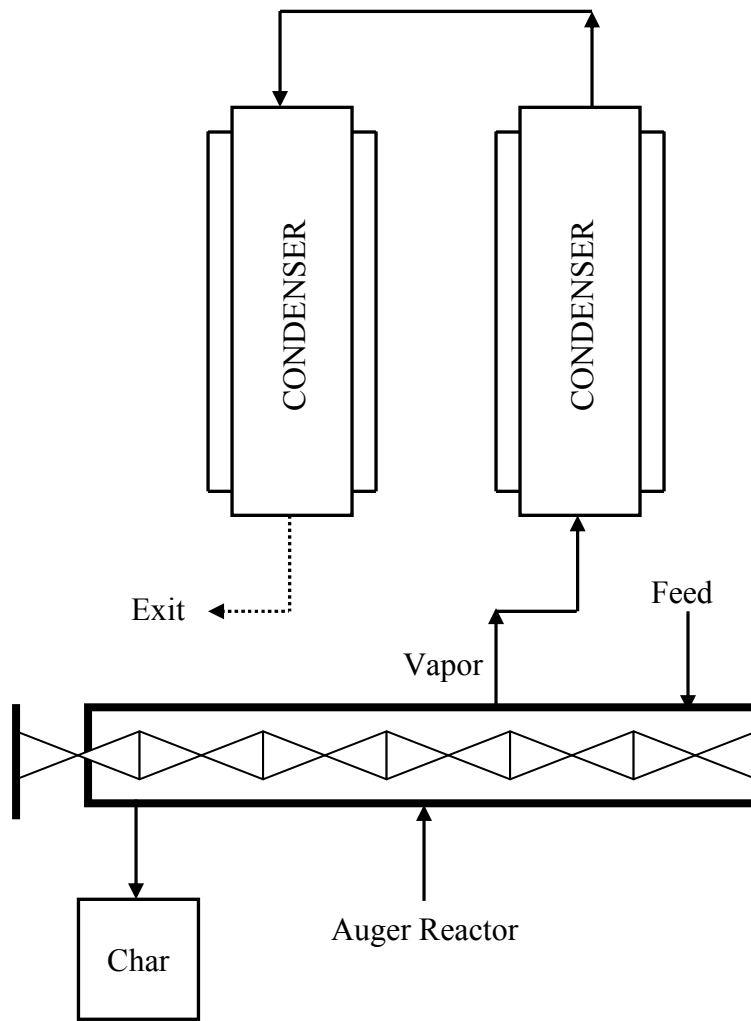


Figure 3.3 A Rough Schematic of the Mississippi State University (MSU) Small-Scale Auger Reactor System



Figure 3.4 Gas Analysis Setup Used with the Mississippi State University (MSU) Small-Scale Auger Reactor System

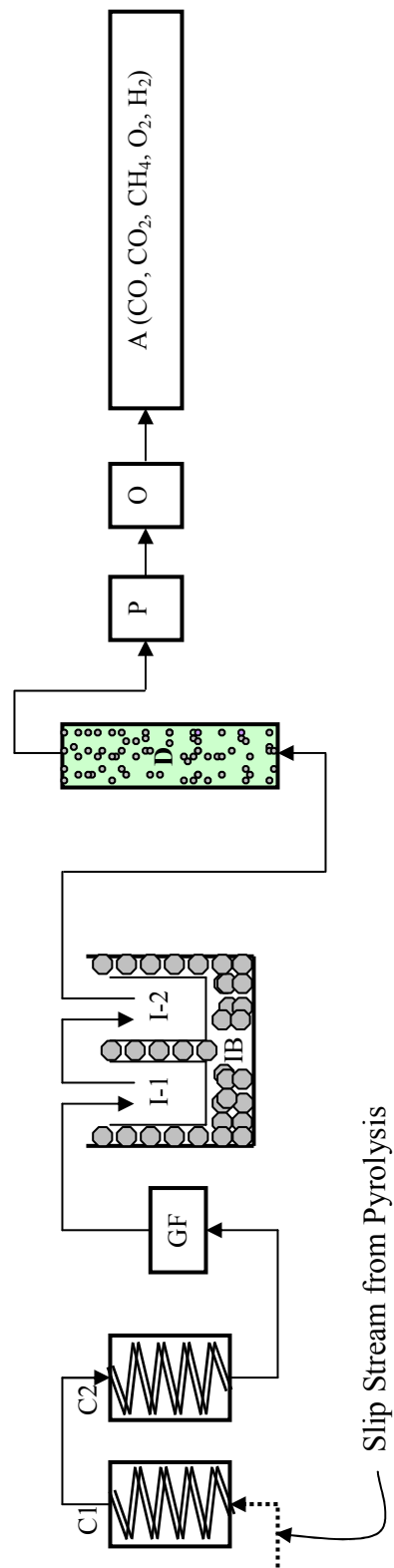


Figure 3.5 Gas Sampling and Analysis Train of Pyrolysis Conducted at Mississippi State University (MSU)

[Notations Used: A-Gas Analyzer, C1&C2-Spiral Tube Condensers, D-Desiccant (Anhydrous CaSO₄), GF-Glass Filter, I-1& I-2-Greensburg Impingers, IB-Ice Bath, O-Oil Filter, and P-PreFilter]



Figure 3.6 A Pictorial View of the Renewable Oil International (ROI[®]) Large-Scale Auger Reactor System (Obtained with Permission)



Figure 3.7 A Pictorial View of the National Renewable Energy Laboratory (NREL) Entrained Flow Reactor (Obtained with Permission)

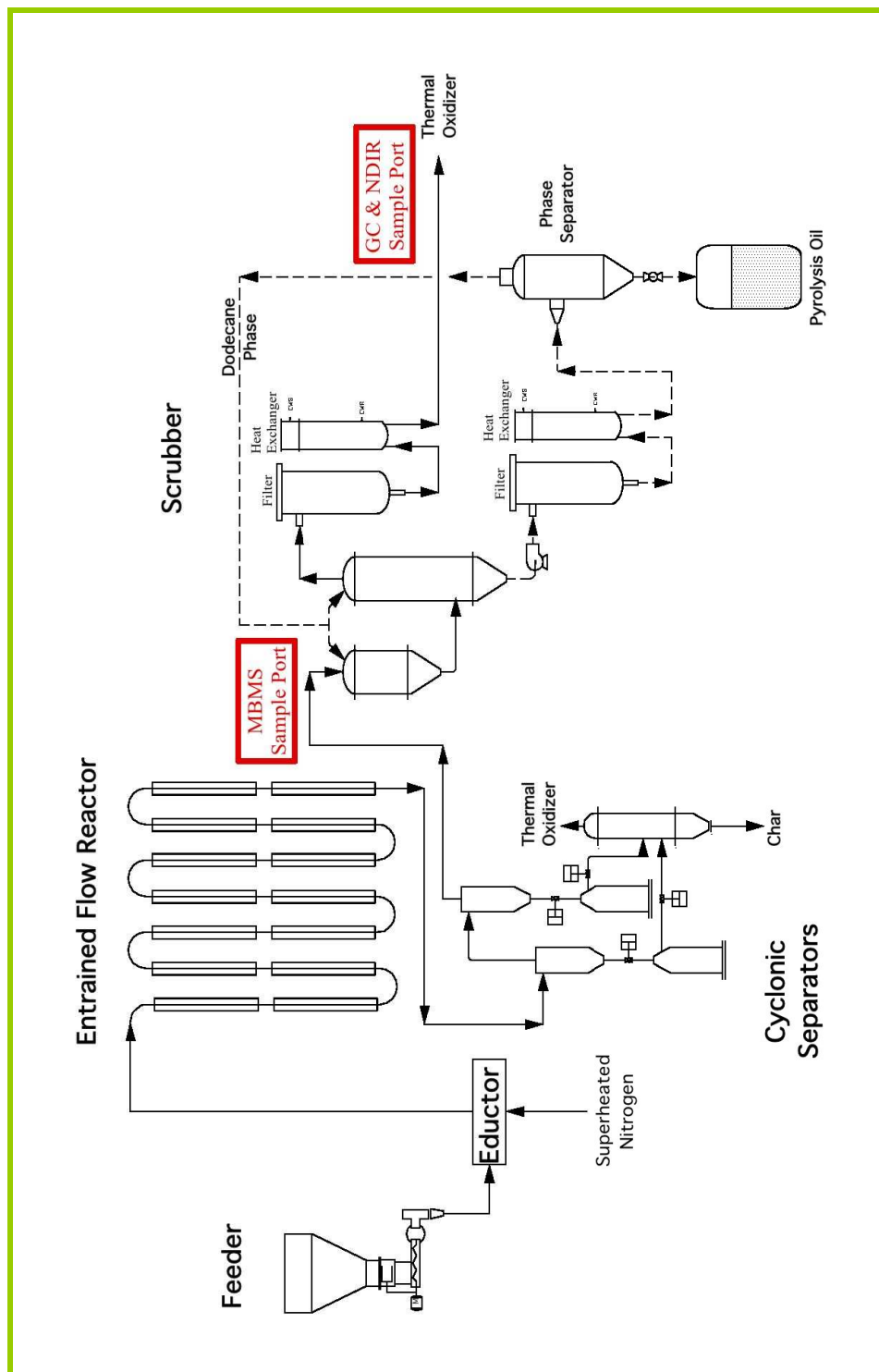


Figure 3.8 Process Flow Diagram (PFD) of the National Renewable Energy Laboratory (NREL) Entrained Flow Reactor (Obtained with Permission)

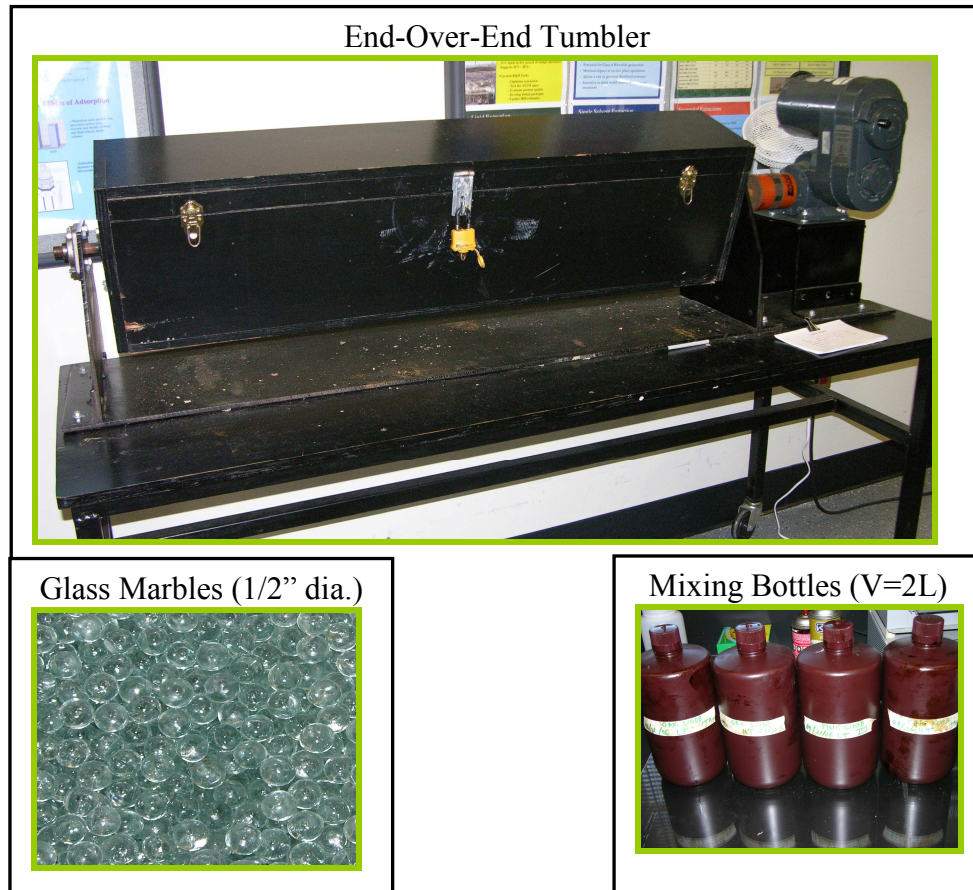


Figure 3.9 Mixing Equipment Used for Mississippi State University (MSU) Pyrolysis Oils



Figure 3.10 Nylon (6/6) Filter Mediums Used for Pyrolysis Oil Filtration

(Source: <http://www.smallparts.com/>)



Figure 3.11 Millipore[®] Vacuum Filtration Apparatus Used for Pyrolysis Oil Filtration



Figure 3.12 Fisher Scientific Vortex Mixer Utilized for Mixing Additives

(Source: <http://www.fishersci.com/>)



Figure 3.13 Ventilated Hood Used for Ambient ($\sim 25^{\circ}\text{C}$) Stability Testing in Phase IV



Figure 3.14 Gravity Convection Oven Used for Accelerated ($80\pm 2^{\circ}\text{C}$) Stability Testing in Phases II-IV

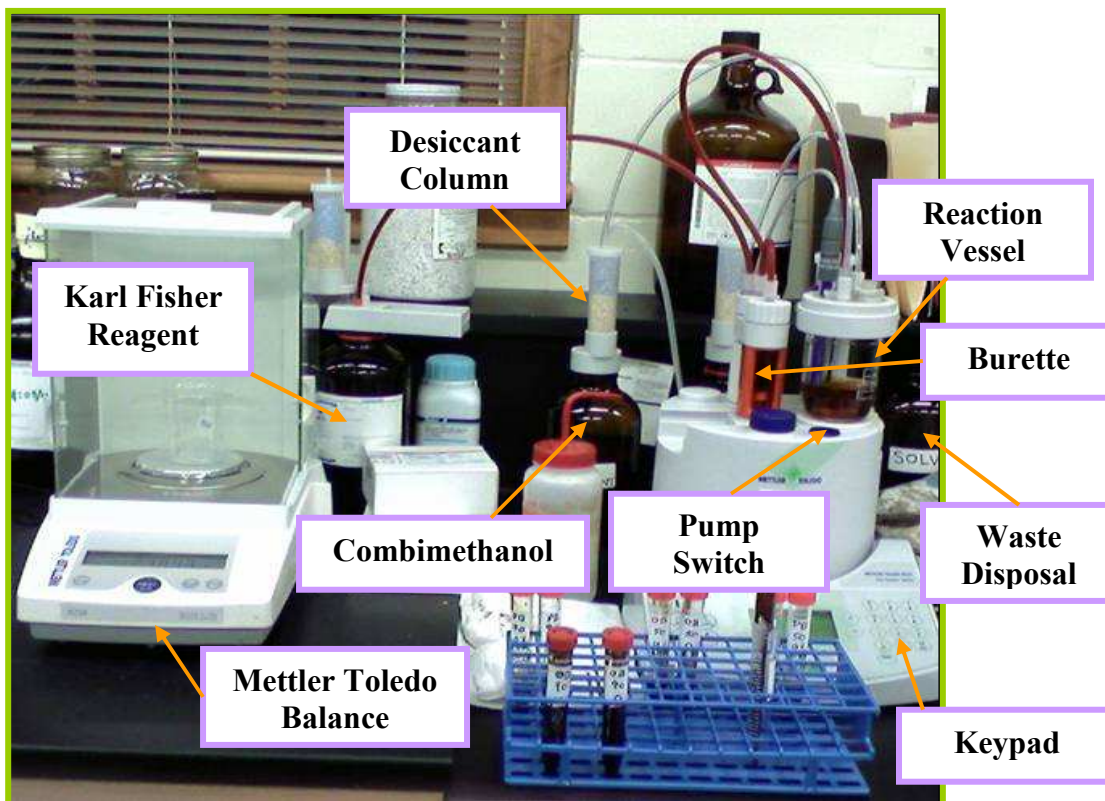


Figure 3.15 A Pictorial View of the Mettler Toledo[®] Volumetric Karl Fisher Apparatus (Model: DL31) Used in this Study

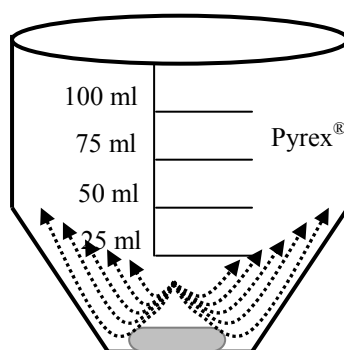


Figure 3.16 Reaction Vessel Used in DL31 Karl Fisher Apparatus

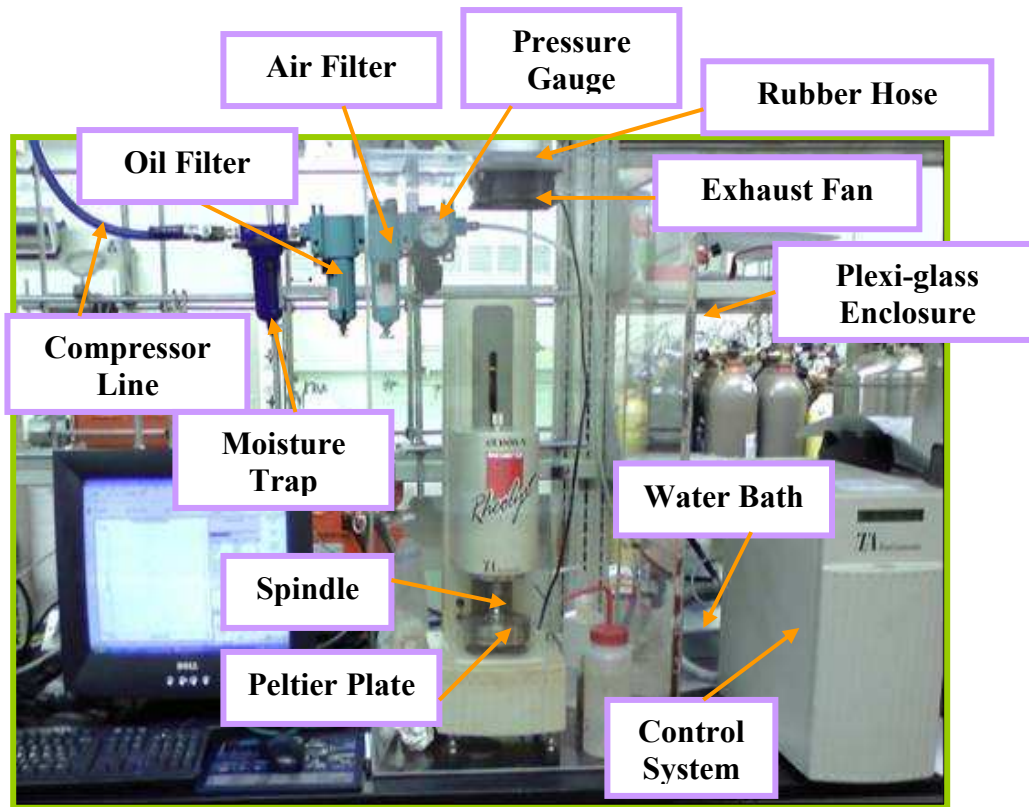


Figure 3.17 A Pictorial View of the TA Instruments[®] Rheometer Apparatus (Model: AR1000-N) Used in this Study

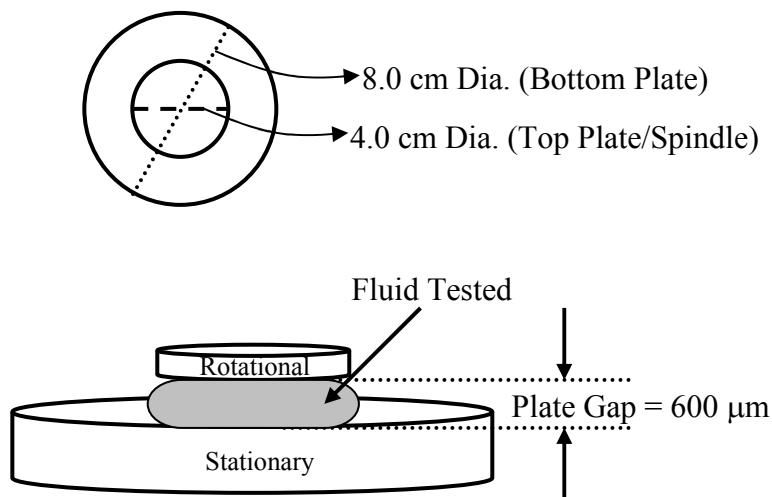


Figure 3.18 Top and Side Views of the Disk-Plate or Parallel Plate Geometry Used in AR1000-N Rheometer

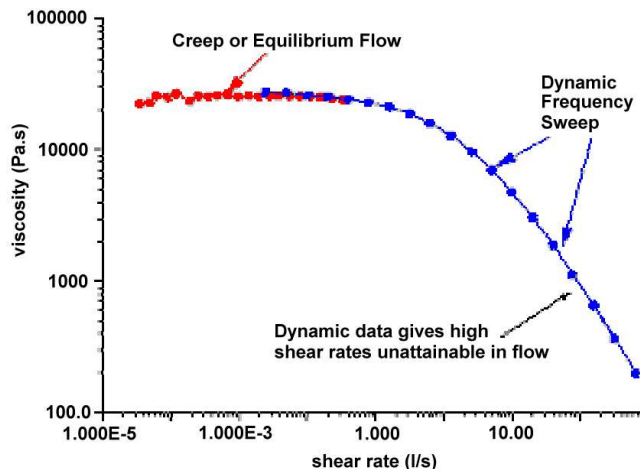


Figure 3.19 A Typical Profile of Viscosity versus Shear Rate (SR) of a Fluid Exhibiting both Newtonian ($SR < 1 \text{ s}^{-1}$) and Pseudoplastic ($SR > 1 \text{ s}^{-1}$) Behavior as Generated by AR1000-N Rheometer

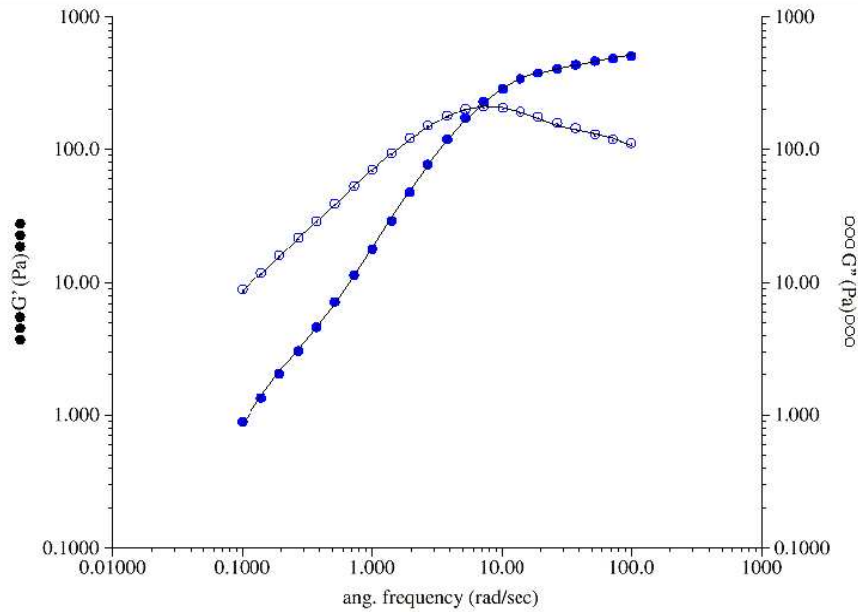


Figure 3.20 A Typical Profile of Modulus (G' -Storage and Loss- G'') versus Angular Frequency of a Polymer as Generated by AR1000-N Rheometer



Figure 3.21 Kimax[®] Volumetric Flask (Capacity=1 ml) Used for Density Measurements

(Source: <http://www.fishersci.com>)

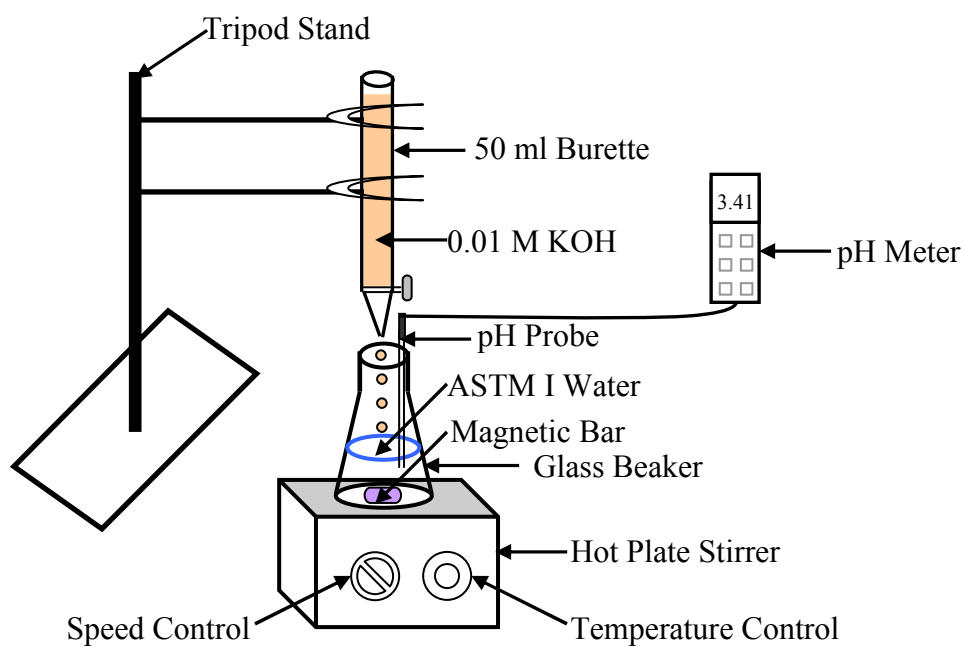


Figure 3.22 A Pictorial View of the Acid Value Testing Apparatus Used in this Study

CHAPTER IV

RESULTS AND DISCUSSION

Pyrolysis Oil Production (Phase I)

Introduction

As discussed previously, Mississippi State University (MS) pyrolysis oils (16) were produced using a small-scale auger reactor by varying feedstock, vapor residence time, and pyrolysis temperature. The four feed stocks utilized were pine wood, pine bark, oak wood, and oak bark. The pyrolysis temperatures utilized were 400 and 450 °C. The residence times were qualitatively described as slow and fast depending on the distance of the gas collection port from the feed port. However, vapor residence time was observed to be an insignificant variable due to the lack of difference in properties of the oils that were collected from different gas ports. More explanation on the insignificance of vapor residence time is provided in this phase. Reactor yields with respect to oil, water, char, and gases are discussed apart from pyrolysis oil fractionation, reactor off-gas analysis, and reactor temperature control.

Fractionation of Pyrolysis Oil

Typically, a pyrolysis reactor produces four fractions as shown in Table 4.1, which include: a) organic rich pyrolysis fraction (oil) b) aqueous rich pyrolysis fraction (water) c) char and d) unaccounted mass (in the form of non-condensables and tars). The

organic rich fraction (ORF) which was collected from condensers 1, 3, 4, and 5 and were combined. This ORF consisted of both organic and aqueous phases with the water content ranging from 15-25% (by mass) as per the Karl Fisher analysis. An aqueous rich fraction (ARF) or water was collected from condenser 2 and it contained mostly water (>50 wt.%), extractives, and acids as reported by the Forest Products Laboratory at Mississippi State University (FP-MSU). This ARF fraction was discarded by FP-MSU and not included in any subsequent analysis. Thus, the pyrolysis oil yields without ARF ranged from 16.5% (oak bark) to 29.8% (oak wood). Likewise, high char yields (41.57-59.26 wt.%) and low oil yields (29.68-33.25 wt.%) from the slow pyrolysis of pine bark are reported in the literature (Sensoz, 2003).

A significant weight loss in the form of non-condensables (discussed later) was observed for each run even though the reactor gas passed through a series of condensers (5). Pyrolysis oil is produced by the rapid condensation of a complex stream of volatile and non-volatile organics, water vapor, mist, particulate matter, and aerosols (Bridgwater, 1999). Consequently, proper condensation is very difficult and generally results in low oil yields. Infact, for the MSU small-scale auger reactor system, pyrolysis oil was observed to condense in the stack beyond the last condenser reflecting incomplete condensation and accounting for the high losses. Pyrolysis oil collected from different condenser ports indicated that both 'organic and aqueous' rich fractions can be separated. Proper cooling of the condensers is essential to regulate the vapor inlet and outlet temperatures. The 'organic and aqueous' rich fractions eventually separated during the condensation process because of the difference in the boiling points (b.p's) of water and oil. Thus, the ARF was collected from condenser 2 whereas the ORF was collected from condensers 1, 3, 4, and

5 which were combined. The ORF or pyrolysis oil is largely composed of levoglucosan, guaiacol, and other lignaceous (lignin derived) compounds. The list of major compounds (out of the 30 analyzed) present in the ORF as quantitatively analyzed by GC-MS is shown in Table 4.2 (Ingram et al., 2008). Five compounds were present in significant ($\geq 1\%$) quantities for at least one feed stock as shown in the table. Levoglucosan is the most significant compound present in all the feed stocks ranging from 8.21% (oak bark) to 21.60% (oak wood). With the exception of levoglucosan, a similar chemical composition was observed for 'wood and bark' oils derived from 'pine or oak' feed stocks.

The fractionation of pyrolysis oil vapor was achieved by independently controlling the 5 condenser temperatures. The condenser 1 was maintained slightly above 100 °C to separate heavy organics from water and the light organics. The heavy organics are deemed to be the organic compounds with high b.p.'s and high molecular weights (m.w's). However, the light organics are deemed to be the organic compounds with low b.p's and low m.w's. The condenser 1 had the highest log mean temperature difference (LMTD) where most of the ORF was collected. However, condenser 2 was maintained slightly above 60 °C and hence mostly water and volatile compounds (light organics) collectively known as ARF was collected from this condenser. The vapor inlet temperature for the condenser 2 was slightly greater than 100 °C whereas its vapor outlet temperature was close to 60 °C. For most pyrolysis runs the temperatures of condensers 3-5 were maintained close to ambient temperature (25 °C). Even though these condensers were maintained at ambient temperature, small quantities of pyrolysis oil in the form of heavy organics were collected in them. This is attributed to the inefficient condensation, secondary char catalyzed reactions, and to the poor heat and mass transfer. These time-

dependent secondary reactions seem to be responsible for the network polymerization and repolymerization of pyrolysis oil vapor (Bridgwater and Peacocke, 2000). Here, mass transfer term refers to the uncontrolled carryover of char fines during the vapor transport process, which seem to have a great potential to retain oil in their porous structure. Regardless, of the above anomalies observed majority of the pyrolysis oil vapor was collected in condensers '1 and 2' as 'ORF and ARF' respectively.

The water content in both ORF and ARF seems to be derived from the moisture in the original feed stocks as well as the molecular cracking reactions that occurred during pyrolysis. Although the water content of heavy organics collected from condensers 3, 4, and 5 was not tested individually they are expected to have the lowest concentration level. Thus, the fractionation technique can be beneficial in increasing the fuel value of the pyrolysis oils by minimizing the water content. During this study, the oil fractions collected from condensers 1, 3, 4, and 5 were combined and this mixture was collectively known as ORF or simply pyrolysis oil. This pyrolysis oil was utilized during the stability studies that involved the phases 2-4. As mentioned previously, the fraction collected from condenser 2 was identified as ARF. However, this fraction (ARF) was not utilized during the stability testing.

Auger Reactor Yields

An example of the daily yields obtained from oak wood (high temperature and slow residence) is shown in Figure 4.1 and this is typical of daily yields when values varied around $\pm 5\%$. This particular oil run was completed in a span of 12 days as shown in Figure 4.1; otherwise most runs were completed within a week. Although a strict time

schedule for each run was proposed, inconsistent delays occurred in between pyrolysis oil runs due to unexpected reactor troubleshooting, maintenance, and shut down operations. The daily yield data for all the MS pyrolysis oil runs is presented in Appendix A.

The list of the 16 MS pyrolysis oils with respective yields are provided in Table 4.1. The total pyrolysis oil yields were determined by the addition of both ORF and ARF yields as shown in this table. A lowest pyrolysis oil yield of 42.8% was achieved for pine bark produced at high temperature and fast residence as shown in Table 4.1. A highest pyrolysis oil yield of 62.9% was achieved for oak wood produced at low temperature and slow residence. As shown in this table pine bark had the lowest oil yields among all the feed stocks tested. This is attributed to the nature of the feedstock and the difficulty in controlling the pyrolysis temperature. Otherwise similar oil yields were obtained from the beginning to the end of most runs as illustrated in Figure 4.1.

The average yields of oil (ORF), water (ARF), char, and unaccounted mass from each feedstock for all residence times and pyrolysis temperatures combined are shown in Figure 4.2. The wooden feed stocks showed high ARF yields compared to the bark feed stocks as shown in this figure. This is justified by the higher holocellulosic content of wooden feed stocks compared to the bark feed stocks (Sjostrum, 1993).

High char yields were obtained for bark feed stocks compared to the wooden feed stocks as visualized from Figure 4.2. This is attributed to the higher lignin content of bark feed stocks compared to the wooden feed stocks (Sjostrum, 1993). Subsequently, a low char yield of 17.3% was achieved for oak wood oil produced at high temperature and fast residence. A high char yield of 43.2% was achieved for pine bark oil produced at low temperature and fast residence time. Significantly high yields of char were obtained from

the small-scale auger reactor system due to the slow pyrolysis conditions. This trend obtained is in agreement with the results published in the literature for fluidized bed, fixed bed, and transport reactor systems (Scott et al 1988; Sensoz, 2003; Blasi et al. 1999).

The lowest (13.44%) and highest (32.32%) yields of unaccounted mass (UM) were obtained for the pine bark oils. The lowest yield of UM was observed for the pine bark oil produced at low temperature and fast residence. Contrarily, the highest yield of UM was obtained for the pine bark oil produced at high temperature and slow residence. A major portion of this UM is non-condensable gases while a minor portion is in the form of condensable tars. These tars are suspected to have polyaromatic compounds such as naphthalenes, anthracenes, and phenanthrenes. Thus, a fraction of UM collected as tarry pyrolyzate during the condenser cleaning operation is shown in Figure 4.3. This fraction indicates the presence of heavy tar like substances obtained after excessive cracking and network polymerization reactions in the pyrolysis vapor.

Influence of Reactor Conditions

The influence of pyrolysis temperature and residence time on the reactor yields is illustrated by the oak wood run in Figures 4.4-4.5. Graphs for all other oil runs are presented in Appendix A. Pyrolysis temperature was observed to significantly affect the yields of ORF and UM as shown in Figure 4.4. However, residence time had a limited effect on the pyrolysis oil (low temperature) yields as shown in Figure 4.5. At a high pyrolysis temperature (450 °C) cracking of long-chain compounds may have occurred during the gas release and transfer process. Non-condensable gases could increase

resulting in lower yields of pyrolysis oil. Likewise an increase in the gas yields with a corresponding decrease in the liquid yields at high pyolysis temperatures have been reported (Blasi et al., 1999). Both pyrolysis temperature and residence time however did not have a significant impact on the char yields of oak wood.

Reactor Off-Gas Analysis

Generally, low yields of pyrolysis oil were observed because of the low condensation efficiencies. The low condensation efficiencies subsequently resulted in higher percentages of UM. The gases analyzed by the Nova[®] portable analyzer were (CO, CO₂, O₂, and CH₄). Here, it should be noted that the NOVA analyzer reports all carbon compounds in the gas as CH₄ including the compounds greater than C₂. The normalized gas composition obtained for the pine bark oil (low temperature and fast residence) is shown in Table 4.3. As shown in this table, highest percentage of the reactor off-gas is attributed to methane. On the other hand the lowest percentage of the reactor off-gas is attributed to hydrogen which is observed to be below detection limit (BDL) of the analyzer. Evidently a picture depicting the tarry condensate (yellow colored) built on the borosilicate glass filter used during gas analysis has been shown in Figure 4.6.

Reactor Temperature Control

An example of ‘reactor temperature (y) versus reactor length (x)’ for the five ceramic band heaters has been provided in Figure 4.7. There are six zones due to the band heating along the entire length of the reactor and are identified by A to F. Band heating apparently resulted in dismal temperature control and consequently the temperature between any two successive bands varied widely as illustrated in Figure 4.7. The zonal

temperatures were all controlled (overshooting/undershooting) as per the set point temperatures using the ceramic band heaters. The heaters 2-4 were mostly temperature controlled as pyrolysis was expected to occur in the zones C-E at either 400 or 450 °C. A maximum temperature fluctuation of ± 50 °C was observed for the zone C during the reactor operation. However, a minimum temperature fluctuation of ± 25 °C was observed for the zones A, B, and F as the heaters 1 and 5 were least operated. Because of this inherent variation in the zonal temperatures, several hotspots were created during the reactor operation. Hence, it is expected that these hotspots resulted in increased thermal gradients and decreased pyrolysis efficiency. Further an illustration of ‘zonal temperature (y) versus run time (x)’ for the five ceramic band heaters has been provided in Figure 4.8. As visualized from this figure, the temperature of zone E was most difficult to control during the reactor operation. Consequently, the variability in temperature obtained for this zone is the maximum.

Reactor Residence Time

As widely reported in the literature, vapor residence time is the primary control variable used during the slow and fast pyrolysis of most reactor systems. Based on the steady state assumptions, the theoretical derivation shown below indicates the fractional difference (31.58%) in residence times of slow and fast pyrolysis that occurred in Mississippi State University (MSU) small-scale auger reactor. This number seems to be large enough to suggest the significance of variable residence time on the oil composition and its properties. However, for the MSU auger reactor, dual isotopic (^{13}C & ^1H) nuclear magnetic resonance spectroscopy (NMR) of the pyrolysis oil samples (obtained from

slow and fast pyrolysis oil ports) provided inconclusive evidence during the spectral analysis based on the relative abundance of important functional groups. Some of these functional groups included carboxyls, carbonyls, hydroxyls, ethers, alkyls, aryls, aliphatics, and ethers. Hence, residence time is deemed to be insignificant during the variable minimization process as also evidenced by the viscosity test results during the preliminary testing phase.

Assuming each batch of the lignocellulosic feedstock was pyrolyzed in plug flow mode the gas and vapor residence time can be defined in Equation 1 as follows.

$$\begin{aligned}\tau &= (\text{Reactor Volume})/(\text{Volumetric Flow Rate of Gas and Vapor}) \\ &= V/Q\end{aligned}\tag{4-1}$$

As depicted in Figure 4.9 for fast pyrolysis occurring from port 1 the Equation 1 can be written as,

$$\begin{aligned}\tau_1 &= (\text{Reactor Volume})_1/(\text{Volumetric Flow Rate of Gas and Vapor})_1 \\ &= V_1/Q_1\end{aligned}\tag{4-2}$$

As depicted in Figure 4.9 for slow pyrolysis occurring from port 2 the Equation 1 can be written as,

$$\begin{aligned}\tau_2 &= (\text{Reactor Volume})_2/(\text{Volumetric Flow Rate of Gas and Vapor})_2 \\ &= V_2/Q_2\end{aligned}\tag{4-3}$$

The gas and vapor residence time averaged over slow and fast residence times can be written in Equation 4 as follows.

$$\tau_{\text{avg}} = (\tau_1 + \tau_2)/2\tag{4-4}$$

The relative difference between actual and average residence times can then be defined in Equation 5 as follows.

$$(\tau_2 - \tau_1) / (\tau)_{\text{avg.}} = 2(\tau_2 - \tau_1) / (\tau_1 + \tau_2) \quad (4-5)$$

Thus, back substituting the residence times in Equation 5 in terms of reactor volumes, gas, and vapor flow rates from Equations 2-3 will provide Equation 6 as follows.

$$(\tau_2 - \tau_1) / (\tau)_{\text{avg.}} = 2(V_2/Q_2 - V_1/Q_1) / (V_1/Q_1 + V_2/Q_2) \quad (4-6)$$

Assuming that approximately similar volumetric flow rates of gas and vapor are released through ports 1 and 2, $Q_1 \sim Q_2 = Q$.

Naturally the above assumption will simplify Equation 6 to Equation 7 as follows.

$$(\tau_2 - \tau_1) / (\tau)_{\text{avg.}} = 2(V_2 - V_1) / (V_1 + V_2) \quad (4-7)$$

Since the MSU auger reactor geometry is cylindrical as shown in Figure 4.9, its total volume (V) then becomes, $V = (\pi/4)D^2L$.

Where,

D = Inside diameter

L = Total length of the reactor

Consequently, the distances of ports 1 and 2 from the feed entrance can be expressed in terms of the partial reactor lengths as follows.

L_1 = Distance of port 1 from the feed entrance

L_2 = Distance of port 2 from the feed entrance

Making the above substitutions in Equation 7 leads to Equation 8 as follows.

$$(\tau_2 - \tau_1) / (\tau)_{\text{avg.}} = 2(L_2 - L_1) / (L_1 + L_2) \quad (4-8)$$

The actual distance of separation between ports 1 and 2 as shown in Figure 4.9 has been measured to be 6" implying $L_2 - L_1 = 6''$. Thus, Equation 8 will provide a fractional difference of 31.58% in the slow and fast residence times as calculated below.

$$(\tau_2 - \tau_1) / (\tau)_{\text{avg.}} = 2(L_2 - L_1) / (L_1 + L_1 + 6) = 2(6'') / (16'' + 16'' + 6'') = 0.3158$$

The above calculation is based on the assumption that a feed particle is completely pyrolyzed into a complex stream (gas, vapor, steam, aerosol, and mist) before reaching slow (2) and fast (1) pyrolysis ports as a charred particle. However, the complex vapor-cracking and other secondary reactions are expected to occur as a function of reactor length and consequently vary the composition of gas and vapor stream released from ports 1 and 2. Practically, the distance of separation (6") between these two ports might not be significant enough to have caused a variation in the composition of chemical compounds. Furthermore, it was also observed during the reactor runs that there was a back flow of excess volumes of gas and vapor from the chamber to the feeder. This phenomenon seems to indicate that all the moles of gas formed from a feed batch during the pyrolysis reaction were not timely released (partly due to the horizontal positioning of the reactor) from the ports 1 and 2 before the charred particles traveled the distances of L_1 and L_2 . Consequently, it was hypothesized earlier that the NMR analysis of pyrolysis oils obtained from pyrolysis ports (1 and 2) did not reveal a significant difference in terms of their chemical composition.

Preliminary Stability Testing (Trial Runs)

Introduction

Preliminary testing was performed using wood and bark derived Mississippi State University (MS) pyrolysis oils (16). The main purpose of this testing was to perform three tasks that are: 1) study the stability of frequently tested or aged oils 2) study the stability of refrigerated oils and 3) to ultimately combine oils with similar pyrolysis conditions. Refrigerated oils were stored at 4 °C in a dark refrigerator. Frequently tested

oils were removed from the refrigerator before testing and brought to room temperature (~25 °C) by natural convection as discussed previously. After the testing was performed these oils were placed back in the refrigerator. So these oils frequently underwent the transitioning in their temperature that is from 4 °C to 25 °C and back. This process continued until the end of test duration. The test duration of the task 1 lasted for about four months. Task 2 was performed to compare the stability of refrigerated oils with the frequently tested oils but they were tested only in the beginning and end of the test duration (4 months). Due to the time lags involved during the pyrolysis oil production, storage, and utilization, the tasks 1 and 2 were necessary to ensure that the oil stability during its refrigeration is unaffected. The task 3 was conducted to evaluate the effects of pyrolysis temperature and residence time on the oil viscosity and water content and combine the oils with similar production conditions. Statistical analysis of variance (ANOVA) and least significant difference (LSD) tests were conducted to evaluate the significance of pyrolysis conditions on the mean viscosity and mean water content of the pyrolysis oils.

Stability of Frequently Tested Oils (Aged)

The viscosity of frequently tested wood pyrolysis oils showed a consistent increase as a function of aging time. An example of this trend is shown for MS oak wood (OW) pyrolysis oils in Figure 4.10. This particular figure shows the stability performance of the frequently tested OW oils in reference with the refrigerated OW oils. The oils produced at a particular pyrolysis temperature (low or high) showed an identical response [$cP=f(\text{days})$] regardless of the residence time. The viscosity of high temperature oils is

consistently higher than that of the low temperature oils as shown in the figure. At a particular pyrolysis temperature the viscosity of the fast residence OW oils is consistently lower than the slow residence OW oils. These trends are attributed to the overall slow pyrolysis that was conducted due to which secondary polymerization reactions are hypothesized to have occurred in the oils. Normally, in well controlled pyrolysis conditions (fast residence time and fast cooling time) a higher number of thermolytic cracking reactions are expected to occur at a high pyrolysis temperature than the low pyrolysis temperature. The secondary polymerization reactions are also kept minimal in such a controlled pyrolysis process. Consequently, low viscosity and high water content of the high temperature oils is to be expected than the low temperature oils.

The water content of the frequently tested OW pyrolysis oils showed a mild increase as a function of aging time as indicated in Figure 4.11. After 60 days, the increase in the average water content (six reps) with aging time became slightly more apparent. Nevertheless, a maximum increase of 9-10% in the water content is observed for the OW oil (OW-LT-FR) after an aging time of 120 days. At a particular pyrolysis temperature the water content of the slow residence OW oils is consistently lower than the fast residence OW oils. The water content of low temperature oils is consistently higher than the high temperature oils as shown in the figure. This trend indicates that certain amount of water content is truly beneficial in lowering the pyrolysis oil viscosity.

The pH and density of the frequently tested wood pyrolysis oils did not increase with aging time. An example of the flat response in pH and density obtained for the MS OW pyrolysis oils is shown in Figures 4.12-4.13. As seen the pH and density of the OW oils do not vary significantly regardless of the pyrolysis condition utilized.

Stability of Refrigerated Oils (Fresh)

The viscosity of the frequently tested MS wood oils (aged) as compared to the refrigerated MS wood oils is relatively unaffected as shown in Figures 4.14-4.17. These figures are obtained from the oil viscosity measurements performed at the end of test duration. Here, aged oils refer to the oils that were frequently tested for their properties over a period of 4 months. However, refrigerated oils refer to the oils that are constantly stored at 4 °C in a dark refrigerator. Aged pine wood oils showed slightly higher viscosity than the refrigerated pine wood (PW) oils as shown in Figure 4.14. However, the viscosity of the refrigerated oak wood (OW) oils did not differ significantly from that of the aged oak wood oils as shown in Figure 4.15. The viscosity trends obtained in Figures 4.10 and 4.14 apparently indicate that the stability of the refrigerated oils in comparison with the aged oils is relatively unaffected over a prolonged storage period of 4 months. The PW oils regardless of pyrolysis conditions showed Newtonian flow behavior as seen from Figures 4.14 and 4.16. Contrarily, the OW oils regardless of pyrolysis conditions showed non-Newtonian flow behavior as seen from Figures 4.15 and 4.17. The influence of residence time on the viscosity of PW and OW pyrolysis oils is not apparent as shown in Figures 4.14-4.15. However, the influence of pyrolysis temperature on the viscosity of PW and OW pyrolysis oils is apparent as shown in Figures 4.16-4.17. These trends reveal that the pyrolysis oils with the same temperature and different residence times do not differ significantly from each other. However, the pyrolysis oils with the same residence time and different temperature differ significantly from each other. These trends have been statistically verified using ANOVA and LSD tests which are discussed in the next

section. Hence, the pyrolysis oils with the same residence time are combined by retaining the variables feedstock and pyrolysis temperature.

Statistical Modeling

Statistical analysis of variance (ANOVA) is performed using the viscosity and water content data of 16 MS pyrolysis oils. These oils are produced from pine bark, pine wood, oak bark, and oak wood. The reactor conditions are low temperature (LT=400 °C), high temperature (HT=450 °C), slow residence time (SR), and fast residence time (FR). No additives were added to the oils during their viscosity and water content measurements. The viscosity and water content data is obtained by performing direct measurements on the oils. Both the viscosity and water content models are statistically significant at the observed significance level (OSL) of 0.05. A slightly lower regression coefficient ($R^2=0.73$) is obtained for the viscosity model compared to the water content model ($R^2=0.87$) as the oil viscosity is measured only once as a function of shear rate and temperature. However, the number of replicates used for water content is six.

Viscosity Model (ANOVA)

The variable, level, and treatment information for the ANOVA viscosity model is shown in Table 4.4. A total number of 192 observations were utilized. The response variable (viscosity) used in this model is obtained at the shear rates of 0.1, 1, 10, and 100 s^{-1} and measurement temperatures of 25, 50, and 80 °C. The ANOVA model obtained for oil viscosity is shown in Table 4.5. The degrees of freedom (DF) utilized for the error are 137. A very high value of mean square error (MSE=573008) is obtained due to the fact that Newtonian and non-Newtonian oils are both present in the viscosity dataset. The

mean viscosity of the 16 MS pyrolysis oils obtained from the model is ~402 cP. The residence time did not significantly affect the viscosity of pyrolysis oils. However, feedstock and pyrolysis temperature significantly affected the viscosity of pyrolysis oils.

An observed significance level (OSL) of 0.05 is used during the LSD t-tests for the mean viscosity of pyrolysis oils. The mean viscosity of bark oils (PB and OB) is significantly higher than the mean viscosity of wood oils (PW and OW) as shown in Table 4.6. Similarly, the mean viscosity of high temperature (450 °C) pyrolysis oils is significantly higher than the mean viscosity of low temperature (400 °C) pyrolysis oils as shown in Table 4.7. However, the mean viscosity of slow residence (SR) pyrolysis oils does not differ significantly from the mean viscosity of fast residence (FR) pyrolysis oils as shown in Table 4.8. All the viscosity measurement temperatures differ significantly from each other as shown in Table 4.9. The lowest and the highest mean viscosities are observed for 80 and 25 °C respectively. The shear rates of 1, 10, and 100 s⁻¹ do not differ significantly based on their mean viscosity as shown in Table 4.10. As expected the highest mean viscosity of the pyrolysis oils is obtained at a shear rate of 0.1 s⁻¹.

Water Content Model (ANOVA)

The variable, level, and treatment information for the ANOVA water content model is shown in Table 4.11. A total number of 96 observations were utilized. The response variable (% water content) used in this model is obtained from the Karl Fisher analysis of 16 MS pyrolysis oils. The ANOVA model obtained for oil water content is shown in Table 4.12. The degrees of freedom (DF) utilized for the error are 80. A low value of MSE (5.66) is obtained as compared to the viscosity model. The mean water

content of the pyrolysis oils obtained from the model is ~20 wt.%. As seen from the previous model also the residence time did not significantly affect the water content of pyrolysis oils. However, feedstock and pyrolysis temperature significantly affected the water content of pyrolysis oils.

An OSL of 0.05 is used during the LSD t-tests for the mean water content of pyrolysis oils. The mean water content of all the pyrolysis oils (PW, PB, OW and OB) differs significantly from each other as shown in Table 4.13. The lowest and the highest mean water content is obtained for OW and PB oils respectively. Similarly, the mean water content of low temperature (400 °C) pyrolysis oils is significantly higher than the mean water content of high temperature (450 °C) pyrolysis oils as shown in Table 4.14. However, the mean water content of slow residence (SR) pyrolysis oils does not differ significantly from the mean water content of fast residence (FR) pyrolysis oils as shown in Table 4.15.

In summary, the viscosity values obtained using viscometer were found to map with the values obtained from rheometer for the same spindle revolutions per minute (rpm) and wood pyrolysis oils evaluated. The MS pyrolysis oils produced from each feedstock with similar residence times were combined to eliminate the variable vapor residence time. Thus, the 16 MS pyrolysis oils were reduced to half after retaining variables feedstock and pyrolysis temperature. However, during the phases II-IV, only four MS pyrolysis oils produced at low temperature from each feedstock will be utilized.

Additive Prescreening (Phase II)

Introduction

As discussed in Chapter 3, additive prescreening was performed using pine wood pyrolysis oil (high temperature) to down select the best three additives including methanol. The viscosity of control (0 wt.% additive) and additive (10 wt.%) blended pyrolysis oils were analyzed as a function of shear rate. Consequently, the flow behavior of pyrolysis oils if Newtonian or non-Newtonian was determined. The rheological definitions of Newtonian and non-Newtonian liquids have been discussed in Chapter 2. The viscosity, water content (Karl Fisher), and pH of 27 pyrolysis oils (control and additive blended) were analyzed as a function of storage time (0-192 hr). A storage temperature of 80 °C was utilized to accelerate the aging reactions that commonly occur in pyrolysis oils. These aging reactions ultimately result in an increase in the viscosity and water content of pyrolysis oils. Hence, depending on the significance of viscosity and water content elevation the pyrolysis oils were observed to be either partially polymerized (stable) or completely polymerized (unstable). The statistical analysis of variance (ANOVA) models obtained for viscosity and water content of pyrolysis oils are discussed in this phase. The least significant difference (LSD) analysis was also conducted for the mean viscosity and the mean water content of pyrolysis oils. Consequently, due importance was given to anisole (ANS), glycerol (GLY), and methanol MEH in this discussion as these additives were chosen to be the best performing additives.

Influence of Shear Rate on the Pyrolysis Oil Viscosity

The influence of shear rate and storage time on the pyrolysis oil viscosity was analyzed for the control and additive blended pyrolysis oils. Most pyrolysis oils exhibited Newtonian flow behavior for storage times less than 48hr independent of the shear rate. After 48hr the pine wood pyrolysis oils exhibited non-Newtonian flow behavior due to the rapid acceleration of polymerization reactions. This behavior of pyrolysis oils is more dominant at low shear rates ($\leq 20\text{s}^{-1}$) than the high shear rates ($>20\text{ s}^{-1}$) because of the pseudoplastic nature of these oils. The viscosity versus shear rate data obtained for the control (CTL) and additive blended oils (anisole-ANS, glycerol-GLY, and methanol-MEH) at a measurement temperature of $25\text{ }^{\circ}\text{C}$ is shown in Figures 4.18-4.21. Amongst all the additives tested GLY exhibited unique characteristics in the oil flow properties as shown in Figure 4.20. The GLY blended oil exhibited Newtonian properties for all the storage times tested. Furthermore, the transitioning in its flow behavior (Newtonian to non-Newtonian) as compared to the other oils was not observed beyond aging time of 48hr. This anomalous behavior of GLY is attributed to its hygroscopic nature and its tendency to form hydrogen bonding with water as reported (Dashnau et al., 2006). Water is known to be present in abundant quantities in the pyrolysis oil (Maschio et al., 1992). Hence, the hygroscopic nature of GLY can be beneficial in producing homogeneous oil. As explained earlier wood pyrolysis oil is a heterogeneous mixture of hydrophilic and hydrophobic lignocellulosic compounds (Ba et al., 2004; Boucher et al., 2000). Consequently, the viscosity measurements can be difficult to ascertain. Inaccurate measurements of the pyrolysis oil viscosity even at room temperature due to their instability, volatility, and complex multiphase behavior have been reported in the

literature (Radovanovic, et al., 2000). In support of this finding, ANS (Figure 4.19) shows variations (cross over or overlapping) in the viscosity-shear rate profiles especially for storage times exceeding 12hr. Consequently, a systematic increase in the ANS oil viscosity as a function of storage time did not occur at all shear rates as compared to GLY and MEH in Figures 4.20-4.21.

The viscosity increase (%) of CTL, ANS, GLY, and MEH blended oils as a function of shear rate is shown in Figures 4.22-4.25. This increase is computed by the percentage change in viscosity (25 °C) with storage time (0 to 192 hr). Among all the above oils CTL is observed to show the highest increase in viscosity for the shear rates of 10-200 s⁻¹ (Note Y-axis scale). Further, the highest increase in viscosity for CTL and MEH blended oil are observed at low shear rates (≤ 10 s⁻¹) as shown in Figures 4.22 and 4.25. This is likely due to the low shearing effect on the pyrolysis oil structure and its internal fluidic resistance. Subsequently, the viscosity increase reached a plateau at high shear rates of ≥ 20 s⁻¹ for CTL and MEH blended oil. A uniform increase in viscosity was observed for ANS and GLY blended pyrolysis oils as a function of shear rate (≤ 20 s⁻¹) as shown in Figures 4.23-4.24. The pyrolysis oils that were aged to 192 hr consistently exhibited non-Newtonian behavior at low shear rates of ≤ 10 s⁻¹. Once the shear rate exceeded 10 s⁻¹ the flow behavior was close to Newtonian for ANS and GLY blended oils. This is apparently due to the breakdown and realignment of internal fluidic structure of pyrolysis oil. Evidence of this trend can be seen from Figures 4.18-4.19, and 4.21 shown previously.

Influence of Additive on the Oil Viscosity (Initial)

The additive GLY with greater than 99% purity showed Newtonian flow properties with a viscosity around 700 cP as shown in Figure 4.26. The high viscosity of GLY caused an increase 22-25% in the initial (0 hr) oil viscosity after its mixing. At the expense of this initial increase in viscosity GLY seems to maintain the oil properties for long storage times exceeding 48 hr. At 0 hr a similar increase in the oil viscosity as that of GLY was observed for resorcinol (RSL). A highest increase 592-598% in oil viscosity after additive mixing is observed for polyethylene glycol (PEG) apparently due to its high molecular weight (~20000 g/mol). The use of high molecular weight additives is not apparently found in the literature. However, they are included in this research to study the effects of increasing the oxygen content of additive on the stability of pyrolysis oils.

The viscosity of ANS and MEH as measured by the TA rheometer was found near (1-2) cP. This low viscosity of ANS and MEH decreased the initial oil viscosity significantly because of their dilution effect. Consequently, ANS lowered the oil viscosity by 46-50% and MEH lowered the oil viscosity by 70-75% within the shear rate range of 1-200 s⁻¹. A similar decrease in the initial oil viscosity as that of MEH 70-75% is observed for ethanol (ETH), methyl formate (MEF), and methyl ethyl ketone (MEK) after their mixing. These low molecular weight additives seem to be beneficial in minimizing the viscosity increase and thus aging of pyrolysis oils as reported (Diebold and Czernik, 1997; Diebold 2000).

Influence of Temperature on the Pyrolysis Oil Viscosity

The influence of measurement temperature on the viscosity of CTL, ANS, GLY, and MEH blended pyrolysis oils is shown in Figures 4.27-4.30. The viscosity of the oils in these figures corresponds to a shear rate 100 s^{-1} . A high shear rate is selected because a fully developed flow of the pyrolysis oil is expected to occur at this rate. The flow behavior of non-Newtonian liquids as a function of shear rate is already discussed in Chapter 2. A drastic but consistent decrease in viscosity can be seen for all the pyrolysis oils as the measurement temperature is raised from 25 to 80 $^{\circ}\text{C}$. Consequently, non-linear response of viscosity as a function of measurement temperature can be visualized at storage times of 0, 96, and 192 hr. Furthermore, a consistent increase in viscosity (cP) is observed as a function of storage time (hr) regardless of measurement temperature ($^{\circ}\text{C}$). This trend was observed for CTL, GLY, and MEH in Figures 4.27 and 4.29-4.30. However, in the case of ANS the increase in viscosity from 96 to 192 hr was not significant as shown in Figure 4.28. Since, the increase in viscosity indicates the chemical changes that likely occur in pyrolysis oils, ANS blended oil seems to be more stable at 192 hr, than control (CTL) and other blended oils (GLY and MEH). At 192 hr, a sharp decrease (high slope) in viscosity as a function of temperature ($-\Delta\mu/\Delta T$ or $\text{cP}/^{\circ}\text{C}$) is observed for ‘CTL and GLY’ compared to ‘ANS and MEH’. This suggests that the chemical structural changes that might result by the addition of ANS and MEH are far more significant than GLY. For most additives tested the viscosity decrease ($-\Delta\mu/\Delta T$) became increasingly rapid as the storage time was increased with the exception of ANS.

Exponential fit is used to correlate the oil viscosity (CTL, ANS, GLY, and MEH) with measurement temperature as shown in Table 4.16. Subsequently, these models

(temperature versus viscosity) are observed to have a high regression coefficient (≥ 0.98). A highest drop in oil viscosity is observed for GLY at 192 hr as the temperature is raised from 25 to 80 °C. However, a lowest drop in oil viscosity is observed for ANS at 192 hr as the temperature is raised from 25 to 80 °C. The mathematical model $\{\mu = a[\exp(-b \cdot T)]\}$ coefficient (a) and index (b) of ANS (192 hr), GLY (192 hr), and MEH (192 hr) seems to suggest that 'a' has a greater influence on the oil viscosity drop $[(\Delta\mu/\mu)\%]$ than 'b'.

It can be inferred from the above mathematical model that the coefficient 'a' becomes the limiting factor at low temperatures for a potential bio-fuel application. Consequently, in cold climatic regions (arbitrarily ≤ 10 °C) the pumping of pyrolysis oil can be difficult due to its high viscosity. To avoid this problem pyrolysis oil needs to be stored at a temperature higher than the ambient temperature to initiate the flow. It can be inferred from the above mathematical model that the index 'b' becomes the limiting factor at high temperatures for a potential bio-fuel application. Consequently, in the hot climatic regions where average temperature is arbitrarily ≥ 30 °C, pyrolysis oils can be used relatively easily as bio-fuels provided they do not become polymerized and phase-separated.

Most chemical and thermal changes in the additive blended pyrolysis oils seem to occur between 0 and 96 hr rather than 96 to 192 hr based on the increase in numerical value of coefficient 'a'. A relatively high numerical value of exponential index 'b' suggests that the viscosity decrease as a function of temperature is most drastic for GLY. Likewise, a relatively low numerical value of exponential index 'b' indicates that the viscosity decrease as a function of temperature is least drastic for ANS. A consistent decrease in the index b with storage time is observed for ANS only. This trend seems to

indicate that lowering the viscosity drop of ANS blended pyrolysis oil might be beneficial where prolonged heating is required.

Influence of Storage Time on the Pyrolysis Oil Viscosity

The influence of storage time on the viscosity of control (CTL) and additive blended oils (ANS, GLY, and MEH) is shown in Figures 4.31-4.34. The viscosity of the oils in these figures corresponds to a shear rate 100 s^{-1} . The increase in viscosity as a function of storage time ($+\Delta\mu/\Delta t$ or cP/hr) for most additives including ANS, GLY, and MEH is generally high during the initial storage period of 24-48 hr. That also means most polymerization reactions occur during this period as indicated by a sharp increase in the viscosity. The CTL and GLY oils seem to show a continued increase in viscosity ($+\Delta\mu/\Delta t$) as shown in Figures 4.31 and 4.33. But the increase is more drastic for CTL as compared to GLY. The above trend indicates that CTL and GLY do not attain chemical equilibrium (minimum Gibbs free energy, $\Delta G < 0$) within the 192 hr aging period. Further the viscosity of 'CTL and GLY' increased by '210% and 162%' as the storage time is increased from 96 to 192 hr. The viscosity increase ($+\Delta\mu/\Delta t$) of ANS blended oil apparently stabilized after 24 hr as shown in Figure 4.32. This trend implies that ANS reached chemical equilibrium within 24 hr that is much faster than most additives tested in this research. The viscosity increase ($+\Delta\mu/\Delta t$) of MEH blended oil however stabilized after 96 hr as shown in Figure 4.34. This trend implies that MEH reached chemical equilibrium within 96 hr aging period.

The viscosity increase ($+\Delta\mu/\Delta t$) is negligible beyond 48 hr for most additives especially ketones and esters as shown in Table 4.17. This trend is observed for certain

additives only among alcohols, ethers, and cyclic compounds. They are polyethylene glycol (PEG), ethanol (ETH), methyl tertiary butyl ether (MTBE), anisole (ANS), ethylene glycol dimethyl ether (EGD), decahydronaphthalene (DHN), and tetrahydronaphthalene (THN). However, the viscosity of aldehydes [acetaldehyde (ACH) and 2-furaldehyde (2FL)] continued to increase beyond 48 hr as seen for CTL and ANS. The viscosity increase ($+\Delta\mu/\Delta t$) is far more drastic in the case of 2FL as shown in Figure 4.35. Such an increase in the viscosity is attributed to the severe polymerization of the pyrolysis oil components.

Influence of Additive on the Viscosity Increase (%)

The influence of additive on the viscosity increase (%) of pyrolysis oils is explored specifically for 6 groups of additives as shown in Table 4.17. Generally, the cyclic compounds showed the highest viscosity increase while ketones favored the lowest viscosity increase as indicated in Figure 4.36. The viscosity increase (%) with storage time (0 to 192 hr) of all the additive blended oils at a shear rate of 100 s^{-1} is shown in this figure. Among all the oils aged to 192 hr, specifically ANS blended oil had the lowest viscosity increase (60%) while 2-furaldehyde (2FL) blended oil had the highest ($1.5 \times 10^3\%$). The viscosity increase ($2.2 \times 10^3\%$) of the RSL peak as shown in Figure 4.36 is obtained for storage times of 0 and 24 hr as this oil was observed to completely polymerize at 48 hr. The highest viscosity increase in the case of RSL at the shortest aging period (24 hr) could be due to the presence of two hydroxyl groups on the aryl unit. The resulting phenoxide ion (mono/di) during resonance stabilization of resorcinol could be participating in the higher order polymerization reactions. However, with anisole the

phenoxide ion formation is restricted because of the presence of a lone methoxyl group in its aromatic structure.

The furfuryl alcohol (FAL) peak shown in Figure 4.36 corresponds to the 96 hr aging period. The FAL blended pine wood oil just like the RSL blended oil was observed to completely polymerize at the longest aging period of 192 hr. Hence, viscosity measurements were not possible for these oils for the aging periods beyond 24 hr for RSL and 96 hr for FAL. The additives (RSL and FAL) are chemically known to have a tendency of resin formation irreversibly in the presence of heat and acids (Jain and Jain, 1995; Brockmann et al., 2009). Consequently, the RSL and FAL mixed pine wood pyrolysis oils (pH: 2-4) when stored at a temperature of 80 °C, seem to develop a tendency to polymerize at a much faster rate than most additives utilized in this research. These additives are projected to be useful in a niche application such as the utilization of phenolic fraction of pyrolysis oil to preserve wood.

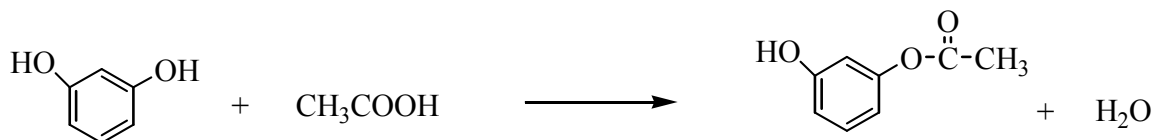
As shown in Table 4.17, the chemical additives RSL and FAL are included in the additive group of alcohols while 2FL is included in the additive group of aldehydes. Resorcinol (RSL) has a lone aromatic ring while FAL and 2FL both have single aliphatic rings as shown in Table 3.6. Hence, each of these compounds is observed to closely emulate the viscosity increase of other cyclic compounds such as cyclohexane (CHX), decahydronaphthalene (DHN), and xylene (XYL). Except for RSL, FAL, and 2FL; all the additives performed better than CTL (5.05 x 10²%) by at least a factor of 1.1 (CHX) and utmost a factor of 8.4 (ANS). Among all the storage times (0, 12, 24, 48, 96, and 192 hr) tested the highest increase in viscosity is observed from 96 to 192 hr. The trend in viscosity increase seems to continue if aged beyond 192 hr for some additives that were

ineffective during oil stabilization. An example of this trend was shown in Figure 4.35 for 2FL. The chemical reactions continue to occur in the unstable pyrolysis oils until they become completely polymerized (solid-like). As indicated in Figure 4.37, polyethylene glycol (PEG) among alcohols had consistently higher viscosity than CTL for all the storage times tested. Among all the additives utilized, PEG is the only additive showing such anomalous behavior due to its high molecular weight.

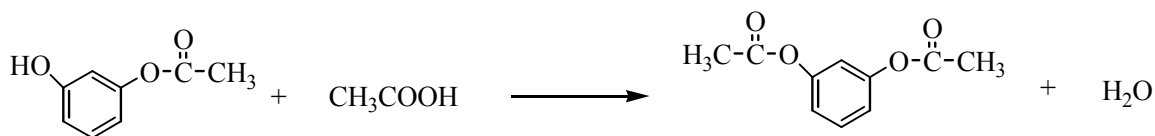
The change in the initial viscosity (increase/decrease) of pyrolysis oils after additive mixing was closely monitored during this investigation. Correspondingly RSL, GLY, and PEG increased the oil viscosity by 20, 23, and 595% respectively. These numbers seem to correlate well with the increasing number of oxygen atoms in the additives (2-RSL, 3-GLY, and 455-PEG). The percentage increase in viscosity shown by RSL (110.1 g/mol) is lower than that of GLY (92.1 g/mol) in spite of its higher molecular weight. This trend can be justified by the ability of hydroxyl groups towards participation in a network polymerization reaction such as esterification. The chemical reactions of additives (RSL, GLY, and PEG) with a 1^o alcohol or a carbonyl compound (acid and ester) present in the pyrolysis oil are schemed below. Hence, methanol, acetic acid, methyl acetate, and also water are considered because they are available (high %abundance) in the pyrolysis oils as reported (Maschio et al., 1992; Bridgwater, 1999; Oasmaa et al., 2003).

Resorcinol (RSL)-Esterification Rxns

- Step 1: Resorcinol + Acetic Acid → Resorcinol Monoacetate + Water

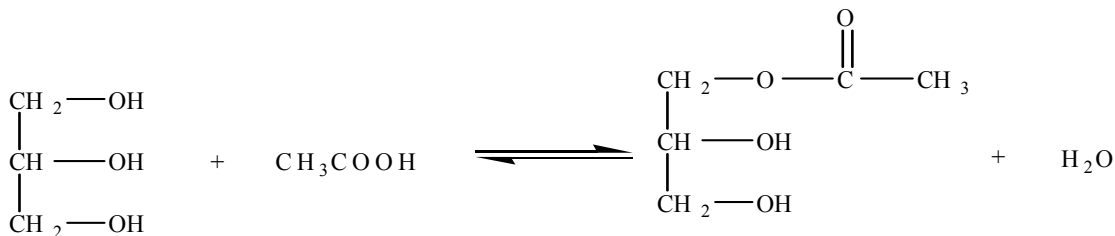


- Step 2: Resorcinol Monoacetate + Acetic Acid → Resorcinol Diacetate + Water

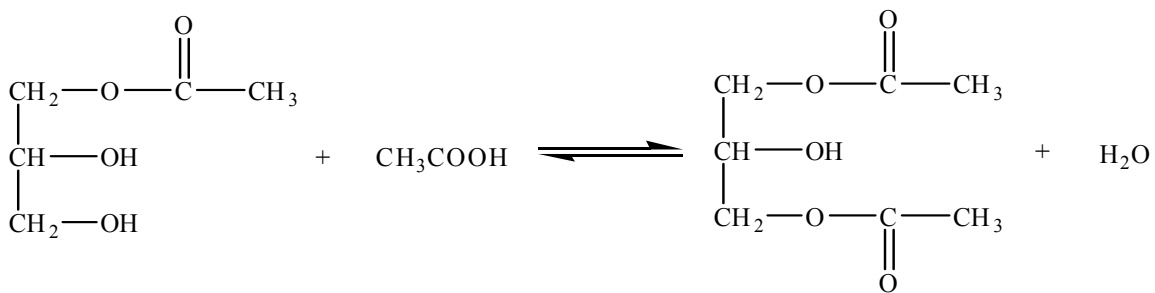


Glycerol (GLY)-Esterification Rxns

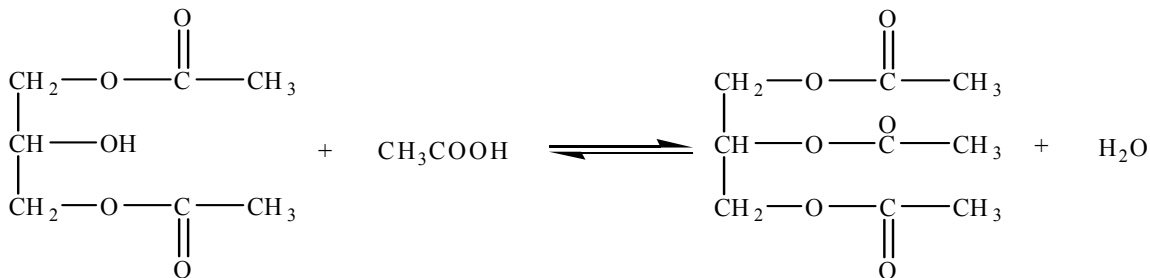
- Step 1: Glycerol + Acetic Acid ⇌ Glycerol Monoacetate (Monoacetin) + Water



- Step 2: Monoacetin + Acetic Acid ⇌ Glycerol Diacetate (Diacetin) + Water

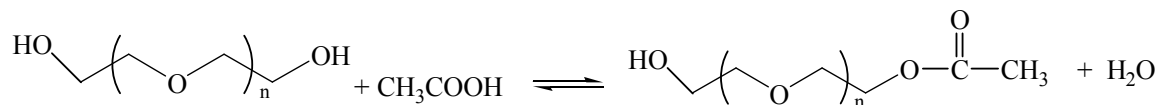


- Step 3: Diacetin + Acetic Acid ⇌ Glycerol Triacetate (Triacetin) + Water

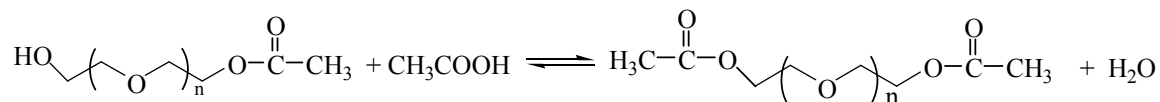


Polyethylene Glycol (PEG)-Esterification Rxns

- Step 1: PEG + Acetic Acid \rightleftharpoons Polyethylene Glycol Monoacetate (PGM) + Water



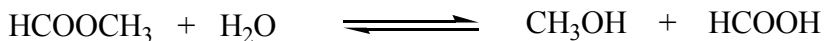
- Step 2: PGM + Acetic Acid \rightleftharpoons Polyethylene Glycol Diacetate (PGD) + Water



The above chemical reactions can ultimately contribute to a small increase in the initial oil viscosity with the exception of PEG (20000 g/mol). At the same time these reactions can prevent the complex polymerization reactions that are known to occur and destabilize the pyrolysis oils. The occurrence of complex polymerization reactions in the pyrolysis oils is imminent without the use of chemical additives (low/high molecular weight) at right concentrations. Hence, these complex polymerization reactions can contribute to a significant increase in the oil viscosity as a function of storage time and storage temperature. In contrast to the previous trends, the chemical additives namely anisole (ANS), ethanol (ETH), methyl ethyl ketone (MEK), methyl formate (MEF), and methanol (MEH) decreased the initial oil viscosity by 48, 68, 69, 70, and 71% respectively. Such decreases in the initial oil viscosity due to low molecular weight additives can be largely attributed to their physical dilution and reaction effects. Furthermore, the involvement of low molecular weight additives in the chemical reactions comprising of hydrolysis, esterification, acetalization, and acylation is schemed below.

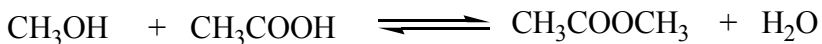
Ester (MEF)-Hydrolysis Rxn

- Methyl Formate + Water \rightleftharpoons Methanol + Formic Acid

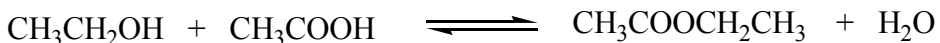


Alcohols (MEH and ETH)-Esterification Rxns

- Methanol + Acetic Acid \rightleftharpoons Methyl Acetate + Water

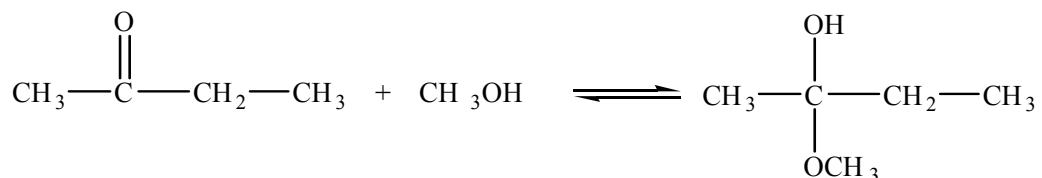


- Ethanol + Acetic Acid \rightleftharpoons Ethyl Acetate + Water

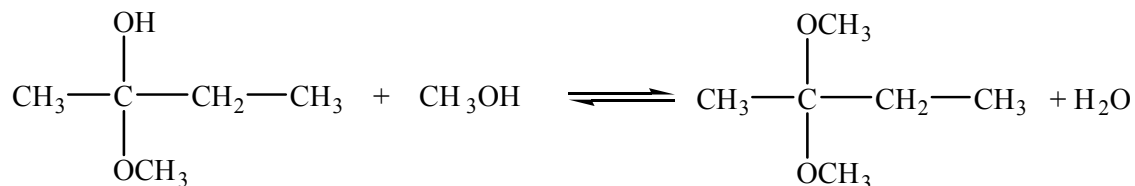


Ketone (MEK)-Acetalization Rxns

- Step 1: Methyl Ethyl Ketone + Methanol \rightleftharpoons Hemiacetal

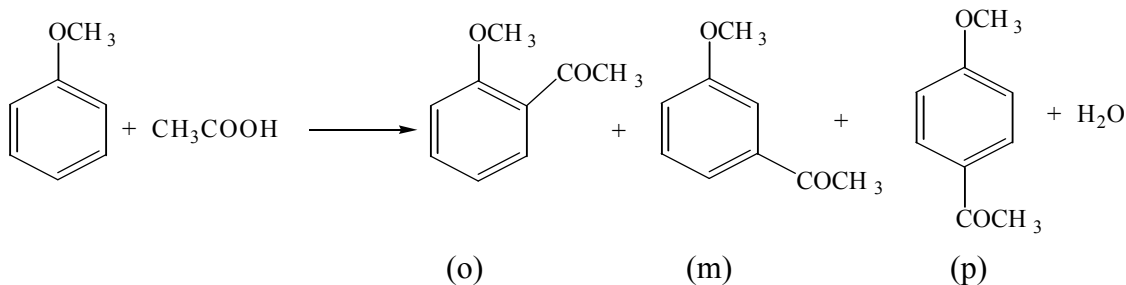


- Step 2: Hemiacetal + Methanol \rightleftharpoons Acetal + Water

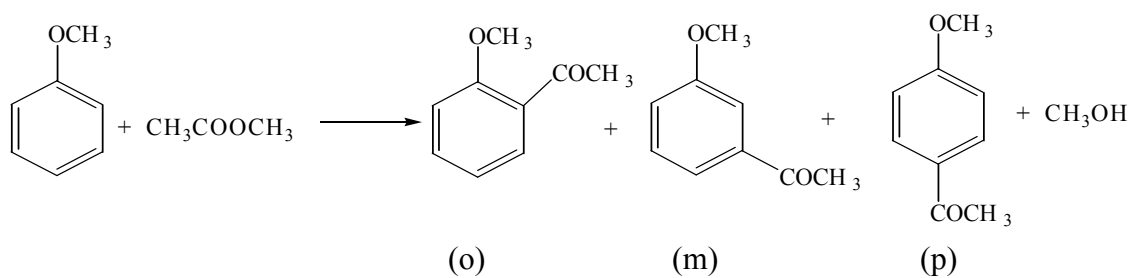


Aryl Ether (ANS)-Electrophilic Aromatic Substitution or Acylation Rxns

- Anisole + Acetic Acid \Rightarrow Methoxyacetophenone (o/p \gg m) + Water



- Anisole + Methyl Acetate \Rightarrow Methoxyacetophenone (o/p \gg m) + Methanol



The complex polymerization reactions that occur in the pyrolysis oils (>200 compounds) due to their prolonged storage can not be well established by using a single analytical tool or even kinetic studies (Mohan et al., 2006, Meier et al., 2002, Czernik, 1994). However, those reactions are expected to largely manifest in the form of viscosity, molecular weight and water content increases in the oils. The measurement of viscosity and water content at different storage times, storage temperatures, and additive concentrations was considered in this research. Therefore, the aim of this research was to study and predict the overall stability of pyrolysis oils as they aged.

Rheological Modeling (Shear Stress vs. Shear Rate)

The shear stress (dyne.cm^{-2}) of control and additive blended pyrolysis oils (ANS, GLY, and MEH) is plotted as a function of shear rate (s^{-1}) as shown in Figures 4.38-4.39. Different models were attempted to best fit the shear stress (y) versus shear rate (x) data using the TA advantage[®] data analysis software. Ultimately, two models with minimum standard error, maximum accuracy, and repeatability were selected. They are Power Law (PL) and Herschel Bulkley (HB) models as shown in Table 4.18. The PL or Ostwald de Waele model adequately described the flow behavior of pyrolysis oils at 0 hr. However, HB model adequately described the flow behavior of pyrolysis oils at 192 hr. This

transformation in the model with a storage time increase (0 to 192 hr) could very well be explained by the polymeric and phase changes that occurred during the prolonged heating of pyrolysis oils at 80 °C.

The standard error of PL models is observed to be lower than that of the HB models as shown in Table 4.18. The rate indices (n's) of PL models are close to unity which is in conformance with the Newtonian characteristics of pine wood pyrolysis oils. The ANS and GLY rate indices (n's) are close to unity with a minimal yield stress (τ_0) for the HB models. This trend indicates that ANS and GLY blended oils exhibit Newtonian properties at both 0 and 192 hr. The limiting viscosity (K) of GLY blended oil is observed to be similar to that of CTL for both storage times of 0 and 192 hr. Consequently, the original molecular structure of the pine wood pyrolysis oil might be less altered by GLY addition when compared to ANS or MEH addition. This phenomenon needs to be established by using a dynamic tool such as molecular modeling. The yield stress of CTL oil is twice high as that of MEH blended oil at 192 hr subsequently indicating a higher extent of polymerization. The PL exponents or rate indices (n's) of CTL and MEH models at 192 hr indicated Bingham Plastic flow behavior under the class of HB liquids. A similar classification is available for softwood and hardwood derived pyrolysis oils in the literature (Perez et al., 2006). As such, the Bingham plastic liquids are non-Newtonian liquids with a critical yield stress. These liquids begin to flow once the critical yield stress is exceeded. The flow behavior of both control and additive blended pyrolysis oils is affected by the unstable polymeric reactions. However, these reactions seem to be kinetically more favored for control oil rather than the additive blended pyrolysis oils.

Influence of Additive on the Water Content of Pyrolysis Oils

The influence of chemical additives on the water content of pyrolysis oils has been explored in this research using Karl Fisher analysis. All the additives (26) generally performed better than CTL for the storage times (6) tested. The water content increase (%) of pyrolysis oils with storage time (0 to 192 hr) is shown in Figure 4.40. Generally, the influence of storage time on the water increase of pyrolysis oils was more pronounced until 24 hr after which the water content reached a plateau. An example of this trend is shown in Figure 4.41 for alcohols.

At initial storage time (0 hr) all the additives consistently performed better than CTL, which had a maximum water content of 12.5 wt.%. The addition of alcohols had a beneficial effect on the stability of pyrolysis oils by lowering their initial water content by 8-16%. The addition of cyclic compounds to the pyrolysis oils resulted in the least decrease in their initial water content (2-3%). Generally, esters among all the additive groups produced the highest decrease in the initial water content of pyrolysis oils. Furthermore, methyl formate (MEF) decreased the initial water content of pyrolysis oil by 22.4% which was the maximum. The typical behavior for water content of control and additive blended pine wood pyrolysis oils as a function of storage time is depicted in Figure 4.42. The initial lowering in the water content is likely due to the consumption of some of the water molecules in hydrogen bonding (intermolecular) with the additive molecules. Consequently, this drop seems to increase with the hygroscopicity or hydrophilicity of additive. But during the aging reactions of pyrolysis oils at 80 °C the water molecules are expected to break away from the hydrogen bonding and hence

become available as free water for the Karl Fisher analysis. Contrarily, the water content of control oil continued to show an increase during the entire aging period (192 hr).

At final storage time (192 hr) all the additives performed better than CTL by decreasing oil water content except 2-furaldehyde (2FL), which resulted in the same amount of water as CTL (14.7 wt.%). Among ethers, ethyl ether (EEE) performed better than CTL by showing 17% less water. Furthermore, EEE resulted in the least amount of water among all the additives selected. Among alcohols, the water content measurements of resorcinol (RSL) and furfuryl alcohol (FAL) blended oils were not possible at 192 hr because these oils completely polymerized at storage times of 24 hr (RSL) and 96 hr (FAL). Hence, the RSL and FAL peaks shown in Figure 4.40 correspond to the water content increases (%) obtained at these storage times (RSL: 0-24 hr, FAL: 0-96 hr). The FAL and RSL blended oils are observed to be the least stable oils in this phase.

The water content of pyrolysis oils is observed to increase significantly for the pyrolysis oils that are aged to 192 hr. An increase of 17.9% in the water content is observed for the CTL oil. A minimum water content increase of 1.9% is observed for decahydronaphthalene (DHN) as shown in Figure 4.40, while a maximum increase of 38% is observed for ethyl acetate (ETA). Although, DHN significantly minimized the water content increase of pine wood pyrolysis oil, the viscosity increase due to its addition is observed to be high (352%) as previously shown in Figure 4.36. Hence, DHN is not a suitable additive for stabilizing pyrolysis oils.

As a general trend, both esters and aldehydes are observed to have the highest water content increase (0 to 192 hr) compared to the other additive groups (4) tested. Cyclic compounds on the contrary seem to show the lowest water content increase.

Regardless, the water content of pyrolysis oils (27) during the entire storage period (192 hr) did not reach the critical levels of 30-35 wt.%. Hence, phase-separation of the oils was not apparent but they showed varying degrees of polymerization in viscosity or water content increases. The pine wood pyrolysis oils produced from the auger reactor were quickly quenched and fractionated into aqueous rich and organic rich fractions. Thus, the multiple effect condensers (series) removed most of the water present in the pyrolysis oil to a concentration level of 12 wt.% or less for wood derived pyrolysis oils, and 18 wt.% or less for bark derived pyrolysis oils. However, a further increase (2-4 wt.%) in the water content beyond these concentrations during storage (ambient or accelerated) is not expected to significantly affect the oil stability.

Influence of Additive on the pH of Pyrolysis Oils

The pH of pyrolysis oils is not observed to significantly vary with storage time. An example of the pH of control and additive blended pyrolysis oils obtained initially (0 hr) is shown in Figure 4.43. The lowest initial pH (2.3) can be observed for ethyl acetate (ETA) blended pyrolysis oil. However, the highest initial pH (3.0) is observed for glycerol (GLY), furfuryl alcohol (FAL), cyclohexane (CHX) and tetrahydronaphthalene (THN) blended pyrolysis oils. Similar pH values within the experimental margin of error ($\pm 5\%$) are obtained at 192 hr for the above additive blended oil samples. There is a high likelihood that the experimental occur during pH measurements increased with storage time because of an increase in the oil viscosity. Consequently, the oils aged to 192 hr are associated with the maximum error. Among ketones, cyclopentanone (CPE) blended pyrolysis oil is observed to have the lowest pH for all aging periods. Among ethers, ANS

blended pyrolysis oil is observed to have the lowest pH for all aging periods. The difference in pH of the CPE and ANS blended oils from the respective group additives is distinguishable as the storage time is increased beyond 48 hr.

Most additives were observed to have an insignificant impact on the pH of pyrolysis oils with the exception of GLY, FAL, CHX, and THN. These additives showed a mild increase (6.6%) in the initial oil pH due to mixing. A typical example of oil pH as a function of storage time can be seen from Figure 4.44. There seems to be a slight decrease in the pH of alcohol blended pyrolysis oils as the storage time is increased from 0 to 48 hr. However, most of these changes in pH are found within the experimental margin of error ($\pm 5\%$). Hence, it is surmised that a total acid value test would better reveal the differences in acidic concentration of aged pyrolysis oils.

Statistical Analysis

Statistical analysis of variance (ANOVA) is conducted using the stability data (viscosity and water content) of pyrolysis oils. During the analysis, RSL and FAL data is excluded as these additives completely polymerized the pine wood pyrolysis oils at storage times of 24 and 96 hr respectively. This task was essential to bring a balanced data analysis of the oil storage stability. After excluding RSL and FAL, the 24 additives were further reclassified into 8 chemical groups as shown in Table 4.19. This task was performed to minimize the convolution of additives during the least significant difference (LSD) testing. A critical value of 1.97 (t) is used for all LSD comparisons during the viscosity data analysis. It should be recalled that the viscosity testing was performed in single replicate whereas duplicate testing was conducted for water content. Hence, to

increase the statistical confidence in the ANOVA model predictions, the viscosity data obtained at different shear rates (1, 2, 10, 20, 100, 200 s⁻¹) and measurement temperatures (25, 50, and 80 °C) was combined. The resulting ANOVA model produced better analysis of the viscosity results when the above shear rates (6) and measurement temperatures (3) were combined for the 24 additives. Likewise, the water content data collected at storage times (0 and 192 hr) is combined to perform ANOVA. A critical value of 1.99 (t) is used for all LSD comparisons during the analysis of oil water content.

Alcohols are the single largest group chosen in this study as they are known to stabilize the pyrolysis oils effectively (Oasmaa and Czernik, 1999; Doshi et al., 2005, Oasmaa et al., 2004). Furthermore, an additive concentration of 5-10% has been reported to stabilize the pyrolysis oils effectively (Diebold, 2000; Oasmaa et al., 2004). Hence, an additive concentration of 10% was utilized during prescreening studies or phase 2. Furthermore, additive concentration ($0 \leq X \leq 20$, X=additive concentration in wt.%) has been optimized during phase 3 of this research by utilizing the prescreened additives from phase 2. During statistical analysis, each group shown in Table 4.19 is treated as a block based on the functional group and chemical structure of additives. This is imperative to study the impact of different additives on the stability of pyrolysis oils.

Different ANOVA models were evaluated for viscosity and water content data by varying the number of interactions of treatment variables. Eventually, those models were selected, which closely predicted with the experimental data trends as previously seen. The treatment variables used for the ultimate viscosity model are chemical additive group (BLK), shear rate, viscosity temperature, and additive. The percentage increase in viscosity (PINC) from 0 to 192 hr is considered as the response variable after

transforming the viscosity data using a natural logarithmic function (Ln_ePINC). This transformation was essential to increase the normality of the viscosity data. The mean response variable is later used as a statistical index to compare the storage stability of different pyrolysis oils.

The treatment variables used for the water content model are additive group (BLK), additive, and storage time. The water content data obtained from the Karl Fisher analysis of pyrolysis oils is used as a response variable. The water content data obtained at smaller storage times did not show a significant variation. Hence, to maximize the variation in the water content of pyrolysis oils, the storage times of 0 and 192 hr are only utilized during statistical analysis. Both viscosity and water content models (ANOVA) are statistically significant at an observed significance level (OSL) or p-value of 0.05. The same OSL or p-value is used to check the significance of treatment variables and their interactions. Both these models possess a high regression coefficient ($R^2 > 0.98$) indicating a strong fit between the response and treatment variables. Additionally, a very low mean square error (MSE) is obtained for both the models even though a minimum number of replicates were used.

Viscosity Model (ANOVA)

The variable, level, and treatment input information of the viscosity model is shown in Table 4.20. The extended SAS[®] output of the viscosity model is shown in Tables 4.21-4.25. A total of 450 observations (Shear Rate*Measurement temperature *Additive= $6*3*25$) are used in this model. The ANOVA model obtained for the treatment variables and their interactions (2-way) is shown in Table 4.21. All the

variables and interactions are observed to significantly affect the viscosity of pyrolysis oils.

The LSD comparisons obtained for the mean viscosity of different additive groups (Blocks) within 95% confidence limits is shown in Table 4.22. The control in comparison with all the additive groups is observed to differ significantly with respect to the mean viscosity. The highest difference in mean viscosity (+1.02) is observed for ‘control and alcohols’ indicating that alcohols result in the least viscosity increase (VI) among all the additive groups. The means of different additive groups are observed to differ significantly ($\alpha=0.05$) except ‘ethers and esters’, ‘ethers and aldehydes’, and ‘esters and aldehydes’.

The LSD output obtained for the treatment variable ‘shear rate’ is shown in Table 4.23. All the shear rates ranging 1-100 s^{-1} were observed to significantly differ with respect to the mean VI of pyrolysis oils. However, the shear rates of 100 and 200 s^{-1} do not differ significantly with respect to their mean VI. These two trends are attributed to the complete transformation in pyrolysis oil flow behavior (Newtonian to non-Newtonian) usually observed at storage times of 96 and 192 hr. The LSD output obtained for the treatment variable ‘viscosity temperature’ is shown in Table 4.24. The mean viscosity increases of all the pyrolysis oils differed significantly as a function of measurement temperature. Consequently, the highest mean VI is obtained at 50 $^{\circ}C$ whereas the lowest mean VI is obtained at 80 $^{\circ}C$. The anomalously high value of mean VI at 50 $^{\circ}C$ compared to 25 $^{\circ}C$ is not discounted as the mean response variable used is based on the % calculation. However, experimental evidence clearly indicated that the

actual viscosity of pyrolysis oils is inversely proportional to the measurement temperature.

The LSD output obtained for the treatment variable ‘additive’ is shown in Table 4.25. Among all the additives (24) analyzed, 2-furaldehyde (2FL) showed the highest mean VI while anisole (ANS) showed the lowest. Further, 2-furaldehyde (2FL) and xylene (XYL) blended oils are observed to have significantly higher mean VI than that of control (CTL) and they all differed significantly from each another. This trend is attributed to a high degree polymerization caused by the additives 2FL and XYL. The chemical additives ‘methyl ethyl ketone (MEK) and ethyl ether (EEE)’ do not differ significantly in increasing the oil mean viscosity. Likewise, the chemical additives ‘ethyl ether (EEE) and acetaldehyde (ACH)’ do not differ significantly in increasing the oil mean viscosity. Hence, the stabilizing effect of these four additives can not be verified independently due to their convolution in the mean VI, the representation of which is shown by ‘line and dotted’ circles in Table 4.25. Here, convolution is defined as the overlapping in the mean viscosity increase of different additives. The additives (9) that are convoluted with respect to their mean VI include acetaldehyde (ACH), ethylene glycol dimethyl ether (EGD), ethyl ether (EEE), ethyl acetate (ETA), methyl ethyl ketone (MEK), methyl acetate (MEA), 2-propanol (2PL), tetrahydronaphthalene (THN), and tetrahydrofuran (THF).

Generally, alcohols showed the best performance based on the increase in oil mean viscosity. The alcohols ‘ethanol (ETH), polyethylene glycol (PEG), and glycerol (GLY)’ differed significantly with respect to the mean VI and are found in the top four additives (ANS included) based on the lowest mean VI. Methanol produced relatively

low mean VI whereas additives '2-propanol (2PL) and t-butanol (TBL)' showed relatively high mean VI. The participation of the lone hydroxyl group (2PL-2⁰ and TBL-3⁰) in a simple polymerization reaction such as esterification seems to be sterically hindered by the adjacent methyl groups. As a result, 2PL and TBL were relatively ineffective in preventing the complex polymerization reactions and also the high VI.

The relatively high molecular weight (MW) additives such as ANS, GLY, PEG, and CHX have performed better than the relatively low MW additives such as MEH, 2PL, ACT. This trend could be due to the fact that low MW additives did not perform well at large storage times exceeding 48 hr. High MW additives on the contrary are expected to cause the least VI of pyrolysis oils at these storage times. The best three additives based on their lowest mean VI are ANS, GLY, and PEG. However, MEH is selected as a base evaluation additive in precedence of PEG during the phases 3-4 of this research.

Water Content Model (ANOVA)

The variable, level, and treatment information of the water content model is shown in Table 4.26. The extended SAS[®] output of the water content model is shown in Tables 4.27-4.30. A total of 100 observations (additive*storage time*replicate = 25*2*2) are used in this model. The ANOVA model obtained for the treatment variables is shown in Table 4.27. All the variables are observed to significantly affect the water content of pyrolysis oils.

The LSD comparisons obtained for the mean water content of different additive groups (Blocks) within 95% confidence limits is shown in Table 4.28. The control in

comparison with all the additive groups is observed to differ significantly with respect to the mean water content. The highest difference in mean water content (+2.09) is observed for ‘control and ethers’ indicating that ethers resulted in the least amount of water among all the additive groups. The means of different additive groups are observed to differ significantly ($\alpha=0.05$) except ‘alcohols and aromatics’, ‘alcohols and aldehydes’, ‘heterocyclics and aldehydes’, ‘heterocyclics and monocyclics’, ‘aromatics and aldehydes’, and ‘aldehydes and monocyclics’.

The LSD output obtained for the treatment variable ‘storage time’ is shown in Table 4.29. Both the storage times (0 and 192 hr) are observed to significantly affect the mean water content of pyrolysis oils with 192 hr being the highest. The LSD output obtained for the treatment variable ‘additive’ is shown in Table 4.30. Control (CTL) is observed to have the highest mean water content (13.63%) among all the pyrolysis oils. But it is well below the critical water content (30%) needed to phase separate the pyrolysis oils. Generally, ethers are observed to have the lowest mean water content among all the additive groups evaluated. Further, the chemical additives ‘Isopropyl ether (IPE), methyl butyl tertiary ether (MTB), methyl formate (MEF), and ethyl ether (EEE)’ do not differ significantly from each other with respect to the mean oil water content. The lowest mean water content of ether blended pyrolysis oils is probably due to the fact that ethers did not take part in simple polymerization reactions (Ex: esterification) that usually release water as a byproduct. That also means the two lone-paired e^- of the oxygen atom (Ether = $R^1-\ddot{O}-R^2$, where $R^1, R^2 =$ Alkyl Groups, $O=$ oxygen) are available to form

hydrogen bonding (intermolecular) with the surrounding water molecules. Hence, the availability of free water during the Karl Fisher reaction might be decreased.

All the additives except 'CTL, IPE, MTB, MEF, and EEE' showed a high degree of convolution in the LSD output as shown in Table 4.30. Here, convolution is defined as the overlapping in the mean water content of different additives. A higher degree of convolution in the water content model compared to the viscosity model seems to be because of the small variability in the water content data. Because of this limitation the best three additives (ANS, GLY, and MEH) for phase 3 studies are chosen based on the mean viscosity model only.

Concentration Optimization (Phase III)

Introduction

As discussed in Chapter 3, concentration optimization was performed using pine wood pyrolysis oil (low temperature) to optimize the concentration of prescreened additives from phase 2. The prescreened additives include anisole (ANS), glycerol (GLY), and methanol (MEH). By varying additive concentration the chemical and physical properties of the 13 pyrolysis oils (1-control and additive blended-12) were analyzed. They include viscosity, storage modulus, loss modulus, water content, and pH. A storage temperature of 80 °C was utilized to evaluate the stability of pyrolysis oils as a function of additive concentration and storage time. The additive concentrations are 0, 5, 10, 15, and 20 wt.% and storage times are 0, 24, 96, and 192 hr. Statistical analysis of variance (ANOVA) is utilized to specifically model the effects of additive concentration on the viscosity (cP) increase and water content (%) increase of pine wood pyrolysis oils.

Rheological Flow Behavior of Pyrolysis Oils

The rheological flow behavior of the pine wood pyrolysis oils is studied in this phase as a function of shear rate, shear stress, additive concentration, and storage time. As seen in phase 2, most pyrolysis oils exhibit Newtonian behavior during the initial aging period (0-24 hr) independent of additive concentration. However, during the final aging period (96-192 hr) a complete transformation in the oil flow behavior that is from Newtonian to pseudoplastic or shear thinning is observed. This phenomenon can be explained by the accelerated aging reactions that occur during the oil storage. Further, the viscosity (25 °C) of pyrolysis oils is observed to increase dramatically at low shear rates ($\leq 10 \text{ s}^{-1}$) because of the apparent transformation of their flow behavior from 24 to 96 hr. However, at high shear rates exceeding 10 s^{-1} , the increase in oil viscosity as a function of storage time is not significant. At the initial storage time (0 hr) all the additives [ANS (A10), GLY (G10), and MEH (M10)] with 10 wt.% concentration are observed to closely emulate Newtonian behavior as shown in Figure 4.45. However, at the final storage time (192 hr), these additives exhibit pseudoplastic behavior with the exception of GLY as shown in Figure 4.46. The Newtonian flow behavior of GLY at 192 hr is observed only when its concentration exceeded 5 wt.% (G5) as shown in Figure 4.47. To ascertain this unique flow characteristic of GLY blended oils shear stress (SS) as a function of shear rate (SR) is considered.

The SS as a function of SR for control (CTL) and GLY blended pyrolysis oils (5-20 wt.%) is shown in Figures 4.48-4.52. Similar trends (SS vs. SR) are obtained for CTL (0 wt.%) and GLY (5 wt.%) oils at all storage times as shown in Figures 4.48-4.49. A linear correlation between SS and SR is nearly achieved for GLY at 10 wt.%

concentration as shown in Figure 4.50. However, as the GLY concentration is increased above 10 wt.% a perfectly linear relationship between SS and SR is obtained at all storage times as shown in Figures 4.51-4.52. At small storage times (≤ 24 hr), similar values of SS are obtained for all the shear rates and GLY concentrations. However, at low shear rates (≤ 1 s⁻¹) and large storage times (≥ 96 hr), the low concentrations of GLY (<10 wt.%) seems to produce a stronger dependency of SS on the SR. Furthermore, at all storage times and GLY concentrations of 15 and 20 wt.%, the pine wood pyrolysis oils exhibit Bingham plastic characteristics, but with minimal yield stresses ranging from 0.01-1.0 dyne/cm². These trends imply that the GLY blended oils (>5 wt.%) have a greater tendency to retain the Newtonian flow behavior of pyrolysis oils regardless of the aging period. Among the three additives tested, GLY only showed the above trends indicating its superior flow and stabilizing properties for relatively long aging periods.

Temperature Effects on the Oil Viscosity

The effects of measurement temperature on the viscosity of CTL (0 wt.%) and GLY (10 wt.%) blended oils are shown in Figures 4.53-4.58. Each figure shows the oil viscosity measured at shear rates of 1 s⁻¹ (SR1), 10 s⁻¹ (SR10), and 100 s⁻¹ (SR100). Furthermore, the oil viscosity at each temperature (25, 50, and 80 °C) is successively shown in Figures 4.53-4.55 (CTL) and Figures 4.56-4.58 (GLY). The viscosity showed a decreasing trend as a function of temperature for all the pyrolysis oils. Generally, the flow behavior of GLY blended oils (≥ 10 wt.%) remained Newtonian for all the storage times. Contrarily, the additive blended pyrolysis oils (ANS and MEH) behaved like

Newtonian at small storage times and exhibited pseudoplastic tendency at large storage times.

As shown in Figure 4.53, the pyrolysis oil (CTL) remained stable during the initial aging period (0-24 hr) as the increase in viscosity is negligible. Further the effect of shear rate is not apparent during this period. But beyond the initial aging period the CTL viscosity increased rapidly until 96 hr. During the middle aging period (24-96 hr) most chemical changes that occurred in the oil are indicated by a sharp viscosity increase. However, the viscosity of the oil seems to level off during the final aging period (96-192 hr) suggesting that the chemical reactions are nearly complete. After the initial aging period viscosity (25 °C) of CTL oil is dependent on the shear rate because of the transformation in flow behavior from Newtonian to pseudoplastic. The above trend also occurred for ANS and MEH blended pyrolysis oils at low temperature (25 °C) and high concentrations (≥ 10 wt.%). However, at high temperatures (50 and 80 °C) and low additive concentrations (≤ 5 wt.%) the above trend was observed with a lower consistency for ANS and MEH blended pyrolysis oils. A similar trend in the oil viscosity as that of 25 °C is observed at 50 °C from Figure 4.54, but the oil viscosities measured are consistently lower for all the shear rates. However, the oil viscosity did not reach a plateau when measured at 80 °C regardless of the storage time as shown in Figure 4.55. The oil viscosity at 80 °C is consistently lower than that of 25 and 50 °C establishing the inverse proportionality between viscosity and temperature. At a high temperature of 80 °C the effect of shear rate on the oil viscosity decreased significantly during the middle aging period as visualized from Figure 4.55. After which a continued increase in the oil viscosity is observed during the final aging period nevertheless of shear rate.

These trends seem to indicate that the unblended oil (CTL) underwent a major change in its chemical structure at a high temperature (80 °C). Such a structural change is responsible for the continued increase in oil viscosity during the entire aging period. The above trend is most likely associated with ANS and MEH blended oils but not GLY blended oils. Consequently, the variation in viscosity due to the temperature is observed to be negligible for GLY blended pyrolysis oils independent of shear rate. An example of this trend is shown for GLY (10 wt.%) in Figures 4.56-4.58. This trend also repeated for glycerol blended oils (>10 wt.%) implicating that addition of GLY will be beneficial for lowering the pumping costs. Furthermore, the addition of GLY by a mandatory level of 10 wt.% is expected to result in the fewest changes in the oil properties as a function of temperature.

Additive Concentration Effects on the Oil Viscosity

The effect of ANS concentration (5, 10, and 15 wt.%) on the oil viscosity is shown in Figures 4.59-4.61. Further, each figure represents the oil viscosity as a function of shear rate [1 s^{-1} (SR1), 10 s^{-1} (SR10), and 100 s^{-1} (SR100)] and storage time (0, 24, 96, and 192 hr). The ANS concentration of 10 wt.% seems to result in the most stable oil as its viscosity reached a plateau during the final aging period. This trend is independent of the shear rate as shown in Figure 4.60. Contrarily, the ANS concentrations of 5 and 15 wt.% steadily increased the oil viscosity during the entire aging period. This trend is independent of shear rate as shown in Figures 4.59 and 4.61. The effect of GLY concentration ($\geq 5 \text{ wt.}\%$) on the viscosity of pyrolysis oils is shown in Figures ‘4.56 and 4.62-4.64’ for the shear rates of 1, 10, and 100 s^{-1} . By increasing the GLY concentration

from 5 to 15 wt.%, the viscosity dependence on shear rate is completely eliminated at higher glycerol levels as shown in Figures 4.62-4.63. Further increase in the GLY concentration from 15 to 20 wt.% did not produce a marked decrease in oil viscosity for all the storage times and shear rates as shown in Figures 4.63-4.64. The effect of MEH concentration (5, 10, and 15 wt.%) on the oil viscosity is shown in Figures 4.65-4.67 for the shear rates of 0.1, 1, and 100 s⁻¹. The MEH concentrations of 5 and 10 wt.% seem to produce more stable pyrolysis oils than MEH 15 wt.% as the viscosity increase seems to level off during the final aging period as shown in Figures 4.65-4.66. However, the viscosity of MEH 15 wt.% oil revealed a continued increase during the entire aging period as shown in Figure 4.67. Generally, ANS and GLY produced the lowest viscosity increase during middle and final aging periods whereas, MEH produced the least viscosity increase during the initial storage period. This could be due to the fact that methanol is converted from a primary alcohol to a primary ester relatively fast during the aging process. However, due to the presence of three hydroxyl groups (-OH), the esterification reaction in GLY is expected to occur at a slower rate compared to MEH. The gas chromatography and mass spectrometry (GC-MS) evidence from the literature indicated higher concentrations of esters 'methylacetate and methylstearate' in the aged oils (room and accelerated temperature-80 °C) compared to the raw pyrolysis oils. Thus, the net increase in ester concentration of pyrolysis oils with aging time is due to the involvement of methanol in the methylation reaction (Diebold and Czernik, 1997; Boucher et al. II, 2000).

The increase in oil viscosity (%) obtained as a function of storage time (0 to 192 hr) at a shear rate of 100 s⁻¹ is shown in Figure 4.68. A concentration of 10 wt.% (C10)

produced the least increase in viscosity of ANS and MEH blended oils. However, a concentration of 20 wt.% (C20) produced the least increase in viscosity of GLY blended oils. All additive concentrations (C5 through C20) of GLY and MEH performed better than CTL (C0) as indicated by a lower viscosity increase. However, the ANS concentrations of 5 wt.% (C5) and 15 wt.% (C15) did not perform better than CTL (C0) as indicated by a higher viscosity increase. This sporadic behavior of ANS (5 wt.%) or C5 and ANS (15 wt.%) or C15 blended oils is attributed to the excessive polymerization and phase separation as explained later.

Moduli Studies

Dynamic or oscillatory testing was performed at 25 °C to evaluate the effects of additive, concentration, and storage time on the moduli properties of pine wood pyrolysis oils. The moduli measurements (dyne/cm²) include storage modulus (G') and loss modulus (G''). The definitions of G' and G'' are already discussed in Chapter 3 of this document. A wide range of angular frequency ($\omega = 0.3$ to 30 rad/s) was used to understand the structural properties of pyrolysis oils. Consequently, the moduli (G' and G'') data is used to qualitatively interpret the pyrolysis oil stability based on its structural properties. Higher storage moduli ($G' > G''$) values indicate the presence of a solid-like network in the pyrolysis oils. Contrarily, higher loss moduli ($G'' > G'$) values indicate the presence of a gel-like network in the pyrolysis oils. The presence of a strong or a weak network in the pyrolysis oils is a direct function of the extent or degree of polymerization (DP). The DP of a polymer has been defined as the number of repeat units present in a

polymer chain (Rosen, 1982). Generally, it should be noted that gel-like behavior is observed for the pyrolysis oils based on their moduli values.

A large increase in G' and G'' ($G'' \gg G'$) is observed for CTL and ANS (15 wt.%) or A15 blended pyrolysis oils as the storage time is increased from 24 to 96 hr. A graphical depiction of this trend is shown for A15 in Figures 4.69-4.70. A small increase in the modulus values can be seen during the initial and final aging periods. However, the most increase in the modulus values can be visualized during the middle aging period. This indicates that most structural changes in the pyrolysis oil occur during the middle aging period as stated previously. A steep increase in G' and G'' can be seen over 3-4 orders of magnitude during the initial aging period. This suggests that the modulus (storage or loss) of pyrolysis oil is a strong function of frequency due to its pristine and stable nature. However, during the final aging period relatively flatter response of moduli as a function of frequency is obtained over 1-2 orders of magnitude. Evidently, the modulus dependency on the frequency is reduced because of the polymeric nature of significantly aged oils. Among oils blended with ANS, GLY, and MEH at 15 wt.% concentration (A15, G15, and M15) the flatter response of moduli versus frequency was obtained for A15 only at 96 and 192 hr. This is indicative of the fact that A15 resulted in the least stable pyrolysis oil at these storage times. Contrarily, the modulus of G15 and M15 showed a strong dependency on the frequency regardless of storage time as shown in Figures 4.71-4.74.

The DP of pyrolysis oil is expected to increase with storage times regardless of its chemical stability. This trend can be visualized for G15 and M15 blended pyrolysis oils as shown in Figures 4.71-4.74. Among the additive blended oils (15 wt.%), the G15 oil

seems to be the most stable pyrolysis oil as visualized from Figures 4.71-4.72. The increase in G' (dyne/cm²) for G15 oil as a function of ω (rad/s) is observed over 4-5 orders of magnitude. Clearly the modulus (G' or G'') of G15 is observed to vary the least as a function of storage time followed by M15 as shown in Figures 4.73-4.74. This trend indicates that the chemical structure of GLY blended pyrolysis oils compared to ANS and MEH blended oils, remains relatively unaffected for long storage times. The modulus (G' and G'') for ANS blended oil reached a maximum of $\sim 100,000$ dyne/cm². However, the moduli for GLY and MEH blended oils were well below 100 and 1000 dyne/cm² respectively. This large difference in the modulus seems to indicate that alcohols (GLY and MEH) play a better role of maintaining the oil stability (low DP) as a function of storage time.

Discrete data distribution (G' vs. ω) is obtained for G15 (96 hr) and M15 (0 hr) oils as shown in Figures 4.71 and 4.73. The lack of established structural network is predicted to be responsible for the anomalous behavior of these oils. However, ANS addition to the pyrolysis oils resulted in a complete data distribution (G' vs. ω) even at the beginning of test (0 hr). This seems to indicate that ANS has a stronger tendency to form a structural network with the pine wood pyrolysis oil. An example of this trend is shown in Figure 4.69 for A15. In general, complete distribution (G' vs. ω) was attained for most oils when the storage time exceeded 24hr.

Anisole or methoxy benzene is known to be present in the pyrolysis oil but seemingly in small quantities (Bridgwater, 1996). By increasing the concentration of ANS as an additive, aromatic substitution in the presence of an electrophile or a nucleophile is likely to occur in the pyrolysis oil. An electrophile also Lewis acid is an

electron-deficient species whereas a nucleophile or a Lewis base is an electron-rich species. Depending on the position of substitution (o-ortho, p-para, and m-meta) the methoxy group in anisole can act as an electron donating (o/p directing) or electron withdrawing group (m directing). Electron donation to the aromatic ring is expected to occur by the positive inductive effect (+I) whereas the electron withdrawing from the aromatic ring is expected to occur by the electronegative effect (-I). Hence, a negative or a positive charge resonates on the carbon atoms of benzene ring due to these inductive effects. This charge is eventually balanced by forming a bond with the oppositely charged species from the pyrolysis oil. The possible reactions of ANS are discussed in Chapter 2.

The high stability of GLY blended oil among all the oils can be seen from Figures 4.75-4.76. At a concentration of 15 wt.% (G15) and a storage time of 192 hr, GLY resulted in the lowest values of moduli (G' and G'') along with a strong dependency on the frequency (ω). The presence of triple hydroxyl groups in GLY favors the structural formation or alignment of fresh pyrolysis oil through hydrogen bonding. Another possibility is the formation of a glyceryl ester (discussed in Chapter 2) by reacting with a carboxylic acid during the aging process.

The effects of additive, concentration, and frequency on the moduli properties of pine wood pyrolysis oils are shown in Figures 4.77-4.82. These oils were aged to 192 hr and the moduli measurements were performed at 25 °C. Generally, it is observed that the modulus (storage or loss) of pyrolysis oils decreased as the additive concentration is increased. This is attributed to the greater stabilizing effects of higher concentrations of an additive. The gel-like behavior of the pyrolysis oils (pine wood) is established since their loss modulus (G'') is observed to be much greater than their storage modulus (G')

regardless of additive and concentration. Similar results of moduli are reported for hardwood pyrolysis oil rich in fibers measured at 30 °C (Perez et al., 2006). The authors have also shown that the increased dependency of modulus on the frequency means weaker cross-links are present in the softwood bark oil with the structural network not fully established. The moduli test results obtained in this study indicate the following trend for the additives regardless of their concentrations.

$$X (\text{GLY}) \ll X (\text{MEH}) \ll X (\text{ANS}), \text{ Where } X = G', G''$$

The above relationship indicates that the most stable oils are obtained by the addition of GLY and the least stable oils are obtained by the addition of ANS.

Among all the ANS blended oils, ANS (10 wt.%) or A10 resulted in lowest modulus for the frequency range evaluated as shown in Figures 4.77-4.78. This indicates that A10 produces the most stable oil among the ANS blended oils by minimizing the extent of polymerization. As shown in Figure 4.77, ANS (5 wt.%) or A5 and A10 show identical response (G' vs. ω) at high frequencies (≥ 5 rad/s). The pyrolysis oils showed near identical response (G'' vs. ω) at ANS concentrations of 5 wt.% (A5), 10 wt.% (A10), and 20 wt.% (A20). Also, CTL (0 wt.%) or A0 and ANS (15 wt.%) or A15 do not differ significantly with respect to $G'-G''$ suggesting that A15 resulted in the least stable oil. Hence, increasing the ANS concentration above 10 wt.% was not beneficial in stabilizing the pine wood pyrolysis oils. To ascertain this behavior of ANS, $G'-G''$ data is plotted as a function of angular strain (%) as shown in Figures 4.83-4.84. Here, angular strain can be defined as the rate of change of angular displacement (Zong-da, 1984). Clearly, A10 provided the highest stability based on its linear viscoelastic (LVE) response. Among all

the concentrations used, the LVE response indicates that A10 blended oil requires the highest amount of energy to totally disrupt its chemical structure.

As shown in Figures 4.79-4.80, GLY concentrations exceeding 5 wt.% (G5) did not show a significant variation in the modulus. This trend is valid for both G' and G'' with the G' showing minimal variation especially at higher frequencies. This phenomenon occurred in the case of GLY only indicating that a concentration of 10 wt.% (G10) is sufficient to stabilize the pyrolysis oil. The concentrations of 0 wt.% (G0) and 5 wt.% (G5) resulted in the least stable GLY blended oils. Nevertheless, among all the additives at 5 wt.% concentration G5 seems to produce the most stable oil. The moduli response as a function of strain (%) obtained for the additive blended oils (5 wt.%) is shown in Figures 4.85-4.86. Clearly, G5 needs the highest amount of energy to disrupt its chemical structure much beyond the critical strain (2.5%).

A steady decrease in the modulus as a function of additive concentration can be seen for MEH in Figures 4.81-4.82. This behavior is unique to MEH only indicating that 20 wt.% (M20) concentration resulted in the most stable pyrolysis oil (MEH blended). That also means M20 blended oil is least susceptible to the chemical changes that occur during the storage. The MEH concentrations of 5 wt.% (M5) and 10 wt.% (M10) do not seem to differ significantly with respect to G' - G'' . The sinusoidal curve like response obtained for M5 and M10 blended oils indicates the presence of multiple phases. Furthermore, these phases are expected to release different packets of elastic energy when subjected to angular strain. The multiple phases (sol-gel) reported to be present in the oil are heavy compounds, waxy crystals, aqueous droplets, and char particles (Perez et al., 2006). The multi-phase behavior of the fresh and stored pine bark oils is verified by

the microscopic images obtained as shown in Figures 4.87-4.88. The images obtained at a higher magnification (200X) clearly indicate the presence of crystalline and particulate matter, the formation of which seems to be related with the aging time.

Additive Concentration Effects on Oil Water Content

A typical example of the concentration and storage time effects on the water content of pine wood pyrolysis oils is shown for ANS in Figure 4.89. The water concentration for all the pine wood oils ranged from 8-20 wt.%. Anomalously low concentration of water is obtained at 192 hr for A5 and A15 blended oils as shown in this figure. Further these oils showed a very high increase in viscosity compared to CTL as shown in Figure 4.68. Excessive polymerization and phase separation is suspected to be the reason for the anomalous behavior of A5 and A15 blended oils. A relatively high concentration of water is obtained for A15 oil aged to 96 hr and A20 oil aged to 192 hr. Otherwise, a small increase (15-35 wt.%) in the water content is generally observed during the initial storage period of 24 hr independent of additive type and concentration.

High concentration of water in the pyrolysis oil is not beneficial for its fuel application as water is known to have a high latent heat of vaporization (2260 kJ/kg at 100 °C). Furthermore, pyrolysis oils with water content exceeding 30 wt.% are reported to become unstable by phase separation (Oasmaa and Czernik, 1999). Majority of the pyrolysis oils in this study however are observed to have water concentrations well below this critical level. That could be partly due to the fractionation process employed during the pyrolysis oil production and partly due to the stabilization techniques involved. Hence, most pine wood pyrolysis oils remained chemically stable as their water content

was relatively unaffected with storage time or additive concentration. Phase separation in A5 and A15 blended oils however occurred at a water concentration lower than 30 wt.% due to their accelerated degradation. This phenomenon is possible as softwood pyrolysis oils are known to phase-separate based on the network strength of multiple phases rather than the high water concentration (Perez et al., 2006).

Additive Concentration Effects on Oil pH

A typical example of the concentration effects on the pH of pine wood pyrolysis oils is shown for ANS in Figure 4.90. The pH of all the pyrolysis oils ranged from 2.0 and 3.5 as reported in the literature (Oasmaa and Czernik, 1999). The high oil viscosity and probe sensitivity seem to be responsible for a low pH resolution (Bridgwater, 1999; Oasmaa et al., 2003). Finally, a systematic increase in the additive concentration (0-20 wt.%) did not have a profound impact on the pH of pyrolysis oils.

Statistical Analysis

Statistical analysis of variance (ANOVA) modeling is conducted using viscosity and water content data of the pine wood pyrolysis oils. Modeling is performed to identify the three most optimal additive concentrations for a range of concentrations (0-20 wt.%). These three concentrations are expected to provide the highest stability to the pine wood pyrolysis oils. Hence, two ANOVA models are evaluated in this phase using the viscosity and water content data. Fisher's least significant difference (LSD) test is utilized to analyze the performance of treatment variables. The critical values of parameter (t) utilized for viscosity and water content models during the LSD test are 1.99 and 2.02 respectively. Two-way interactions are necessarily included to increase the model

accuracy. Consequently, the regression coefficient (R^2) obtained for both the models is significantly high. A statistical significance level of $\alpha=0.05$ ($\text{Pr}>F$) is used to study the main and interaction effects. Both the models are observed to be statistically significant. Although unbalanced factorial treatment designs with multiple levels were used the LSD test results mostly corroborated the experimental results.

Viscosity Model (ANOVA)

The variable, level, and treatment information of the viscosity model is provided in Table 4.31. A total of 135 observations are utilized. The treatment variables considered are additive (ADD), measurement temperature (VTEMP), shear rate (SRATE), and concentration (CLEVEL). The viscosity difference or VD ($\Delta\text{cP}=\text{Final-Initial}$) obtained as a function of storage time (0 to 192 hr) is used as the response variable. The extended SAS[®] output corresponding to the viscosity model is provided in Tables 4.32-4.36. The additives (ANS, GLY, and MEH) prescreened from phase 2 are utilized with five concentrations (0, 5, 10, 15, 20 wt.%). The shear rates selected for the viscosity model so as to represent the complete flow behavior of pyrolysis oils are 1, 10, and 100 s^{-1} .

All the treatment variables significantly affect the VD of pyrolysis oils as shown by the ANOVA model in Table 4.32. However, ADD*VTEMP interaction is not significant. That also means the performance of each additive is uniquely different regardless of the measurement temperature. The mean VD of ANS is significantly higher than GLY and MEH as shown in Table 4.33. Additive concentrations of 10, 15, and 20 wt.% do not differ significantly in their performance as shown in Table 4.34. The above trend suggests that 10 wt.% is the most optimal additive concentration to stabilize pine

wood pyrolysis oils. Pyrolysis oil CTL (0 wt.%) is observed to be the least stable oil based on its highest mean VD.

All the measurement temperatures (25, 50, and 80 °C) are observed to significantly affect the mean VD as shown in Table 4.35. The lowest mean VD of pyrolysis oils is obtained at 80 °C while the highest is obtained at 25 °C. A drop of 60% in mean VD is obtained by increasing the VTEMP from 25 to 50 °C. A slightly higher drop (63%) in mean VD is obtained by increasing the VTEMP from 50 to 80 °C. The non-linear viscosity drop as a function of VTEMP indicates the presence of multiple phases in the pyrolysis oil. Those phases seem to slowly disperse into a homogeneous phase as the temperature is raised above 25 °C. Consequently, for large storage times, pyrolysis oils including CTL are completely Newtonian at 80 °C compared to being non-Newtonian at 25 and 50 °C. A typical example of this behavior is shown for CTL and ANS (10 wt.%) oils in Figures 4.91-4.92. Furthermore it is reported that pyrolysis oil undergoes structural changes in the form of precipitation and dissolution at temperatures of 39.2 and 43 °C (Ba et al., 2004 I, II; Chaala et al., 2004). Pyrolysis oils which are not amended and heated for prolonged periods are expected to undergo the above phase changes at a rate higher than the amended pyrolysis oils.

At a low shear rate of 1 s^{-1} highest mean VD is observed as shown in Table 4.36. However, at high shear rates of 10 and 100 s^{-1} lowest mean VD is obtained. Highest mean VD at low shear rates is because the flow behavior of the pyrolysis oils is mostly pseudoplastic. This is especially true for ANS and MEH with storage times greater than 24 hr. However, the mean VD at high shear rates does not differ significantly because the flow behavior becomes nearly Newtonian.

Water Content Model (ANOVA)

The variable, level, and treatment information of the water content model is shown in Table 4.37. A total of 60 observations (ADD*STIME*CLEVEL*REP = 3*2*5*2) are utilized with the treatment variables as shown in this table. The response variable used to model the treatment variables is water content difference (WCD=wt.%). This variable is obtained at the storage times of 24 and 96 hr. Water content difference ($\Delta\text{wt.\%}=\text{Final-Initial}$) from '0 to 192 hr' could not be included in this model because of the presence of outliers in the dataset. The inherent sampling and measurement error of the excessively polymerized or multi-phased oils during Karl Fisher analysis seems to be responsible for the presence of outliers. The extended SAS[®] output corresponding to the water content model is provided in Tables 4.38-4.41. The water content model is observed to be statistically significant ($\alpha=0.05$) with the inclusion of main and interactive effects as shown in Table 4.38. A slightly lower R^2 (0.84) but still a moderately good fit is obtained for the water content model as compared to the viscosity model R^2 (0.91). This is possibly because of the lower number of observations used for the water content model.

All chemical additives (ANS, GLY, and MEH) are observed to differ significantly with respect to the mean WCD as shown in Table 4.39. Methanol (MEH) resulted in the lowest mean WCD (1.08 wt.%) followed by GLY (1.56 wt.%) and ANS (2.18 wt.%). The mean WCD of pyrolysis oils at 96 hr is observed to be significantly higher than the mean WCD at 24 hr as shown in Table 4.40. This implies that the polymerization reactions and the associated phase changes increase as the oil aging increases. As shown in Table 4.41, the additive concentrations of 0 and 5 wt.% showed the lowest mean WCD without

differing significantly from each other. However, the additive concentrations of 10, 15, and 20 wt.% showed the highest mean WCD without differing significantly from each other. This WCD trend is nearly contrary to what is found for the VD trend in Table 4.34. The utilization of a high concentration of additive (ANS, GLY, and MEH) seems to moderately control the viscosity of pyrolysis oils at the expense of a slight increase in their water content. However, this slight increase (2-4 wt.%) in the water content is not detrimental to the phase stability of pyrolysis oils. A slight increase in water content of the additive blended oils is normally achieved by the simple polymeric reactions such as etherification, acetalization, and esterification reactions. But these reactions are more likely to decrease the oil viscosity by preventing excessive polymerization (Diebold, 2000; Diebold and Czernik, 1997; Oasmaa et al, 2004).

Based on the viscosity and water content ANOVA models obtained the additive concentrations of 0 wt.% (low), 5 wt.% (medium), and 10 wt.% (high) are selected for further studies in phase 4 or final stability testing. The most optimal additive concentration for the pine wood pyrolysis oils seems to be 10 wt.%. The above additive concentrations are expected to effectively stabilize the pyrolysis oils produced from different feed stocks, reactor variables, and stored at different conditions.

Final Stability Testing (Phase IV)

Introduction

As discussed in Chapter 3, the storage stability of pyrolysis oils (9) down selected from trial runs (Figure 3.1) is evaluated during this phase. These oils are produced at Mississippi State University (MS), National Renewable Energy Laboratory (NR), and

Renewable Oil International (RI). The study oils are stored at ambient (25 °C) and accelerated (80 °C) temperatures to evaluate their long-term and short-term storage stability. The storage times utilized at these temperatures are 0, 1, 2, 4, 6 months and 0, 24, 48, 96, 192 hours. Consequently, the designations used in this phase for these storage times are M0, M1, M2, M4, M6, H0, H24, H48, H96, and H192. Each month in this study is defined as 30 days. The physical and chemical properties of pyrolysis oils namely viscosity, water content, pH, density, and acid value are measured in phase 4 to assess their storage stability. Statistical analysis of variance (ANOVA) is conducted using viscosity and water content data to evaluate the effects of pyrolysis and storage conditions on the storage stability of oils. The pyrolysis conditions include feedstock, pyrolysis temperature, and residence time. The storage conditions include light, filtration, storage time, additive, and concentration. The additives utilized are anisole (ANS) glycerol (GLY), and methanol (MEH) with their concentrations of 0, 5, and 10 wt.%.

Stability of Wood and Bark Derived Oils (MS) as a Function of Shear Rate

The storage stability of Mississippi State University (MS) pyrolysis oils derived from pine wood (PW), oak wood (OW), oak bark (OB), and pine bark (PB) is discussed in this section. The viscosity versus shear rate relationship is used to analyze the storage stability of MS pyrolysis oils. All the viscosity plots in this phase are depicted for a measurement temperature of 25 °C. A very few research papers seem to have reported the dynamic viscosity at a measurement temperature of 25 °C and a range of shear rates. The measurement of dynamic viscosity of pine wood bio-oil and bio-diesel blend at 25 °C is reported by Perez and others [2007]. Furthermore, the measurement of dynamic viscosity

of hardwood oil (mixture of apple, oak, and cherry) as a function of shear rate is reported by Tzanetakis and others [2008]. The measurement of dynamic viscosity at 25 °C for a range of range of shear rates is given paramount importance in this investigation. Consequently, an improved assessment of the stability behavior of pyrolysis oils is possible based on their complete flow behavior as a function of storage time. As such, conclusions made by previous researchers seem to be subjective and highly dependent on a single point increase or decrease in viscosity for the spindle shear rate considered. During this investigation the viscosity of pyrolysis oils is observed to be strongly related with shear rate and storage time.

The viscosity of PW derived oil (stored at 25 °C) as a function of shear rate is shown in Figure 4.93. Among the 9 oils studied, PW oil only retained Newtonian flow behavior during the entire 6 month (M6) storage period. Additionally, the viscosity increase as a function of storage time is negligibly small. This behavior of the PW oil seems to indicate that it is the most stable pyrolysis oil. However, at a storage temperature of 80 °C, the PW oil retained Newtonian flow behavior for a maximum period of 48 hour (H48) as shown in Figure 4.94. Beyond H48 a significant increase in viscosity is observed for all the shear rates. The flow behavior of PW oil is increasingly non-Newtonian after an aging period of H48. Further the oil viscosity at accelerated storage temperature seems to steadily increase from 0 hr (H0) to 96 hr (H96) as compared to the ambient storage temperature. The oil viscosity increased appreciably as the storage time is doubled from H96 to 192 hr (H192). This behavior of PW derived oils is nearly identical to that obtained during the phases 2 and 3. The viscosity of MS PW oil reached a maximum of 300-400 cP for any shear rate during the M6 (ambient) and H48

(accelerated) aging periods. The viscosity values obtained for both these storage times are approximately equivalent. Beyond H48 the chemical changes in the PW oil seem to occur at a drastic rate rendering the oil least stable. For the oil to become utterly unstable complete polymerization or phase-separation needs to occur. Complete polymerization at times for bark derived oils has caused them to solidify. Similarly, phase-separated oils are measured with high water content exceeding 30 wt.%. These two phenomena are not detected with the MS pine wood oils beyond an aging period of H48. Nevertheless, the chemical changes occurring after H48 are manifested in the change in flow behavior (Newtonian to non-Newtonian) as well as the extent of polymerization indicated by a sharp viscosity increase. Hence, to increase the stability of additive free pyrolysis oils beyond M6 of storage time chemical additives are necessary.

The viscosity of MS OW pyrolysis oils (controls and additive blended) is plotted as a function of shear rate as shown in Figures 4.95-4.100. As shown in Figures 4.95-4.96, the flow behavior of OW controls (CTL's 1-3) changed from slightly shear-thinning (H0) to completely shear-thinning (H192). These figures suggest that the filtration effect on the stability of MS oak wood oil control (CTL3) is negligible. This is perhaps due to its low percentage of solids as reported by Ingram and others [2008]. A filter size of 20 μm is used for this oil which is also the smallest possible filter size achieved among all the MS oils as shown in Table 3.4. Hence, higher percentage of particulate removal is expected for the MS oak wood oil. The variation in viscosity due to the sampling error of oil controls (CTL1 and CTL2) is negligible as seen from Figures 4.95-4.96. Chemical additives namely anisole (ANS), glycerol (GLY), and methanol (MEH) significantly improved the stability of OW oils as compared to the controls (CTL's 1-3). Generally,

additive concentration of 10 wt.% performed better than 5 wt.% as shown in Figures 4.97-4.100. At H0 the viscosity of OW oils is relatively unaffected for all the additives, concentrations, and shear rates. However, the superior stability performance of higher additive concentration (10 wt.%) is apparent at a storage time of H192 from Figures 4.98 and 4.100. Anisole produced the most stable oil at both low (5 wt.%) and high (10 wt.%) concentrations in the respective groups. A transformation in the flow behavior from clearly non-Newtonian to almost Newtonian is observed for Glycerol (10 wt.%) blended MS oak wood oil as shown in Figures 4.99-4.100. This trend suggests a marked improvement in the OW oil stabilizing properties by the addition of GLY (10 wt.%). The viscosity of MEH blended (5 and 10 wt.%) OW oil is observed to be strongly dependent on the shear rate as shown in Figures 4.98 and 4.100. This behavior likely indicates that MEH blended oil is the least stable oil among the additive blended MS OW oils. Due to the very low viscosity of MEH (~1 cP) it seems to have a better dilution effect at H0 compared to ANS and GLY as shown in Figures 4.97 and 4.99. But MEH does not seem to be beneficial in stabilizing the OW oils at longer storage times as shown in Figures 4.98 and 4.100. No visual signs of phase-separation or solidifications were observed during the storage of MS oak wood pyrolysis oils. Evidently, MS wood pyrolysis oils showed greater stability than the MS bark pyrolysis oils which are discussed below.

The viscosity of MS oak bark pyrolysis oils is plotted as a function of shear rate as shown in Figures 4.101-4.102. The viscosity of these non-Newtonian (shear thinning) oils increased slightly during the first 30 days (M1) as shown in Figure 4.101. Afterwards the viscosity of OB oils decreased sharply due to excess water formation from polymerization. This happened until 120 days (M4) after which the OB oil became

completely polymerized causing an increase in the viscosity as shown for M6 in Figure 4.101. In a similar fashion the viscosity of OB oils increased during the first 48 hours (H48) as shown in Figure 4.102. Afterwards the viscosity of OB oils decreased sharply due to the excess water formation until H192 as shown in this figure. Phase separation seems to have occurred at both the storage temperatures due to excess water formation from the polymerization reactions. Furthermore, this phase separation likely caused the light phase to move upwards and heavy phase to gravitate at the bottom of sample vial. Phase separation in OB pyrolysis oils did not resemble the classical oil-water mixture with a well defined interphase. Hence, the light phase is expected to contain both low molecular weight organics (holocellulose derived) and water content (maximum). Contrarily, heavy phase is expected to contain high molecular weight organics (lignin derived) and water content (minimum). This complex phase separation in pyrolysis oils imposed significant challenges during the viscosity and water content measurements.

Polymerization and phase separation also occurred in MS pine bark oils ultimately causing them to be the least stable oils with a maximum storage life of M1 at ambient temperature (25 °C) or H24 at accelerated temperature (80 °C). The filtered bark control samples (CTL3) are observed to exhibit near Newtonian flow behavior during the monthly and hourly testing. An example of this trend obtained at ambient storage temperature is shown for PB CTL3 in Figures 4.103-4.104. However, additive blended PB oils exhibited non-Newtonian flow behavior regardless of storage time and concentration as shown in Figures 4.105-4.108. An exception to this trend is GLY (10 wt.%) that showed near Newtonian behavior at H192.

Fluorescent light does not seem to significantly affect the overall stability of PB pyrolysis oils (CTL1-light exposed and light protected-CTL2) as seen from Figures 4.103-4.104. It is suspected that the impact of light through photo-oxidation reactions is negligible compared to the highly oxidized state of pyrolysis oils. This trend is generally observed for all the pyrolysis oils in this study. Similar results are reported for light exposed oil samples derived from beech wood oil (Meier et al., 2002). Filtration of CTL3 sample however seems to have a positive impact on increasing the stability of all the pyrolysis oils. A typical example of this trend can be visualized from Figure 4.103-4.104 where the filtered oil sample (CTL3) significantly lowered the viscosity of pine bark derived oils. Bark derived oils are reported to have higher amount of particulate solids than the wood derived oils (Ingram et al., 2008). Hence, filtration of the bark oils to remove the particulate solids and tarry agglomerates is projected to increase their long-term storage stability.

As expected, GLY (~700 cP) addition to fresh MS PB oils substantially increased their viscosity compared to ANS and MEH blended oils. This behavior can be visualized from Figures 4.105-4.106. However, the GLY and MEH blended (5 wt.%) oils showed identical flow behavior at M6 as shown in Figure 4.107. Additionally, GLY blended (10 wt.%) oil resulted in the lowest viscosity at M6 among all the PB derived oils as shown in Figure 4.108. This is accompanied by a near identical Newtonian flow behavior for an aging period of 180 days (M6) as indicated. Anisole blended (5 and 10 wt.%) pine bark pyrolysis oils showed the highest viscosity for most shear rates as seen from Figures 4.107-4.108. This suggests that GLY blended PB oils are the most stable oils followed by MEH blended PB oils. Contrarily, amongst the additive blended PB pyrolysis oils ANS

blended oils are least stable. Additionally their viscosity is strongly related with shear rate when compared to the GLY and MEH blended PB oils as shown in the above figures.

The water content of bark derived oils is significantly greater than the wood derived oils as measured. Hence, GLY addition in effect is expected to produce more stable bark oils than ANS and MEH. Due to the hygroscopic nature of GLY the miscibility of light and heavy phases can be increased and consequently oil homogeneity. A marked decrease in the viscosity of additive blended PB oils (5 and 10 wt.%) as a function of storage time can be visualized from Figures 4.105-4.108. As the storage time is increased from M0 to M6 it is likely that the additive blended PB oils caused a substantial increase in the water content which helped in lowering their viscosity significantly. This phenomenon as explained earlier is consistent with the additive free PB oils (CTL's 1-3). Polymerization and phase separation of the additive blended PB oils is rather responsible for the sharp decrease in viscosity and not by the physical dilution of additives.

By nature the pyrolysis oils are produced with a certain amount of water in them regardless of feedstock and reactor conditions. But when the existing water content exceeds the network tolerance level then pyrolysis oil structure becomes unstable and consequently phase separation occurs (Perez et al., 2006). Excess water in the oils that causes phase separation mainly comes from the polymerization reactions during their storage. Karl Fisher analysis (water content) of the bark derived oils is discussed separately in this phase. The complex chemical structure of bark derived oils followed by the presence of multiple phases makes these oils significantly less stable compared to the wood derived oils (Sjostrum, 1993; Perez et al., 2006; Ingram et al., 2008). Experiment

wise the challenges during the viscosity measurements of bark derived oils is substantially minimized by the utilization of chemical additives. A typical example of sheared pine bark oil after the viscosity test is performed is shown in Figure 4.110. This figure clearly demonstrates the presence of multiple phases in the pine bark oil as well the structural deformation achieved after the viscosity test is concluded.

Comprehensively, all the three additives (ANS, GLY, and MEH) performed well in maintaining or increasing the pyrolysis oil stability based on the viscosity-shear rate data. The stability performance of these additives is much dependent upon feedstock, additive concentration, and storage conditions. Feedstock is concluded to be the single most important variable having the highest impact on the oil storage properties. This is apparently due to the variation in the holocellulosic and lignin content of biomass (Shafizadeh, 1982).

Stability of Wood Derived Oils (RI and NR) as a Function of Storage Time

The viscosity of Renewable Oil International (RI) pine wood (PW) oil at a shear rate of 100 s^{-1} and a measurement temperature of $25 \text{ }^{\circ}\text{C}$ is plotted as shown in Figures 4.110-4.111. The viscosity of National Renewable Energy Laboratory (NREL) oak wood (OW) oil at a shear rate of 100 s^{-1} and a measurement temperature of $25 \text{ }^{\circ}\text{C}$ is plotted as shown in Figures 4.112-4.113. A high shear rate of 100 s^{-1} is chosen to represent fully developed flow behavior of oils especially that are non-Newtonian. As a general trend it is observed that the oil viscosity increased as a function of storage time regardless of additive concentration. The viscosity increase becomes more significant for storage times exceeding 120 days or 48 hr. Accelerated storage time of 48 hr and ambient storage time

of 180 days seem to be approximately equivalent based on the viscosity data. This is verified statistically using least significant difference (LSD) test of the mean response variables (viscosity and water content). Similar trends are obtained for PW and OW oils as seen from Figures 4.110-4.113. The PW/OW oil controls (CTL's 1-3) showed the highest rate of increase in viscosity as a function of storage time making them the least stable oils. This phenomenon is more apparent at accelerated storage temperature (80 °C) as shown in Figures 4.111 and 4.113. Approximately 33.33% increase in viscosity is observed for NR OW control oils as shown in Figure 4.112. This increase is observed to be the largest for OW oils (stored at 25 °C) as their storage time is increased from 120 to 180 days. The effects of filtration (CTL3) and light (CTL1) is not apparent from these figures as the differences in viscosity are small among the control oils. Besides the viscosities used in these graphs are based on a single shear rate of 100 s⁻¹. However, the filtration and light effect on the oil stability is studied broadly for the 9 study oils based on the LSD test of mean viscosity. Until 96 hr or 120 days, the viscosity of all the additive concentrations is consistently lower than control oils with the exception of GLY (5 and 10 wt.%). The viscosity values obtained for GLY at concentrations of 5 and 10 wt.% are nearly identical but still lower than the control oils (CTL's 1-3). This suggests that 5 wt.% concentration of GLY is sufficient to stabilize either RI PW or NR OW oils. The viscosity of PW showed a minimum increase with storage time when the ANS or MEH concentration is 10 wt.%. Likewise OW oils showed a minimum increase with storage time when the MEH concentration is 10 wt.%. In fact the OW oils showed approximately same increase in viscosity with storage time regardless of ANS concentration (5 or 10 wt.%). This suggests that 5 wt.% of ANS is sufficient to stabilize

NR OW oils. The above trends are however verified statistically using LSD test of mean viscosity and mean water content. The viscosity of fresh and aged OW and PW oils in this study ranged from 50-1100 cP at a measurement temperature of 25 °C and a shear rate of 100 s⁻¹. Czernik and Bridgwater [2004] have reported the viscosity of pyrolysis oils to range from 35 to 1000 cP at a measurement temperature of 40 °C. Feedstock and process conditions have been reported to cause such a wide variation in the oil viscosity.

Stability of Wood Derived Oils (MS, NR, and RI) as a Function of Additive Conc.

The viscosity increase (%) of MS and NR pyrolysis oils as a function of additive (MEH) concentration is shown in Figure 4.114. The viscosity increase (%) of RI pyrolysis oils as a function of additive (ANS, GLY, MEH) concentration is shown in Figure 4.115. The storage times of 0 days (M0) and 180 days (M6) are considered to compute the viscosity increase of oils stored at ambient temperature (25 °C). The storage times of 0 hr (H0) and 192 hr (H192) are considered to compute the viscosity increase of oils stored at accelerated temperature (80 °C). Pyrolysis oil control (CTL2-0 wt.%) is used to compare the performance of methanol (0, 5 and 10 wt.%) blended oils as shown in Figure 4.114. As a general trend increase in MEH concentration decreased the viscosity or increased the storage stability of OW oils independent of storage temperature and reactor type (auger or entrained flow). A concentration of 10 wt.% MEH seems to result in the most stable OW oils. The viscosity increase obtained for the RI control oils (CTL's 1-3) is nearly identical at a storage temperature of 25 °C as shown in Figure 4.115. However, at 80 °C smallest increase in viscosity is obtained for filtered control (CTL3) implying that filtration of oils significantly affects their long-term storage

stability. As expected control oils (CTL1 and CTL2) do not differ significantly from each other based on their viscosity increase (ambient/accelerated). Anisole (10 wt.%) resulted in the lowest RI oil viscosity increase among all the additives and concentrations. This behavior was observed for both the storage temperatures. In conclusion the stability of RI PW oils is expected to increase as the additive concentration is increased. Based on the viscosity increase of RI PW oils the additive performance is summarized as follows.

Additive (wt.%) @ 25 °C

- ANS (10) > ANS (5) > GLY (10) > GLY (5) > MEH (5) > MEH (10)

Additive (wt.%) @ 80 °C

- ANS (10) > ANS (5) > GLY (10) > MEH (10) > GLY (5) > MEH (5)

Karl Fisher Analysis

The water content (wt.%) of NR OW and MS OB oils as a function of additive concentration and storage time is shown in Figures 4.116-4.119. Both these oils are produced at low pyrolysis temperature. Light and filtration do not seem to significantly impact the oil water content as shown in Figures 4.116 and 4.118. These figures also indicate that the water content remains relatively unaffected when the oils are stored at ambient storage temperature. This trend is independent of storage time, feed stock, and additive concentration. However, at accelerated storage temperature, water content showed a progressive increase with storage time regardless of additive concentration and feed stock. This trend (water increase) obtained from Figures 4.117 and 4.119 is similar to the trend (viscosity increase) obtained for RI PW and NR OW oils from Figures 4.111 and 4.113. A major increase in water content for most NR OW oils is obtained during the

0-24 and 96-192 hour periods as shown in Figure 4.117. This trend seems to indicate that most polymerization reactions occur in these two storage periods. Likewise a major increase in water content for most MS OB oils is obtained during the 96-192 hour period as shown in Figure 4.119. The above trends are independent of additive concentration with the exception of ANS. Similar trends are reported for water content during the phases 2-3 of this research. Anisole seems to have a beneficial effect in lowering the water content of pyrolysis oils during the long-term storage. Additionally ANS addition to MS OB oils caused a sharp initial drop in the water content as shown in Figures 4.118-4.119. This anomalous behavior of ANS could not be established with the tools utilized in this research. Nevertheless this behavior prompted for the acid value testing of oil samples that are blended with ANS. Generally higher water content of OB samples at 192 hr (Figure 4.119) compared to the OW samples at 192 (Figure 4.117) indicates that OW samples possess greater long-term storage stability than the OB samples. The range of water content obtained for OW samples is 18-25 wt.% and 12-35 wt.% for OB samples. Similar values for the water content of pyrolysis liquids is reported in the literature (Oasmaa et al., 2003; Czernik and Bridgwater, 2004; Oasmaa et al., 2004, Oasmaa and Kuoppala, 2003).

The water content increase of MS OB oils (controls and additive blended) is shown in Figure 4.120. The increase in water content of oils is computed as shown in this figure. A slight variation in the water content is observed among the control oils (CTL1 and CTL2) stored at 80 °C. This variation in water content is attributed to the multiphase nature of bark oils. Filtration is not observed to significantly affect the water content of OB oil (CTL3). Large peaks are obtained for ANS blended (5 and 10 wt.%) oils

compared to all the other oils. As explained previously, a sharp drop in the water content of ANS blended samples during the initial storage period is responsible for this trend. This trend is contrary to the low peaks of viscosity obtained for RI PW oils in Figure 4.115. The chemical reactions are possibly arrested by the ANS addition during the initial threshold period which is roughly H24 or M1. After this period the unstable polymeric reactions might increase significantly to affect the storage stability of ANS blended oils. At ambient storage temperature the water content increase of additive blended samples (A5, A10, G5, G10, and M10) is comparatively higher than all the control oils (CTL's 1-3). Similarly, at accelerated storage temperature the water content increase of additive blended samples (A5 and A10) is comparatively higher than all the controls. This increase in water content generally seems to positively affect the storage stability of oils by lowering their viscosity. Czernik and Bridgwater [2004] have indicated that the presence of water in pyrolysis oils advantageously lowers their viscosity. Consequently, it enhances the flow properties of oils. The increase in water content (wt.%) of PW oils as a function of MEH concentration is shown in Figure 4.121. The water content increase of oils is computed at different storage temperatures as shown in this figure. The water content generally showed an increasing trend with a systematic increase in the MEH concentration. This trend in contrast to the viscosity trend from Figure 4.114 suggests that chemical additives increase the stability of pyrolysis oils by the addition of small quantities (< 5 wt.%) of water. This addition of water to the pyrolysis oil physically implies that the viscosity of the oil is lowered. However, chemically it suggests that simpler chemical reactions occur at the expense of complex polymeric reactions. This phenomenon is in accordance with the findings of other researchers (Diebold and

Czernik, 1997; Diebold, 2000). The combination of RI PW oils and MEH (10 wt.%) resulted in the highest water content increase independent of storage temperature. A similar increase in the water content is obtained for MS PW oils at MEH concentrations of 5 and 10 wt.%.

Density of Pyrolysis Oils

The density of all the pyrolysis oils in this study ranged from 1.05 to 1.35 g/ml. Pyrolysis liquids are known to have similar values of density as reported by other researchers (Oasmaa and Czernik, 1999; Oasmaa et al., 2004). The density of NR OW pyrolysis oils (low temperature) as a function of storage time is shown in Figures 4.122-4.123. The density of these oils is observed to be independent of storage temperature, storage time, light, filtration, and additive concentration.

During this study the density of the entrained flow reactor pyrolysis oils is observed to be slightly lower than those of auger reactor produced pyrolysis oils. Due to a very high concentration of water (50-60 wt.%), NR OW pyrolysis oils (high temperature) have the least density among all the oils. A slight decrease in the density of ANS blended oil samples is observed but within the margin of experimental error.

Density of MS bark derived oils was relatively difficult to measure compared to the wood oils due to their higher flow resistance. Similarly, oils that were aged to long storage times also offered higher flow resistance during density measurements. This is apparently due to their high viscosity. The high viscosity was caused by the increasing number of polymerization reactions that occurred with storage time.

pH of Pyrolysis Oils

The pH of all the pyrolysis oils in this study ranged from 1.80 to 3.80. Glycerol blended oil samples are observed to have the highest pH. Pyrolysis liquids are reported to have similar values of pH by other researchers (Oasmaa and Czernik, 1999; Oasmaa and Kuoppala, 2003; Czernik and Bridgwater, 2004). The pH of NR OW pyrolysis oils is shown in Figures 4.124-4.125. The pH of these oils is observed to be independent of storage temperature, storage time, light, filtration, and additive concentration.

The measurement error of pH is relatively high for samples with multiphase behavior and high solid content. The longest analysis time of the pH probe is observed for the highly polymerized oil samples. Frequent cleaning and calibration of the probe during the pH measurements minimized the error in readings.

Acid Value of Pyrolysis Oils

Small changes in the pH units can be cumbersome to quantify the changes in acid $[H^+]$ concentration. Hence, acid value testing of pyrolysis oils is performed to better understand these changes. This testing facilitates fast and accurate readings as the oil sample is significantly diluted in an aqueous medium. As mentioned previously the acid value of control (CTL1) and ANS blended oil samples (10 wt.%) is determined during this independent study. These oil samples are stored at 25 °C for a period of 0 (M0), 90 (M3), and 180 (M6) days. The breakthrough curves are obtained by plotting the pH change (final-initial) against titrant volume (0.01 N KOH). A sharp rise in the pH differential indicates that the acid-base reaction is complete.

The breakthrough curves obtained for the NR PW oils are shown in Figures 4.126-4.127. A systematic shift (forward) in the breakthrough volume of titrant is observed for both these samples. This implies that the acid concentration of the PW samples continuously increased with storage time. The breakthrough curves obtained for the NR OW oils are shown in Figures 4.128-4.129. A similar trend as that of PW oils is observed for OW oils but the increase in the breakthrough volume of aged OW samples (M3 and M6) did not differ significantly. This suggests that the maximum increase in acid concentration occurred during the 0-90 day storage period (M0 to M3).

A plot of the acid value (mg KOH consumed /g oil) as a function of storage time for both PW and OW oils is shown in Figure 4.130. The acid value of NR PW oil samples (CTL1 and A10) did not differ significantly from each other. However, a progressive increase in their acid concentration as a function of storage time can be visualized. Contrarily, NR OW oil samples (CTL1 and A10) showed a flatter response in acid value as the storage time is increased. However, the acid values of both OW samples are observed to be significantly different with CTL1 sample showing a higher acid value for all the storage times (M0, M3, and M6). The progressive increase in the acid value of NR PW oils compared to NR OW oils indicates their lower storage stability. Statistical LSD test of the viscosity data as discussed later in Table 4.46 well supports this trend. The range of acid values obtained for the NR wood oils is 74.6-97.2. These values are found to map with the range reported by other researchers (Oasmaa and Czernik, 1999; Scholze, 2002).

Weight Loss of Pyrolysis Oils

The weight loss of NR oak wood oil samples (low temperature) measured as a function of storage time (days and hours) is shown in Figures 4.131-4.132. The initial and final weights are monitored before and after insertion in the hood (days) or oven (hours). Negligible weight losses (<0.1 wt.%) due to sample volatilities is observed for the oil samples. This trend is observed to be independent of oil type, storage time, storage temperature, and additive concentration. A progressive decrease in the oil sample weight (g) as a function of storage time can be seen due to the successive sampling. A sharp decrease in sample weights of sample can be seen for the samples stored at 80 °C as shown in Figure 4.132 compared to the samples stored at 25 °C as shown in Figure 4.131. This is because of the difficulty in pouring precise amounts of more viscous samples.

Data Quality Control

Analytical standards were run frequently for every test during the phases 2-4 of this research. The experimental tests included viscosity, water content, density, pH, and acid value. Standard checks were essential to frequently calibrate the instrumentation and monitor the accuracy during data collection. Consequently, viscosity tests were run using Brookfield® silicone oil standards for each set of pyrolysis oils (15-20). The viscosity test was run only once for each oil sample as the main objective of this research was to study the oil stability both qualitatively and quantitatively. Hence, a range of shear rates were used to measure viscosity rather than a single shear rate. In fact, the control samples (CTL1 and CTL2) used during this research generally produced near identical flow behavior during viscosity tests of the respective pyrolysis oils. The testing time lag

between the samples stored at 80 °C was minimized significantly by using a single replicate. Aquastar® water standard was used during water content measurements or Karl Fisher analysis. Both concentration and percent water tests were performed for every set of pyrolysis oil samples analyzed (10-15). American Society for Testing and Material (ASTM) type I water was used during density calibration. Density calibrations were performed each time the cleaning operations of the volumetric flasks were conducted. Fisher Scientific buffers were used during pH and acid value measurements. The pH probe calibration was performed twice (before and after) every time the oil samples were analyzed. All the pH measurements were performed using the probes that were purchased from the same manufacturer. This minimized the error when they needed to be changed. Due to the viscous nature of pyrolysis oils frequent replacement of the pH probes was necessary.

Statistical Analyses and Modeling

The experimental design used during phase 4 constitutes 3*5*4 factorial arrangement of treatments (additive concentration, storage time, and shear rate) in a completely randomized design for each feedstock (pine wood, oak wood, and oak bark). Three types of statistical models were applied to the Mississippi State University pyrolysis oil viscosity data (normalized) during this phase. They included analysis of variance (ANOVA), response surface regression (RSREG), and general linear model (GLM). Eventually, the second order GLM model was chosen as it resulted in the best regressed fit ($R^2 \geq 70.39$). The principle of hierarchy was considered during the inclusion of non-significant ($\alpha=0.05$) model terms. The general equation with second order applied

during modeling is provided in Table 4.42. Consequently, the model parameters and their estimates obtained for the pine wood (methanol), oak wood (glycerol), and oak bark (anisole) pyrolysis oils are shown in Table 4.43. The wood derived oils have lower mean viscosity than the bark derived oils indicating their higher stability. The root mean square error and coefficient of variation for the oak derived oils is higher than the pine wood derived oil. This trend is to be expected as the oak derived oils are non-Newtonian compared to the pine wood oil that is Newtonian. The model equations obtained for the above oils are shown in Table 4.44. The canonical analysis of response surface (RSREG procedure) revealed a minimum value of viscosity (85.91 cP) for the methanol blended pine wood oil. This value is obtained at a storage time of 3.97 months and methanol concentration of 11.78 wt.%. Likewise, a minimum value of viscosity (50.13 cP) is obtained for the glycerol blended oak wood oil. This value is obtained at a shear rate of 57.20 s^{-1} and a storage time of 1.58 months. Furthermore, canonical analysis of response surface revealed a stationary value of viscosity (9.58 cP) for the anisole blended oak bark oil. This value is obtained at a shear rate of 57.40 s^{-1} and anisole concentration of 4.49 wt.%. The response surfaces obtained for pine wood, oak wood, and oak bark oils from the GLM models resembled closely with a plane, valley, and saddle respectively.

Pine Wood Pyrolysis Oil (MSU)

The linear relationship of viscosity as a function of shear rate and storage time (month) was seen earlier in Figure 4.93 for the additive-free MS pine wood pyrolysis oil. This trend was attributed to its Newtonian-like flow properties as well as its superior stability compared to all the other oils. A nearly identical surface response was obtained

for this particular oil when the viscosity was plotted as function of methanol concentration and storage time as shown in Figure 4.133 (a and b). However, the curvature in the response decreased significantly with storage time as visualized from Figure 4.133 (c). This is due to a significant increase in the shear rate from 10 to 100 s⁻¹. Generally, at large shear rates it is hypothesized that the pyrolysis oil network flows well with minimal resistance. The polyaromatic plate-like structure of the pyrolysis oils seems to exhibit slipping behavior as a result of high shear rate. Furthermore, an increase in the methanol concentration from 0 to 10 wt.% also decreased the oil viscosity and consequently improved its flow characteristics. Regardless of shear rate studied the storage time does not seem to affect the increase in oil viscosity significantly. This trend further confirms that the pine wood oils of MS are the most stable pyrolysis oils at ambient storage conditions.

The contour plots as shown in Figure 4.134 (a-c) indicate that the region of minimum viscosity or high stability starts from a methanol concentration of ~8 wt.%. This trend can be visualized from the dashed contour lines in this figure. Based on the model predictions the minimum viscosity of oil decreased by 13.41% as the shear rate was increased from 1 to 100 s⁻¹. This much drop in viscosity can be understood well by the slipping behavior of the pyrolysis oil network. At low shear rates of 1 and 10 s⁻¹ the minimum viscosity region of the pine wood pyrolysis oil is predicted at high methanol concentrations (≥8 wt.%) and large storage times (>2 months). At a high shear rate of 100 s⁻¹ the minimum viscosity region of the pine wood pyrolysis oil is predicted at high methanol concentrations (≥8 wt.%) and storage times exceeding 0.5 months. This

discrepancy in storage times is justified by the differences in the flow behavior of pyrolysis oil as a function of shear rate.

Oak Wood Pyrolysis Oil (MSU)

As seen earlier from Figure 4.95, additive-free, oak wood oil is clearly non-Newtonian. Further effort has been made in this part to model and understand its flow behavior as a function of glycerol concentration, storage time, and shear rate. The effect of increasing glycerol concentration is much obvious on the viscosity of oak wood pyrolysis oil. Hence, as glycerol concentration was increased from 0 to 10 wt.% the surface response region of minimum viscosity became increasingly parallel with the storage time vs. shear rate plane as shown in Figure 4.135. Glycerol is likely reacting with catalytic acids from the pyrolysis oil as explained previously and eventually lowering the viscosity. Glycerol concentration in excess of 5 wt.% seems to be necessary in effectively stabilizing the oak wood derived pyrolysis oils. As observed from the surface cross sections the decrease in viscosity as a function of shear rate ($\geq 0.1 \text{ s}^{-1}$ and $\leq 50 \text{ s}^{-1}$) is attributed to the pseudoplastic (shear-thinning) flow behavior of oak wood oil. However, the increase in viscosity as function of shear rate ($\geq 50 \text{ s}^{-1}$ and $\leq 100 \text{ s}^{-1}$) or dilatant (shear-thickening) flow behavior could not be experimentally verified. Such anomalous flow behavior of shear-thinning followed by shear-thickening has been reported to occur in suspensions such as blood, paint, ink and cement (Larson, 1999). Analogically, glycerol blended oak wood oil can be considered as a suspension with the fresh oak derived oils (wood and bark) reported to contain significantly higher amount of solids than pine wood (Ingram et al., 2008). Further, the aging process of pyrolysis oils is

expected to influence the formation of micelles, reaction clusters, and waxy crystals due to the increase in number of covalent bonds (Perez et al., 2006). The impact of shear rate on the viscosity of oak wood pyrolysis oil remained relatively unaffected for each concentration of glycerol. Storage time is primarily responsible for showing an increasing trend in viscosity at low glycerol concentrations (0 and 5 wt.%). This trend suggests that the viscosity increasing complex polymerization reactions continue to occur with time in pyrolysis oils when low concentrations of additives are utilized. However, at high concentration (10 wt.%) of glycerol these reactions are minimized as indicated (Figure 4.135 c) by the non-significant effect of storage time on the oak wood oil viscosity.

The contour plots as shown in Figure 4.136 (a-c) indicate the region of minimum viscosity in the form of a dashed circle. As the glycerol concentration increased from 0 to 10 wt.% the minimum viscosity dropped by 15.04% as predicted by the model. Furthermore, the region of minimum viscosity positioned more towards large storage times (≤ 4 months) on the ordinate. Such a shift in the region of minimum viscosity indicates the higher stability of oak wood oils blended with large concentrations (≥ 10 wt.%) of glycerol.

Oak Bark Pyrolysis Oil (MSU)

As seen earlier from Figure 4.102, additive-free, oak bark oil is clearly non-Newtonian as a function of storage time (hour). This oak bark derived oil apparently exhibited a very complex flow behavior due to polymerization and phase-separation that occurred during its storage. Further effort has been made in this part to model and understand its flow behavior as a function of anisole concentration, storage time, and

shear rate. A saddle-like surface response as a function of storage time can be visualized from Figure 4.137 (a-c) for the oak bark oil. As the anisole concentration increased from 0 to 10 wt.% the saddle surface twisted more towards high concentration region resulting in a lower viscosity prediction. The complex flow behavior of oak bark oil is partly responsible for obtaining the saddle-like surface. Both pseudoplastic and dilatant behavior of flow can be visualized as previously observed with the oak wood oil. Once again the dilatant flow behavior of oak bark oil with shear rates of 50 s^{-1} plus could not be established experimentally but predicted to occur because of its high percentage of suspended particulate matter (Ingram et al., 2008). The particulate matter such as char and aggregates in the pyrolysis oil formed due to pyrolysis and aging reactions are apparently non-dissolvable even by the addition of an external additive. Hence, during the viscosity measurements they play a significant role in exhibiting complex flow behavior. Beyond anisole concentration of 8 wt.% this two-pronged flow behavior (pseudoplastic and dilatant) is substantially minimized as seen from the surface cross sections. Addition of anisole to the oak bark oil in excess of the above concentration resulted in the least viscosity increase among all the pyrolysis oils. As a function of storage time the viscosity increase of anisole blended oak bark oil is substantially minimized due to the slow polymerization reactions consuming anisole.

The plots as shown in Figure 4.138 (a-c) indicate the region of 'low and high' viscosity in the form of 'solid and dashed' contour lines. The low viscosity contour is observed at high concentration ($\geq 8 \text{ wt.}\%$) of anisole where as the high viscosity contour occurred at low shear rates ($\leq 1 \text{ s}^{-1}$). Regardless of the anisole concentration utilized the positioning of saddle point is unaffected with respect to the storage time and shear rate

coordinates. As the storage time is increased from 0 to 192 hr the low viscosity dropped by 43.89% as predicted by the model. Likewise, the high viscosity also dropped by 43.84% as predicted by the model. Such a high drop in viscosity of oak bark oil (anisole) compared to the pine wood oil (methanol) and oak wood oil (glycerol) is attributed to the aromatic nature of anisole. Because of this phenomenon the oak bark oil viscosity dropped significantly with the increase in aging time and anisole concentration. Having said that anisole does seem to exhibit interesting behavior as a function of concentration. Small concentration of anisole (≤ 5 wt.%) did not result in a favorable drop in oil viscosity but instead showed an increasing trend. Contrarily, beyond the above concentration the oil viscosity showed a decreasing trend. High concentrations of anisole (≥ 8 wt.%) and large shear rates (≥ 50 s⁻¹) resulted in a maximum drop in the oil viscosity. Hence, high concentrations of anisole are needed to stabilize oak bark oil effectively.

The aromatic structure of anisole seems to increase the formation and slipping of plate-like structures present in the pyrolysis oil. Consequently, anisole blended oak bark pyrolysis oil (≥ 8 wt.%) resulted in low viscosity measurements at large shear rates (≥ 50 s⁻¹). The above trend is well supported by the lowest Herschel-Bulkley rate index ($n=0.87$) obtained for the anisole blended pine wood oil (storage time = 192 hr) as shown earlier in Table 4.18. Pyrolysis oil network has been reported to be comprised of strong aromatic networks (interconnected) that are formed either from the pyrolysis reaction or as a result of prolonged storage. These networks are primarily lignin derivatives or oligomeric molecules such as tetramers, pentamers, hexamers, heptamers, and octamers as structurally illustrated (Bayerbach and Meier, 2009). The presence of secondary forces (weak) such as hydrogen bond, dipole interactions, and van der Waals forces in the

pyrolysis oil network is expected to favor the formation of aromatic structures in layers though not in a completely organized fashion. As reported for the softwood bark derived oil these weak forces are strongly affected (decreased) by an external factor such as temperature (Boucher et al., 2000). Likewise, moderate to high shear rates are also expected to decrease the weak forces and hence the oil viscosity.

In an attempt to understand the weak forces present in the pyrolysis oil, molecular modeling was performed using ‘Spartan 06’ Wavefunction Incorporated. Specifically, Hartee-Fock (3-21G) method of calculations was chosen with the lowest interaction energy possible between the two molecules. Evidence of hydrogen bonding can be observed in a planar fashion between anisole and lignin precursors (guaiacol and syringol) as shown in Figure 4.139. Guaiacol and syringol units are chosen during modeling as they are the backbones of lignin structure and as explained in Chapter II. Lignin is known to have the highest polydispersity index (M_w/M_n) among all the lignocellulosic components of wood (Sjostrom, 1993; Brady, 2002). In the case of guaiacol, the oxygen atom from the methoxyl group of anisole is observed to form a hydrogen bond with one of the hydrogen atoms from the methoxyl group of guaiacol. Similarly, the oxygen atom from the methoxyl group of syringol is observed to form a hydrogen bond with the hydrogen atom (meta position) of aromatic anisole. Both the above cases reveal the formation of plate-like structures by the addition of anisole to the pyrolysis oil. Furthermore, the delocalized nature of electrons from the π -orbitals of benzene ring is expected to create dipole-induced interactions in the pyrolysis oil leading to stronger attractions between adjacent aromatic molecules. Hence, it is highly possible

that plate-like structures similar to the graphite structure continue to exist in the anisole blended pyrolysis oil.

As a general conclusion of this study, addition of aromatic additives such as anisole in high concentrations (8-10 wt.%) is beneficial in optimizing the stability of hardwood-derived oils (Ex: Oak) when compared to the softwood-derived oils (Ex: Pine), due to their significantly lower range of lignin content. Contrarily, addition of alcoholic additives such as methanol and glycerol in high concentrations (8-10 wt.%) is beneficial in optimizing the stability of softwood-derived oils.

Pyrolysis Oil Application

Pine wood produced the most stable pyrolysis oil during the storage period of six months. The increase in pine wood oil viscosity during the six months (25 °C) is approximately equivalent to the increase obtained during 48 hrs (80 °C). Glycerol also known as glycerin is the obvious additive of choice as it provided the highest stability to pine wood oil when stored beyond 24 hrs. So, in effect, to stabilize pine wood derived pyrolysis oils beyond 6 months, glycerol (8-10 wt.%) is necessary to meet the American Society for Testing and Materials (ASTM) long-term storage stability requirements (≥ 1 yr). Based on the viscosity data obtained at 80 °C and 192 hrs, a shelf-life of at least 1 year (25 °C) has been predicted for the pine wood pyrolysis oil blended with glycerol (10 wt.%). A set of favorable conditions involving the production, fractionation, distillation, storage, and pumping of pyrolysis oil as a potential bio-fuel have been identified. Additionally, the projected energy costs of glycerin blended pyrolysis oil as a function of its concentration are shown.

Production

Auger reactor systems can be cost-effective overall when it comes to their flexibility in design and operation. However, the transfer of heat to the biomass particle seems to be somewhat limited due to the time-lags involved during band heating. On the other hand induction heating of dried biomass (negligible bound moisture) accompanied by an acid catalyst is thought to increase the heat transfer and pyrolysis efficiencies. A uniform biomass particle size distribution (PSD) is also projected to increase the thermo-chemical conversion efficiencies and minimize the plugging and coking problems. Apart from these benefits a uniformly sized value-added by product (bio-char) can be produced from the reactor that can be utilized directly in an industrial waste water treatment application. Excess flow rates of inert gas such as nitrogen or argon are needed to: 1) obtain a precise control of the residence time and 2) minimize the vapor cracking reactions.

Fractionation and Distillation

Multiple-effect condensers can be beneficial in fractionating pyrolysis oil vapor upstream into broadly aqueous rich and organic rich fractions. However, the temperature of each condenser has to be controlled carefully according to the product type, composition, and quality desired. The aqueous rich fraction can be further distilled downstream into water and light volatile compound such as acetic acid especially since it is known to be present in significantly large quantities (~10 wt.%) in the pyrolysis oil (Maschio et al., 1992). However, the downside of such a distillation process is that it can be cost consuming and labor intensive. The distillation of organic rich fraction is

contrarily difficult due to the complex polymerization reactions that are known to occur during the process (Adjaye et al., 1992).

Storage and Pumping

Corrosion is one of the major concerns involved during the storage and pumping of pyrolysis oil due to its low pH (Czernik and Bridgwater, 2004). Only a mild improvement (<1 log unit) in the pH is possible even at high concentrations (10-20 wt.%) of an additive such as a trihydric alcohol (glycerol). Hence, the storage and pumping equipment needs to be specially constructed for this application. Stainless steel or ultra high molecular weight polyethylene (UHMPE) seems to be the obvious choice of material of construction due to their high corrosion resistivity and mechanical strength. A sun light protective coating to the large-scale storage equipment might be useful in preventing photo-oxidation of pyrolysis oil as well as prolonged heating of the oil. Addition of glycerol (8-10 wt.%) to the pine wood pyrolysis oil is beneficial in retaining its Newtonian flow properties for relatively long time periods. So, effectively the pumping constraints of variable shear rate and viscosity resulting from the non-Newtonian oil can be eliminated during its long-term storage (≥ 1 yr). The viscosity of the pine wood oil blended with glycerol (10 wt.%) was observed to be 300 cP (measured @ 25 °C) for the entire storage period of six months with a measurement error of $\pm 1\%$. Additionally, quick preheating of pine wood oil at a low temperature (50 °C) will decrease its viscosity significantly ($>50\%$) while minimizing the power consumption.

Projected Energy Costs

The disposal of glycerin a waste byproduct from the bio-diesel industry is of major concern as reported (Johnson and Taconi, 2007). Currently the demand for this crude glycerin in the market is much lower than its production capacity. Consequently, there is excess glycerin readily available for its application. Further, the cost of crude glycerin obtained from the bio-diesel industry is projected to be 0.05 \$/lb (0.53 \$/gal). Synthetic glycerin or glycerol by itself can cost anywhere from 0.5-1.5 \$/gallon. Hence, by the direct utilization of crude glycerin from bio-diesel industry the costs of additive could well be minimized. However, the downside is that the crude glycerin contains impurities such as water, salts, heavy metals, and alcohol in it (Hedtke, 1996; Johnson and Taconi, 2007). Among these impurities at least alcohol can be beneficial in lowering the viscosity of pyrolysis oil. Studies have reported that the pyrolysis oil stability can be increased by the use of low molecular weight alcohols such as methanol and ethanol (Diebold and Czernik, 1997). The pyrolysis oil production or selling cost has been reported to vary from 0.5-2.5 \$/gallon depending upon the feedstock cost and production capacity (Ringer et al., 2006). So, the overall costs of glycerin blended pyrolysis oil is estimated to range from 1.03-3.03 \$/gallon. A plot of energy cost (\$/GJ) as a function of glycerol concentration (wt.%) and bio-crude cost (\$/gal) is shown in Figure 4.140. This plot reveals that as the concentration of crude glycerin and the bio-crude cost increase a significant reduction in the energy cost can be truly achieved.

Calculations

Density of crude glycerin = 1.20 g/cc (assumption)

Density of crude pine wood oil = 1.19 g/cc (Ingram et al., 2008)

Heating value of crude glycerol = 20.9 KJ/g (Johnson and Taconi, 2007)

Heating value of crude pine wood oil = 18.7 KJ/g (Ingram et al., 2008)

$$\text{Mixture heating value} = \sum_{i=1}^2 x_i * HV_i$$

Where,

X_i = Mass fraction of a mixture component

HV_i = Heating value of a mixture component

$$\text{Mixture density} = \sum_{i=1}^2 x_i * \rho_i$$

Where,

X_i = Mass fraction of a mixture component

ρ_i = Density of a mixture component

Table 4.1

Average Reactor Yields (mass %) of the 16 Mississippi State University Pyrolysis Oils

Feed Stock	Temperature	Residence Time	ARF[#]	ORF^{##}	Char	UM^{###}
Pine Wood	Low	Slow	29.6	19.1	19.8	31.5
Pine Wood	Low	Fast	33.9	21.3	18.9	25.9
Pine Wood	High	Slow	29.7	22.1	17.5	30.7
Pine Wood	High	Fast	28.8	22.2	18.4	30.6
Oak Wood	Low	Slow	33.1	29.8	20.9	16.3
Oak Wood	Low	Fast	32.8	29.0	19.6	18.5
Oak Wood	High	Slow	31.9	21.4	17.3	29.5
Oak Wood	High	Fast	34.1	24.6	18.2	23.2
Pine Bark	Low	Slow	23.1	21.1	28.6	27.2
Pine Bark	Low	Fast	23.9	19.4	43.2	13.4
Pine Bark	High	Slow	20.7	22.4	24.5	32.3
Pine Bark	High	Fast	23.7	19.1	32.6	24.5
Oak Bark	Low	Slow	27.3	16.5	26.1	30.2
Oak Bark	Low	Fast	27.6	22.8	29.6	20.0
Oak Bark	High	Slow	26.1	19.4	24.5	30.0
Oak Bark	High	Fast	25.6	21.2	21.3	31.9
# Aqueous rich fraction (ARF) obtained from condenser 2						
## Organic rich fraction (ORF) obtained from condensers 1, 3, 4, and 5						
### Unaccounted mass (UM) mostly in the form of non-condensables						

Table 4.2

Gas Chromatographic-Mass Spectrometer (GC-MS) Analysis of Mississippi State University Pyrolysis Oils Produced at High Temperature and Slow Residence Time (Ingram et al., 2008)

Pyrolysis Oil Component	Retention Time (min)	Concentration (mass %)			
		PW ^I	PB ^{II}	OW ^{III}	OB ^{IV}
Phenol	15.46	0.77	0.87	0.50	0.68
2-Methylphenol	18.01	0.37	0.24	0.25	0.31
3-Methylphenol	18.71	0.71	0.85	0.40	0.57
2-Methoxyphenol (o-Guaiacol)	19.23	0.39	0.28	0.22	0.34
2,4-Dimethylphenol	21.11	0.27	0.22	0.12	0.14
2-Methoxy-4-methylphenol (4-Methylguaiacol)	22.51	0.54	0.51	0.18	0.30
4-Methyl-1,2-benzenediol (4-Methylcatechol)	24.36	0.65	0.46	0.76	0.57
2-Methoxy-4-(1-propenyl) phenol [Isoeugenol]	29.79	0.62	0.46	0.15	0.42
Oleic Acid	44.73	0.39	0.21	0.21	0.36
Furfural	10.18	0.47	0.85	1.10	0.71
3-Methyl-1,2-cyclopentanedione	17.15	1.00	0.49	0.93	0.77
1,2-Benzendiol	22.44	3.79	4.46	2.25	2.23
3-Methyl-1,2-benzenediol (3-Methylcatechol)	25.24	2.44	2.81	1.11	1.19
1,6-Anhydro-beta-D-glucopyranose (Levoglucosan)	33.26	14.20	21.50	21.60	8.21
I-Pine Wood (PW), II-Pine Bark (PB), III-Oak Wood (OW), IV-Oak Bark (OB)					

Table 4.3

Normalized Gas Composition (vol.%) of Mississippi State University Pine Bark-Low Temperature-Fast Residence (PB-LT-FR) Pyrolysis Oil

Time (min)	CO (%)	CO ₂ (%)	CH ₄ (%)	H ₂ (%)	O ₂ (%)
0	30.64	19.57	46.91	BDL	2.88
1	30.03	19.10	48.11	BDL	2.76
2	29.90	19.09	48.79	BDL	2.22
3	29.68	18.89	49.46	BDL	1.97
4	29.53	18.78	49.87	BDL	1.82
5	29.24	18.78	50.25	BDL	1.73
6	29.09	18.72	50.50	BDL	1.68
7	29.08	18.75	50.51	BDL	1.66
8	28.81	18.79	50.75	BDL	1.64
9	28.61	18.91	50.85	BDL	1.63
10	28.43	18.95	50.99	BDL	1.63
BDL=Below detection limit					

Table 4.4

Variable-Level-Treatment Input for the Mean Viscosity Model of Additive Free Mississippi State University (MS) Fresh Pyrolysis Oils (16)

Variable Used	Levels	Treatments
FEEDSTOCK	4	Oak Bark (OB), Oak Wood (OW) Pine Bark (PB), Pine Wood (PB)
PYROLYSIS TEMPERATURE ($^{\circ}\text{C}$)	2	400, 450
RESIDENCE TIME	2	Slow, Fast
VISCOSITY TEMPERATURE ($^{\circ}\text{C}$)	3	25, 50, 80
SHEAR RATE (s^{-1})	4	0.1, 1, 10, 100
<ul style="list-style-type: none"> • Response variable used for this model is the oil viscosity (cP) • Number of observations used = 192 		

Table 4.5

Analysis of Variance (ANOVA) Model Obtained for the Mean Viscosity of Additive Free Mississippi State University (MS) Fresh Pyrolysis Oils (16)

Source	DF	SS	MS	F Value	Pr > F
Model	54	213287357.1	3949765.9	6.89	<0.0001
Error	137	78502062.8	573007.8		
Corrected Total	191	291789419.8			
FEEDSTOCK (FS)	3	18711489.56	6237163.19	10.88	<0.0001
PYR. TEMPERATURE (PT)	1	9009867.00	9009867.00	15.72	0.0001
RESIDENCE TIME (RT)	1	105187.69	105187.69	0.18	0.6690
VISC. TEMPERATURE (VT)	2	20844679.03	10422339.52	18.19	<0.0001
SHEAR RATE (SR)	3	37940427.94	12646809.31	22.07	<0.0001
FS*PT	3	8264485.08	2754828.36	4.81	0.0032
FS*VT	6	15432020.84	2572003.47	4.49	0.0004
FS*SR	9	36424346.15	4047149.57	7.06	<0.0001
PT*VT	2	7148818.16	3574409.08	6.24	0.0026
PT*SR	3	13111038.29	4370346.10	7.63	<0.0001
VT*SR	6	23730665.22	3955110.87	6.90	<0.0001
FS*PT*VT	6	8411317.64	1401886.27	2.45	0.0281
FS*PT*SR	9	14153014.46	1572557.16	2.74	0.0056
Regression coefficient (R^2) = 0.73					
Coefficient of variation = 188.32					
Root mean square error = 756.97					
Mean viscosity (cP) = 401.97					
<ul style="list-style-type: none"> • Observed significance level (α) = 0.05 • Residence time (RT) is not statistically significant 					

Table 4.6

Least Significant Difference (LSD) Output of Feedstock Based on the Mean Viscosity (V) of Additive Free Mississippi State University (MS) Fresh Pyrolysis Oils (16)

t-Grouping	Mean V	N	Feedstock
A	810.7	48	PB
A	599.1	48	OB
B	112.0	48	PW
B	86.0	48	OW
Means with the same letter are not significantly different			
N=Number of observations			
PB=Pine Bark, OB=Oak Bark PW=Pine Wood, OW=Oak Wood			
Observed significance level (α) = 0.05			
Error degrees of freedom = 137			
Error mean square = 573007.8			
Critical value of t = 1.98			
LSD = 305.55			

Table 4.7

Least Significant Difference (LSD) Output of Pyrolysis Temperature (PT) Based on the Mean Viscosity (V) of Additive Free Mississippi State University (MS) Fresh Pyrolysis Oils (16)

t-Grouping	Mean V	N	PT (°C)
A	618.6	96	450
B	185.3	96	400
N=Number of observations			
Observed significance level (α) = 0.05			
Error degrees of freedom = 137			
Error mean square = 573007.8			
Critical value of t = 1.98			
LSD = 216.05			

Table 4.8

Least Significant Difference (LSD) Output of Residence Time (RT) Based on the Mean Viscosity (V) of Additive Free Mississippi State University (MS) Fresh Pyrolysis Oils (16)

t-Grouping	Mean V	N	RT
A	425.4	96	SR
A	378.6	96	FR
Means with the same letter are not significantly different			
N=Number of observations			
SR=Slow Residence Time FR=Fast Residence Time			
Observed significance level (α) = 0.05			
Error degrees of freedom = 137			
Error mean square = 573007.8			
Critical value of t = 1.98			
LSD = 216.05			

Table 4.9

Least Significant Difference (LSD) Output of Viscosity Temperature (VT) Based on the Mean Viscosity (V) of Additive Free Mississippi State University (MS) Fresh Pyrolysis Oils (16)

t-Grouping	Mean V	N	VT ($^{\circ}$C)
A	828.6	64	25
B	350.8	64	50
C	26.4	64	80
N=Number of observations			
Observed significance level (α) = 0.05			
Error degrees of freedom = 137			
Error mean square = 573007.8			
Critical value of t = 1.98			
LSD = 264.61			

Table 4.10

Least Significant Difference (LSD) Output of Shear Rate (SR) Based on the Mean Viscosity (V) of Additive Free Mississippi State University (MS) Fresh Pyrolysis Oils (16)

t-Grouping	Mean V	N	SR (s ⁻¹)
A	1161.7	48	0.1
B	265.4	48	1
B	106.3	48	10
B	74.5	48	100
Means with the same letter are not significantly different			
N=Number of observations			
Observed significance level (α) = 0.05			
Error degrees of freedom = 137			
Error mean square = 573007.8			
Critical value of t = 1.98			
LSD = 305.55			

Table 4.11

Variable-Level-Treatment Input for the Mean Water Content Model of Additive Free Mississippi State University (MS) Fresh Pyrolysis Oils (16)

Variable Used	Levels	Treatments
FEEDSTOCK	4	Oak Bark (OB), Oak Wood (OW) Pine Bark (PB), Pine Wood (PB)
PYROLYSIS TEMPERATURE (°C)	2	400, 450
RESIDENCE TIME	2	Slow, Fast
<ul style="list-style-type: none"> • Response variable used for this model is the oil viscosity (cP) • Number of replicates used = 6 • Number of observations used = 96 		

Table 4.12

Analysis of Variance (ANOVA) Model Obtained for the Mean Water Content of Additive Free Mississippi State University (MS) Fresh Pyrolysis Oils (16)

Source	DF	SS	MS	F Value	Pr > F
Model	15	3035.90	202.39	35.76	<0.0001
Error	80	452.74	5.66		
Corrected Total	95	3488.65			
FEEDSTOCK (FS)	3	1491.44	497.15	87.85	<0.0001
PYR. TEMPERATURE (PT)	1	733.83	733.83	129.67	<0.0001
RESIDENCE TIME (RT)	1	12.33	12.33	2.18	0.1439
FS*PT	3	342.76	114.25	20.19	<0.0001
FS*RT	3	236.15	78.72	13.91	<0.0001
PT*RT	1	28.65	28.65	5.06	0.0272
FS*PT*RT	3	190.75	63.58	11.24	<0.0001
Regression coefficient (R^2) = 0.87					
Coefficient of variation = 11.82					
Root mean square error = 2.38					
Mean water content (wt.%) = 20.13					
<ul style="list-style-type: none"> Observed significance level (α) = 0.05 Residence time (RT) is not statistically significant 					

Table 4.13

Least Significant Difference (LSD) Output of Feedstock Based on the Mean Water Content (WC) of Additive Free Mississippi State University (MS) Fresh Pyrolysis Oils (16)

t-Grouping	Mean WC	N	Feedstock
A	25.27	24	PB
B	21.50	24	OB
C	19.43	24	PW
D	14.35	24	OW
N=Number of observations			
PB=Pine Bark, OB=Oak Bark PW=Pine Wood, OW=Oak Wood			
Observed significance level (α) = 0.05			
Error degrees of freedom = 80			
Error mean square = 5.66			
Critical value of t = 1.99			
LSD = 1.37			

Table 4.14

Least Significant Difference (LSD) Output of Pyrolysis Temperature (PT) Based on the Mean Water Content (WC) of Additive Free Mississippi State University (MS) Fresh Pyrolysis Oils (16)

t-Grouping	Mean WC	N	PT (°C)
A	22.90	48	400
B	17.37	48	450
N=Number of observations			
Observed significance level (α) = 0.05			
Error degrees of freedom = 80			
Error mean square = 5.66			
Critical value of t = 1.99			
LSD = 0.97			

Table 4.15

Least Significant Difference (LSD) Output of Residence Time (RT) Based on the Mean Water Content (WC) of Additive Free Mississippi State University (MS) Fresh Pyrolysis Oils (16)

t-Grouping	Mean WC	N	RT
A	20.49	48	FR
A	19.78	48	SR
Means with the same letter are not significantly different			
N=Number of observations			
FR=Fast Residence Time SR=Slow Residence Time			
Observed significance level (α) = 0.05			
Error degrees of freedom = 80			
Error mean square = 5.66			
Critical value of t = 1.99			
LSD = 0.97			

Table 4.16

Mathematical Models Obtained for Viscosity of Pine Wood Pyrolysis Oils as a Function of Temperature

Pyrolysis Oil	Conc. (%)	Temp. (°C)	Storage Time (hr)	I Model Coefficients		II R ²	III (Δμ/μ)%
				a	b*10 ⁻²		
Control (CTL)	0	25, 50, 80	0	1257	5.1	0.99	94.0
			96	3950	5.4	0.99	95.0
			192	7693	5.4	0.98	94.9
Anisole (ANS)	10	25, 50, 80	0	526	4.3	0.98	90.5
			96	850	3.8	0.99	87.8
			192	757	3.5	0.99	85.0
Glycerol (GLY)	10	25, 50, 80	0	1616	5.4	0.98	94.9
			96	3305	5.6	0.99	95.5
			192	5491	5.8	0.98	96.0
Methanol (MEH)	10	25, 50, 80	0	261	3.7	0.99	86.6
			96	685	4.6	0.99	92.1
			192	763	4.2	0.98	90.3
I-Model coefficients are obtained from the exponential equation $\mu = a[\exp(-b \cdot T)]$ where μ =oil viscosity, T=temperature in °C							
II-R ² represents the goodness of fit or the regression coefficient of the exponential model							
III-(Δμ/μ)% represents the percentage viscosity drop obtained by raising the temperature of the oil from 25 to 80 °C							

Table 4.17

Chemical Classification of Additives Selected for Prescreening Studies

Chemical Group (Number of Additives)	Additives Selected (SAS Code)
Aldehyde (2)	Acetaldehyde (ACH) and 2-Furaldehyde (2FL)
Alcohol (8)	Methanol (MEH), Resorcinol (RSL), 2-Propanol (2PL), Glycerol (GLY), Tertiary Butanol (TBL), Polyethylene Glycol (PEG), Furfuryl Alcohol (FAL), and Ethanol (ETH)
Cyclic (5)	Tetrahydrofuran (THF), Cyclohexane (CHX), Decahydronaphthalene (DHN), Tetrahydronaphthalene (THN), and Xylene (XYL)
Ether (5)	Ethyl Ether (EEE), Isopropyl Ether (IPE), Anisole (ANS), Ethylene Glycol Dimethyl Ether (EGD), and Methyl Tertiary Butyl Ether (MTB)
Ester (3)	Methyl Formate (MEF), Methyl Acetate (MEA), and Ethyl Acetate (ETA)
Ketone (3)	Acetone (ACT), Cyclopentanone (CPE), and Methyl Ethyl Ketone (MEK)

Table 4.18

Rheological Models Obtained for Shear Stress of Pine Wood Pyrolysis Oils as a Function of Shear Rate

MPO	Additive	MT	ST	St	RM	τ_0	K	n	SE
MS-PW-HT	Control	25	80	0	PL	0	427	0.98	1.36
MS-PW-HT	Control	25	80	192	HB	87.27	1768	1.05	3.16
MS-PW-HT	Anisole	25	80	0	PL	0	241	0.96	1.72
MS-PW-HT	Anisole	25	80	192	HB	0.15	585	0.87	7.33
MS-PW-HT	Glycerol	25	80	0	PL	0	458	1.01	1.28
MS-PW-HT	Glycerol	25	80	192	HB	1.84	1815	0.95	2.55
MS-PW-HT	Methanol	25	80	0	PL	0	120	0.98	1.99
MS-PW-HT	Methanol	25	80	192	HB	38.17	196	1.00	7.07
MPO=Mixed pyrolysis oil MS-PW-HT=Mississippi State-Pine Wood-High Temperature MT=Measurement temperature in $^{\circ}\text{C}$ ST=Storage temperature in $^{\circ}\text{C}$ St=Storage time in hour RM=Rheological model PL=Power law [$\tau=K(\gamma)^n$] HB=Herschel Bulkley [$\tau=\tau_0+K(\gamma)^n$] τ =Shear stress in dyne.cm $^{-2}$ τ_0 =Yield stress in dyne.cm $^{-2}$ K=Consistency index or limiting viscosity in centipoise (cP) γ =Shear rate in sec $^{-1}$ n=Power law exponent or rate index SE=Standard error									

Table 4.19

Chemical Classification of Additives Used for Statistical Analysis of Variance (ANOVA)

Chemical Group (Number of Additives)	Additives Selected (SAS Code)
Aldehyde (1)	Acetaldehyde (ACH)
Alcohol (6)	Methanol (MEH), 2-Propanol (2PL), Glycerol (GLY), Tertiary Butanol (TBL), Polyethylene Glycol (PEG), and Ethanol (ETH)
Aromatic (2)	Anisole (ANS) and Xylene (XYL)
Monocyclic (3)	Tetrahydrofuran (THF), Cyclohexane (CHX), and 2-Furaldehyde (2FL)
Ether (4)	Ethyl Ether (EEE), Isopropyl Ether (IPE), Ethylene Glycol Dimethyl Ether (EGD), and Methyl Tertiary Butyl Ether (MTB)
Ester (3)	Methyl Formate (MEF), Methyl Acetate (MEA), and Ethyl Acetate (ETA)
Heterocyclic (2)	Decahydronaphthalene (DHN) and Tetrahydronaphthalene (THN)
Ketone (3)	Acetone (ACT), Cyclopentanone (CPE), and Methyl Ethyl Ketone (MEK)
Note: Resorcinol (RSL) and furfuryl alcohol (FAL) were not included during statistical analysis as these additives completely polymerized the pyrolysis oils at 192 hr	

Table 4.20

Variable-Level-Treatment Input for the Mean Viscosity Model of
Pine Wood Pyrolysis Oils (High Temperature)

Variable Used	Levels	Treatments
BLK=Additive Group	9	1-Control, 2-Ether, 3-Ketone, 4-Alcohol, 5-Heterocyclic, 6-Aromatic, 7-Ester, 8-Aldehyde, and 9-Monocyclic
SRATE=Shear Rate (s ⁻¹)	6	1, 2, 10, 20, 100, 200
VTEMP=Viscosity Temperature (°C)	3	25, 50, 80
ADD=Additive	25	2FL, 2PL, ACH, ACT, ANS, CHX, CPE, *CTL, DHN, EEE, EGD, ETA, ETH, GLY, IPE, MEA, MEF, MEH, MEK, MTB, PEG, TBL, THF, THN, XYL
<ul style="list-style-type: none"> • CTL=Pyrolysis oil control (0% Additive) • Response variable used for the mean viscosity model is obtained by the natural logarithmic value of percentage increase in viscosity (PINC) from 0 to 192 hr 		

Table 4.21

Analysis of Variance (ANOVA) Model Obtained for the Mean Viscosity Increase (%) of
Pine Wood Pyrolysis Oils (High Temperature)

Source	DF	SS	MS	F Value	Pr > F
Model	217	594.41	2.74	796.80	< 0.0001
Error	232	0.80	0.003439		
Corrected Total	449	595.21			
#BLK	8	39.58	4.95	1439.01	<0.0001
SRATE	5	224.18	44.84	13042.10	<0.0001
VTEMP	2	39.72	19.86	5776.43	<0.0001
##ADD	24	163.93	6.83	1986.83	<0.0001
SRATE*VTEMP	10	24.51	2.45	712.89	<0.0001
SRATE*ADD	120	29.57	0.25	71.69	<0.0001
VTEMP*ADD	48	72.92	1.52	441.93	<0.0001
Regression coefficient (R ²) = 0.99					
Coefficient of variation = 0.95					
Root mean square error (RMSE) = 0.06					
Mean Ln _c PINC = 6.14					
<ul style="list-style-type: none"> • #BLK refers to a group of additive as shown in Table 4.8 • ##Resorcinol (RSL) and furfuryl alcohol (FAL) blended pyrolysis oil samples were polymerized completely at 24 and 96 hr respectively. Hence, viscosity ANOVA model was run with 24 additives and control (CTL) • Observed significance level (α) = 0.05 					

Table 4.22

Least Significant Difference (LSD) Output of Additive Group (BLK) Based on the Mean Viscosity Increase (%) of Pine Wood Pyrolysis Oils (High Temperature)

Additive Group Comparison*	Mean Difference in LnPINC	Confidence Limits (95%)		Significance Level [$\alpha=0.05$]
1-2	+0.63	+0.60	+0.66	***
1-3	+0.78	+0.74	+0.81	***
1-4	+1.02	+0.99	+1.05	***
1-5	+0.38	+0.35	+0.42	***
1-6	+0.30	+0.27	+0.33	***
1-7	+0.64	+0.61	+0.67	***
1-8	+0.63	+0.59	+0.67	***
1-9	+0.23	+0.20	+0.26	***
2-3	+0.15	+0.13	+0.17	***
2-4	+0.39	+0.38	+0.41	***
2-5	-0.24	-0.27	-0.22	***
2-6	-0.33	-0.35	-0.30	***
2-7	+0.01	-0.01	+0.03	----
2-8	+0.00	-0.03	+0.03	----
2-9	-0.40	-0.42	-0.38	***
3-4	+0.25	+0.23	+0.26	***
3-5	-0.39	-0.42	-0.37	***
3-6	-0.47	-0.50	-0.45	***
3-7	-0.14	-0.16	-0.11	***
3-8	-0.15	-0.18	-0.12	***
3-9	-0.55	-0.57	-0.53	***
4-5	-0.64	-0.66	-0.62	***
4-6	-0.72	-0.74	-0.70	***
4-7	-0.38	-0.40	-0.36	***
4-8	-0.39	-0.42	-0.36	***
4-9	-0.79	-0.81	-0.77	***
5-6	-0.08	-0.11	-0.05	***
5-7	+0.26	+0.23	+0.28	***
5-8	+0.25	+0.21	+0.28	***
5-9	-0.15	-0.18	-0.13	***
6-7	+0.34	+0.31	+0.36	***
6-8	+0.33	+0.29	+0.36	***
6-9	-0.07	-0.10	-0.05	***
7-8	-0.01	-0.04	0.02	----
7-9	-0.41	-0.43	-0.39	***
8-9	-0.40	-0.43	-0.37	***
*Additive Group	1-Control, 2-Ether, 3-Ketone, 4-Alcohol, 5-Heterocyclic, 6-Aromatic, 7-Ester, 8-Aldehyde, and 9-Monocyclic			

Table 4.23

Least Significant Difference (LSD) Output of Shear Rate (s^{-1}) Based on the Mean Viscosity Increase (%) of Pine Wood Pyrolysis Oils (High Temperature)

t-Grouping	Mean LnPINC	N	Shear Rate (s^{-1})
A	7.28	75	1
B	6.85	75	2
C	6.10	75	10
D	5.83	75	20
E	5.42	75	100
E	5.39	75	200
N=Number of observations Means with the same letter are not significantly different			
Pseudoplastic Region: 1-20 s^{-1} Newtonian Region: 100-200 s^{-1}			

Table 4.24

Least Significant Difference (LSD) Output of Temperature ($^{\circ}C$) Based on the Mean Viscosity Increase (%) of Pine Wood Pyrolysis Oils (High Temperature)

t-Grouping	Mean LnPINC	N	Viscosity Temperature ($^{\circ}C$)
A	6.55	150	50
B	6.03	150	25
C	5.86	150	80
N=Number of observations			

Table 4.25

Least Significant Difference (LSD) Output of Control and Additives Based on the Mean Viscosity Increase (%) of Pine Wood Pyrolysis Oils (High Temperature)

t-Grouping	Mean LnPINC	N	Additive
A	7.89	18	2FL (2-Furaldehyde)
B	7.69	18	XYL (Xylenes)
C	6.77	18	CTL (Control)
D	6.71	18	DHN (Decahydronapthalene)
E	6.34	18	IPE (Isopropyl Ether)
F	6.26	18	MEF (Methyl Formate)
F	6.25	18	TBL (t-Butanol)
G	6.18	18	MEK (Methyl Ethyl Ketone)
GH	6.16	18	EEE (Ethyl Ether)
H	6.14	18	ACH (Acetaldehyde)
IJ	6.12	18	EGD (Dimethyl Ether)
IJ	6.10	18	2PL (2-Propanol)
JK	6.09	18	MEA (Methyl Acetate)
KL	6.06	18	THN (Tetrahydronapthalene)
LM	6.03	18	ETA (Ethyl Acetate)
M	6.01	18	THF (Tetrahydro Furan)
N	5.95	18	ACT (Acetone)
N	5.94	18	MTB (Methyl t-Butyl Ether)
O	5.86	18	MEH (Methanol)
O	5.84	18	CPE (Cyclopentanone)
P	5.72	18	CHX (Cyclohexane)
Q	5.63	18	ETH (Ethanol)
R	5.36	18	PEG (Polyethylene Glycol)
S	5.29	18	GLY (Glycerol)
T	5.24	18	ANS (Anisole)
N=Number of observations			
Means with the same letter are not significantly different			
2FL: 2670.44% (Maximum PINC)			
ANS: 188.67% (Minimum PINC)			

Table 4.26

Variable-Level-Treatment Input for the Mean Water Content Model of Pine Wood Pyrolysis Oils (High Temperature)

Variable Used	Levels	Treatments
BLK=Additive Group	9	1-Control, 2-Ether, 3-Ketone, 4-Alcohol, 5-Heterocyclic, 6-Aromatic, 7-Ester, 8-Aldehyde, and 9-Monocyclic
STIME=Storage Time (hr)	2	0, 192
ADD=ADDITIVE	25	2FL, 2PL, ACH, ACT, ANS, *CTL, CHX, CPE, DHN, EEE, EGD, ETA, ETH, GLY, IPE, MEA, MEF, MEH, MEK, MTB, PEG, TBL, THF, THN, and XYL
<ul style="list-style-type: none"> *CTL=Pyrolysis oil control (0% Additive) Response variable used for the mean water content model was obtained as wt.% water during Karl Fisher analysis 		

Table 4.27

Analysis of Variance (ANOVA) Model Obtained for the Mean Water Content (wt.%) of Pine Wood Pyrolysis Oils (High Temperature)

Source	DF	SS	MS	F-Value	Pr > F
Model	33	201.87	6.12	118.93	<0.0001
Error	66	3.39	0.0514		
Corrected Total	99	205.27			
*BLK	8	23.18	2.90	56.33	<0.0001
STIME	1	143.59	143.59	2791.69	<0.0001
**ADD	24	35.10	1.46	28.44	<0.0001
Regression coefficient (R^2) = 0.98					
Coefficient of variation = 1.85					
Root mean square error (RMSE) = 0.23					
Mean water content (%) = 12.25					
<ul style="list-style-type: none"> *BLK refers to a group of additive as shown in Table 4.14 **Resorcinol (RSL) and furfuryl alcohol (FAL) blended pyrolysis oil samples were polymerized completely at 24 and 96 hr respectively. Therefore, water content ANOVA model was run with 24 additives and control (CTL) Observed significance level (α) = 0.05 					

Table 4.28

Least Significant Difference (LSD) Output of Additive Group (BLK) Based on the Mean Water Content (wt.%) of Pine Wood Pyrolysis Oils (High Temperature)

Additive Group Comparison*	Mean Difference in Water Content (wt.%)	Confidence Limits (95%)		Significance Level [$\alpha=0.05$]
1-2	+2.09	+1.84	+2.34	***
1-3	+1.50	+1.24	+1.76	***
1-4	+1.28	+1.04	+1.53	***
1-5	+0.93	+0.65	+1.21	***
1-6	+1.19	+0.92	+1.47	***
1-7	+1.87	+1.61	+2.13	***
1-8	+1.18	+0.85	+1.50	***
1-9	+0.96	+0.69	+1.22	***
2-3	-0.59	-0.76	-0.42	***
2-4	-0.81	-0.95	-0.66	***
2-5	-1.16	-1.36	-0.96	***
2-6	-0.90	-1.09	-0.70	***
2-7	-0.22	-0.39	-0.04	***
2-8	-0.92	-1.17	-0.66	***
2-9	-1.13	-1.30	-0.96	***
3-4	-0.22	-0.38	-0.06	***
3-5	-0.57	-0.78	-0.36	***
3-6	-0.31	-0.52	-0.10	***
3-7	+0.37	+0.19	+0.56	***
3-8	-0.33	-0.59	-0.07	***
3-9	-0.54	-0.73	-0.36	***
4-5	-0.35	-0.54	-0.17	***
4-6	-0.09	-0.28	+0.09	----
4-7	+0.59	+0.43	+0.75	***
4-8	-0.11	-0.35	+0.14	----
4-9	-0.32	-0.48	-0.16	***
5-6	+0.26	+0.04	+0.49	***
5-7	+0.94	+0.74	+1.15	***
5-8	+0.25	-0.03	+0.52	----
5-9	+0.03	-0.18	+0.24	----
6-7	+0.68	+0.47	+0.89	***
6-8	-0.02	-0.29	+0.26	----
6-9	-0.23	-0.44	-0.02	***
7-8	-0.70	-0.96	-0.44	***
7-9	-0.91	-1.10	-0.73	***
8-9	-0.21	-0.48	+0.05	----
*Additive Group	1-Control, 2-Ether, 3-Ketone, 4-Alcohol, 5-Heterocyclic, 6-Aromatic, 7-Ester, 8-Aldehyde, and 9-Monocyclic			

Table 4.29

Least Significant Difference (LSD) Output of Storage Time (hr) Based on the Mean Water Content (wt.%) of Pine Wood Pyrolysis Oils (High Temperature)

t-Grouping	Mean Water Content (wt.%)	N	Storage Time (hr)
A	13.44	50	192
B	11.05	50	0
N=Number of observations			

Table 4.30

Least Significant Difference (LSD) Output of Control and Additives Based on the Mean Water Content (wt.%) of Pine Wood Pyrolysis Oils (High Temperature)

t-Grouping	Mean Water Content (%)	N	Additive
A	13.63	4	CTL (Control)
B	12.91	4	2FL (2-Furaldehyde)
B	12.91	4	GLY (Glycerol)
BC	12.74	4	MEH (Methanol)
BC	12.70	4	DHN (Decahydronaphthalene)
BC	12.69	4	THN (Tetrahydronaphthalene)
BC	12.65	4	ANS (Anisole)
BC	12.65	4	ETH (Ethanol)
BC	12.63	4	THF (Tetrahydro Furan)
CD	12.45	4	CHX (Cyclohexane)
CD	12.45	4	ACH (Acetaldehyde)
CD	12.42	4	EGD (Dimethyl Ether)
DE	12.26	4	CPE (Cyclopentanone)
DE	12.22	4	MEK (Methyl Ethyl Ketone)
DE	12.22	4	XYL (Xylenes)
EF	12.08	4	MEA (Methyl Acetate)
EF	12.06	4	2PL (2-Propanol)
EF	11.96	4	ETA (Ethyl Acetate)
F	11.89	4	ACT (Acetone)
F	11.89	4	TBL (t-Butanol)
F	11.80	4	PEG (Polyethylene Glycol)
G	11.35	4	IPE (Isopropyl Ether)
G	11.30	4	MTB (Methyl t-Butyl Ether)
G	11.21	4	MEF (Methyl Formate)
G	11.07	4	EEE (Ethyl Ether)
N=Number of observations			
Means with the same letter are not significantly different			

Table 4.31

Variable-Level-Treatment Input for the Mean Viscosity Model of Pine Wood Pyrolysis Oils (Low Temperature)

Variable Used	Levels	Treatments
ADD=Additive	3	ANS, GLY, MEH
VTEMP=Viscosity Temperature ($^{\circ}\text{C}$)	3	25, 50, 80
SRATE=Shear Rate (s^{-1})	3	1, 10, 100
CLEVEL=Additive Concentration (wt.%)	5	0*, 5, 10, 15, 20
<ul style="list-style-type: none"> * Pyrolysis oil control (0% Additive) Response variable used for the viscosity model is obtained as a difference (increase) in viscosity ($\text{VD}=\text{cP}$) from 0 to 192 hr 		

Table 4.32

Analysis of Variance (ANOVA) Model Obtained for the Mean Viscosity Difference (cP) of Pine Wood Pyrolysis Oils (Low Temperature)

Source	DF	SS	MS	F Value	Pr > F
Model	46	69022.06	1500.48	18.98	<0.0001
Error	88	6956.07	79.05		
Corrected Total	134	75978.13			
ADD	2	3116.28	1558.14	19.71	<0.0001
VTEMP	2	13844.07	6922.03	87.57	<0.0001
SRATE	2	12149.35	6074.67	76.85	<0.0001
CLEVEL	4	14455.66	3613.91	45.72	<0.0001
ADD*VTEMP	4	677.53	169.38	2.14	0.0821*
ADD*SRATE	4	1972.79	493.20	6.24	0.0002
ADD*CLEVEL	8	5090.31	636.29	8.05	<0.0001
VTEMP*SRATE	4	3099.56	774.89	9.80	<0.0001
VTEMP*CLEVEL	8	6639.04	829.88	10.50	<0.0001
SRATE*CLEVEL	8	7977.47	997.18	12.62	<0.0001
Regression coefficient (R^2) = 0.91					
Coefficient of variation = 61.02					
Root mean square error (RMSE) = 8.89					
Mean increase in viscosity (VD) = 14.57 cP					
<ul style="list-style-type: none"> Observed significance level (α) = 0.05 ADD*VTEMP interaction is merely not significant 					

Table 4.33

Least Significant Difference (LSD) Output of Additive Based on the Mean Viscosity Difference (cP) or VD of Pine Wood Pyrolysis Oils (Low Temperature)

t-Grouping	Mean VD	N	Additive
A	21.23	45	ANS
B	12.41	45	GLY
B	10.08	45	MEH
N=Number of observations Means with the same letter are not significantly different			

Table 4.34

Least Significant Difference (LSD) Output of Additive Concentration (wt.%) Based on the Mean Viscosity Difference (cP) or VD of Pine Wood Pyrolysis Oils (Low Temperature)

t-Grouping	Mean VD	N	Additive Concentration (%)
A	29.62	27	0
B	24.30	27	5
C	8.06	27	15
C	7.02	27	10
C	3.86	27	20
N=Number of observations Means with the same letter are not significantly different			

Table 4.35

Least Significant Difference (LSD) Output of Measurement Temperature (⁰C) Based on the Mean Viscosity Difference (cP) or VD of Pine Wood Pyrolysis Oils (Low Temperature)

t-Grouping	Mean VD	N	Temperature (⁰C)
A	28.29	45	25
B	11.28	45	50
C	4.15	45	80
N=Number of observations			

Table 4.36

Least Significant Difference (LSD) Output of Shear Rate (s^{-1}) Based on the Mean Viscosity Difference (cP) or VD of Pine Wood Pyrolysis Oils (Low Temperature)

t-Grouping	Mean VD	N	Shear Rate (s^{-1})
A	27.90	45	1
B	9.25	45	10
B	6.56	45	100
N=Number of observations Means with the same letter are not significantly different			

Table 4.37

Variable-Level-Treatment Input for the Mean Water Content Model of Pine Wood Pyrolysis Oils (Low Temperature)

Variable Used	Levels	Treatments
ADD=ADDITIVE	3	ANS, GLY, MEH
STIME=Storage Time (hr)	2	24, 96
CLEVEL=Additive Concentration (wt.%)	5	0*, 5, 10, 15, 20
<ul style="list-style-type: none"> * Pyrolysis oil control (0% Additive) Response variable used for the mean water content model is obtained as a difference (increase) in water content (WCD=wt.%) from 0 to 24 hr and 0 to 96 hr respectively The water content (wt.%) of the pyrolysis oils was determined during Karl Fisher analysis 		

Table 4.38

Analysis of Variance (ANOVA) Model Obtained for the Mean Water Content Difference (wt.%) of Pine Wood Pyrolysis Oils (Low Temperature)

Source	DF	SS	MS	F Value	Pr > F
Model	21	63.96	3.05	9.58	<0.0001
Error	38	12.09	0.32		
Corrected Total	59	76.05			
ADD	2	12.17	6.09	19.13	<0.0001
STIME	1	5.31	5.31	16.69	0.0002
CLEVEL	4	7.41	1.85	5.83	0.0009
ADD*STIME	2	3.97	1.98	6.23	0.0046
ADD*CLEVEL	8	20.83	2.60	8.18	<0.0001
STIME*CLEVEL	4	14.28	3.57	11.22	<0.0001
Regression coefficient (R^2) = 0.84					
Coefficient of variation = 35.09					
Root mean square error (RMSE) = 0.56					
Mean water content Increase (WCD) = 1.61 wt.%					
• Observed significance level (α) = 0.05					

Table 4.39

Least Significant Difference (LSD) Output of Additive Based on the Mean Water Content Difference (wt.%) or WCD of Pine Wood Pyrolysis Oils (Low Temperature)

t-Grouping	Mean WCD	N	ADDITIVE
A	2.18	20	ANS
B	1.56	20	GLY
C	1.08	20	MEH
N=Number of observations WCI=Water content increase (wt.%)			

Table 4.40

Least Significant Difference (LSD) Output of Storage Time (hr) Based on the Mean Water Content Difference (wt.%) or WCD of Pine Wood Pyrolysis Oils (Low Temperature)

t-Grouping	Mean WCD	N	Storage Time (hr)
A	1.90	30	96
B	1.31	30	24

N=Number of observations
WCI=Water content increase (wt.%)

Table 4.41

Least Significant Difference (LSD) Output of Additive Concentration (wt.%) Based on the Mean Water Content Difference (wt.%) or WCD of Pine Wood Pyrolysis Oils (Low Temperature)

t-Grouping	Mean WCD	N	Additive Concentration (%)
A	1.96	12	20
A	1.92	12	15
A	1.78	12	10
B	1.30	12	5
B	1.08	12	0

N=Number of observations
WCI=Water content increase (%)
Means with the same letter are not significantly different

Table 4.42

General Linear Model (GLM) Selected during the Statistical Analyses

Y =	$\beta_0 + \beta_1 * X_1 + \beta_2 * X_2 + \beta_3 * X_3 + \beta_{11} * X_1^2 + \beta_{22} * X_2^2 + \beta_{33} * X_3^2 + \beta_{12} * X_1 * X_2 + \beta_{13} * X_1 * X_3 + \beta_{23} * X_2 * X_3 + \epsilon$
Where,	<p>Y = Response variable [normalized viscosity (cP)] β_0 = Intercept $\beta_1, \beta_2, \beta_3, \beta_{11}, \beta_{22}, \beta_{33}, \beta_{12}, \beta_{13}, \beta_{23}$ = Model coefficients Main Effects: X_1 = Additive concentration (wt.%) X_2 = Storage time (months or hours) X_3 = Shear rate (s^{-1}) Interactions (2-way) = 6 = ($X_i * X_j$), where i, j = 1, 2, 3 ϵ = Model error [$\epsilon \sim N(0, \sigma^2)$]</p>

Table 4.43

General Linear Model (GLM) Parameters and their Estimates Obtained for Additive Blended Mississippi State University Pyrolysis Oils Stored at 25 and 80 °C

Model Parameter	Estimate		
	Pine Wood (Methanol)	Oak Wood (Glycerol)	Oak Bark (Anisole)
R-Square	0.947589	0.829641	0.703892
Coefficient of Variation	2.595264	4.451718	19.11449
Root MSE	0.130533	0.237922	1.032262
Mean Viscosity (cP)	152.88	209.45	221.50

Table 4.44

General Linear Model (GLM) Equations Obtained for Additive Blended Mississippi State University Pyrolysis Oils Stored at 25 and 80 °C

Pine Wood (Methanol)	V =	$5.658845627 - 0.165201115*CONC - 0.078023169*ST - 0.001260168*SR - 0.005913793*CONC*ST - 0.000230230*CONC*SR + 0.000534730*ST*SR + 0.0085*CONC*CONC + 0.015219439*ST*ST$
Oak Wood (Glycerol)	V =	$5.416358149 + 0.003709052*CONC - 0.008624682*ST - 0.051377938*SR - 0.011157328*CONC*ST - 0.000813883*ST*SR + 0.035113939*ST*ST + 0.000460375*SR*SR$
Oak Bark (Anisole)	V =	$6.462615975 + 0.657875*CONC - 0.003007813*ST - 0.189387853*SR - 0.071075*CONC*CONC + 0.001646917*SR*SR$
Where,		
V = Normalized Viscosity (cP)		
CONC = Additive Concentration = 0, 5, 10 wt.%		
ST = Storage Time = 0, 1, 2, 4, 6 months [Pine Wood and Oak Wood]		
ST = Storage Time = 0, 24, 48, 96, 192 hours [Oak Bark]		
SR = Shear Rate = 0.1, 1, 10, 100 s ⁻¹		

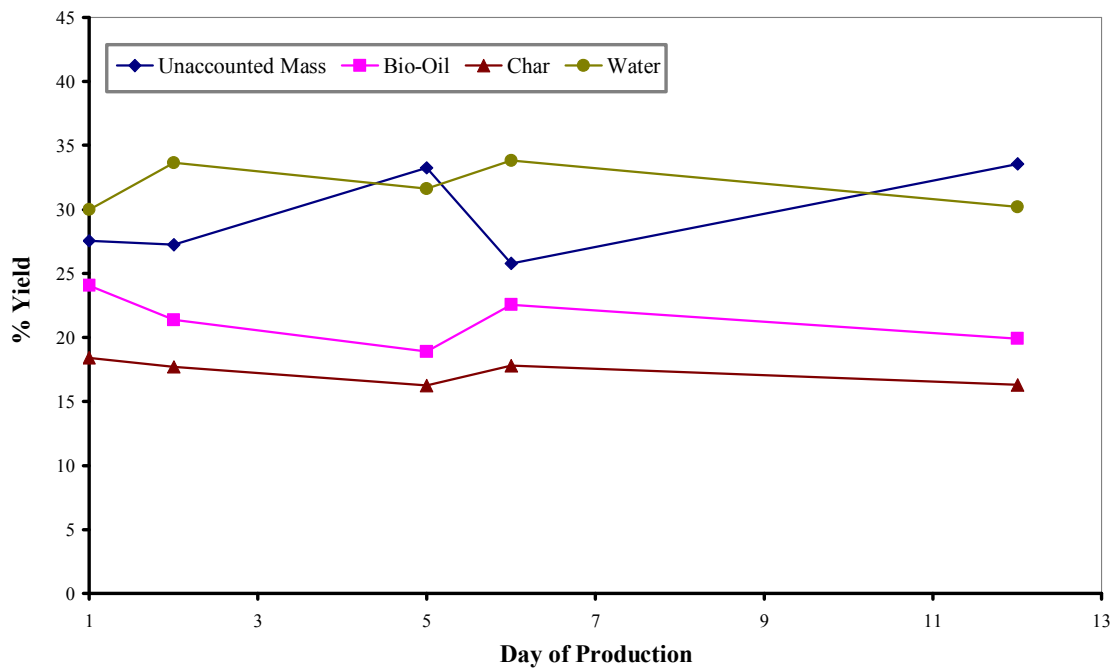


Figure 4.1 Daily Reactor Yields of Oak Wood-High Temperature-Slow Residence (OW-HT-SR) Pyrolysis Oil

[*This test run was completed over a span of 12 days with the reactor operating for 5 days]

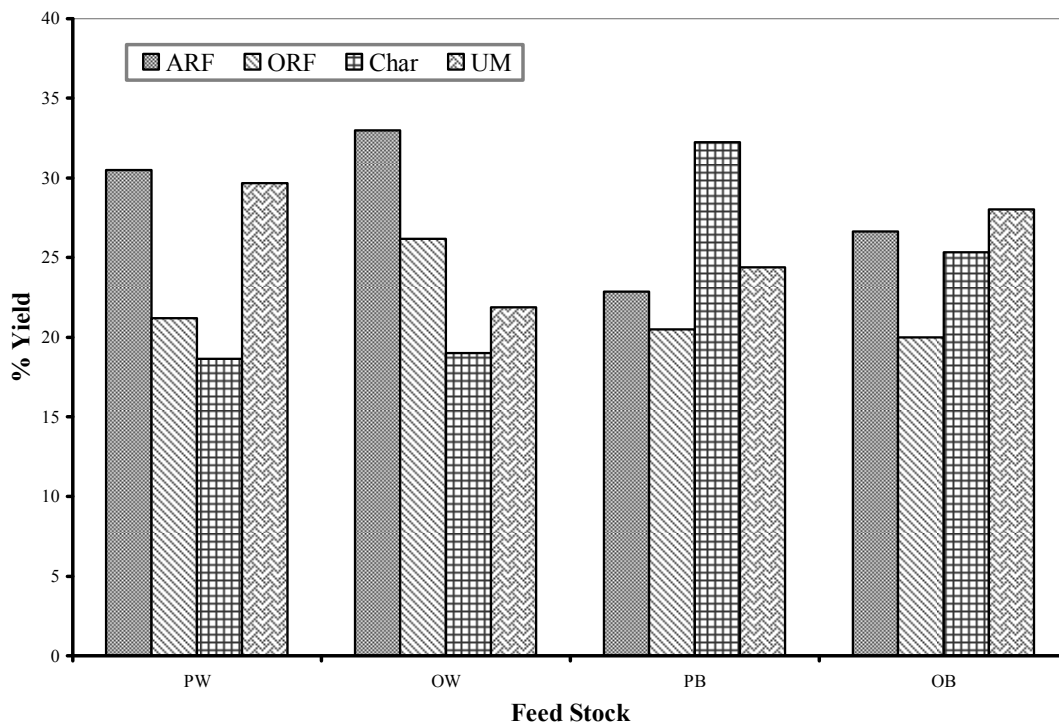


Figure 4.2 Average Yields of Four Fractions (Water-ARF, Oil-ORF, Char, and Unaccounted Mass-UM) Obtained from Auger Reactor

[*The four feed stocks utilized were pine wood (PW), oak wood (OW), pine bark (PB), and oak bark (OB)]



Figure 4.3 Tarry Pyrolyzate Collected from the Mississippi State University Auger Reactor Condensers

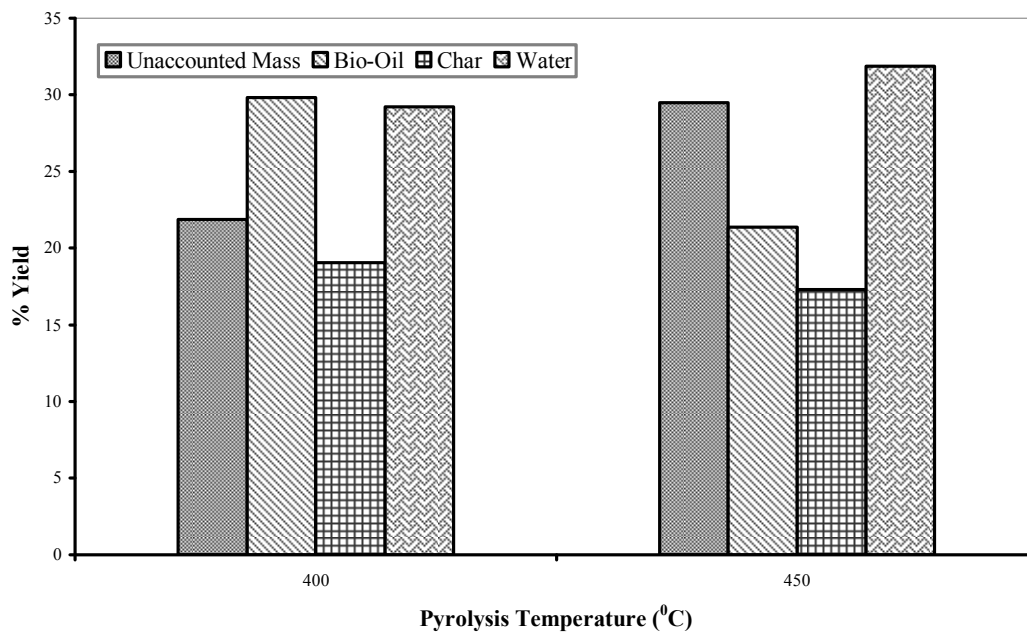


Figure 4.4 Influence of Pyrolysis Temperature on the Average Reactor Yields of Mississippi State University-Oak Wood-Slow Residence (MS-OW-SR) Pyrolysis Oils

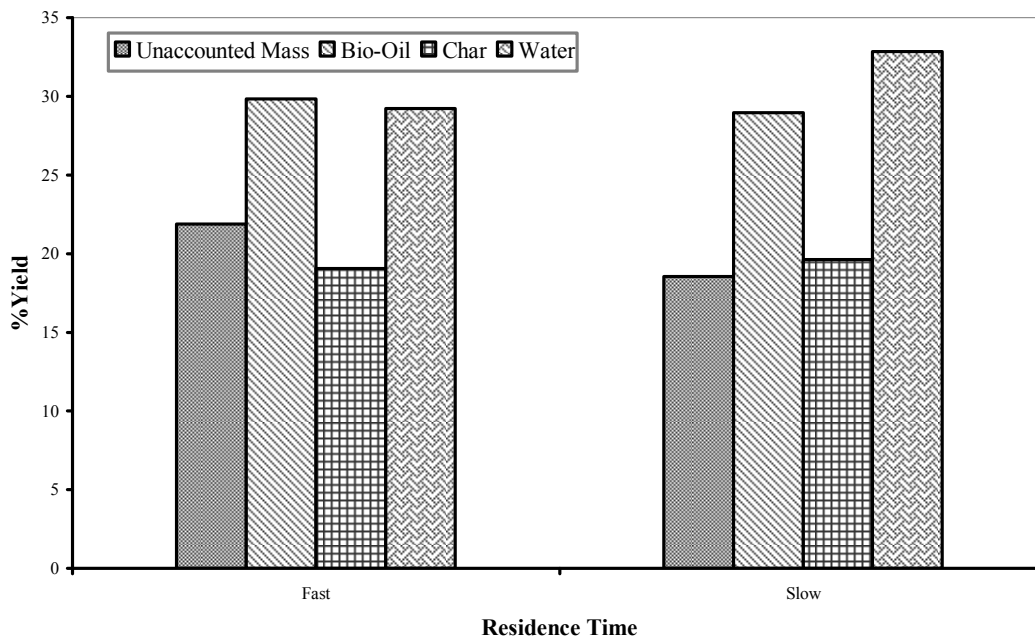


Figure 4.5 Influence of Residence Time on the Average Reactor Yields of Mississippi State University-Oak Wood-Low Temperature (MS-OW-LT) Pyrolysis Oils



Figure 4.6 Tarry Mass Collected During Gas Analysis of Mississippi State University Pine Bark-Low Temperature-Fast Residence (PB-LT-FR) Pyrolysis Oil

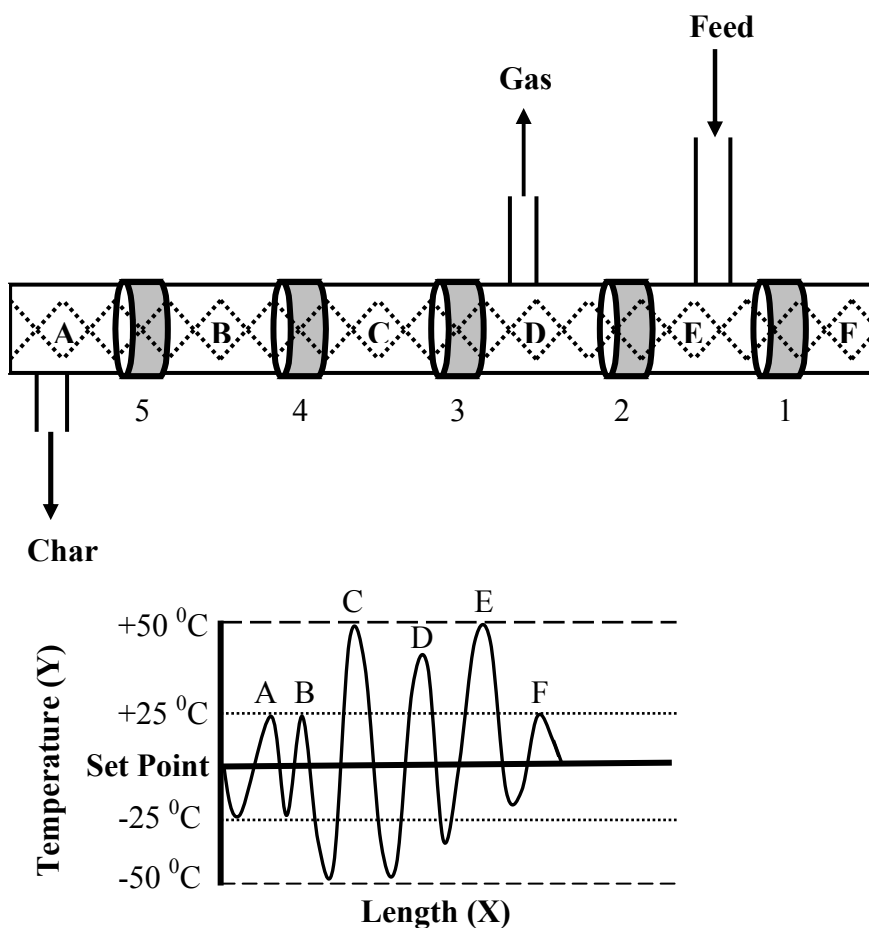


Figure 4.7 Temperature Variation of the Ceramic Band Heaters (1-5) Observed as a Function of Reactor Length

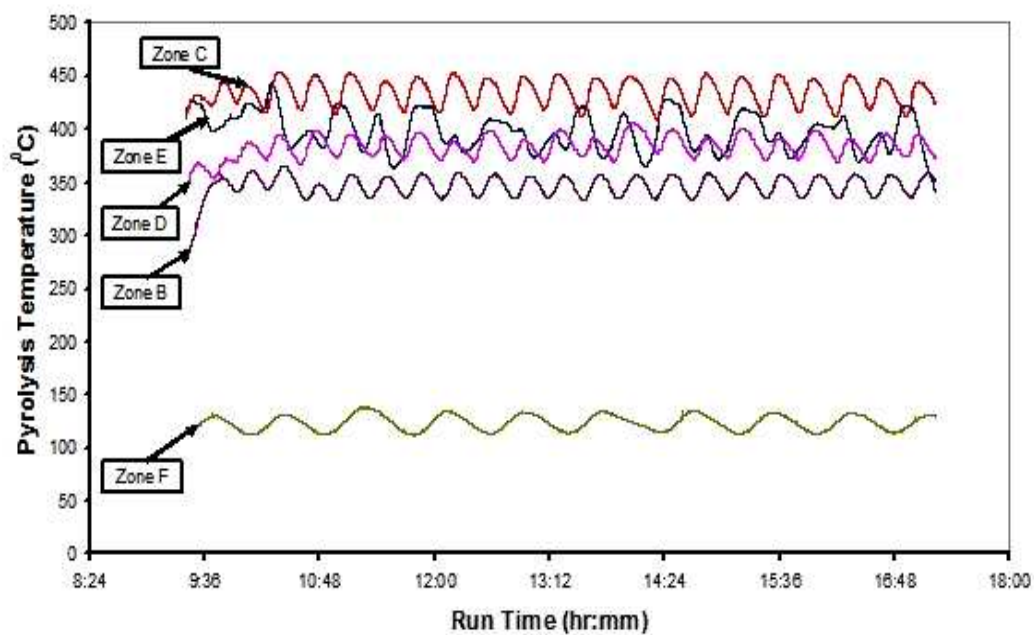


Figure 4.8 Zonal (B-F) Temperature Profile Obtained as a Function of Run Time

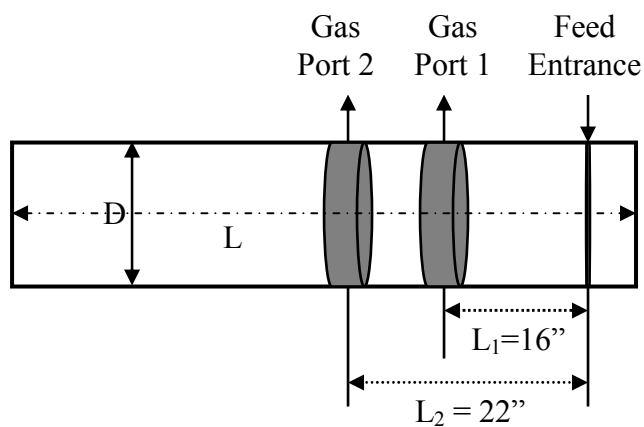


Figure 4.9 Approximate Distances of Gas and Vapor Collection Ports from the Feed Entrance of Mississippi State University (MSU) Small-Scale Auger Reactor

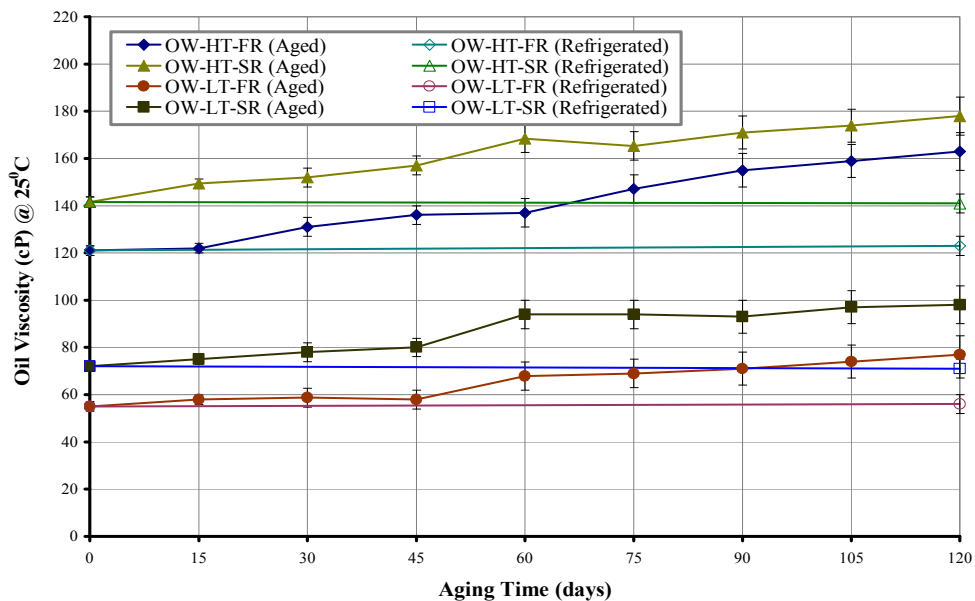


Figure 4.10 Viscosity (cP) as a Function of Aging Time (days) of Oak Wood (OW) Pyrolysis Oils of Mississippi State University

[*Temperature (LT-Low and High-HT) and Time (SR-Slow and Fast-FR)]

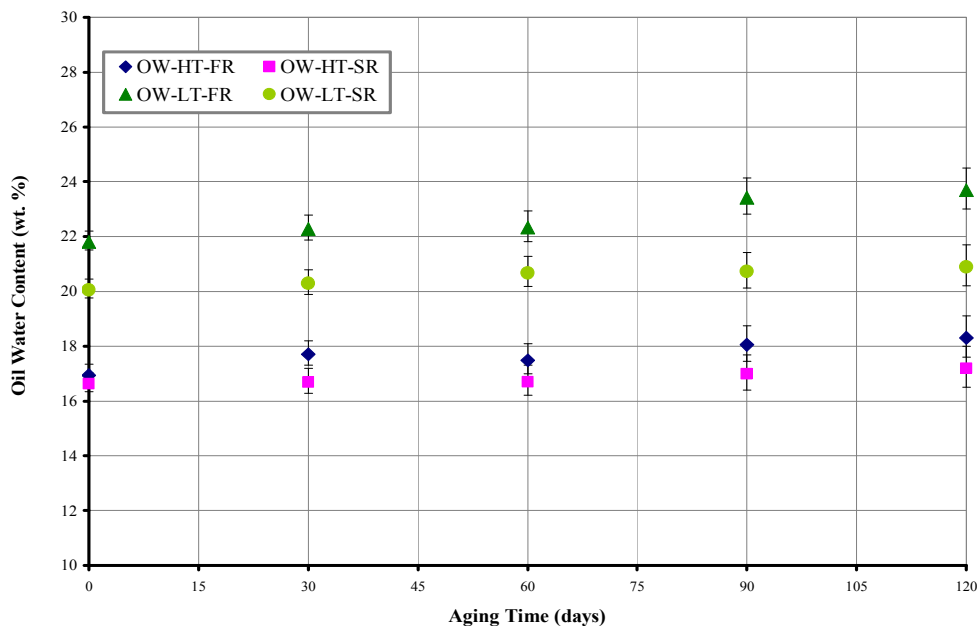


Figure 4.11 Water Content (wt.%) as a Function of Aging Time (days) of Oak Wood (OW) Pyrolysis Oils of Mississippi State University

[*Temperature (LT-Low and High-HT) and Time (SR-Slow and Fast-FR)]

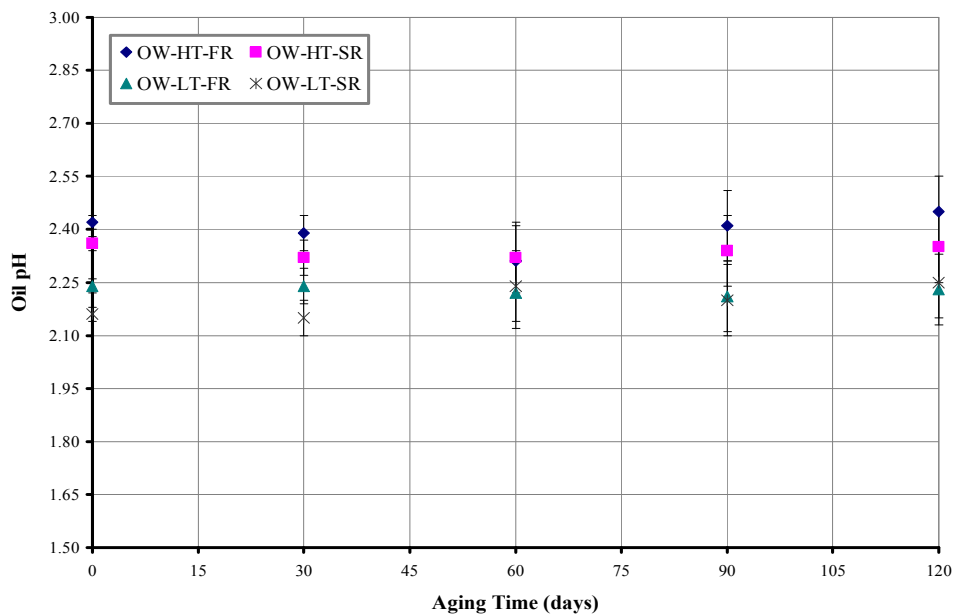


Figure 4.12 Acidity (pH) as a Function of Aging Time (days) of Oak Wood (OW) Pyrolysis Oils of Mississippi State University

[*Temperature (LT-Low and High-HT) and Time (SR-Slow and Fast-FR)]

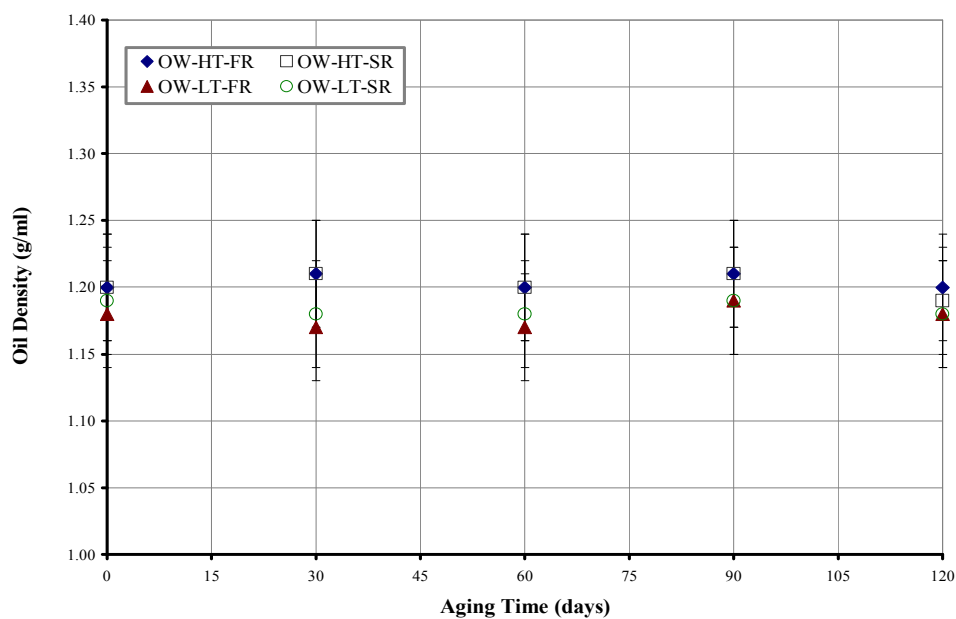


Figure 4.13 Density (g/ml) as a Function of Aging Time (days) of Oak Wood (OW) Pyrolysis Oils of Mississippi State University

[*Temperature (LT-Low and High-HT) and Time (SR-Slow and Fast-FR)]

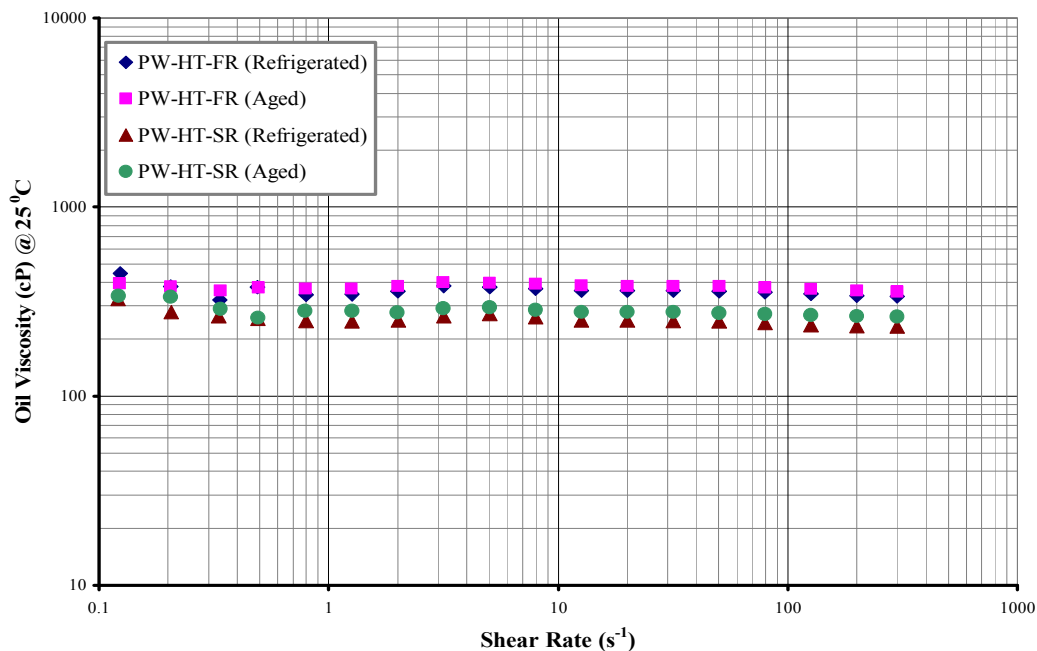


Figure 4.14 Viscosity (cP) as a Function of Shear Rate (s^{-1}) and Residence Time (SR-Slow and Fast-FR) of Pine Wood (PW) High Temperature (HT) Pyrolysis Oils of Mississippi State University

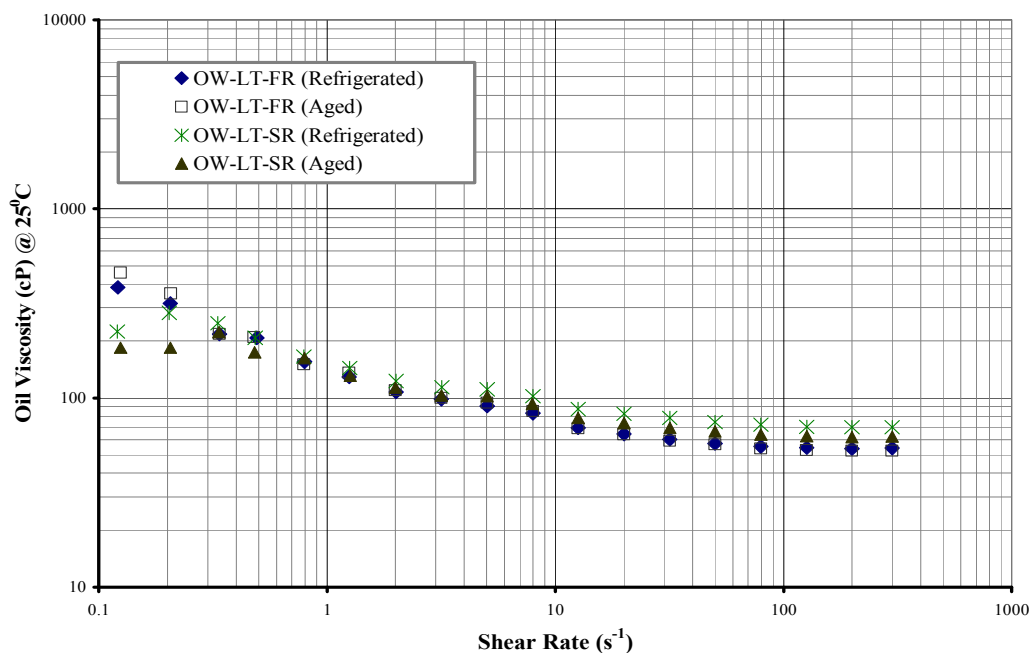


Figure 4.15 Viscosity (cP) as a Function of Shear Rate (s^{-1}) and Residence Time (SR-Slow and Fast-FR) of Oak Wood (OW) Low Temperature (LT) Pyrolysis Oils of Mississippi State University

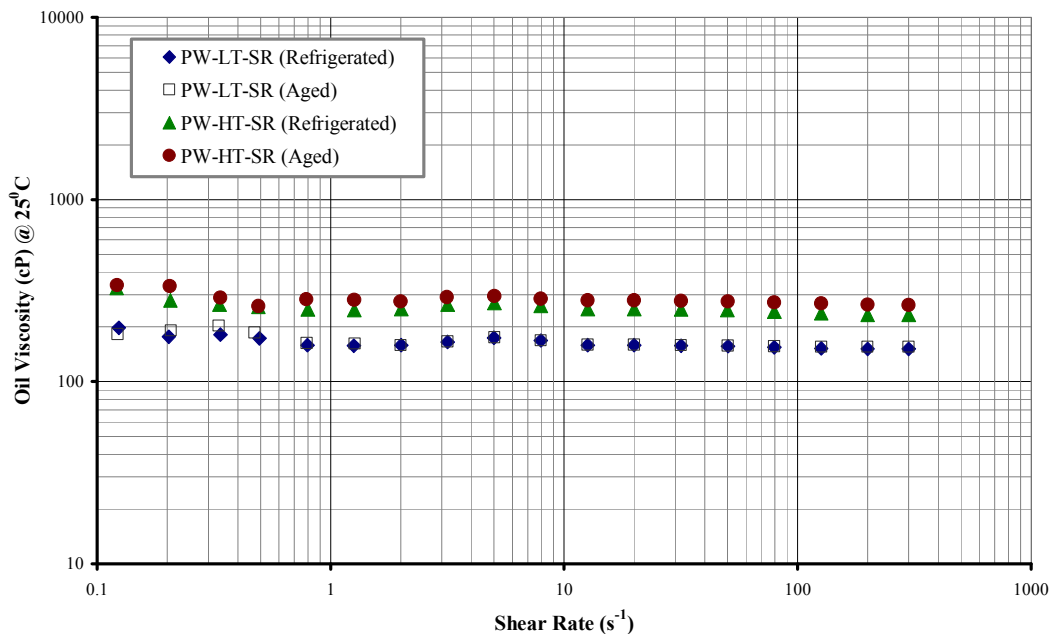


Figure 4.16 Viscosity (cP) as a Function of Shear Rate (s^{-1}) and Pyrolysis Temperature (LT-Low and High-HT) of Pine Wood (PW) Slow Residence (SR) Pyrolysis Oils of Mississippi State University

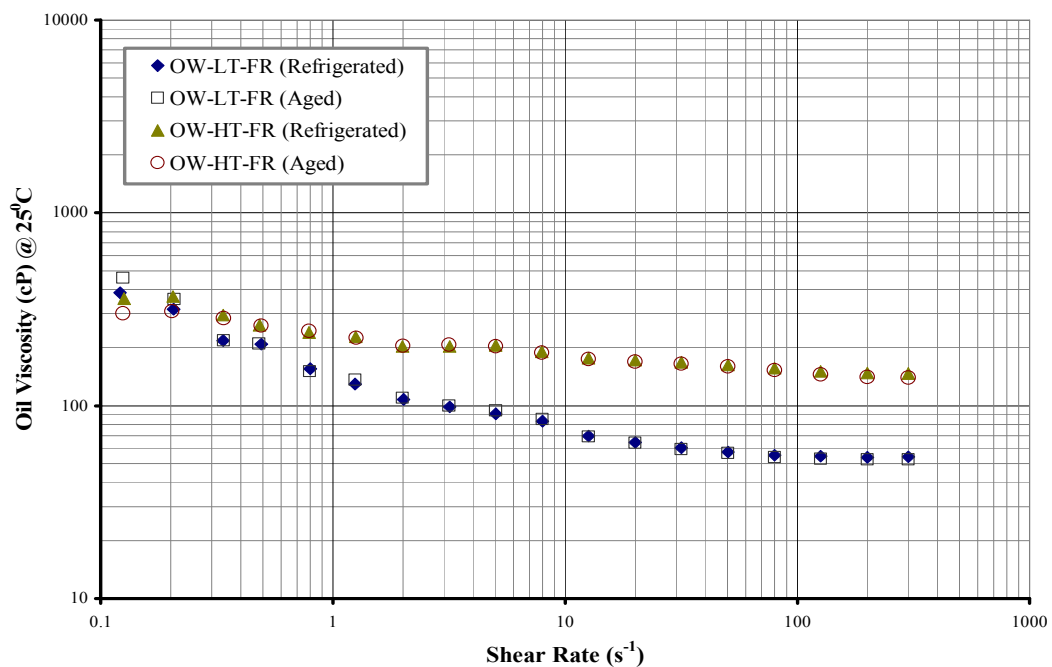


Figure 4.17 Viscosity (cP) as a Function of Shear Rate (s^{-1}) and Pyrolysis Temperature (LT-Low and High-HT) of Oak Wood (OW) Fast Residence (FR) Pyrolysis Oils of Mississippi State University

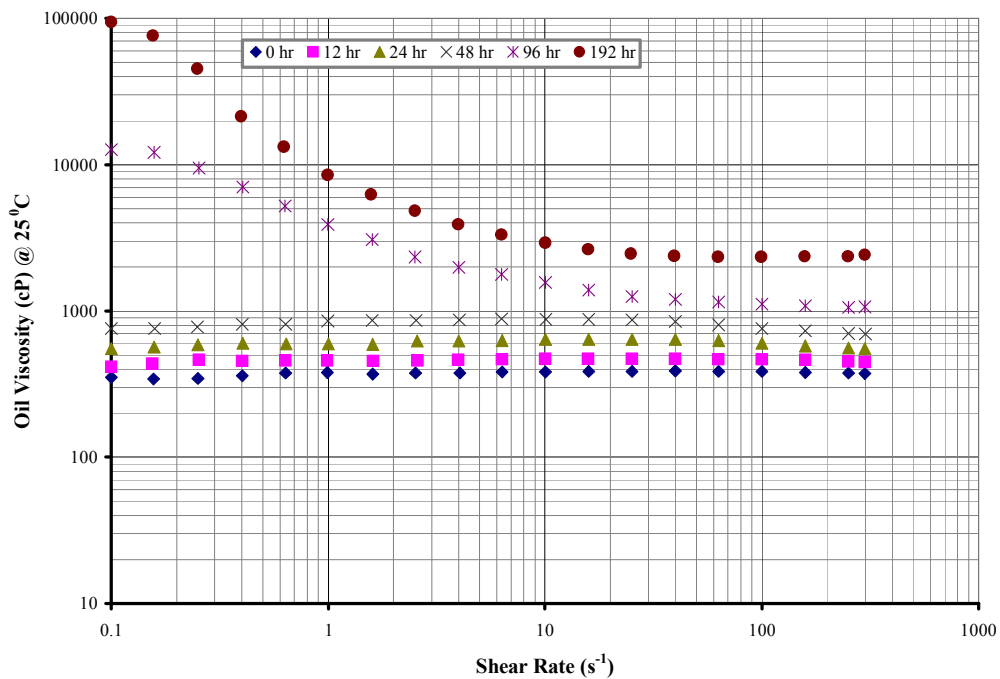


Figure 4.18 Viscosity (cP) of Pine Wood Pyrolysis Oil Control (0 wt.%) Measured as a Function of Shear Rate (s^{-1}) and Storage Time (hr)

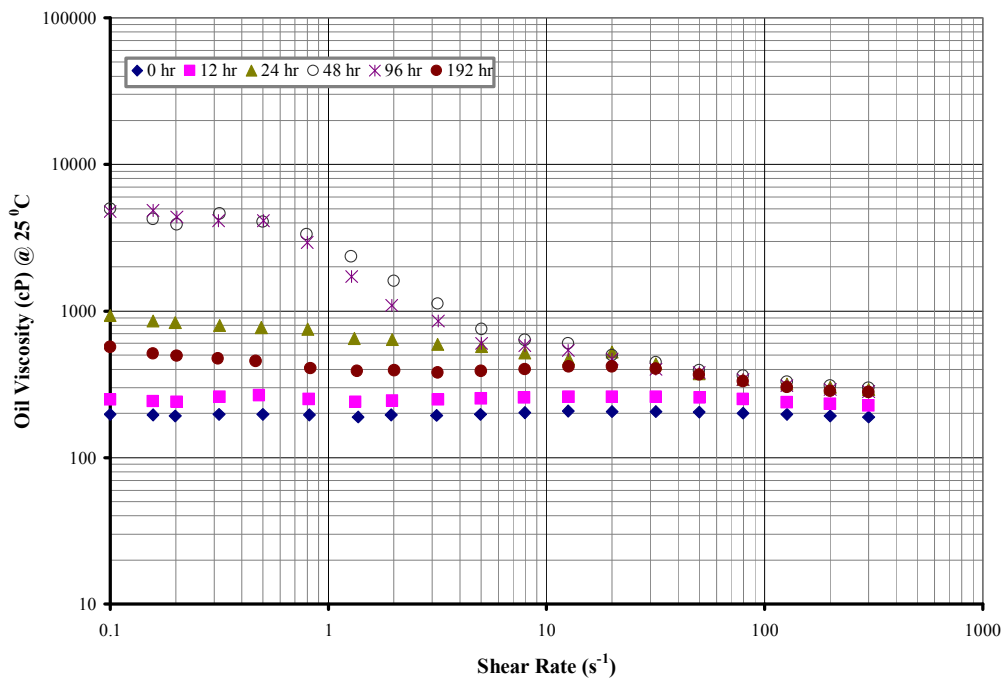


Figure 4.19 Viscosity (cP) of Anisole Blended Pine Wood Pyrolysis Oil (10 wt.%) Measured as a Function of Shear Rate (s^{-1}) and Storage Time (hr)

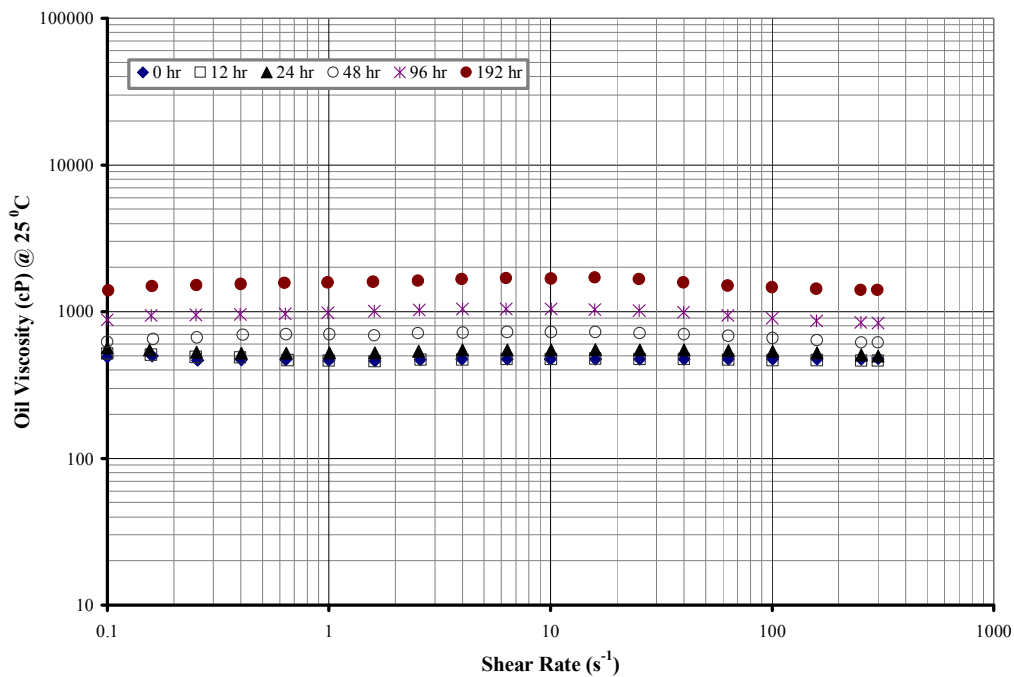


Figure 4.20 Viscosity (cP) of Glycerol Blended Pine Wood Pyrolysis Oil (10 wt.%) Measured as a Function of Shear Rate (s^{-1}) and Storage Time (hr)

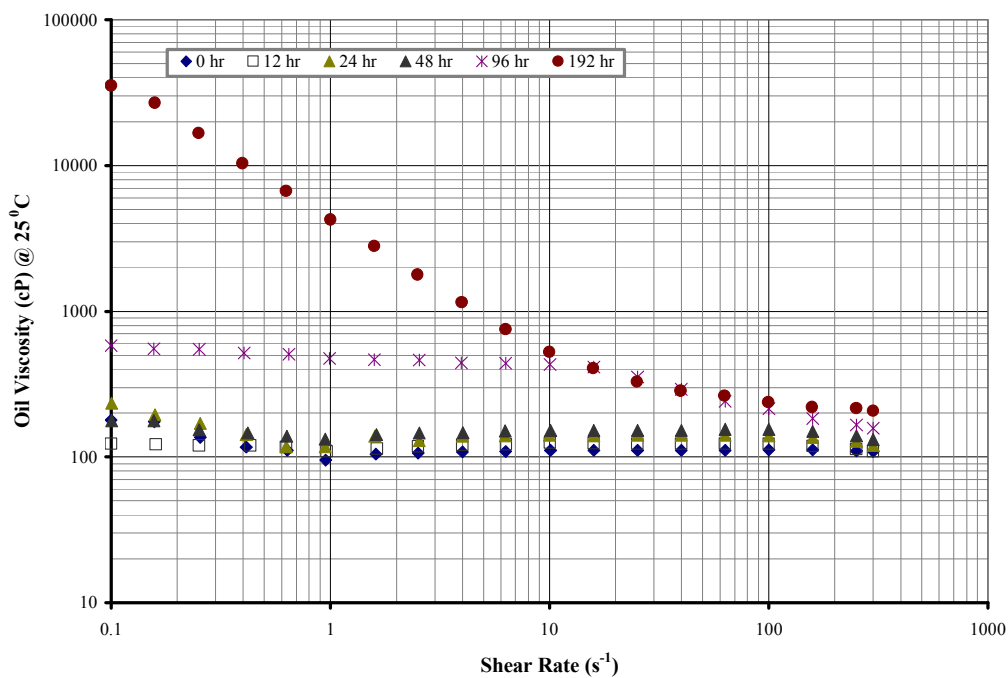


Figure 4.21 Viscosity (cP) of Methanol Blended Pine Wood Pyrolysis Oil (10 wt.%) Measured as a Function of Shear Rate (s^{-1}) and Storage Time (hr)

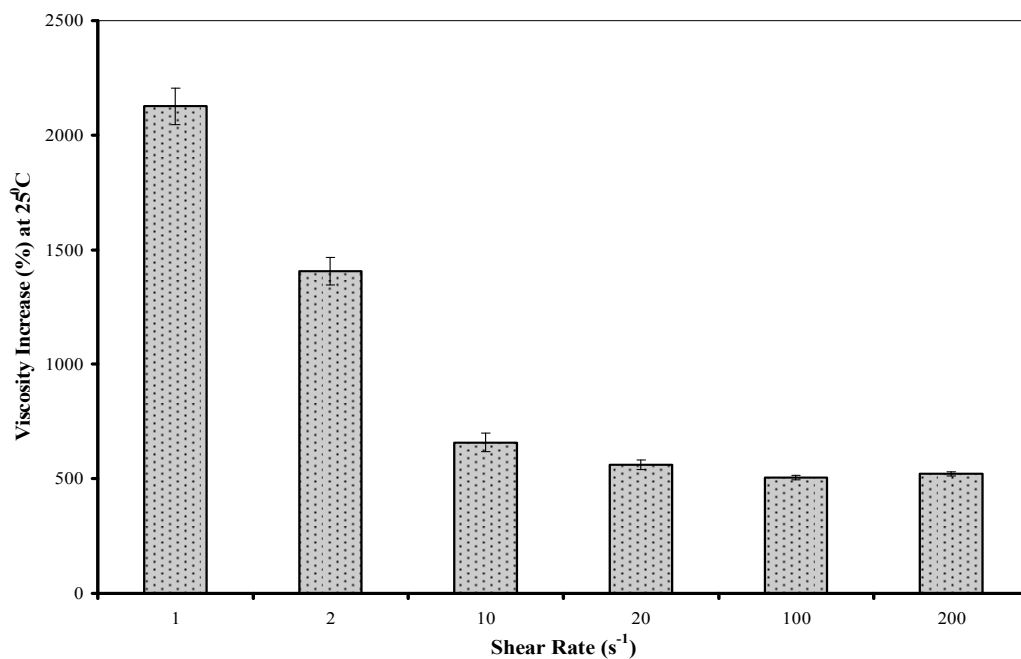


Figure 4.22 Percentage Increase in Viscosity (0 hr vs. 192 hr) of Pine Wood Pyrolysis Oil Control (0 wt.%) Obtained as a Function of Shear Rate (s^{-1})

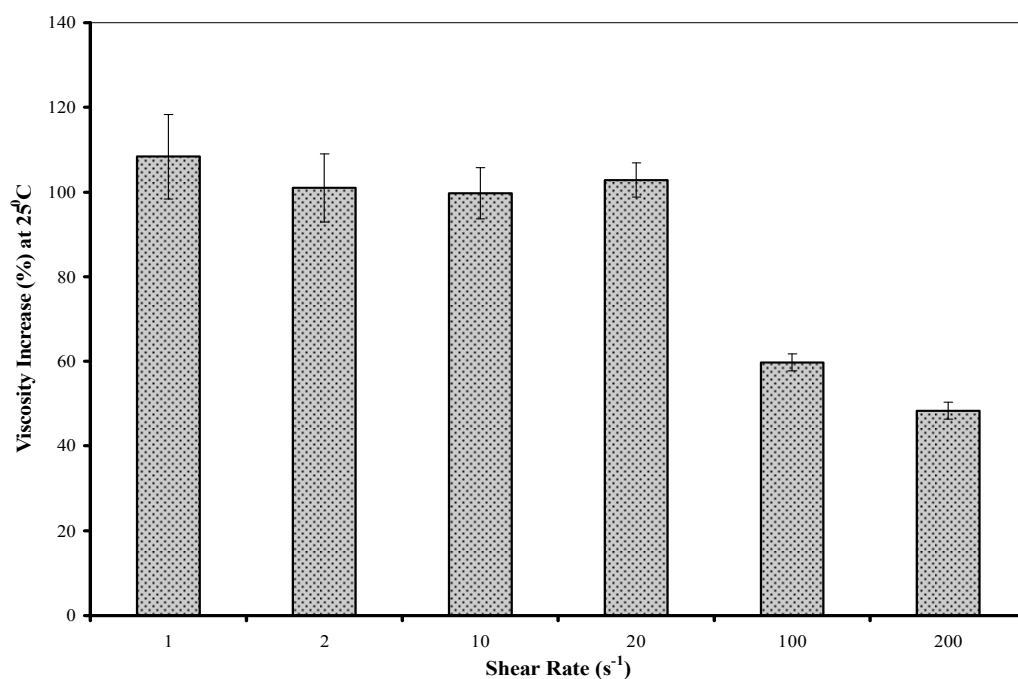


Figure 4.23 Percentage Increase in Viscosity (0 hr vs. 192 hr) of Anisole Blended Pine Wood Pyrolysis Oil (10 wt.%) Obtained as a Function of Shear Rate (s^{-1})

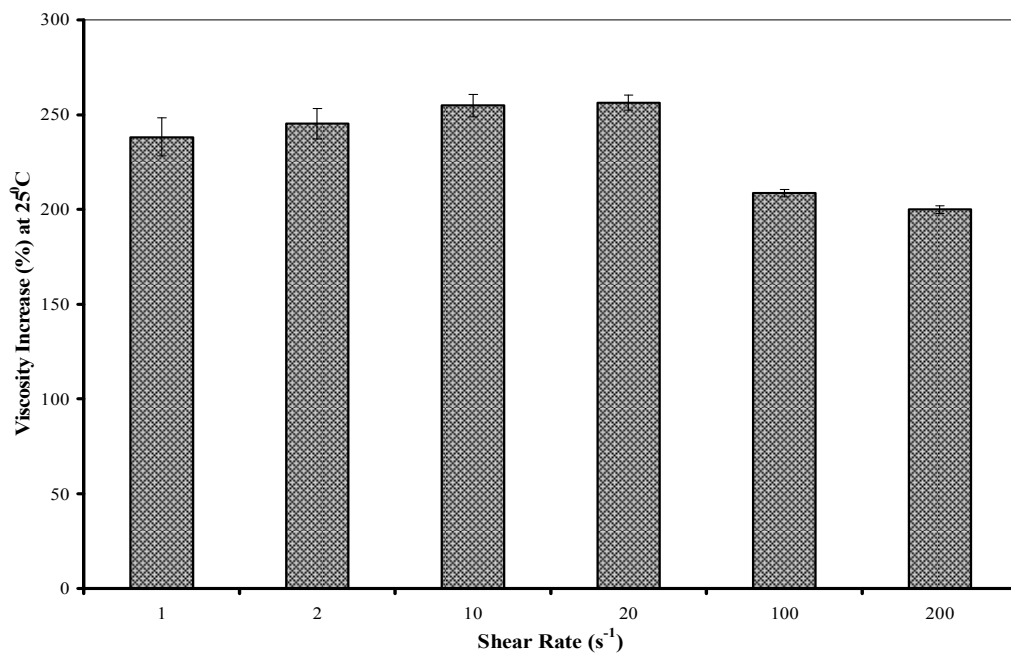


Figure 4.24 Percentage Increase in Viscosity (0 hr vs. 192 hr) of Glycerol Blended Pine Wood Pyrolysis Oil (10 wt.%) Obtained as a Function of Shear Rate (s⁻¹)

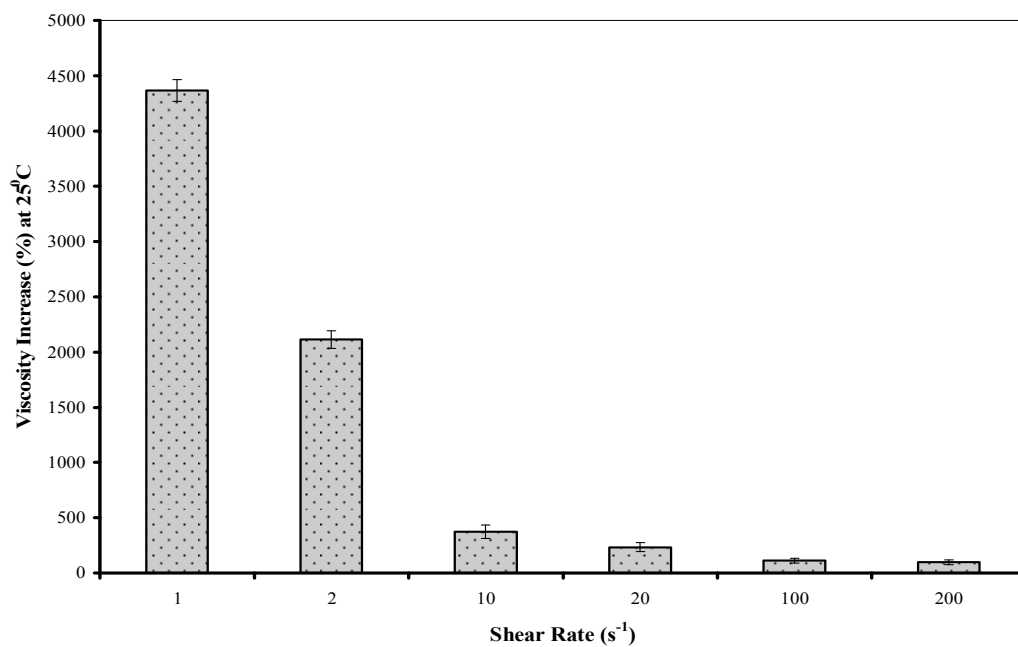


Figure 4.25 Percentage Increase in Viscosity (0 hr vs. 192 hr) of Methanol Blended Pine Wood Pyrolysis Oil (10 wt.%) Obtained as a Function of Shear Rate (s⁻¹)

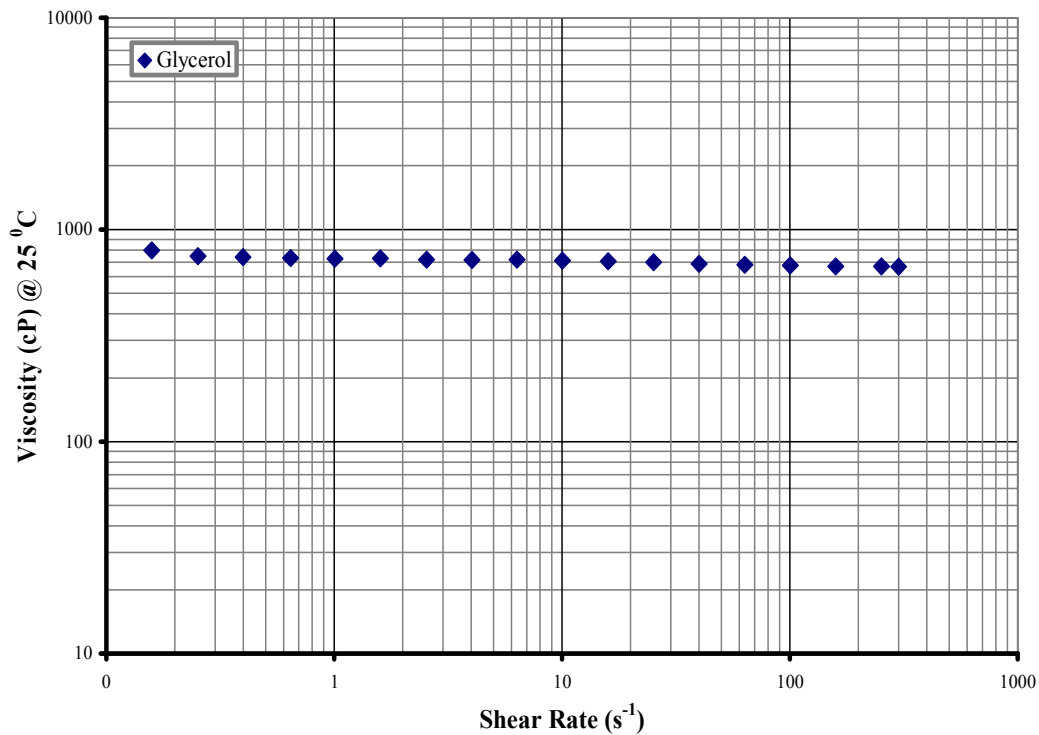


Figure 4.26 Viscosity of Glycerol Measured as a Function of Shear Rate (s^{-1})

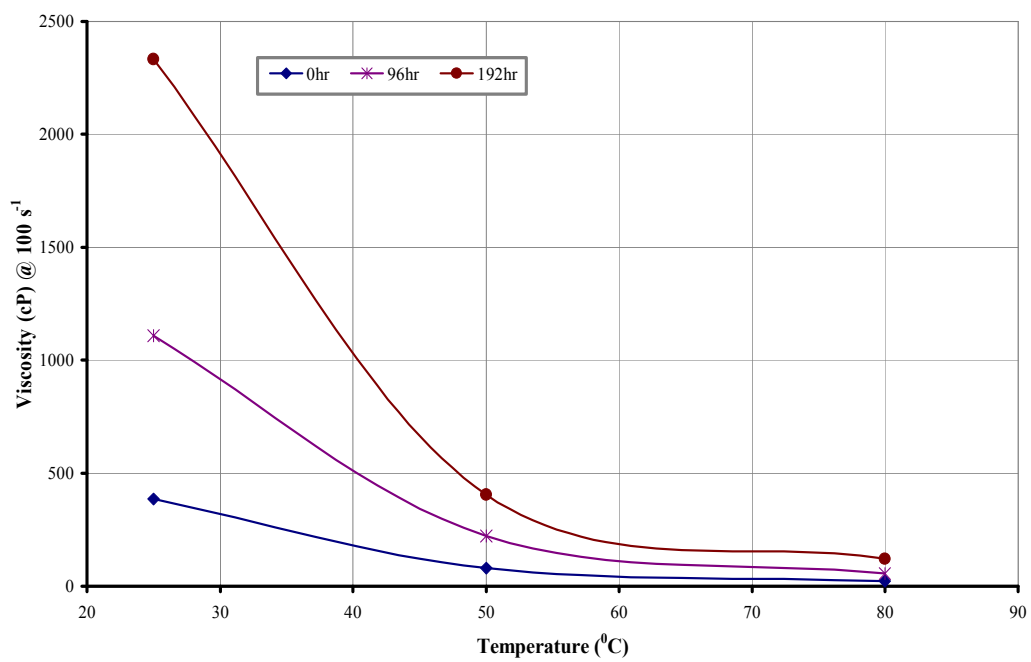


Figure 4.27 Viscosity (cP) of Pine Wood Pyrolysis Oil Control (0 wt.%) Measured as a Function of Temperature ($^{\circ}C$) and Storage Time (hr)

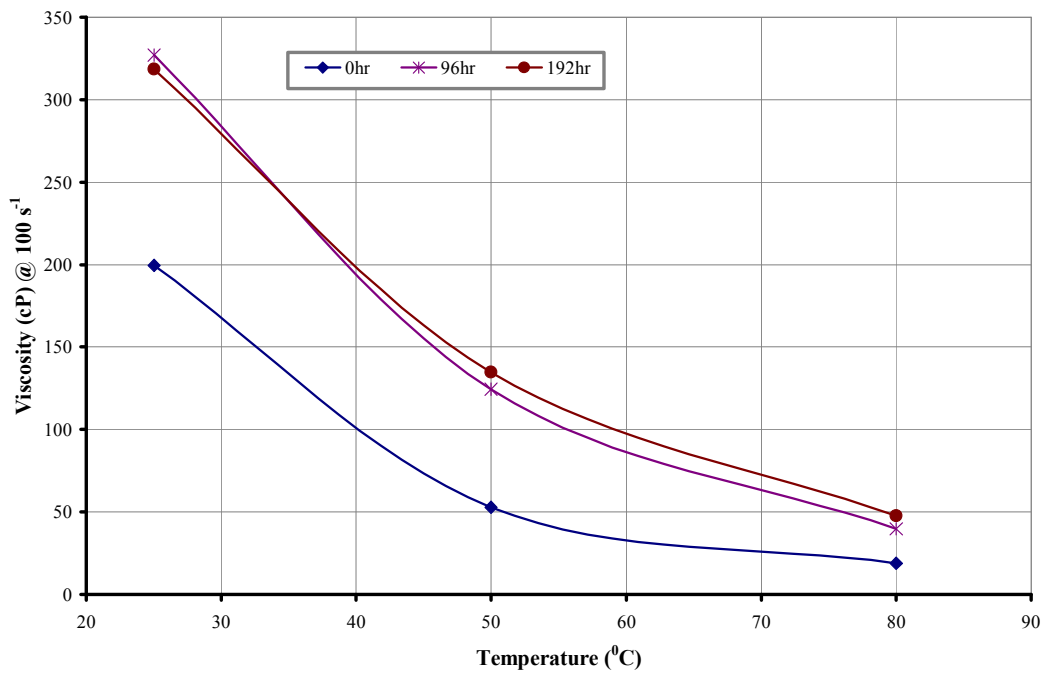


Figure 4.28 Viscosity (cP) of Anisole Blended Pine Wood Pyrolysis Oil (10 wt.%) Measured as a Function of Temperature ($^{\circ}\text{C}$) and Storage Time (hr)

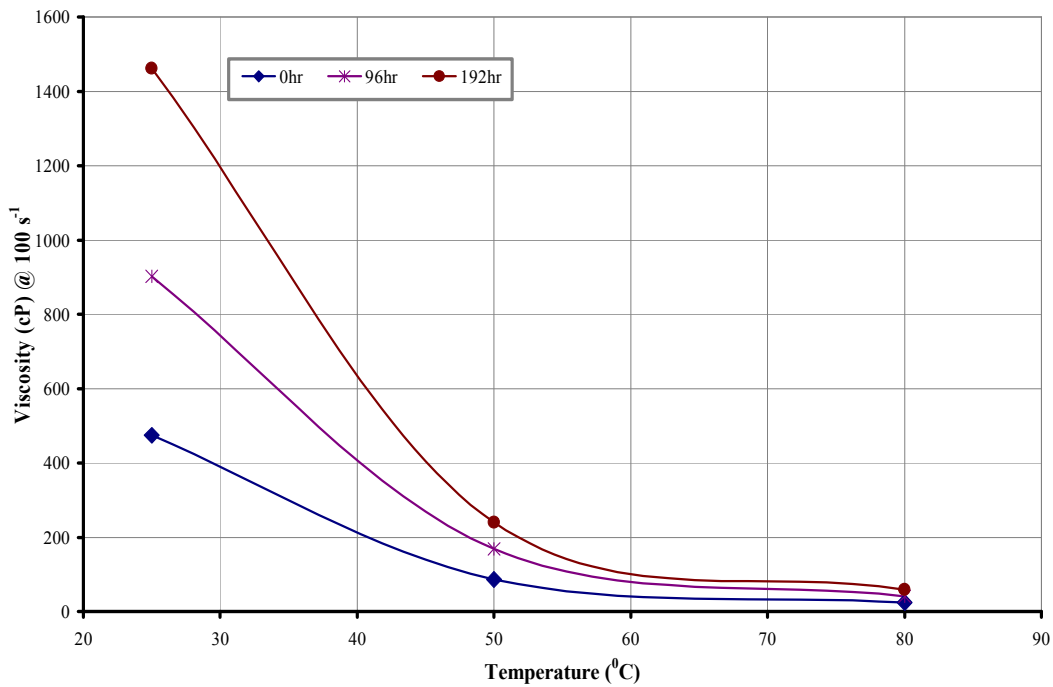


Figure 4.29 Viscosity (cP) of Glycerol Blended Pine Wood Pyrolysis Oil (10 wt.%) Measured as a Function of Temperature ($^{\circ}\text{C}$) and Storage Time (hr)

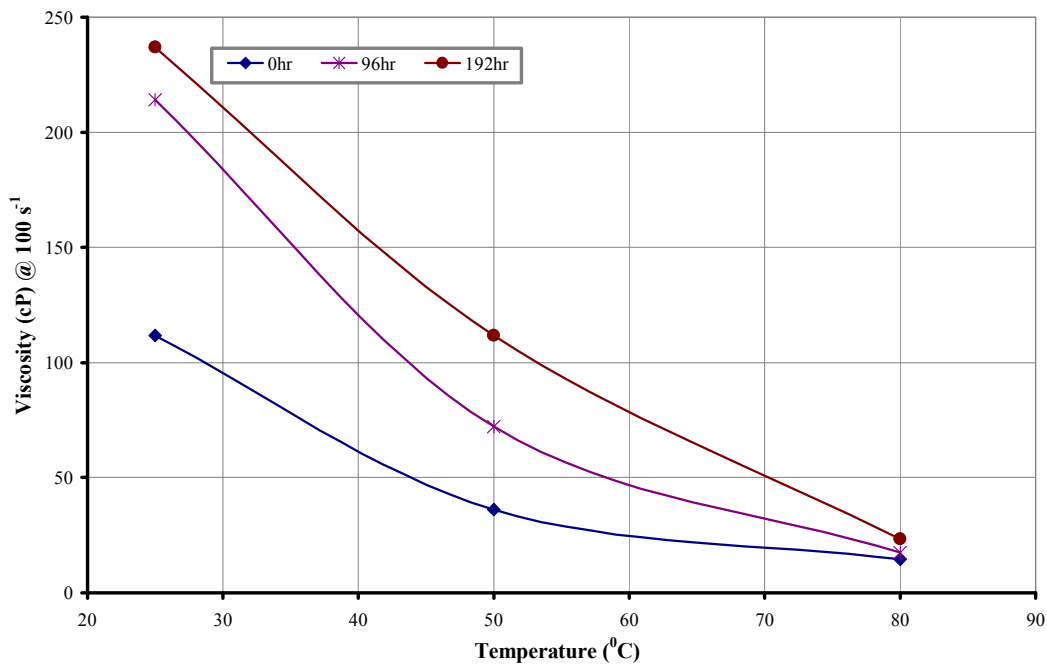


Figure 4.30 Viscosity (cP) of Methanol Blended Pine Wood Pyrolysis Oil (10 wt.%) Measured as a Function of Temperature (°C) and Storage Time (hr)

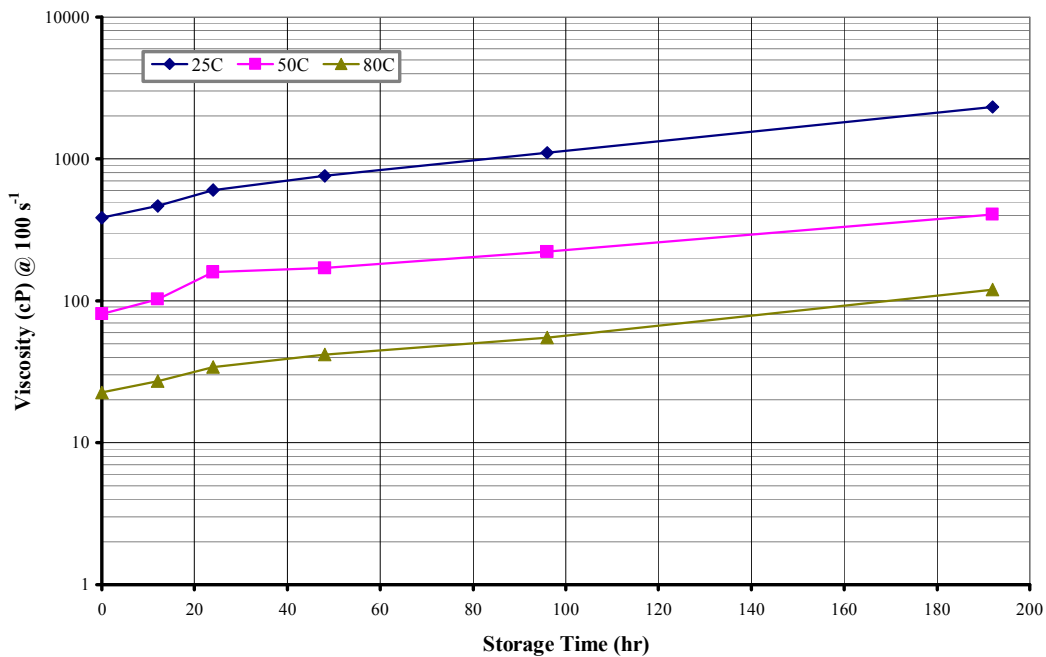


Figure 4.31 Viscosity (cP) of Pine Wood Pyrolysis Oil Control (CTL-0 wt.%) Measured as a Function of Storage Time (hr) and Temperature (°C)

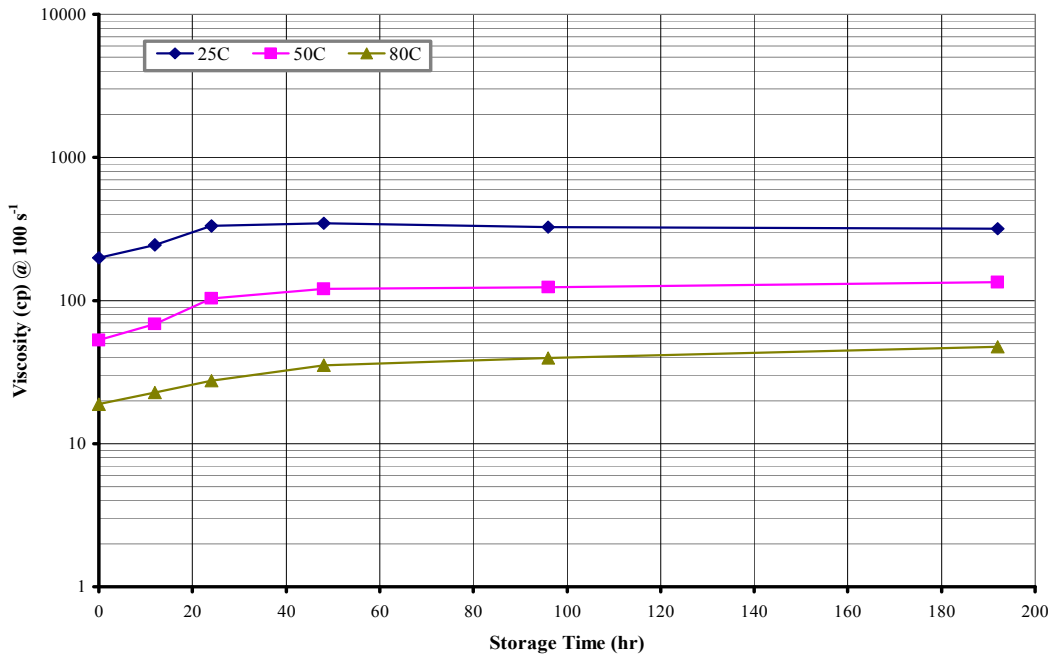


Figure 4.32 Viscosity (cP) of Anisole (ANS) Blended Pine Wood Pyrolysis Oil (10 wt.%) Measured as a Function of Storage Time (hr) and Temperature ($^{\circ}\text{C}$)

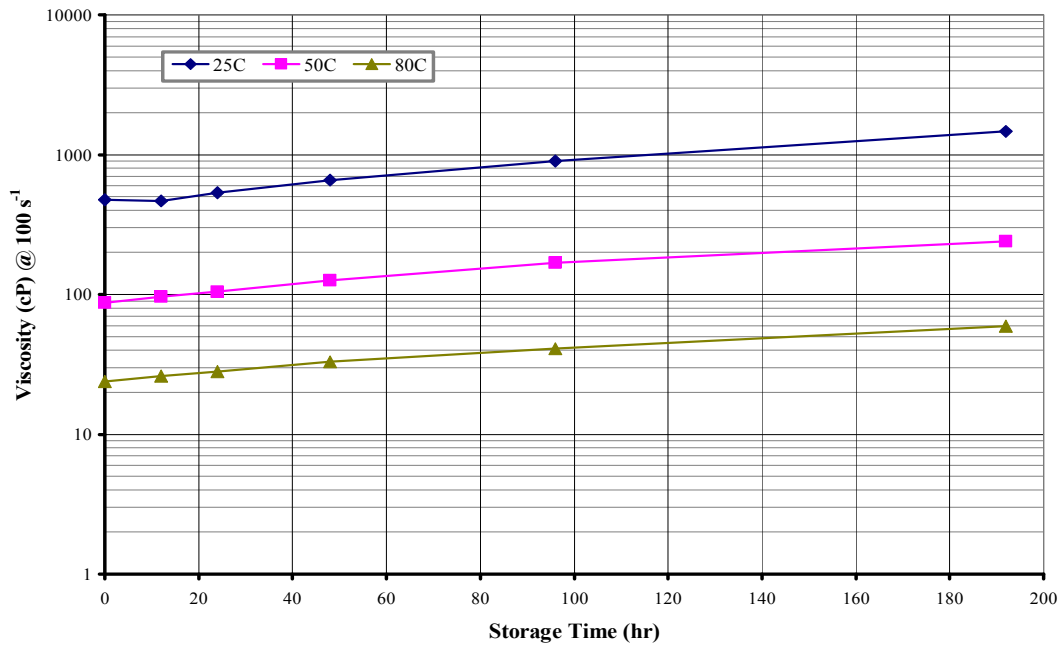


Figure 4.33 Viscosity (cP) of Glycerol (GLY) Blended Pine Wood Pyrolysis Oil (10 wt.%) Measured as a Function of Storage Time (hr) and Temperature ($^{\circ}\text{C}$)

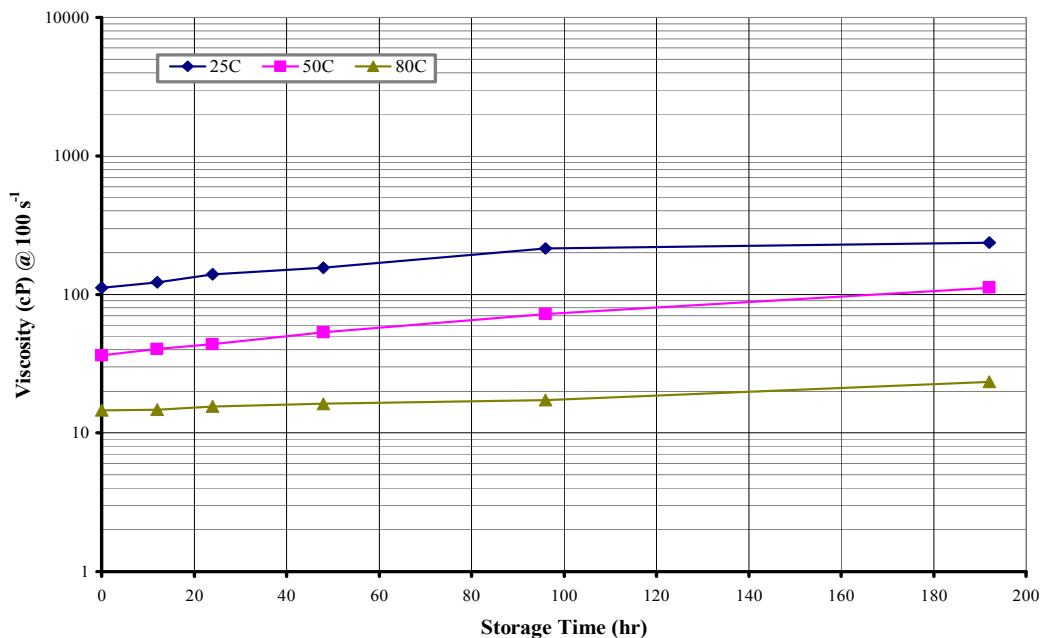


Figure 4.34 Viscosity (cP) of Methanol (MEH) Blended Pine Wood Pyrolysis Oil (10 wt.%) Measured as a Function of Storage Time (hr) and Temperature ($^{\circ}\text{C}$)

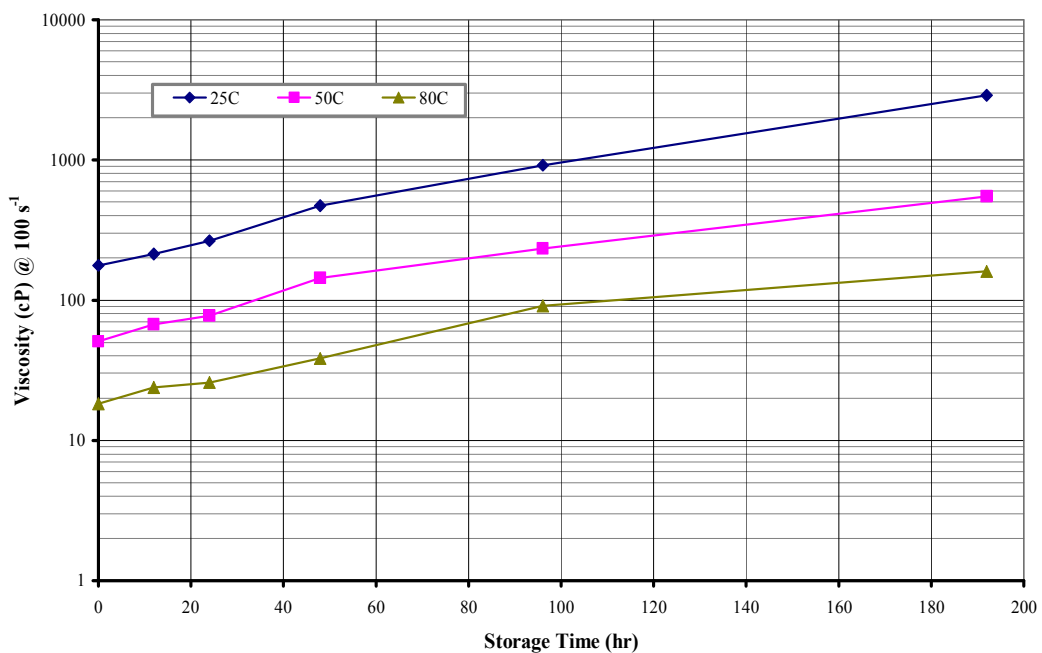


Figure 4.35 Viscosity (cP) of 2-Furaldehyde (2FL) Blended Pine Wood Pyrolysis Oil (10 wt.%) Measured as a Function of Storage Time (hr) and Temperature ($^{\circ}\text{C}$)

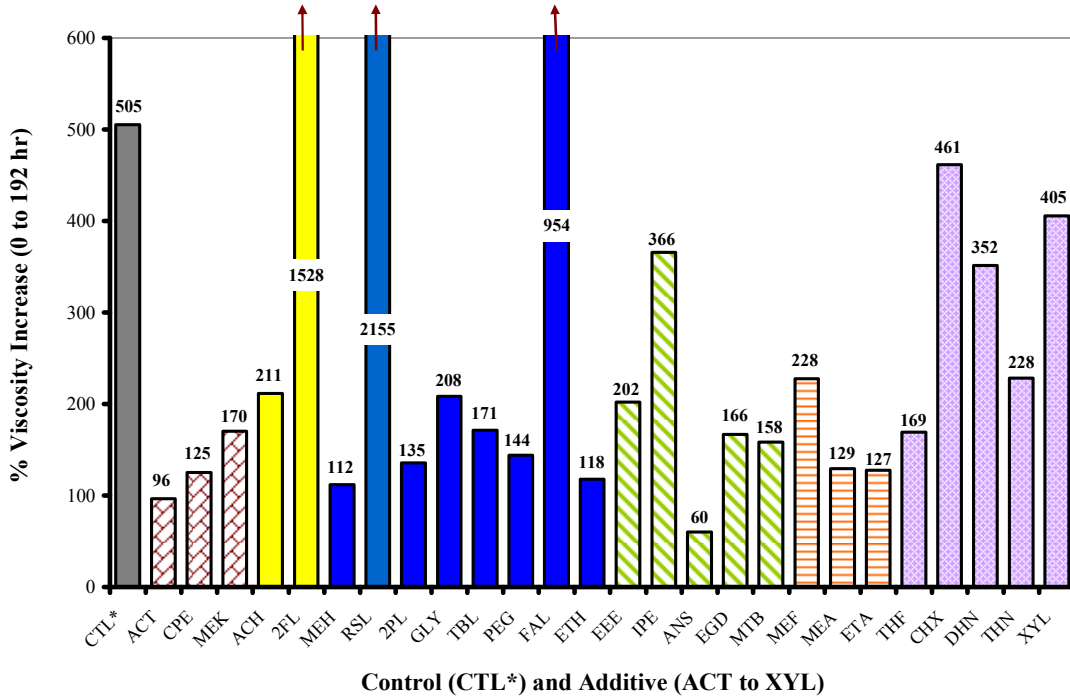


Figure 4.36 Percentage Increase in Viscosity of Control (0 wt.%) and Additive Blended (10 wt.%) Pine Wood Pyrolysis Oils Obtained at a Shear Rate of 100 s^{-1} and a Temperature of $25 \text{ }^{\circ}\text{C}$

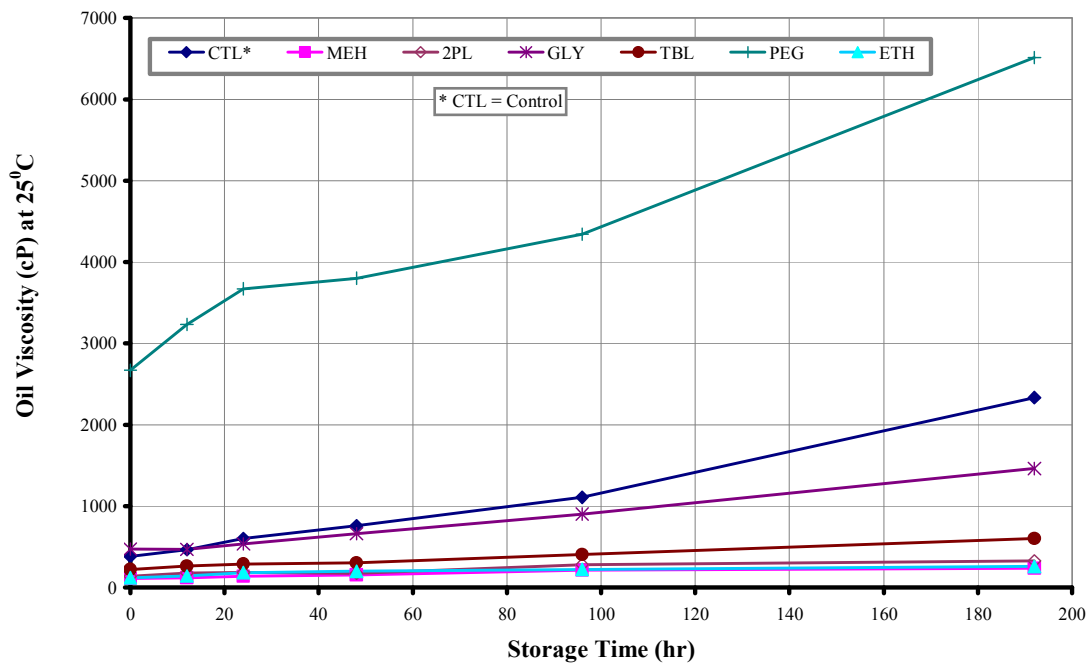


Figure 4.37 Viscosity (cP) of Alcohol Blended Pine Wood Pyrolysis Oils Measured as a Function of Storage Time (hr) [Shear Rate = 100 s^{-1}]

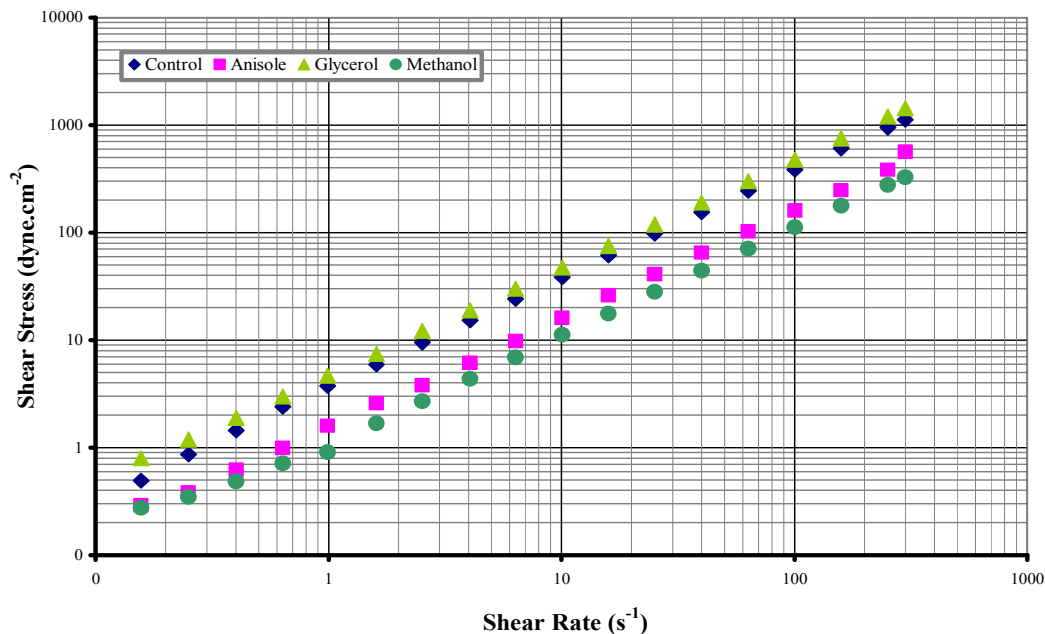


Figure 4.38 Shear Stress versus Shear Rate Profiles of Control, Anisole, Glycerol, and Methanol Blended Pine Wood Pyrolysis Oils at a Storage Time of 0 hr and Measurement Temperature of 25 °C

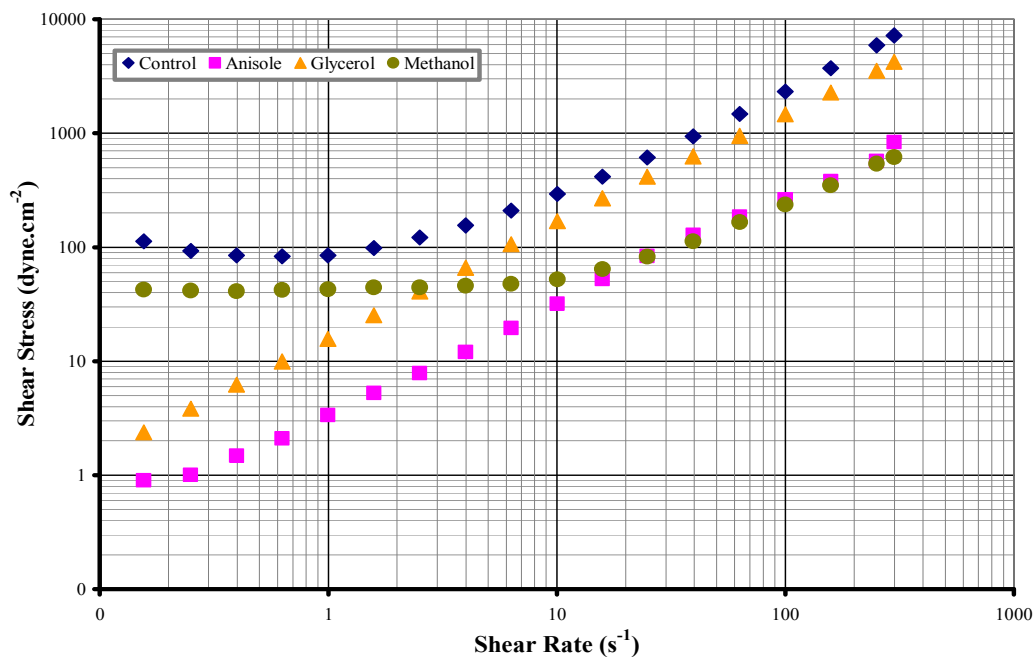


Figure 4.39 Shear Stress versus Shear Rate Profiles of Control, Anisole, Glycerol, and Methanol Blended Pine Wood Pyrolysis Oils at a Storage Time of 192 hr and Measurement Temperature of 25 °C

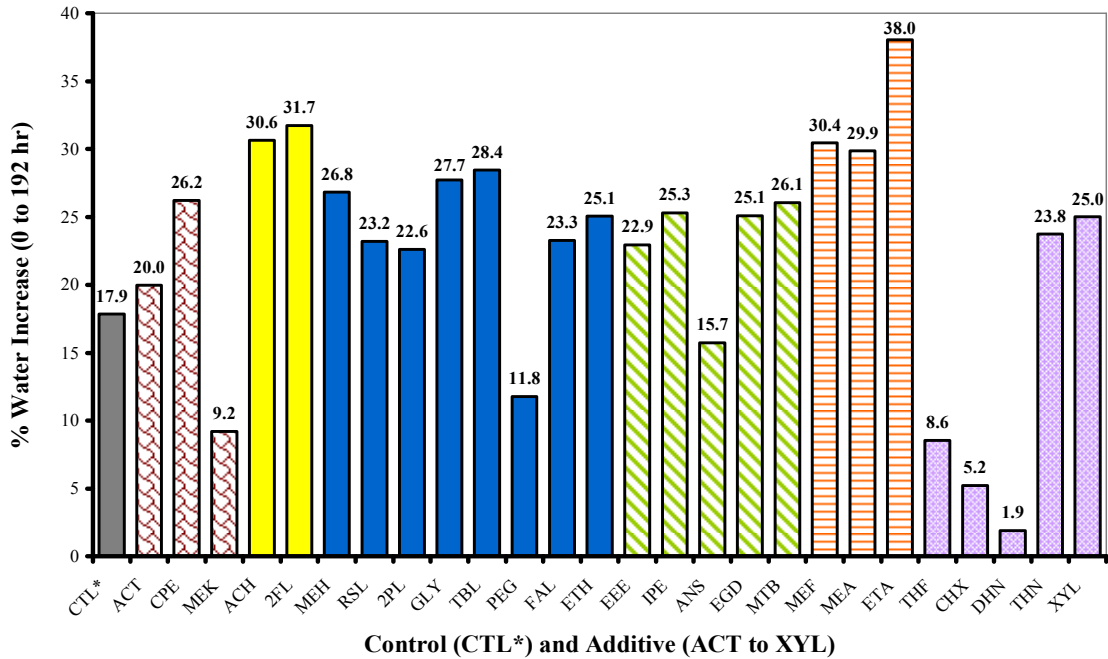


Figure 4.40 Increase in Water Content (%) of Control (0 wt.%) and Additive Blended (10 wt.%) Pine Wood Pyrolysis Oils Measured at Storage Times of 0 and 192 hr

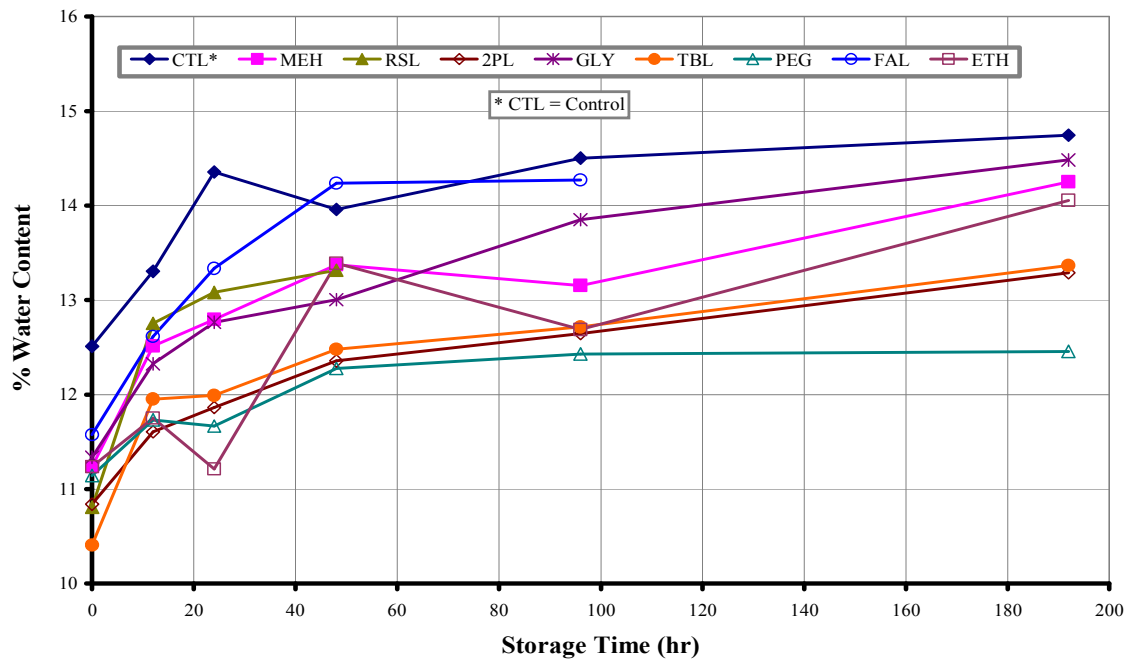


Figure 4.41 Water Content (wt.%) of Alcohol Blended (10 wt.%) Pine Wood Pyrolysis Oils Measured as a Function of Storage Time (hr)

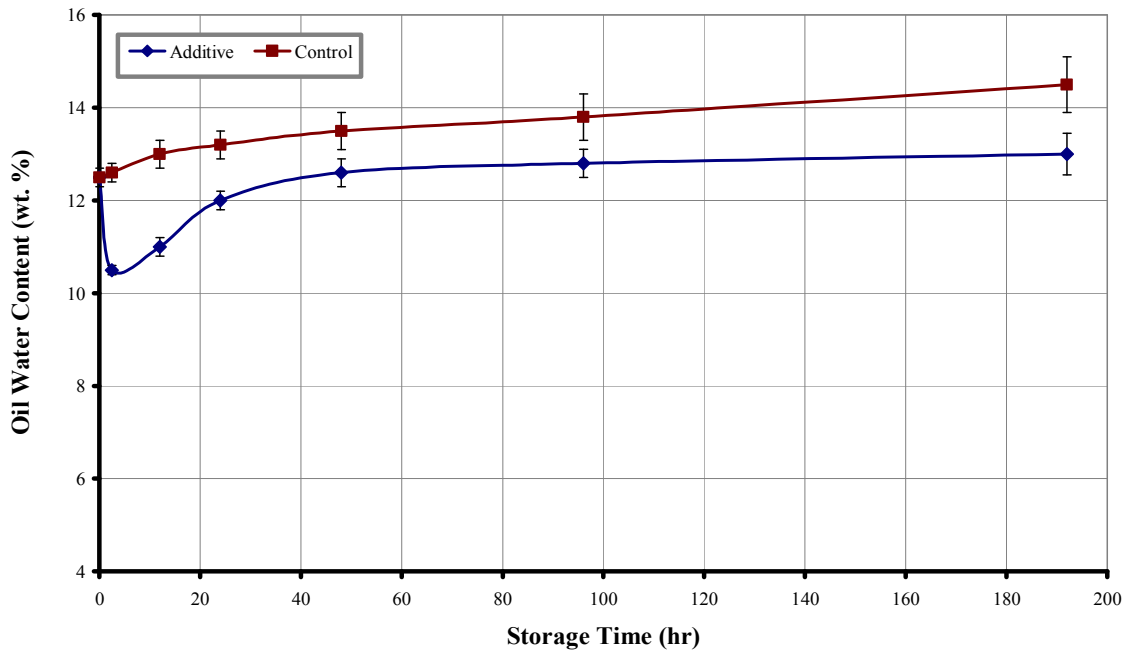


Figure 4.42 Typical Behavior of the Water Content (wt.%) of Additive Blended (10 wt.%) Pine Wood Pyrolysis Oils Measured as a Function of Storage Time (hr)

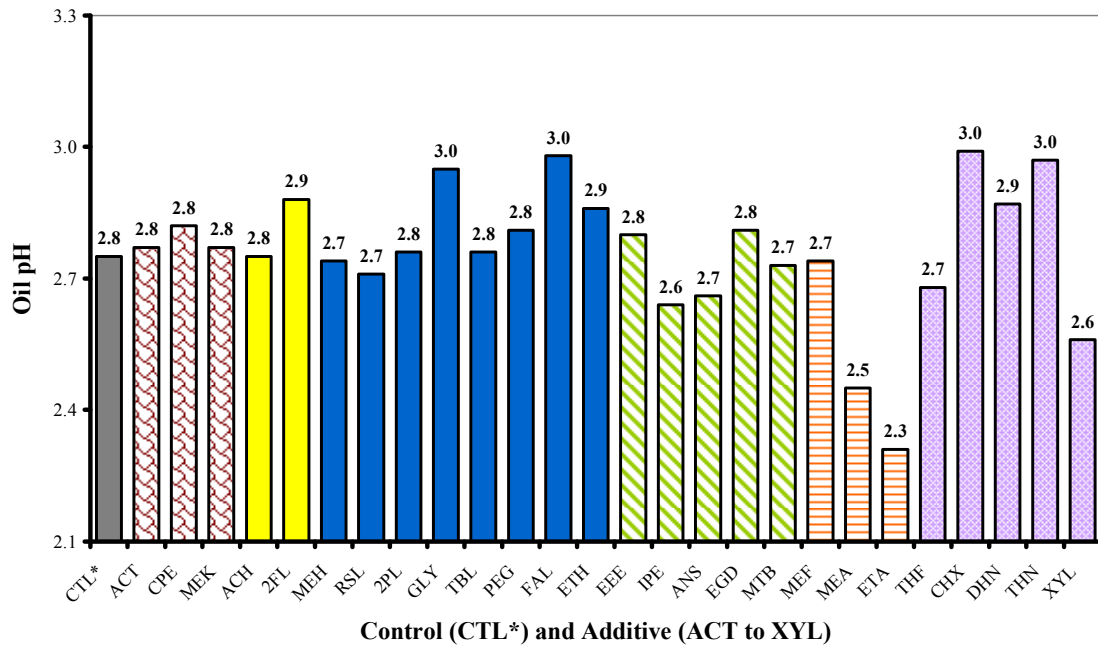


Figure 4.43 The pH of Control (0 wt.%) and Additive Blended (10 wt.%) Pine Wood Pyrolysis Oils Measured at Initial Storage Time (0 hr)

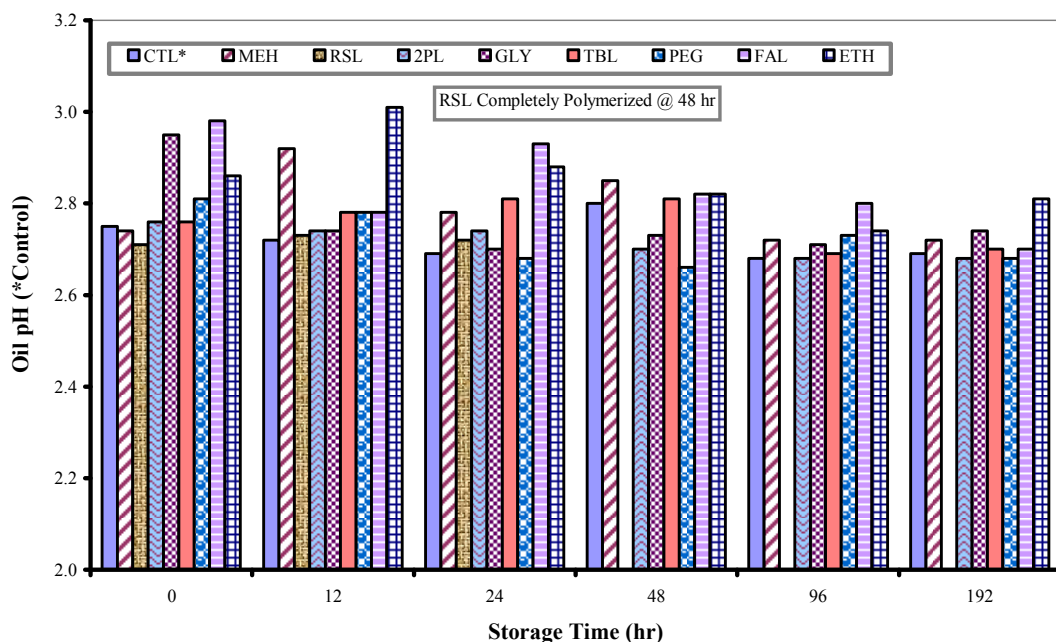


Figure 4.44 The pH of Alcohol Blended (10 wt.%) Pine Wood Pyrolysis Oils Measured as a Function of Storage Time (hr)

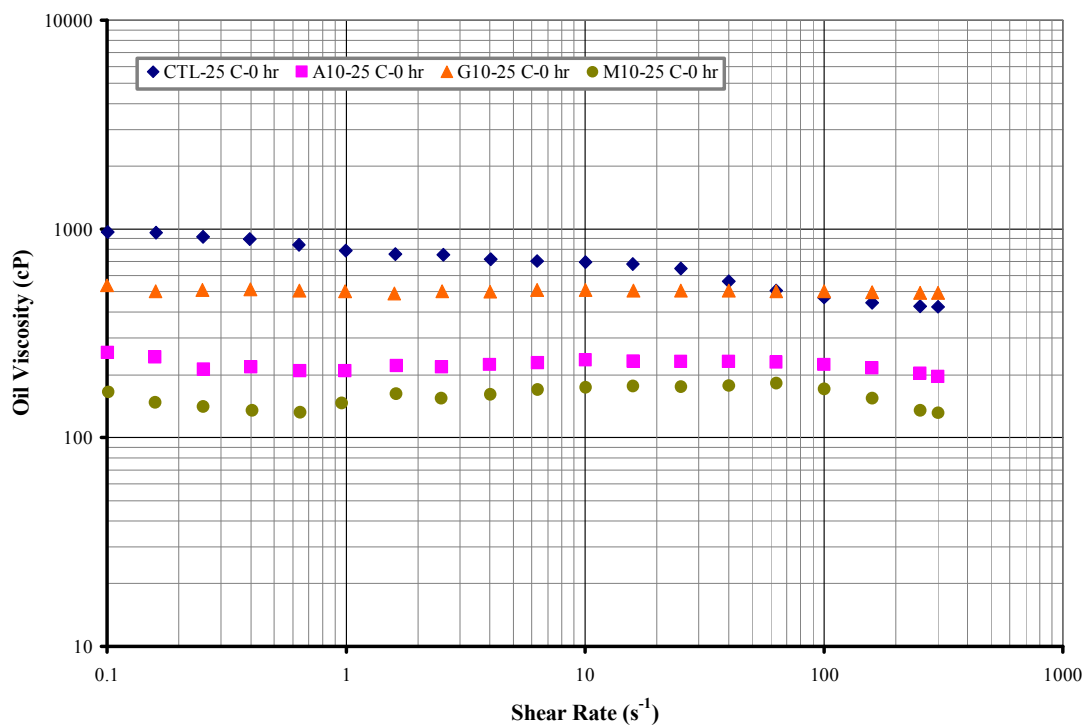


Figure 4.45 Viscosity Measured at 25 °C and 0 hr as a Function of Shear Rate for Control (0 wt.%) and Additive Blended (10 wt.%) Pyrolysis Oils

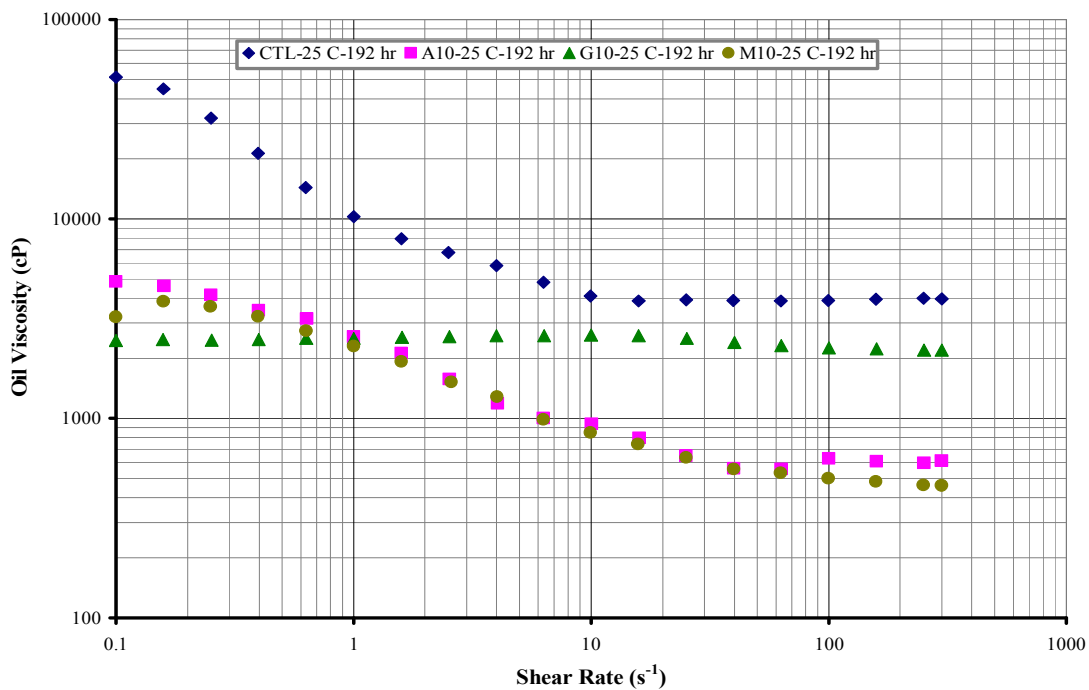


Figure 4.46 Viscosity Measured at 25 °C and 192 hr as a Function of Shear Rate for Control (0 wt.%) and Additive Blended (10 wt.%) Pyrolysis Oils

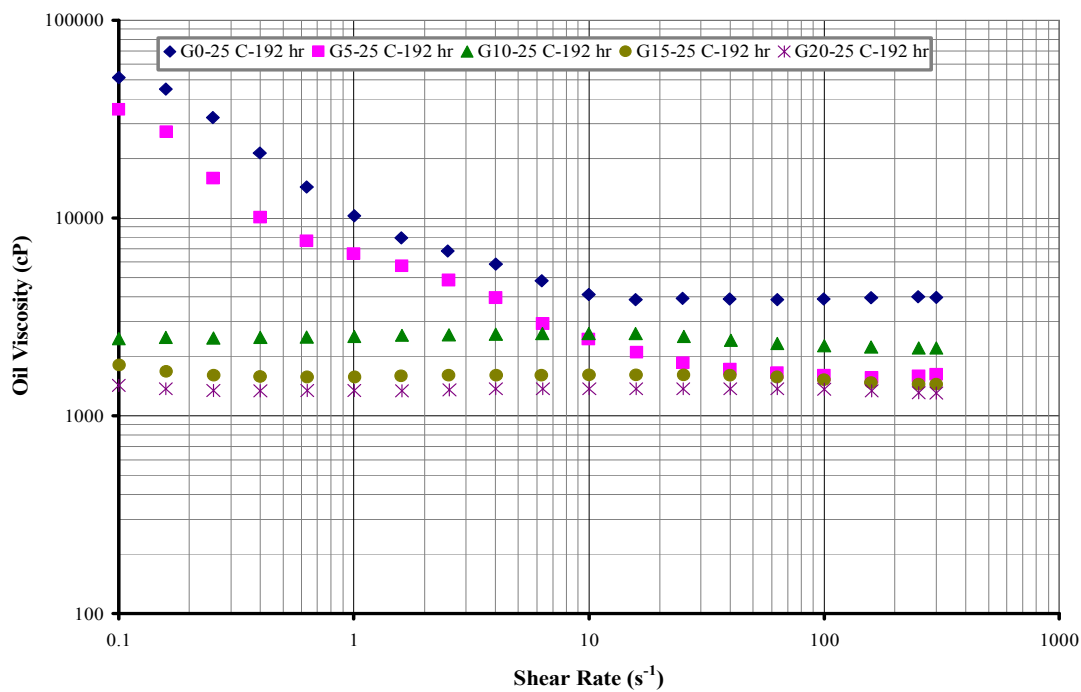


Figure 4.47 Viscosity Measured at 25 °C and 192 hr as a Function of Shear Rate for Glycerol Blended (0-20 wt.%) Pyrolysis Oils

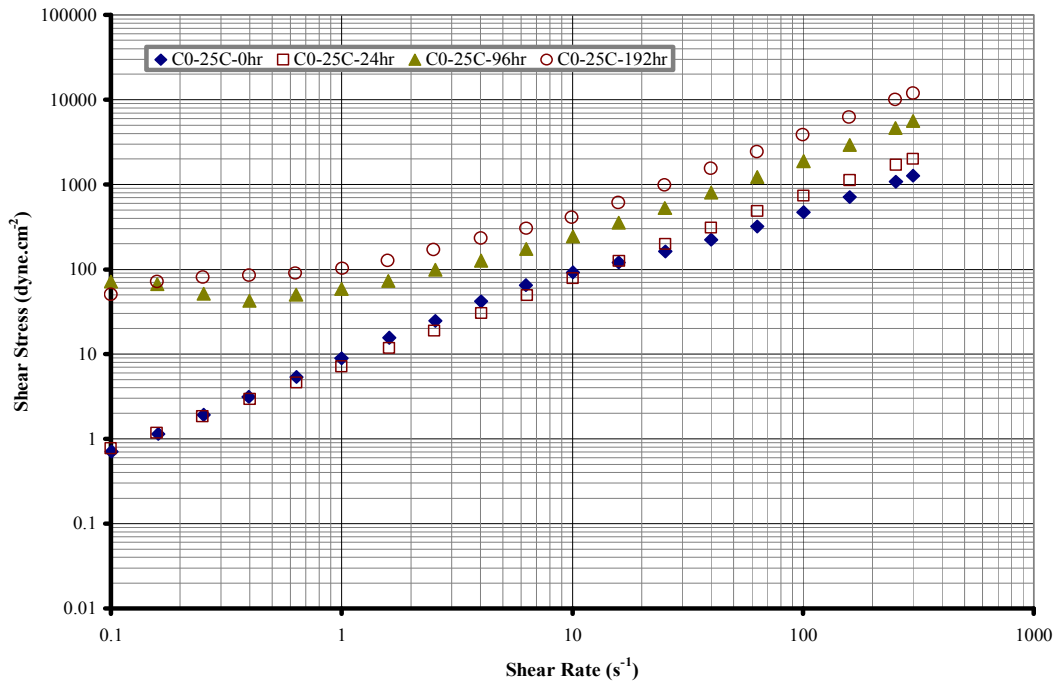


Figure 4.48 Shear Stress Measured at 25 °C as a Function of Shear Rate and Storage Time for Control (0 wt.%) Pyrolysis Oil

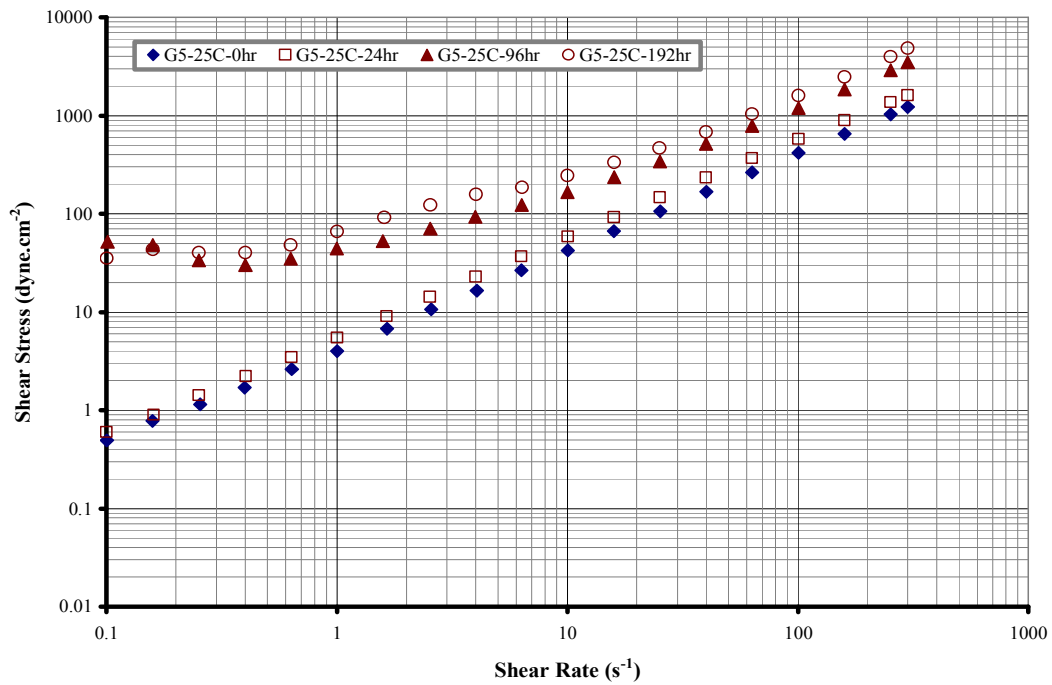


Figure 4.49 Shear Stress Measured at 25 °C as a Function of Shear Rate and Storage Time for Glycerol Blended (5 wt.%) Pyrolysis Oil

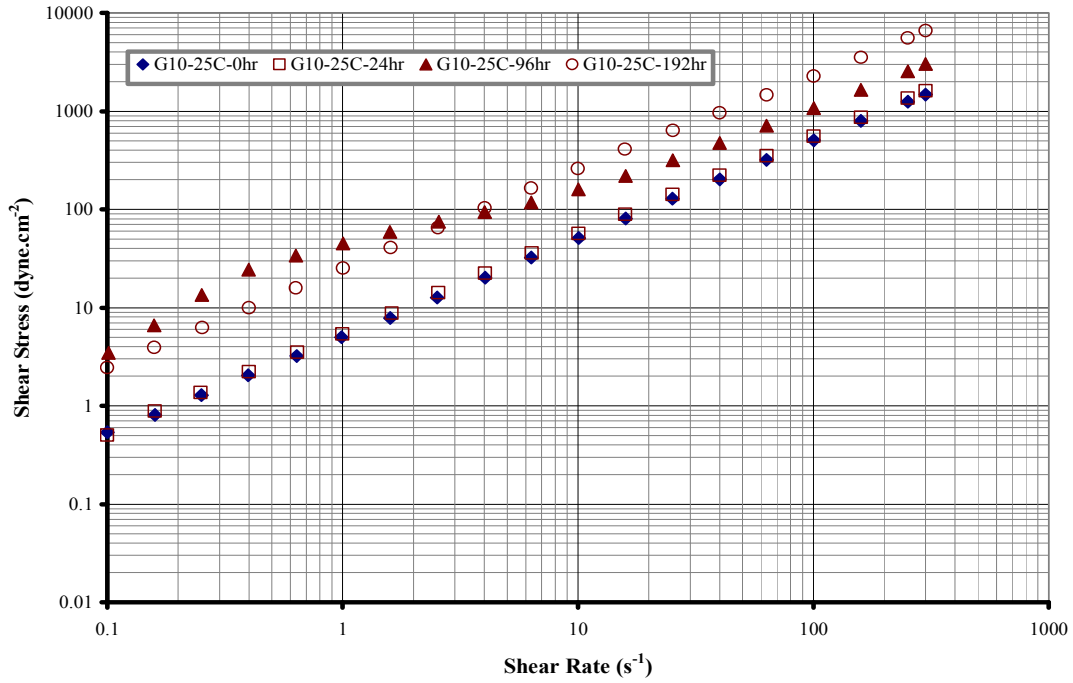


Figure 4.50 Shear Stress Measured at 25 °C as a Function of Shear Rate and Storage Time for Glycerol Blended (10 wt.%) Pyrolysis Oil

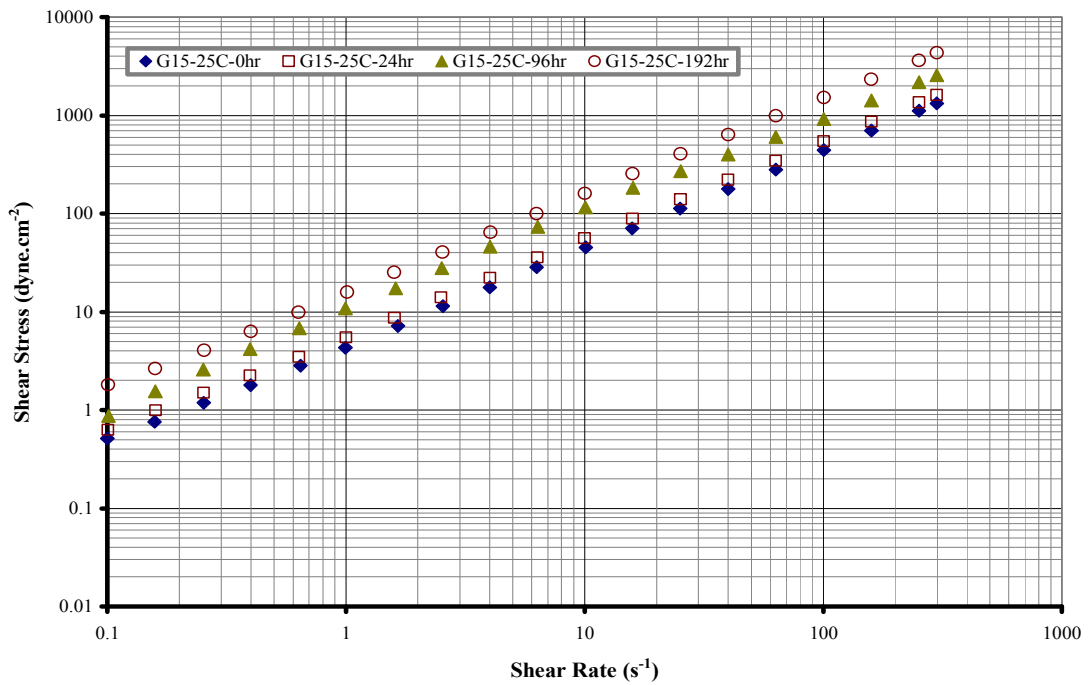


Figure 4.51 Shear Stress Measured at 25 °C as a Function of Shear Rate and Storage Time for Glycerol Blended (15 wt.%) Pyrolysis Oil

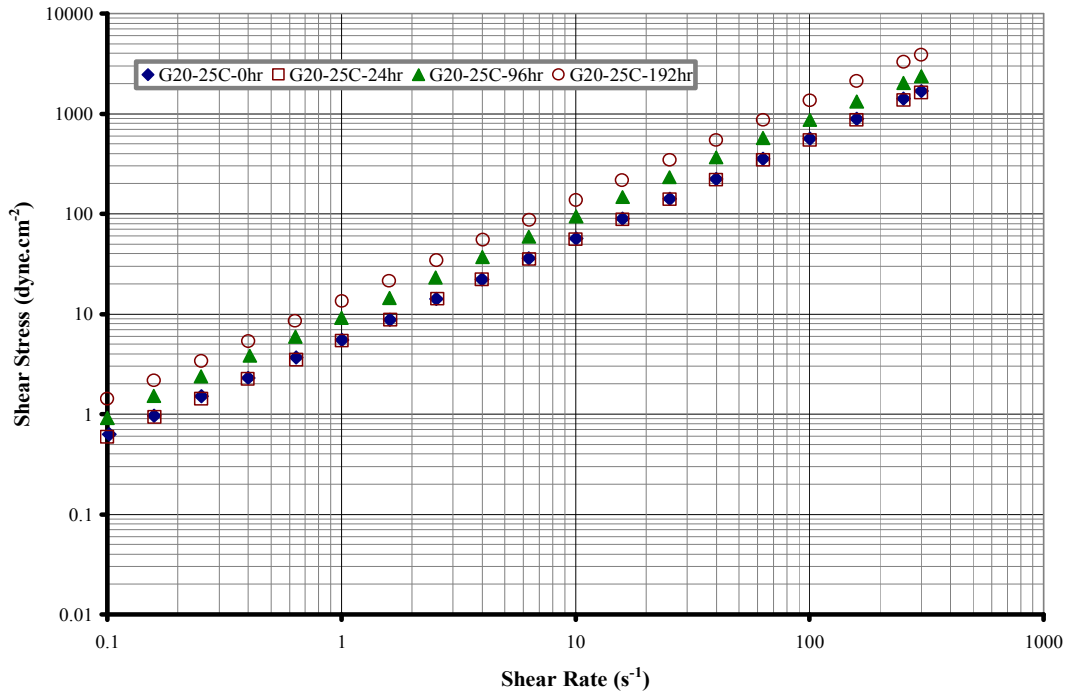


Figure 4.52 Shear Stress Measured at 25 °C as a Function of Shear Rate and Storage Time for Glycerol Blended (20 wt.%) Pyrolysis Oil

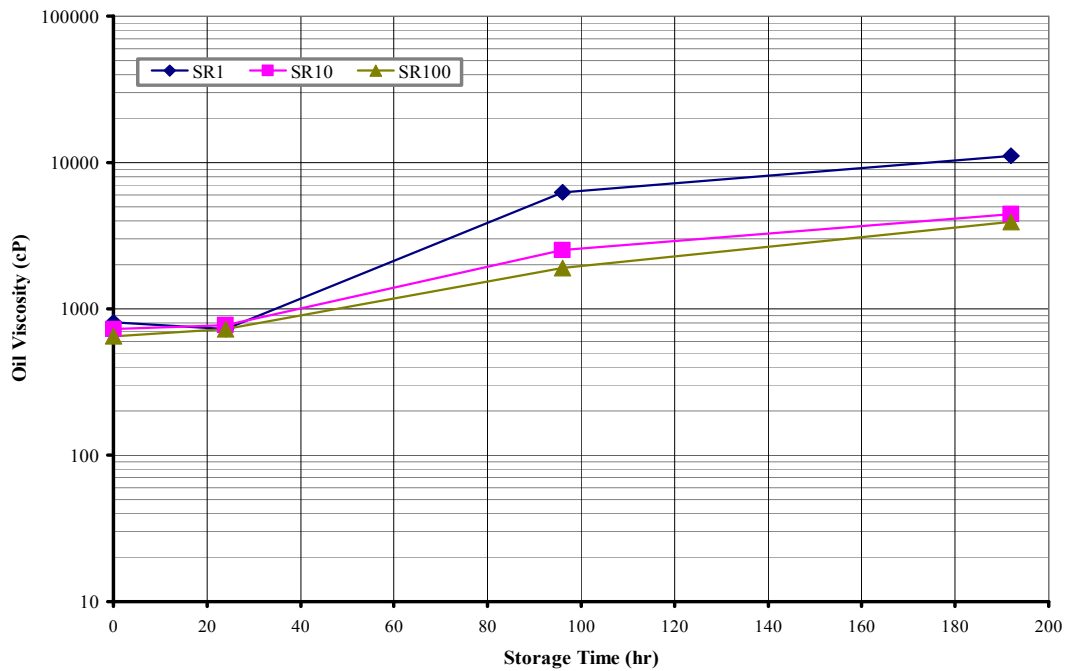


Figure 4.53 Viscosity (cP) Measured at 25 °C as a Function of Shear Rate (SR=s⁻¹) and Storage Time (hr) for Control (0 wt.%) Pyrolysis Oil

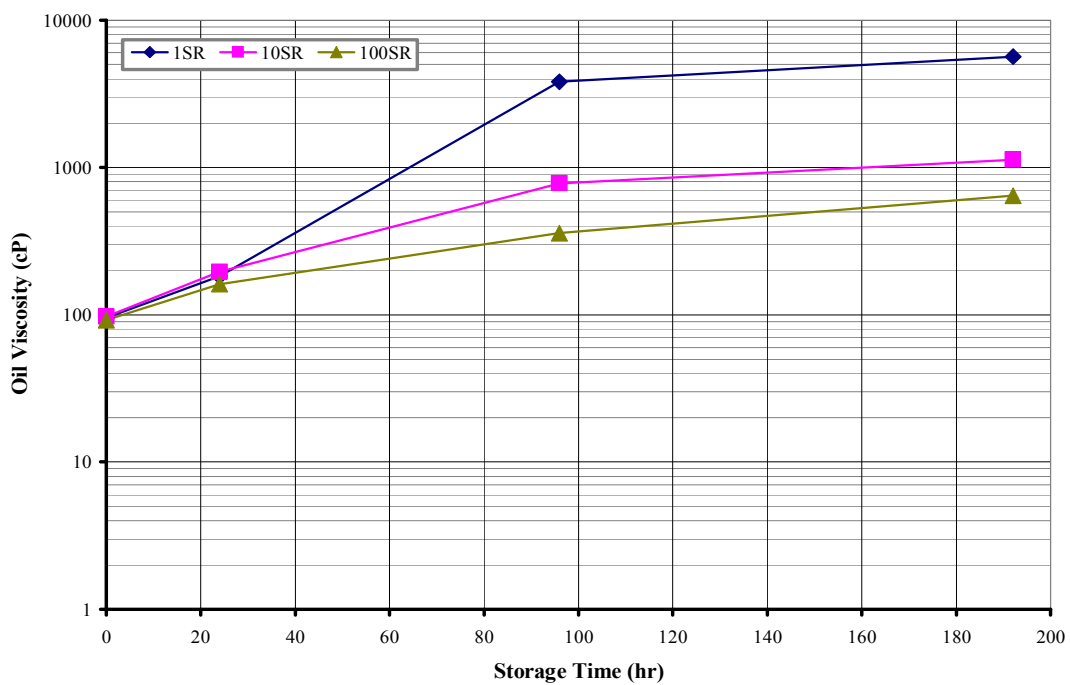


Figure 4.54 Viscosity (cP) Measured at 50 °C as a Function of Shear Rate ($SR=s^{-1}$) and Storage Time (hr) for Control (0 wt.%) Pyrolysis Oil

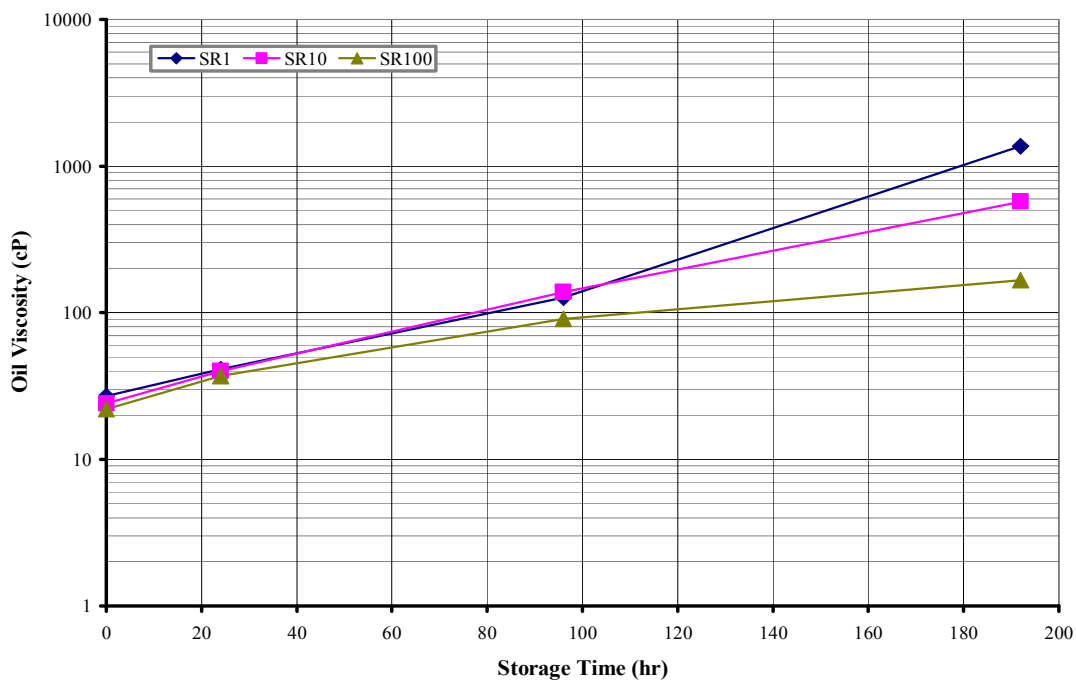


Figure 4.55 Viscosity (cP) Measured at 80 °C as a Function of Shear Rate ($SR=s^{-1}$) and Storage Time (hr) for Control (0 wt.%) Pyrolysis Oil

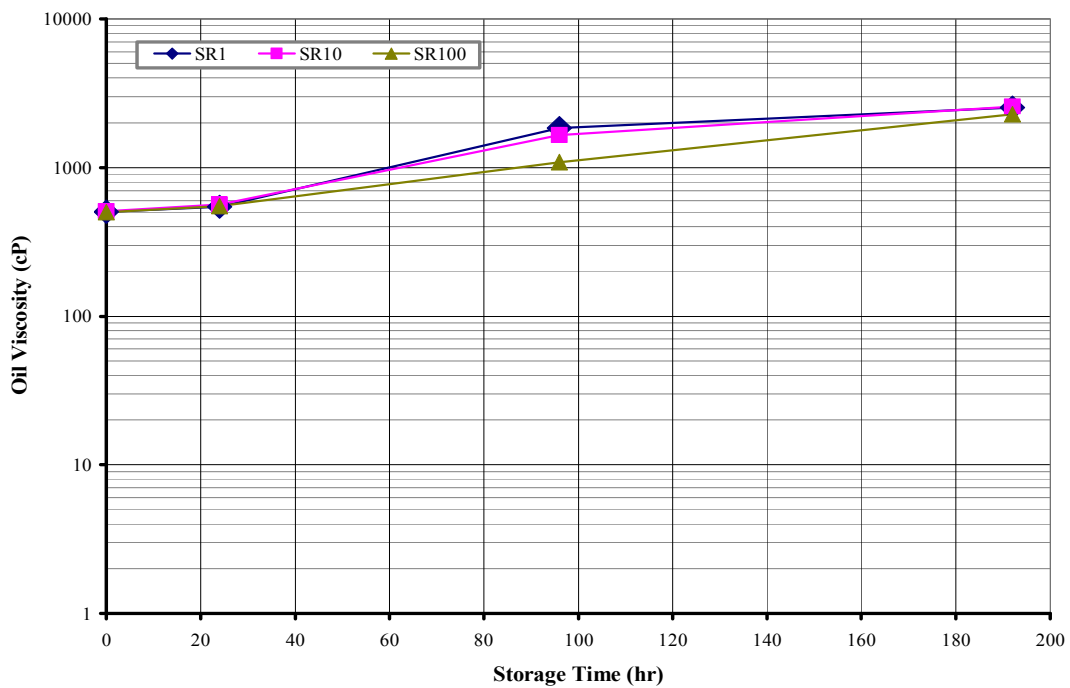


Figure 4.56 Viscosity (cP) Measured at 25 °C as a Function of Shear Rate ($SR=s^{-1}$) and Storage Time (hr) for Glycerol (10 wt.%) Blended Pyrolysis Oil

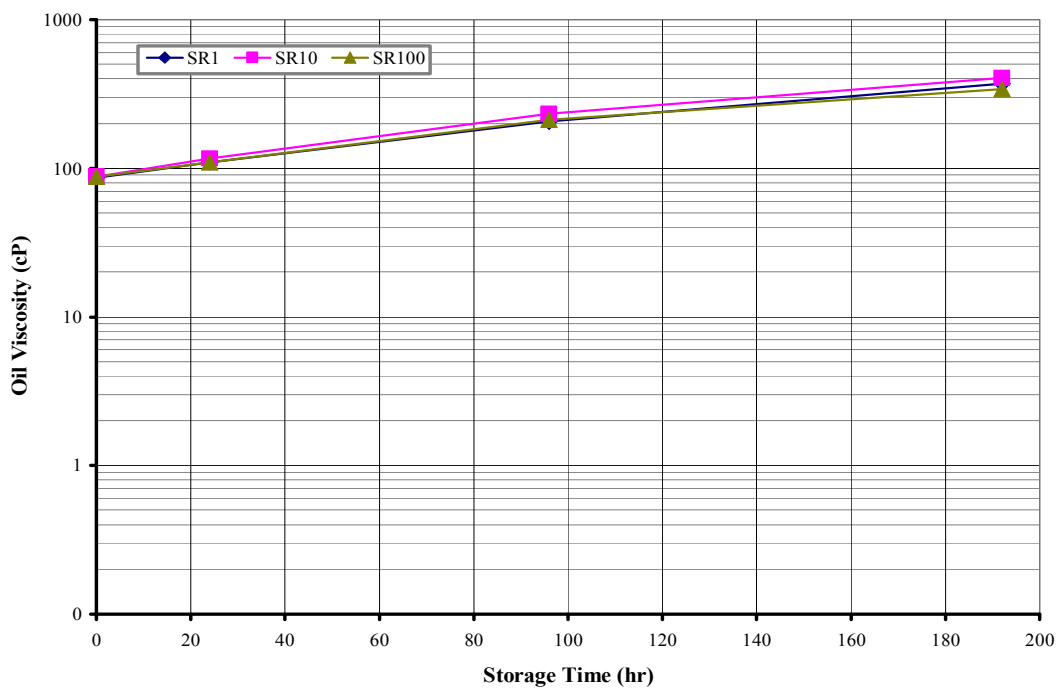


Figure 4.57 Viscosity (cP) Measured at 50 °C as a Function of Shear Rate ($SR=s^{-1}$) and Storage Time (hr) for Glycerol (10 wt.%) Blended Pyrolysis Oil

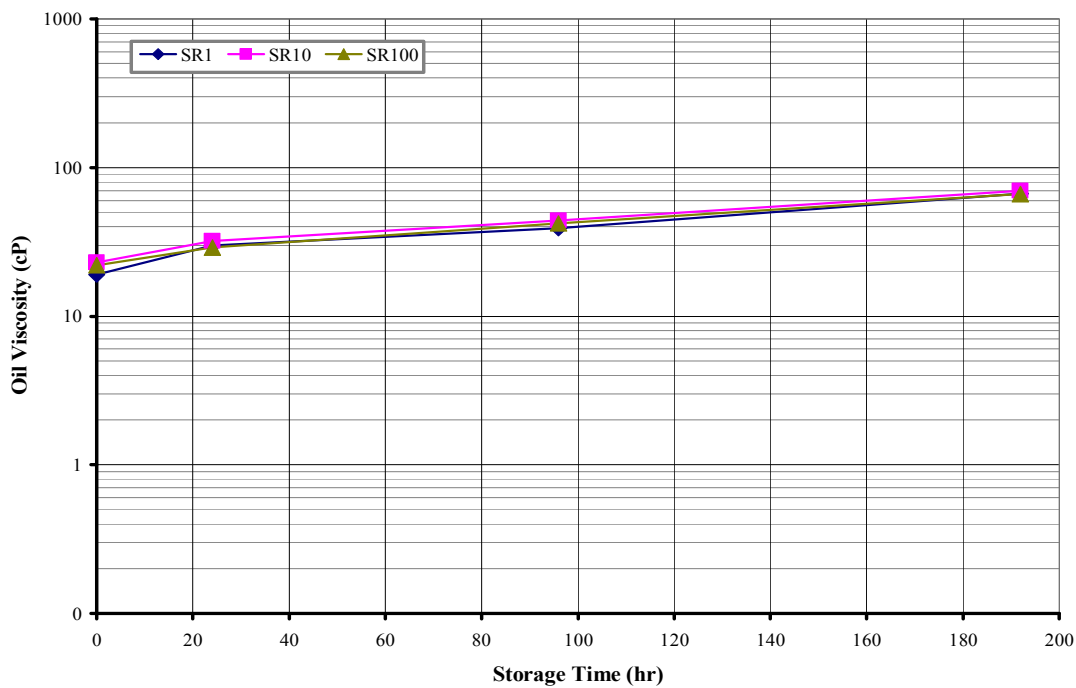


Figure 4.58 Viscosity (cP) Measured at 80 °C as a Function of Shear Rate (SR=s⁻¹) and Storage Time (hr) for Glycerol (10 wt.%) Blended Pyrolysis Oil

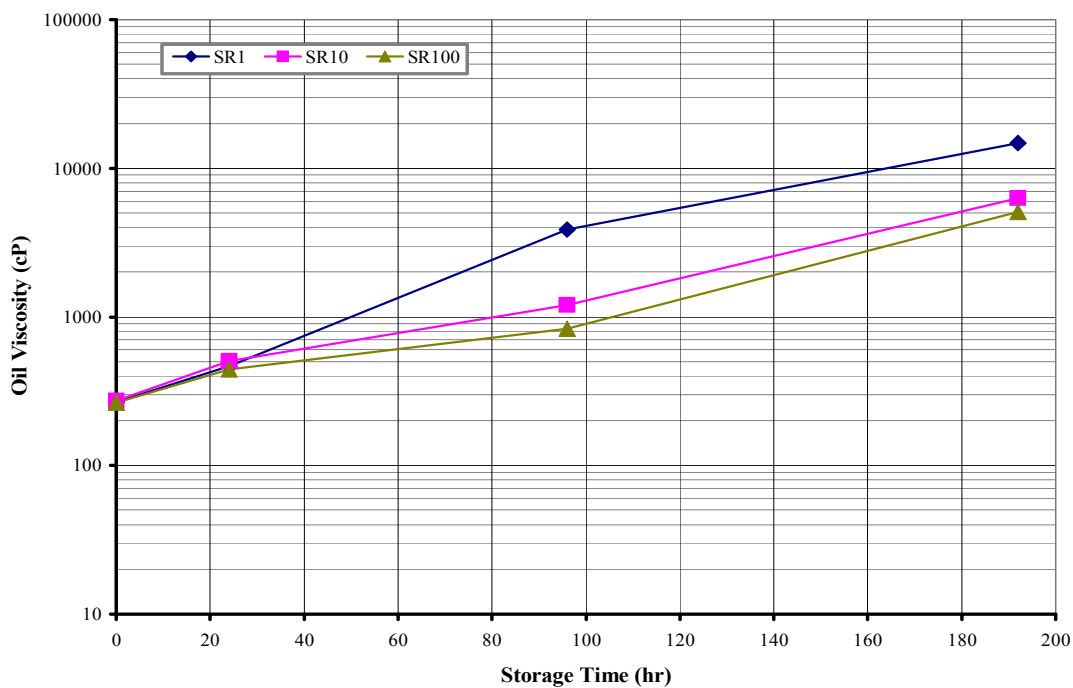


Figure 4.59 Viscosity (cP) Measured at 25 °C as a Function of Shear Rate (SR=s⁻¹) and Storage Time (hr) for Anisole (5 wt.%) Blended Pyrolysis Oil

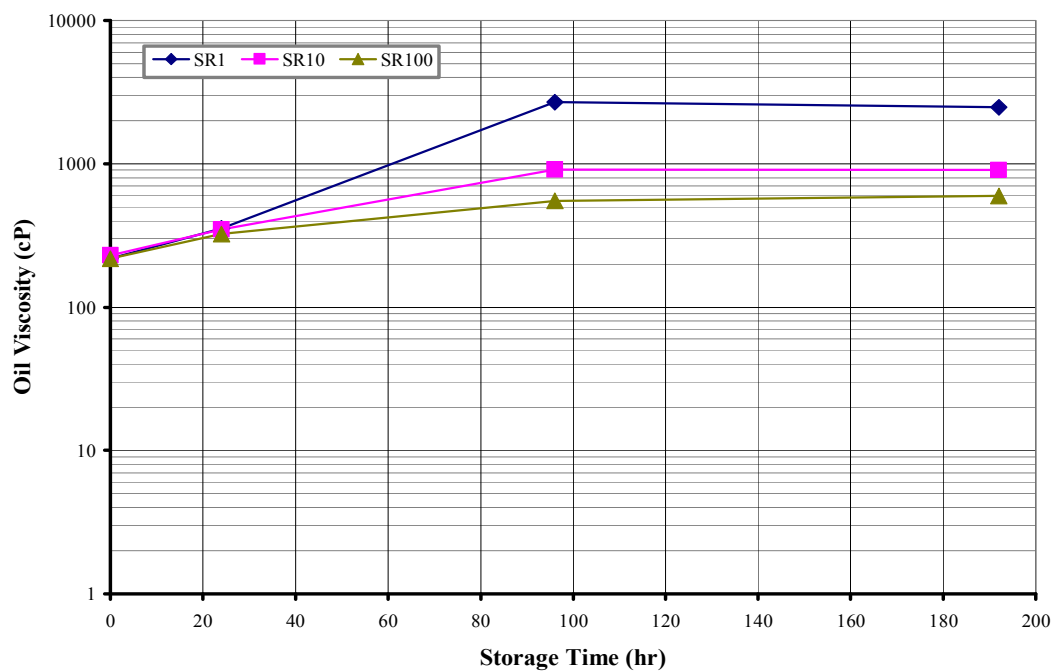


Figure 4.60 Viscosity (cP) Measured at 25 °C as a Function of Shear Rate ($SR=s^{-1}$) and Storage Time (hr) for Anisole (10 wt.%) Blended Pyrolysis Oil

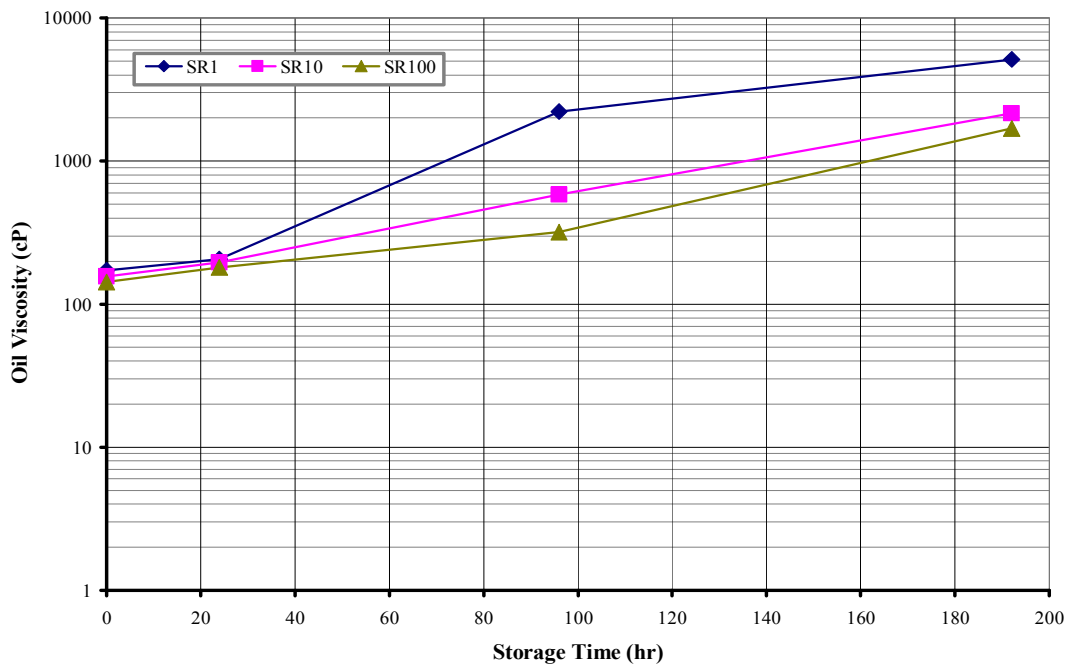


Figure 4.61 Viscosity (cP) Measured at 25 °C as a Function of Shear Rate ($SR=s^{-1}$) and Storage Time (hr) for Anisole (15 wt.%) Blended Pyrolysis Oil

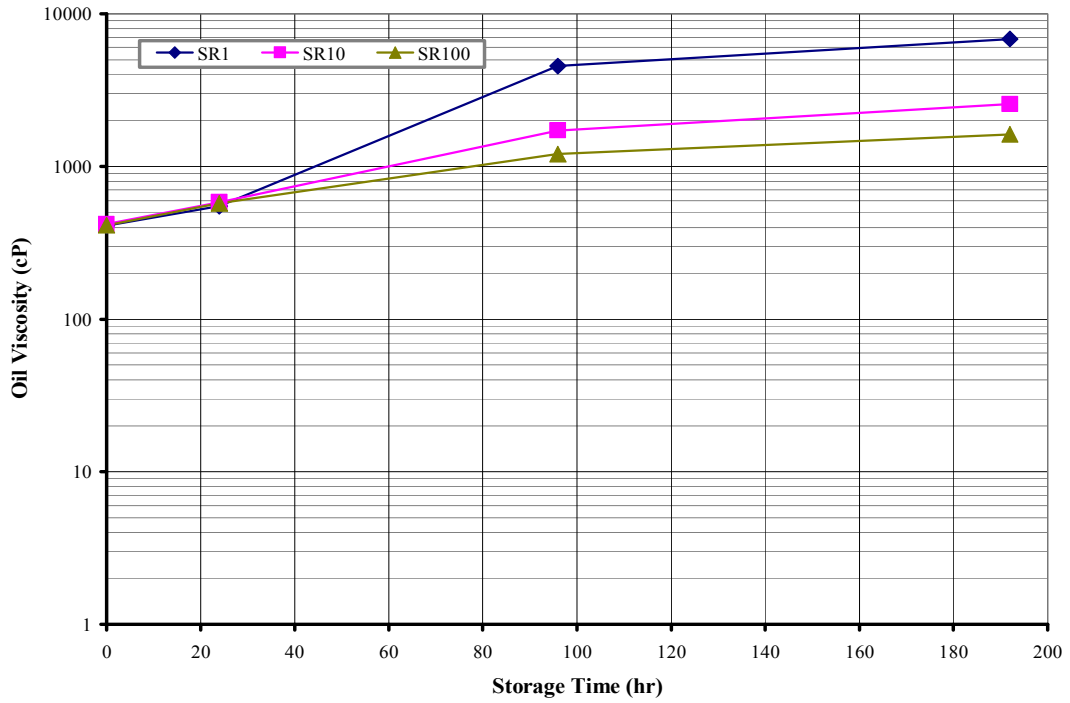


Figure 4.62 Viscosity (cP) Measured at 25 °C as a Function of Shear Rate ($SR=s^{-1}$) and Storage Time (hr) for Glycerol (5 wt.%) Blended Pyrolysis Oil

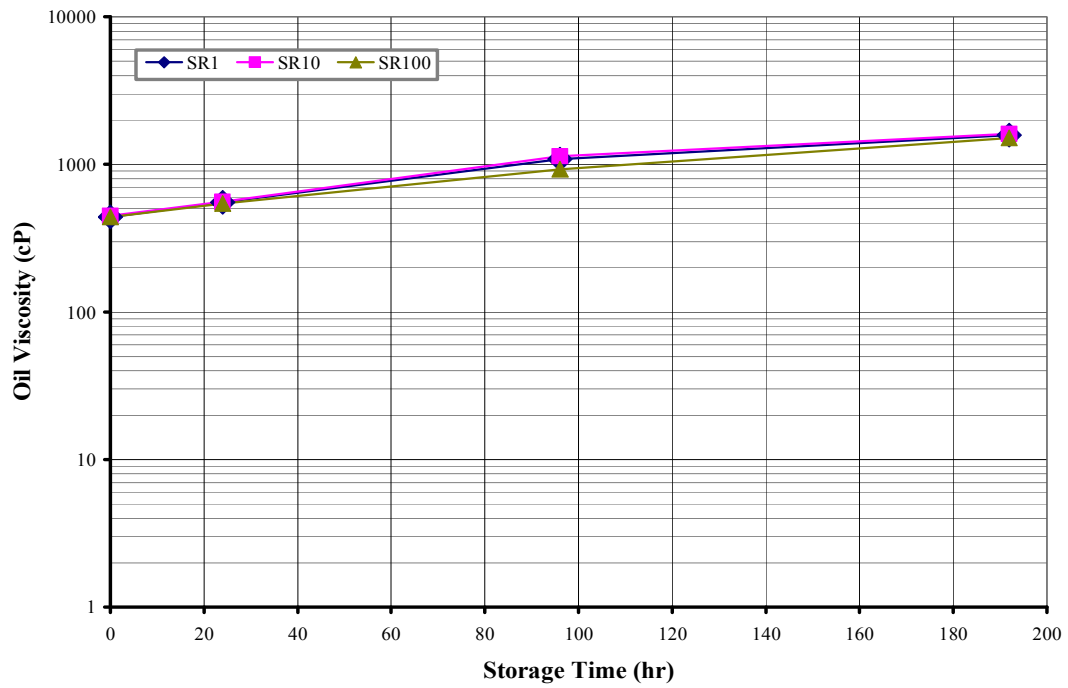


Figure 4.63 Viscosity (cP) Measured at 25 °C as a Function of Shear Rate ($SR=s^{-1}$) and Storage Time (hr) for Glycerol (15 wt.%) Blended Pyrolysis Oil

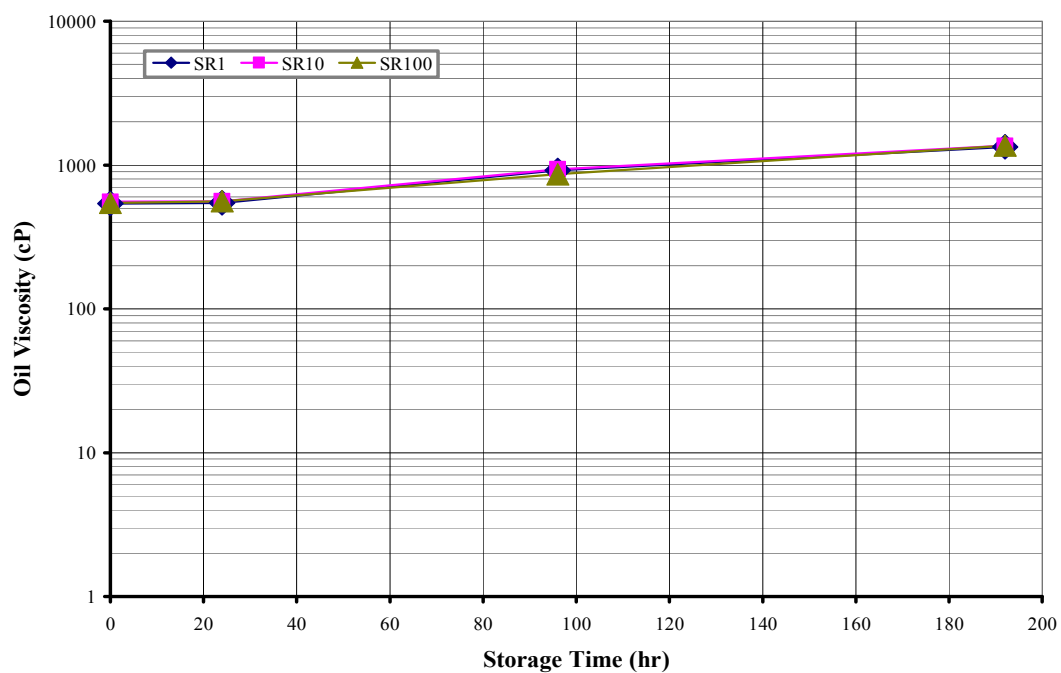


Figure 4.64 Viscosity (cP) Measured at 25 °C as a Function of Shear Rate ($SR=s^{-1}$) and Storage Time (hr) for Glycerol (20 wt.%) Blended Pyrolysis Oil

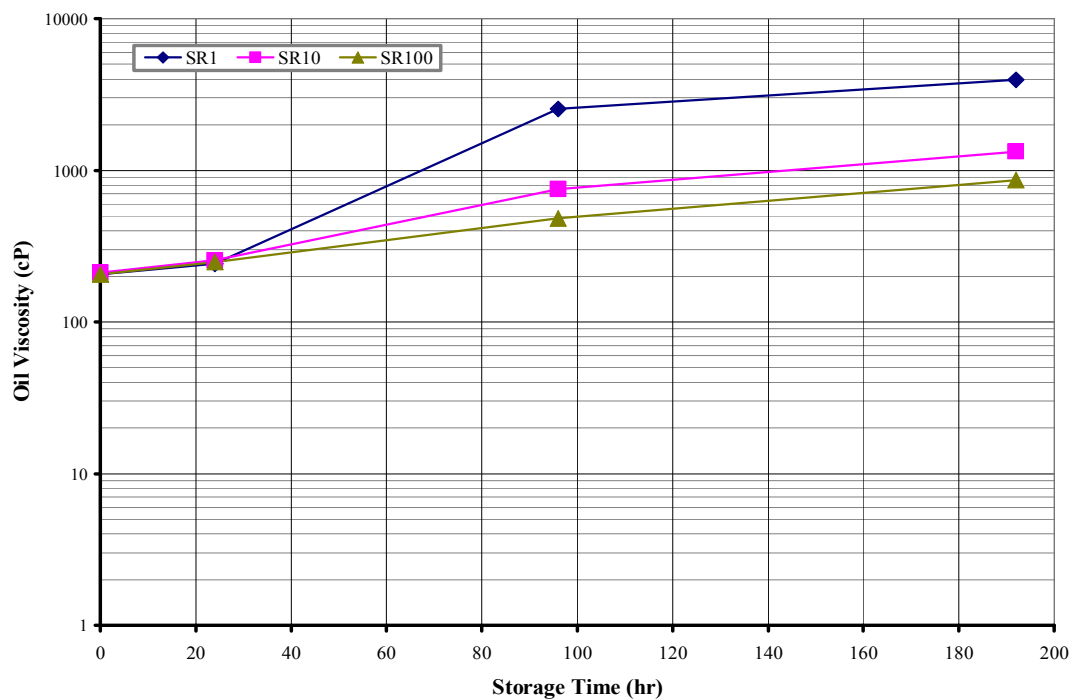


Figure 4.65 Viscosity (cP) Measured at 25 °C as a Function of Shear Rate ($SR=s^{-1}$) and Storage Time (hr) for Methanol (5 wt.%) Blended Pyrolysis Oil

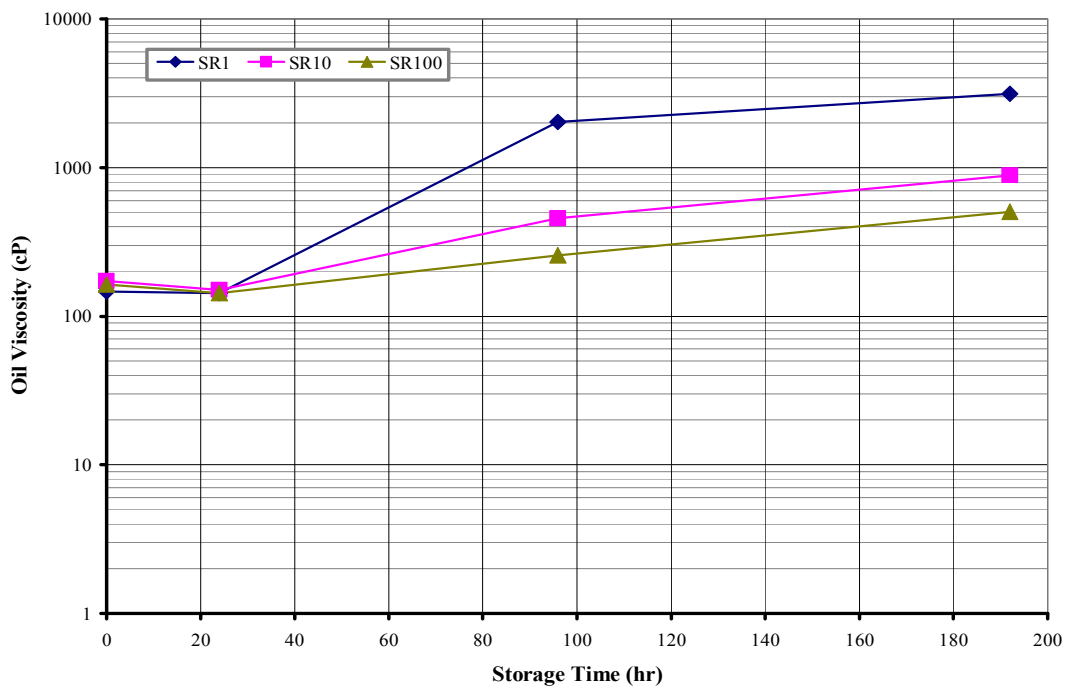


Figure 4.66 Viscosity (cP) Measured at 25 °C as a Function of Shear Rate ($SR=s^{-1}$) and Storage Time (hr) for Methanol (10 wt.%) Blended Pyrolysis Oil

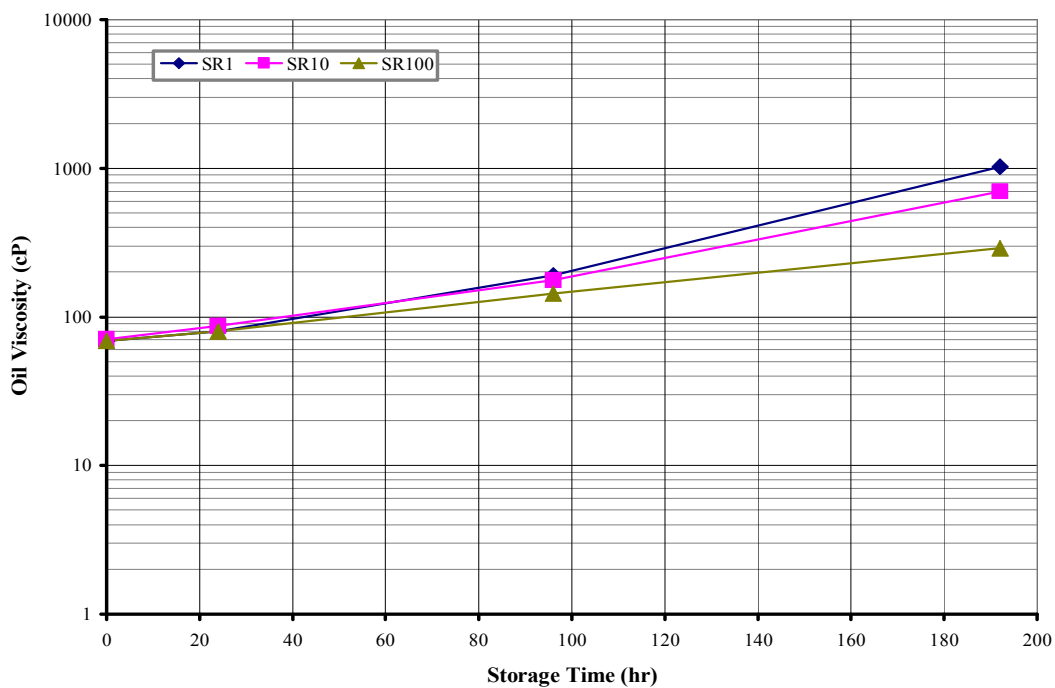


Figure 4.67 Viscosity (cP) Measured at 25 °C as a Function of Shear Rate ($SR=s^{-1}$) and Storage Time (hr) for Methanol (15 wt.%) Blended Pyrolysis Oil

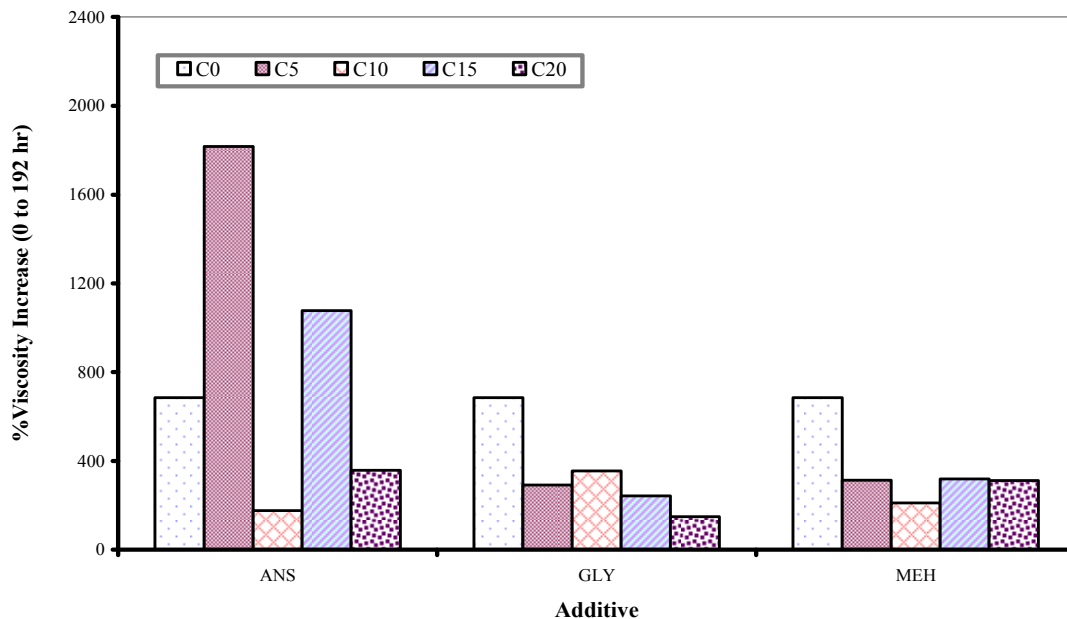


Figure 4.68 Viscosity Increase (%) of Pine Wood Pyrolysis Oils Obtained at 25 °C and 100 s⁻¹ as a Function of Additive Concentration (0-20 wt.%)

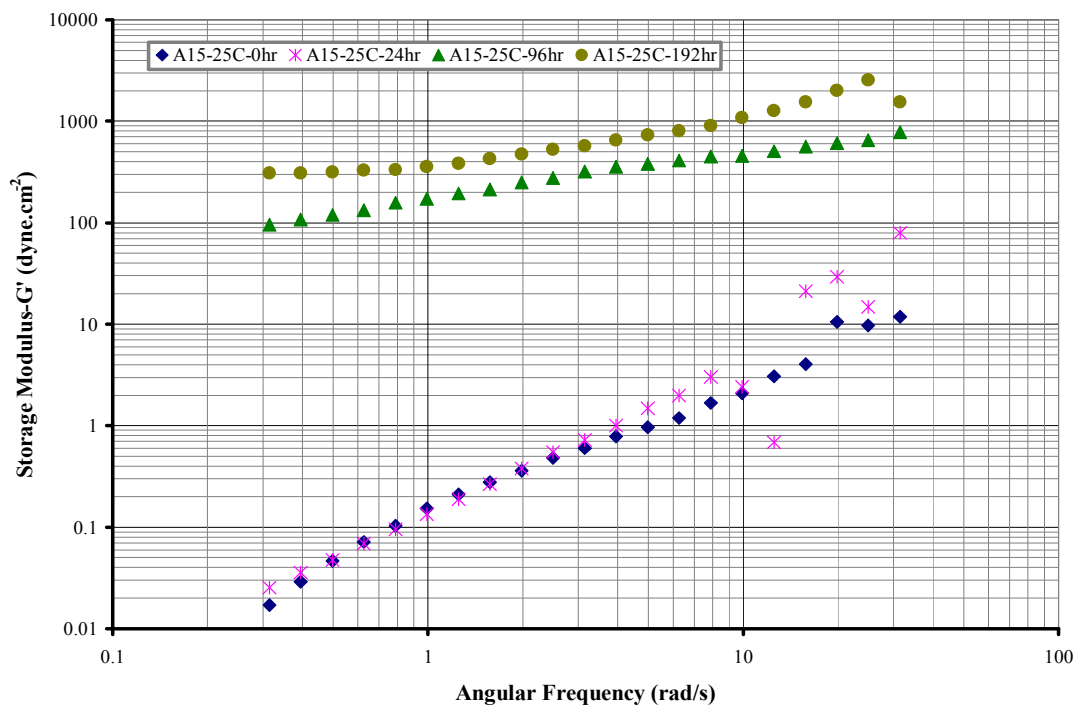


Figure 4.69 Storage Modulus (25 °C) of Anisole Blended Pyrolysis Oil (15 wt.%) Measured as a Function of Frequency and Storage Time

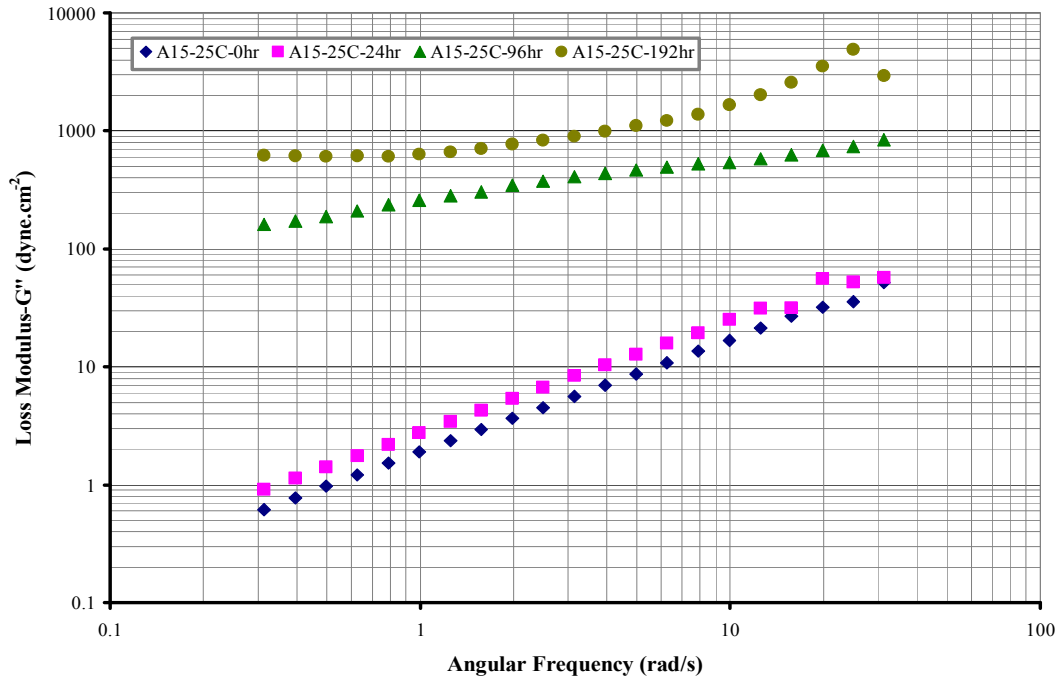


Figure 4.70 Loss Modulus (25 °C) of Anisole Blended Pyrolysis Oil (15 wt.%) Measured as a Function of Frequency and Storage Time

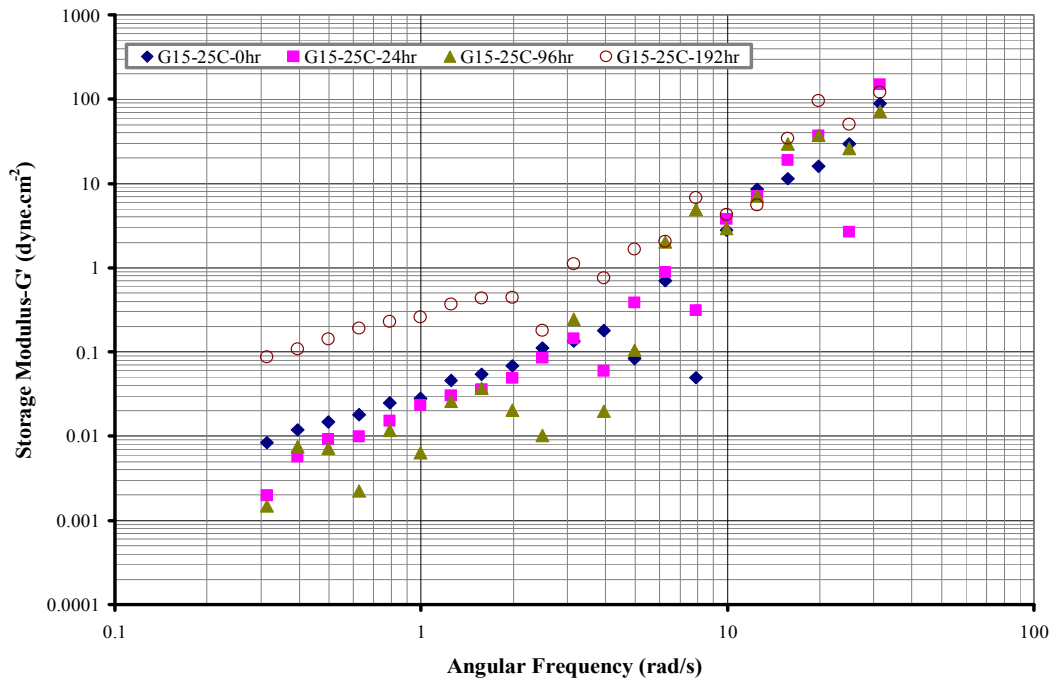


Figure 4.71 Storage Modulus (25 °C) of Glycerol Blended Pyrolysis Oil (15 wt.%) Measured as a Function of Frequency and Storage Time

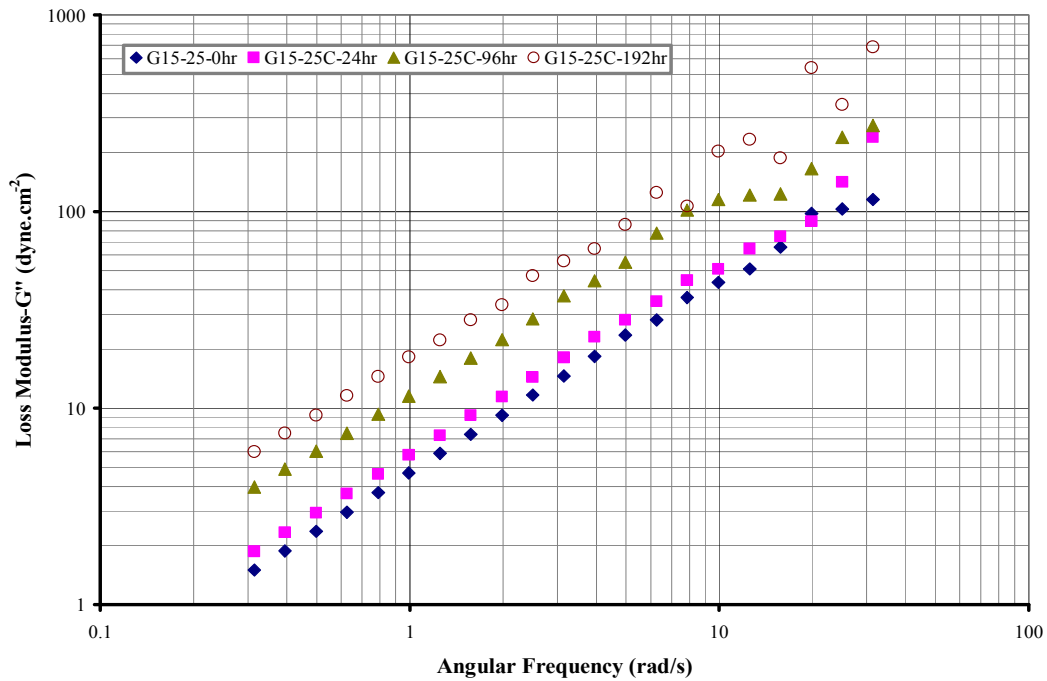


Figure 4.72 Loss Modulus (25 °C) of Glycerol Blended Pyrolysis Oil (15 wt.%) Measured as a Function of Frequency and Storage Time

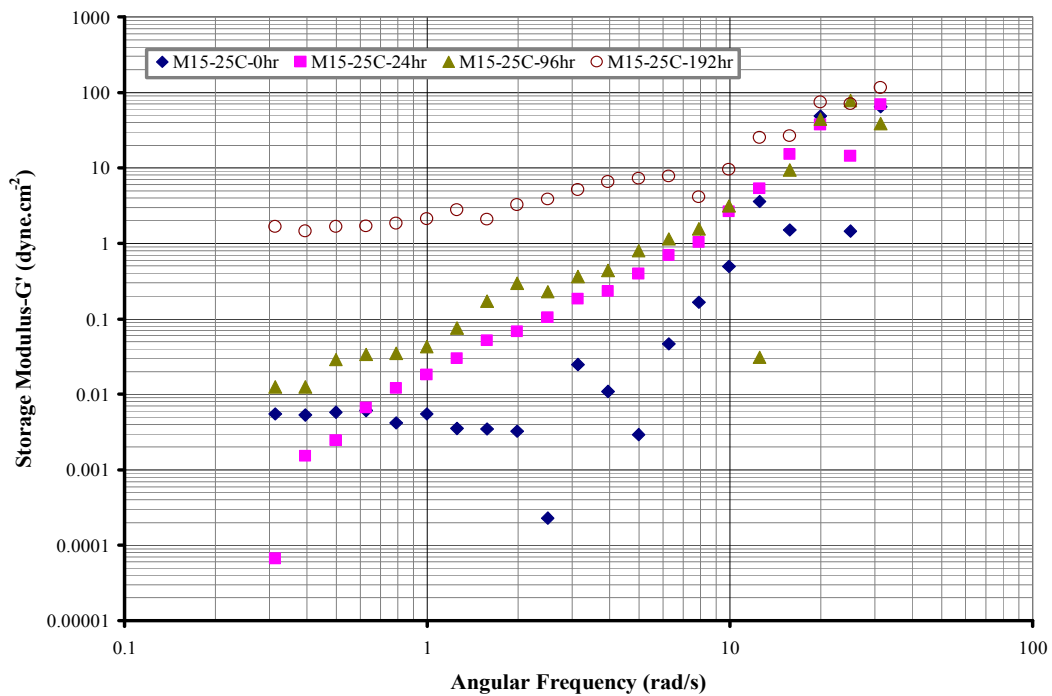


Figure 4.73 Storage Modulus (25 °C) of Methanol Blended Pyrolysis Oil (15 wt.%) Measured as a Function of Frequency and Storage Time

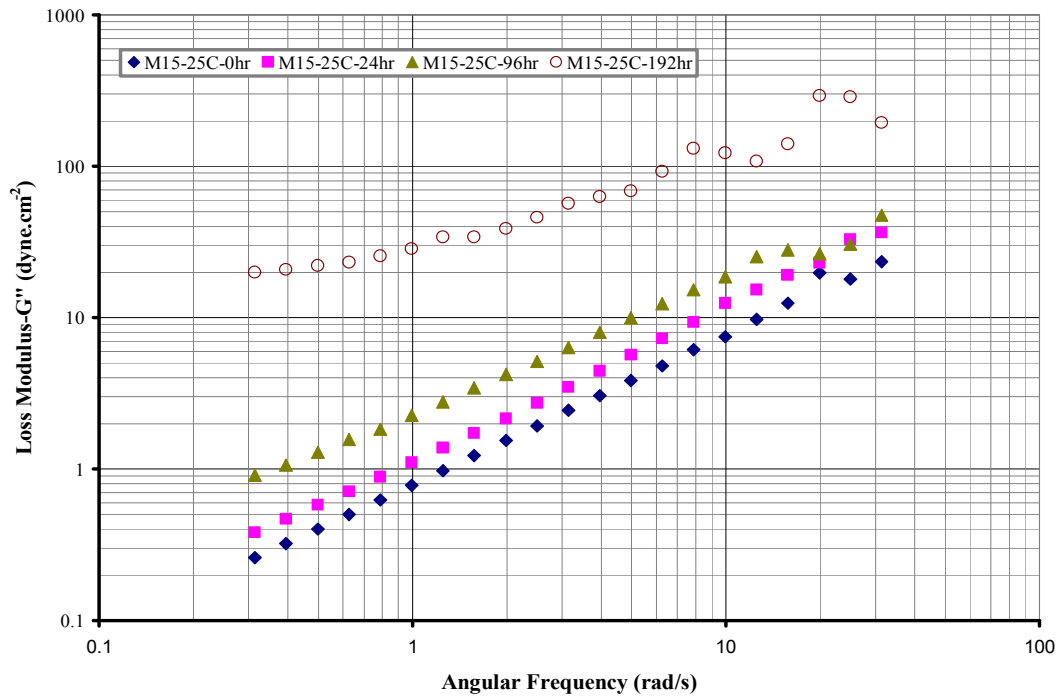


Figure 4.74 Loss Modulus (25 °C) of Methanol Blended Pyrolysis Oil (15 wt.%) Measured as a Function of Frequency and Storage Time

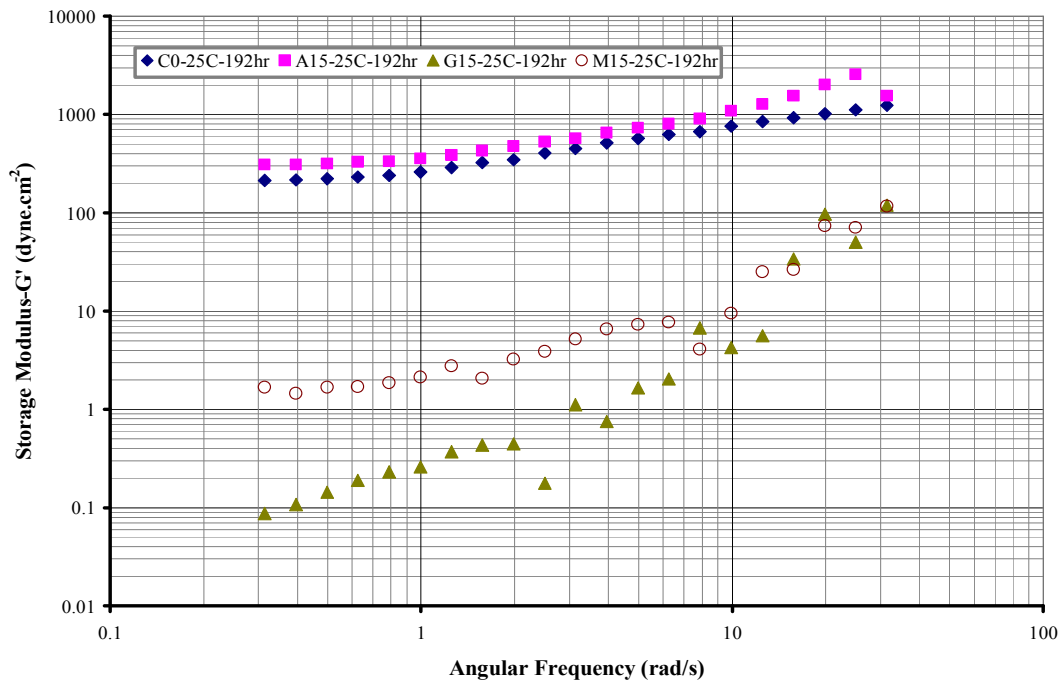


Figure 4.75 Storage Modulus of Control (0 wt.) and Additive Blended Pyrolysis Oils (15 wt.%) Measured at 192 hr and 25 °C

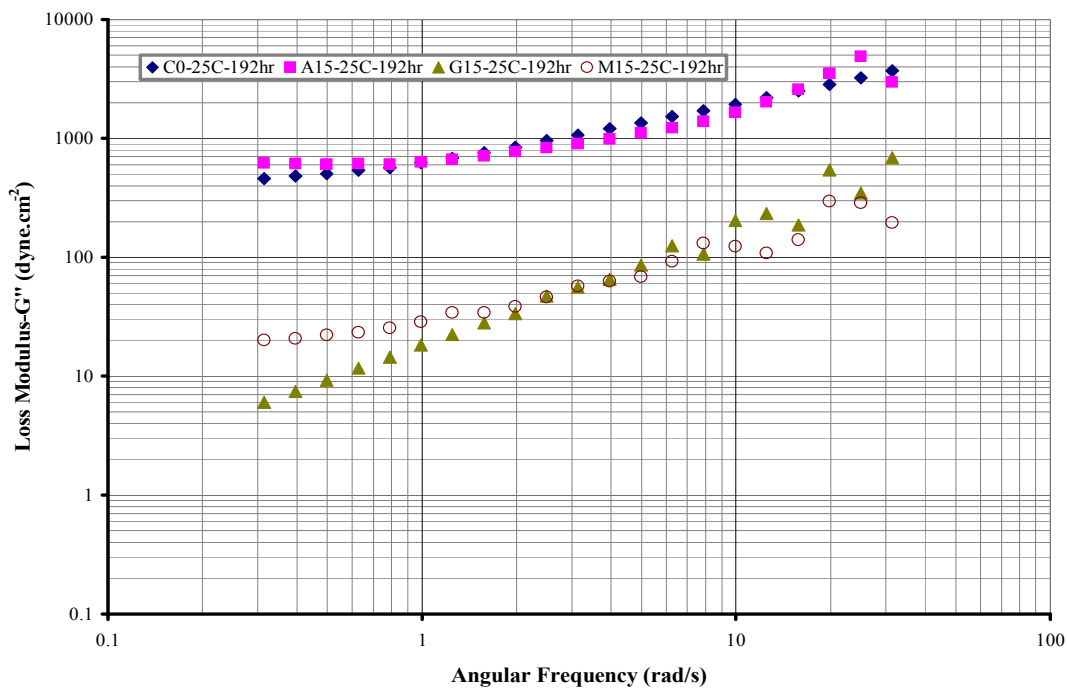


Figure 4.76 Loss Modulus of Control (0 wt.%) and Additive Blended Pyrolysis Oils (15 wt.%) Measured at 192 hr and 25 °C

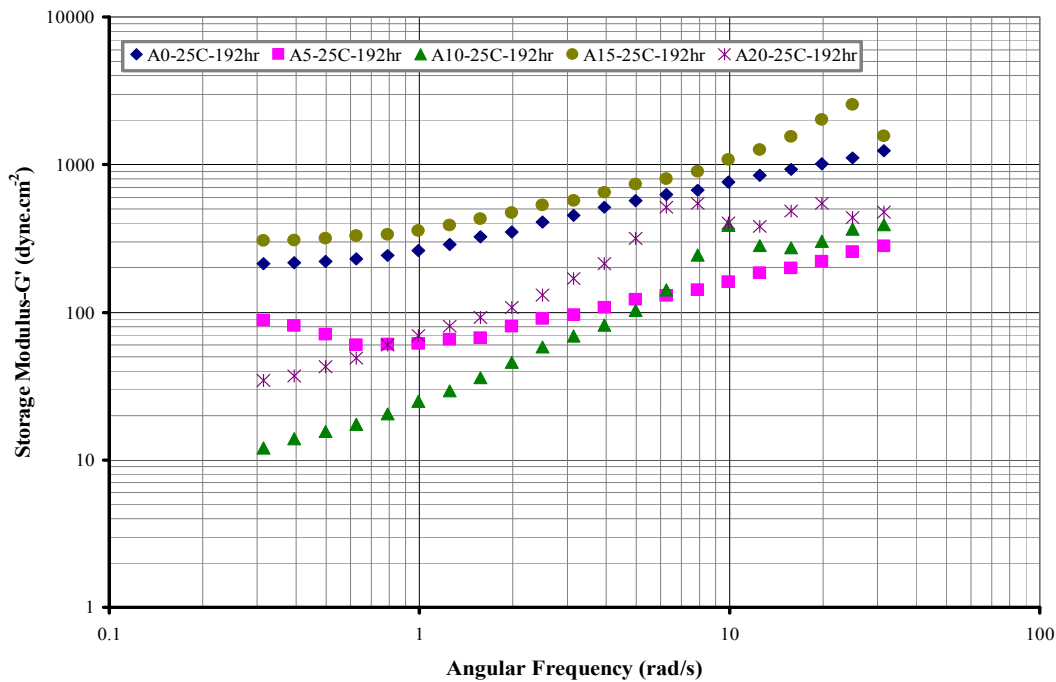


Figure 4.77 Storage Modulus of Anisole Blended Pyrolysis Oil Measured as a Function of Concentration (0-20 wt.%) and Frequency at 192 hr and 25 °C

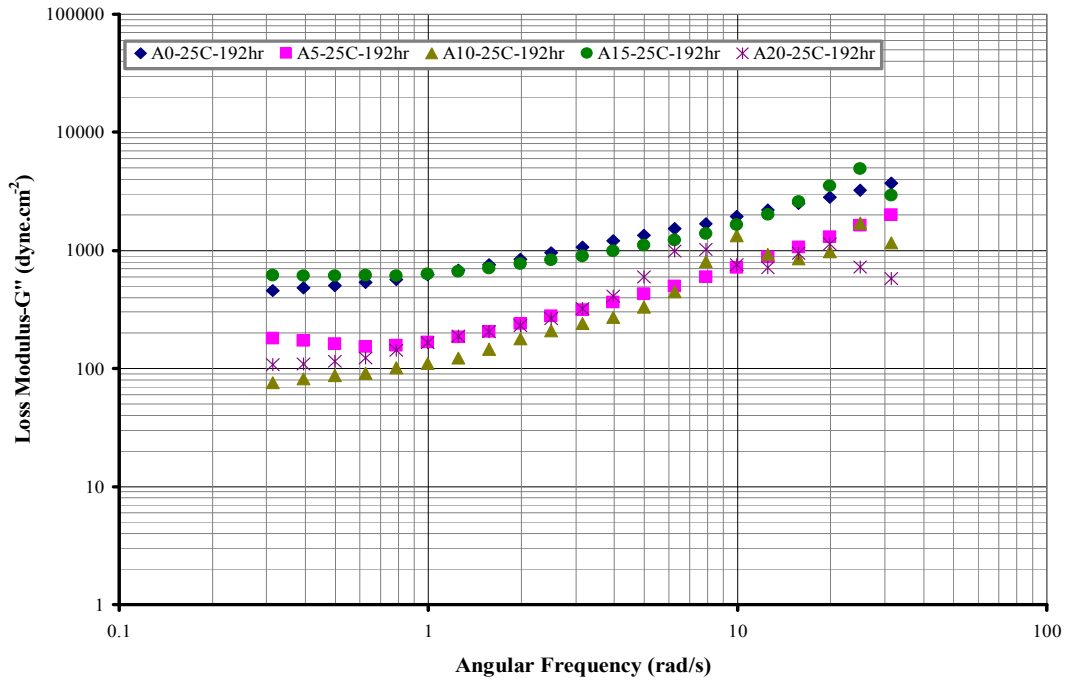


Figure 4.78 Loss Modulus of Anisole Blended Pyrolysis Oil Measured as a Function of Concentration (0-20 wt.%) and Frequency at 192 hr and 25 °C

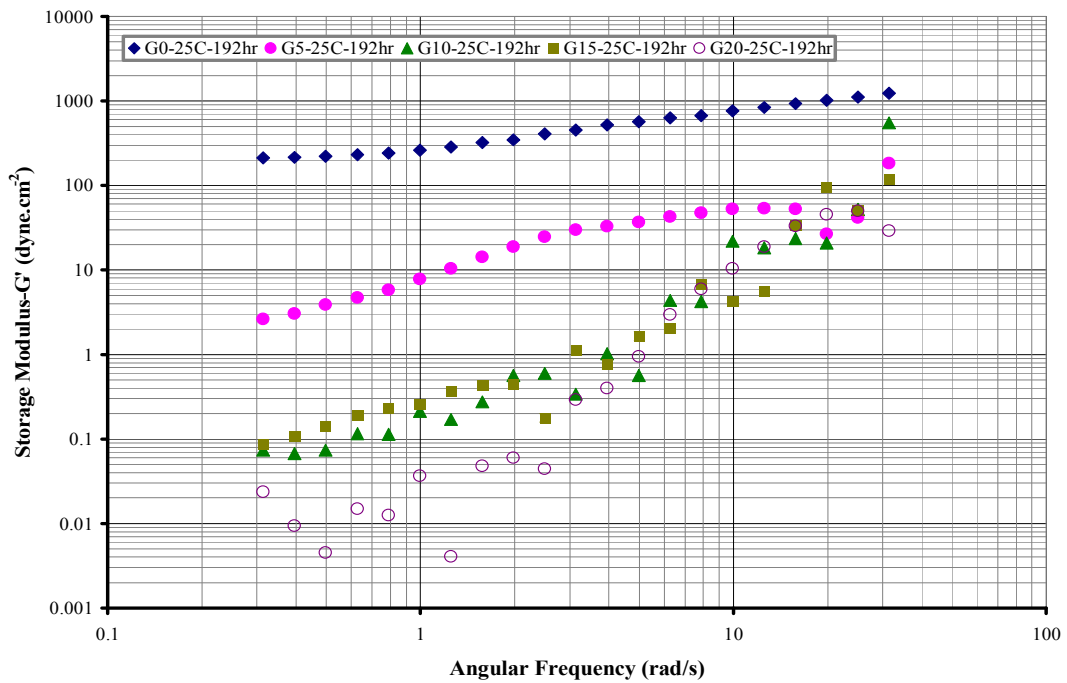


Figure 4.79 Storage Modulus of Glycerol Blended Pyrolysis Oil Measured as a Function of Concentration (0-20 wt.%) and Frequency at 192 hr and 25 °C

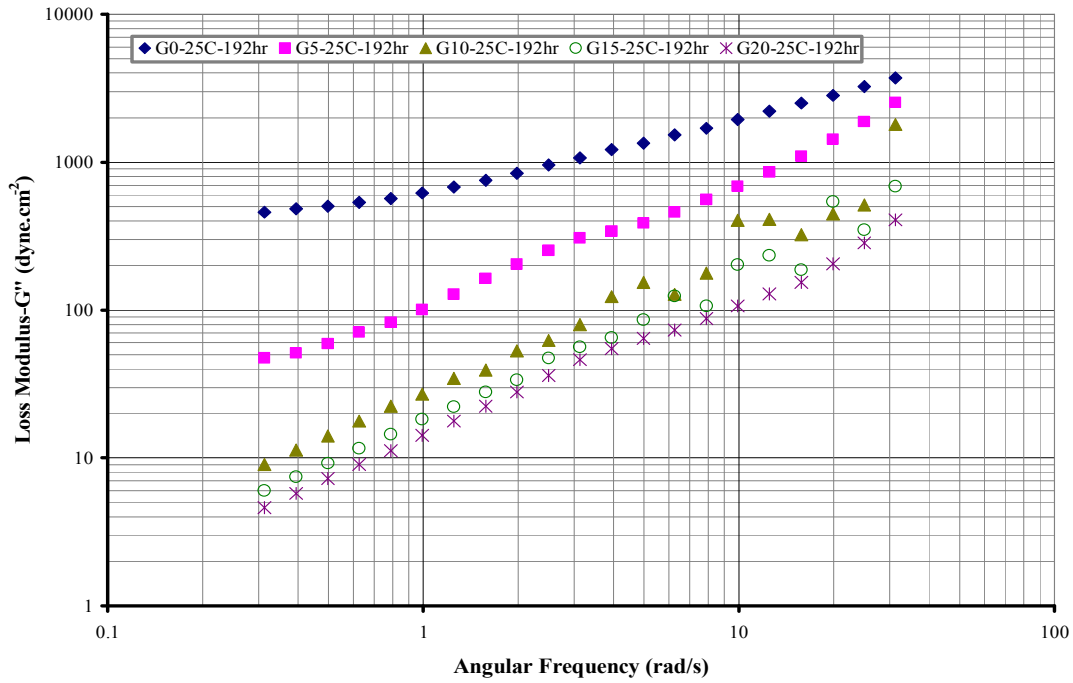


Figure 4.80 Loss Modulus of Glycerol Blended Pyrolysis Oil Measured as a Function of Concentration (0-20 wt.%) and Frequency at 192 hr and 25 °C

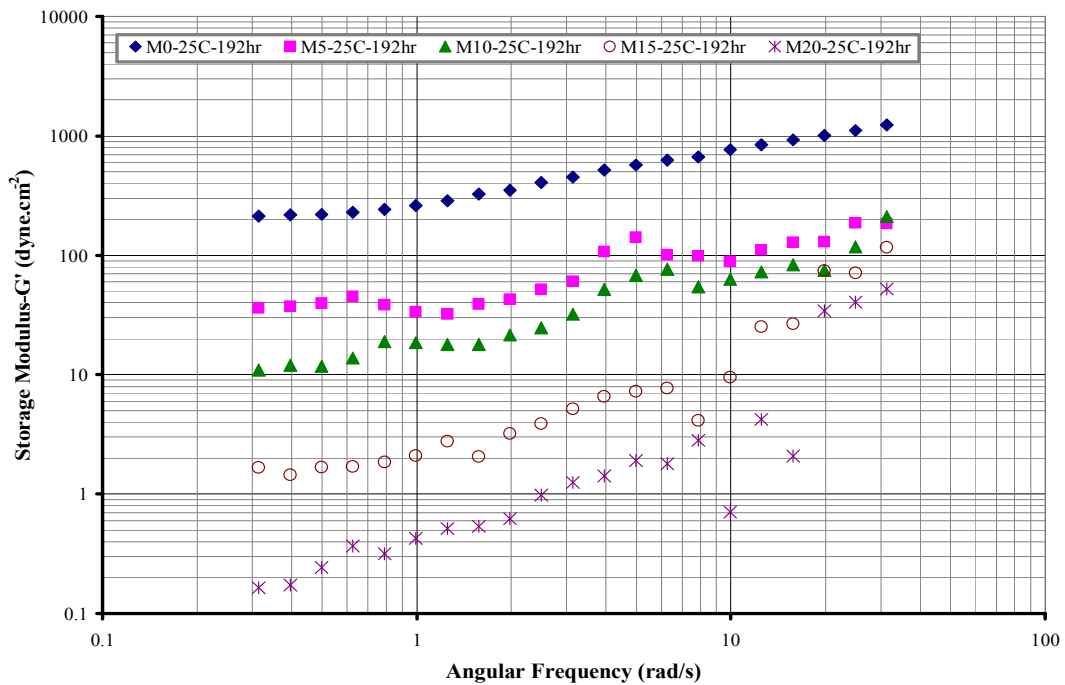


Figure 4.81 Storage Modulus of Methanol Blended Pyrolysis Oil Measured as a Function of Concentration (0-20 wt.%) and Frequency at 192 hr and 25 °C

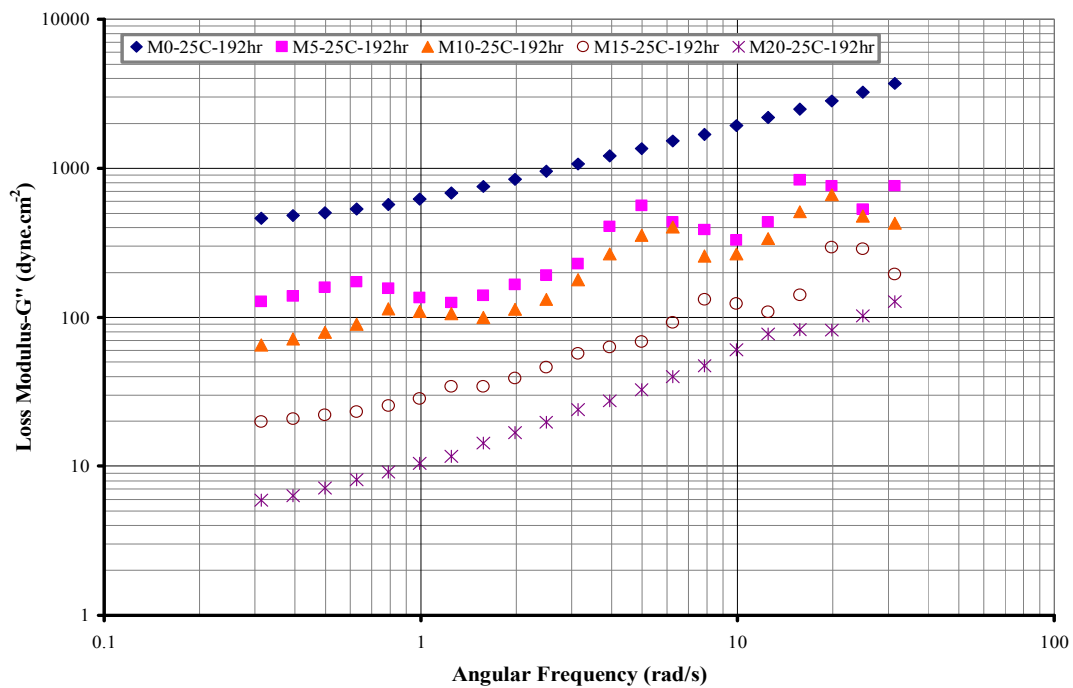


Figure 4.82 Loss Modulus of Methanol Blended Pyrolysis Oil Measured as a Function of Concentration (0-20 wt.%) and Frequency at 192 hr and 25 °C

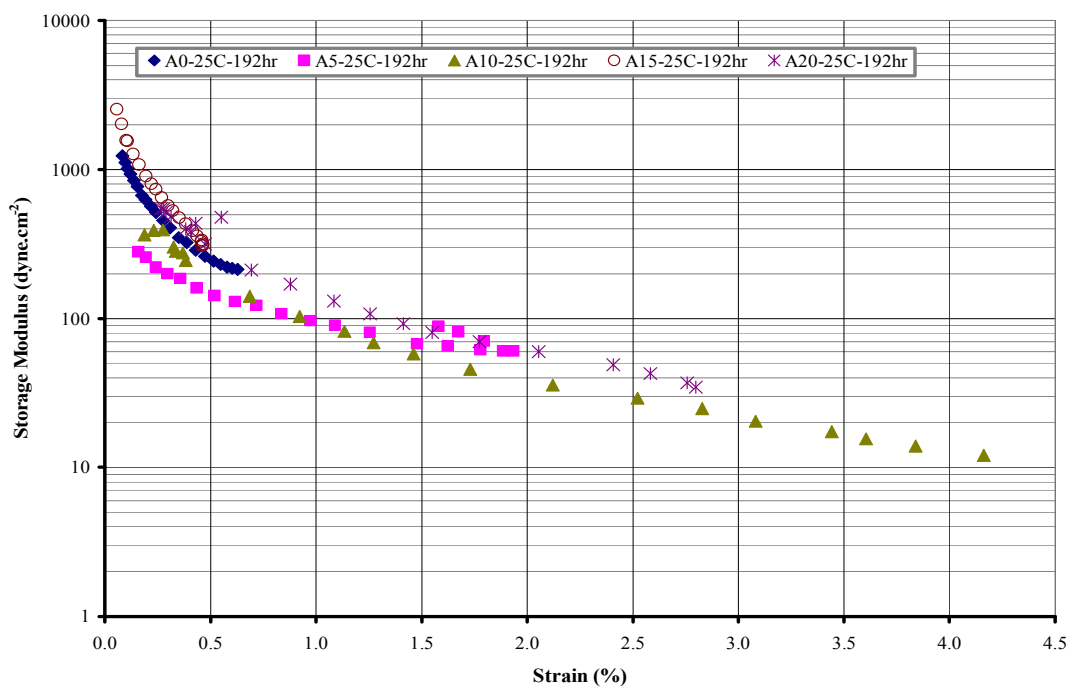


Figure 4.83 Storage Modulus of Anisole Blended Pyrolysis Oil Measured as a Function of Concentration (0-20 wt.%) and Strain at 192 hr and 25 °C

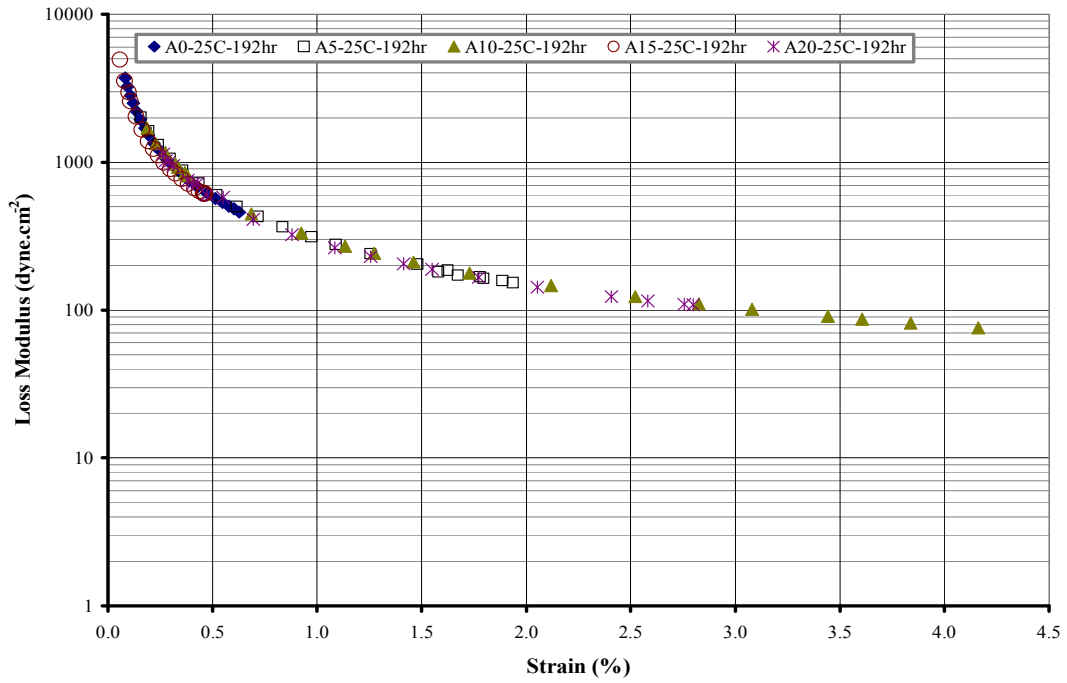


Figure 4.84 Loss Modulus of Anisole Blended Pyrolysis Oil Measured as a Function of Concentration (0-20 wt.%) and Strain at 192 hr and 25 °C

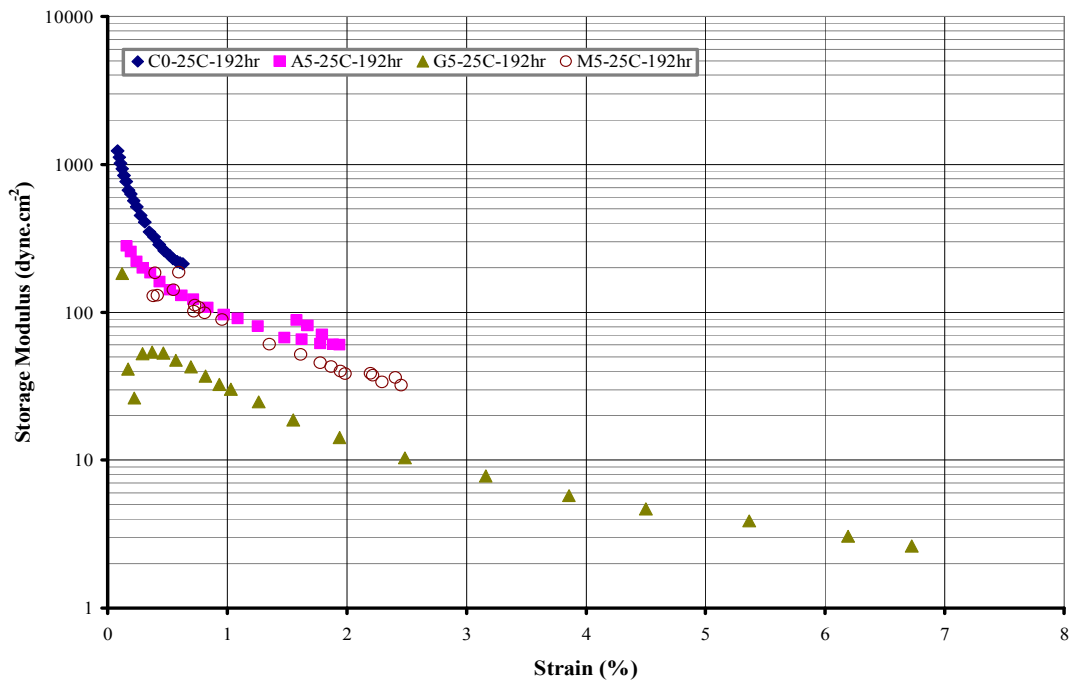


Figure 4.85 Storage Modulus of Control (0 wt.) and Additive Blended (5 wt.%) Pyrolysis Oil Measured as a Function of Strain at 192 hr and 25 °C

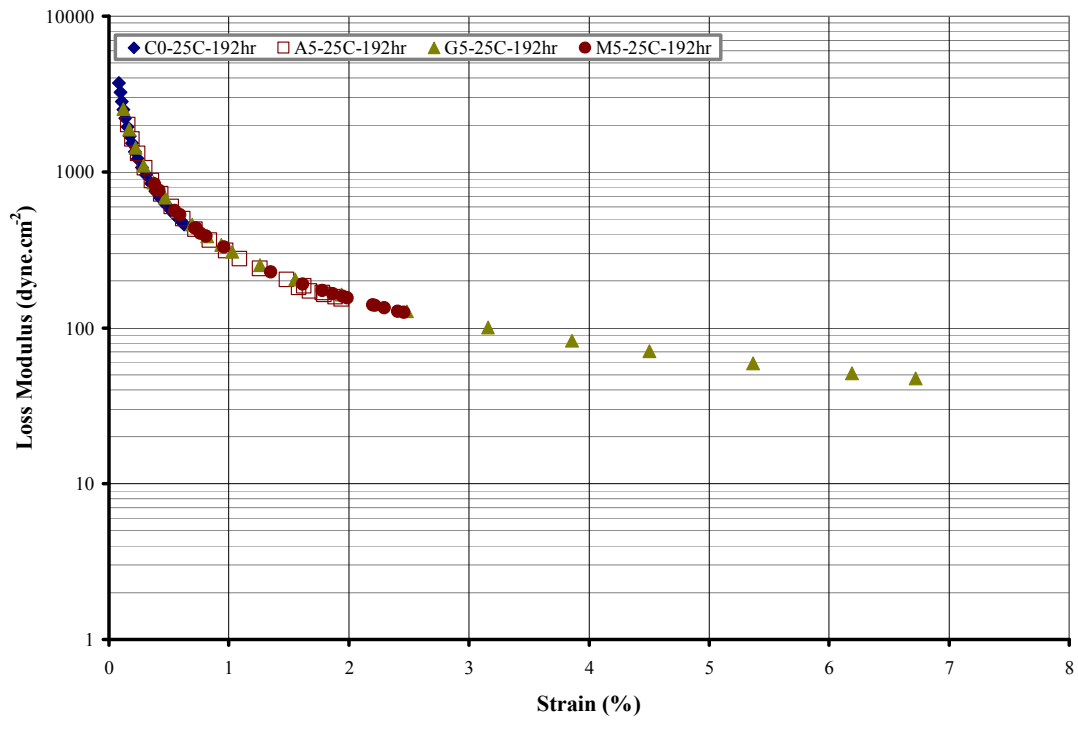


Figure 4.86 Loss Modulus of Control (0 wt.%) and Additive Blended (5 wt.%) Pyrolysis Oil Measured as a Function of Strain at 192 hr and 25 °C

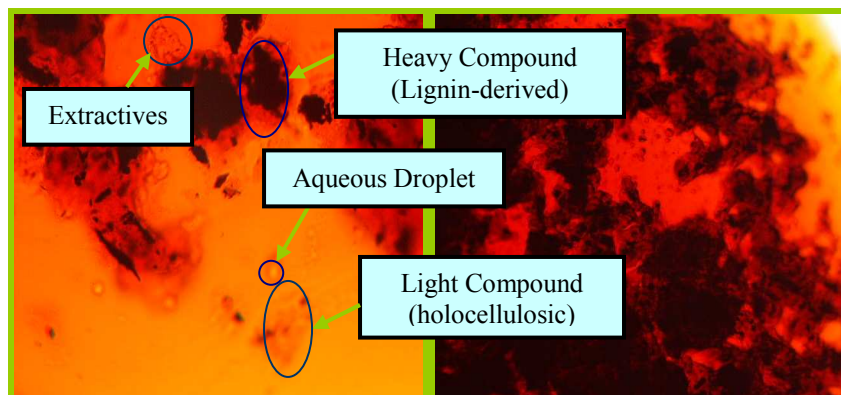


Figure 4.87 Microscopic Images (200X and 40X) Obtained for the Fresh (0 hr) Pine Bark Pyrolysis Oil at 25 °C

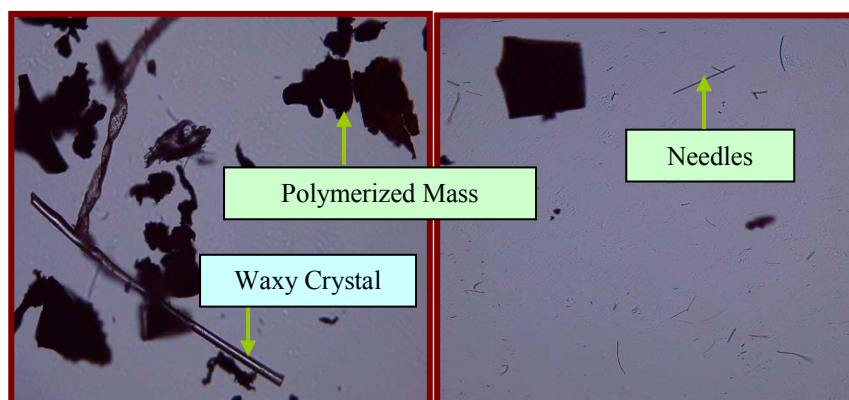


Figure 4.88 Microscopic Images (200X) Obtained for the Aged (192 hr) Pine Bark Pyrolysis Oil at 25 °C

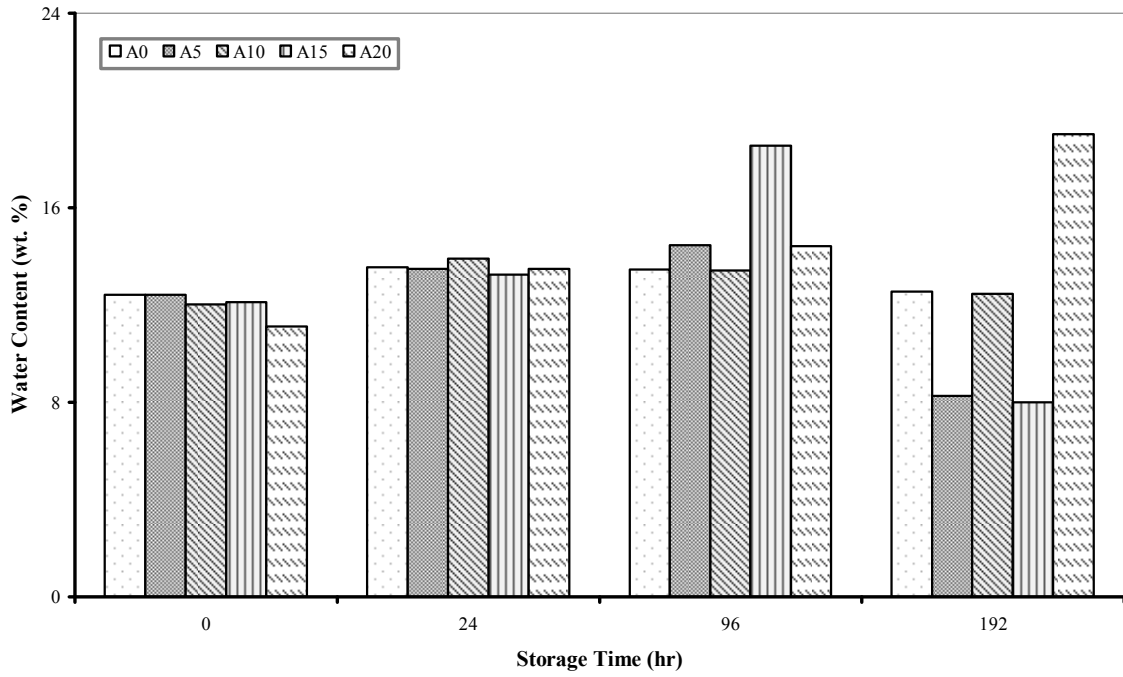


Figure 4.89 Water Content (wt.%) of Anisole Blended Pyrolysis Oil as a Function of Concentration (0-20 wt.%) and Storage Time

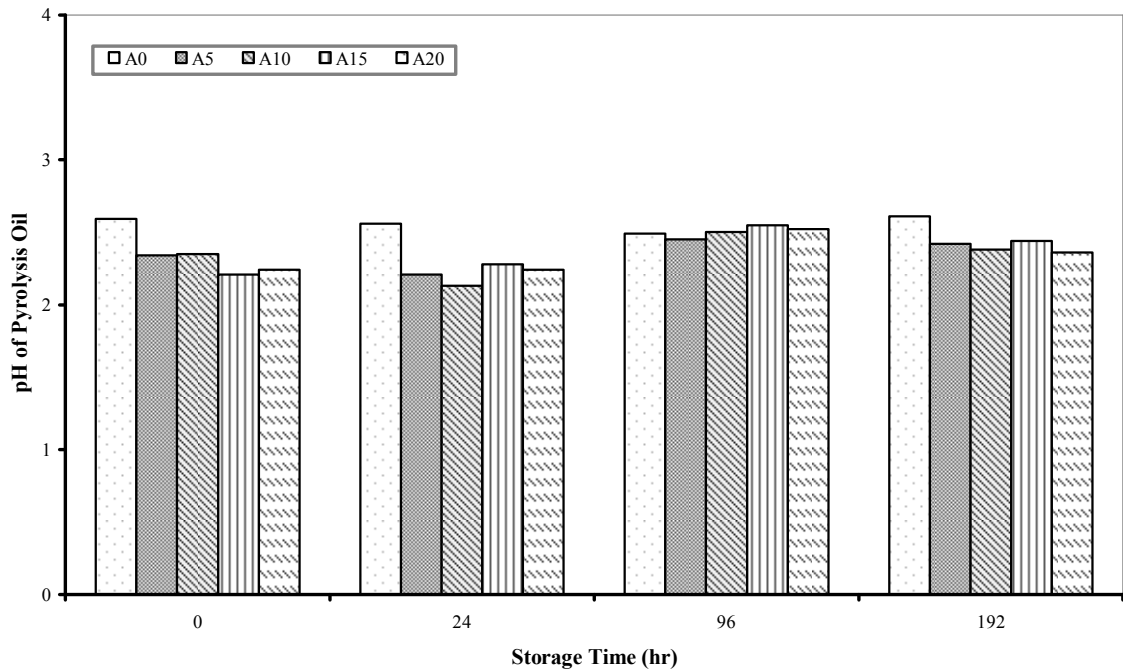


Figure 4.90 pH of Anisole Blended Pyrolysis Oil as a Function of Concentration (0-20 wt.%) and Storage Time

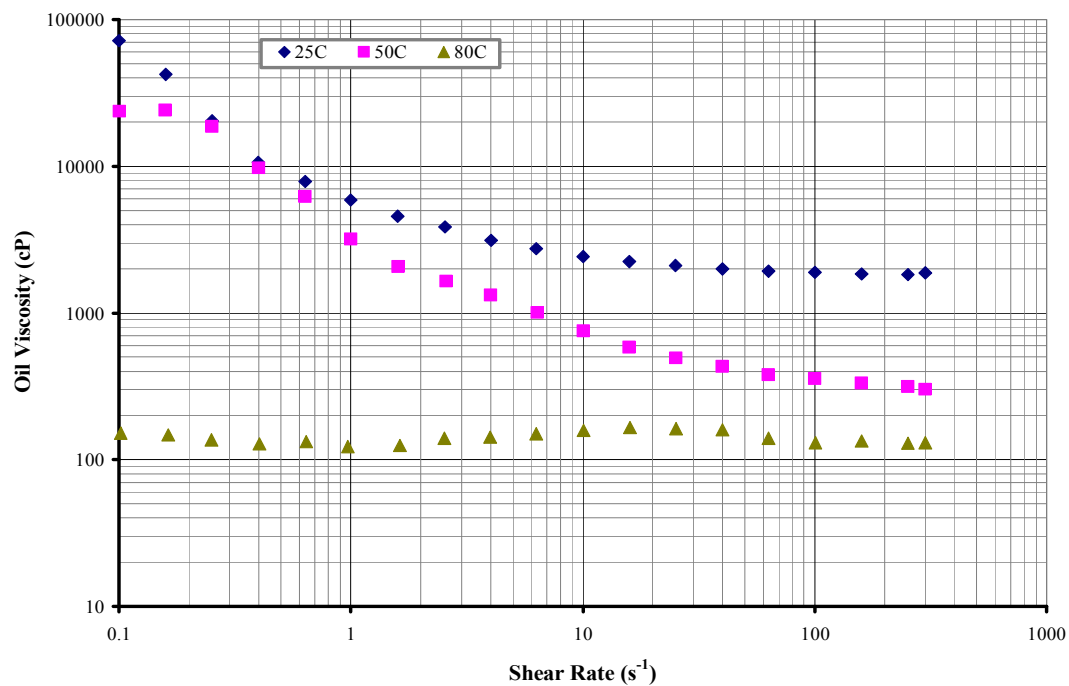


Figure 4.91 Viscosity (cP) of Pine Wood Pyrolysis Oil Control (0 wt.%) Measured at 96 hr as a Function of Shear Rate (s⁻¹) and Temperature (°C)

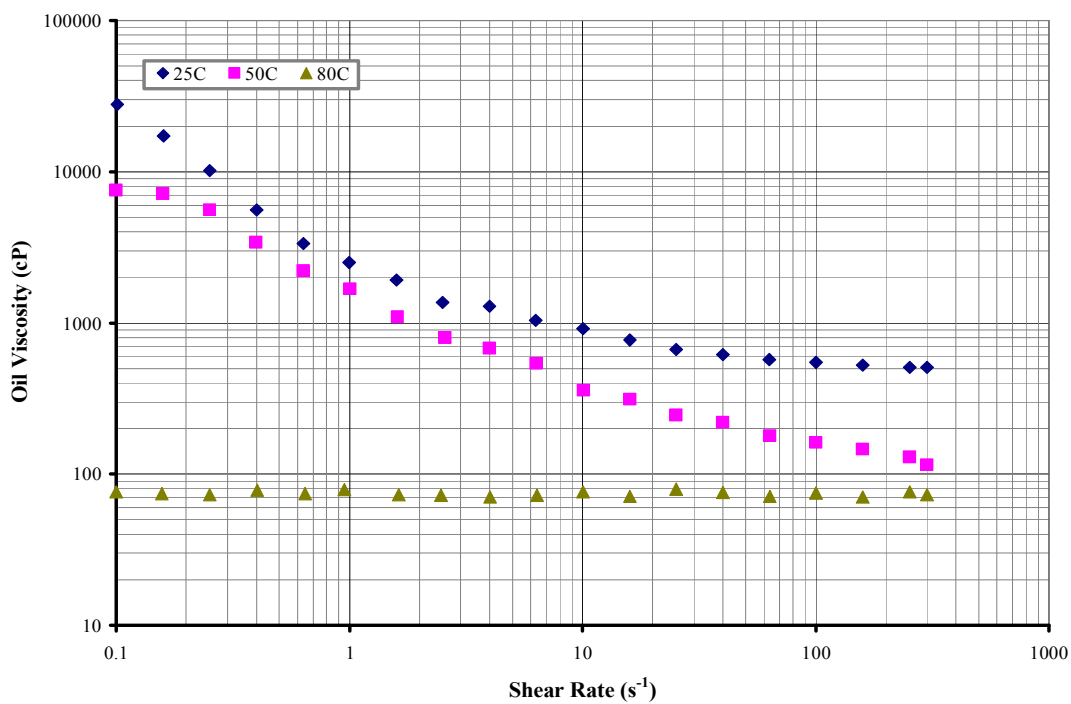


Figure 4.92 Viscosity (cP) of Anisole Blended (10 wt.%) Pine Wood Pyrolysis Oil Measured at 96 hr as a Function of Shear Rate (s⁻¹) and Temperature (°C)

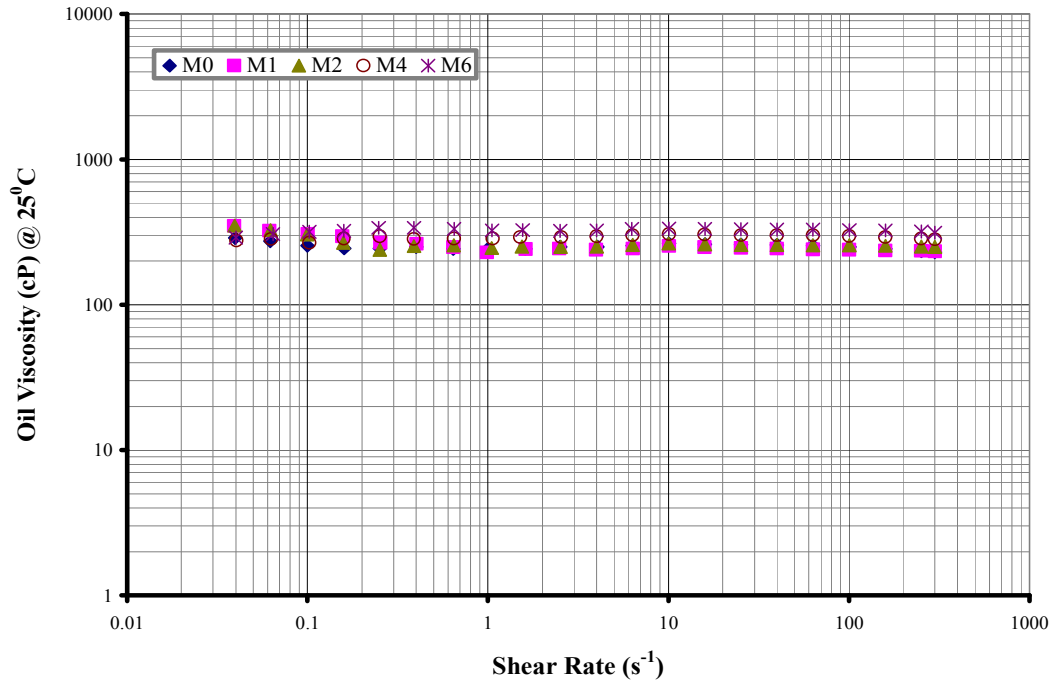


Figure 4.93 Viscosity (cP) of Mississippi State University (MS) Pine Wood Oil Control (CTL2) as a Function of Shear Rate (s⁻¹) and Storage Time (Month-M)

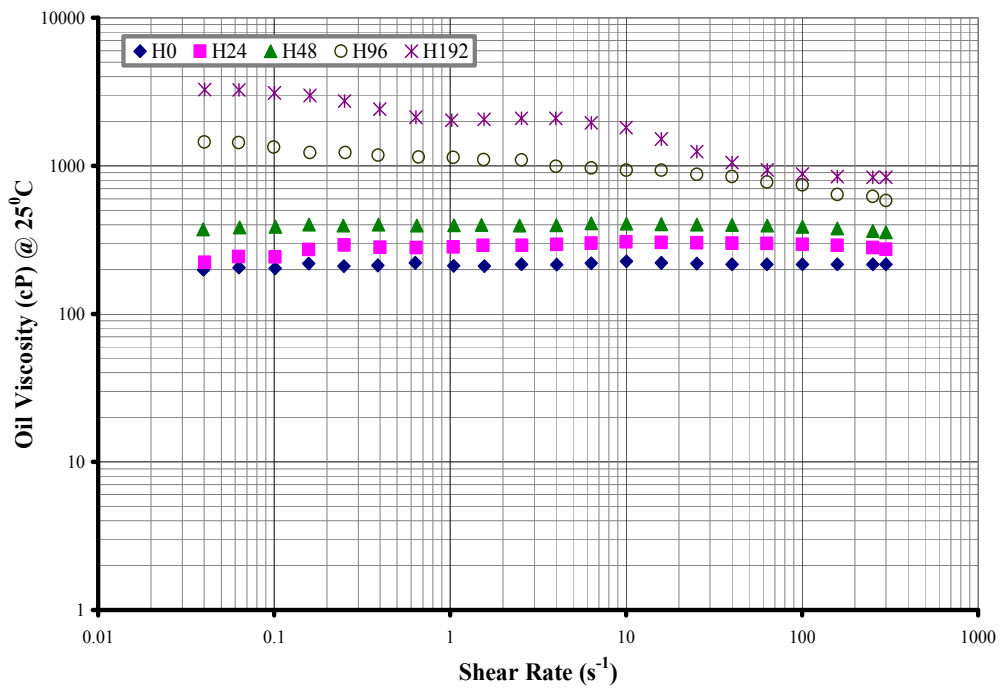


Figure 4.94 Viscosity (cP) of Mississippi State University (MS) Pine Wood Oil Control (CTL2) as a Function of Shear Rate (s⁻¹) and Storage Time (Hour-H)

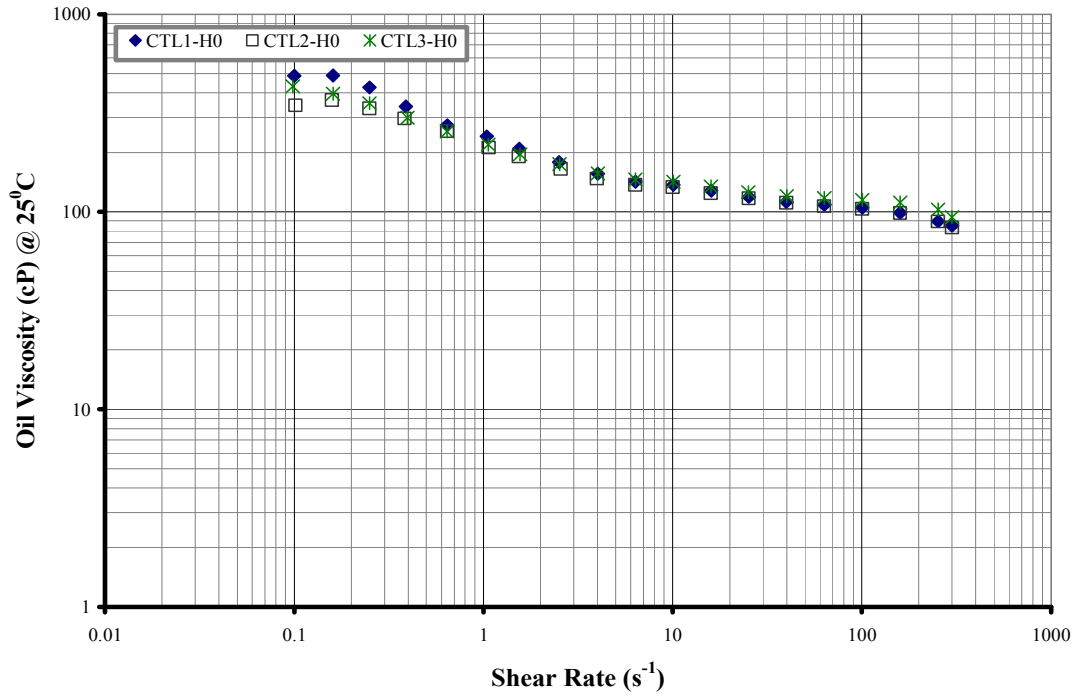


Figure 4.95 Viscosity (cP) as a Function of Shear Rate (s⁻¹) of Mississippi State University (MS) Fresh (0 hr) Oak Wood Oil Controls (CTL's 1-3)

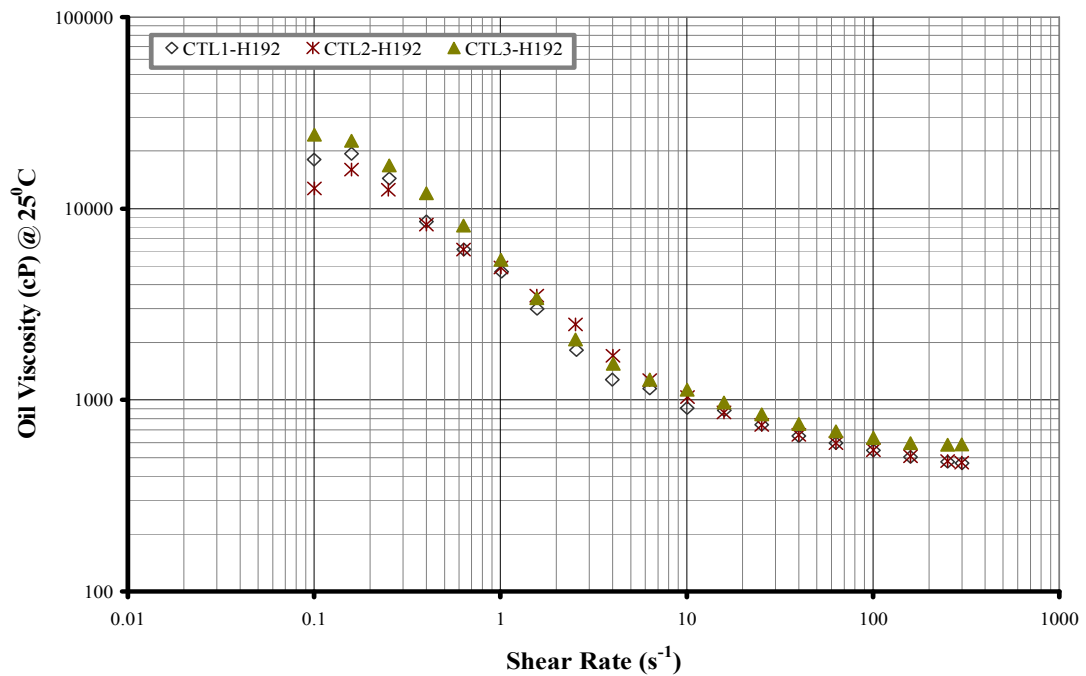


Figure 4.96 Viscosity (cP) as a Function of Shear Rate (s⁻¹) of Mississippi State University (MS) Oak Wood Oil Controls (CTL's 1-3) Aged to 192 hours

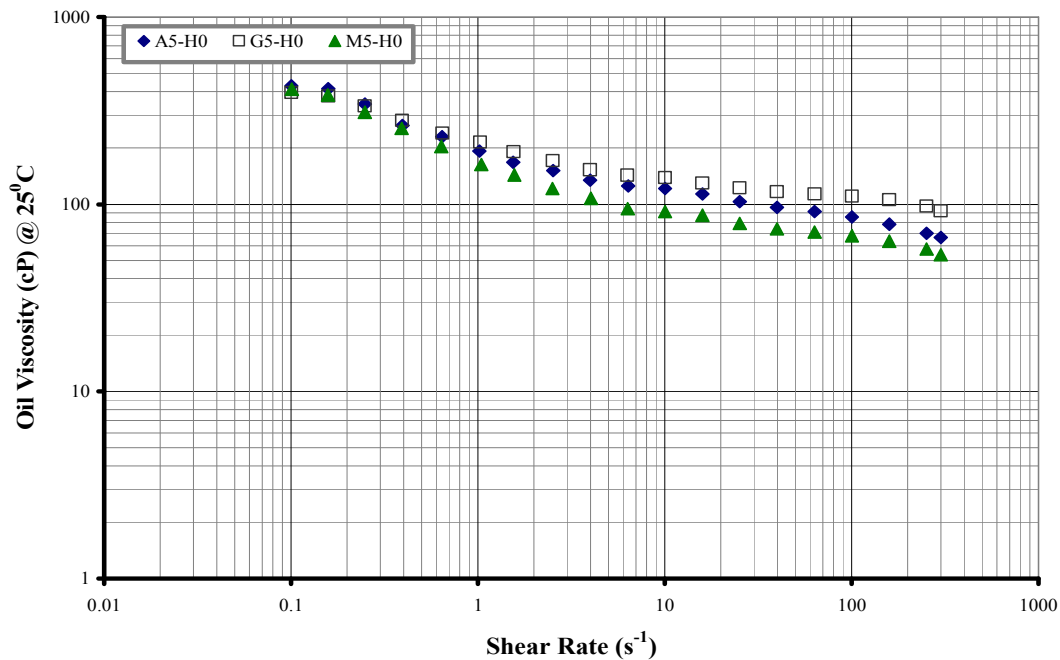


Figure 4.97 Viscosity (cP) as a Function of Shear Rate (s^{-1}) of Additive Blended (5 wt.%) Mississippi State University (MS) Fresh (0 hr) Oak Wood Oils

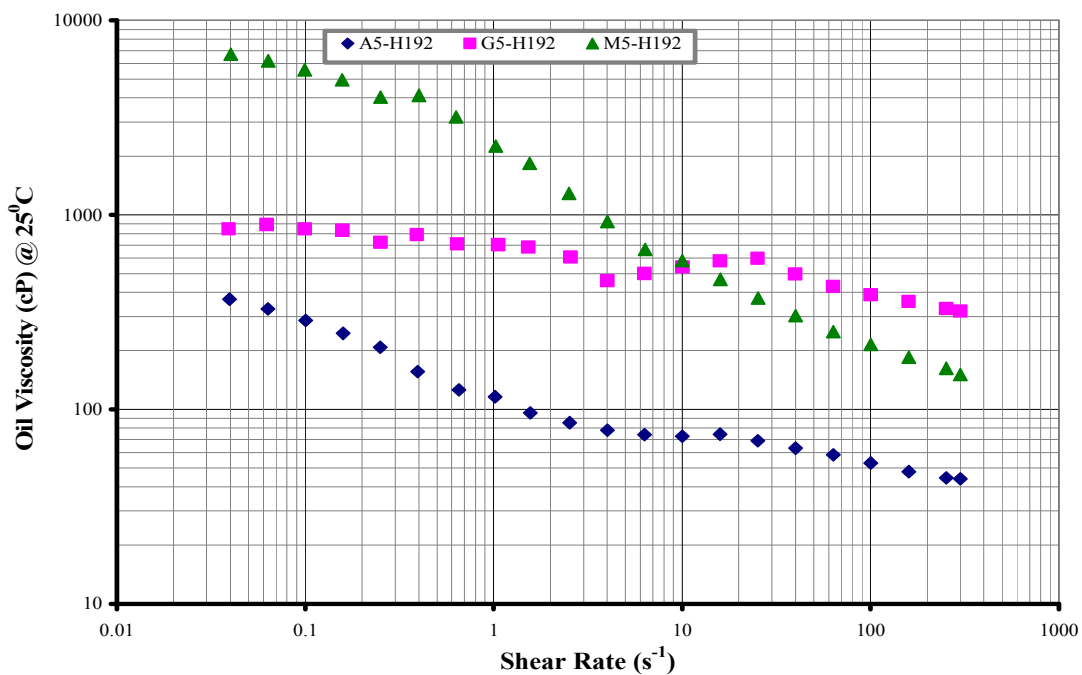


Figure 4.98 Viscosity (cP) as a Function of Shear Rate (s^{-1}) of Additive Blended (5 wt.%) Mississippi State University (MS) Oak Wood Oils Aged to 192 hours

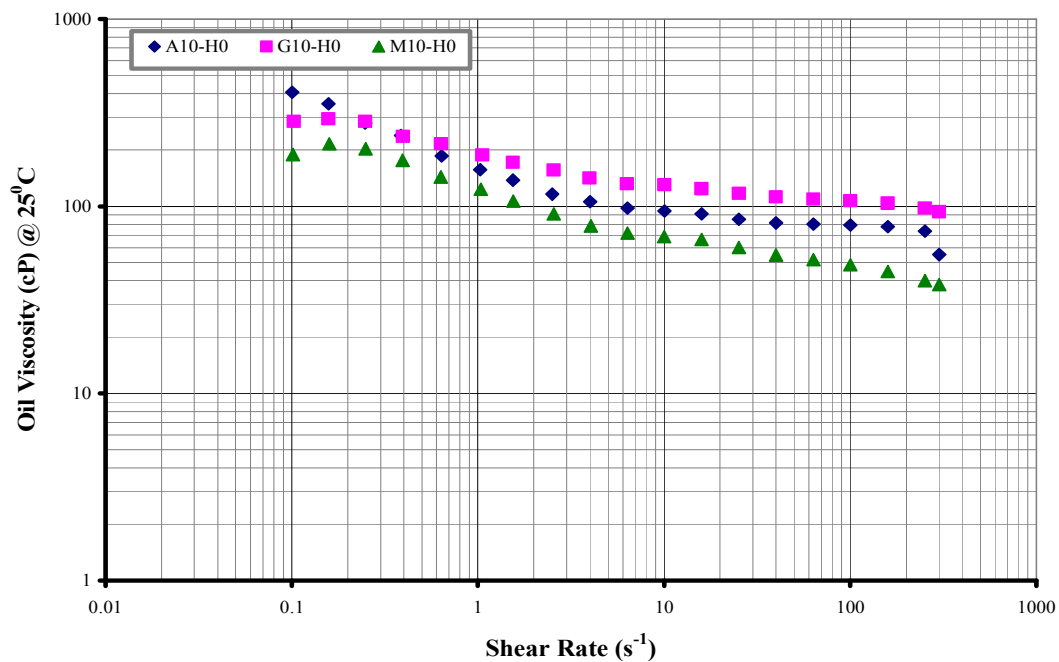


Figure 4.99 Viscosity (cP) as a Function of Shear Rate (s^{-1}) of Additive Blended (10 wt.%) Mississippi State University (MS) Fresh (0 hr) Oak Wood Oils

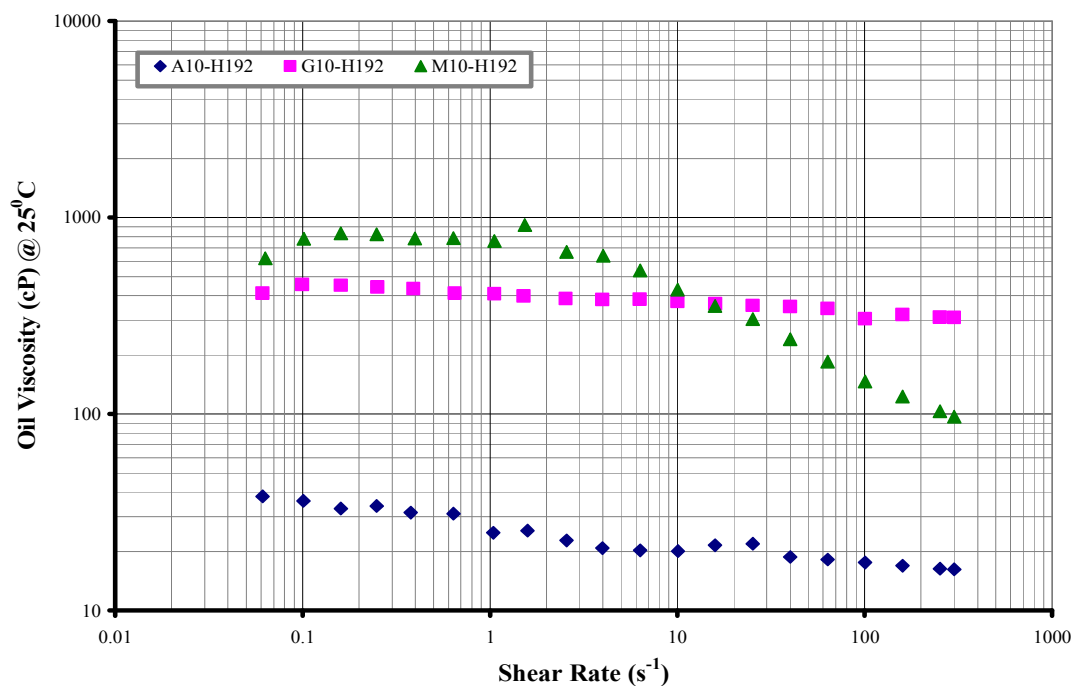


Figure 4.100 Viscosity (cP) as a Function of Shear Rate (s^{-1}) of Additive Blended (10 wt.%) Mississippi State University (MS) Oak Wood Oils Aged to 192 hours

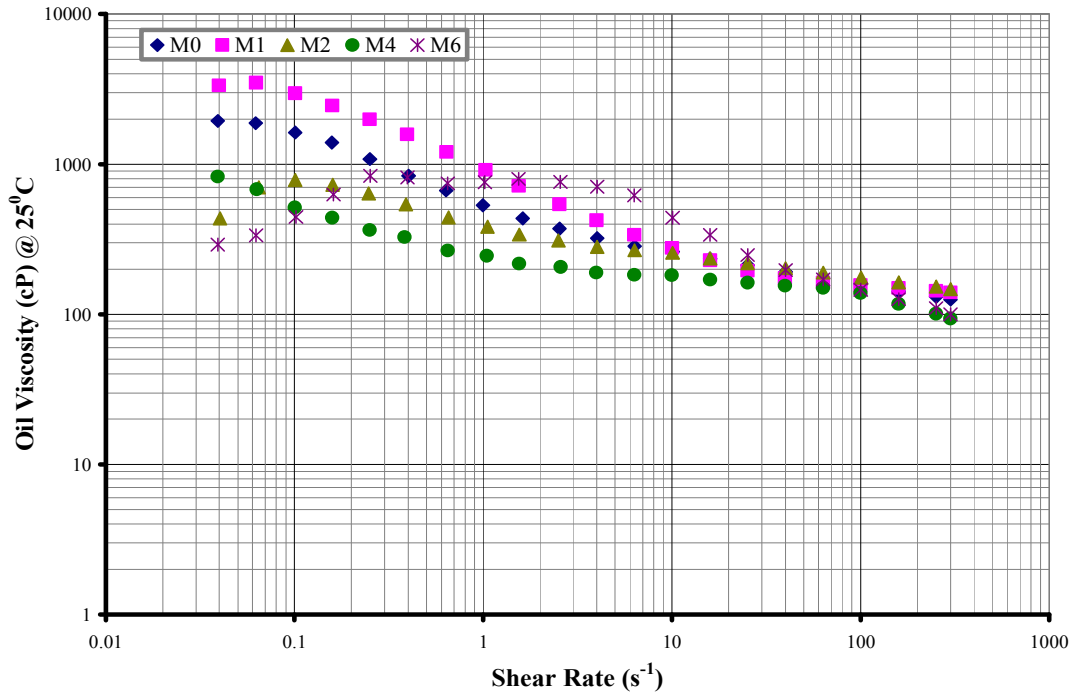


Figure 4.101 Viscosity (cP) of Mississippi State University (MS) Oak Bark Oil Control (CTL2) as a Function of Shear Rate (s^{-1}) and Storage Time (Month-M)

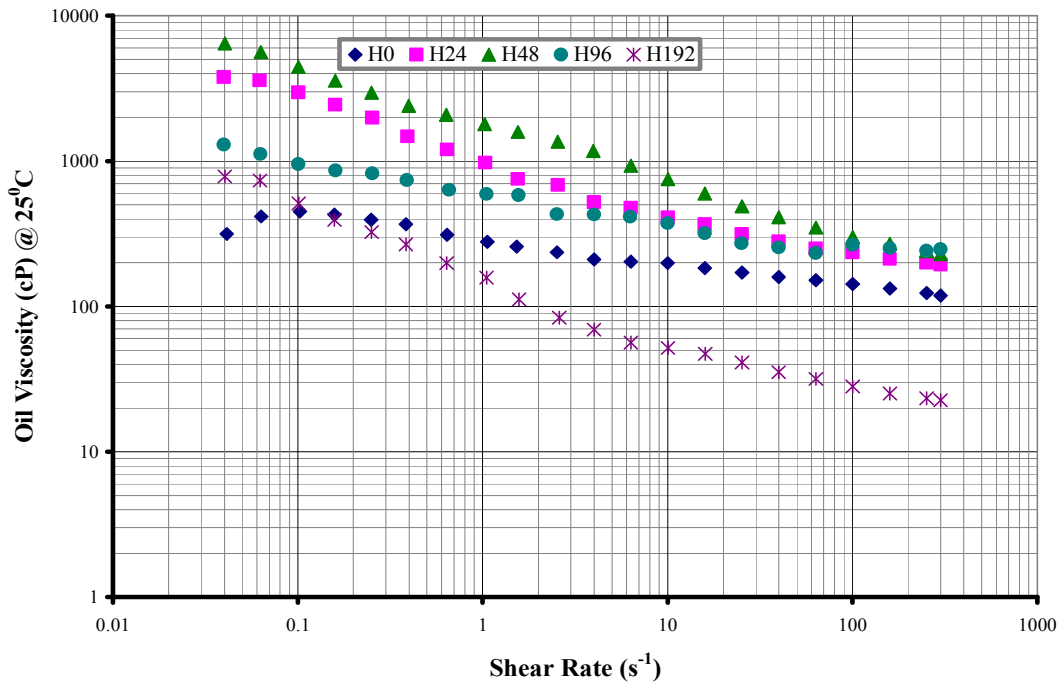


Figure 4.102 Viscosity (cP) of Mississippi State University (MS) Oak Bark Oil Control (CTL2) as a Function of Shear Rate (s^{-1}) and Storage Time (Hour-H)

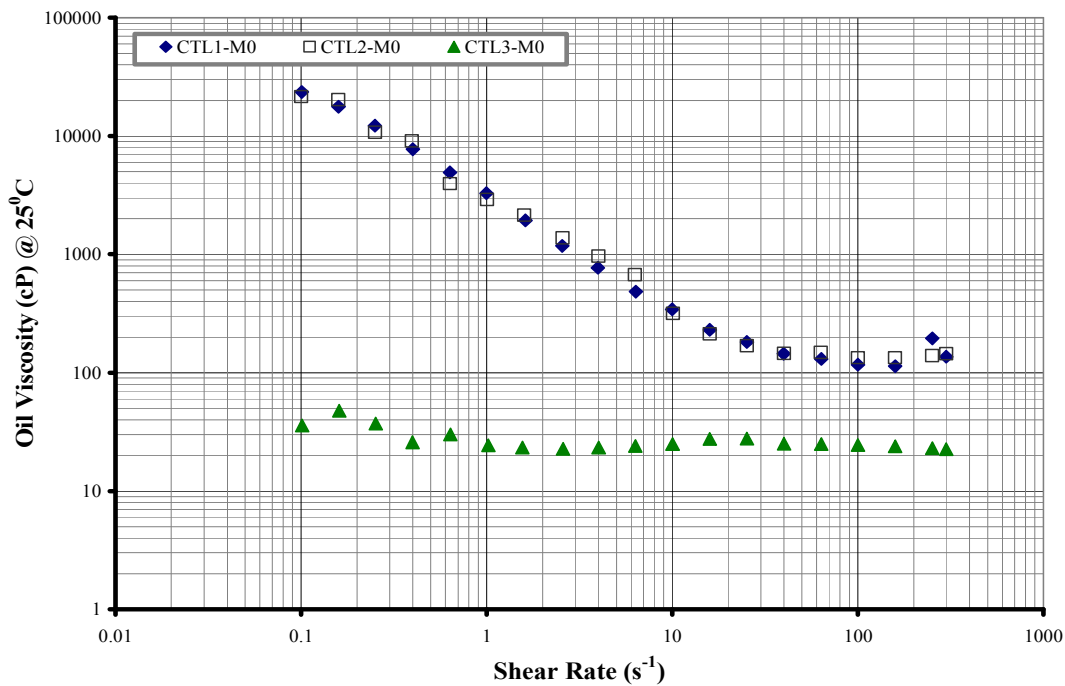


Figure 4.103 Viscosity (cP) as a Function of Shear Rate (s⁻¹) of Mississippi State University (MS) Fresh (0 hr) Pine Bark Oil Controls (CTL's 1-3)

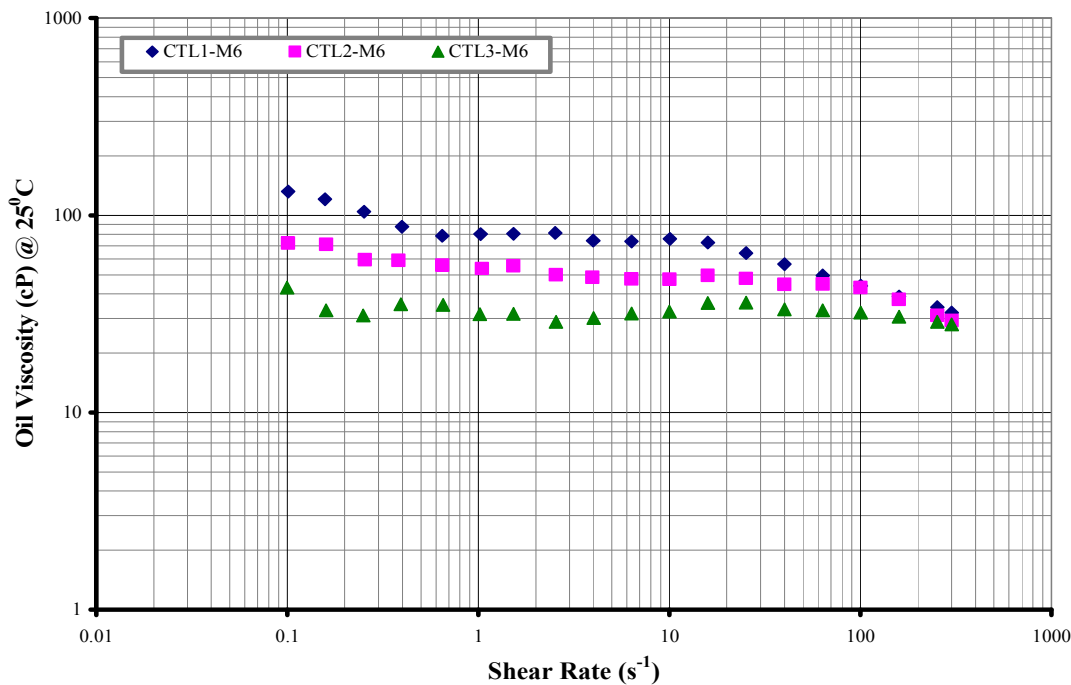


Figure 4.104 Viscosity (cP) as a Function of Shear Rate (s⁻¹) of Mississippi State University (MS) Pine Bark Oil Controls (CTL's 1-3) Aged to 180 days

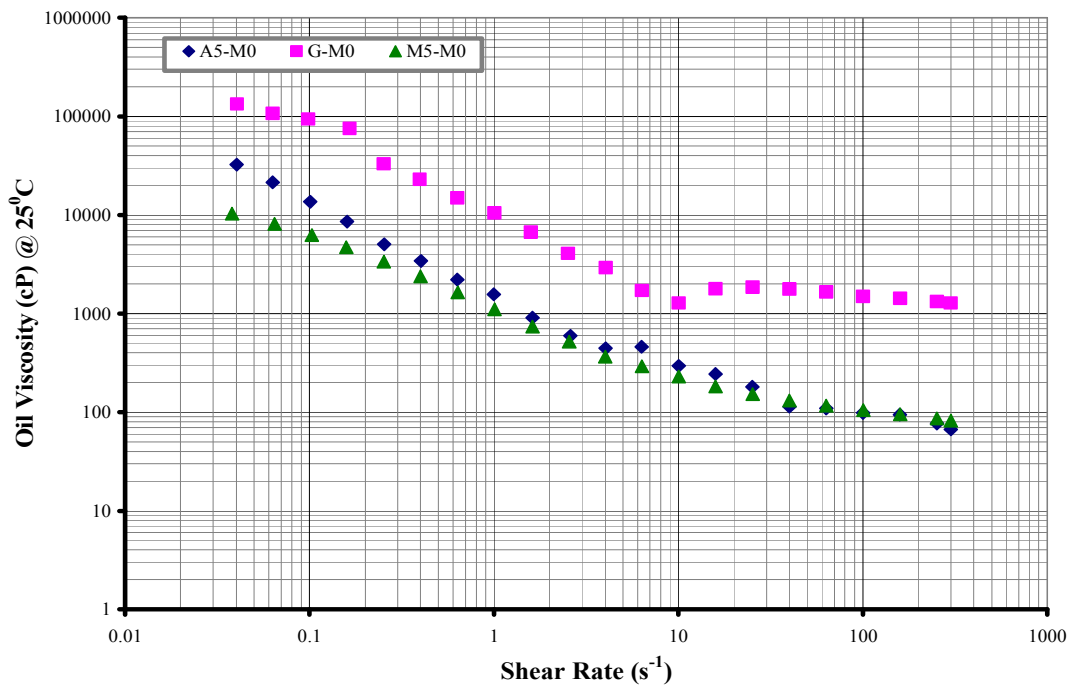


Figure 4.105 Viscosity (cP) as a Function of Shear Rate (s⁻¹) of Additive Blended (5 wt.%) Mississippi State University (MS) Fresh (0 hr) Pine Bark Oil

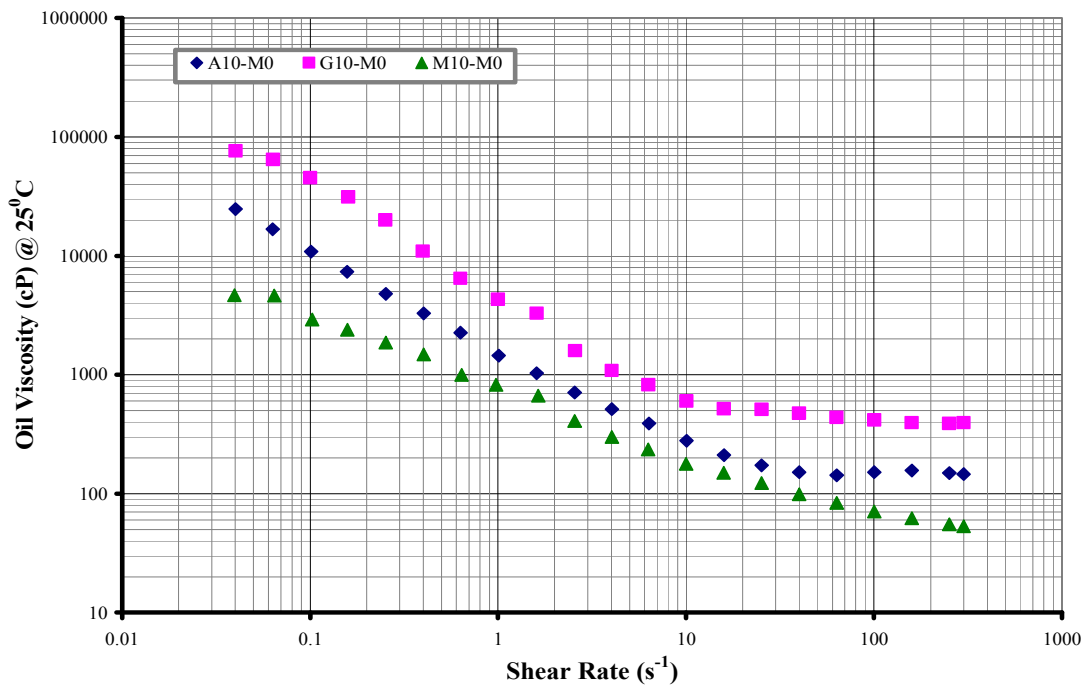


Figure 4.106 Viscosity (cP) as a Function of Shear Rate (s⁻¹) of Additive Blended (10 wt.%) Mississippi State University (MS) Fresh (0 hr) Pine Bark Oil

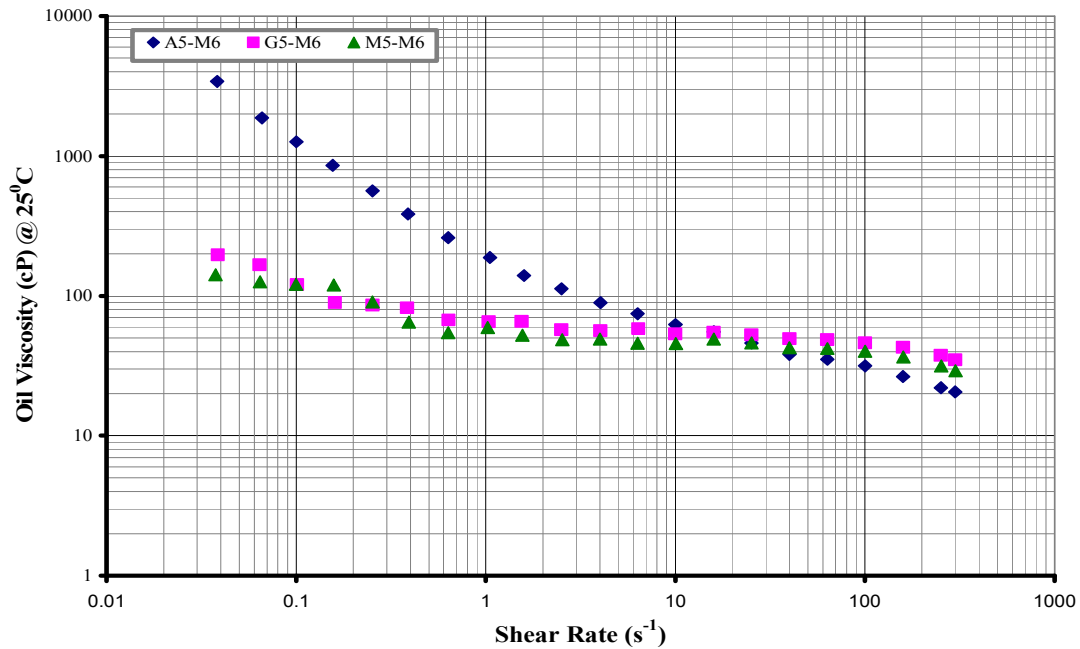


Figure 4.107 Viscosity (cP) as a Function of Shear Rate (s⁻¹) of Additive Blended (5 wt.%) Mississippi State University (MS) Pine Bark Oil Aged to 180 days

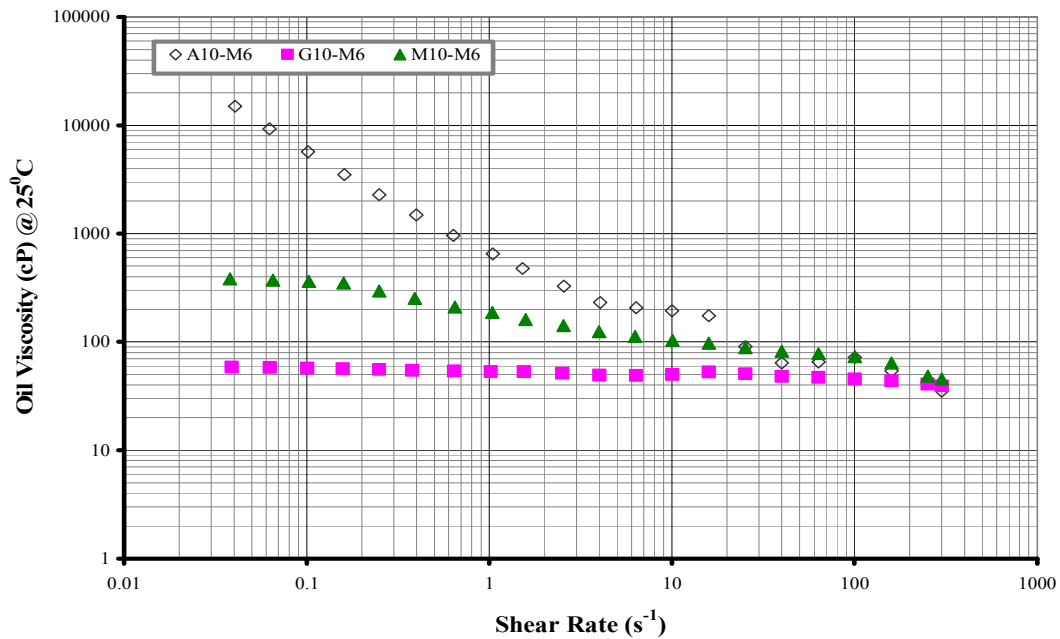


Figure 4.108 Viscosity (cP) as a Function of Shear Rate (s⁻¹) of Additive Blended (10 wt.%) Mississippi State University (MS) Pine Bark Oil Aged to 180 days



Figure 4.109 Rheometer Spindle Revealing the Sheared Pine Bark Pyrolysis Oil

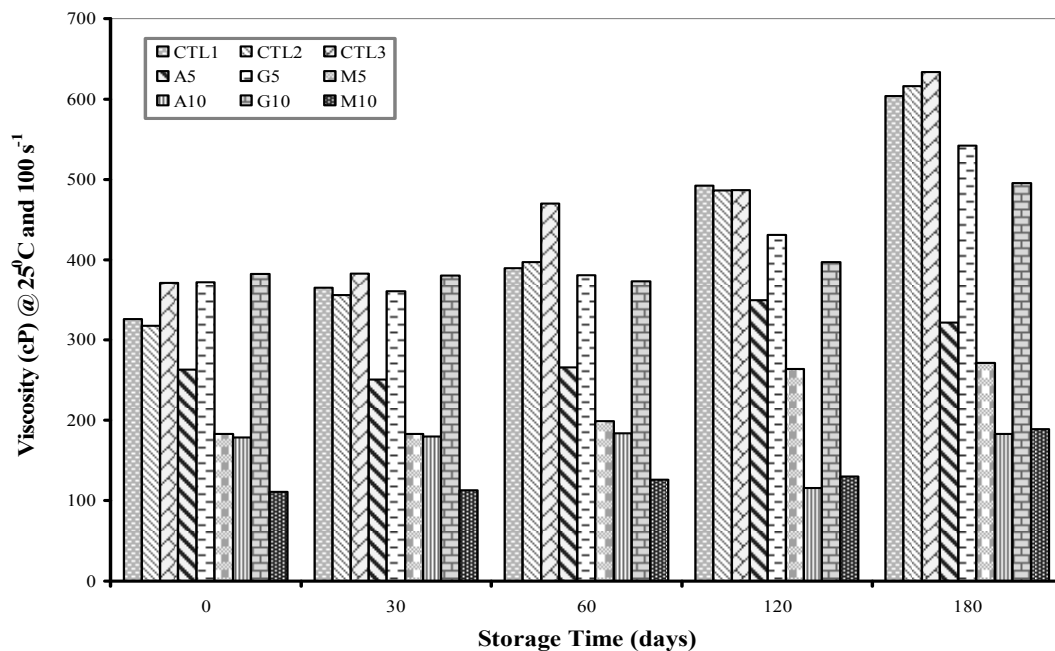


Figure 4.110 Viscosity (cP) as a Function of Storage Time (days) of Renewable Oil International (RI) Low Temperature Pine Wood Pyrolysis Oils (Controls and Additive Blended)

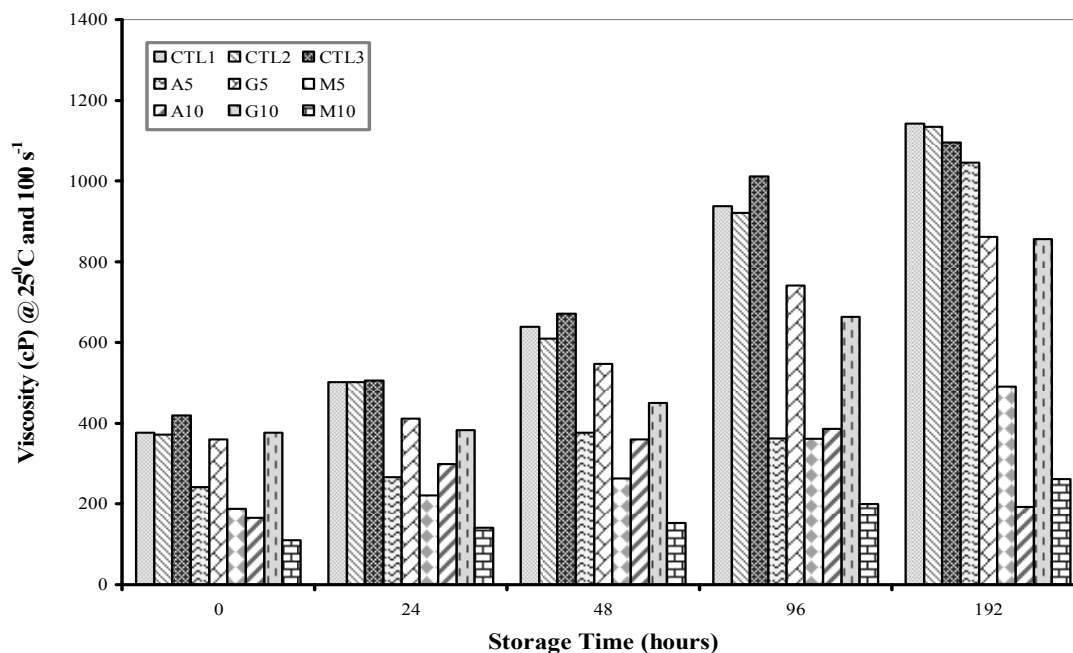


Figure 4.111 Viscosity (cP) as a Function of Storage Time (hours) of Renewable Oil International (RI) Low Temperature Pine Wood Pyrolysis Oils (Controls and Additive Blended)

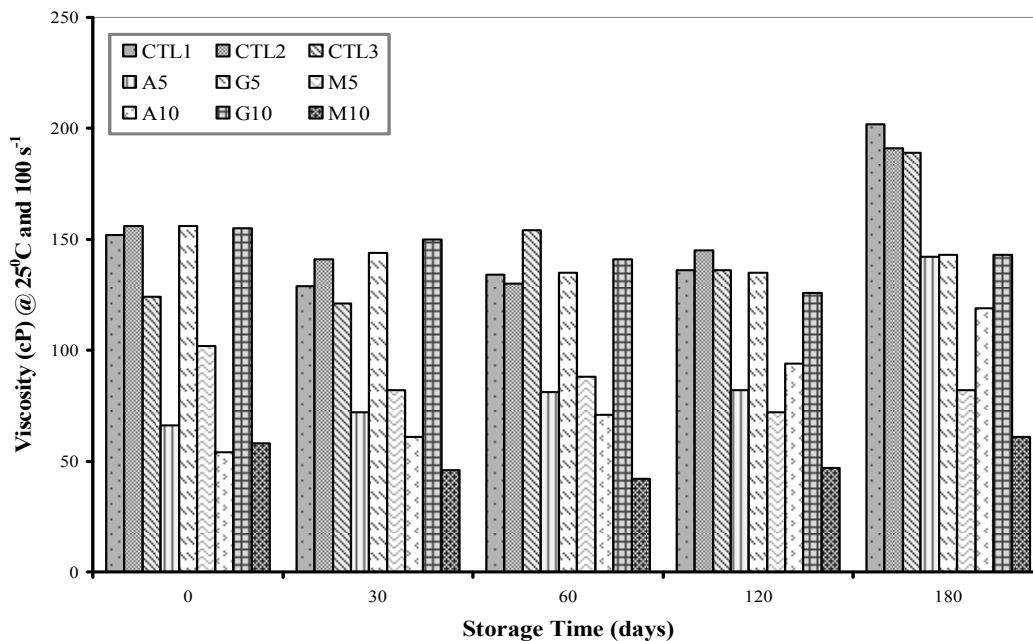


Figure 4.112 Viscosity (cP) as a Function of Storage Time (days) of National Renewable Energy Laboratory (NR) Low Temperature Oak Wood Pyrolysis Oils (Controls and Additive Blended)

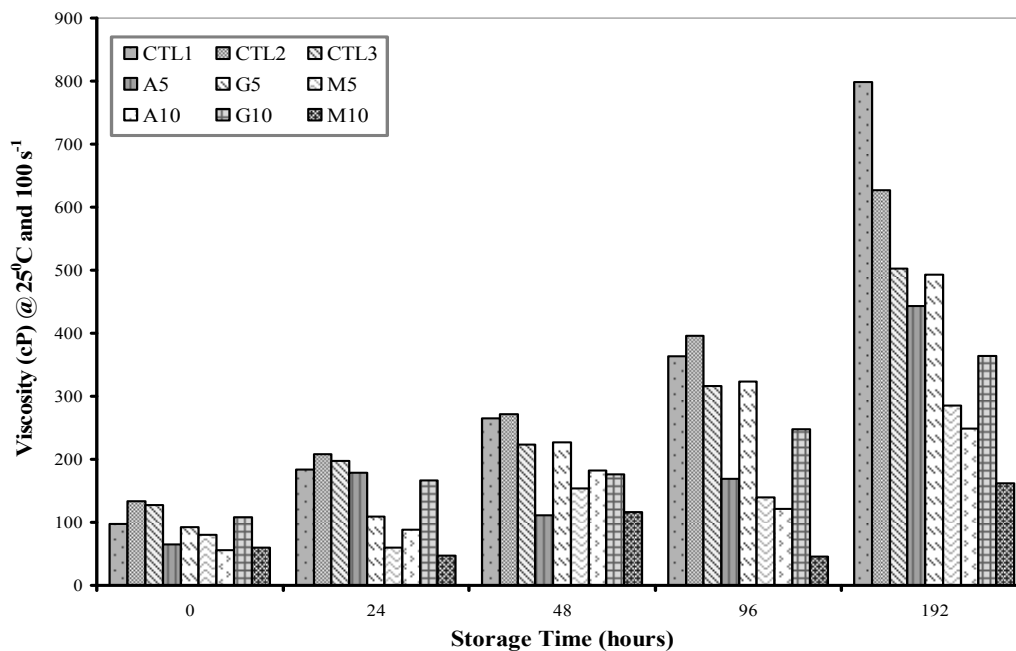


Figure 4.113 Viscosity (cP) as a Function of Storage Time (hours) of National Renewable Energy Laboratory (NR) Low Temperature Oak Wood Pyrolysis Oils (Controls and Additive Blended)

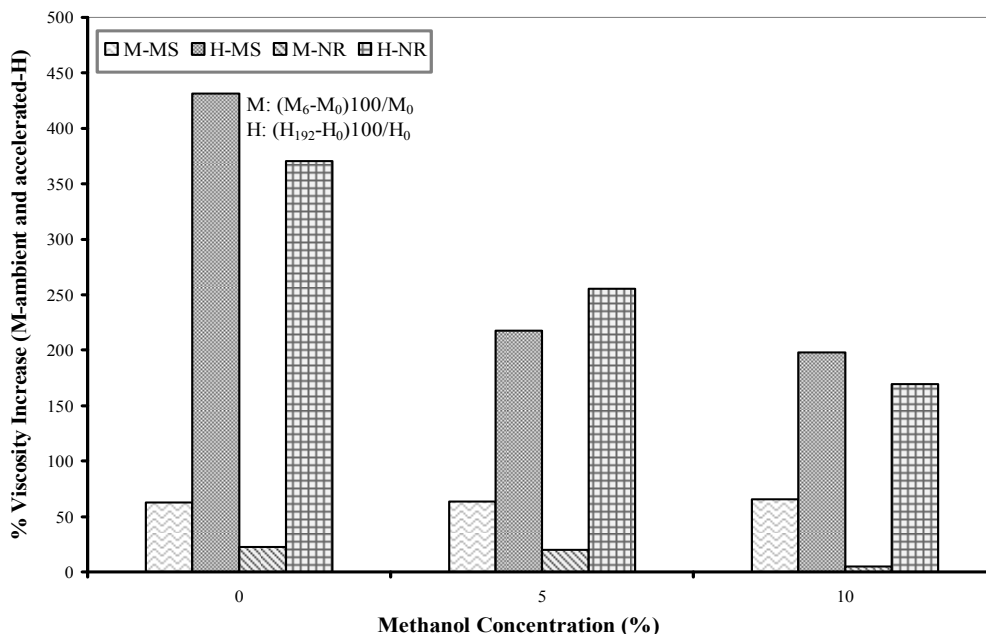


Figure 4.114 Viscosity Increase (%) as a Function of Methanol Concentration (wt.%) of Mississippi State University (MS) and National Renewable Energy Laboratory (NR) Low Temperature Oak Wood Pyrolysis Oils

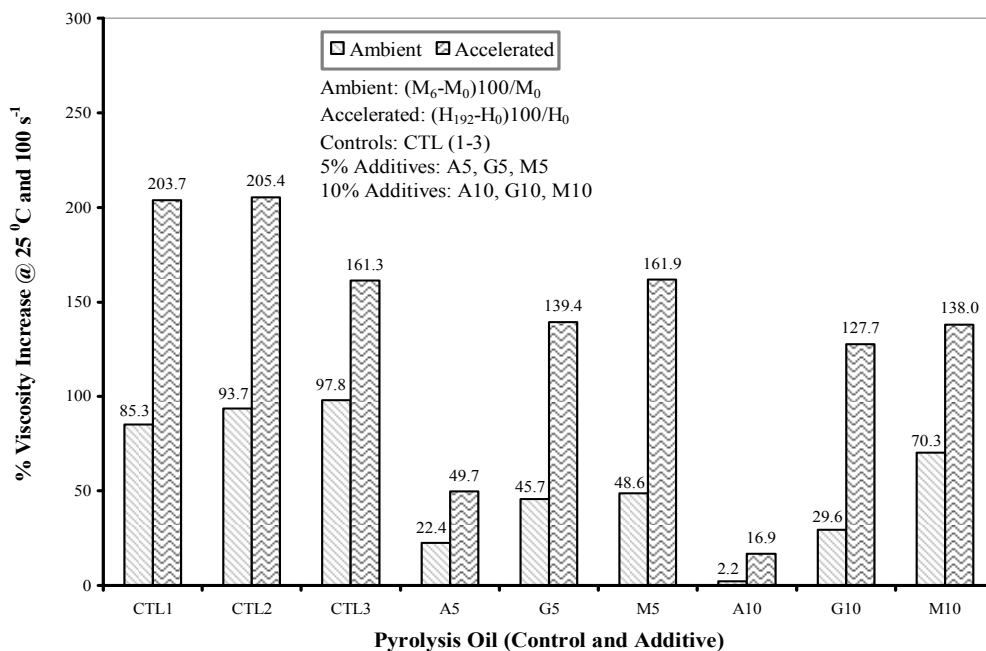


Figure 4.115 Viscosity Increase (%) as a Function of Storage Temperature of Renewable Oil International (RI) Low Temperature Pine Wood Pyrolysis Oils (Controls and Additive Blended)

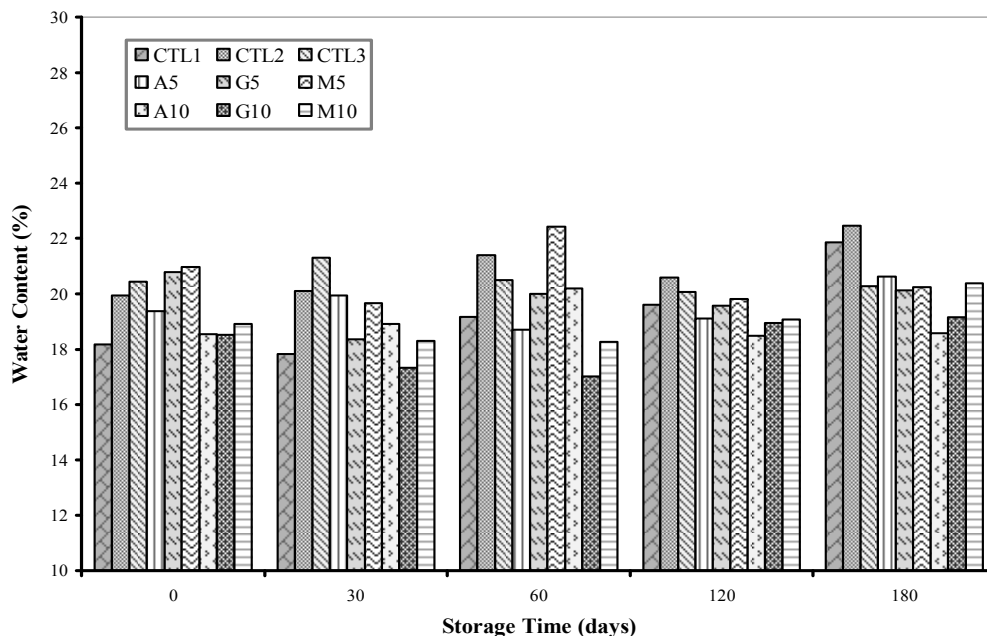


Figure 4.116 Water Content (wt.%) as a Function of Storage Time (days) of National Renewable Energy Laboratory (NR) Low Temperature Oak Wood Pyrolysis Oils (Controls and Additive Blended)

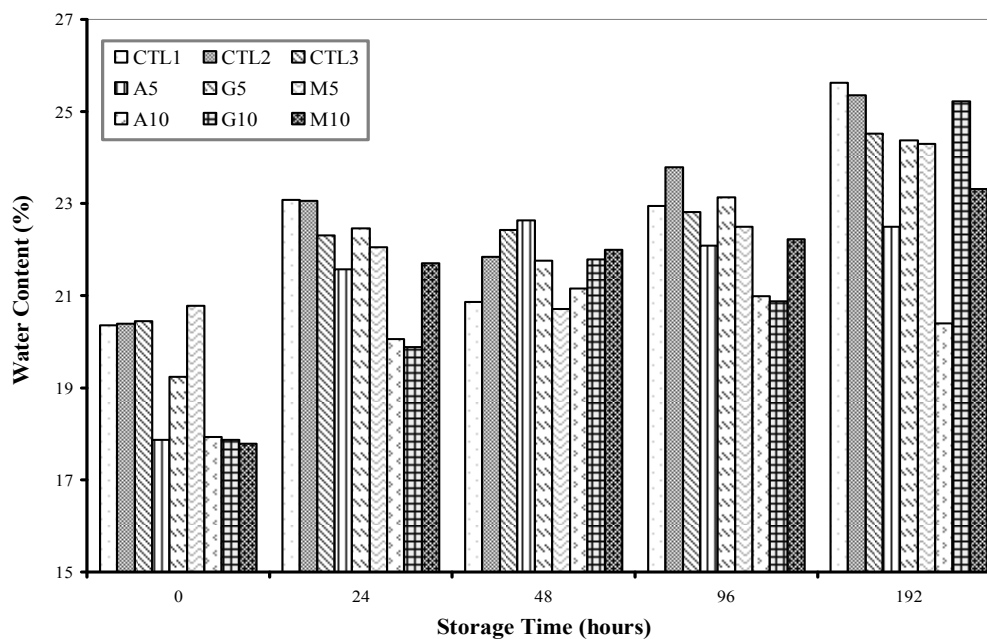


Figure 4.117 Water Content (wt.%) as a Function of Storage Time (hours) of National Renewable Energy Laboratory (NR) Low Temperature Oak Wood Pyrolysis Oils (Controls and Additive Blended)

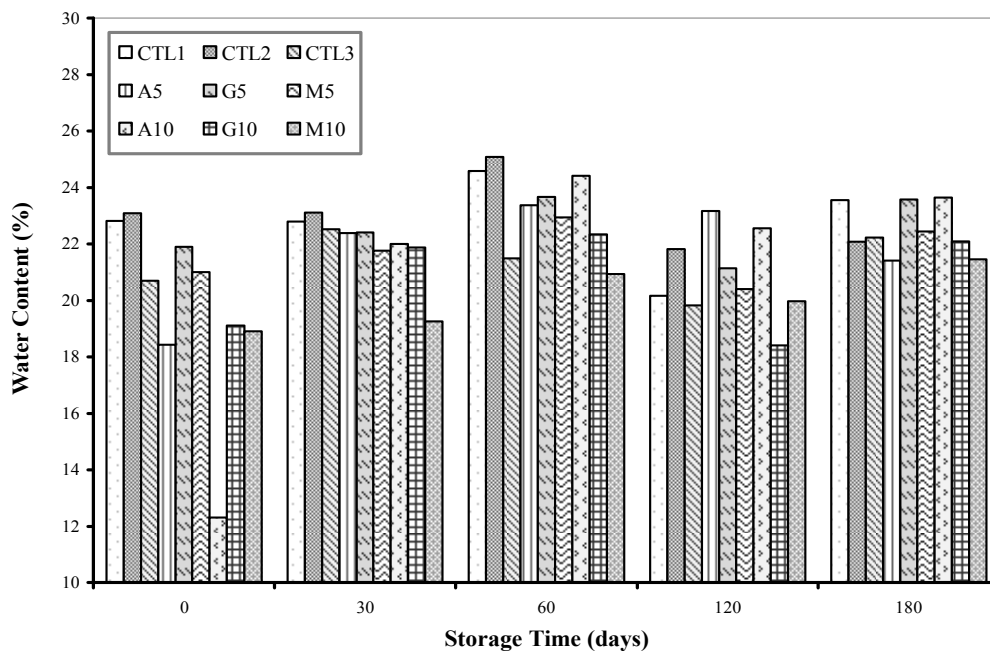


Figure 4.118 Water Content (wt.%) as a Function of Storage Time (days) of Mississippi State University (MS) Low Temperature Oak Bark Pyrolysis Oils (Controls and Additive Blended)

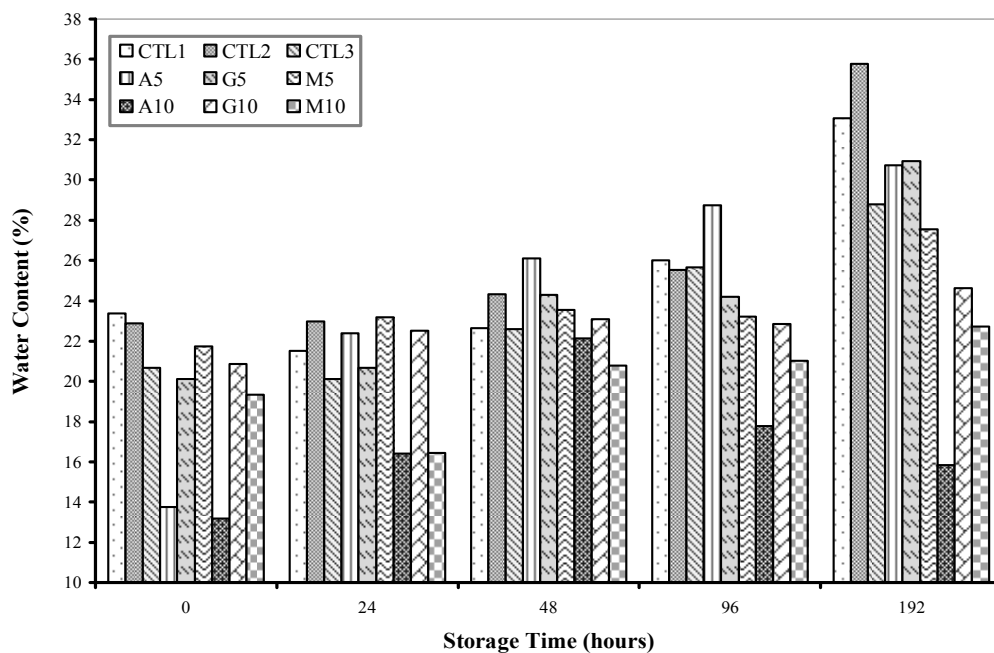


Figure 4.119 Water Content (wt.%) as a Function of Storage Time (hours) of Mississippi State University (MS) Low Temperature Oak Bark Pyrolysis Oils (Controls and Additive Blended)

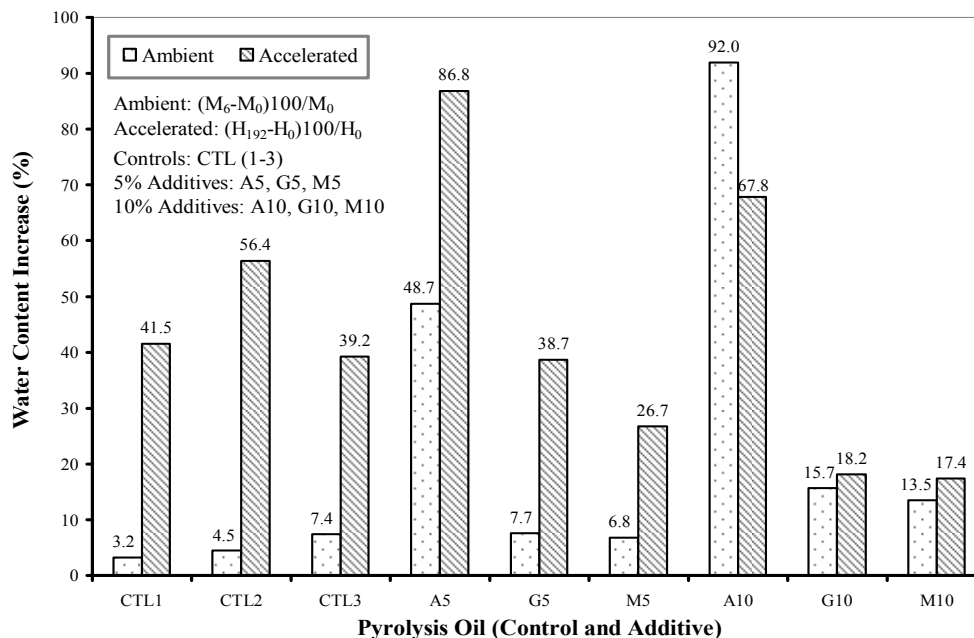


Figure 4.120 Water Content Increase (%) as a Function of Storage Temperature of Mississippi State University (MS) Low Temperature Oak Bark Pyrolysis Oils (Controls and Additive Blended)

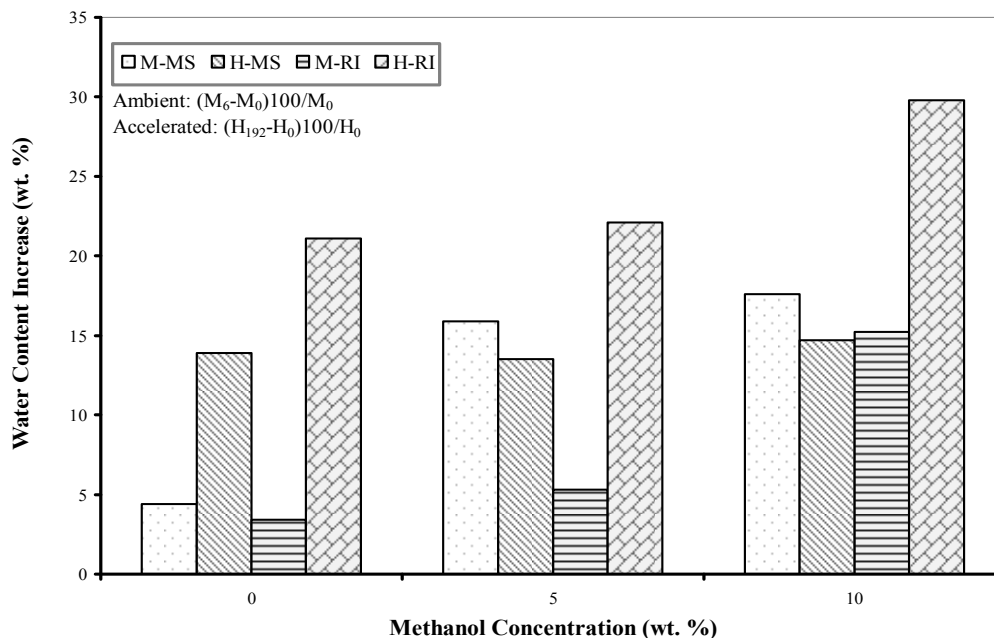


Figure 4.121 Water Content Increase (%) as a Function of Methanol Concentration (wt.%) of Mississippi State University (MS) and Renewable Oil International (RI) Low Temperature Pine Wood Pyrolysis Oils

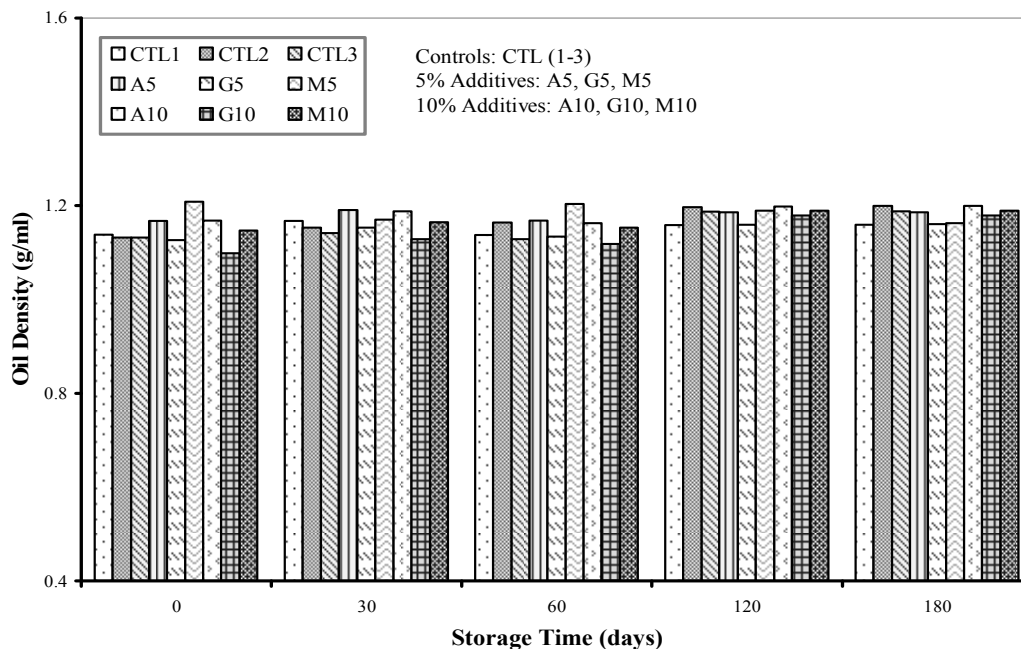


Figure 4.122 Density (g/ml) as a Function of Storage Time (days) of National Renewable Energy Laboratory (NR) Low Temperature Oak Wood Pyrolysis Oils (Controls and Additive Blended)

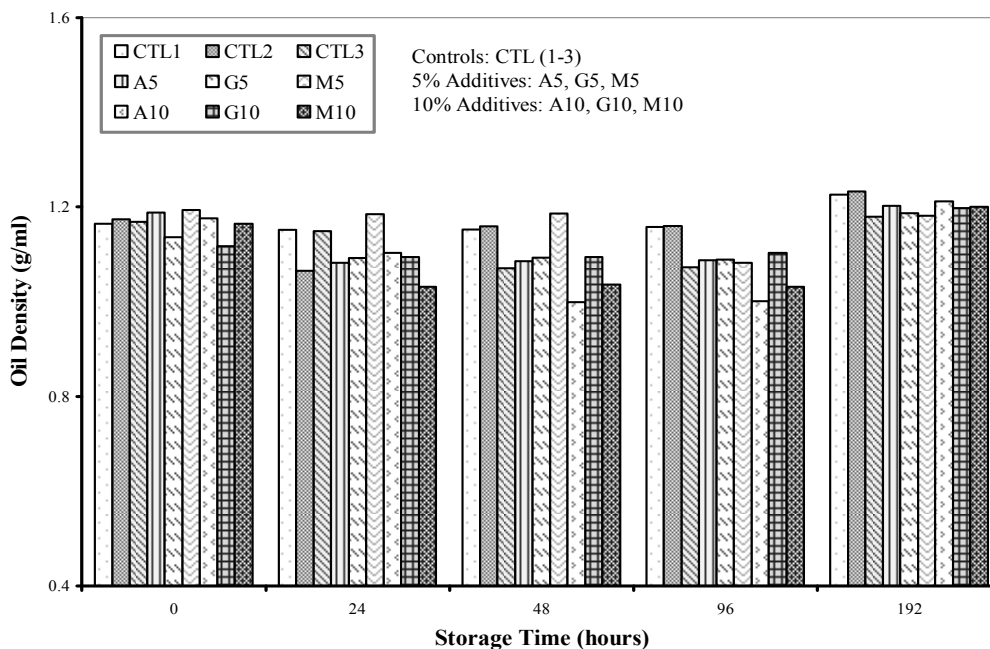


Figure 4.123 Density (g/ml) as a Function of Storage Time (hours) of National Renewable Energy Laboratory (NR) Low Temperature Oak Wood Pyrolysis Oils (Controls and Additive Blended)

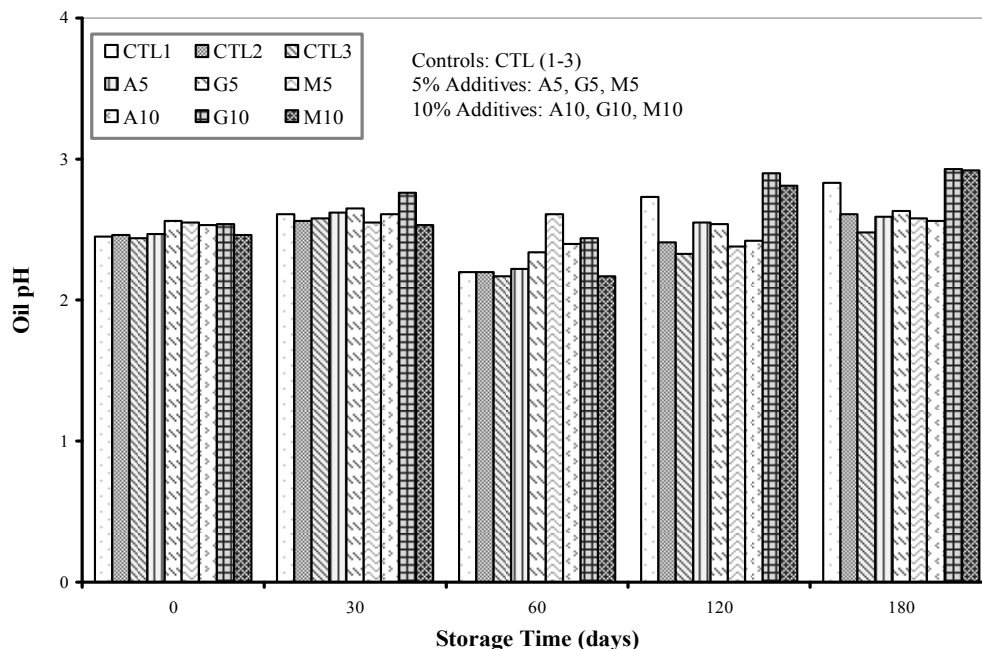


Figure 4.124 pH as a Function of Storage Time (days) of National Renewable Energy Laboratory (NR) Low Temperature Oak Wood Pyrolysis Oils (Controls and Additive Blended)

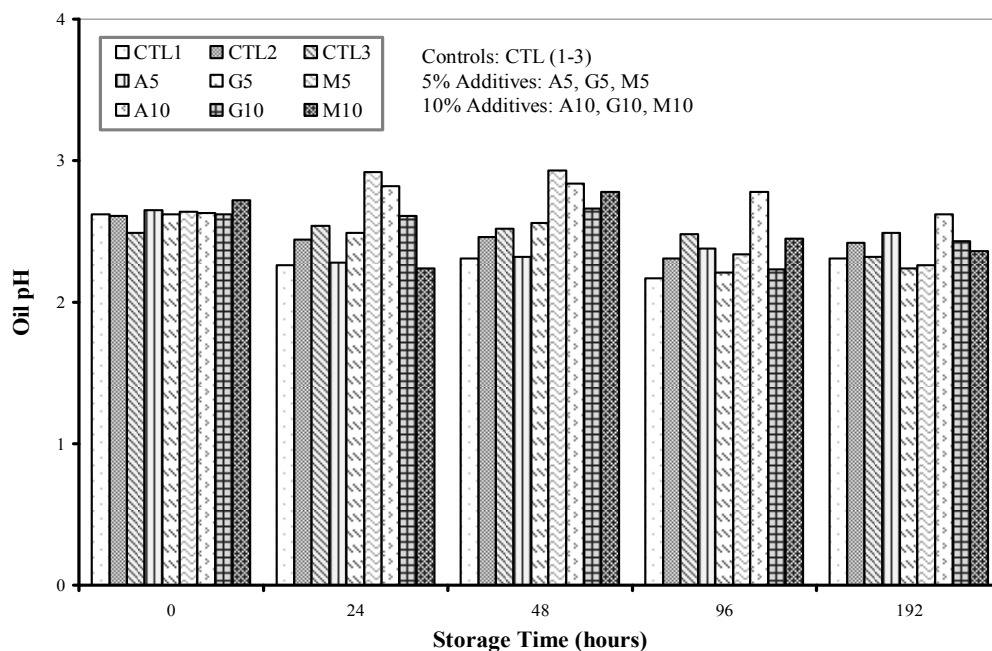


Figure 4.125 pH as a Function of Storage Time (hours) of National Renewable Energy Laboratory (NR) Low Temperature Oak Wood Pyrolysis Oils (Controls and Additive Blended)

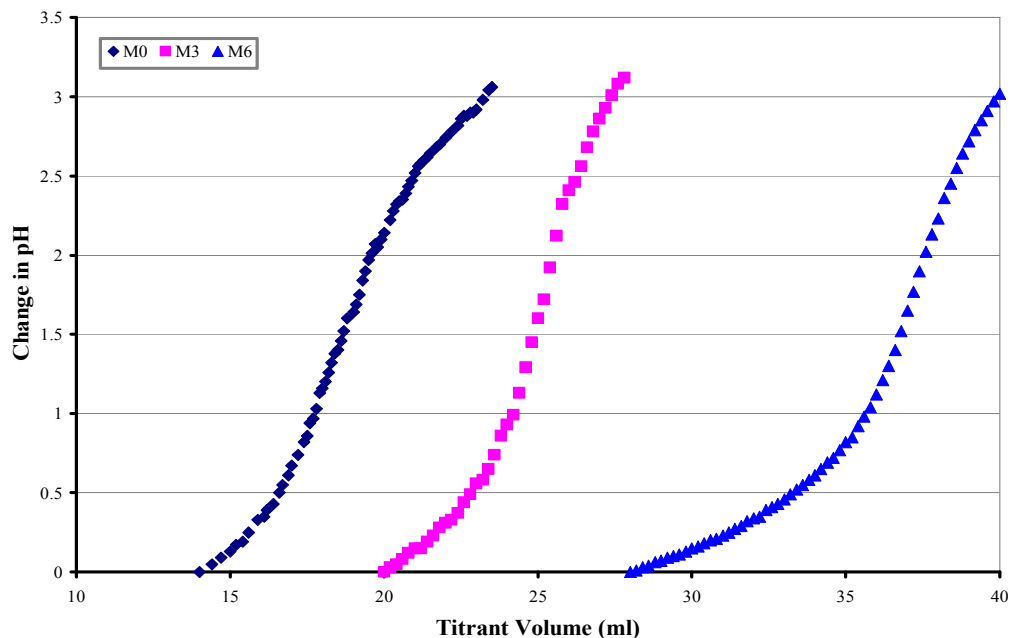


Figure 4.126 Breakthrough Curves of pH as a Function of Storage Time (Month-M) and Titrant Volume (ml) for National Renewable Energy Laboratory (NR) High Temperature Pine Wood Pyrolysis Oil Control (CTL1)

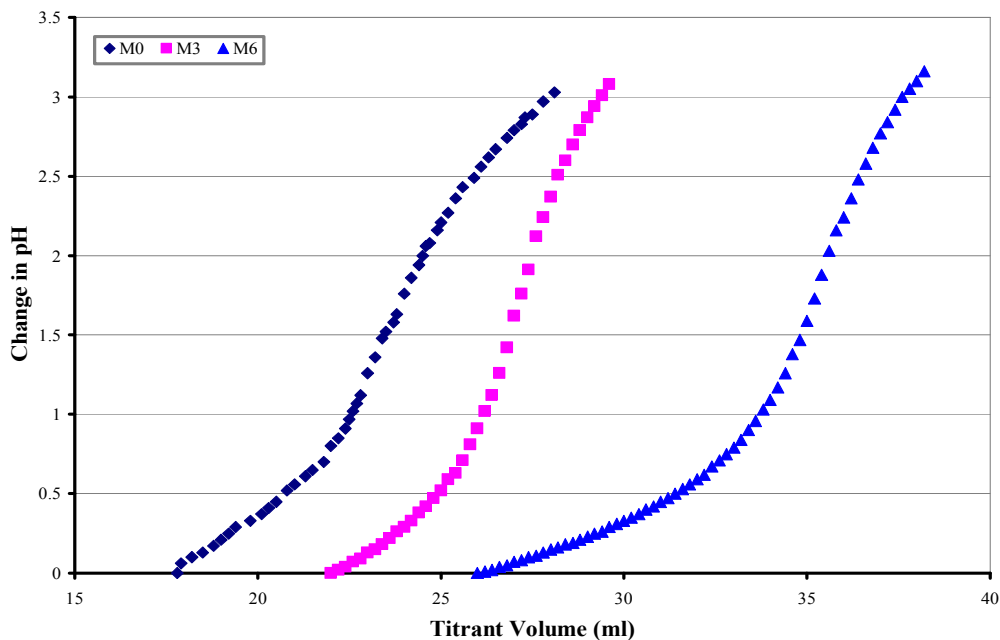


Figure 4.127 Breakthrough Curves of pH as a Function of Storage Time (Month-M) and Titrant Volume (ml) for National Renewable Energy Laboratory (NR) High Temperature Anisole Blended (10 wt.%) Pine Wood Pyrolysis Oil

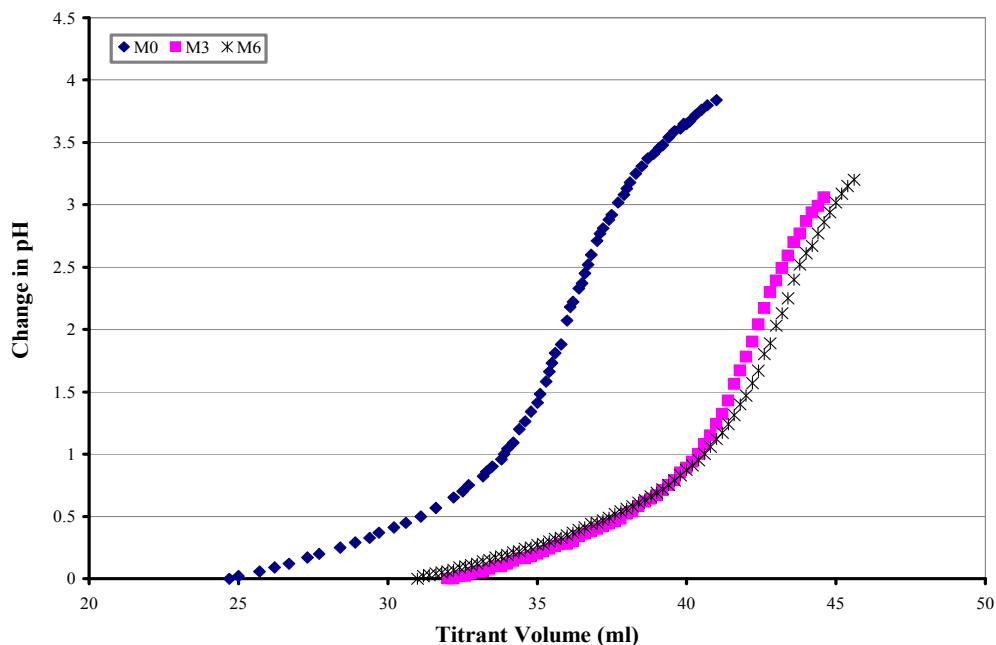


Figure 4.128 Breakthrough Curves of pH as a Function of Storage Time (Month-M) and Titrant Volume (ml) for National Renewable Energy Laboratory (NR) High Temperature Oak Wood Pyrolysis Oil Control (CTL1)

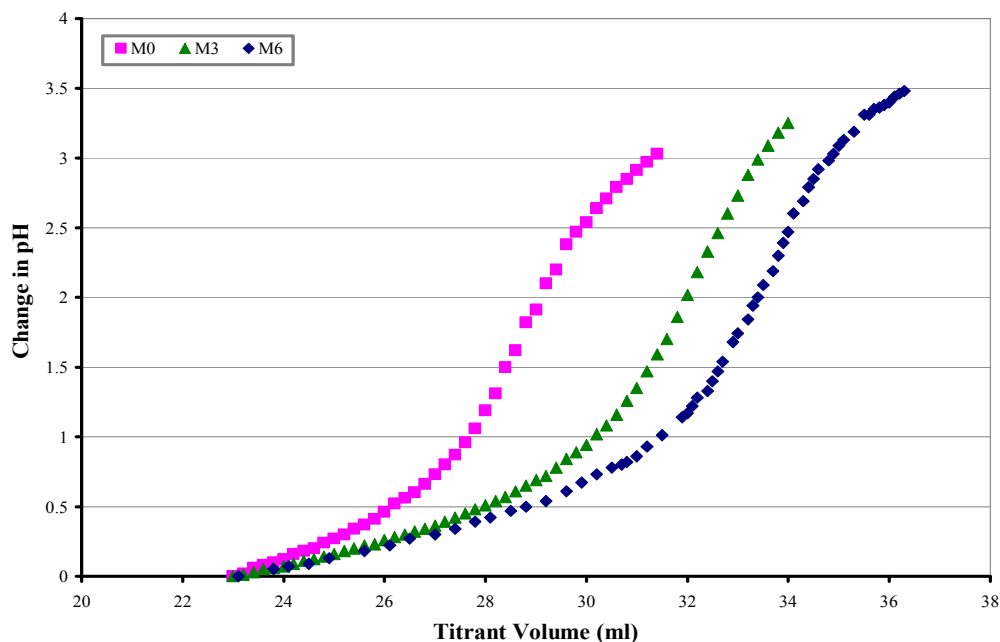


Figure 4.129 Breakthrough Curves of pH as a Function of Storage Time (Month-M) and Titrant Volume (ml) for National Renewable Energy Laboratory (NR) High Temperature Anisole Blended (10 wt.%) Oak Wood Pyrolysis Oil

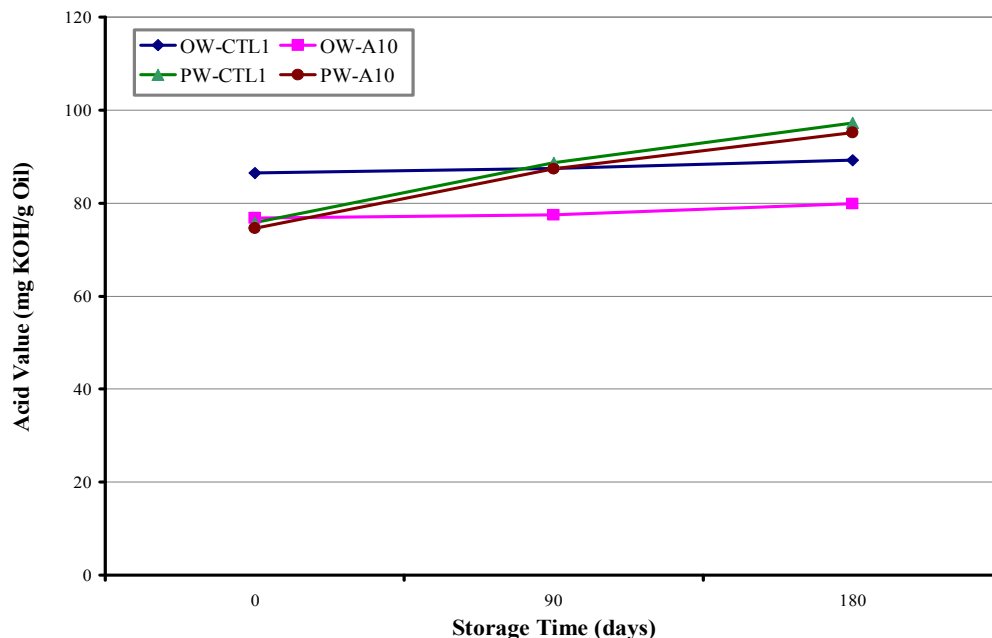


Figure 4.130 Acid Value (mg KOH/g Oil) as a Function of Storage Time for National Renewable Energy Laboratory (NR) High Temperature Pine Wood (PW) and Oak Wood (OW) Pyrolysis Oils (Control-CTL1 and Anisole-10 wt.%)

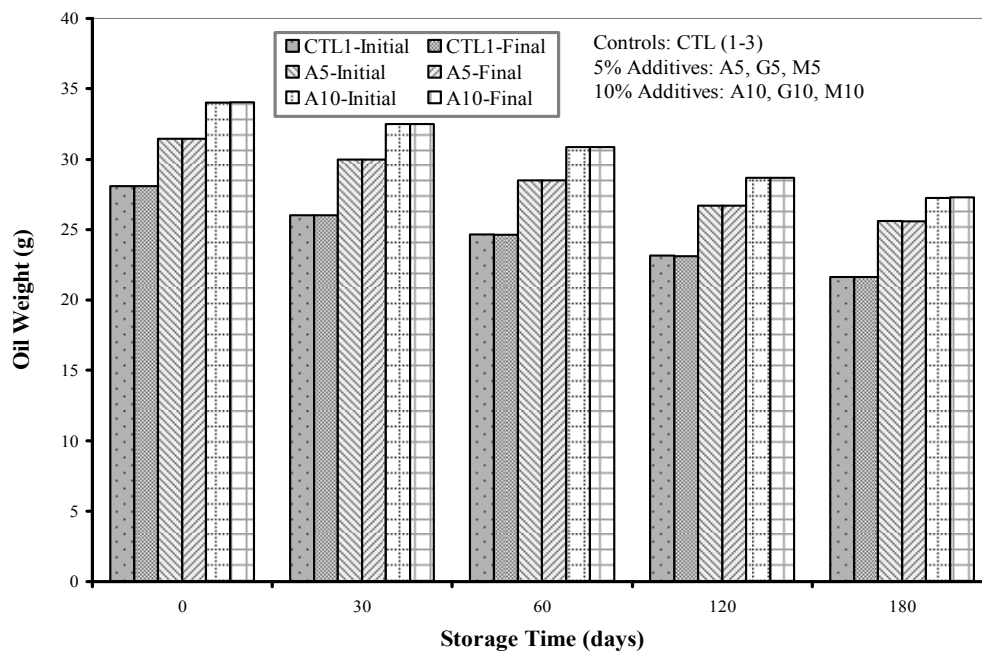


Figure 4.131 Sample Weight as a Function of Storage Time (days) of National Renewable Energy Laboratory (NR) Low Temperature Oak Wood Pyrolysis Oils (Control and Additive Blended)

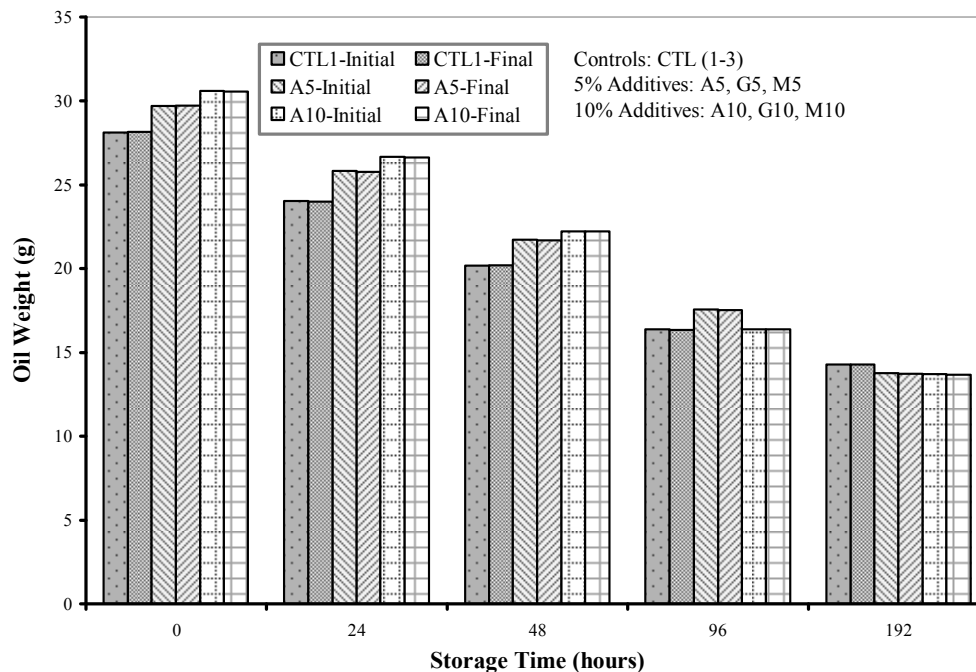


Figure 4.132 Sample Weight as a Function of Storage Time (hours) of National Renewable Energy Laboratory (NR) Low Temperature Oak Wood Pyrolysis Oils (Control and Additive Blended)

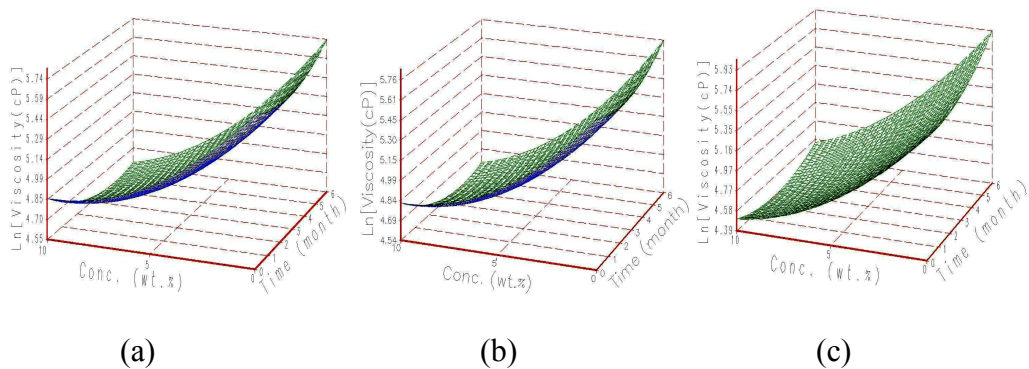


Figure 4.133 Surface Response Plots Obtained for the Normalized Viscosity (cP) of Mississippi State University (MS) Pine Wood Pyrolysis Oil as a Function of Storage Time (month) and Methanol Concentration (wt.%)

[*The above viscosity measurements were performed at 25°C and shear rates of a) 1 s^{-1} b) 10 s^{-1} and c) 100 s^{-1} for the MS pine wood oil stored at 25°C .]

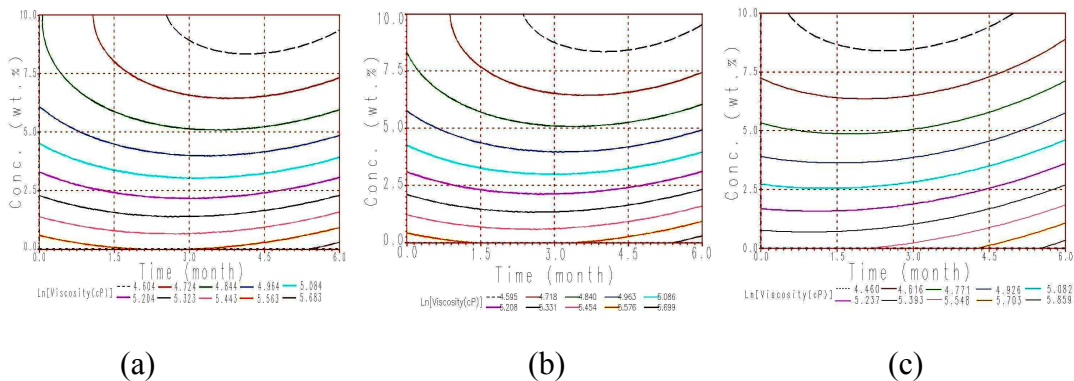


Figure 4.134 Contour Plots Obtained for the Normalized Viscosity (cP) of Mississippi State University (MS) Pine Wood Pyrolysis Oil as a Function of Storage Time (month) and Methanol Concentration (wt.%)

[*The above viscosity measurements were performed at 25°C and shear rates of a) 1 s^{-1} b) 10 s^{-1} and c) 100 s^{-1} for the MS pine wood oil stored at 25°C .]

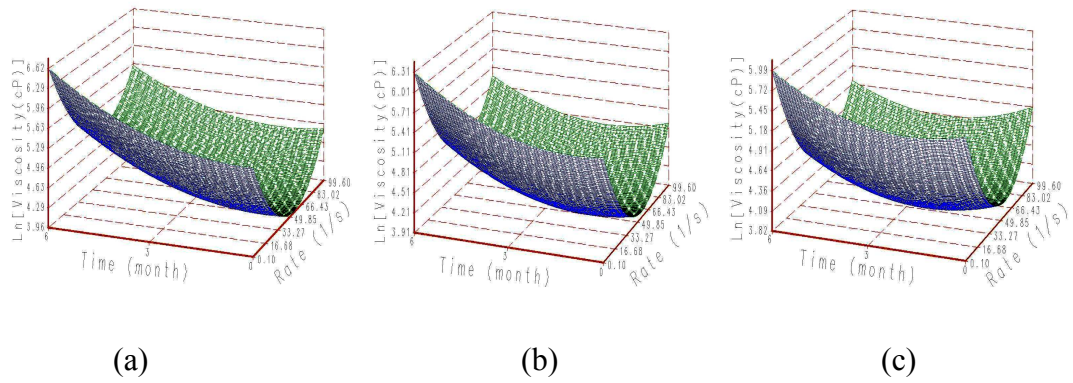


Figure 4.135 Surface Response Plots Obtained for the Normalized Viscosity (cP) of Mississippi State University (MS) Oak Wood Pyrolysis Oil as a Function of Storage Time (month) and Shear Rate (s^{-1})

[*The above viscosity measurements were performed at 25 °C and glycerol concentrations of a) 0 wt.% b) 5 wt.% and c) 10 wt.% for the MS oak wood oil stored at 25 °C.]

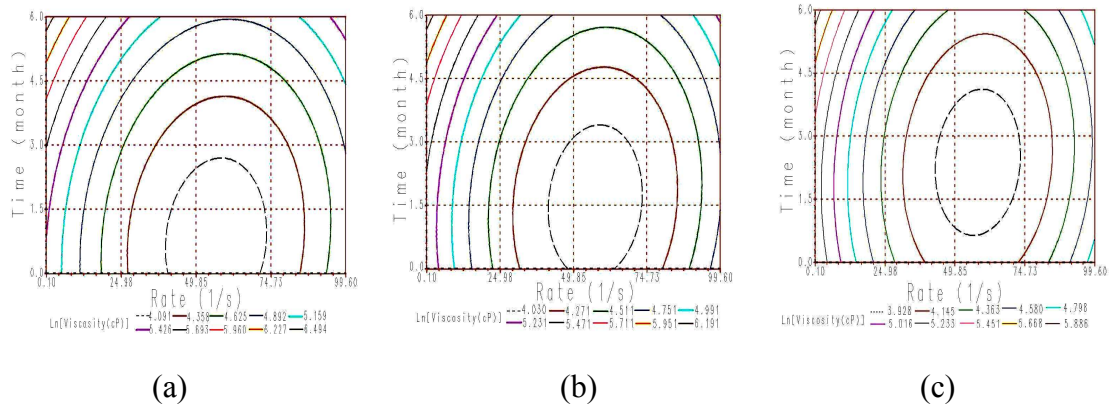


Figure 4.136 Contour Plots Obtained for the Normalized Viscosity (cP) of Mississippi State University (MS) Oak Wood Pyrolysis Oil as a Function of Storage Time (month) and Shear Rate (s^{-1})

[*The above viscosity measurements were performed at 25 °C and glycerol concentrations of a) 0 wt.% b) 5 wt.% and c) 10 wt.% for the MS oak wood oil stored at 25 °C.]

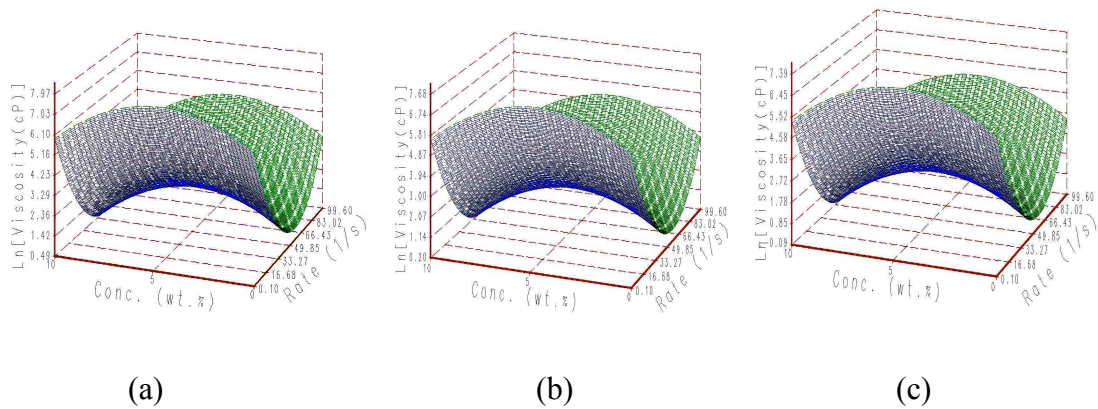


Figure 4.137 Surface Response Plots Obtained for the Normalized Viscosity (cP) of Mississippi State University (MS) Oak Bark Pyrolysis Oil as a Function of Shear Rate (s^{-1}) and Anisole Concentration (wt.%)

[*The above viscosity measurements were performed at 25 $^{\circ}C$ and storage times of a) 0 hr b) 96 hr and c) 192 hr for the MS oak bark oil stored at 80 $^{\circ}C$.]

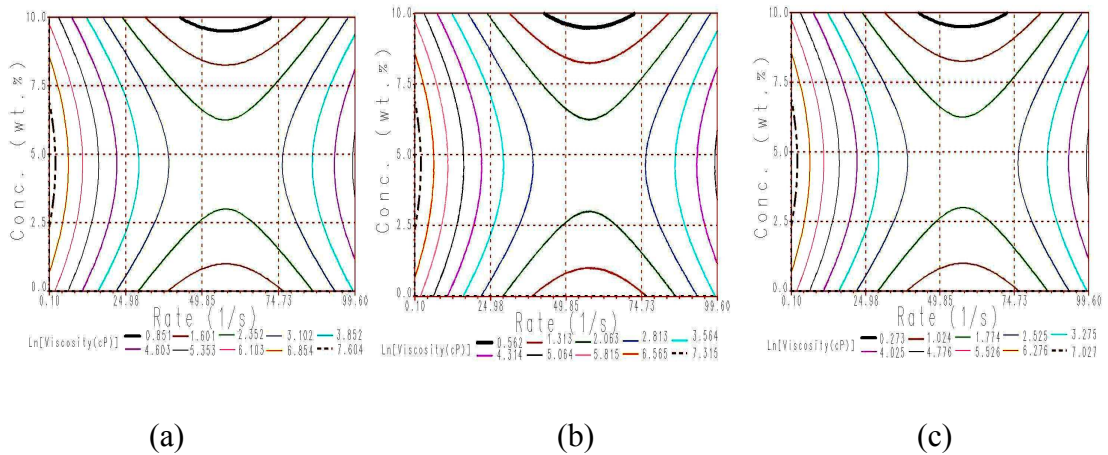


Figure 4.138 Contour Plots Obtained for the Normalized Viscosity (cP) of Mississippi State University (MS) Oak Bark Pyrolysis Oil as a Function of Shear Rate (s^{-1}) and Anisole Concentration (wt.%)

[*The above viscosity measurements were performed at 25 $^{\circ}C$ and storage times of a) 0 hr b) 96 hr and c) 192 hr for the MS oak bark oil stored at 80 $^{\circ}C$.]

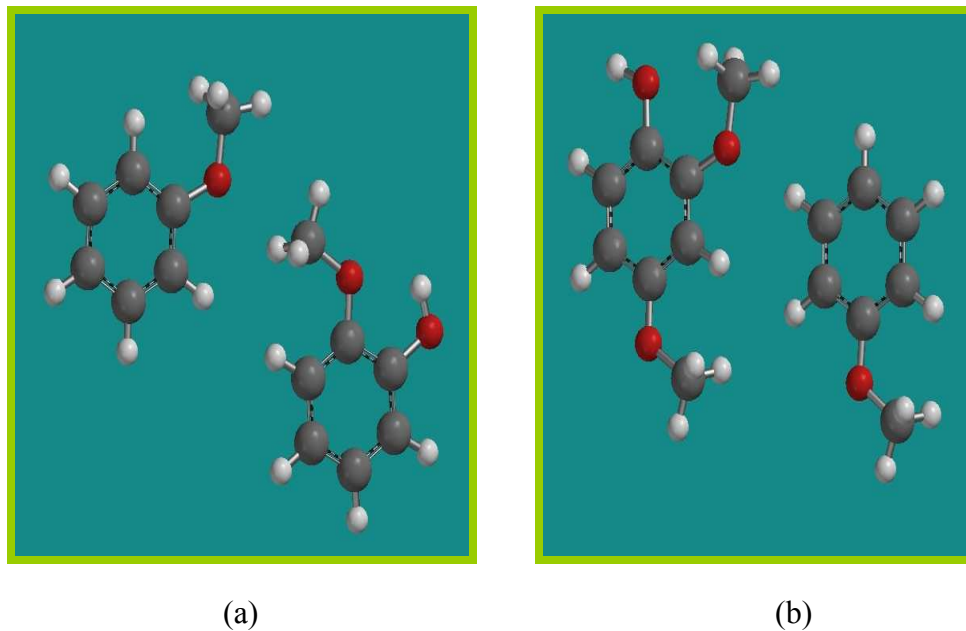


Figure 4.139 Ball and Spoke Models Obtained for the Hydrogen Bonding of Anisole with a) Guaiacol and b) Syringol as Predicted by Spartan Wave Function[©]

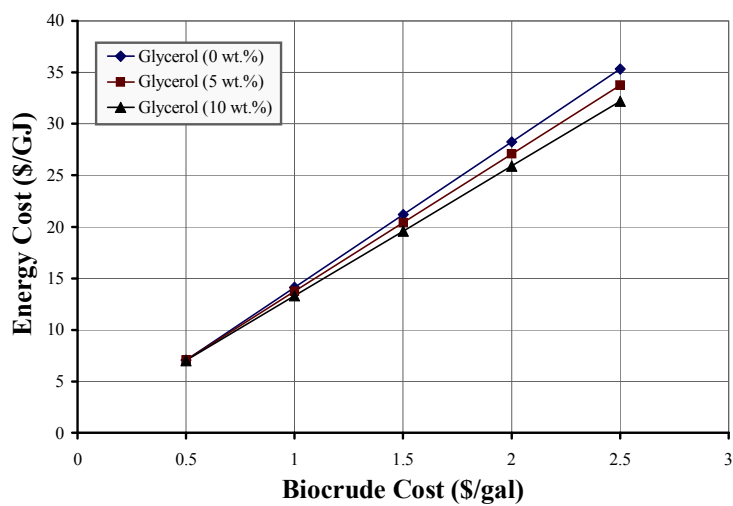


Figure 4.140 Cost of Glycerol Addition to Pine Wood Pyrolysis Oil as a Function of its Concentration (wt.%)

CHAPTER V

CONCLUSIONS AND RECOMMENDATIONS

Conclusions

Based on the results of this study it was determined that pyrolysis oil stability is enhanced through the addition of chemical additives. Of the 26 additives screened, it appears that anisole, glycerol, and the well documented methanol are most effective for pyrolysis oil stability. Specific conclusions for each of the four phases and trial runs of this study are provided below.

1. Of the four feed stocks used in this study [pine wood (PW), pine bark (PB), oak wood (OW), and oak bark (OB)] the highest yield of pyrolysis oil was obtained for OW (62.9%) whereas the highest yield of bio-char was obtained for PB (43.2%). Unfortunately, of this total oil yields, the aqueous-rich fraction ranged from 37.6-52.0 % for OB (min.) and PB (max.) respectively
2. Generally, the oil yields were independent of residence time and pyrolysis temperature. But this is attributed to the inadequate reactor control
3. The pyrolysis oil stream was separated effectively into aqueous-rich and organic-rich fractions by using a multi-stage condenser
4. Significant weight losses in the form of non-condensable gases such as CO, CO₂, CH₄, and tars were observed
5. Refrigeration of pyrolysis oils at 4 °C was observed to slow the rate of increase of oil viscosity by minimizing the unstable polymeric reactions
6. Accelerated storage stability test conducted at 80 °C for a period of 192 hours was effective in distinguishing the stability performance of pyrolysis oils as a function of additive

7. Based on the results of this investigation rheology is an effective tool for predicting pyrolysis oil stability
8. In general, most chemical additives evaluated in this study increased the pyrolysis oil stability with the noted exceptions of resorcinol, furfuryl alcohol, and 2-furaldehyde
9. In general, the low molecular weight additives favored greater stability of pyrolysis oils when compared to the high molecular weight additives
10. Based on the results of this investigation pyrolysis oils can exhibit both Newtonian and non-Newtonian flow properties
11. The Herschel Bulkley and Power Law models can adequately model the rheological behavior of the pyrolysis oils. Anisole blended pyrolysis oil exhibited the lowest viscosity rate index (n) postulated due to its aromatic structure and plate-like movement of the oil sub-layers
12. The addition of chemical additives to the pyrolysis oils can significantly affect their viscosity properties
13. Among the 6 groups of chemical additives evaluated in this study, alcohols had the most significant effect on pyrolysis oil viscosity
14. Addition of anisole seems to mask the pungent odor of pyrolysis oils due to its strong perfumic anise odor
15. Among the 6 groups of chemical additives evaluated in this study, ethers had the most significant impact on pyrolysis oil water content
16. Based on the results obtained in this study phase-separation of pyrolysis oils was not observed except when the oils were aged for prolonged storage periods accompanied by low additive concentrations
17. The pH of pyrolysis oils ranged from 2-3 independent of the additive group selected
18. Glycerol in excess of 5 wt.% showed superior flow and stabilizing properties among all the additives and concentrations tested
19. Pyrolysis oils exhibit gel type flow behavior based on the storage moduli (G') and loss moduli (G'') tests conducted for evaluating structural stability
20. Based on the analysis of variance (ANOVA), 10 wt.% was observed to be the most optimal additive concentration in stabilizing the pyrolysis oils

21. Pine wood pyrolysis oils are deemed to be the most stable pyrolysis oils during this study. In general, the wood derived oils showed greater storage stability than the bark derived oils
22. The artificial light used in this study did not have a significant impact on the oxidative stability of pyrolysis oils. Hence, the chemical and physical properties of the additive free pyrolysis oils were relatively unaffected by light
23. Even though all the additives (anisole, glycerol, and methanol) performed well, their effect on the oil stability is dependent upon the feedstock, concentration, storage, and production conditions. Feedstock is concluded to be the single most important variable affecting the pyrolysis oil properties such as viscosity and water content
24. Acid value testing was observed to be more accurate than pH testing in measuring the acidic content of pyrolysis oils
25. Generally, both the mean viscosity and the mean water content of pyrolysis oils were observed to increase with increasing storage time
26. Aromatic additives in excess of 8 wt.% are beneficial in optimizing the stability of hardwood-derived oils. However, alcoholic additives in excess of 8 wt.% are beneficial in optimizing the stability of softwood-derived oils
27. The results of the filtration study indicated that reduction in particulate concentration increased pyrolysis oil stability. Consequently, filtration had the highest impact on the stability of bark derived oils because of their high solid content compared to the wood derived oils

Recommendations

1. An improved reactor design is necessary to obtain precise control of vapor residence time and pyrolysis temperature to eventually maximize pyrolysis oil yields
2. Pretreatment of biomass prior to auger reactor pyrolysis is projected to increase the pyrolysis oil yields by enhancing the thermal breakdown of lignocellulosics
3. Pyrolysis oils yields in the future need to be reported on a dry weight basis
4. Particulate removal from the pyrolysis process upstream can significantly increase the pyrolysis oil stability

5. A full-scale storage stability study involving the use of glycerol as a pyrolysis oil stabilizer is highly recommended
6. Additive blending studies involving the use of multifunctional chemical additives will be useful in the increased understanding of storage stability of pyrolysis oils
7. Extensive testing of pyrolysis oils for their total acid value is predicted to be useful in better understanding of their storage stability behavior with time
8. A complete life-cycle analysis of the pyrolysis oil is highly recommended for its potential use as a bio-fuel
9. Catalytic hydrodeoxygenation at the expense of high operating costs and lower oil yields is projected to increase the storage stability of pyrolysis oils by reducing the concentration of many volatile and odor causing compounds. Consequently, the pH of the pyrolysis oils can also be improved significantly
10. The thermal stability of pyrolysis oils based on the predetermined temperature of an onsite engine during its performance evaluation is essential in better understanding the complex changes of the oil chemical composition
11. Adsorption studies involving the use of bio-char for removing volatile organics and inorganic heavy metals need to be performed to isolate its potential industrial application

BIBLIOGRAPHY

- Adjaye, J.D., R.K. Sharma, and N.N. Bakshi. "Characterization and Stability Analysis of Wood-Derived Bio-Oil." *Fuel Processing Technology*, 31, 1992, pp. 241-256.
- Agblevor, F. A. and S. Besler. "Inorganic Compounds in Biomass Feedstocks. 1. Effect on the Quality of Fast Pyrolysis Oils." *Energy and Fuels*, 10, 1996, pp. 293-298.
- Ba, T., A., Chaala, M. Garcia-Perez, D. Rodrigue, and C. Roy. "Colloidal Properties of Bio-oils Obtained by Vacuum Pyrolysis of Softwood Bark. I. Characterization of Water-Soluble and Water-Insoluble Fractions." *Energy and Fuels*, 18, 2004, pp. 704-712.
- Ba, T., A., Chaala, M. Garcia-Perez, and C. Roy. "Colloidal Properties of Bio-oils Obtained by Vacuum Pyrolysis of Softwood Bark. II. Storage Stability." *Energy and Fuels*, 18, 2004, pp. 188-201.
- Barton, A.F.M. "CRC Handbook of Solubility Parameters and Other Cohesion Parameters." CRC Press, Boca Raton, FL, 1983, pp. 139-165.
- Bayerbach, R. and D. Meier. "Characterization of the Water-Insoluble Fraction from Fast Pyrolysis Liquids (Pyrolytic Lignin). Part IV: Structure Elucidation of Oligomeric Molecules." *Journal of Analytical and Applied Pyrolysis*, 85, 2009, pp. 98-107.
- Biodiesel Handling and Use Guidelines*, DOE/GO-102006-2288, Second Edition, United States Department of Energy, March 2006.
- Bird, R.B., W.E. Stewart, and E.N. Lightfoot. "Transport Phenomena." John Wiley & Sons, Singapore, 1994, pp. 3-12.
- Blasi, C.D., G. Signorelli, C.D. Russo, and G. Rea. "Product Distribution from Pyrolysis of Wood and Agricultural Residues." *Ind. Eng. Chem. Res.*, 38, 1999, pp. 2216-2224.
- Boucher, M. E., A. Chaala, and C. Roy. "Bio-oils Obtained by Vacuum Pyrolysis of Softwood Bark as a Liquid Fuel for Gas Turbines. Part I: Properties of Bio-oil and its Blends with Methanol and a Pyrolytic Aqueous Phase." *Biomass and Bioenergy*, 19, 2000, pp. 337-350.

- Boucher, M. E., A. Chaala, H. Pakdel, and C. Roy. "Bio-oils Obtained by Vacuum Pyrolysis of Softwood Bark as a Liquid Fuel for Gas Turbines. Part II: Stability and Ageing of Bio-oil and its Blends with Methanol and a Pyrolytic Aqueous Phase." *Biomass and Bioenergy*, 19, 2000, pp. 351-361.
- Brady, T.T. "Fast Pyrolysis- Wood to Gas, Bio-oil, and Fuel-Grade Char." Huskywood LLC, January 2002.
- Bridgwater, A. V. and G. V. C. Peacocke. "Fast Pyrolysis Processes for Biomass." *Renewable and Sustainable Energy Reviews*, 4, 2000, pp. 1-73.
- Bridgwater, A. V. "Principles and Practice of Biomass Fast Pyrolysis Processes for Liquids." *Journal of Analytical and Applied Pyrolysis*, 51, 1999, pp. 3-22.
- Bridgwater, A.V., S. Czernik, J. Diebold, D. Meier, A. Oasmaa, G. Peacocke, J. Piskorz, and D. Radlein. "Fast Pyrolysis of Biomass: A Handbook." CPL Press, Newbury, 1999, pp. 188-189.
- Bridgwater, A., S. Czernik, J. Diebold, D. Meier, A. Oasmaa, C. Peacocke, J. Piskorz, and D. Radlein. "Fast Pyrolysis of Biomass: A handbook." CPL Press, 1999, Newbury, UK, pp. 82-83.
- Bridgwater, A.V. "Production of High Grade Fuels and Chemicals from Catalytic Pyrolysis of Biomass." *Catalysis Today*, 29, 1996, pp. 285-295.
- Brockmann W., P.L. Geiß, J. Klingen, and B. Schröder. "Adhesive Bonding: Materials, Applications, and Technology." Wiley-VCH, Weinheim, 2009, pp. 325-327.
- Buron, H., P. Bru, G. Meunier, and J. A. Ostlund. "New ASTM Method for Heavy Fuel Oil Stability." *PIN*, Measurement and Testing, August/September 2005, pp. 50-51.
- Chaala A., T. Ba, M. G. Perez, and C. Roy. "Colloidal Properties of Bio-oils Obtained by Vacuum Pyrolysis of Softwood Bark: Aging and Thermal Stability." *Energy and Fuels*, 18, 2004, pp. 1535-1542.
- Colo, S.M., P.K.W. Herh, N. Roye, and M. Larsson. "Rheology and the Texture of Pharmaceutical and Cosmetic Semisolids." *American Laboratory*, November 2004, pp. 26-29.
- Czernik, S. and A.V. Bridgwater. "Overview of Applications of Biomass Fast Pyrolysis Oil." *Energy and Fuels*, 18, 2004, pp. 590-598.
- Cernik, S. "Storage of Biomass Pyrolysis Oils." NREL/CP-430-7215, 1994, pp. 67-76.

- Czernik, S., D. K. Johnson, and S. Black. "Stability of Wood Fast Pyrolysis Oil." *Biomass and Bioenergy*, 7, 1-6, 1994, pp. 187-192.
- Das, P., T. Sreelatha, and A. Ganesh. "Bio Oil from Pyrolysis of Cashew Nut Shell-Characterisation and Related Properties." *Biomass and Bioenergy*, 27, 2004, pp. 265-275.
- Dashnau, J.L., N.V. Nucci, K.A. Sharp, and J.M. Vanderkooi. "Hydrogen Bonding and the Cryogenic Properties of Glycerol/Water Mixtures." *J. Phys. Chem. B*, 110, 2006, pp. 13670-13677.
- DeGroot, W.F. and F. Shafizadeh. "Influence of Exchangeable Cations on the Carbonization of Biomass." *J. Anal. Appl. Pyrol.*, 6 (3), 1984, pp. 217-232.
- Demirbas, M.A. "Current Technologies for Biomass Conversion into Chemicals and Fuels." *Energy Sources*, Part A, 28, 2006, pp.1181-1188.
- Demirbas, A. "An Overview of Biomass Pyrolysis." *Energy Sources*, 24, 2002, pp. 471-482.
- Demirbas, A. "Mechanisms of Liquefaction and Pyrolysis Reactions of Biomass." *Energy Convers. Mgmt.*, 41, 2000, pp. 633-646.
- Demirbas, A. and M.M. Küçük. "Delignification of Ailanthus Altissima and Spruce Orientalis with Glycerol or Alkaline Glycerol at Atmospheric Pressure." *Cellulose Chem. Technol.*, 27, 1993, pp. 679-686.
- Diebold, J.P. "A Review of the Chemical and Physical Mechanisms of the Storage Stability of Fast Pyrolysis Bio-Oils." NREL/SR-570-27613, January 2000.
- Diebold, J. P. and S. Czernik. "Additives to Lower and Stabilize the Viscosity of Pyrolysis Oils During Storage." *Energy and Fuels*, 11, 1997, pp. 1081-1091.
- Diebold, J. P., J. W. Scahill, S. Czernik, S. D. Phillips, and C. J. Feik. "Progress in the Production of Hot-Gas Filtered Biocrude Oil at NREL." NREL/TP-431-7971, May 1995.
- Doshi, V. A., H. B. Vuthaluru, and T. Bastow. "Investigations into the Control of Odour and Viscosity of Biomass Oil Derived from Pyrolysis of Sewage Sludge." *Fuel Processing Technology*, 86, 2005, pp. 885-897.
- Dupont Petroleum Laboratory, "80 °C (175 °F) Accelerated Fuel Oil Stability Test." Analytical Method F31-81, February 1981.

- DynaMotive Energy Systems Corporation. "Fast Pyrolysis of Bagasse to Produce Biooil Fuel for Power Generation." Sugar Conference, Dynamotive, 2001.
- Elliott, D.C. "Water, Alkali, and Char in Flash Pyrolysis Oils." *Biomass and Bioenergy*, 7, 1-6, 1994, pp. 179-185.
- Elliott, D.C. and Schiefelbein, G.F. "Liquid Hydrocarbon Fuels from Biomass." *Amer. Chem. Soc.: Div. Fuel Chem. Preprints*, 34(4), 1989, pp.1160-1166.
- Elliott, D.C., and E. Baker. "Hydrotreating Biomass Liquids to Produce Hydrocarbon Fuels X." *Energy from Biomass and Wastes*, Klass, D., IGT, Chicago, 1987, pp. 765-784.
- Evans, R.J., F.A. Agblevor, H.L. Chum, J.B. Wooten, D.B. Chadwick, and S.D. Baldwin. "New Approaches to the Study of Cellulose Pyrolysis." *Prep. Pap.-Am. Chem. Soc., Div. Fuel Chem.*, 36 (2), 1991, pp. 714-724.
- Farag, I.H., C.E. LaClair, and C.J. Barrett. "Technical, Environmental, and Economic Feasibility of Bio-oil in New Hampshire's North Country." Final Report, August 2002, Chemical Engineering Department, University of New Hampshire.
- Fat and Oil Derivatives-Fatty Acid Methyl Esters (FAME)-Determination of Oxidation Stability (Accelerated Oxidation Test)*, DIN EN 14112, Deutsches Institut für Normung, 2003.
- Fratini, E., M. Bonini, A. Oasmaa, Y. Solantausta, J. Teixeira, and P. Baglioni. "SANS Analysis of the Microstructural Evolution During the Aging of Pyrolysis Oils from Biomass." *Langmuir-American Chemical Society*, 22, 2006, pp. 306-312.
- Graham, R.G., B.A. Freel, D.R. Huffman, and M.A. Bergougnou. "Commercial-Scale Rapid Thermal Processing of Biomass." *Biomass and Bioenergy*, 7, 1994, pp. 251-258.
- Gullu, D., A. Demirbas. "Biomass to Methanol via Pyrolysis Process." *Energy Conversion and Management*, 42, 11, July 2001, pp. 1349-1356.
- Handbook of Chemistry and Physics, Edited by Weast, C.R., CRC Press, 56th Edition, Cleveland, OH, 1975.
- Hedtke, D. "Glycerin Processing." *Bailey's Industrial Oil & Fat Products, Volume 5: Industrial and Consumer Nonedible Products from Oils and Fats*, New York: Wiley, Y.H. Hui (Ed.), 1996, pp. 275-308.

- Huber, G. W., S. Iborra, and A. Corma. "Synthesis of Transportation Fuels from Biomass: Chemistry, Catalysts, and Engineering." *Chemical Reviews*, 106, 2006, pp. 4044-4098.
- Ingram, L., D. Mohan, M. Bricka, P. Steele, D. Strobel, D. Crocker, B. Mitchell, J. Mohammad, K. Cantrell, and C.U. Pittman. "Pyrolysis of Wood and Bark in an Augur Reactor: Physical Properties and Chemical Analysis of the produced Bio-oils." *Energy and Fuels*, 22 (1), 2008, pp. 614-625.
- Jain, P.C. and M. Jain. "Engineering Chemistry (Chemistry of Engineering Materials)" Dhanpat Rai & Sons, New Delhi, 1995, pp. 218-221.
- Johnson, D. A. and D. Maclean. "Ablative Fast Pyrolysis: Converting Wood, Agricultural Wastes and Crops into Energy and Chemicals." First Biomass Conference of the Americas: Energy, Environment, Agriculture, and Industry, August-September 1993, pp. 1367-1384.
- Larson, R.G. "The Structure and Rheology of Complex Fluids." Oxford University Press Inc., New York, 1999, pp. 263-314.
- Lashkhi, V.L., L. V. Borenko, I. G. Fuks, B. R. Matveevskii, and O. B. Kopylova. "Colloidal Stability of Motor Oil Additive Packages." *Chemmotology*, Plenum Publishing Corporation, 1987, pp. 649-653.
- Luo, Z., S. Wang, Y. Liao, J. Zhou, Y. Gu, and K. Cen. "Research on Biomass Fast Pyrolysis for Liquid Fuel." *Biomass and Bioenergy*, 26, 2004, pp. 455-462.
- Maschio, G., C. Koufopoulos, and A. Lucchesi. "Pyrolysis, A Promising Route for Biomass Utilization." *Bioresource Technology*, 42, 1992, pp. 219-231.
- McGinnis, G. D. and F. Shafizadeh. "Cellulose." Wood Structure and Composition Edited by Lewin, M. and I. Goldstein, 1991, pp. 139-181.
- Meier D., G. Jesussek, and S. Radtke. "Chemical Stability of Wood Fast Pyrolysis Liquids." Pyrolysis and Gasification of Biomass and Waste: Proceedings of an Expert Meeting, Strasbourg, France, September-October 2002, pp. 221-228.
- Meir, D. and O. Faix. "State of the Art of Applied Fast Pyrolysis of Lignocellulosic Materials-A Review." *Bioresource Technology*, 68, 1999, pp. 71-77.
- Mettler Toledo DL 31/38 Titrators*, Application Brochure 26, Mettler Toledo, Switzerland, 1999.

- Mohan, D., J. Shi, D. D. Nicholas, C. U. Pittman, P. H. Steele, and J. E. Cooper. "Fungicidal Values of Bio-Oils and their Lignin Rich Fractions Obtained from Wood/Bark Fast Pyrolysis." *Chemosphere*, 71, 2008, 456-465.
- Mohan, D., C.U. Pittman, M. Bricka, F. Smith, B. Yancey, J. Mohammad, P. H. Steele, M. F. A. Franco, V. G. Serrano, and H. Gong. "Sorption of Arsenic, Cadmium, and Lead by Chars Produced from Fast Pyrolysis of Wood and Bark during Bio-oil Production." *Journal of Colloid and Interface Science*, 310, 2007, pp. 57-63.
- Mohan, D., C. U. Pittman, and P. H. Steele. "Pyrolysis of Wood/Biomass for Bio-oil: A Critical Review." *Energy and Fuels*, 20, 3, 2006, pp. 848-889.
- Morrison, F.A. "Understanding Rheology." Oxford University Press Inc., New York, 2001, pp. 382-410.
- National Renewable Energy Laboratory (NREL). "An Evaluation and Comparison of Test Methods to Measure the Oxidation Stability of Neat Biodiesel." S.R Westbrook (South West Research Institute), NREL/SR-540-38983, November 2005.
- Oasmaa, A., K. Sipila, Y. Solantausta, and E. Kuoppala. "Quality Improvement of Pyrolysis Liquids: Effect of Light Volatiles on the Stability of Pyrolysis Liquids." *Energy and Fuels*, 19, 2005, pp. 2556-2561.
- Oasmaa, A. and D. Meier. "Norms and Standards for Fast Pyrolysis Liquids 1. Round Robin Test." *J. Anal. Appl. Pyrolysis*, 73, 2005, pp. 323-334.
- Oasmaa, A., E. Kuoppala, J.F. Selin, S. Gust, and Y.Solantausta. "Fast Pyrolysis of Forestry Residue and Pine. 4. Improvement of the Product Quality by Solvent Addition." *Energy and Fuels*, 18, 2004, pp. 1578-1583.
- Oasmaa, A., E. Kuoppala, and Y.Solantausta. "Fast Pyrolysis of Forestry Residue. 2. Physicochemical Composition of Product Liquid." *Energy and Fuels*, 17, 2003, pp. 433-443.
- Oasmaa, A., E. Kuoppala, S. Gust, and Y. Solantausta. "Fast Pyrolysis of Forestry Residue: Effect of Extractives on Phase Separation of Pyrolysis Liquids." *American Chemical Society Journal*, 17(1), January/February 2003, pp. 1-12.
- Oasmaa, A. "Fuel Oil Quality Properties of Wood-Based Pyrolysis Liquids." Academic Dissertation Research Report Series, Report 99, Department of Chemistry-University of Jyvaskyla, Finland, 2003, pp. 32.
- Oasmaa, A. and E. Kuoppala. "Fast Pyrolysis of Forestry Residue. 3 Storage Stability of Liquid Fuel." *Energy and Fuels*, 17, 2003, pp. 1075-1084.

- Oasmaa, A. and S. Czernik. "Fuel Oil Quality of Biomass Pyrolysis Oils-State of the Art for the End Users." *Energy and Fuels*, 13, 1999, pp. 914-921.
- Peacocke, C., D. Meier, S. Gust, A. Webster, A. Oasmaa, and R. McLellan. "Determination of Norms and Standards for Biomass Derived Pyrolysis Liquids." Final Report, Commission of the European Communities, Contract No. 4.1030/C/00-015/2000, 2003.
- Perez, M.G., T.T. Adams, J.W. Goodrum, D.P. Geller, and K.C. Das. "Production and Fuel Properties of Pine Chip Bio-oil/Biodiesel Blends." *Energy and Fuels*, 21, 2007, pp. 2363-2372.
- Perez, M. G., A. Chaala, H. Pakdel, D. Kretschmer, D. Rodrigue, and C. Roy. "Multiphase Structure of Bio-oils." *Energy and Fuels*, 20, 2006, pp. 364-375.
- Perry's Chemical Engineers' Handbook, Edited by Perry, R.H., Green, D.W., and J.O. Maloney, McGraw-Hill, 7th Edition, New York, NY, 1997.
- Pan, W.P. and G.N. Richards. "Influence of Metal Ions on Volatile Products of Pyrolysis of Wood." *J. Anal. Appl. Pyrolysis*, 16, 1989, pp. 117-126.
- Radlein, D., J. Piskorz, and D.S. Scott. "Control of Selectivity in the Fast Pyrolysis of Cellulose." Proceedings of the Biomass for Energy, Industry, and Environment, 6th E.C. Conference, Elsevier Applied Science, New York, 1992, pp. 643-649.
- Radovanovic, M., R. H. Venderbosch, W. Prins, and W. P. M. VanSwaaij. "Some Remarks on the Viscosity Measurement of Pyrolysis Liquids." *Biomass and Bioenergy*, 18, 2000, pp. 209-222.
- Rath, J., M.G. Wolfinger, G. Steiner, G. Krammer, F. Barontini, and V. Cozazni. "Heat of Wood Pyrolysis." *Fuel*, 82 (1), 2003, pp. 81-91.
- Ringer, M., V. Putsche, and J. Scahill. "Large-Scale Pyrolysis Oil Production: A Technology Assessment and Economic Analysis." NREL/TP-510-37779, National Renewable Energy Laboratory, November 2006.
- Rosen, S.L. "Fundamental Principles of Polymeric Materials." John Wiley & Sons, New York, 1982, pp. 202-206.
- Sampling and Analysis of Commercial Fats and Oils-Oil Stability Index (OSI), AOCS Cd 12b-93, Official Methods of Analysis of AOCS, American Oil Chemists' Society, 1993.

- Scholze, B. "Long-term Stability, Catalytic Upgrading, and Application of Pyrolysis Oils –Improving the Properties of a Potential Substitute for Fossil Fuels." Dissertation: University of Hamburg, 2002, pp. 43.
- Schultz, T. P. and F. W. Taylor. "Wood." Biomass Handbook Edited by Kitani, O. and C.W. Hall, Gordon and Breach Science Publications, 1989, pp. 133-141.
- Scott, D.S., P. Majerski, J. Piskorz, and D. Radlein. "A Second Look at Fast Pyrolysis of Biomass-the RTI Process." *Journal of Analytical and Applied Pyrolysis*, 51, 1999, pp. 23-37.
- Scott, D.S., J. Piskorz, M.A. Bergougnou, R. Graham, and R.P. Overend. "The Role of Temperature in the Fast Pyrolysis of Cellulose and Wood." *Ind. Eng. Chem. Res.*, 27, 1988, pp. 8-15.
- Sensoz, S. "Slow Pyrolysis of Wood Barks from Pinus Brutia Ten. and Product Compositions." *Bioresource Technology*, 89, 2003, pp. 307-311.
- Shafizadeh, F. "Introduction to Pyrolysis of Biomass." *Journal of Analytical and Applied Pyrolysis*, 3, 1982, pp. 283-305.
- Sipila, K. and A. Oasmaa. "Improvement of Liquid Quality." Patent Application, FI 19992181, Helsinki, Finland, 1999.
- Sjostrom, E. "Wood Chemistry Fundamentals and Applications." Academic Press Second Edition, 1993, pp. 54-113.
- Standard Test Method for Thermal Oxidation Stability of Aviation Turbine Fuels (JFTOT Procedure)*, ASTM D3241, Annual Book of Standards, American Society for Testing and Materials, West Conshohocken, PA, 2007.
- Standard Test Method for Measuring n-Heptane Induced Phase Separation of Asphaltene-Containing Heavy Fuel Oils as Separability Number by an Optical Scanning Device*, ASTM D7061, Annual Book of Standards, American Society for Testing and Materials, West Conshohocken, PA, 2006.
- Standard Test Method for ASTM Color of Petroleum Products (ASTM Color Scale)*, ASTM D1500, Annual Book of Standards, American Society for Testing and Materials, West Conshohocken, PA, 2004.
- Standard Specification for Middle Distillate Fuel Oil-Military Marine Applications*, ASTM D6985, Annual Book of Standards, American Society for Testing and Materials, West Conshohocken, PA, 2004.

Standard Test Method for Oxidation Stability of Aviation Fuels (Potential Residue Method), ASTM D873, Annual Book of Standards, American Society for Testing and Materials, West Conshohocken, PA, 2003.

Standard Test Method for Assessing Distillate Fuel Storage Stability by Oxygen Overpressure, ASTM D5304, Annual Book of Standards, American Society for Testing and Materials, West Conshohocken, PA, 1992.

Standard Test Method for Distillate Fuel Storage Stability at 43 °C (110 °F), ASTM D4625, Annual Book of Standards, American Society for Testing and Materials, Philadelphia, PA, 1992.

Standard Test Method for Oxidation Stability of Distillate Fuel Oil (Accelerated Method), ASTM D2274, Annual Book of Standards, American Society for Testing and Materials, Philadelphia, PA, 1988.

Standard Test Method for Oxidation Stability of Gasoline (Induction Period Method), ASTM D525, Annual Book of Standards, American Society for Testing and Materials, Philadelphia, PA, 1988.

Standard Test Method for Kinematic Viscosity of Transparent and Opaque Liquids (and the Calculation of Dynamic Viscosity), ASTM D445, Annual Book of Standards, American Society for Testing and Materials, Philadelphia, PA, 1988.

Johnson, D.T. and K.A. Taconi. "The Glycerin Glut: Options for the Value-Added Conversion of Crude Glycerol Resulting from Biodiesel Production." *AICHE, Environmental Progress*, 26 (4), 2007, pp. 338-348.

Tzanetakis, T., N. Ashgriz, D.F. James, and M.J. Thomson. "Liquid Fuel properties of a Hardwood-Derived Bio-oil Fraction." *Energy and Fuels*, 22, 2008, pp. 2725-2733.

United State Department of Energy (U.S DOE). "Biodiesel Handling and Use Guidelines." *Energy Efficiency and Renewable Energy*, DOE/GO-102006-2288, Second Edition, March 2006.

Westbrook, S.R. and R. McCormik. "An Evaluation and Comparison of Test Methods to Measure the Oxidation Stability of Neat Biodiesel." NREL/SR-540-38983, National Renewable Energy Laboratory, Colorado, November 2005.

Young, R.J. and P.A. Lovell. "Introduction to Polymers." CRC Press, Second Edition, 1991, pp. 331-335.

Zabaniotou, A. A. "Pyrolysis of Forestry Biomass By-Products in Greece." *Energy Sources*, 21, 1999, pp. 395-403.

Zaror, C.A. and D.L. Pyle. "The Pyrolysis of Biomass: A General review." *Proc. Indian Acad. Sci. (Engg. Sci.)*, 5 (4), December 1982, pp. 269-285.

Zong-da, Y. "Suggestion of a New Definition of Angular Strain." *Applied Mathematics and Mechanics*, 5 (1), January, 1984.

http://www.methanex.com/products/documents/MxAvgPrice_Sept292008_000.pdf

<http://www.eia.doe.gov/oiaf/aeo/demand.html>

<http://www.chemistry.oregonstate.edu/courses/ch130/latestnews/ch130ln.htm>

http://www.engin.umich.edu/dept/che/research/savage/Fernando/Fernando_main.htm

<http://www.cartage.org.lb/en/themes/sciences/physics/Mechanics/LiquidMechanics/LiquidMechanics/NatureLiquids/NatureLiquids.htm>

<http://webbook.nist.gov/chemistry/name-ser.html>

<http://www.icis.com/>

<http://en.wikipedia.org/>

<http://www.sigmaaldrich.com/>

<http://www.smallparts.com/>

<http://www.fishersci.com/>

APPENDIX A
(PYROLYSIS OIL PRODUCTION-PHASE I)

APPENDIX A

This Appendix presents the results obtained from phase I or Mississippi State University (MSU) pyrolysis oil (bio-oil) production. Pyrolysis oils (16) were produced by varying the feedstock (pine wood-PW, pine bark-PB, oak wood-OW, and oak bark-OB), solid residence time (slow and fast), and pyrolysis temperature (400 and 450 °C). The daily yields (%) of unaccounted mass, bio-oil, char, and water as a function of feedstock and reactor condition is shown in Figures 1-15 for the 16 MSU pyrolysis oils. Further their average yields (%) of unaccounted mass, bio-oil, char, and water as a function of reactor condition for all the runs (complete) is shown in Figures 16-29.

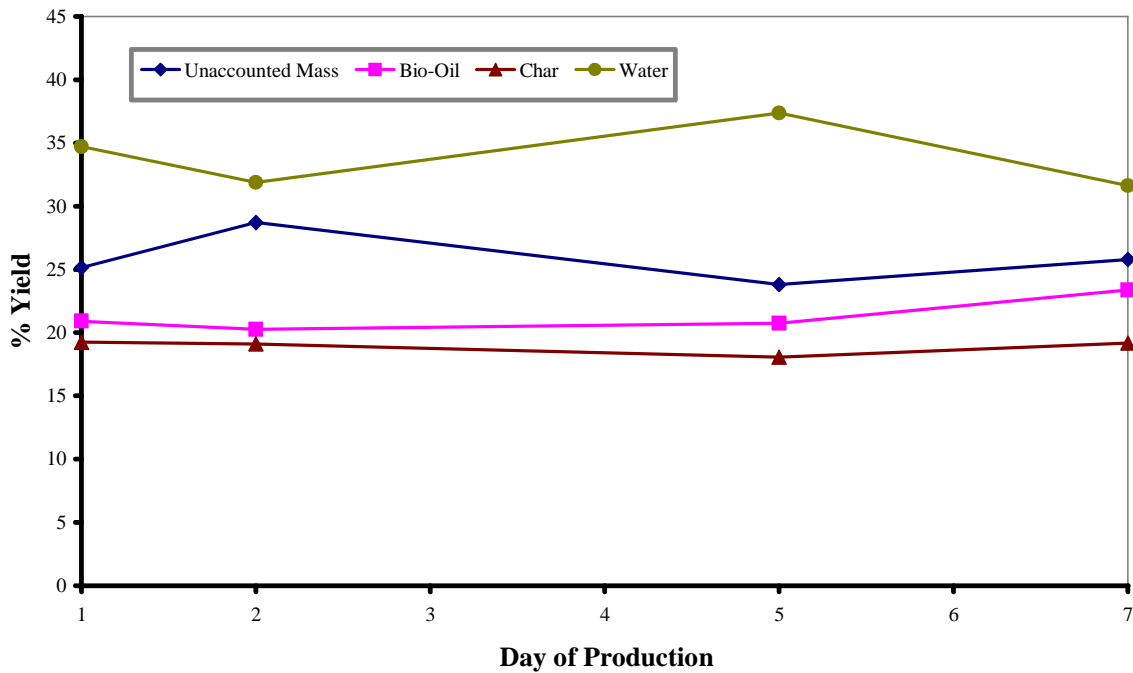


Figure A.1 Reactor Yields of Mississippi State-Pine Wood-Low Temperature-Fast Residence (MS-PW-LT-FR) Bio-Oil

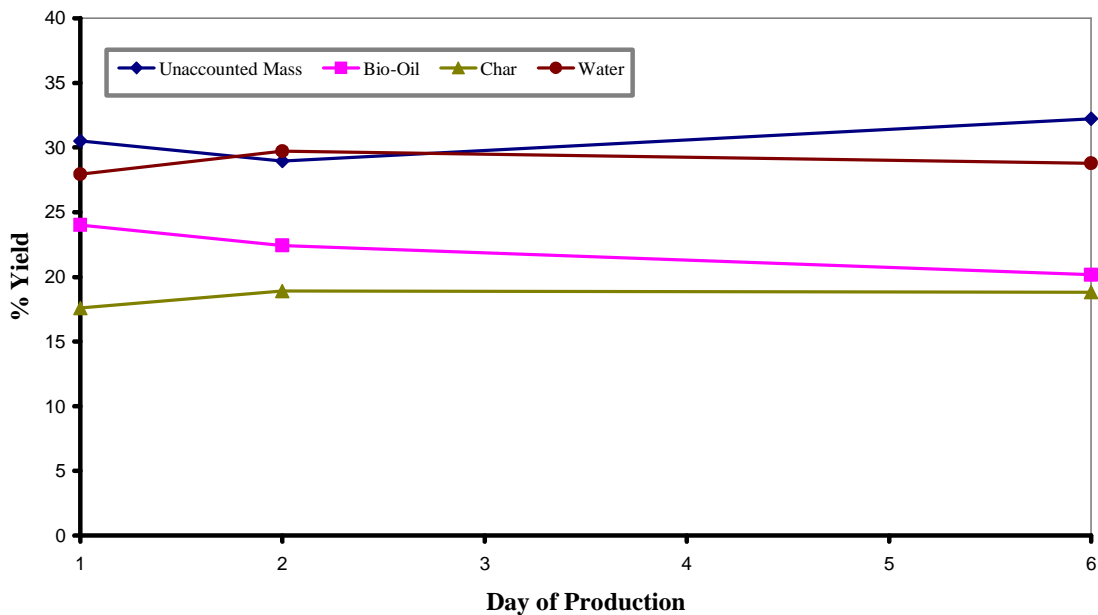


Figure A.2 Reactor Yields of Mississippi State-Pine Wood-High Temperature-Fast Residence (MS-PW-HT-FR) Bio-Oil

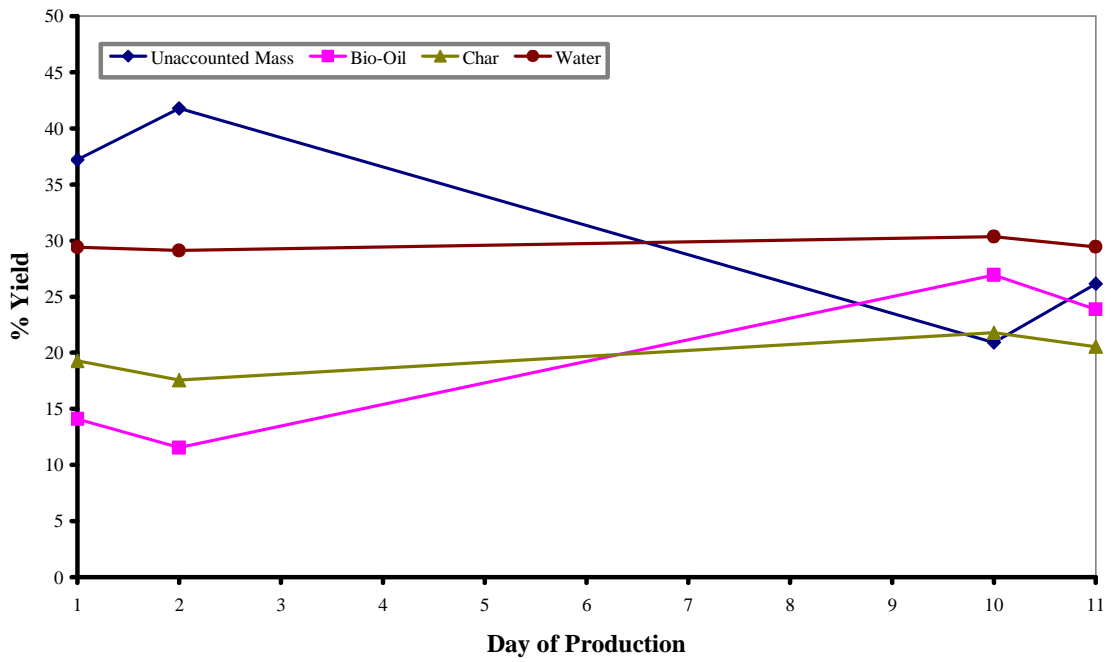


Figure A.3 Reactor Yields of Mississippi State-Pine Wood-Low Temperature-Slow Residence (MS-PW-LT-SR) Bio-Oil

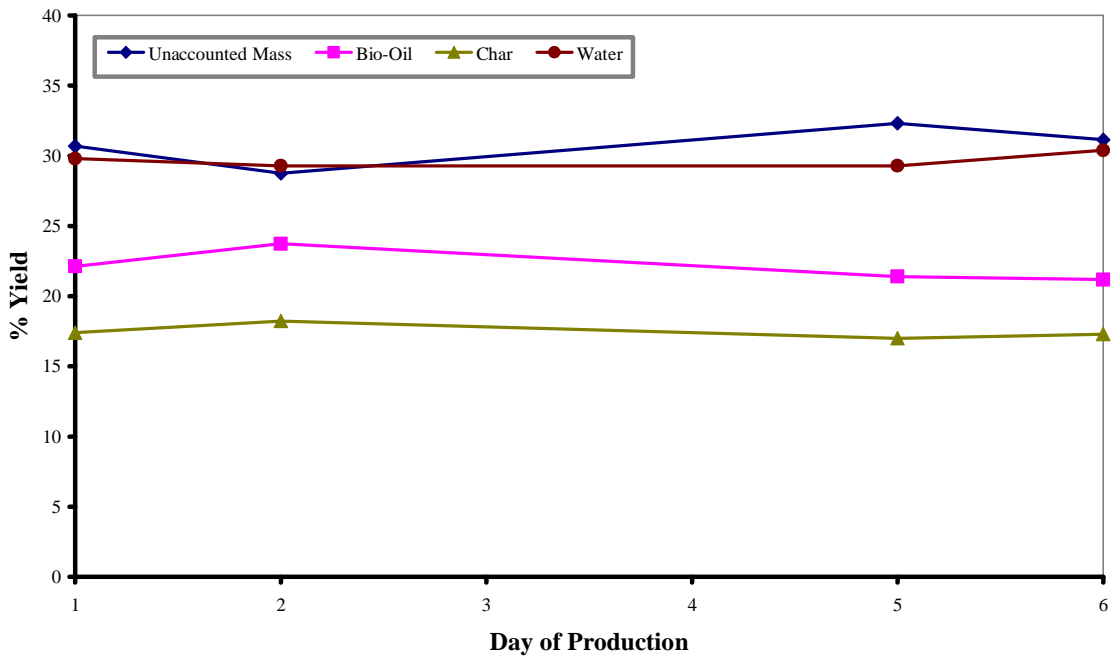


Figure A.4 Reactor Yields of Mississippi State-Pine Wood-High Temperature-Slow Residence (MS-PW-HT-SR) Bio-Oil

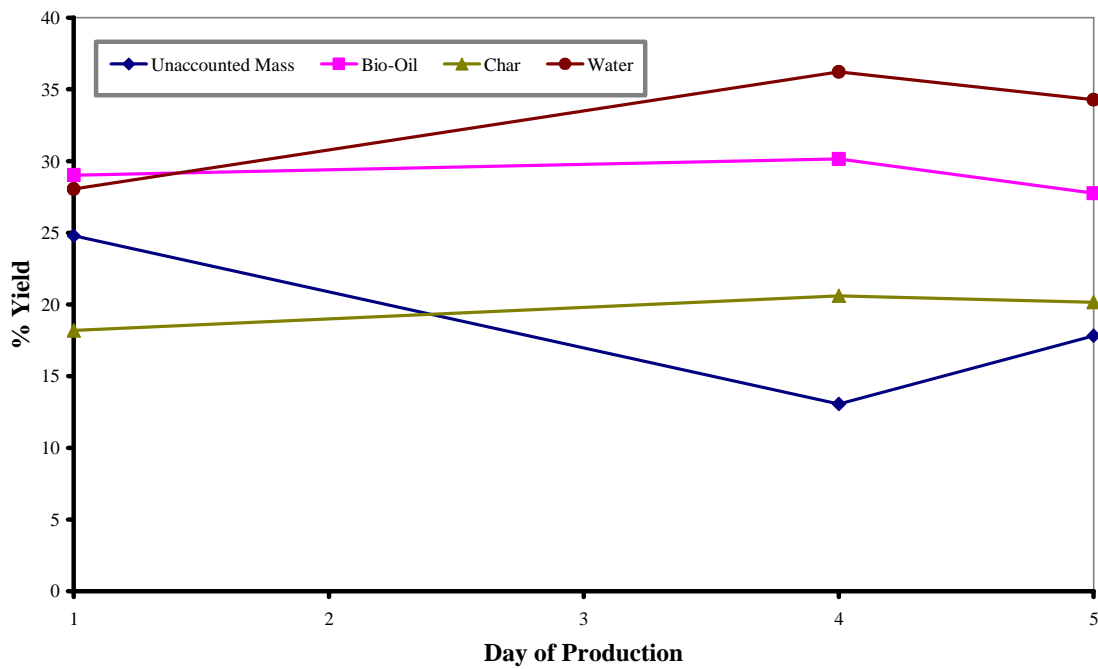


Figure A.5 Reactor Yields of Mississippi State-Oak Wood-Low Temperature-Fast Residence (MS-OW-LT-FR) Bio-Oil

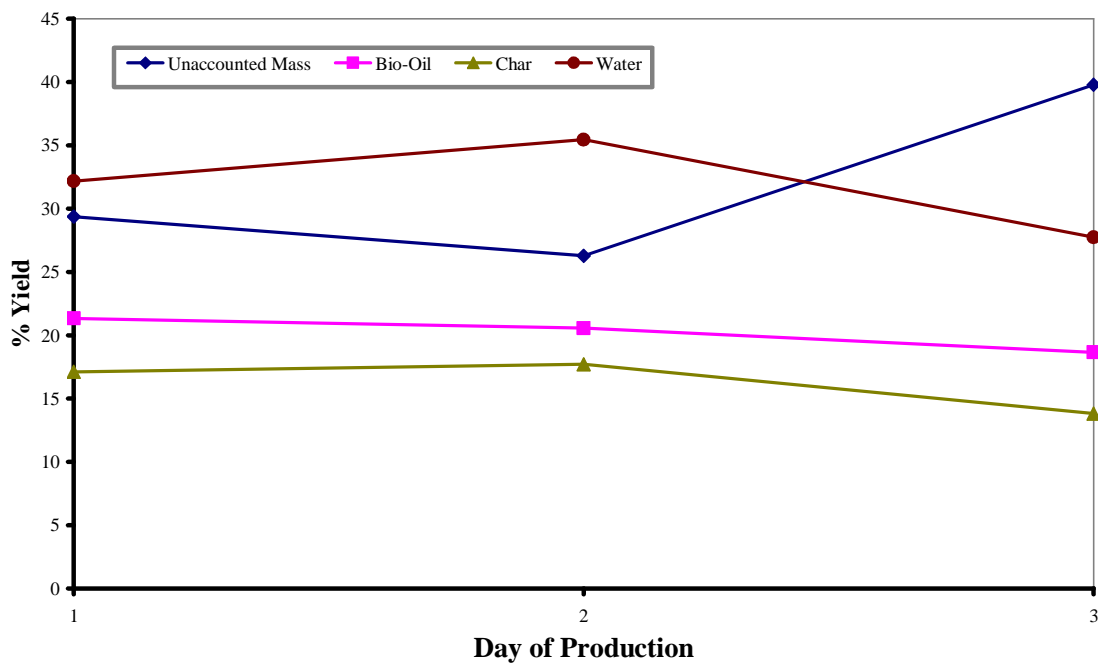


Figure A.6 Reactor Yields of Mississippi State-Oak Wood-High Temperature-Fast Residence (MS-OW-HT-FR) Bio-Oil

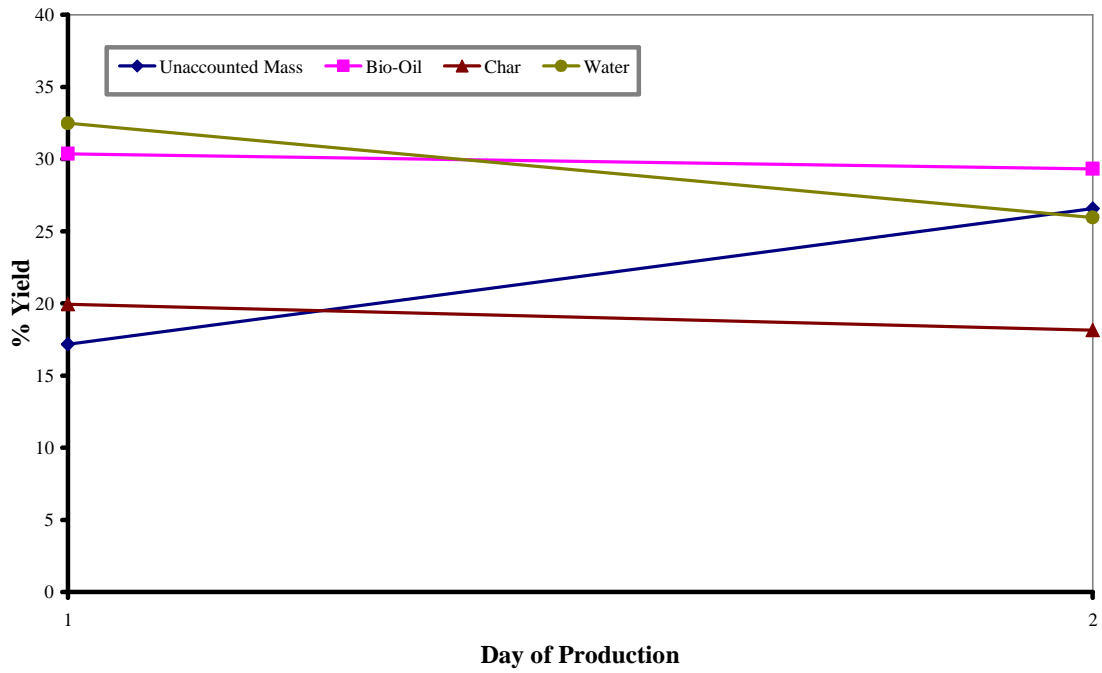


Figure A.7 Reactor Yields of Mississippi State-Oak Wood-Low Temperature-Slow Residence (MS-OW-LT-SR) Bio-Oil

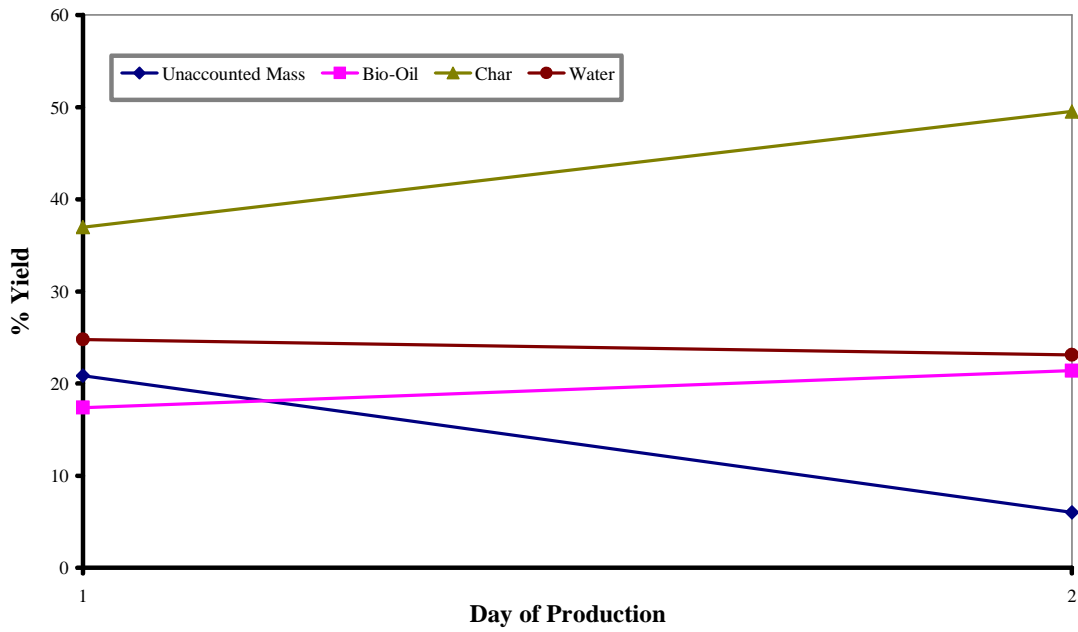


Figure A.8 Reactor Yields of Mississippi State-Pine Bark-Low Temperature-Fast Residence (MS-PB-LT-FR) Bio-Oil

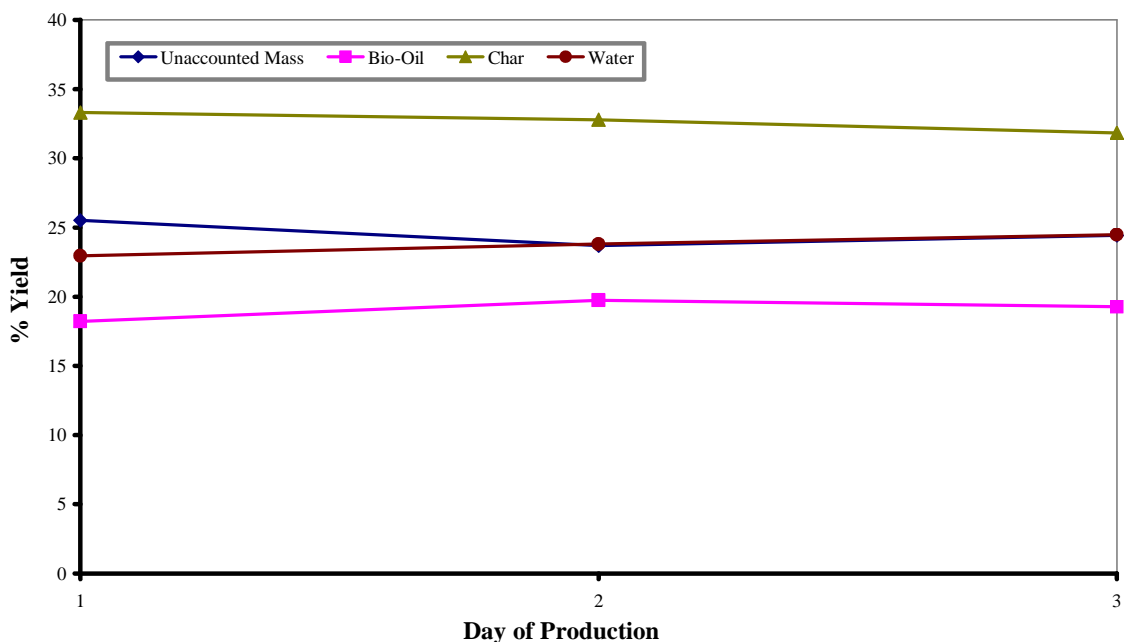


Figure A.9 Reactor Yields of Mississippi State-Pine Bark-High Temperature-Fast Residence (MS-PB-HT-FR) Bio-Oil

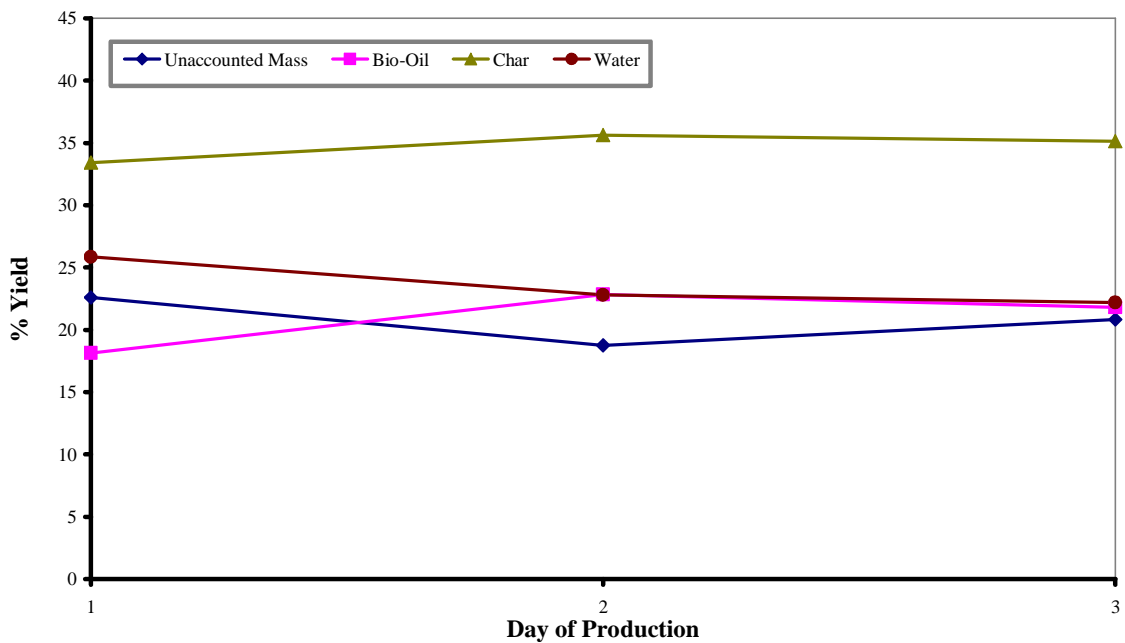


Figure A.10 Reactor Yields of Mississippi State-Pine Bark-Low Temperature-Slow Residence (MS-PB-LT-SR) Bio-Oil

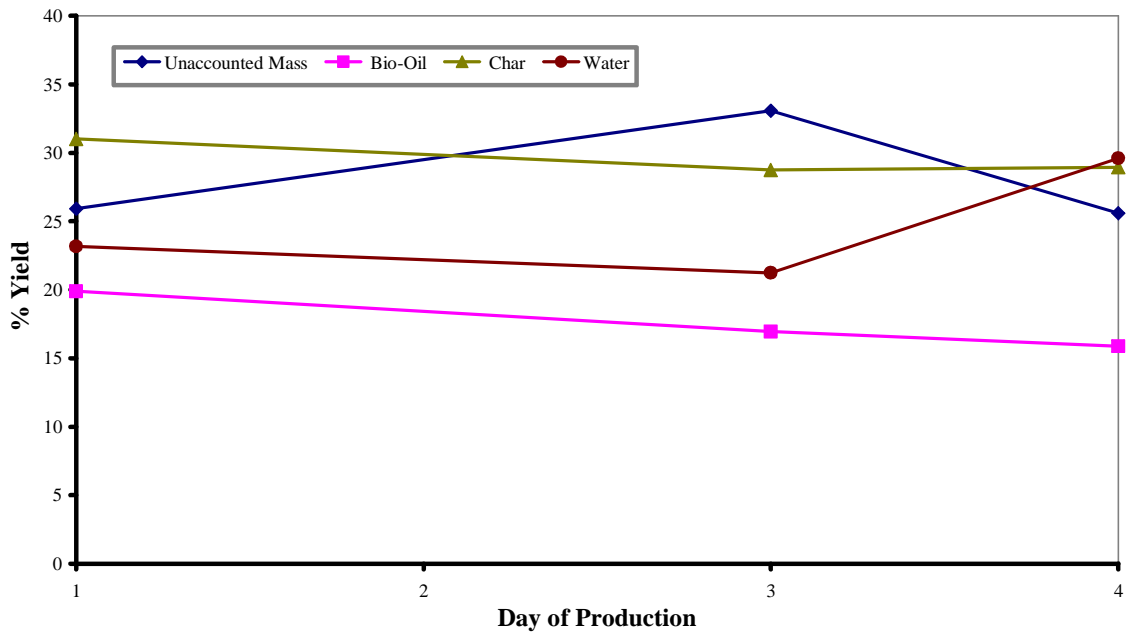


Figure A.11 Reactor Yields of Mississippi State-Pine Bark-High Temperature-Slow Residence (MS-PB-HT-SR) Bio-Oil

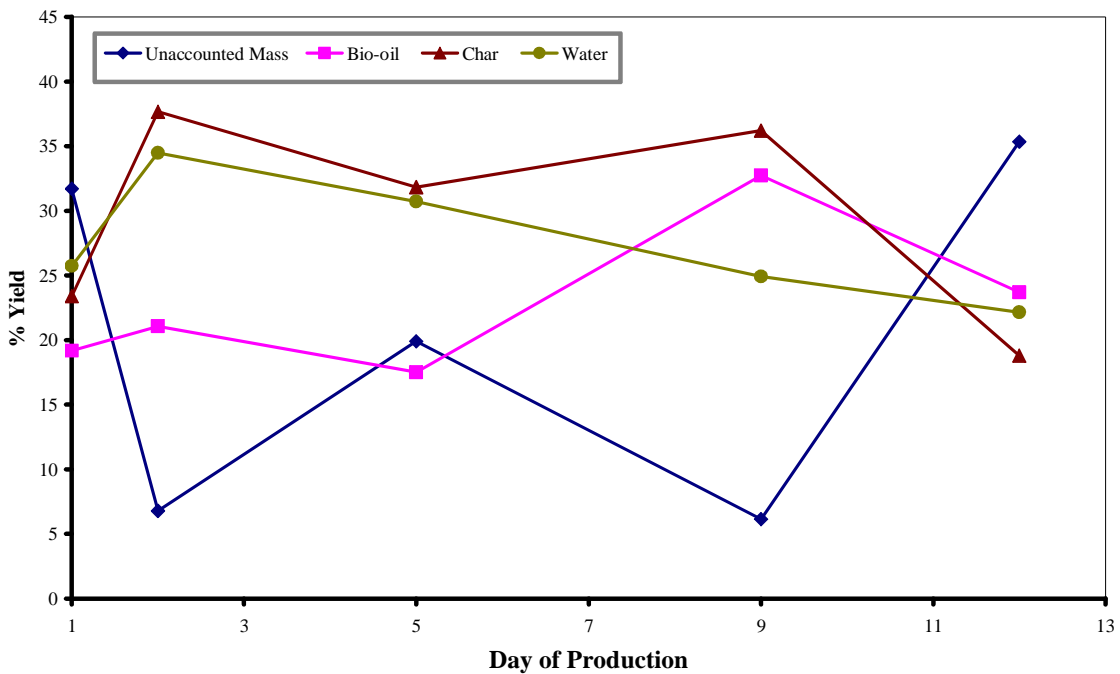


Figure A.12 Reactor Yields of Mississippi State-Oak Bark-Low Temperature-Fast Residence (MS-OB-LT-FR) Bio-Oil

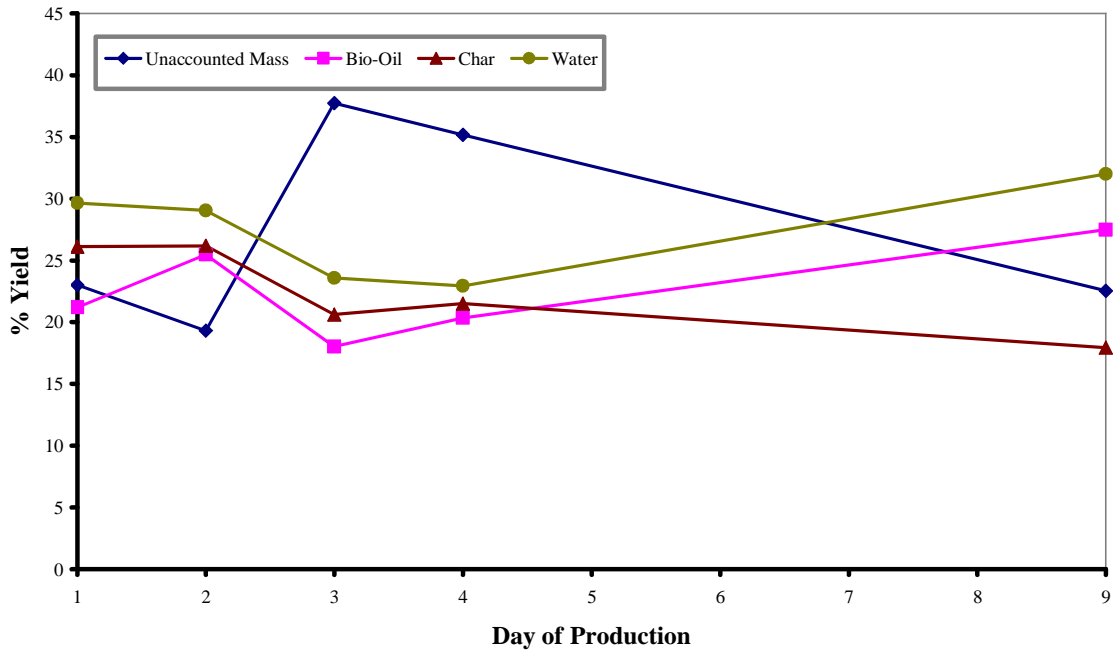


Figure A.13 Reactor Yields of Mississippi State-Oak Bark-High Temperature-Fast Residence (MS-OB-HT-FR) Bio-Oil

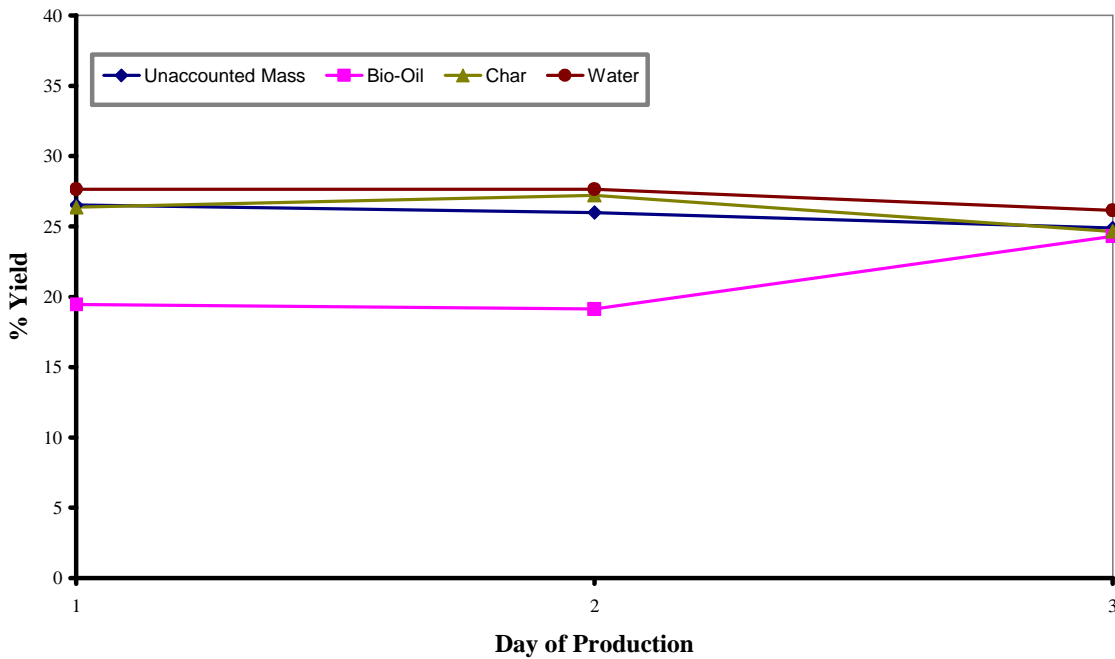


Figure A.14 Reactor Yields of Mississippi State-Oak Bark-Low Temperature-Slow Residence (MS-OB-LT-SR) Bio-Oil

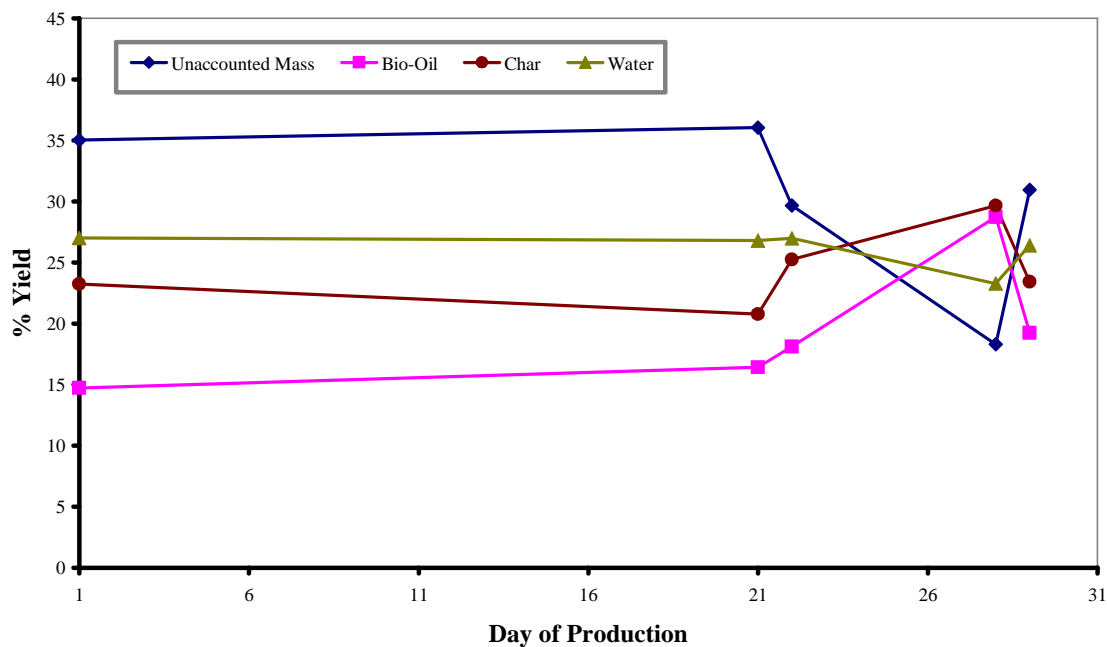


Figure A.15 Reactor Yields of Mississippi State-Oak Bark-High Temperature-Slow Residence (MS-OB-HT-SR) Bio-Oil

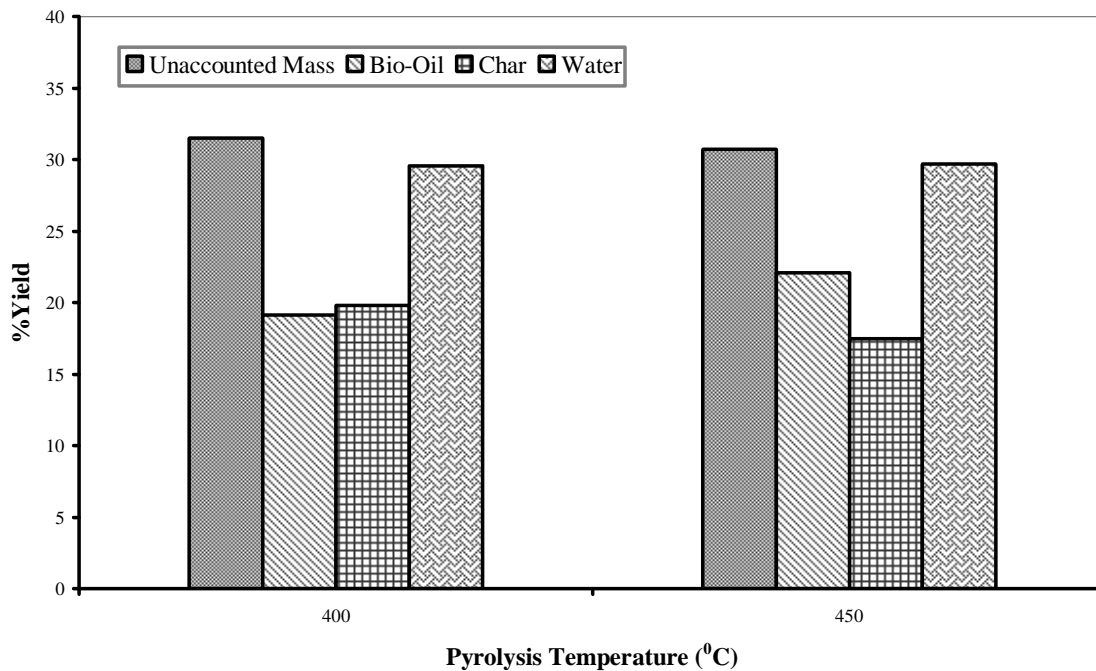


Figure A.16 Average Reactor Yields of Mississippi State-Pine Wood-Slow Residence (MS-PW-SR) Bio-Oils

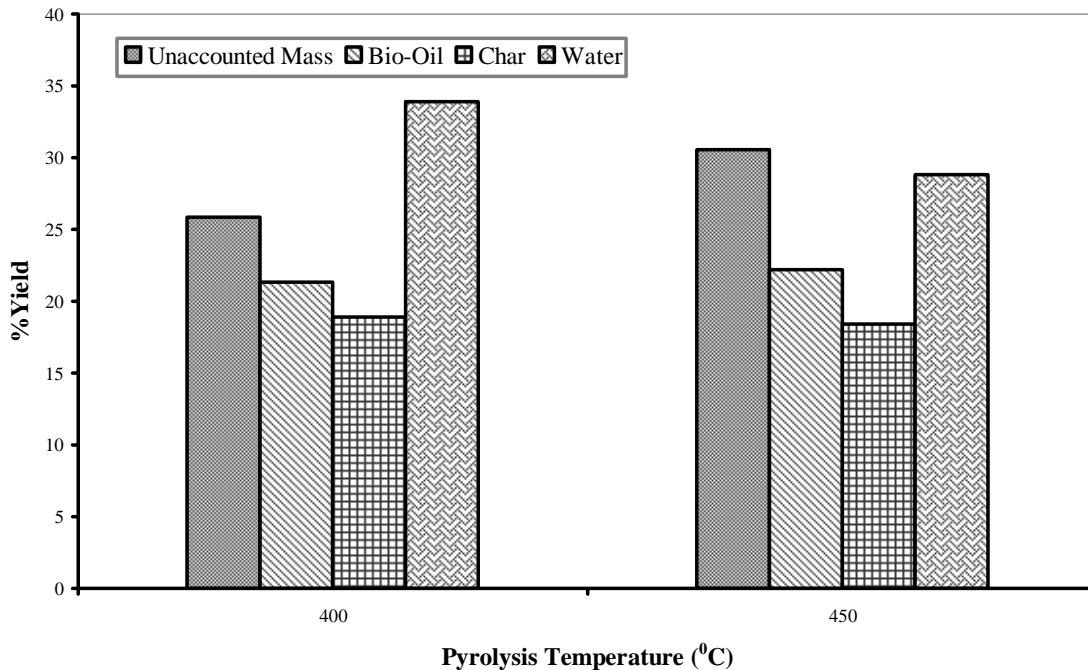


Figure A.17 Average Reactor Yields of Mississippi State-Pine Wood-Fast Residence (MS-PW-FR) Bio-Oils

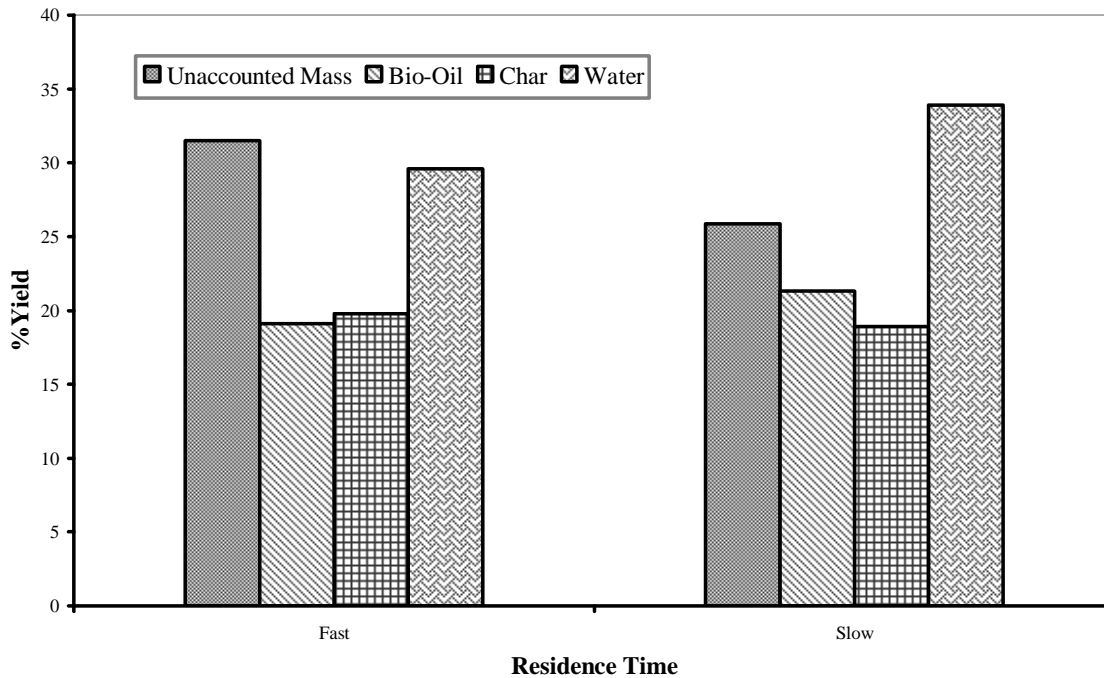


Figure A.18 Average Reactor Yields of Mississippi State-Pine Wood-Low Temperature (MS-PW-LT) Bio-Oils

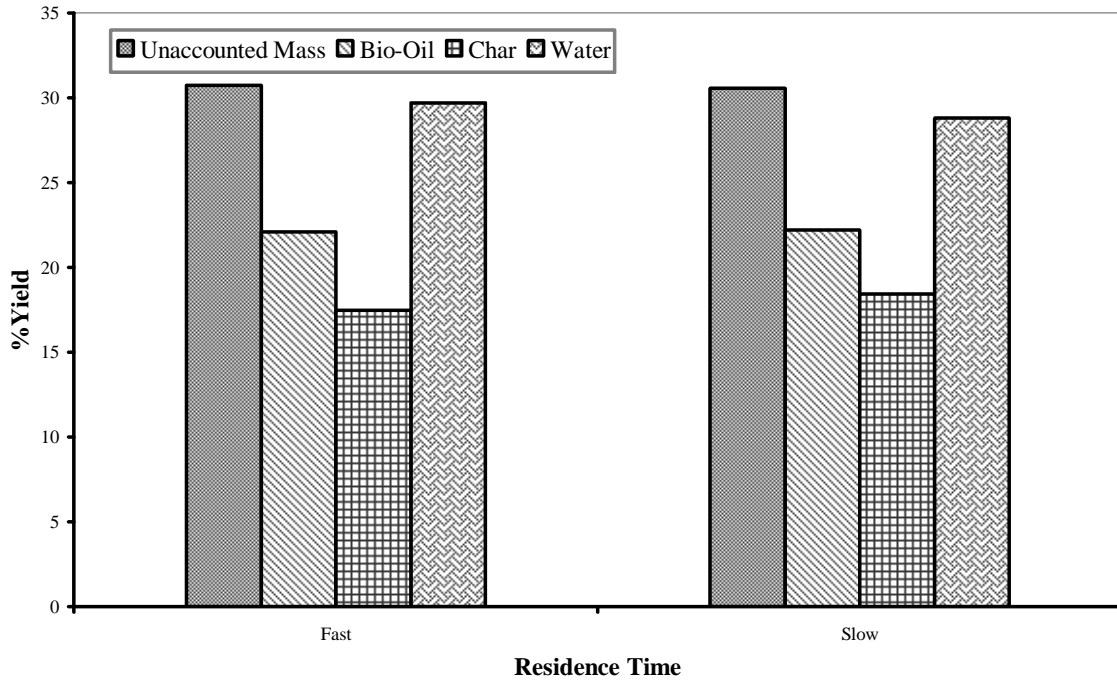


Figure A.19 Average Reactor Yields of Mississippi State-Pine Wood-High Temperature (MS-PW-HT) Bio-Oils

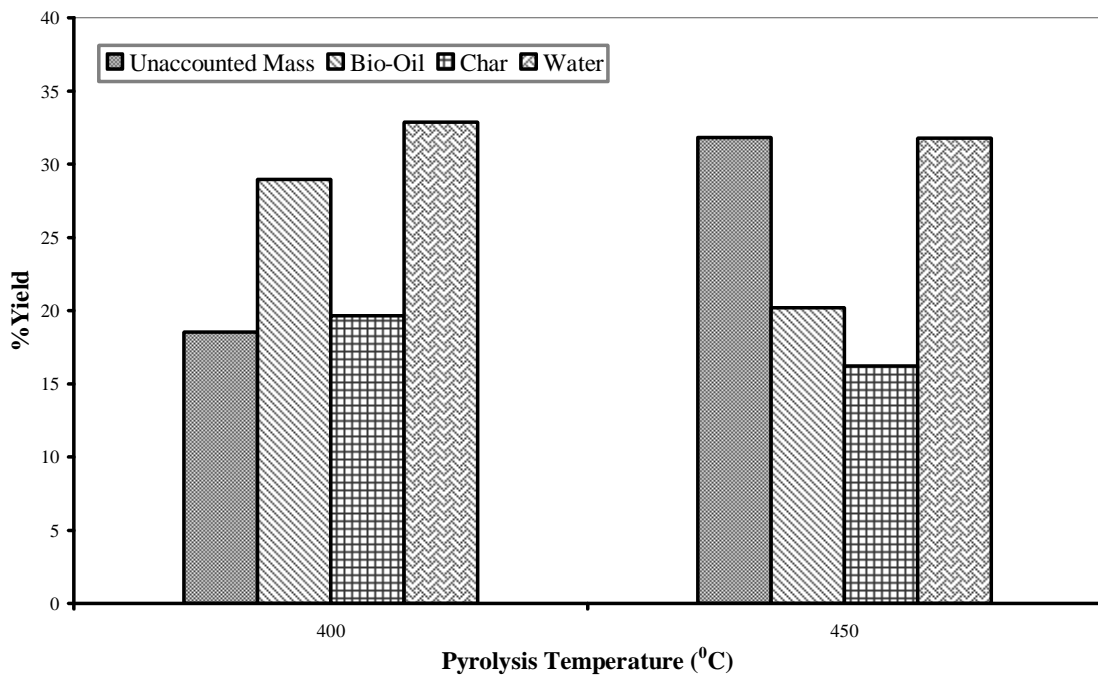


Figure A.20 Average Reactor Yields of Mississippi State-Oak Wood-Fast Residence (MS-OW-FR) Bio-Oils

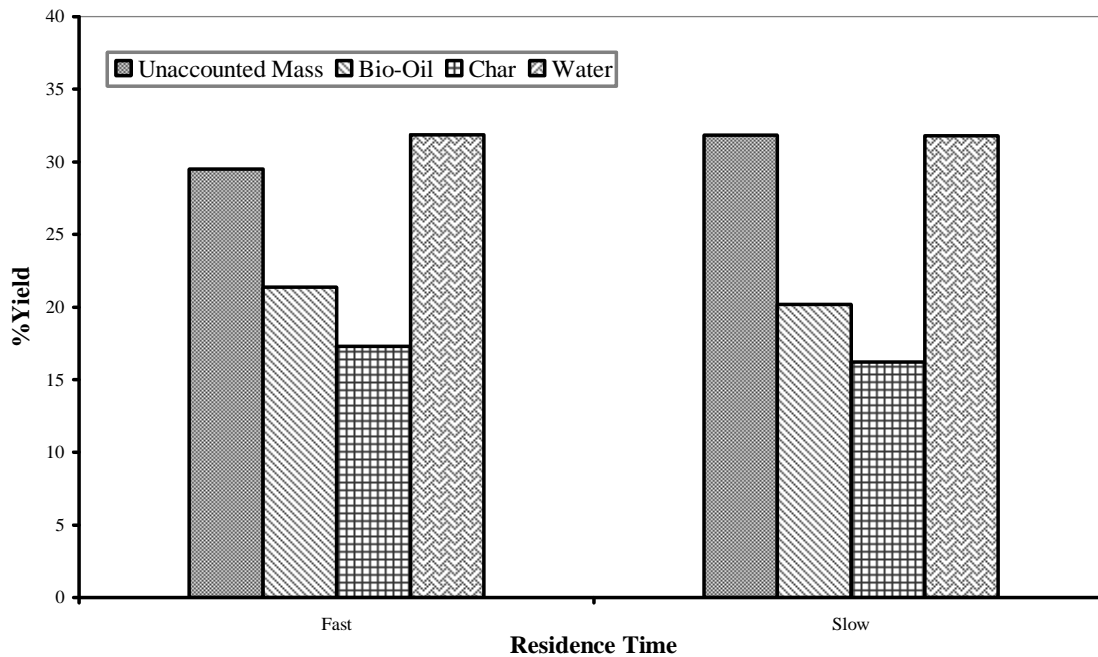


Figure A.21 Average Reactor Yields of Mississippi State-Oak Wood-High Temperature (MS-OW-HT) Bio-Oils

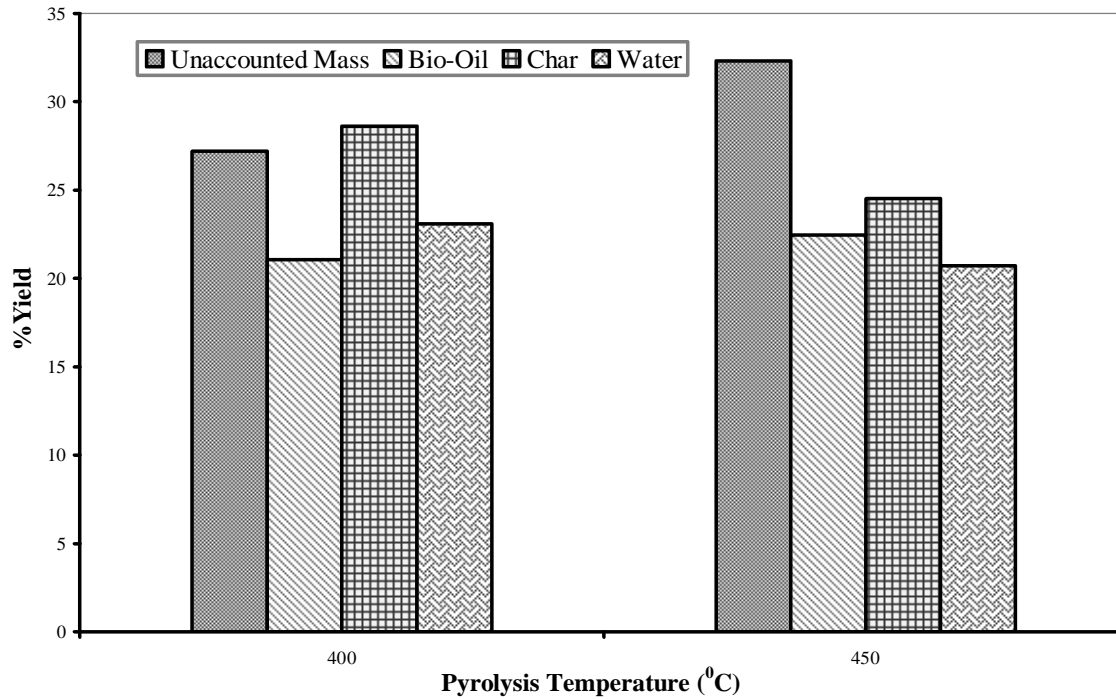


Figure A.22 Average Reactor Yields of Mississippi State-Pine Bark-Slow Residence (MS-PB-SR) Bio-Oils

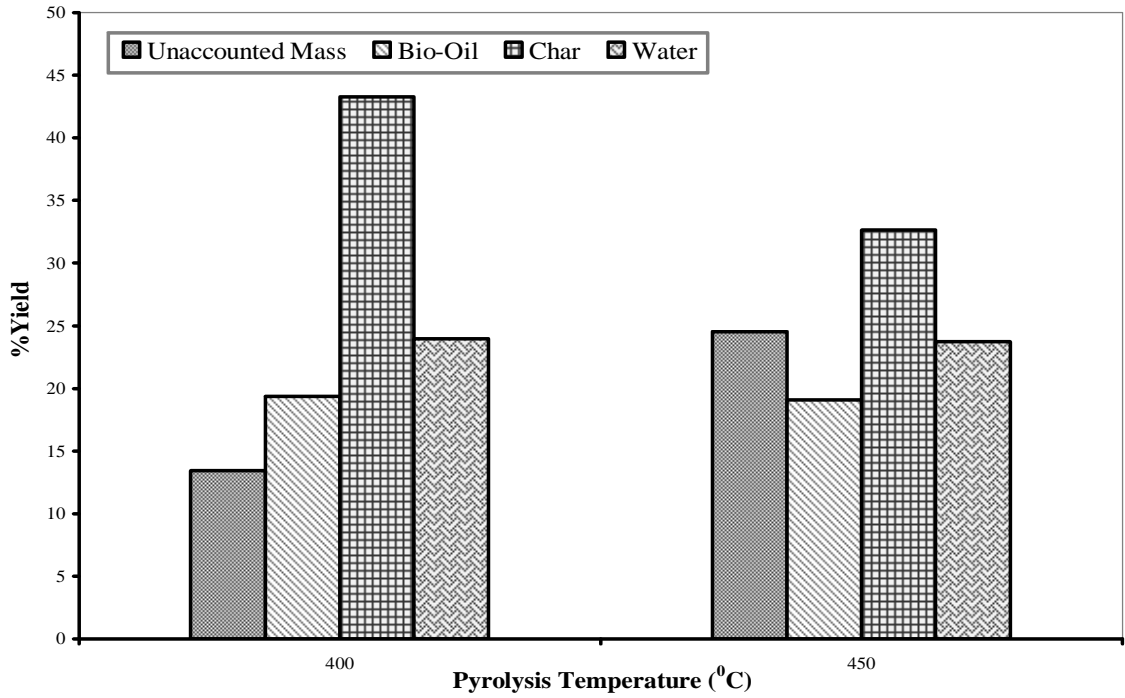


Figure A.23 Average Reactor Yields of Mississippi State-Pine Bark-Fast Residence (MS-PB-FR) Bio-Oils

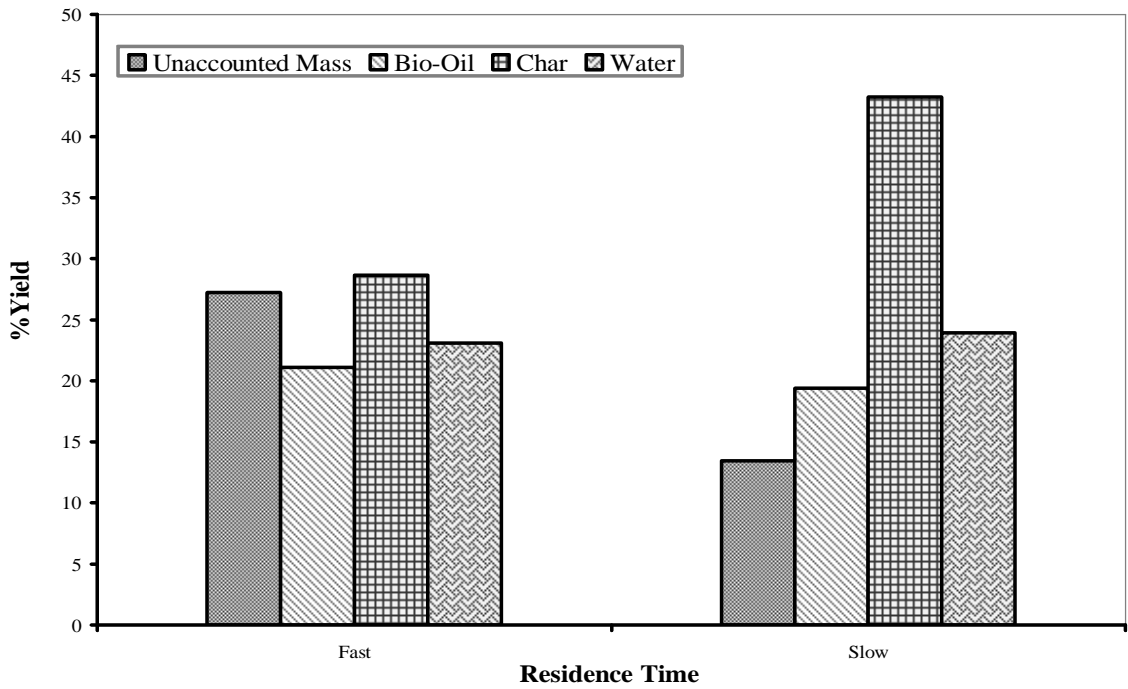


Figure A.24 Average Reactor Yields of Mississippi State-Pine Bark-Low Temperature (MS-PB-LT) Bio-Oils

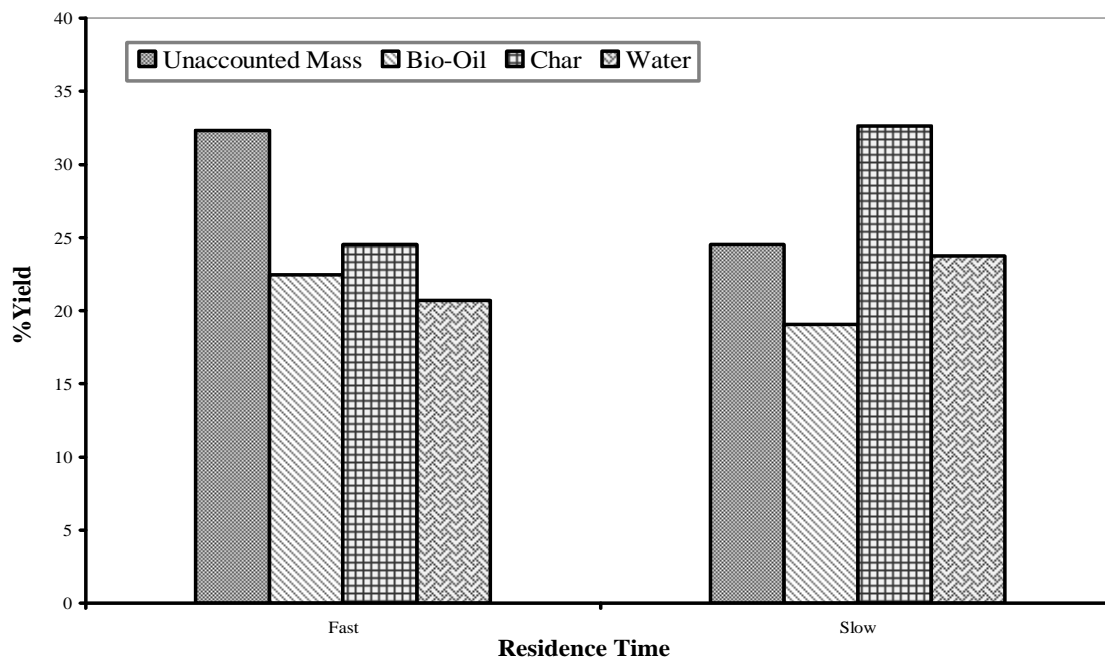


Figure A.25 Average Reactor Yields of Mississippi State-Pine Bark-High Temperature (MS-PB-HT) Bio-Oils

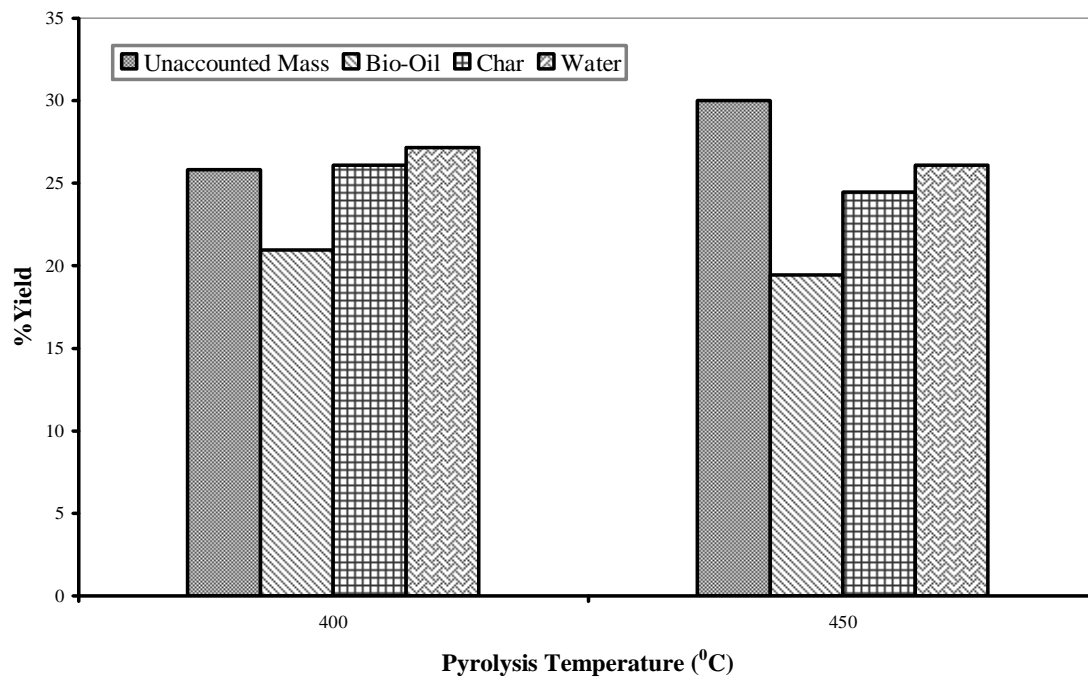


Figure A.26 Average Reactor Yields of Mississippi State-Oak Bark-Slow Residence (MS-OB-SR) Bio-Oils

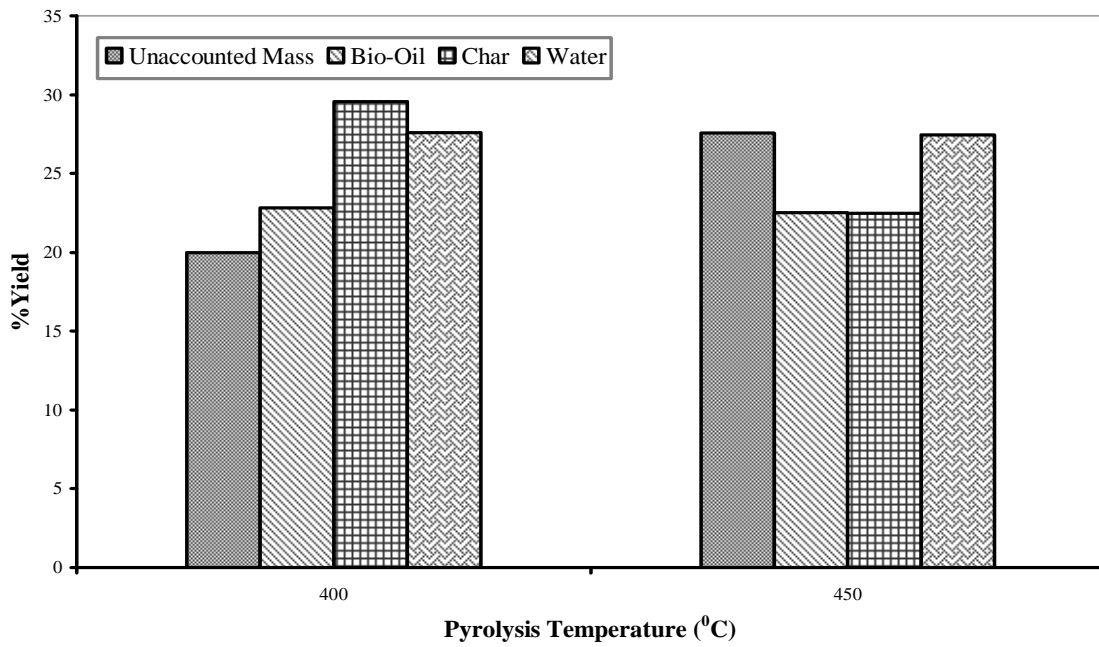


Figure A.27 Average Reactor Yields of Mississippi State-Oak Bark-Fast Residence (MS-OB-FR) Bio-Oils

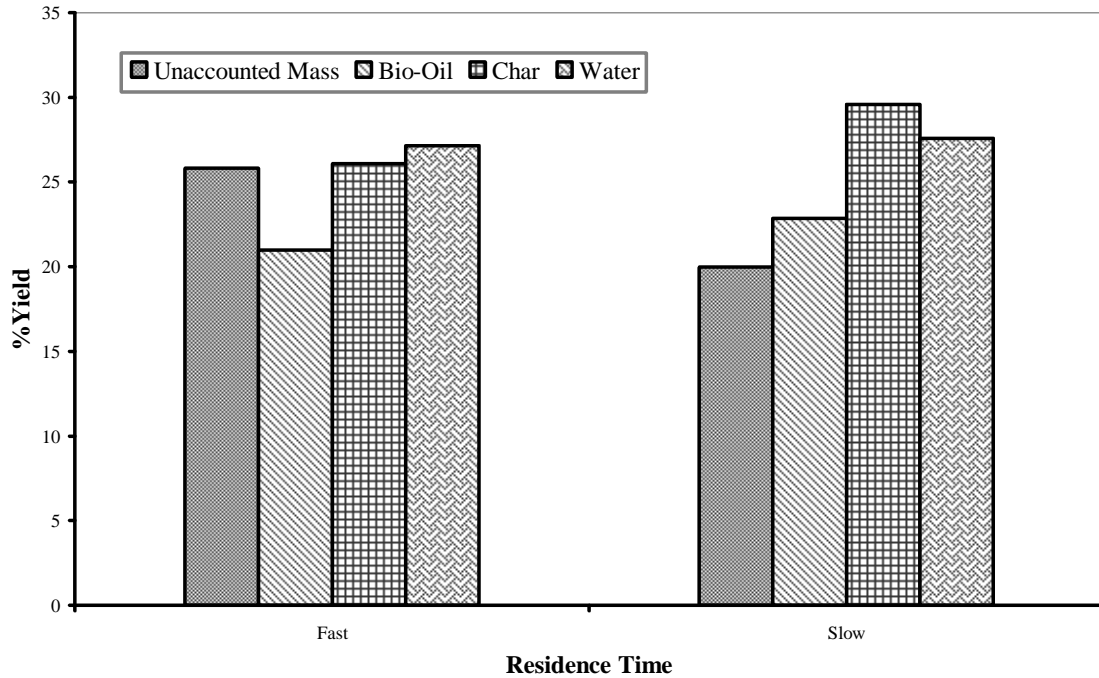


Figure A.28 Average Reactor Yields of Mississippi State-Oak Bark-Low Temperature (MS-OB-LT) Bio-Oils

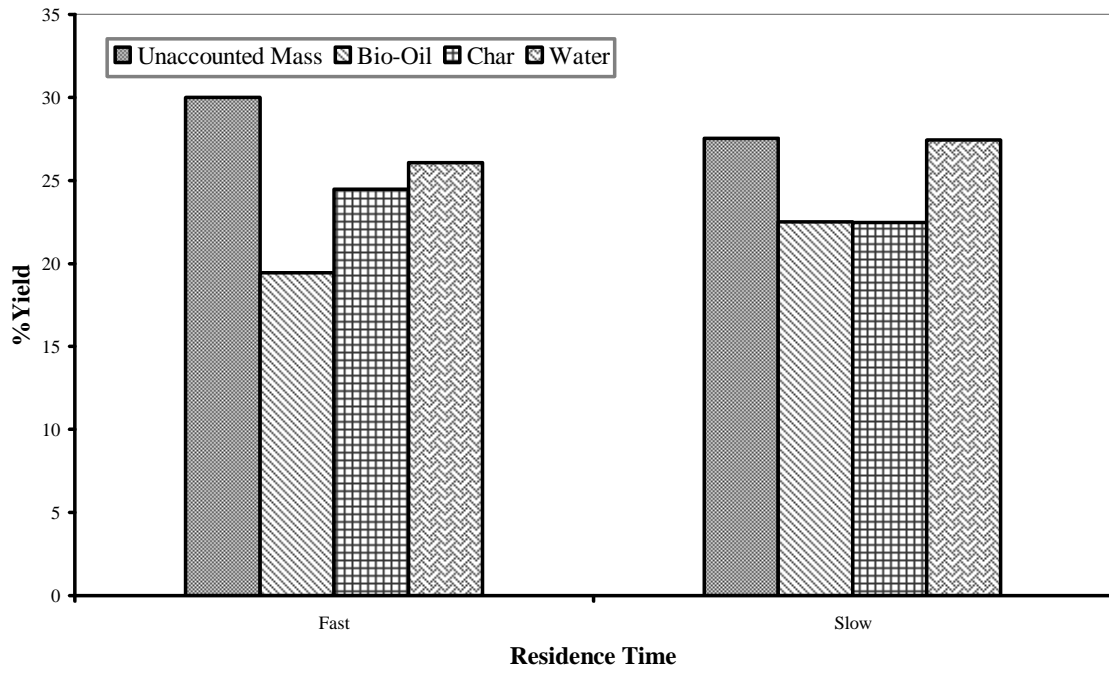


Figure A.29 Average Reactor Yields of Mississippi State-Oak Bark-High Temperature (MS-OB-HT) Bio-Oils

APPENDIX B
(PRELIMINARY STABILITY TESTING-TRIAL RUNS)

APPENDIX B

This Appendix presents the results obtained from preliminary stability testing or trial runs of Mississippi State University (MSU) pyrolysis oils. These trial runs were conducted to evaluate the stability of frequently tested and refrigerated (4 °C) pyrolysis oils. The frequently tested pyrolysis oils underwent the temperature transition from 4 to 25 °C and back. However, the refrigerated oils were constantly stored at 4 °C. Figures 1-4 show the stability of frequently tested pine wood oils as a function of aging time based on their viscosity, water content, pH, and density respectively. The viscosity plot in Figure 1 however reveals the stability performance of frequently tested pine wood oils in reference with the refrigerated pine wood oils. Figures 5-8 represent the viscosity of refrigerated and frequently tested pine wood and oak wood oils alternatively.

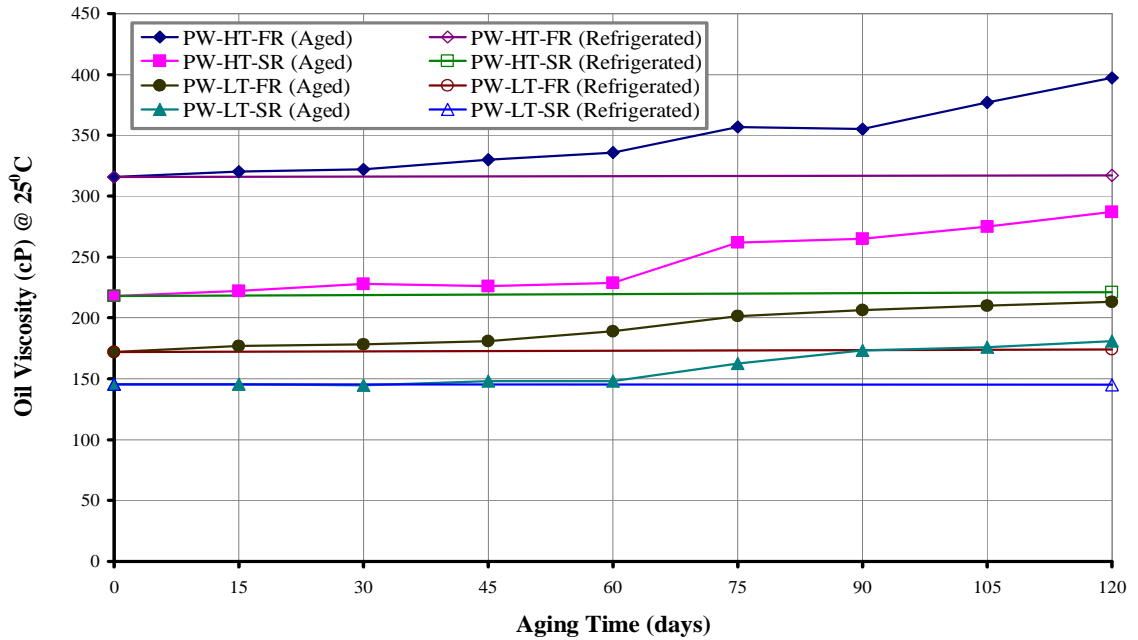


Figure B.1 Viscosity (cP) as a Function of Aging Time (days) of Pine Wood (PW) Pyrolysis Oils [Temperature (LT-Low and High-HT) and Time (SR-Slow and Fast-FR)] of Mississippi State University

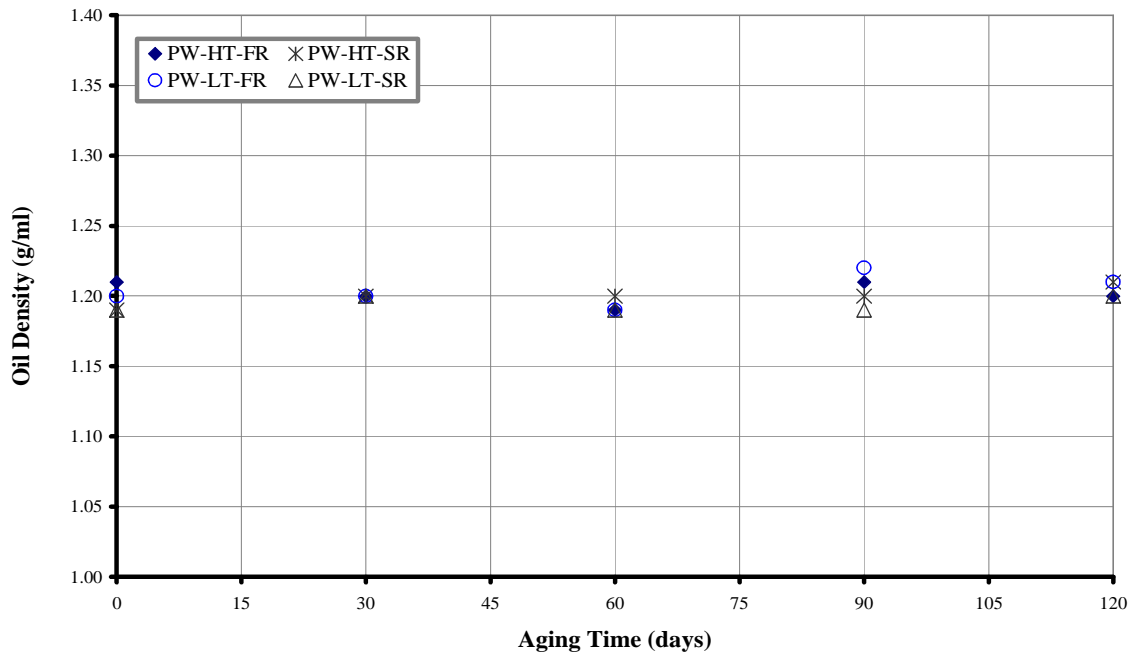


Figure B.2 Density (g/ml) as a Function of Aging Time (days) of Pine Wood (PW) Pyrolysis Oils [Temperature (LT-Low and High-HT) and Time (SR-Slow and Fast-FR)] of Mississippi State University

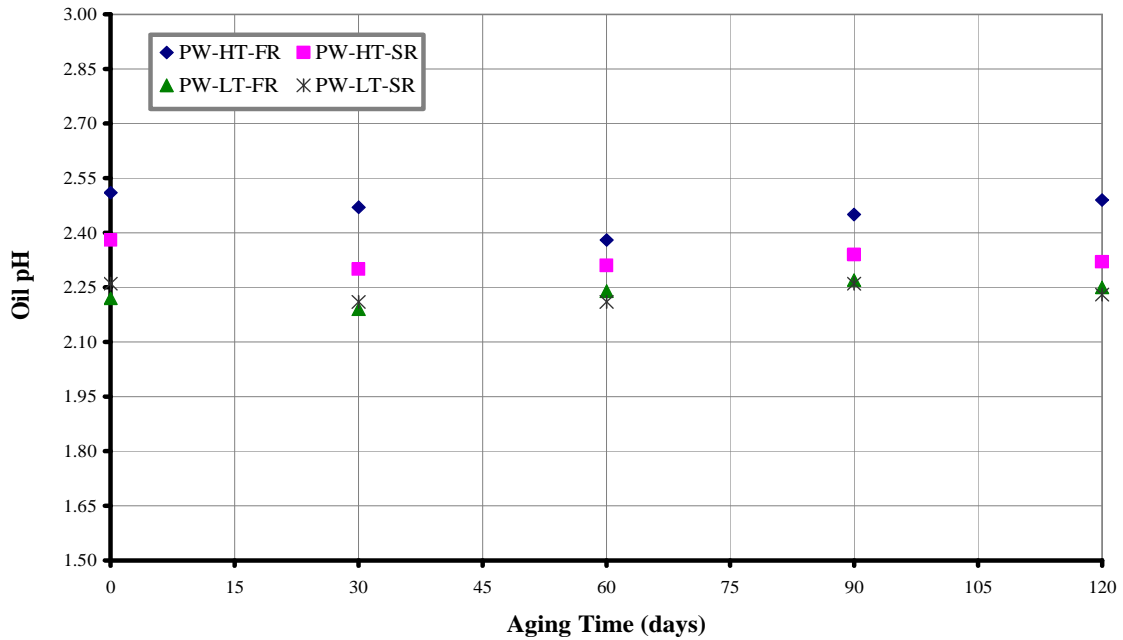


Figure B.3 Acidity (pH) as a Function of Aging Time (days) of Pine Wood (PW) Pyrolysis Oils [Temperature (LT-Low and High-HT) and Time (SR-Slow and Fast-FR)] of Mississippi State University

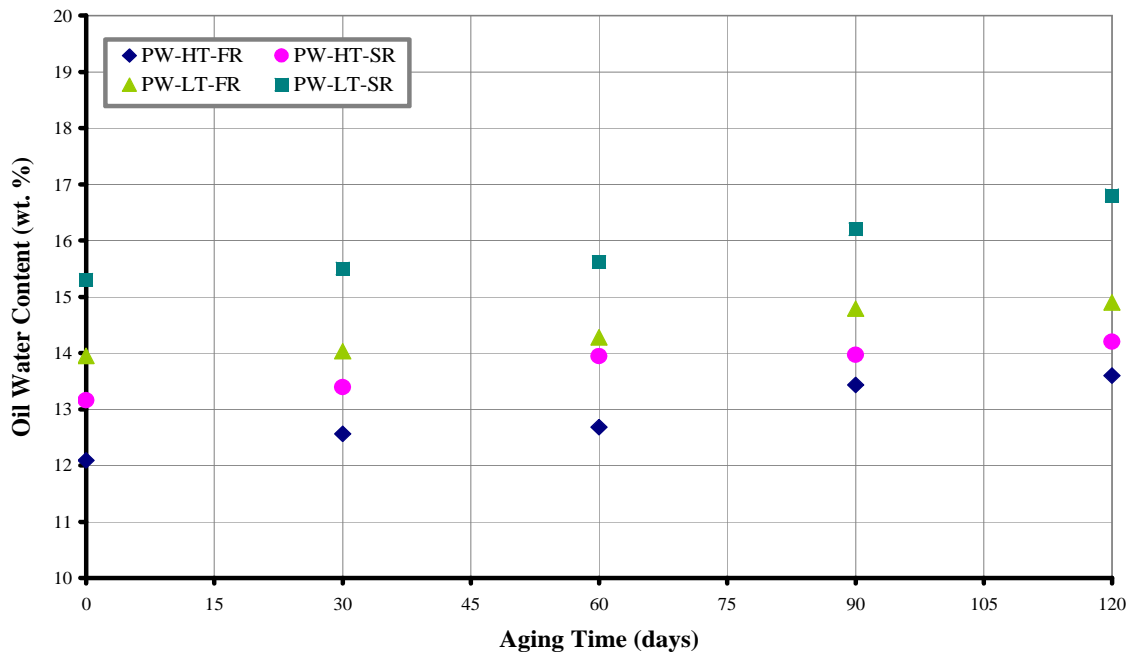


Figure B.4 Water Content (wt.%) as a Function of Aging Time (days) of Pine Wood (PW) Pyrolysis Oils [Temperature (LT-Low and High-HT) and Time (SR-Slow and Fast-FR)] of Mississippi State University

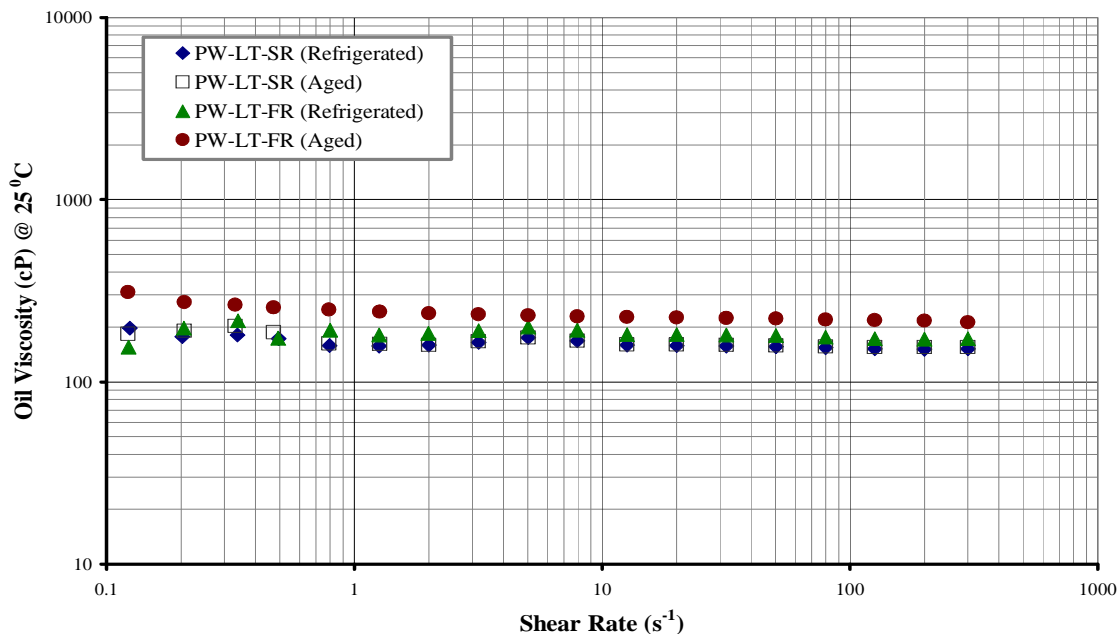


Figure B.5 Viscosity (cP) as a Function of Shear Rate (s^{-1}) and Residence Time (SR-Slow and Fast-FR) of Pine Wood (PW) Low Temperature (LT) Oils of Mississippi State University

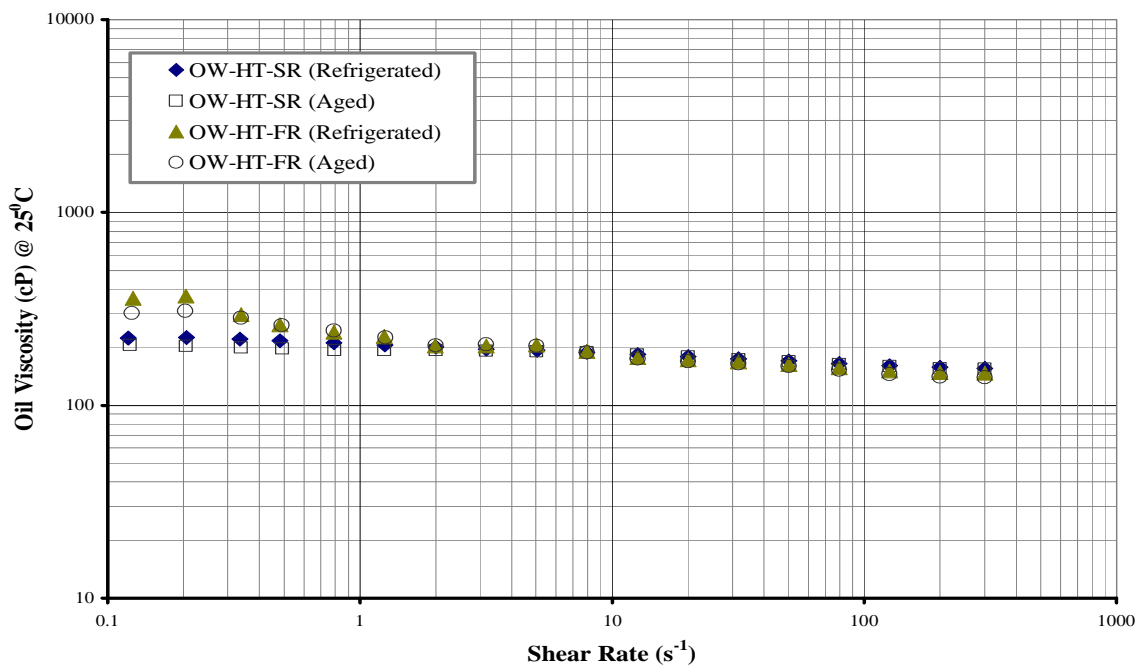


Figure B.6 Viscosity (cP) as a Function of Shear Rate (s^{-1}) and Residence Time (SR-Slow and Fast-FR) of Oak Wood (OW) High Temperature (HT) Oils of Mississippi State University

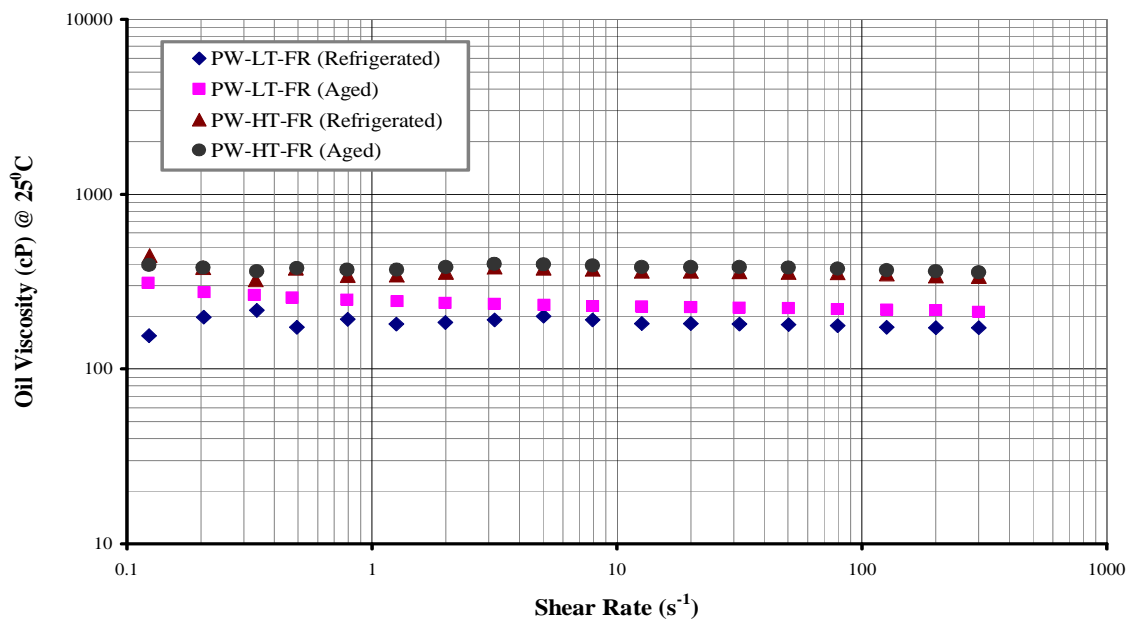


Figure B.7 Viscosity (cP) as a Function of Shear Rate (s^{-1}) and Pyrolysis Temperature (LT-Low and High-HT) of Pine Wood (PW) Fast Residence (FR) Oils of Mississippi State University

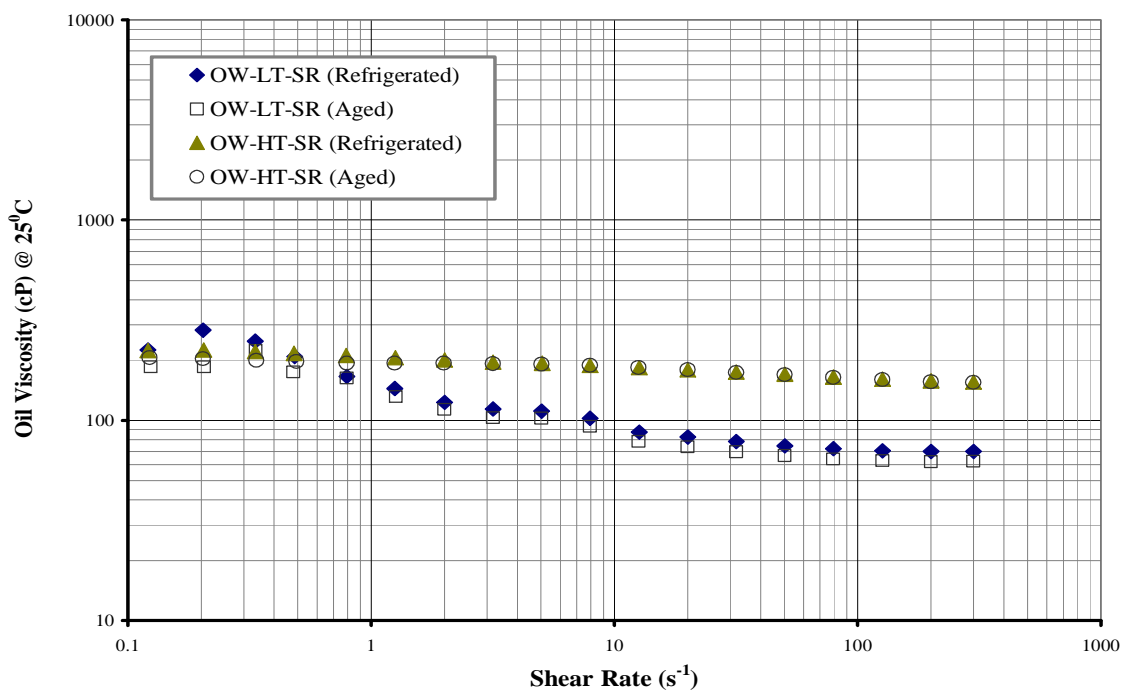


Figure B.8 Viscosity (cP) as a Function of Shear Rate (s^{-1}) and Pyrolysis Temperature (LT-Low and High-HT) of Oak Wood (OW) Slow Residence (SR) Oils of Mississippi State University

APPENDIX C
(ADDITIVE PRESCREENING-PHASE II)

APPENDIX C

This Appendix presents the results obtained from the additive prescreening studies or Phase II. These studies were performed using pine wood pyrolysis oil (high temperature) of Mississippi State University (MSU). The overall objective of this phase was to select three best additives (out of 26) based on their stability performance. An additive concentration of 10 wt.% was utilized during this phase with the storage temperature being 80 °C. The viscosity of additive blended pyrolysis oils as a function of shear rate (s^{-1}) and storage time (hr) is shown in Figures 1-23. The viscosity increase (%) of additive blended pyrolysis oils as a function shear rate (s^{-1}) is shown Figures 24-44. The ‘initial and final’ storage times of ‘0 and 192 hr’ were utilized to compute the viscosity increase (%) in the above figures. It should be noted that the viscosity measurements in Figures 1-44 were performed at a temperature of 25 °C. The viscosity of additive blended pyrolysis oils as a function of storage time (hr) and storage temperature (°C) is shown in Figures 45-66. The viscosity of the pine wood pyrolysis oils in these figures corresponds to a shear rate of 100 s^{-1} .

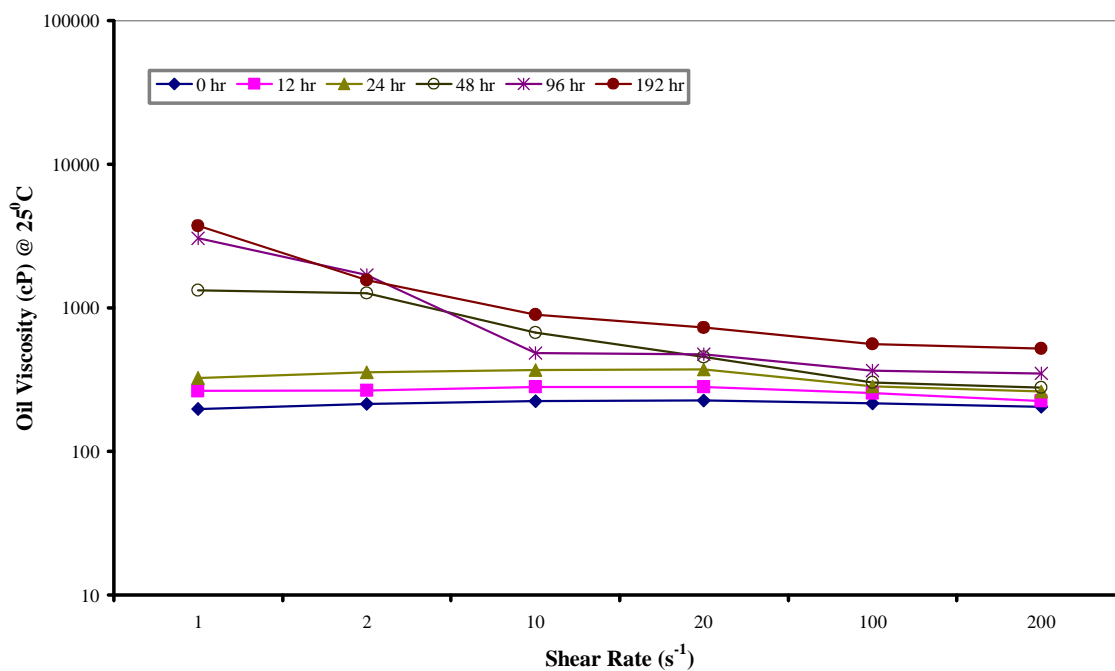


Figure C.1 Viscosity (cP) of Methyl Tertiary Butyl Ether Blended Pyrolysis Oil (10 wt.%) Measured as a Function of Shear Rate (s^{-1}) and Storage Time (hr)

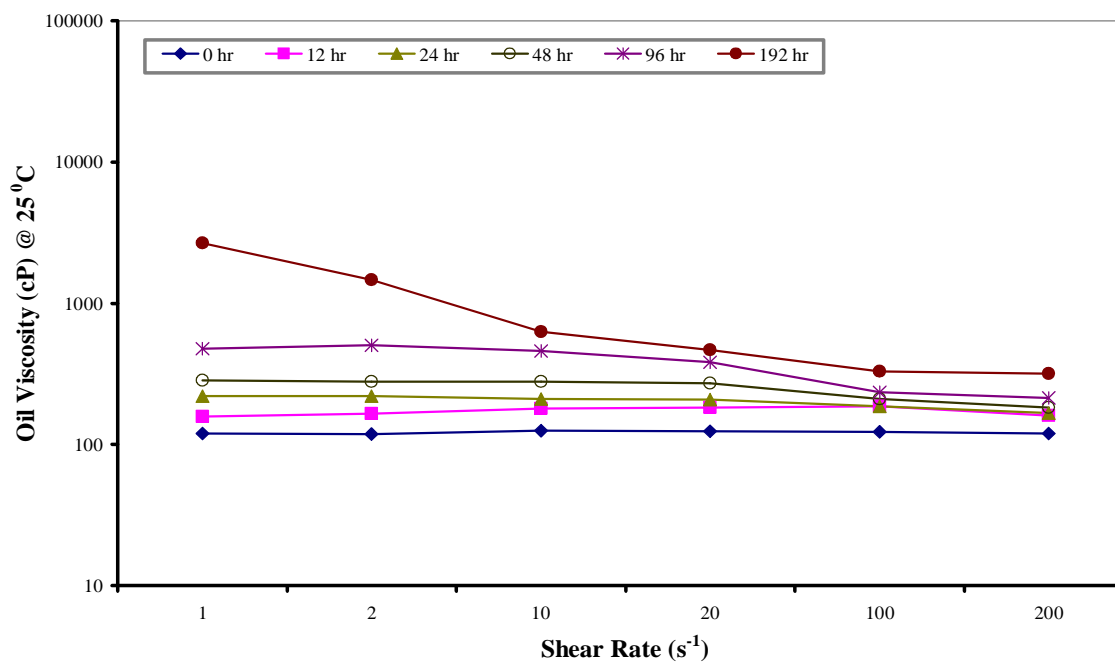


Figure C.2 Viscosity (cP) of Methyl Ethyl Ketone Blended Pyrolysis Oil (10 wt.%) Measured as a Function of Shear Rate (s^{-1}) and Storage Time (hr)

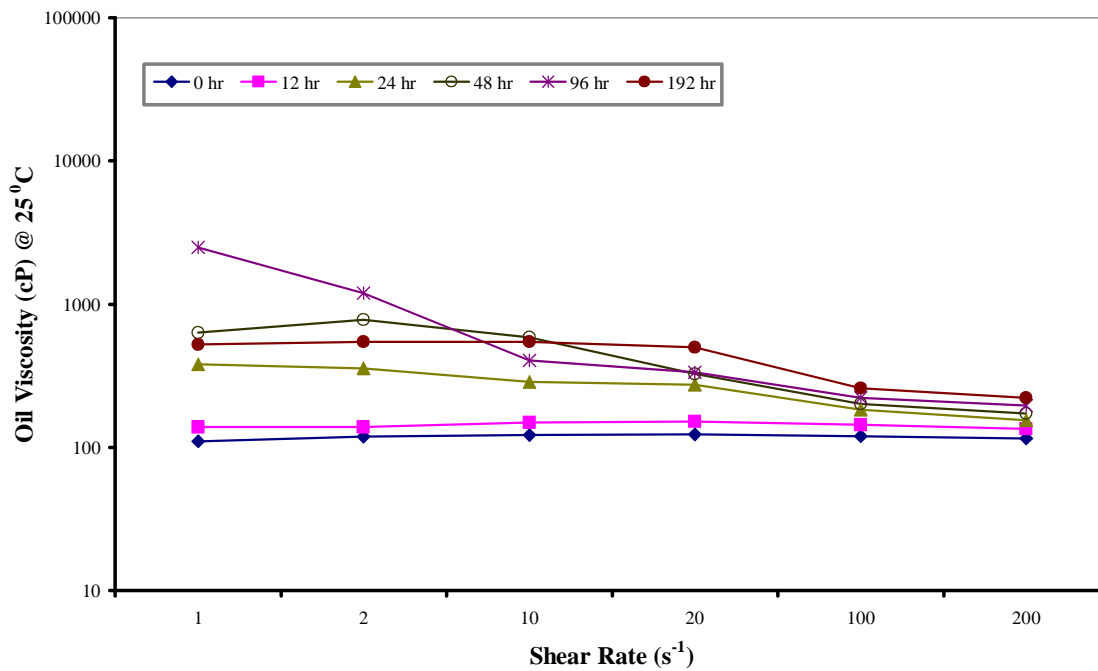


Figure C.3 Viscosity (cP) of Ethanol Blended Pyrolysis Oil (10 wt.%) Measured as a Function of Shear Rate (s⁻¹) and Storage Time (hr)

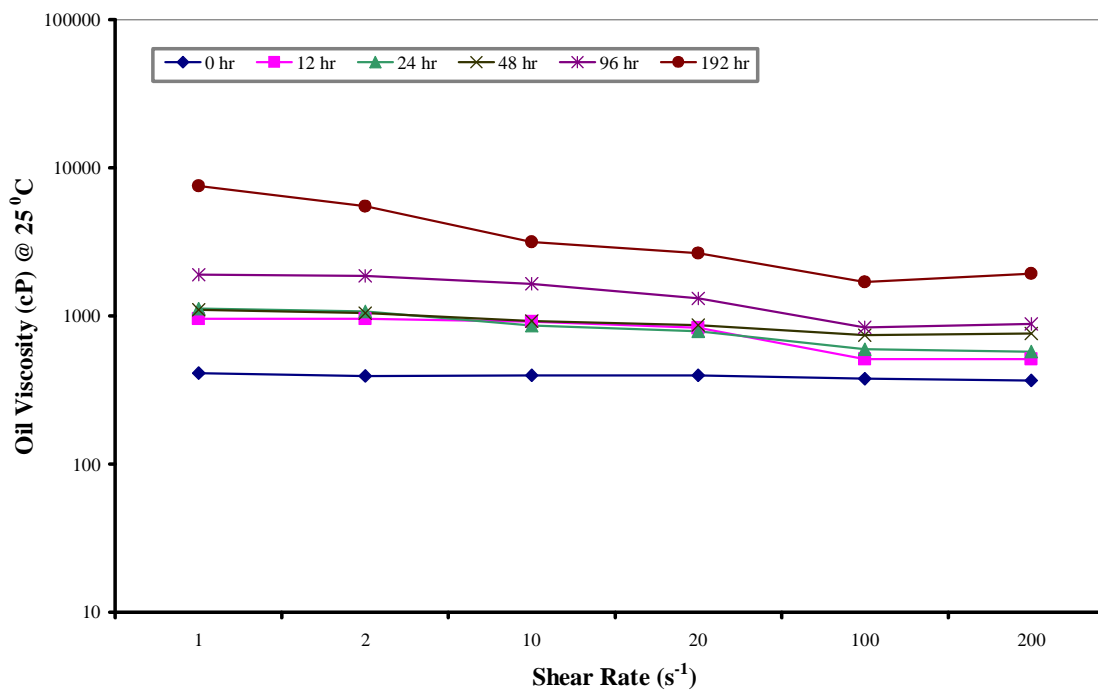


Figure C.4 Viscosity (cP) of Decahydronaphthalene Blended Pyrolysis Oil (10 wt.%) Measured as a Function of Shear Rate (s⁻¹) and Storage Time (hr)

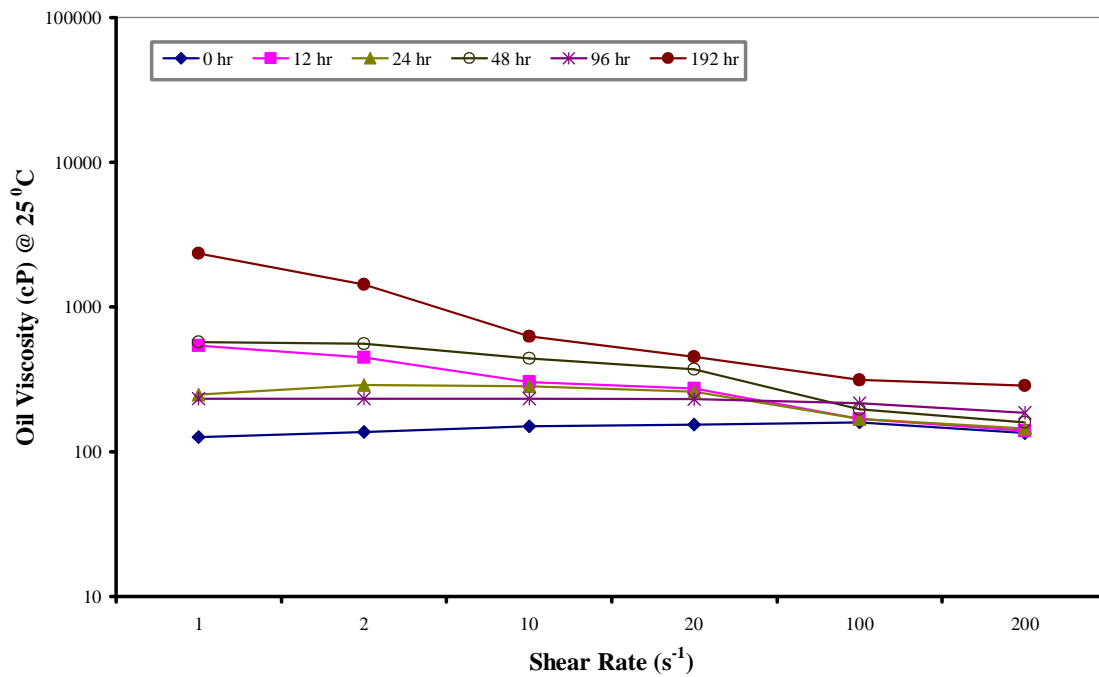


Figure C.5 Viscosity (cP) of Acetone Blended Pyrolysis Oil (10 wt.%) Measured as a Function of Shear Rate (s^{-1}) and Storage Time (hr)

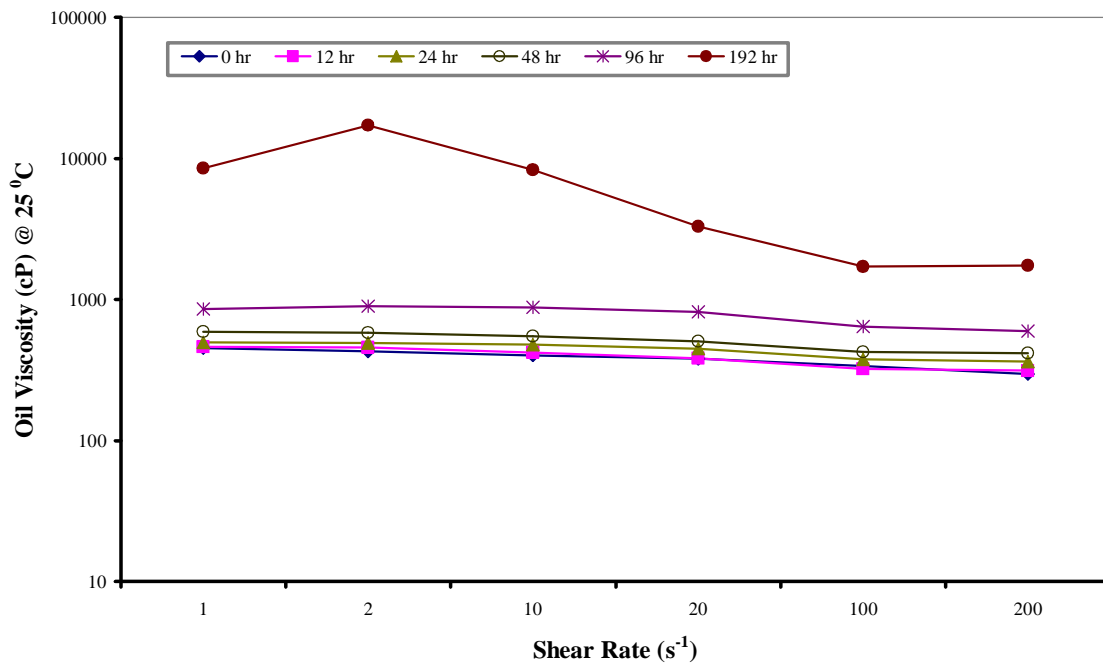


Figure C.6 Viscosity (cP) of Xylene Blended Pyrolysis Oil (10 wt.%) Measured as a Function of Shear Rate (s^{-1}) and Storage Time (hr)

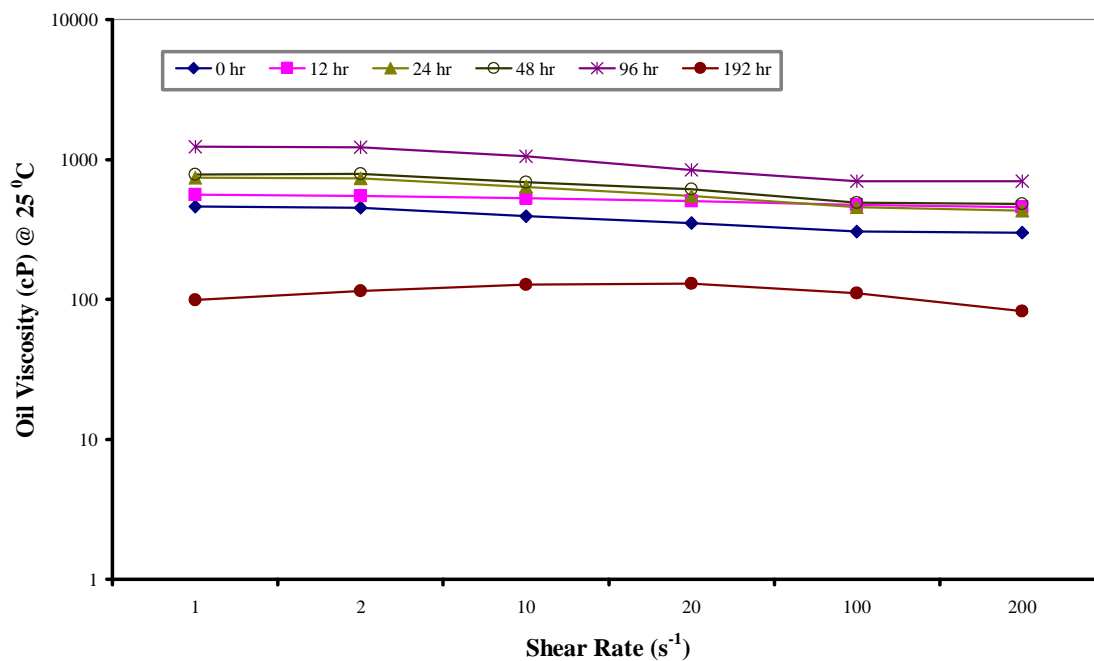


Figure C.7 Viscosity (cP) of Tetrahydronaphthalene Blended Pyrolysis Oil (10 wt.%) Measured as a Function of Shear Rate (s^{-1}) and Storage Time (hr)

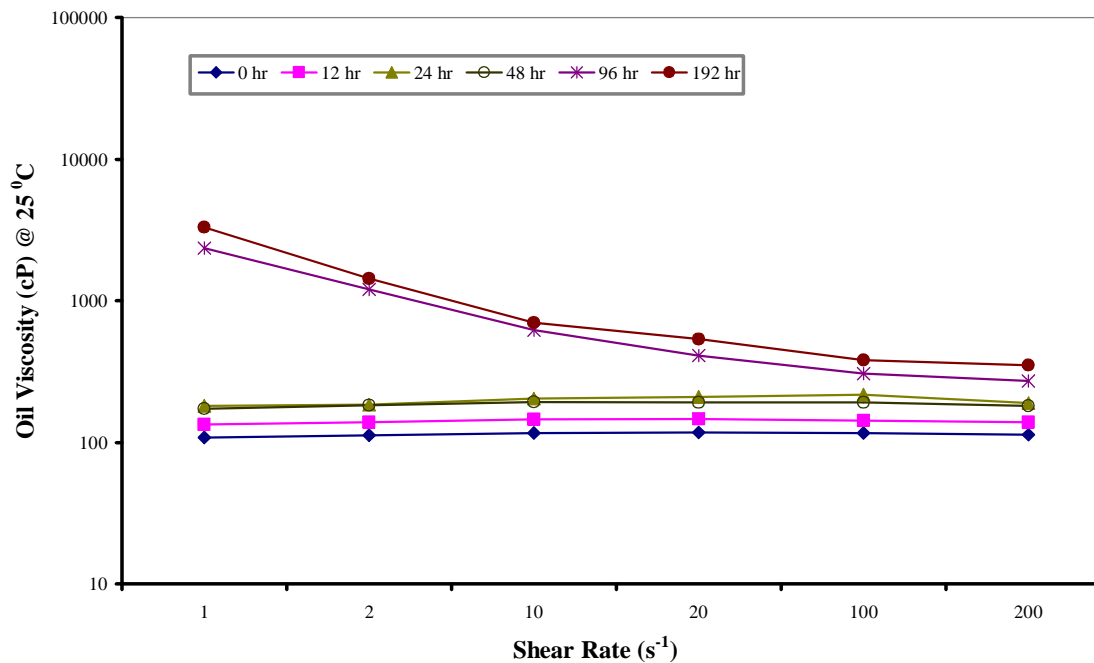


Figure C.8 Viscosity (cP) of Methyl Formate Blended Pyrolysis Oil (10 wt.%) Measured as a Function of Shear Rate (s^{-1}) and Storage Time (hr)

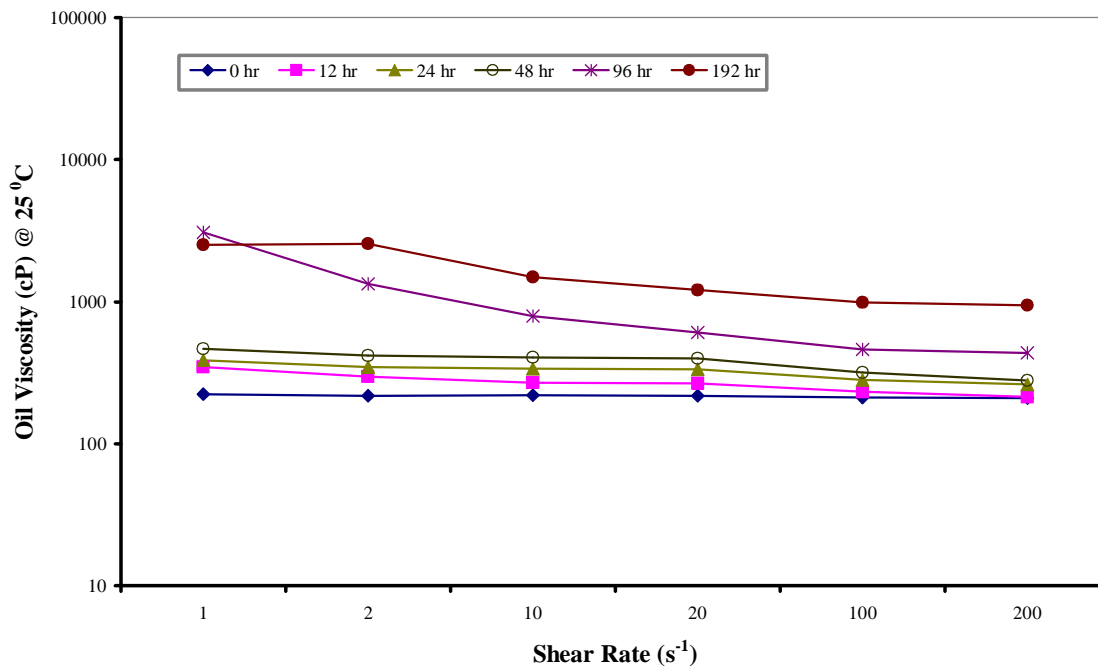


Figure C.9 Viscosity (cP) of Isopropyl Ether Blended Pyrolysis Oil (10 wt.%) Measured as a Function of Shear Rate (s⁻¹) and Storage Time (hr)

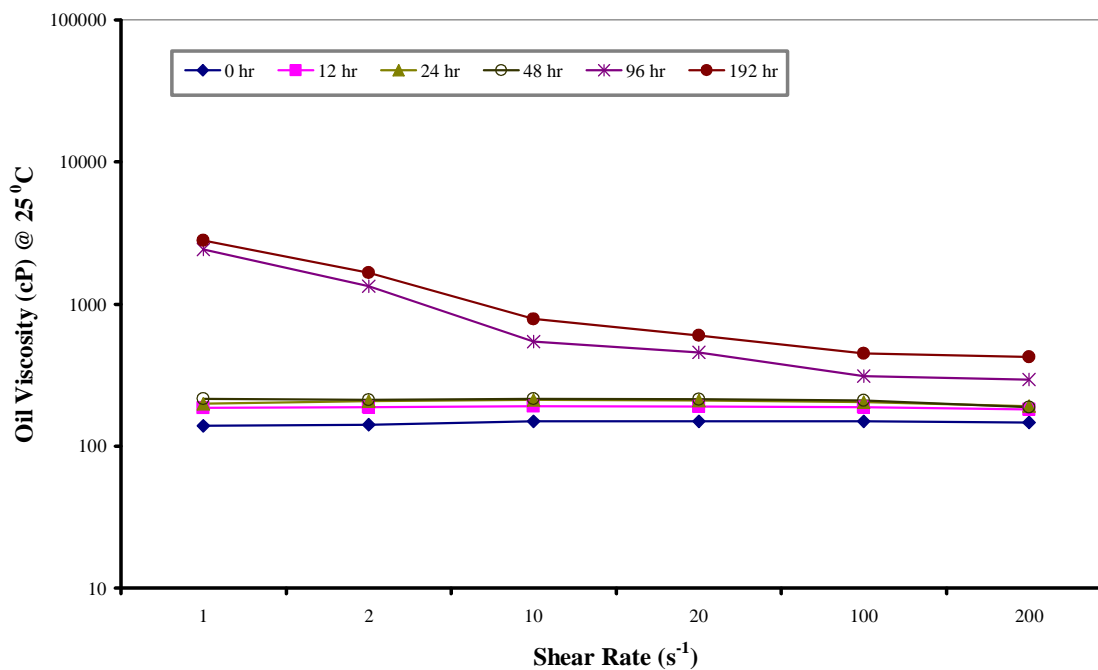


Figure C.10 Viscosity (cP) of Ethyl Ether Blended Pyrolysis Oil (10 wt.%) Measured as a Function of Shear Rate (s⁻¹) and Storage Time (hr)

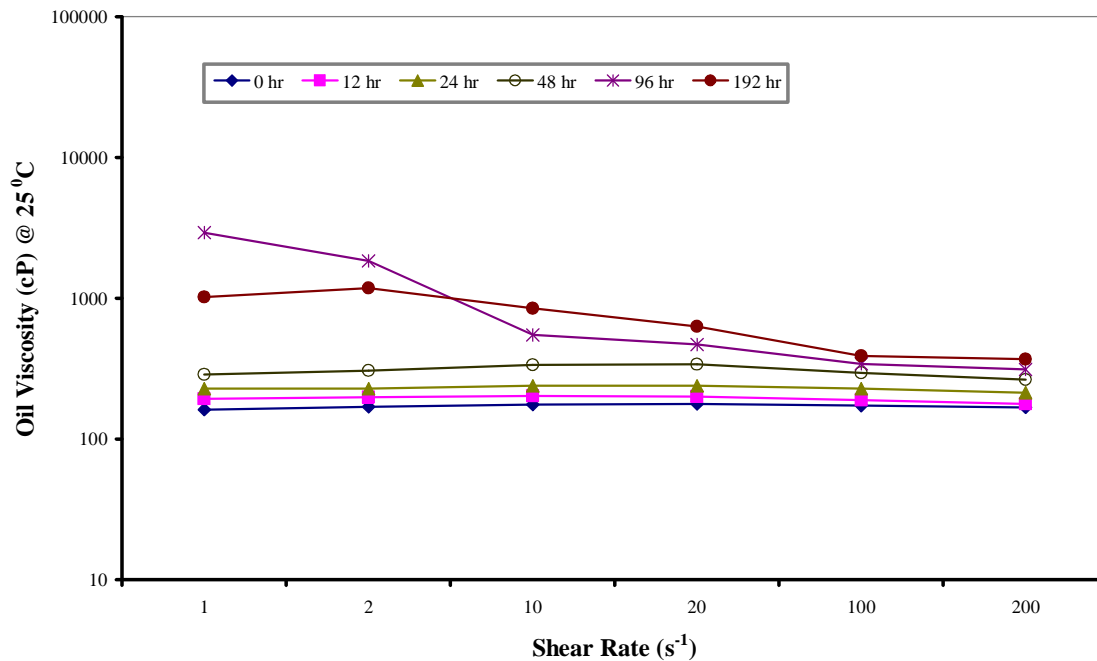


Figure C.11 Viscosity (cP) of Cyclopentanone Blended Pyrolysis Oil (10 wt.%) Measured as a Function of Shear Rate (s⁻¹) and Storage Time (hr)

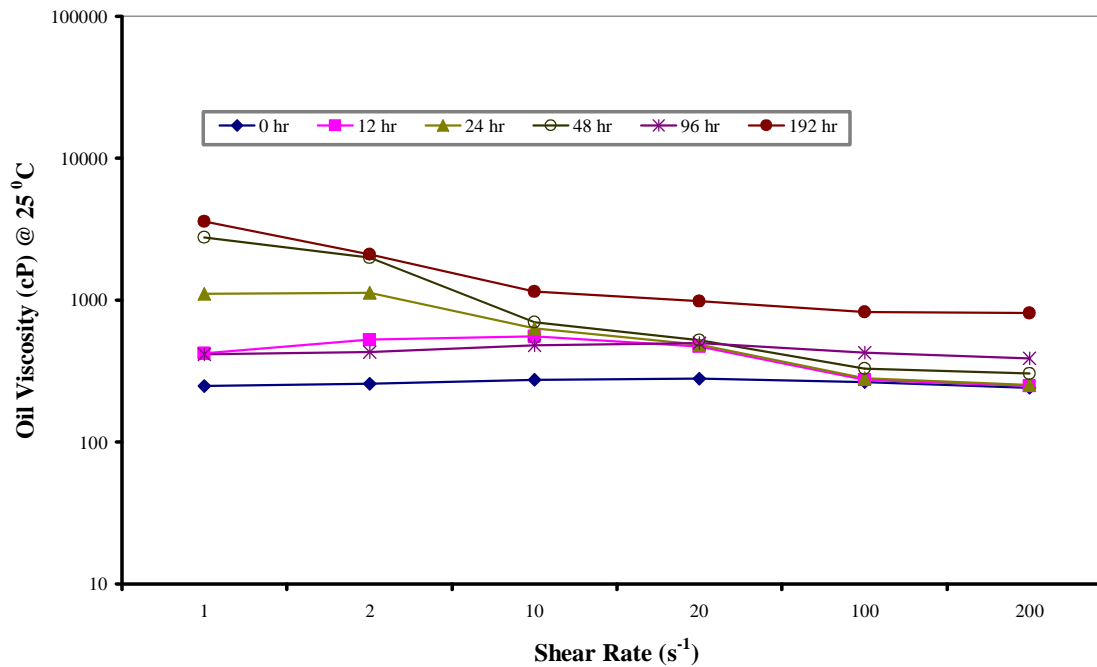


Figure C.12 Viscosity (cP) of Acetaldehyde Blended Pyrolysis Oil (10 wt.%) Measured as a Function of Shear Rate (s⁻¹) and Storage Time (hr)

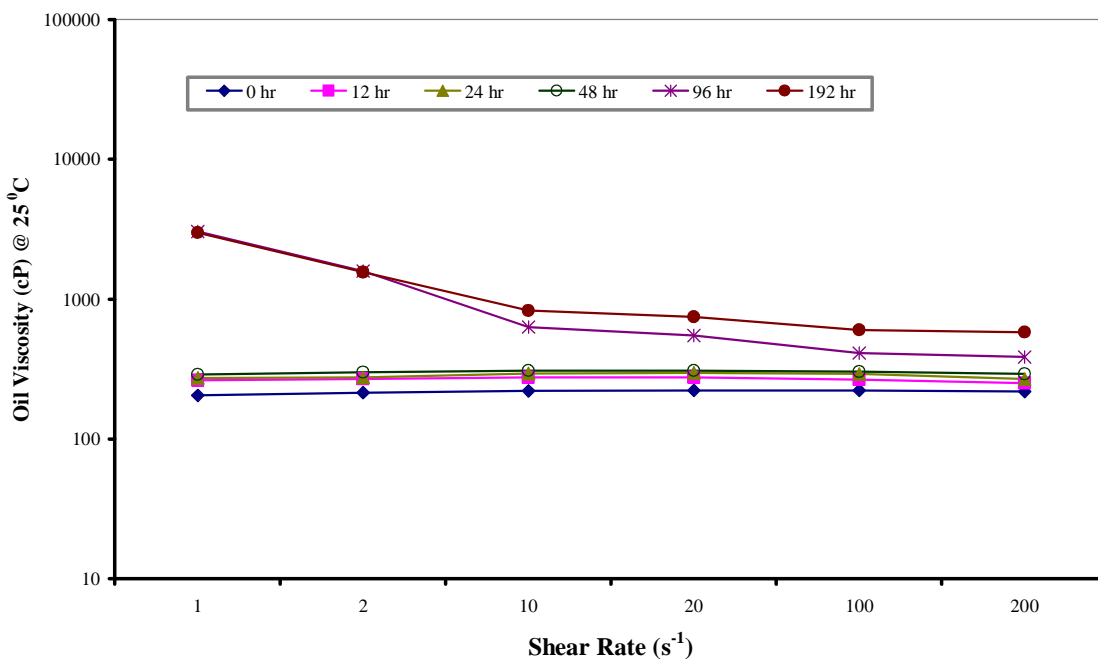


Figure C.13 Viscosity (cP) of t-Butanol Blended Pyrolysis Oil (10 wt.%) Measured as a Function of Shear Rate (s^{-1}) and Storage Time (hr)

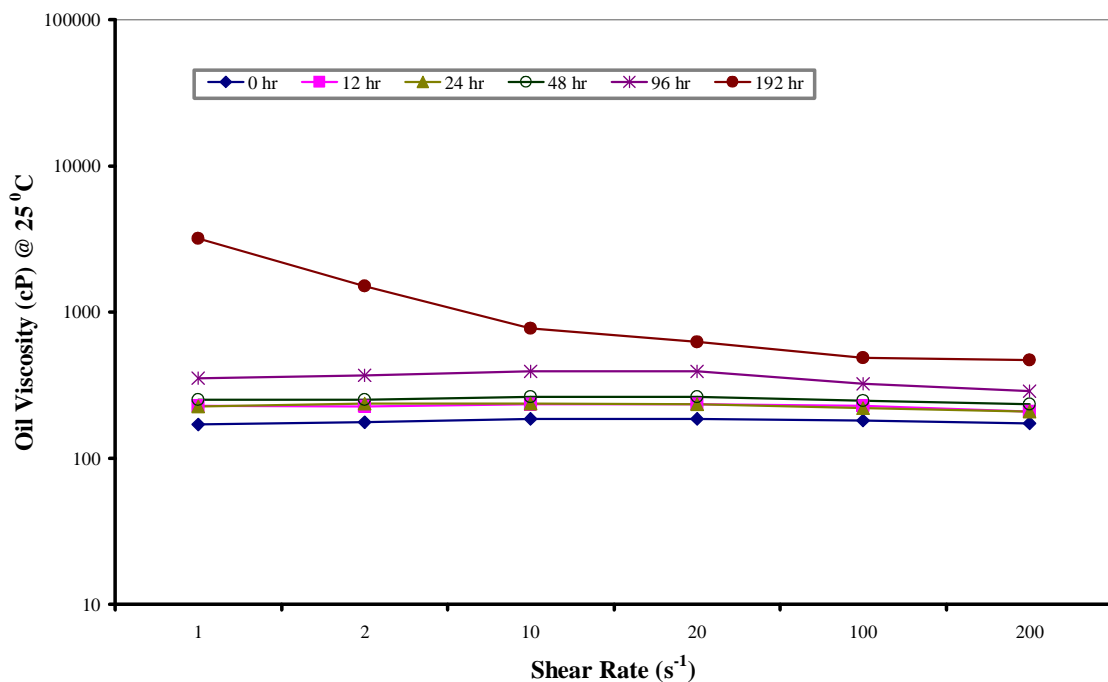


Figure C.14 Viscosity (cP) of Tetrahydrofuran Blended Pyrolysis Oil (10 wt.%) Measured as a Function of Shear Rate (s^{-1}) and Storage Time (hr)

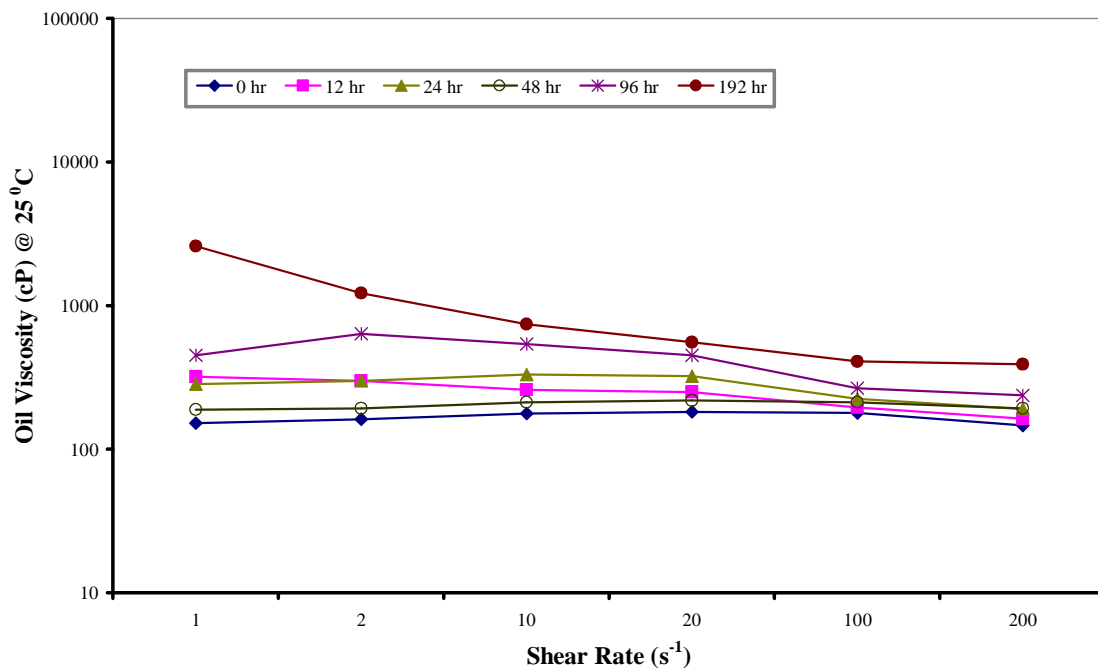


Figure C.15 Viscosity (cP) of Methyl Acetate Blended Pyrolysis Oil (10 wt.%) Measured as a Function of Shear Rate (s⁻¹) and Storage Time (hr)

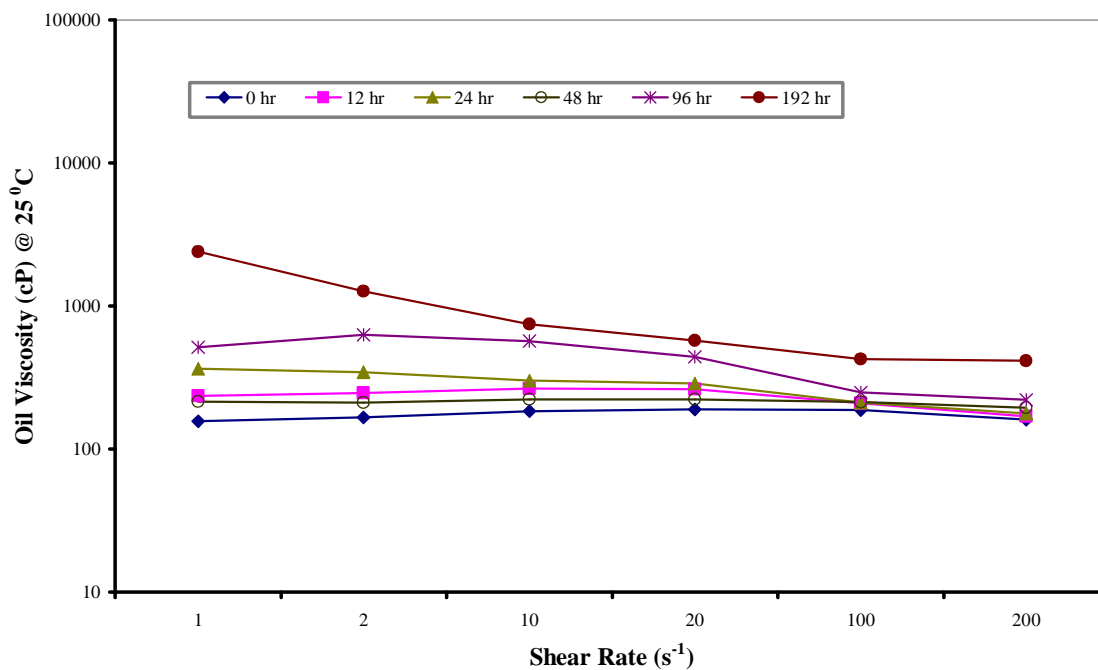


Figure C.16 Viscosity (cP) of Ethyl Acetate Blended Pyrolysis Oil (10 wt.%) Measured as a Function of Shear Rate (s⁻¹) and Storage Time (hr)

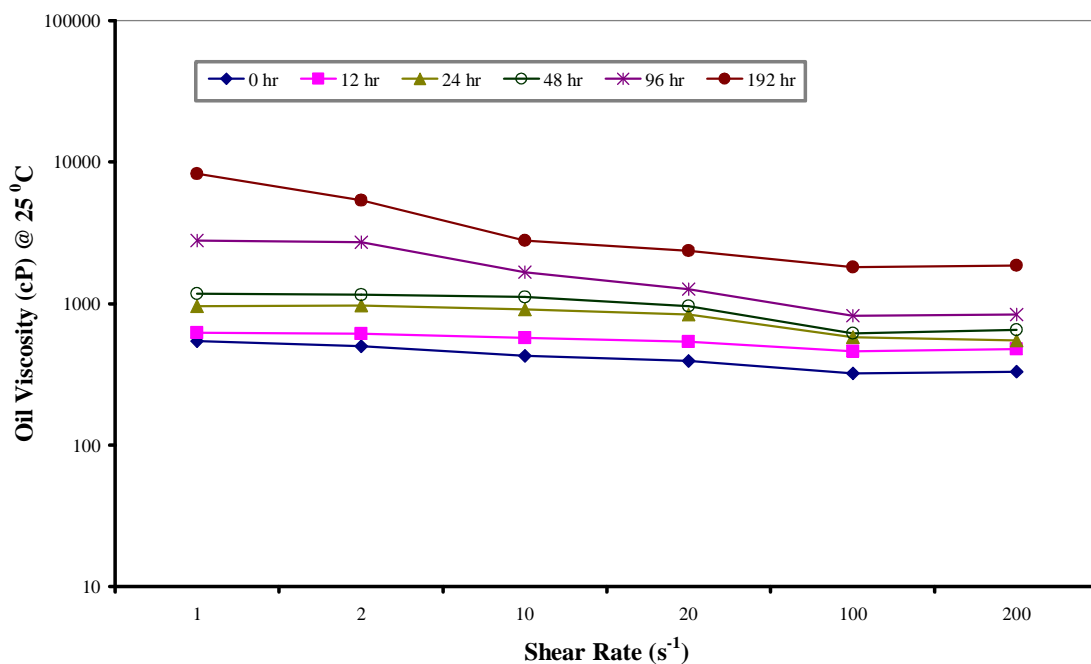


Figure C.17 Viscosity (cP) of Cyclohexane Blended Pyrolysis Oil (10 wt.%) Measured as a Function of Shear Rate (s⁻¹) and Storage Time (hr)

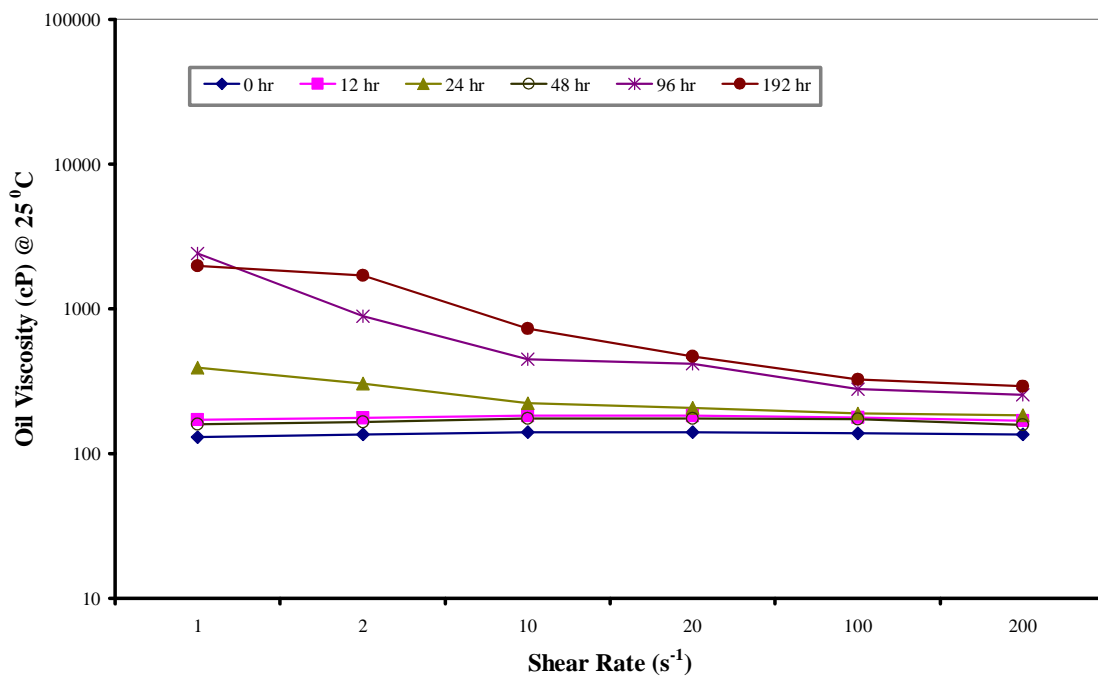


Figure C.18 Viscosity (cP) of 2-Propanol Blended Pyrolysis Oil (10 wt.%) Measured as a Function of Shear Rate (s⁻¹) and Storage Time (hr)

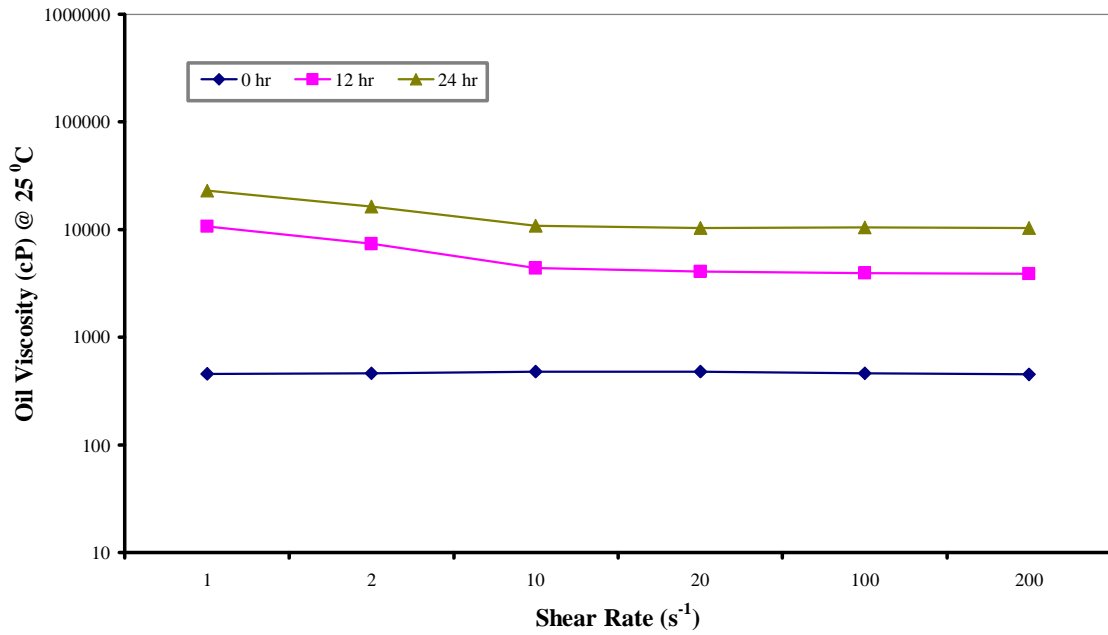


Figure C.19 Viscosity (cP) of Resorcinol Blended Pyrolysis Oil (10 wt.%) Measured as a Function of Shear Rate (s⁻¹) and Storage Time (hr)

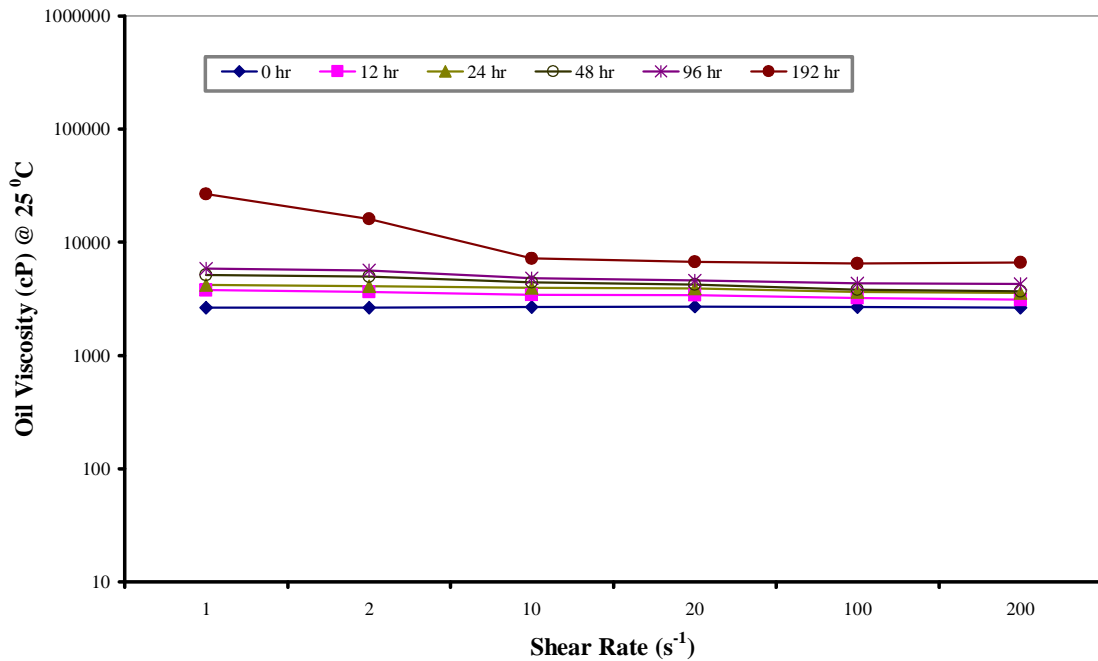


Figure C.20 Viscosity (cP) of Polyethylene Glycol Blended Pyrolysis Oil (10 wt.%) Measured as a Function of Shear Rate (s⁻¹) and Storage Time (hr)

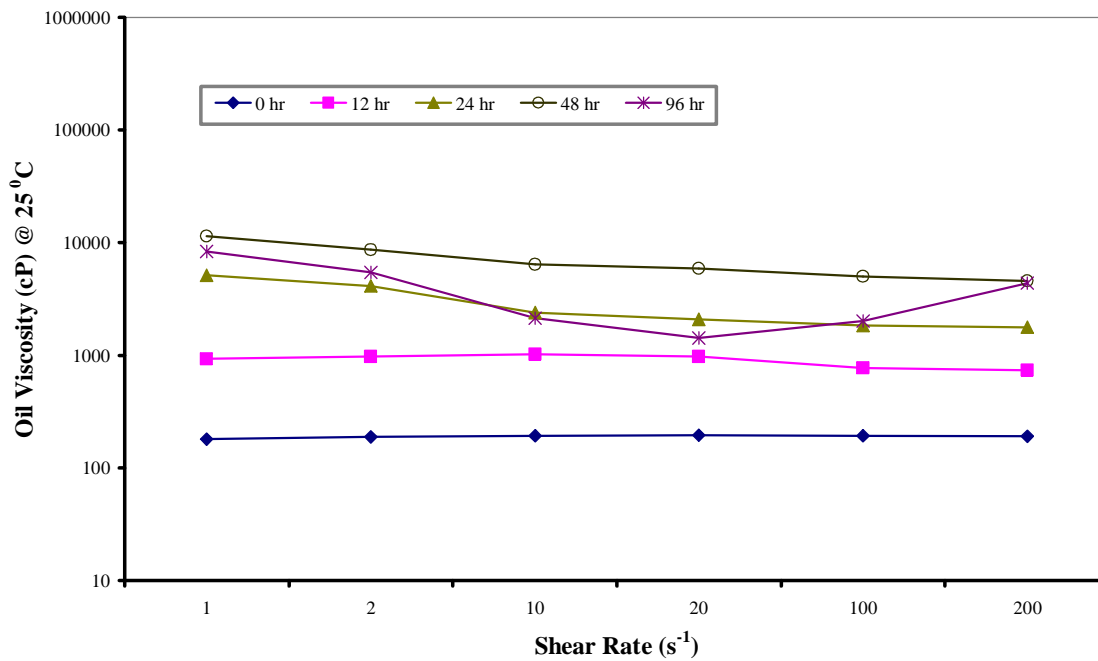


Figure C.21 Viscosity (cP) of Furfuryl Alcohol Blended Pyrolysis Oil (10 wt.%) Measured as a Function of Shear Rate (s^{-1}) and Storage Time (hr)

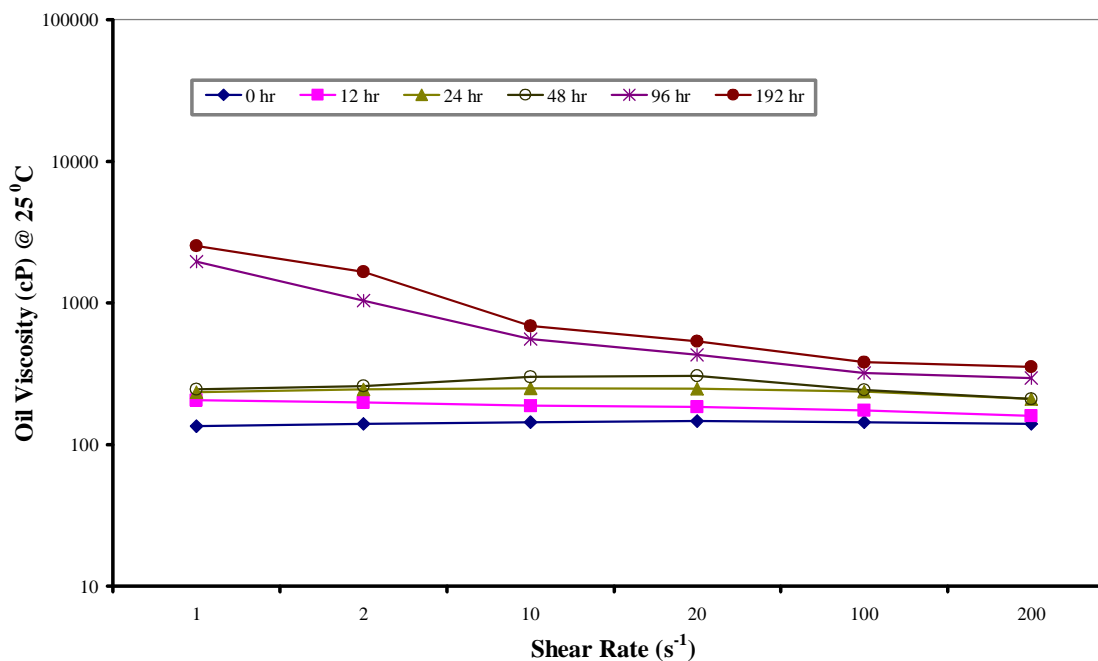


Figure C.22 Viscosity (cP) of Dimethyl Ether Blended Pyrolysis Oil (10 wt.%) Measured as a Function of Shear Rate (s^{-1}) and Storage Time (hr)

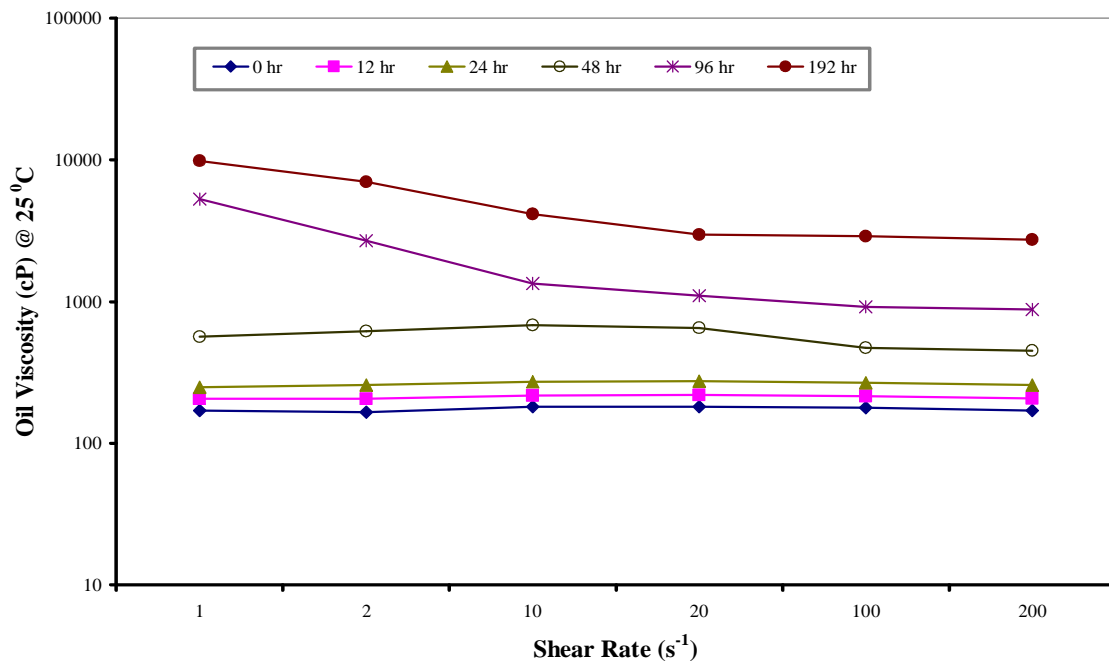


Figure C.23 Viscosity (cP) of 2-Furaldehyde Blended Pyrolysis Oil (10 wt.%) Measured as a Function of Shear Rate (s^{-1}) and Storage Time (hr)

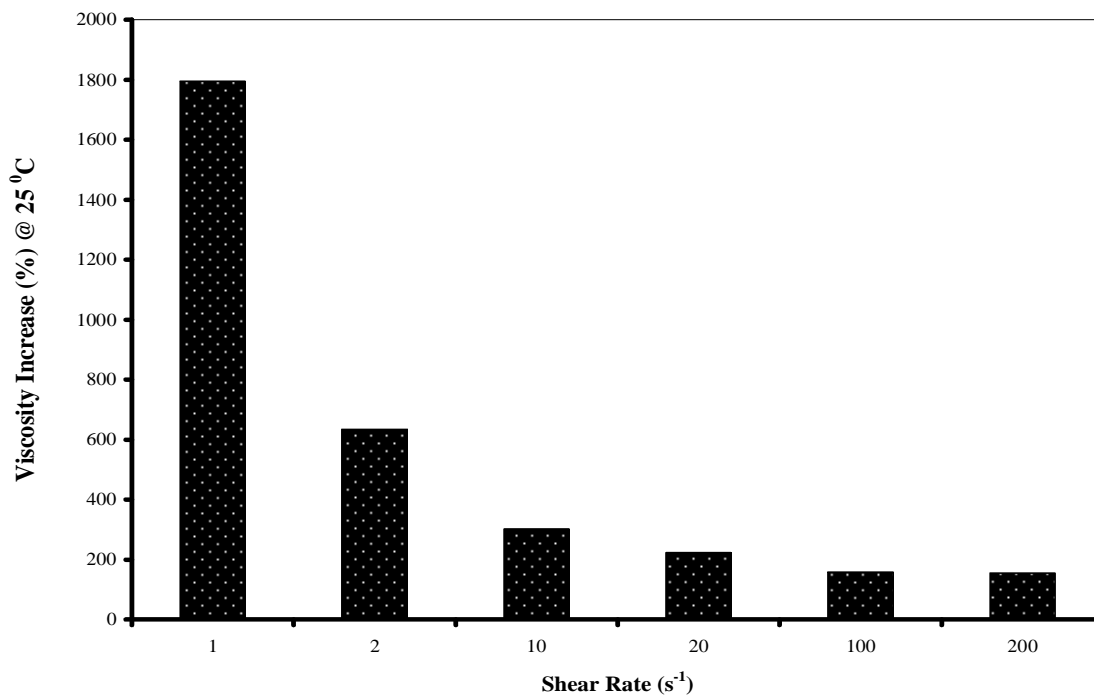


Figure C.24 Percentage Increase in Viscosity (0 hr vs. 192 hr) of Methyl tertiary Butyl Ether Blended Pyrolysis Oil (10 wt.%) Obtained as a Function of Shear Rate (s^{-1})

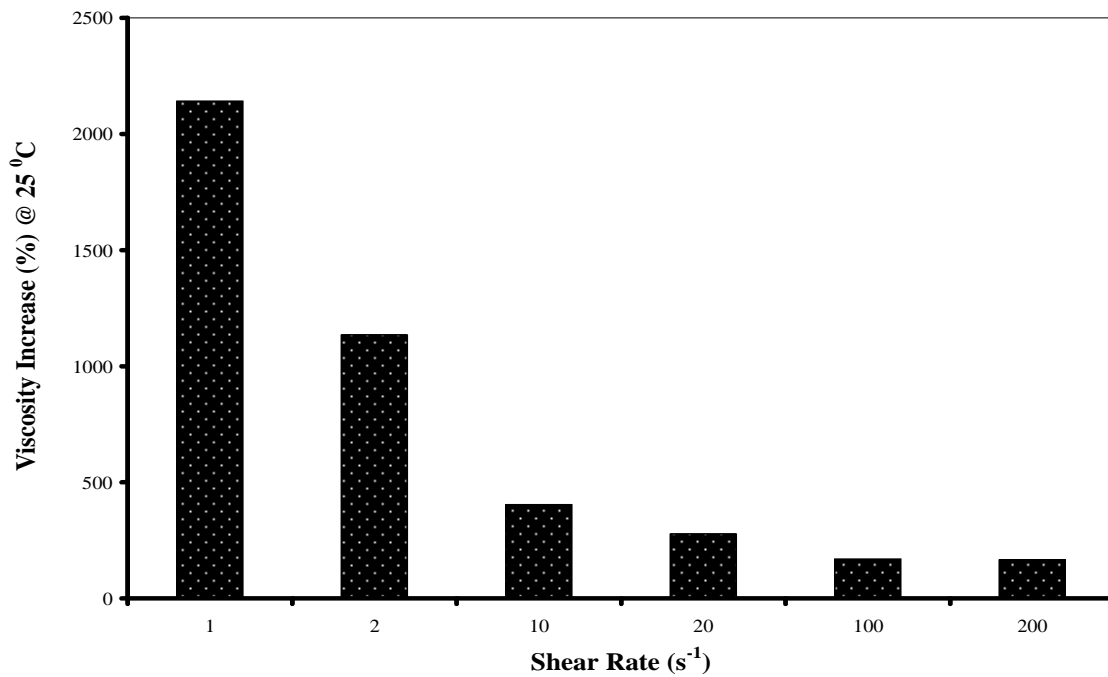


Figure C.25 Percentage Increase in Viscosity (0 hr vs. 192 hr) of Methyl Ethyl Ketone Blended Pyrolysis Oil (10 wt.%) Obtained as a Function of Shear Rate (s⁻¹)

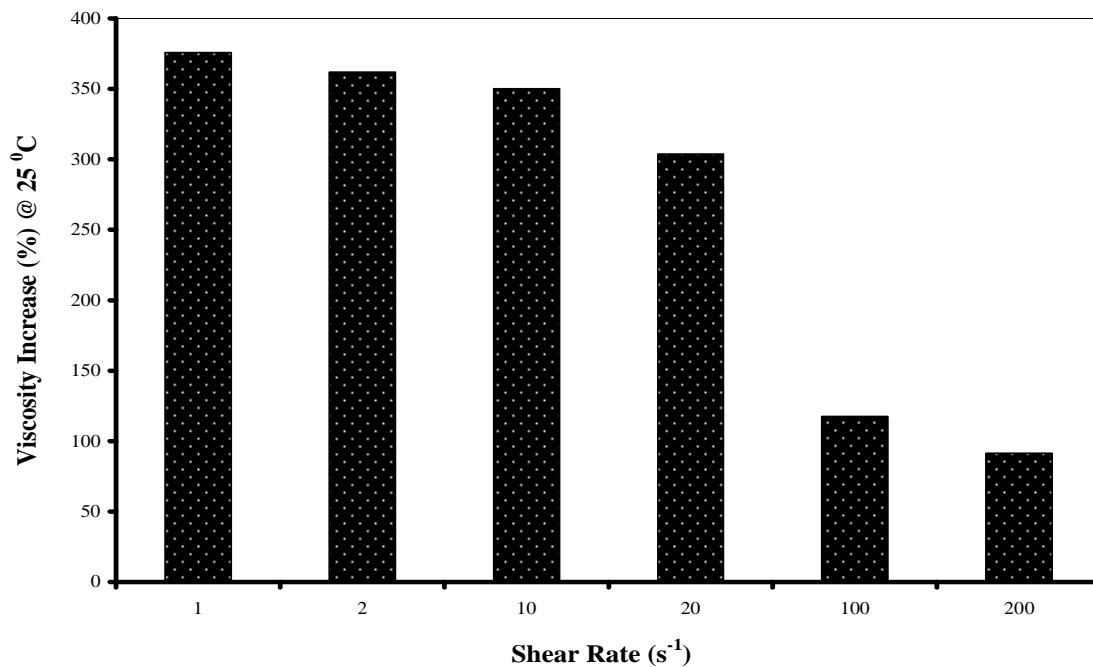


Figure C.26 Percentage Increase in Viscosity (0 hr vs. 192 hr) of Ethanol Blended Pyrolysis Oil (10 wt.%) Obtained as a Function of Shear Rate (s⁻¹)

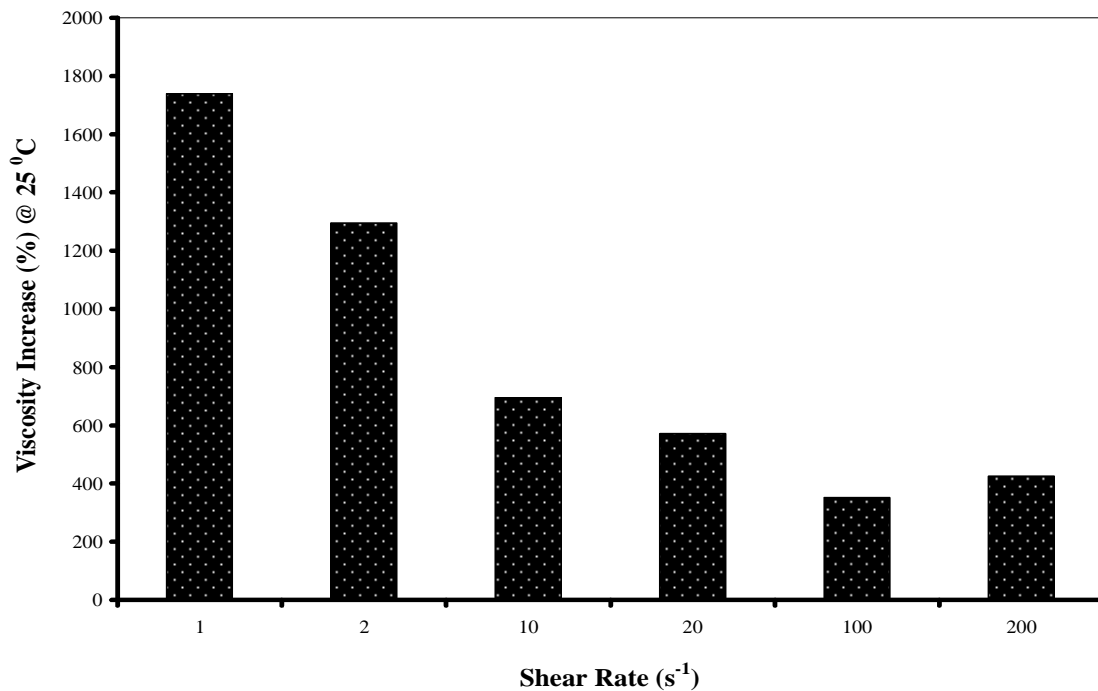


Figure C.27 Percentage Increase in Viscosity (0 hr vs. 192 hr) of Decahydronaphthalene Blended Pyrolysis Oil (10 wt.%) Obtained as a Function of Shear Rate (s^{-1})

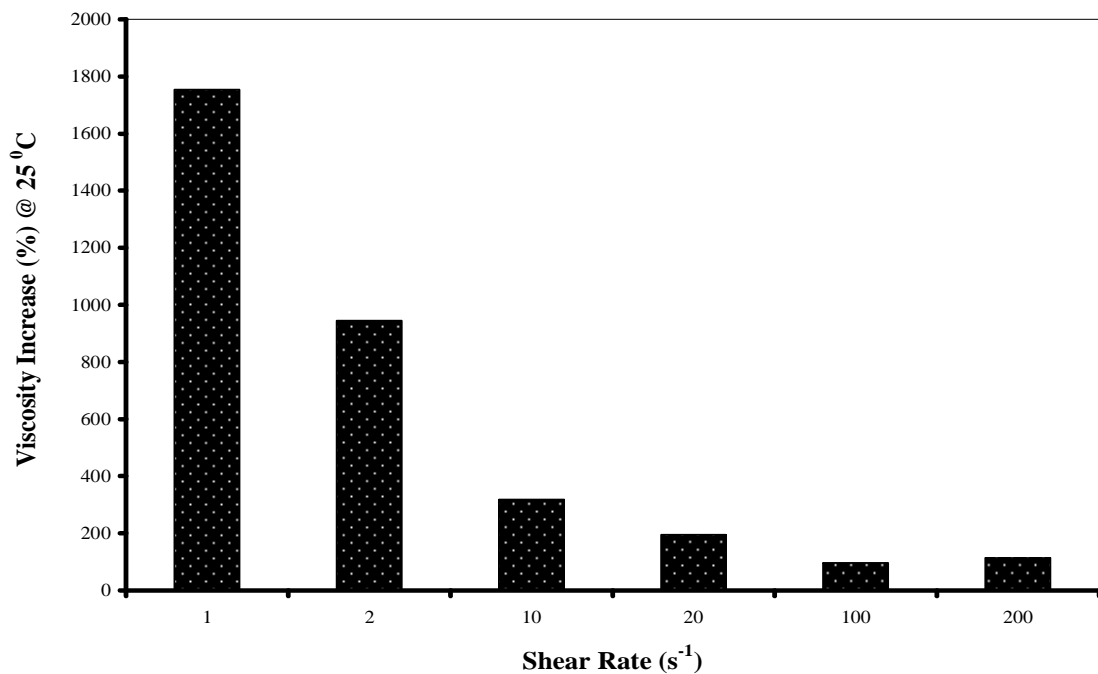


Figure C.28 Percentage Increase in Viscosity (0 hr vs. 192 hr) of Acetone Blended Pyrolysis Oil (10 wt.%) Obtained as a Function of Shear Rate (s^{-1})

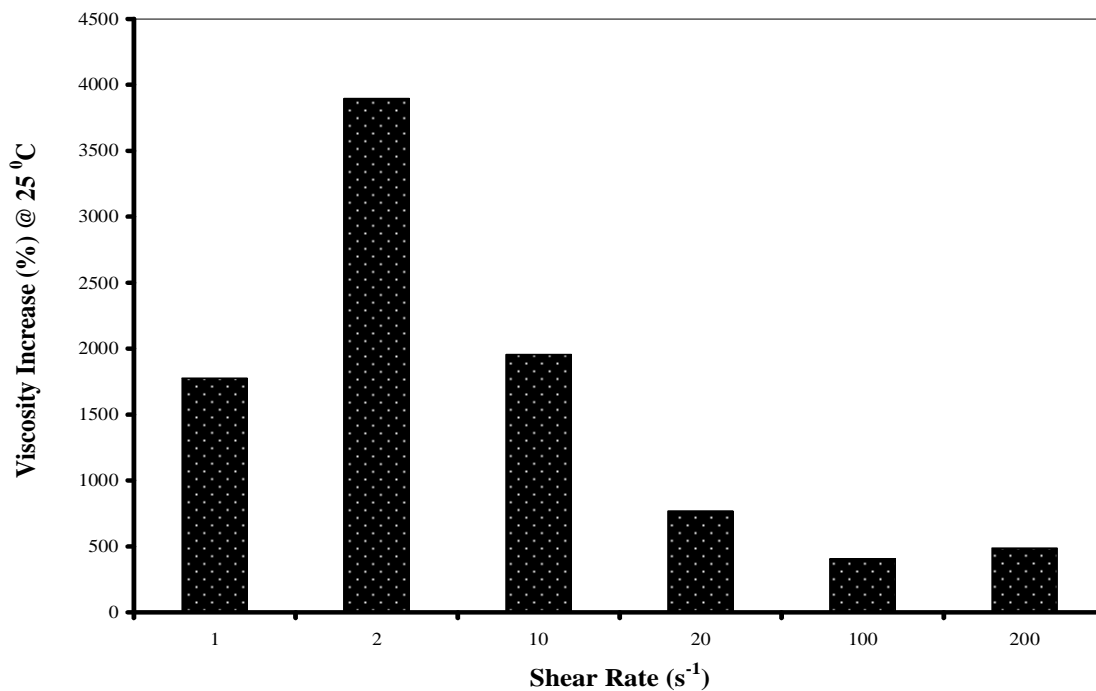


Figure C.29 Percentage Increase in Viscosity (0 hr vs. 192 hr) of Xylene Blended Pyrolysis Oil (10 wt.%) Obtained as a Function of Shear Rate (s^{-1})

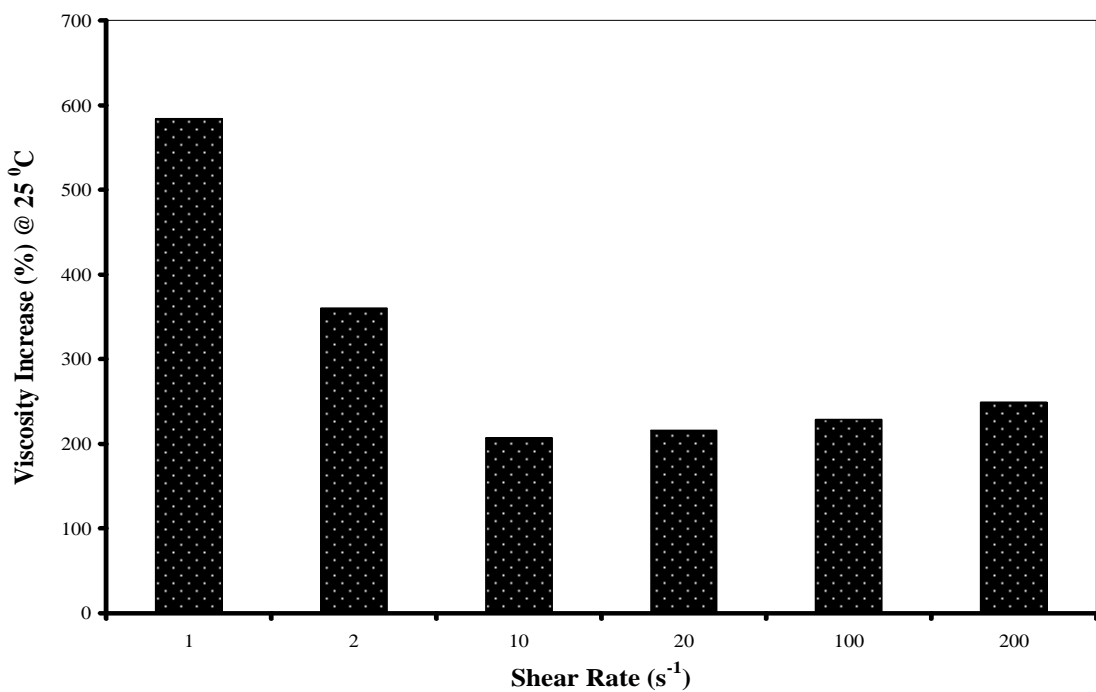


Figure C.30 Percentage Increase in Viscosity (0 hr vs. 192 hr) of Tetrahydronaphthalene Blended Pyrolysis Oil (10 wt.%) Obtained as a Function of Shear Rate (s^{-1})

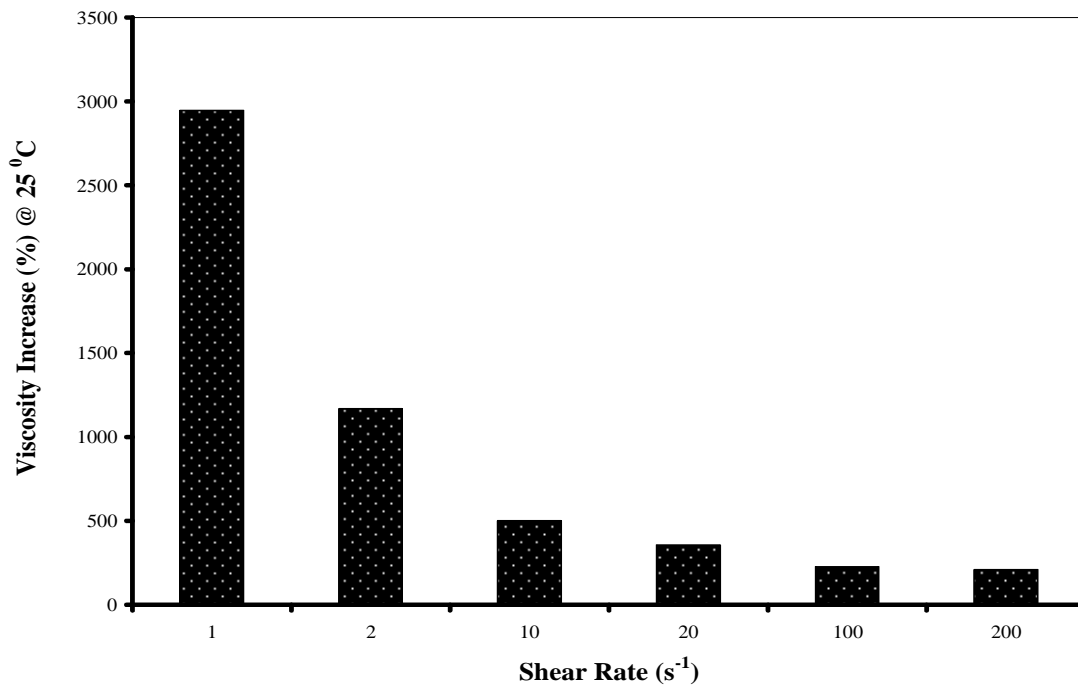


Figure C.31 Percentage Increase in Viscosity (0 hr vs. 192 hr) of Methyl Formate Blended Pyrolysis Oil (10 wt.%) Obtained as a Function of Shear Rate (s⁻¹)

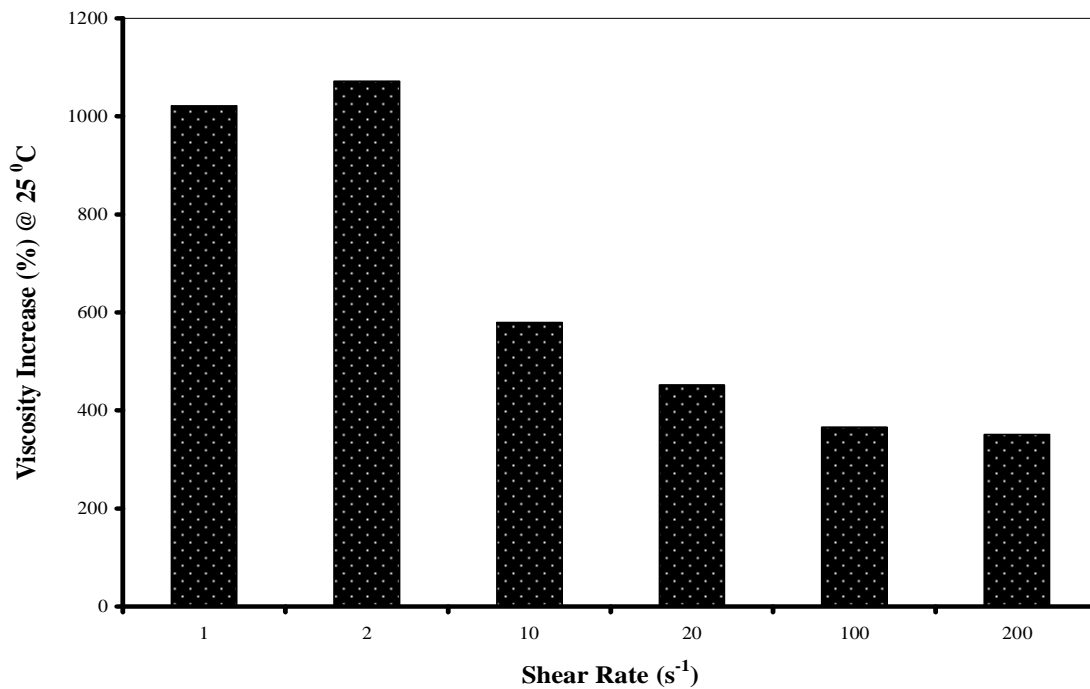


Figure C.32 Percentage Increase in Viscosity (0 hr vs. 192 hr) of Isopropyl Ether Blended Pyrolysis Oil (10 wt.%) Obtained as a Function of Shear Rate (s⁻¹)

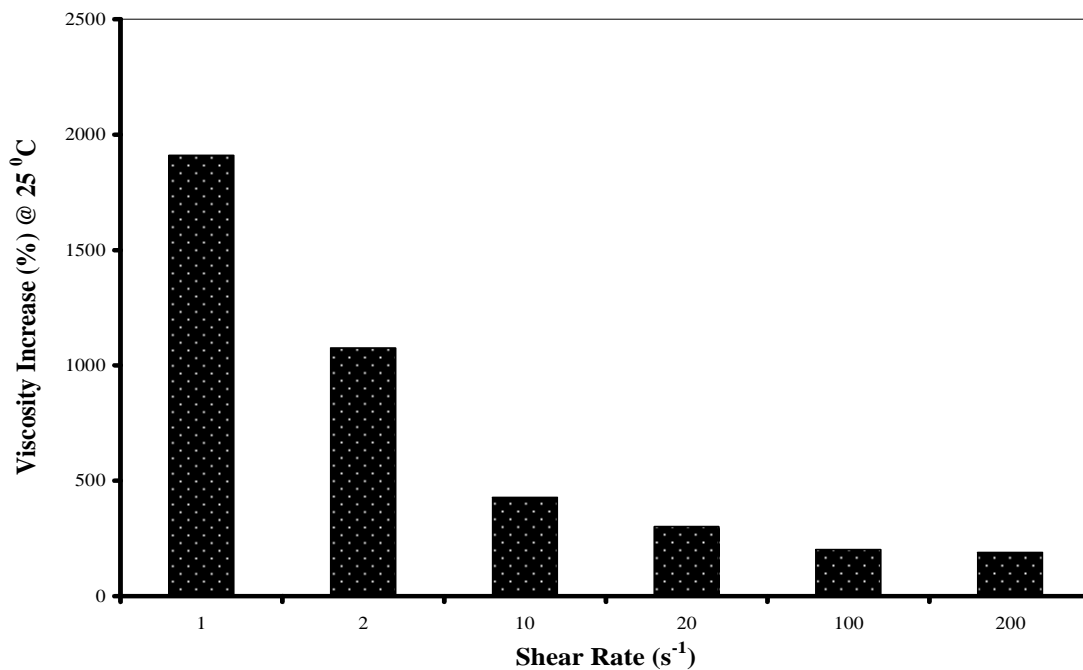


Figure C.33 Percentage Increase in Viscosity (0 hr vs. 192 hr) of Ethyl Ether Blended Pyrolysis Oil (10 wt.%) Obtained as a Function of Shear Rate (s^{-1})

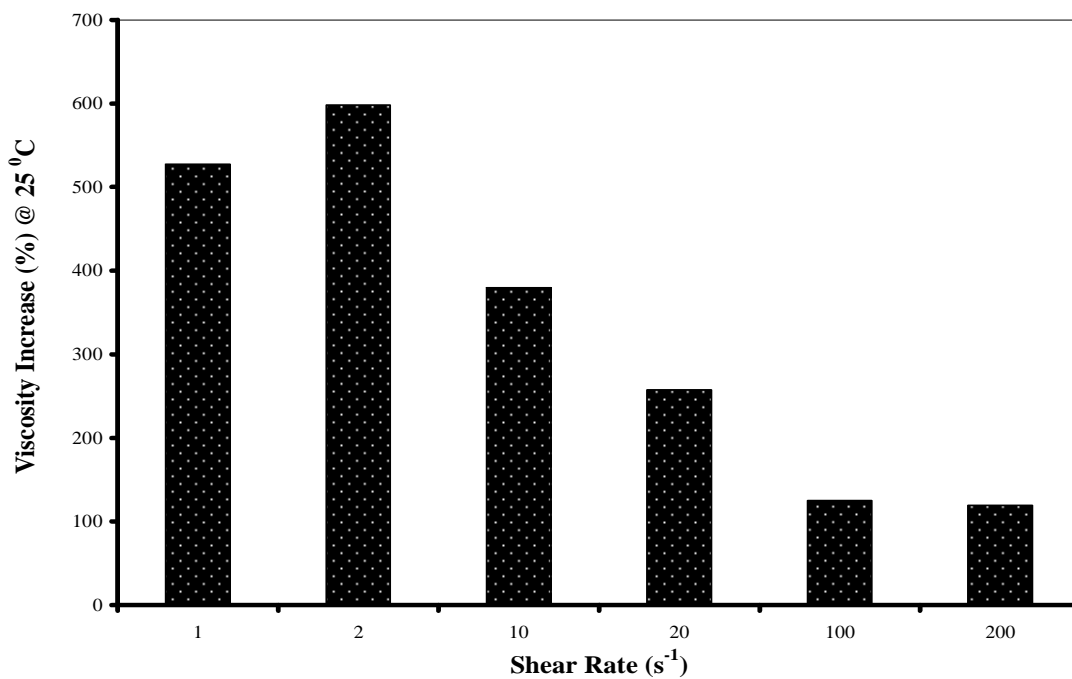


Figure C.34 Percentage Increase in Viscosity (0 hr vs. 192 hr) of Cyclopentanone Blended Pyrolysis Oil (10 wt.%) Obtained as a Function of Shear Rate (s^{-1})

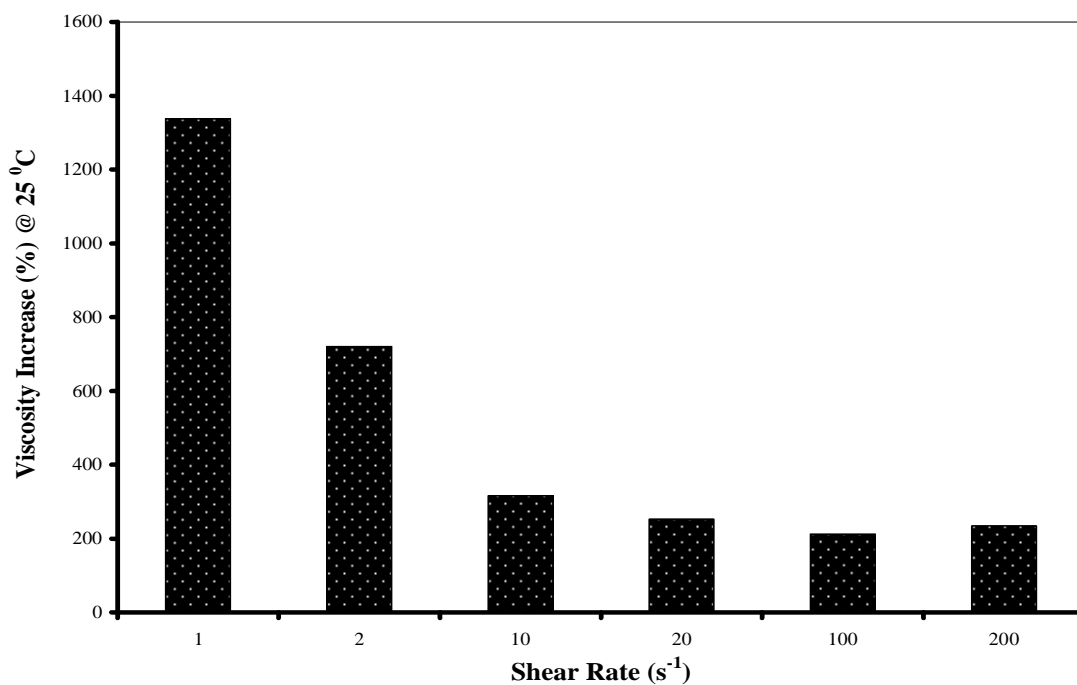


Figure C.35 Percentage Increase in Viscosity (0 hr vs. 192 hr) of Acetaldehyde Blended Pyrolysis Oil (10 wt.%) Obtained as a Function of Shear Rate (s^{-1})

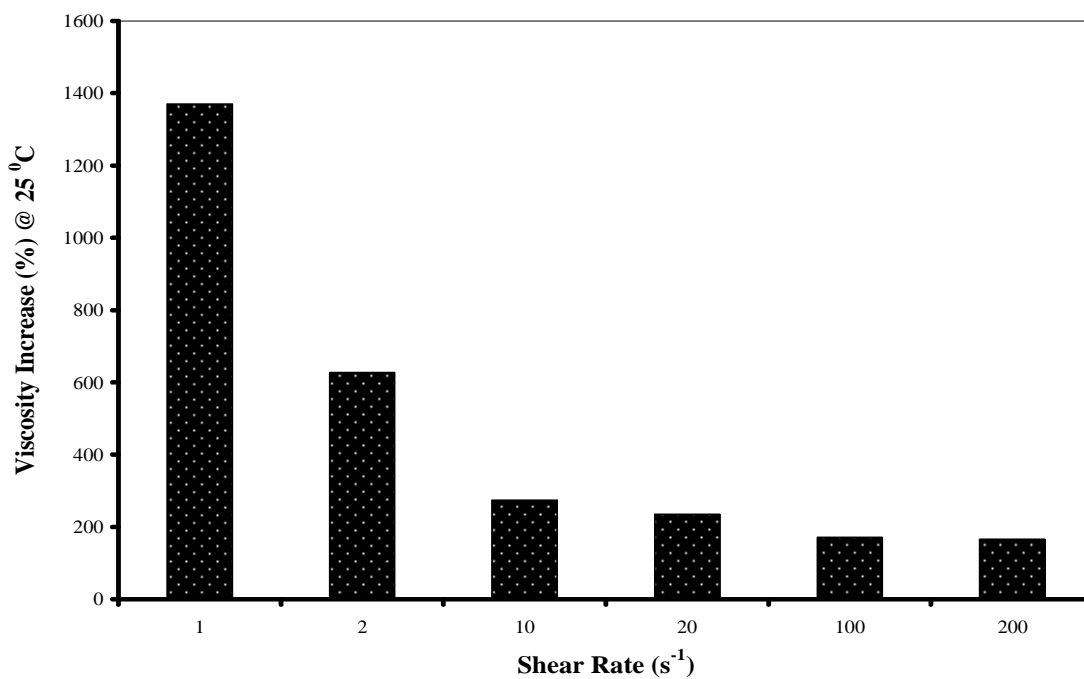


Figure C.36 Percentage Increase in Viscosity (0 hr vs. 192 hr) of t-Butanol Blended Pyrolysis Oil (10 wt.%) Obtained as a Function of Shear Rate (s^{-1})

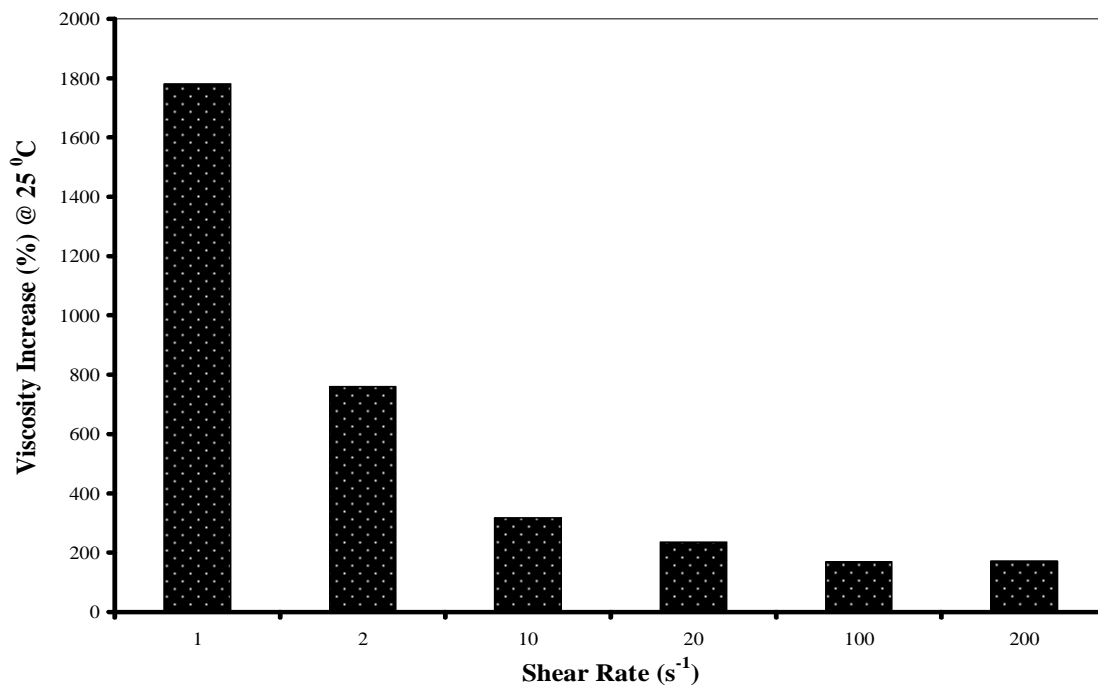


Figure C.37 Percentage Increase in Viscosity (0 hr vs. 192 hr) of Tetrahydrofuran Blended Pyrolysis Oil (10 wt.%) Obtained as a Function of Shear Rate (s^{-1})

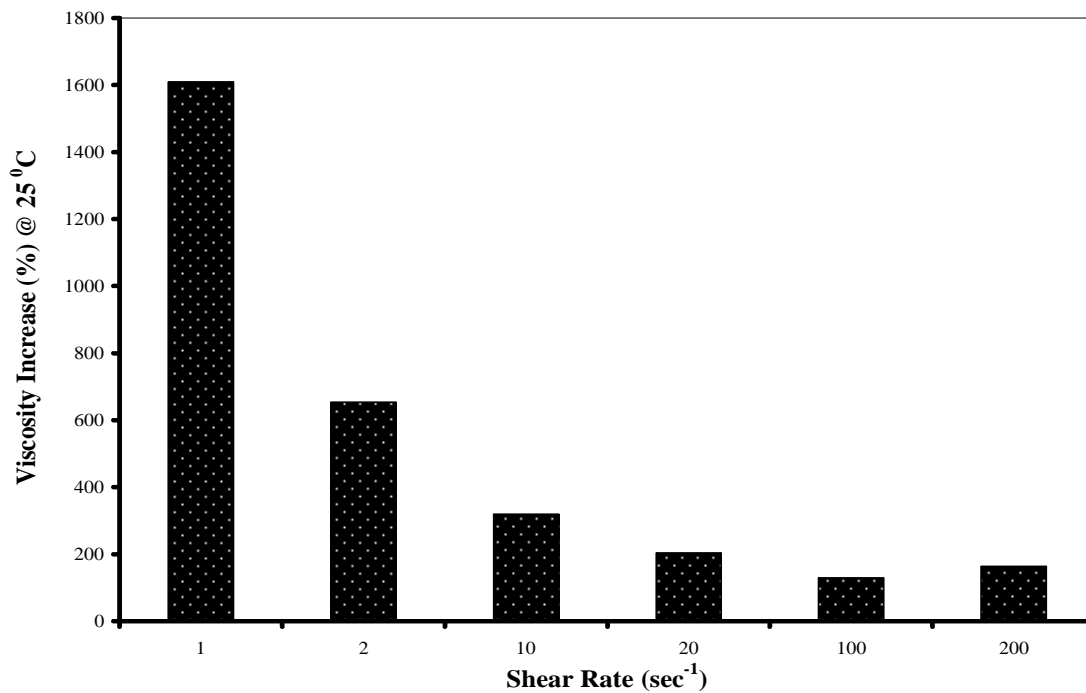


Figure C.38 Percentage Increase in Viscosity (0 hr vs. 192 hr) of Methyl Acetate Blended Pyrolysis Oil (10 wt.%) Obtained as a Function of Shear Rate (s^{-1})

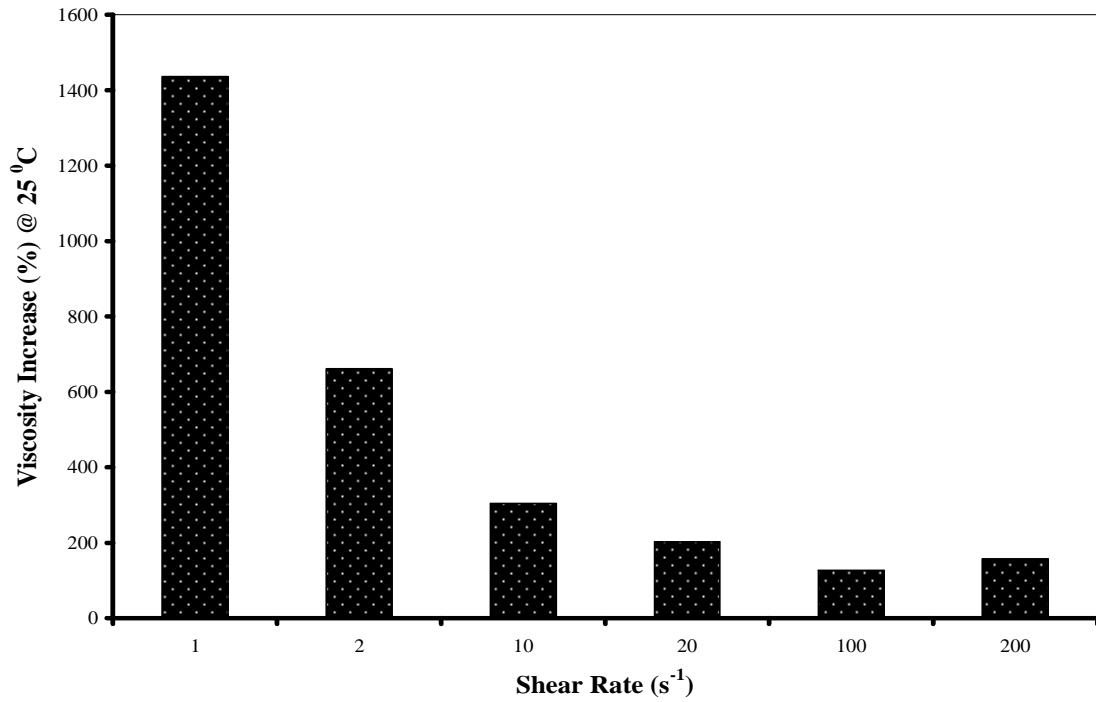


Figure C.39 Percentage Increase in Viscosity (0 hr vs. 192 hr) of Ethyl Acetate Blended Pyrolysis Oil (10 wt.%) Obtained as a Function of Shear Rate (s^{-1})

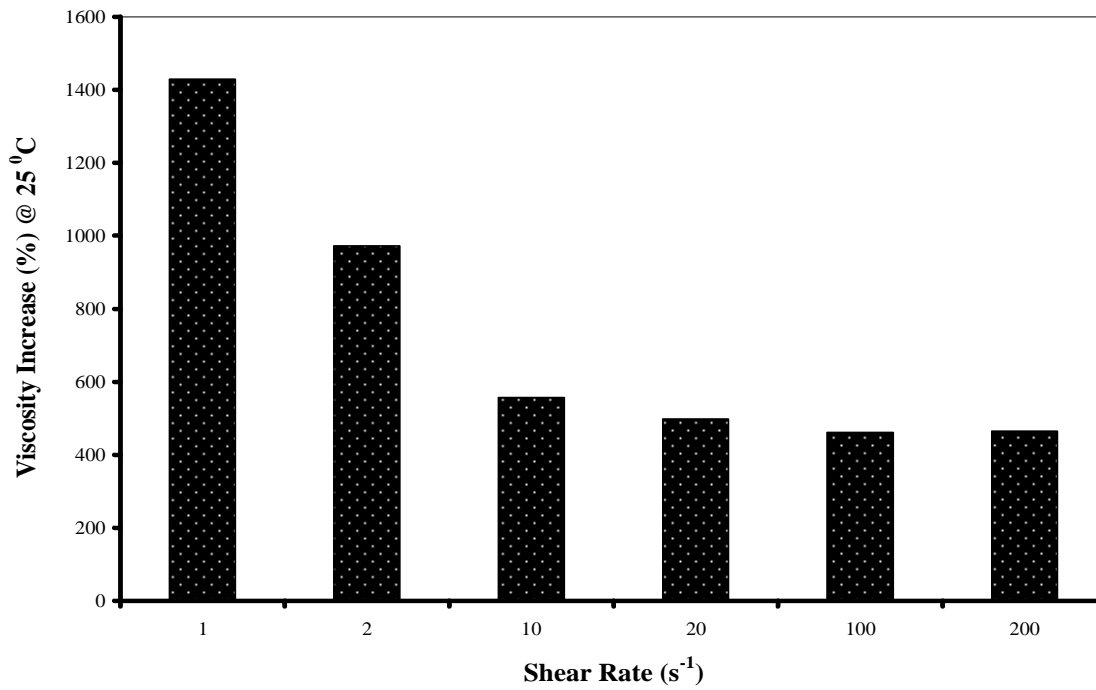


Figure C.40 Percentage Increase in Viscosity (0 hr vs. 192 hr) of Cyclohexane Blended Pyrolysis Oil (10 wt.%) Obtained as a Function of Shear Rate (s^{-1})

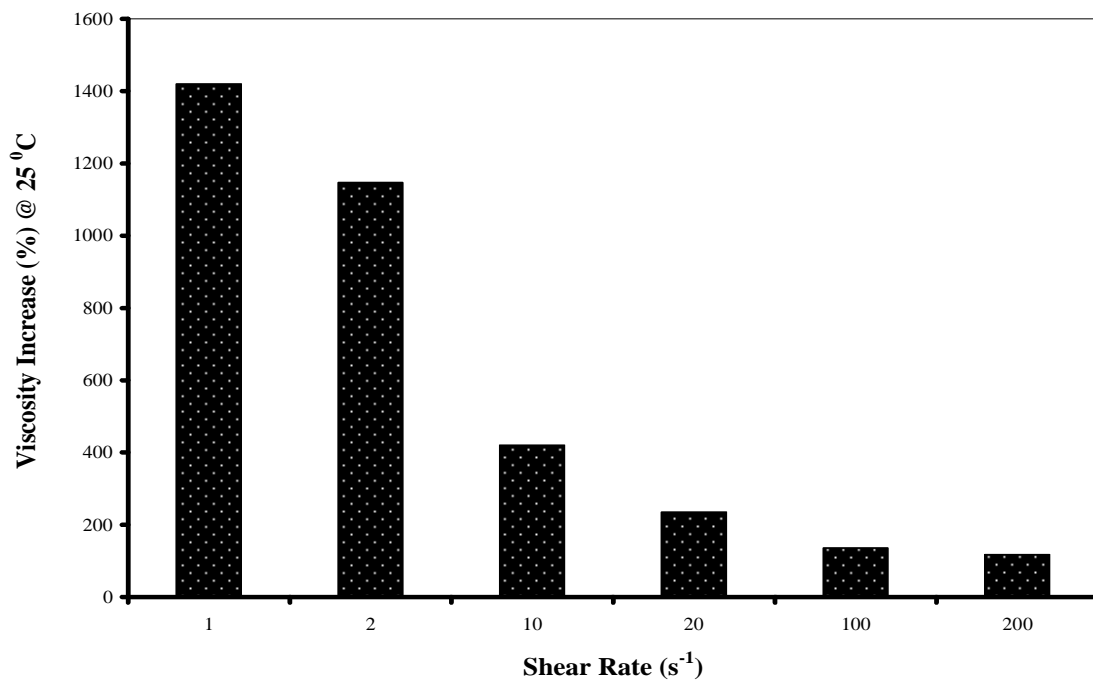


Figure C.41 Percentage Increase in Viscosity (0 hr vs. 192 hr) of 2-Propanol Blended Pyrolysis Oil (10 wt.%) Obtained as a Function of Shear Rate (s^{-1})

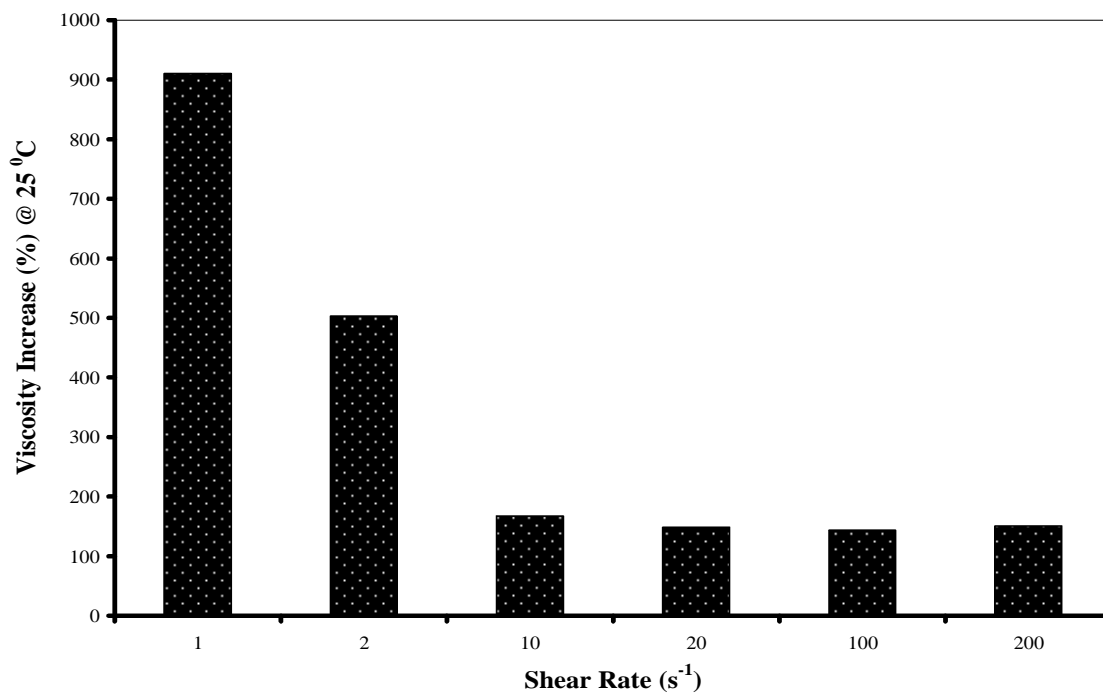


Figure C.42 Percentage Increase in Viscosity (0 hr vs. 192 hr) of Polyethylene Glycol Blended Pyrolysis Oil (10 wt.%) Obtained as a Function of Shear Rate (s^{-1})

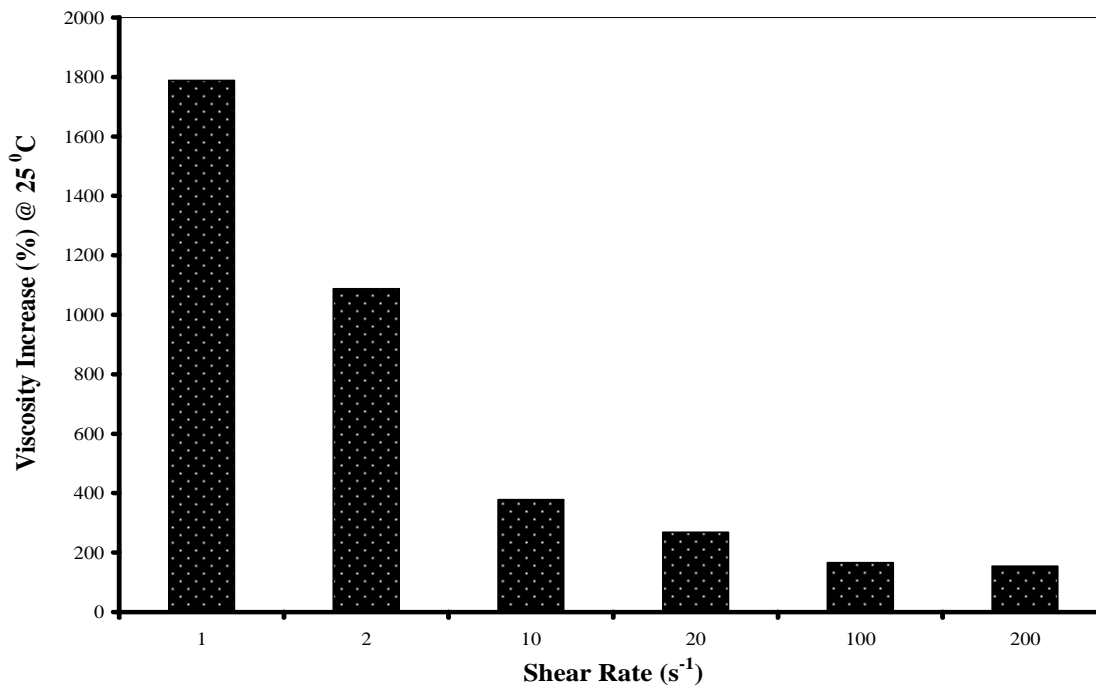


Figure C.43 Percentage Increase in Viscosity (0 hr vs. 192 hr) of Dimethyl Ether Blended Pyrolysis Oil (10 wt.%) Obtained as a Function of Shear Rate (s^{-1})

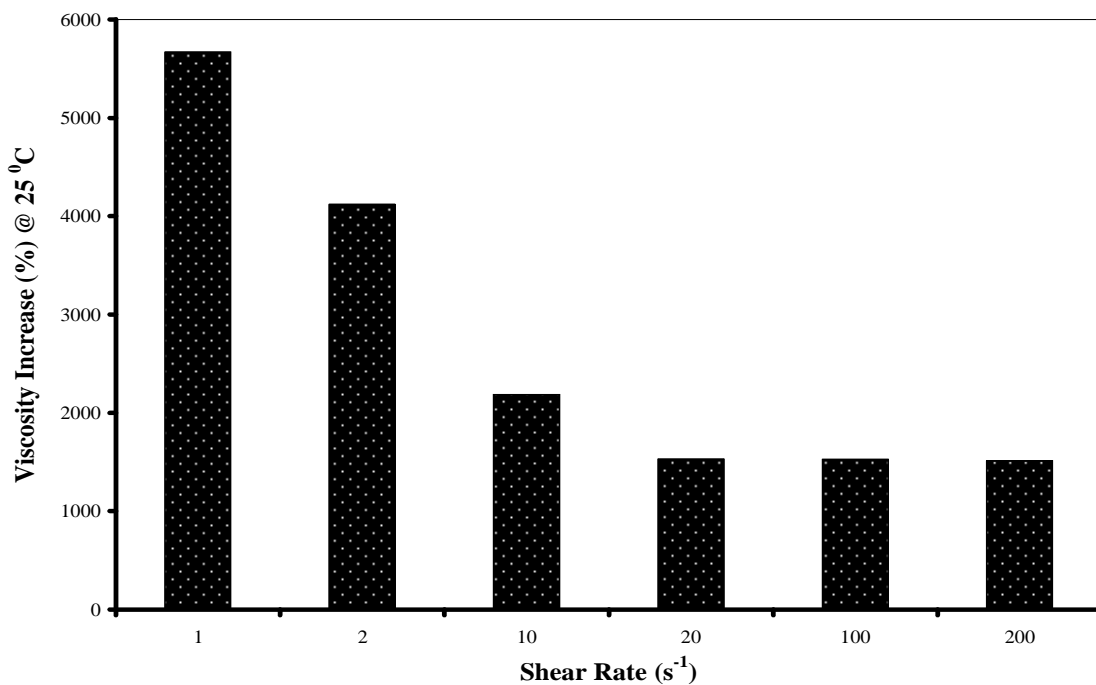


Figure C.44 Percentage Increase in Viscosity (0 hr vs. 192 hr) of 2-Furaldehyde Blended Pyrolysis Oil (10 wt.%) Obtained as a Function of Shear Rate (s^{-1})

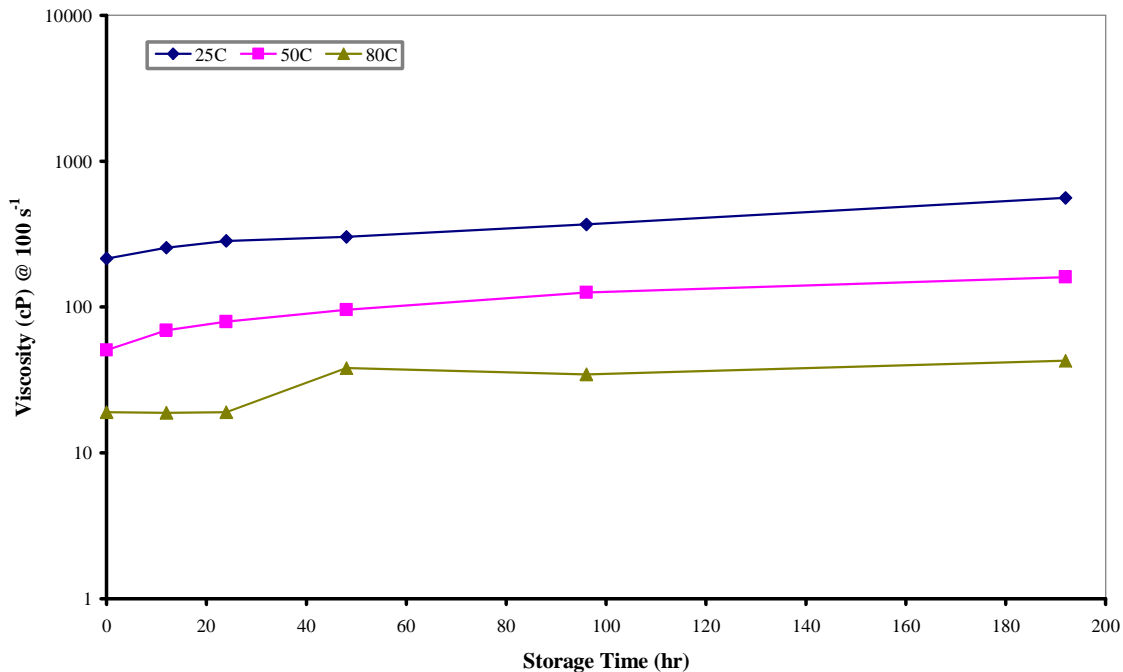


Figure C.45 Viscosity (cP) of Methyl Tertiary Butyl Ether Blended Pyrolysis Oil (10 wt.%) Measured as a Function of Storage Time (hr) and Temperature ($^{\circ}\text{C}$)

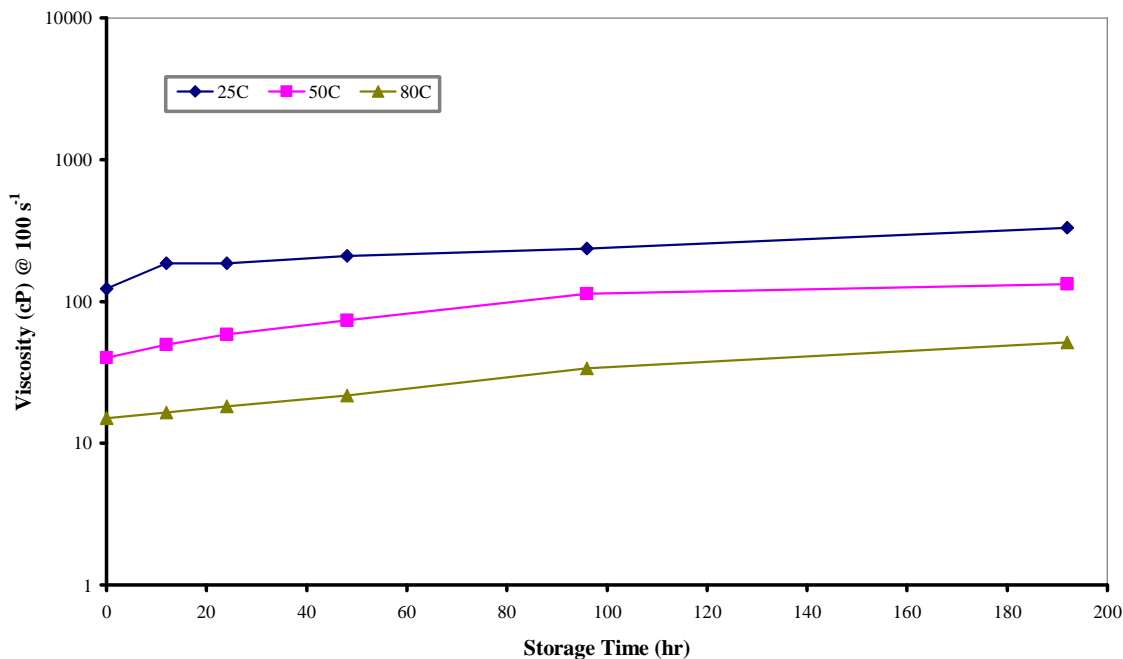


Figure C.46 Viscosity (cP) of Methyl Ethyl Ketone Blended Pyrolysis Oil (10 wt.%) Measured as a Function of Storage Time (hr) and Temperature ($^{\circ}\text{C}$)

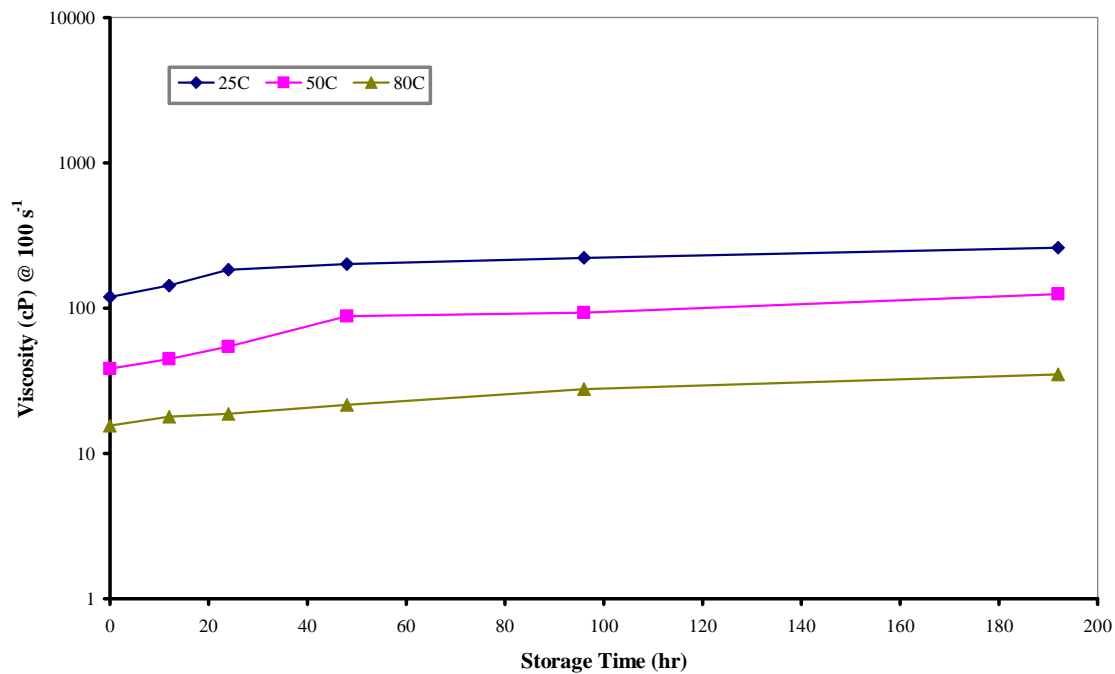


Figure C.47 Viscosity (cP) of Ethanol Blended Pyrolysis Oil (10 wt.%) Measured as a Function of Storage Time (hr) and Temperature ($^{\circ}\text{C}$)

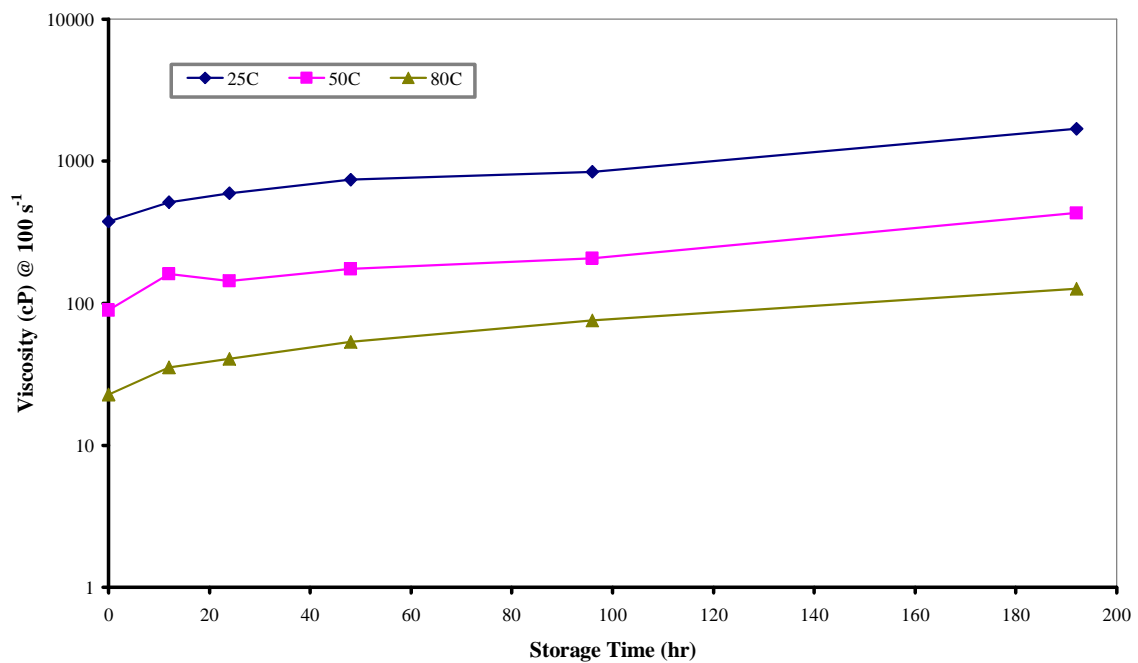


Figure C.48 Viscosity (cP) of Decahydronaphthalene Blended Pyrolysis Oil (10 wt.%) Measured as a Function of Storage Time (hr) and Temperature ($^{\circ}\text{C}$)

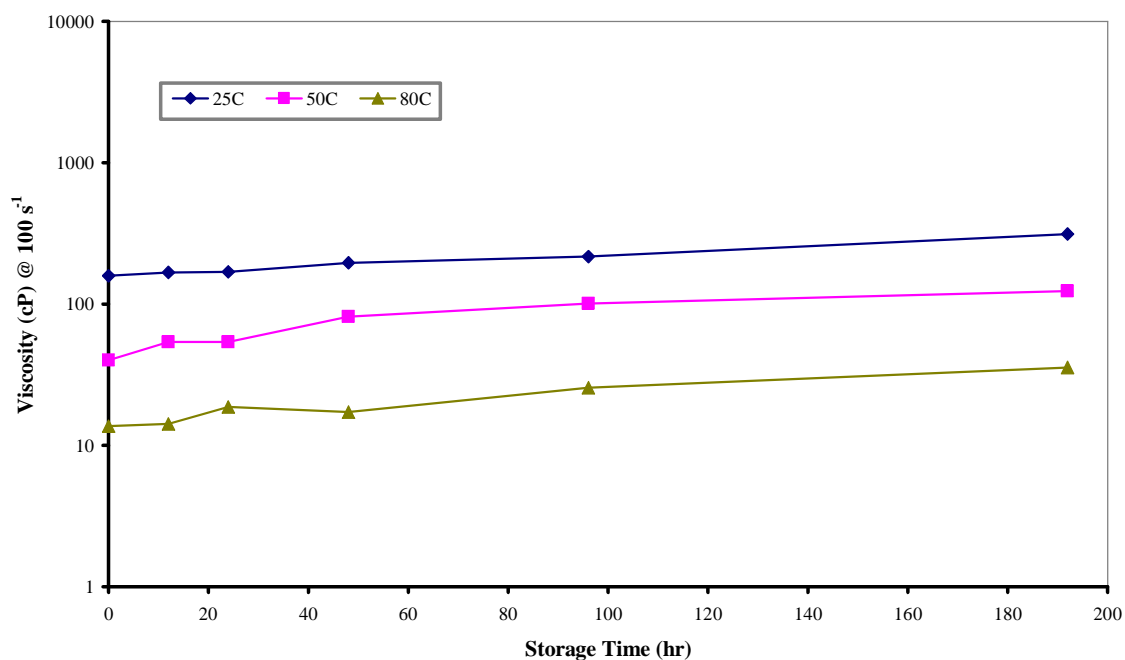


Figure C.49 Viscosity (cP) of Acetone Blended Pyrolysis Oil (10 wt.%) Measured as a Function of Storage Time (hr) and Temperature ($^{\circ}\text{C}$)

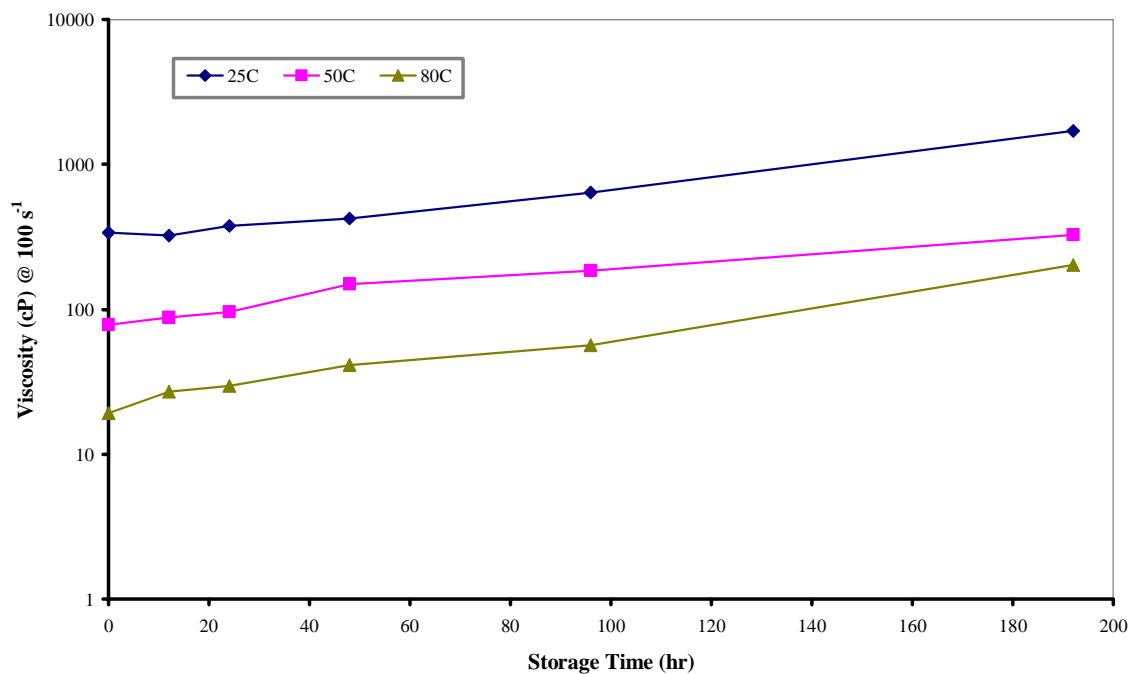


Figure C.50 Viscosity (cP) of Xylene Blended Pyrolysis Oil (10 wt.%) Measured as a Function of Storage Time (hr) and Temperature ($^{\circ}\text{C}$)

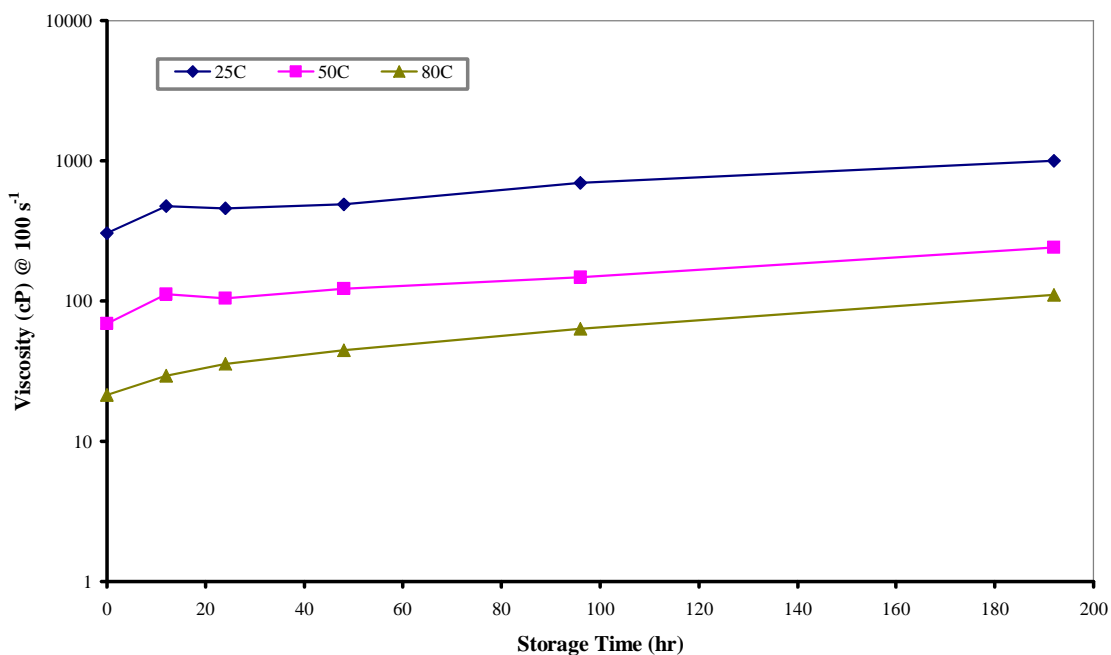


Figure C.51 Viscosity (cP) of Tetrahydronaphthalene Blended Pyrolysis Oil (10 wt.%) Measured as a Function of Storage Time (hr) and Temperature ($^{\circ}\text{C}$)

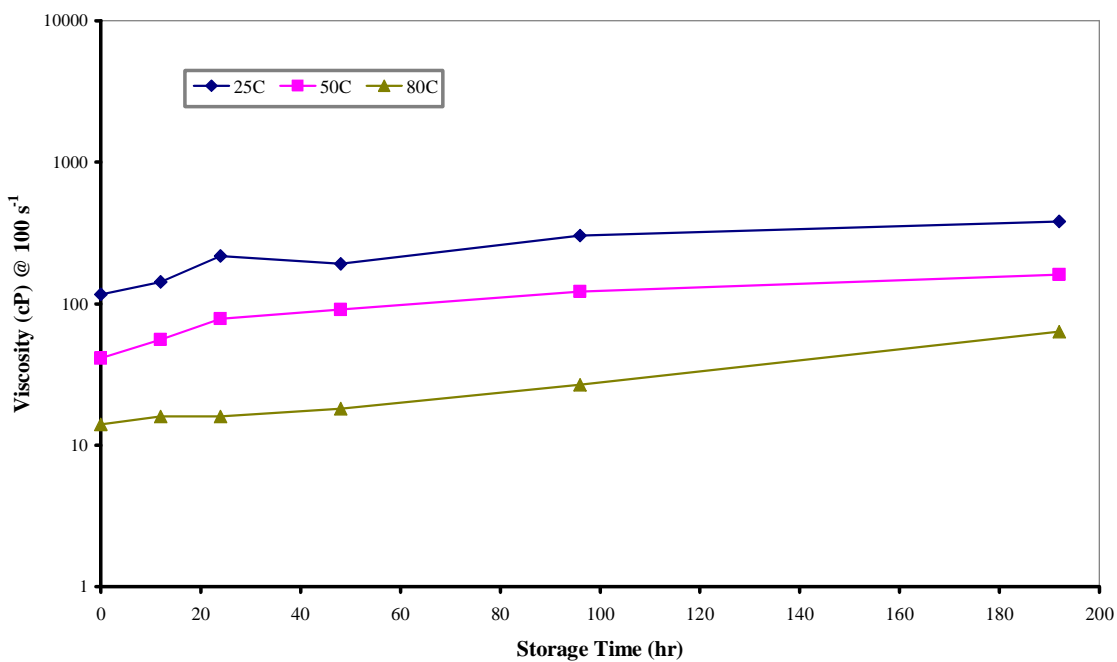


Figure C.52 Viscosity (cP) of Methyl Formate Blended Pyrolysis Oil (10 wt.%) Measured as a Function of Storage Time (hr) and Temperature ($^{\circ}\text{C}$)

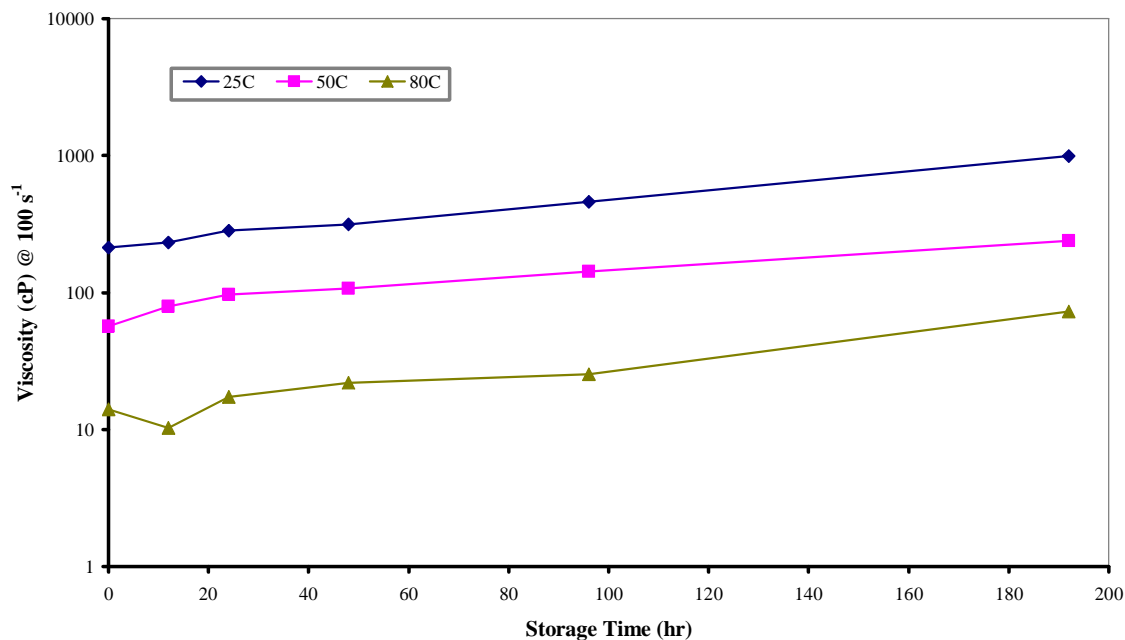


Figure C.53 Viscosity (cP) of Isopropyl Ether Blended Pyrolysis Oil (10 wt.%) Measured as a Function of Storage Time (hr) and Temperature ($^{\circ}\text{C}$)

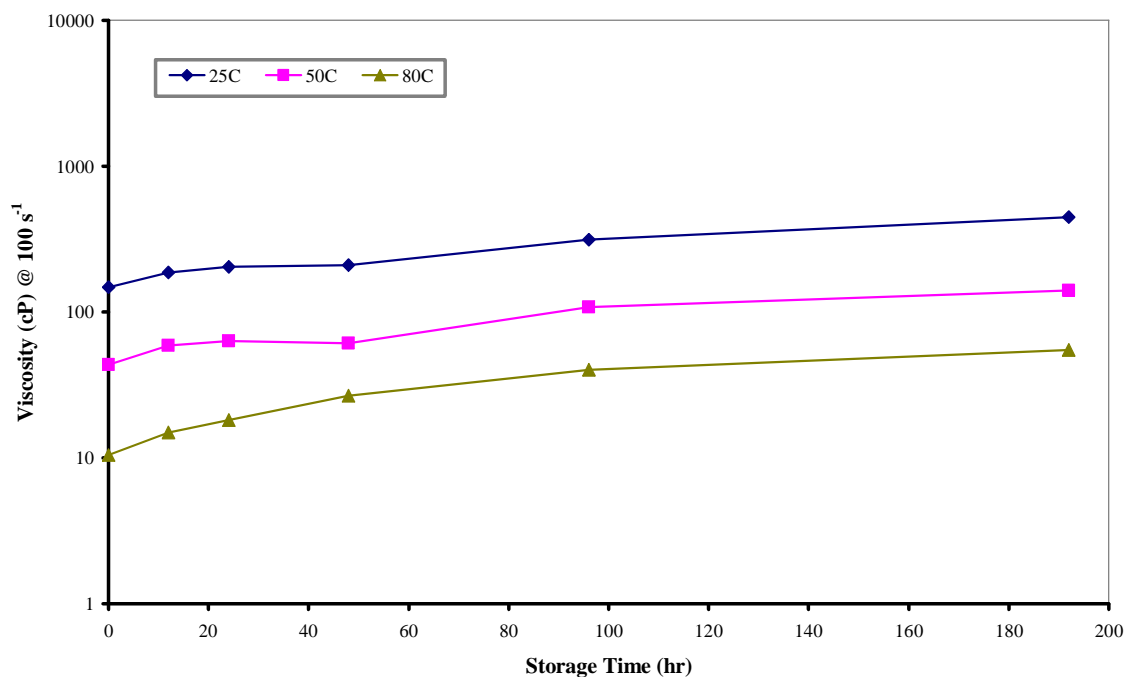


Figure C.54 Viscosity (cP) of Ethyl Ether Blended Pyrolysis Oil (10 wt.%) Measured as a Function of Storage Time (hr) and Temperature ($^{\circ}\text{C}$)

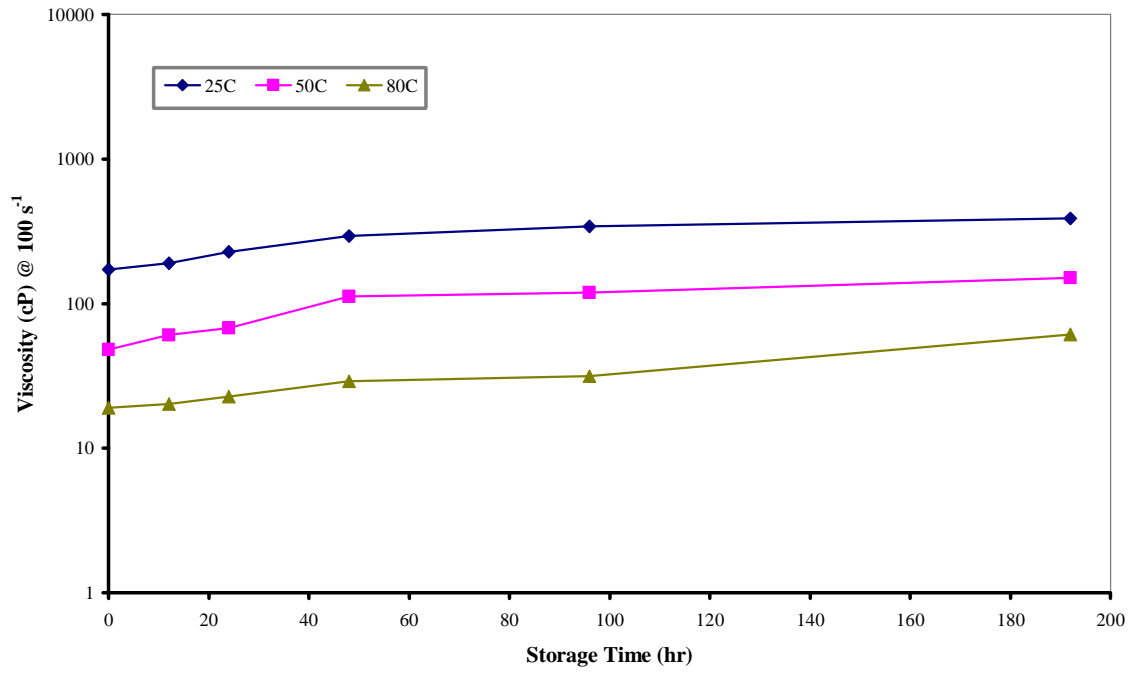


Figure C.55 Viscosity (cP) of Cyclopentanone Blended Pyrolysis Oil (10 wt.%) Measured as a Function of Storage Time (hr) and Temperature ($^{\circ}\text{C}$)

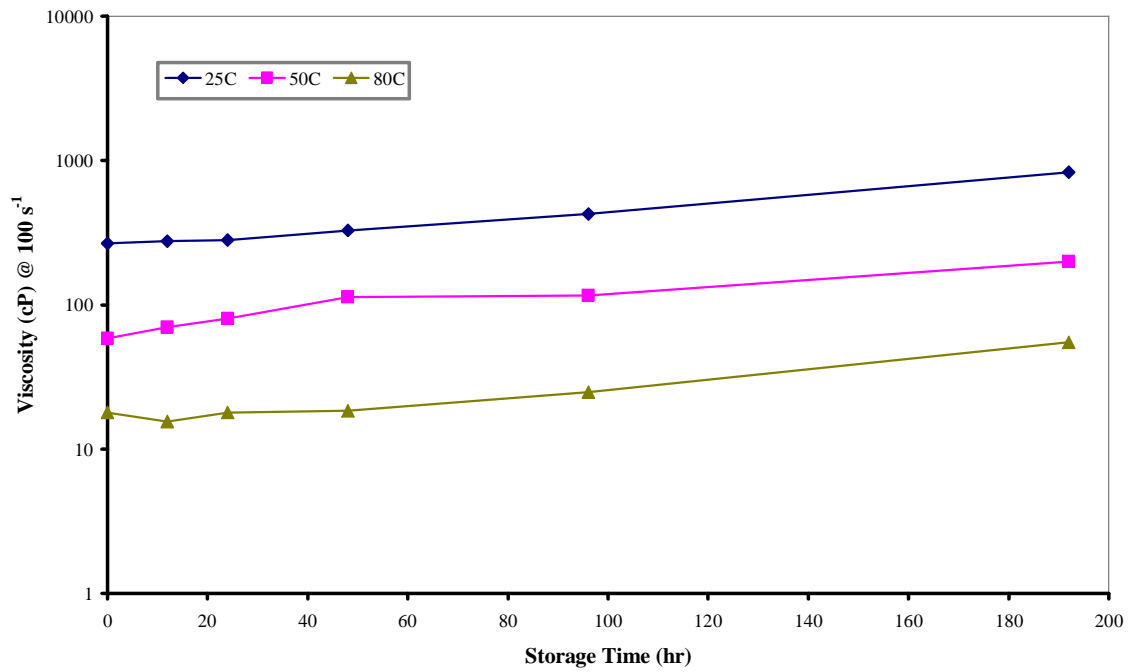


Figure C.56 Viscosity (cP) of Acetaldehyde Blended Pyrolysis Oil (10 wt.%) Measured as a Function of Storage Time (hr) and Temperature ($^{\circ}\text{C}$)

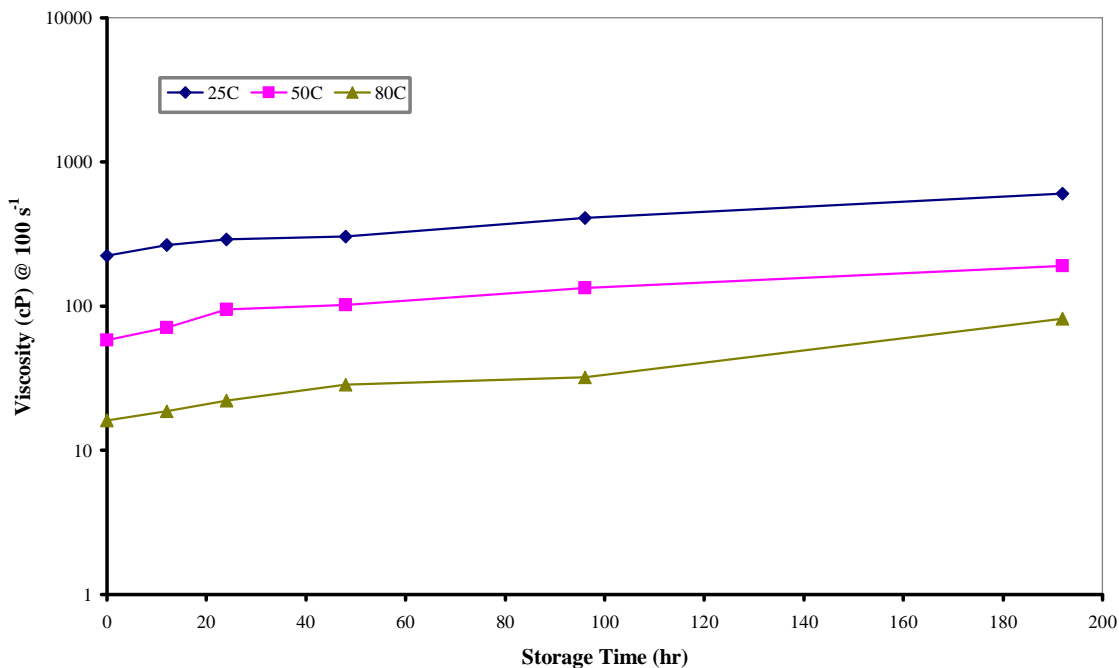


Figure C.57 Viscosity (cP) of t-Butanol Blended Pyrolysis Oil (10 wt.%) Measured as a Function of Storage Time (hr) and Temperature ($^{\circ}\text{C}$)

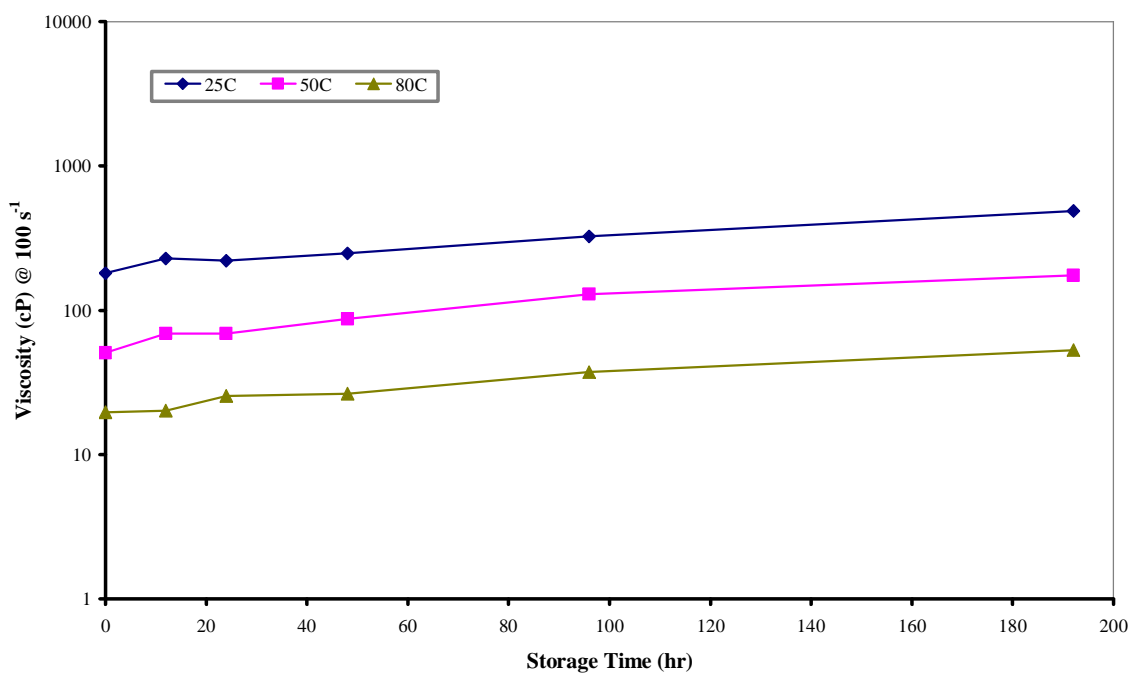


Figure C.58 Viscosity (cP) of Tetrahydrofuran Blended Pyrolysis Oil (10 wt.%) Measured as a Function of Storage Time (hr) and Temperature ($^{\circ}\text{C}$)

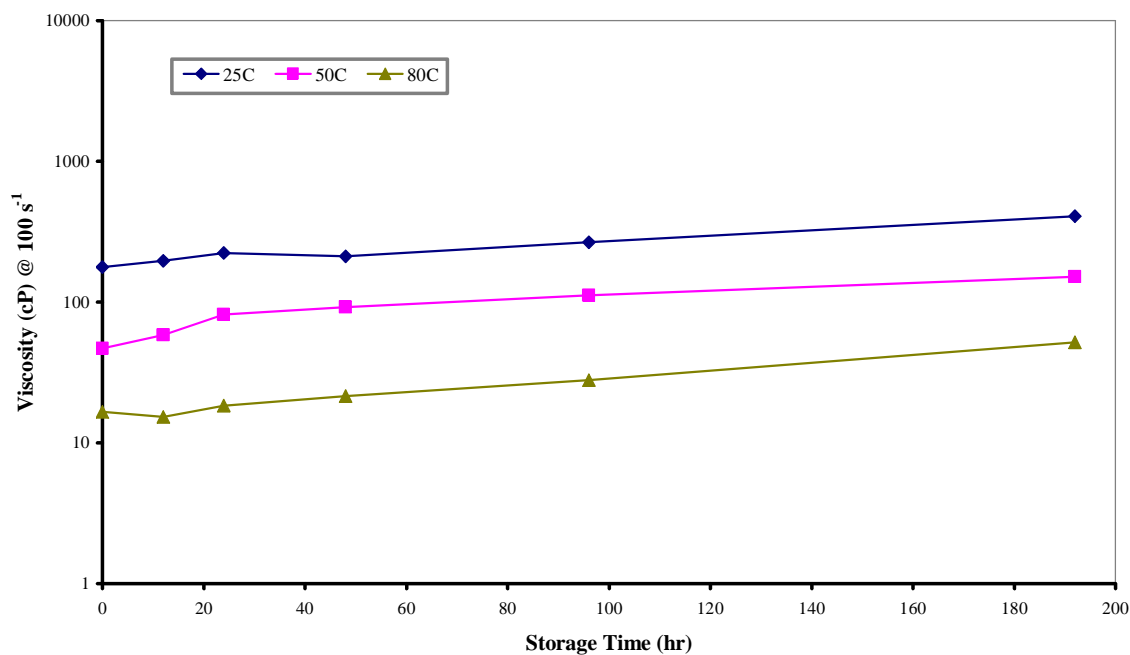


Figure C.59 Viscosity (cP) of Methyl Acetate Blended Pyrolysis Oil (10 wt.%) Measured as a Function of Storage Time (hr) and Temperature ($^{\circ}\text{C}$)

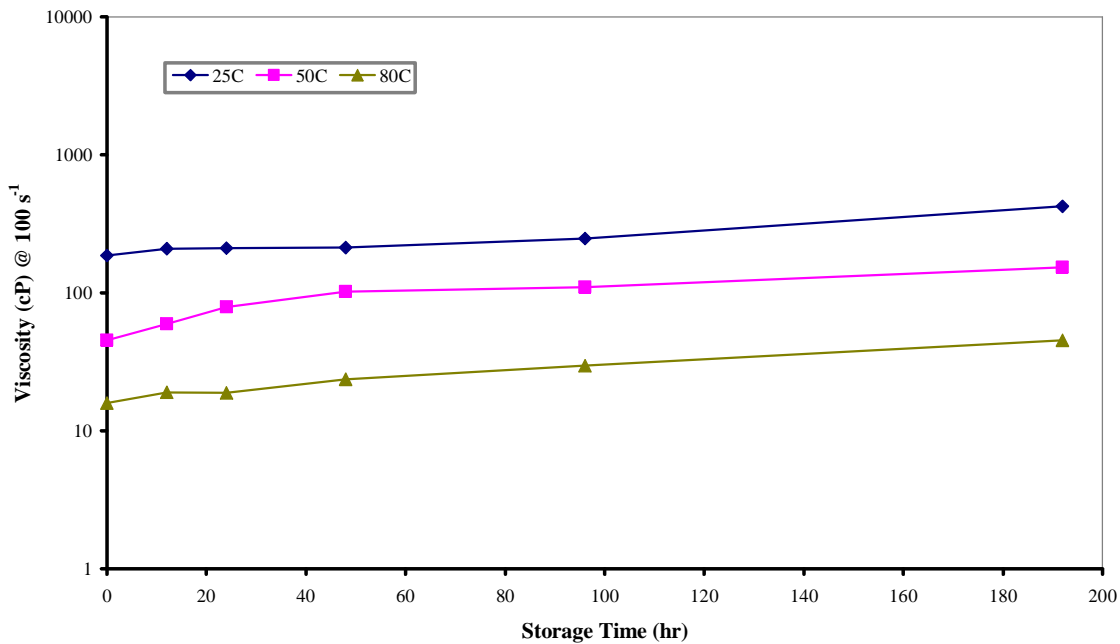


Figure C.60 Viscosity (cP) of Ethyl Acetate Blended Pyrolysis Oil (10 wt.%) Measured as a Function of Storage Time (hr) and Temperature ($^{\circ}\text{C}$)

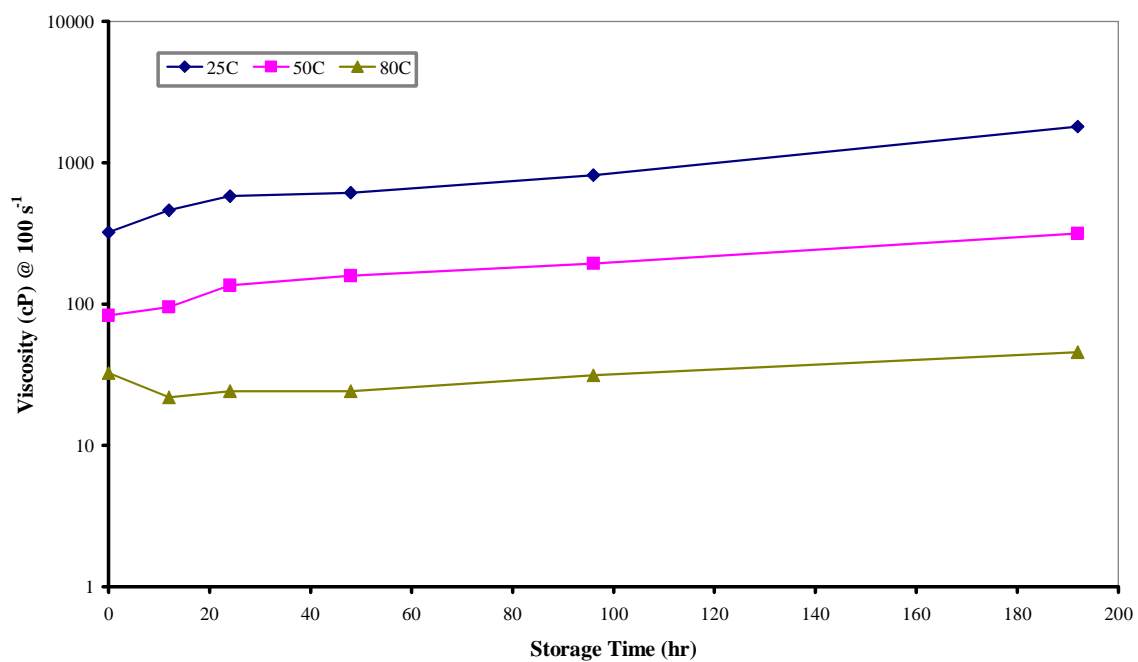


Figure C.61 Viscosity (cP) of Cyclohexane Blended Pyrolysis Oil (10 wt.%) Measured as a Function of Storage Time (hr) and Temperature ($^{\circ}\text{C}$)

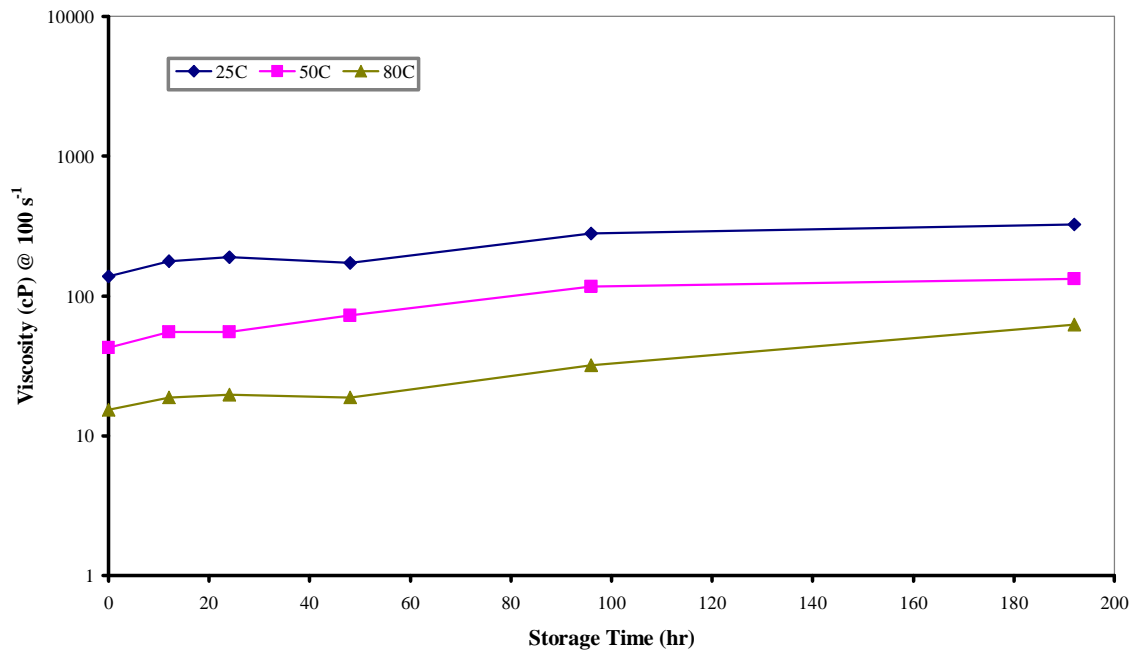


Figure C.62 Viscosity (cP) of 2-Propanol Blended Pyrolysis Oil (10 wt.%) Measured as a Function of Storage Time (hr) and Temperature ($^{\circ}\text{C}$)

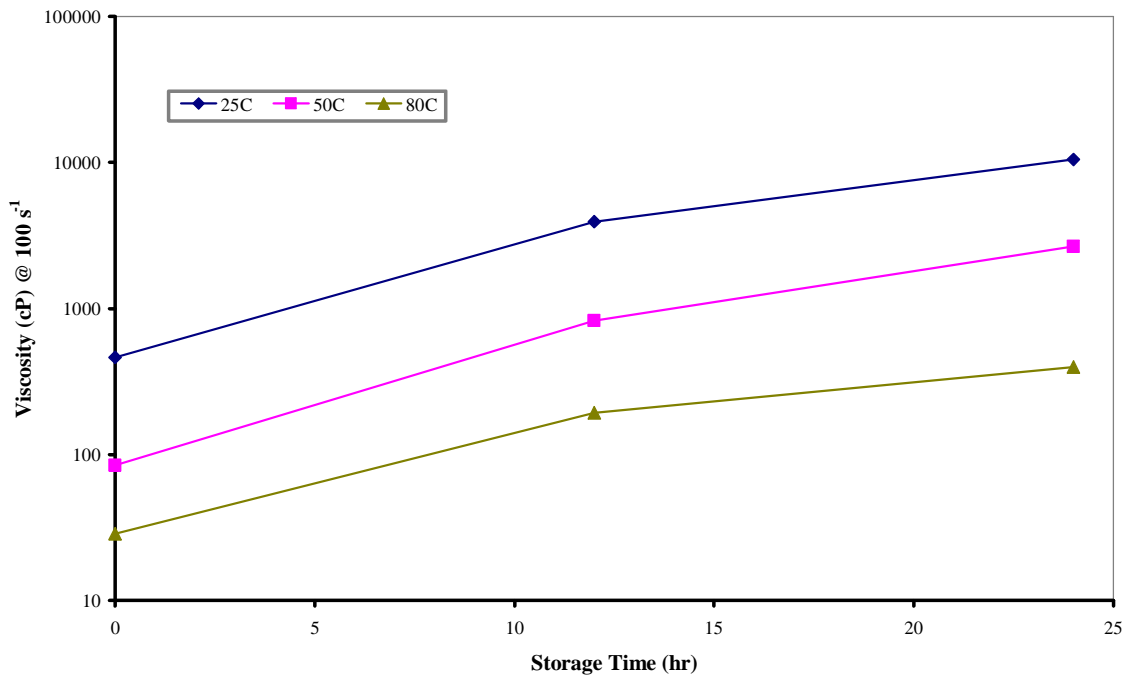


Figure C.63 Viscosity (cP) of Resorcinol Blended Pyrolysis Oil (10 wt.%) Measured as a Function of Storage Time (hr) and Temperature ($^{\circ}\text{C}$)

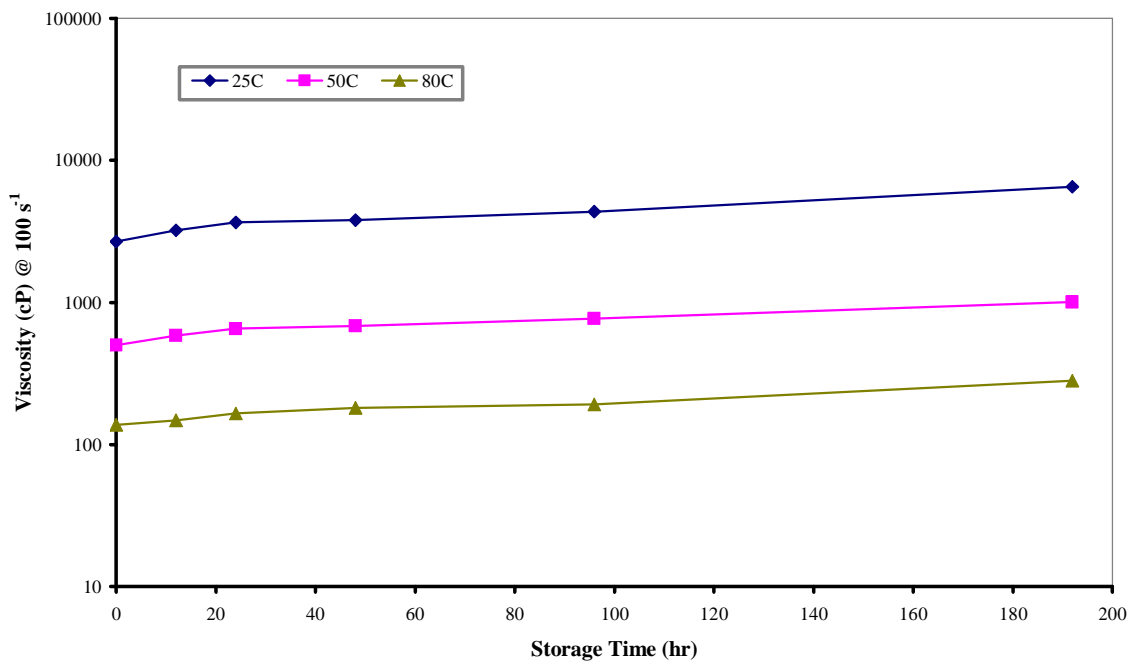


Figure C.64 Viscosity (cP) of Polyethylene Glycol Blended Pyrolysis Oil (10 wt.%) Measured as a Function of Storage Time (hr) and Temperature ($^{\circ}\text{C}$)

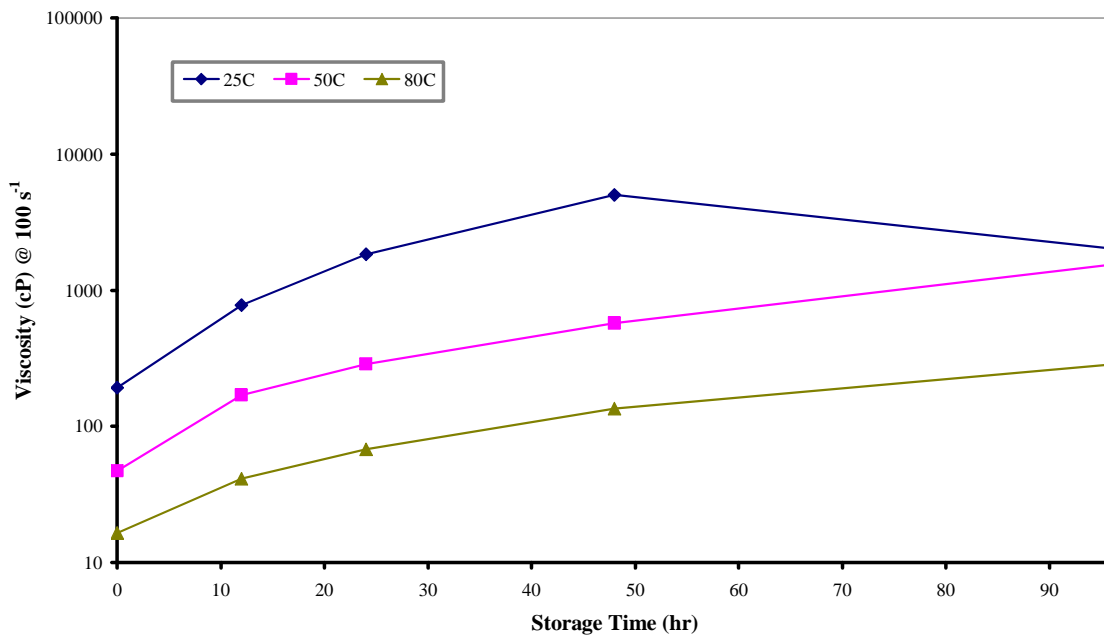


Figure C.65 Viscosity (cP) of Furfuryl Alcohol Blended Pyrolysis Oil (10 wt.%) Measured as a Function of Storage Time (hr) and Temperature ($^{\circ}\text{C}$)

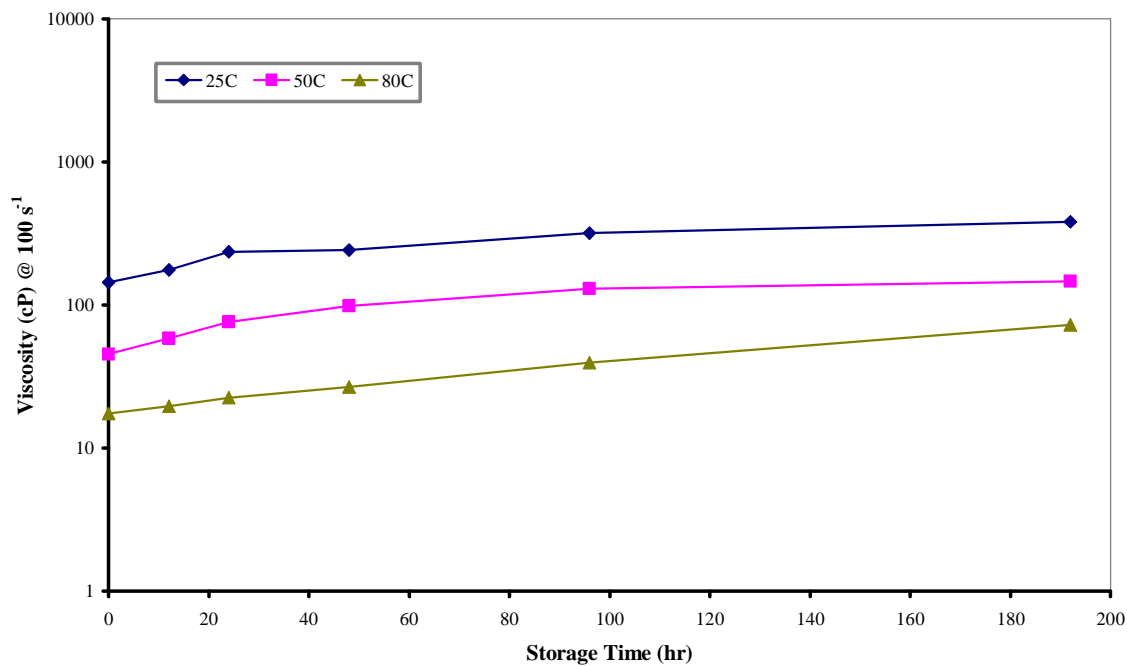


Figure C.66 Viscosity (cP) of Dimethyl Ether Blended Pyrolysis Oil (10 wt.%) Measured as a Function of Storage Time (hr) and Temperature ($^{\circ}\text{C}$)

APPENDIX D
(CONCENTRATION OPTIMIZATION-PHASE III)

APPENDIX D

This Appendix presents the analysis of variance (ANOVA) model input data used during the concentration optimization studies (Phase III). These studies were performed using pine wood pyrolysis oil (low temperature) of Mississippi State University (MSU). The three additives used were anisole (ANS), glycerol (GLY), and methanol (MEH). The overall objective of this phase was to select three best concentrations (low, medium, and high) from a range of concentration (0-20 wt.%). The input data of the viscosity model is shown in Tables 1-3 of this Appendix whereas the input data of the water content model is shown in Tables 4-6 of this Appendix. The interaction or mean response plots of additive concentration level (wt.%) and measurement temperature ($^{\circ}\text{C}$) is shown in Figures 1-3 with the viscosity decrease (cP) as the response variable (Y). The interactions plots of additive concentration level (wt.%) and storage temperature ($^{\circ}\text{C}$) is shown in Figures 4-6 with the water increase (wt.%) as the response variable (Y).

Table D.1

Anisole Input Data of the Analysis of Variance (ANOVA) Viscosity Model

OBS.	ADDITIVE	CLEVEL (wt.%)	VTEMP (⁰ C)	SRATE (s ⁻¹)	VD (cP)
1	ANS	0	25	1	103.34
2	ANS	5	25	1	145.43
3	ANS	10	25	1	22.63
4	ANS	15	25	1	49.69
5	ANS	20	25	1	25.21
6	ANS	0	50	1	55.50
7	ANS	5	50	1	65.21
8	ANS	10	50	1	14.76
9	ANS	15	50	1	34.11
10	ANS	20	50	1	17.87
11	ANS	0	80	1	13.44
12	ANS	5	80	1	70.11
13	ANS	10	80	1	0.62
14	ANS	15	80	1	13.77
15	ANS	20	80	1	0.91
16	ANS	0	25	10	37.33
17	ANS	5	25	10	60.01
18	ANS	10	25	10	6.78
19	ANS	15	25	10	20.09
20	ANS	20	25	10	7.39
21	ANS	0	50	10	10.35
22	ANS	5	50	10	9.98
23	ANS	10	50	10	5.07
24	ANS	15	50	10	6.92
25	ANS	20	50	10	3.49
26	ANS	0	80	10	5.46
27	ANS	5	80	10	9.99
28	ANS	10	80	10	0.81
29	ANS	15	80	10	4.55
30	ANS	20	80	10	0.99
31	ANS	0	25	100	34.25
32	ANS	5	25	100	48.15
33	ANS	10	25	100	3.82
34	ANS	15	25	100	15.42
35	ANS	20	25	100	4.08
36	ANS	0	50	100	5.50
37	ANS	5	50	100	6.16
38	ANS	10	50	100	1.48
39	ANS	15	50	100	3.42
40	ANS	20	50	100	1.39
41	ANS	0	80	100	1.45
42	ANS	5	80	100	6.08
43	ANS	10	80	100	0.65
44	ANS	15	80	100	1.15
45	ANS	20	80	100	0.58

VD = Difference in viscosity at 0 and 192 hr

Table D.2

Glycerol Input Data of the Analysis of Variance (ANOVA) Viscosity Model

OBS.	ADDITIVE	CLEVEL (wt.%)	VTEMP (°C)	SRATE (s ⁻¹)	VD (cP)
46	GLY	0	25	1	103.34
47	GLY	5	25	1	64.31
48	GLY	10	25	1	20.20
49	GLY	15	25	1	11.37
50	GLY	20	25	1	8.02
51	GLY	0	50	1	55.50
52	GLY	5	50	1	39.69
53	GLY	10	50	1	2.87
54	GLY	15	50	1	1.69
55	GLY	20	50	1	0.94
56	GLY	0	80	1	13.44
57	GLY	5	80	1	0.71
58	GLY	10	80	1	0.48
59	GLY	15	80	1	2.27
60	GLY	20	80	1	0.24
61	GLY	0	25	10	37.33
62	GLY	5	25	10	21.45
63	GLY	10	25	10	20.70
64	GLY	15	25	10	11.55
65	GLY	20	25	10	8.10
66	GLY	0	50	10	10.35
67	GLY	5	50	10	7.02
68	GLY	10	50	10	3.16
69	GLY	15	50	10	1.85
70	GLY	20	50	10	1.01
71	GLY	0	80	10	5.46
72	GLY	5	80	10	0.80
73	GLY	10	80	10	0.47
74	GLY	15	80	10	2.48
75	GLY	20	80	10	0.19
76	GLY	0	25	100	34.25
77	GLY	5	25	100	12.08
78	GLY	10	25	100	17.80
79	GLY	15	25	100	10.71
80	GLY	20	25	100	8.12
81	GLY	0	50	100	5.50
82	GLY	5	50	100	2.66
83	GLY	10	50	100	2.52
84	GLY	15	50	100	1.69
85	GLY	20	50	100	0.99
86	GLY	0	80	100	1.45
87	GLY	5	80	100	0.55
88	GLY	10	80	100	0.44
89	GLY	15	80	100	2.40
90	GLY	20	80	100	0.18

VD = Difference in viscosity at 0 and 192 hr

Table D.3

Methanol Input Data of the Analysis of Variance (ANOVA) Viscosity Model

OBS.	ADDITIVE	CLEVEL (wt.%)	VTEMP (°C)	SRATE (s ⁻¹)	VD (cP)
91	MEH	0	25	1	103.34
92	MEH	5	25	1	37.49
93	MEH	10	25	1	29.78
94	MEH	15	25	1	9.58
95	MEH	20	25	1	5.70
96	MEH	0	50	1	55.50
97	MEH	5	50	1	22.17
98	MEH	10	50	1	16.69
99	MEH	15	50	1	1.52
100	MEH	20	50	1	0.96
101	MEH	0	80	1	13.44
102	MEH	5	80	1	0.57
103	MEH	10	80	1	0.55
104	MEH	15	80	1	0.27
105	MEH	20	80	1	0.13
106	MEH	0	25	10	37.33
107	MEH	5	25	10	11.19
108	MEH	10	25	10	7.15
109	MEH	15	25	10	6.24
110	MEH	20	25	10	4.33
111	MEH	0	50	10	10.35
112	MEH	5	50	10	4.84
113	MEH	10	50	10	4.26
114	MEH	15	50	10	1.52
115	MEH	20	50	10	1.00
116	MEH	0	80	10	5.46
117	MEH	5	80	10	0.63
118	MEH	10	80	10	0.58
119	MEH	15	80	10	0.26
120	MEH	20	80	10	0.12
121	MEH	0	25	100	34.25
122	MEH	5	25	100	6.51
123	MEH	10	25	100	3.43
124	MEH	15	25	100	2.20
125	MEH	20	25	100	1.50
126	MEH	0	50	100	5.50
127	MEH	5	50	100	1.77
128	MEH	10	50	100	1.37
129	MEH	15	50	100	0.80
130	MEH	20	50	100	0.54
131	MEH	0	80	100	1.45
132	MEH	5	80	100	0.40
133	MEH	10	80	100	0.43
134	MEH	15	80	100	0.17
135	MEH	20	80	100	0.10

VD = Difference in viscosity at 0 and 192 hr

Table D.4

Anisole Input Data of the Analysis of Variance (ANOVA) Water Content Model

OBS.	ADDITIVE	CLEVEL (wt.%)	STIME (hr)	WCD (wt.%)
1	ANS	0	24	1.00
2	ANS	5	24	1.11
3	ANS	10	24	1.87
4	ANS	15	24	0.90
5	ANS	20	24	2.84
6	ANS	0	24	1.26
7	ANS	5	24	1.01
8	ANS	10	24	1.92
9	ANS	15	24	1.38
10	ANS	20	24	1.93
11	ANS	0	96	0.89
12	ANS	5	96	2.15
13	ANS	10	96	1.36
14	ANS	15	96	6.57
15	ANS	20	96	2.70
16	ANS	0	96	1.17
17	ANS	5	96	1.94
18	ANS	10	96	1.45
19	ANS	15	96	6.29
20	ANS	20	96	3.92
WCD = Difference in water content for 0-24 hr and 0-96 hr storage periods				

Table D.5

Glycerol Input Data of the Analysis of Variance (ANOVA) Water Content Model

OBS.	ADDITIVE	CLEVEL (wt.%)	STIME (hr)	WCD (wt.%)
21	GLY	0	24	1.00
22	GLY	5	24	1.80
23	GLY	10	24	2.38
24	GLY	15	24	0.25
25	GLY	20	24	2.14
26	GLY	0	24	1.26
27	GLY	5	24	1.89
28	GLY	10	24	1.96
29	GLY	15	24	0.32
30	GLY	20	24	1.47
31	GLY	0	96	0.89
32	GLY	5	96	2.01
33	GLY	10	96	2.67
34	GLY	15	96	1.43
35	GLY	20	96	1.65
36	GLY	0	96	1.17
37	GLY	5	96	2.13
38	GLY	10	96	1.94
39	GLY	15	96	1.09
40	GLY	20	96	1.65
WCD = Difference in water content for 0-24 hr and 0-96 hr storage periods				

Table D.6

Methanol Input Data of the Analysis of Variance (ANOVA) Water Content Model

OBS.	ADDITIVE	CLEVEL (wt.%)	STIME (hr)	WCD (wt.%)
41	MEH	0	24	1.00
42	MEH	5	24	0.35
43	MEH	10	24	1.22
44	MEH	15	24	0.74
45	MEH	20	24	1.67
46	MEH	0	24	1.26
47	MEH	5	24	0.00
48	MEH	10	24	1.41
49	MEH	15	24	0.43
50	MEH	20	24	1.52
51	MEH	0	96	0.89
52	MEH	5	96	0.66
53	MEH	10	96	1.59
54	MEH	15	96	1.83
55	MEH	20	96	1.18
56	MEH	0	96	1.17
57	MEH	5	96	0.59
58	MEH	10	96	1.58
59	MEH	15	96	1.76
60	MEH	20	96	0.82
WCD = Difference in water content for 0-24 hr and 0-96 hr storage periods				

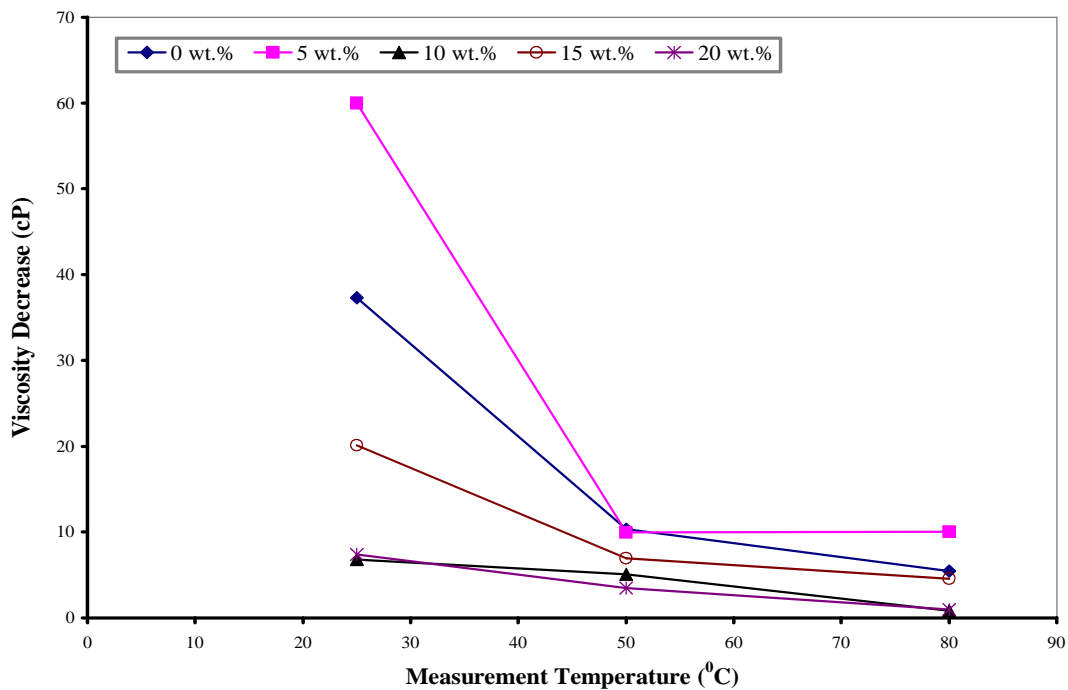


Figure D.1 Viscosity Decrease (cP) of Anisole Blended (wt.%) Pyrolysis Oil Obtained as a Function of Measurement Temperature ($^{\circ}\text{C}$)

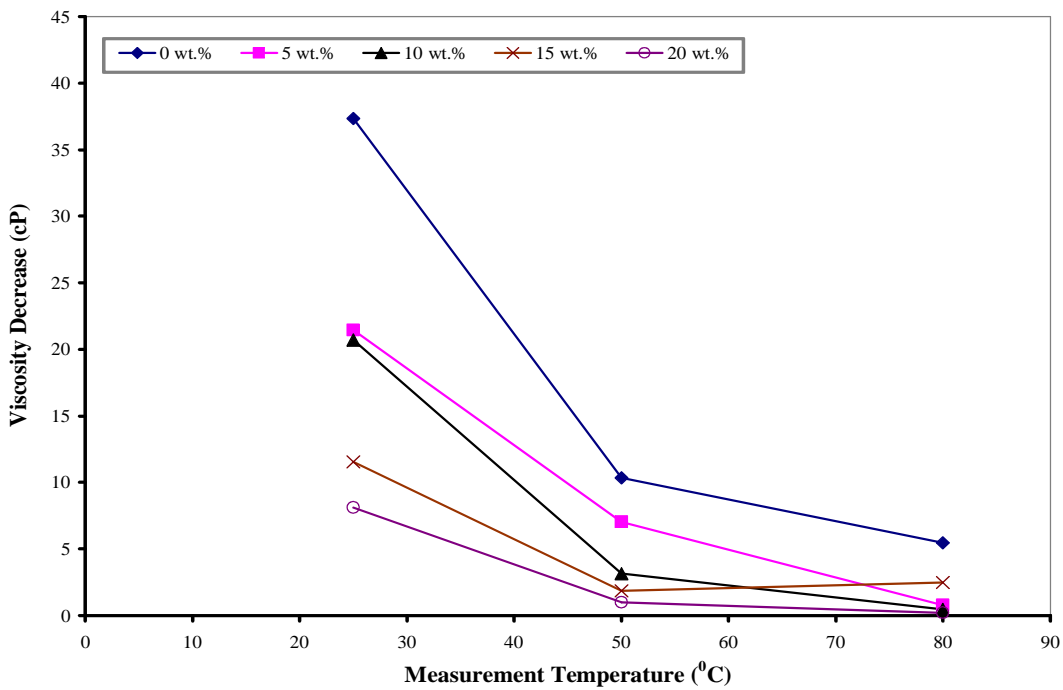


Figure D.2 Viscosity Decrease (cP) of Glycerol Blended (wt.%) Pyrolysis Oil Obtained as a Function of Measurement Temperature ($^{\circ}\text{C}$)

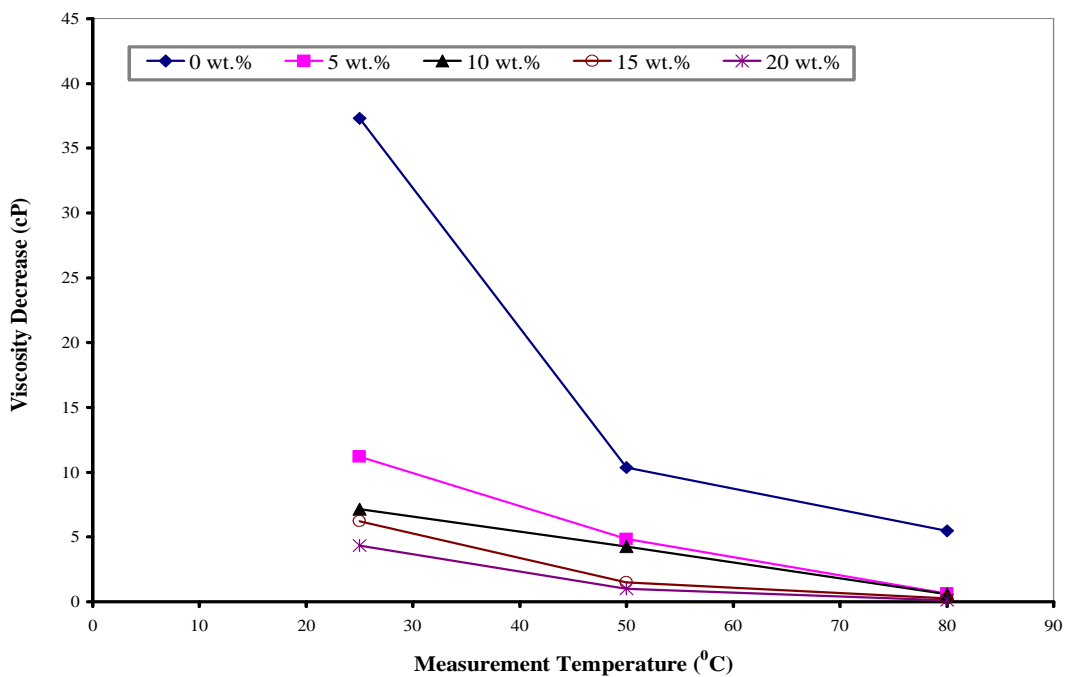


Figure D.3 Viscosity Decrease (cP) of Methanol Blended (wt.%) Pyrolysis Oil Obtained as a Function of Measurement Temperature ($^{\circ}\text{C}$)

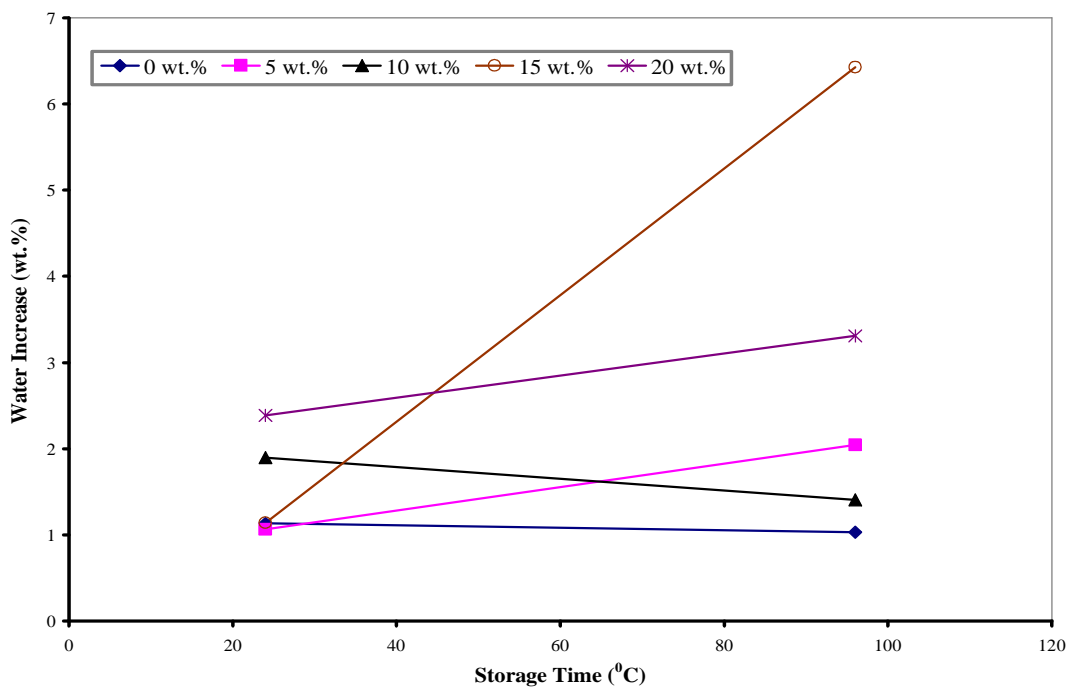


Figure D.4 Mean Water Content Increase (wt.%) of Anisole Blended (wt.%) Pyrolysis Oil Obtained as a Function of Storage Time (hr)

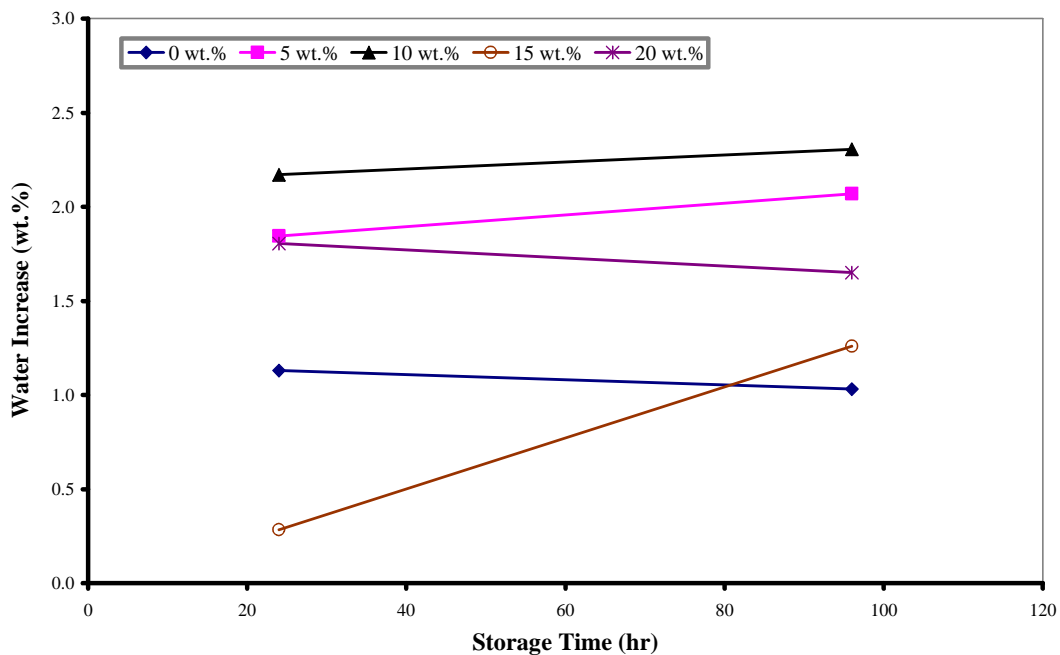


Figure D.5 Mean Water Content Increase (wt.%) of Glycerol Blended (wt.%) Pyrolysis Oil Obtained as a Function of Storage Time (hr)

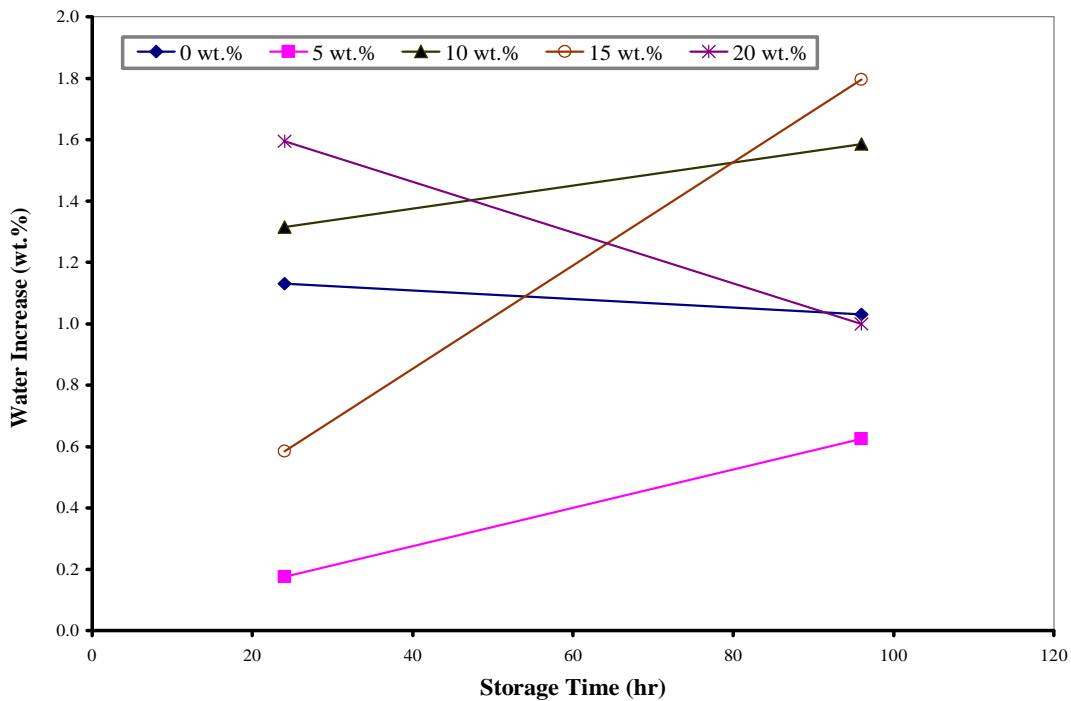


Figure D.6 Mean Water Content Increase (wt.%) of Methanol Blended (wt.%) Pyrolysis Oil Obtained as a Function of Storage Time (hr)

APPENDIX E
(FINAL STABILITY TESTING-PHASE IV)

APPENDIX E

This Appendix presents the viscosity test results of pyrolysis oils obtained from the final stability testing or Phase IV. The pyrolysis oils (9) were produced from four feed stocks and four reactor conditions. The four feed stocks utilized were pine wood (PW), pine bark (PB), oak wood (OW), and oak bark (OB). The four reactor conditions were slow residence time, fast residence time, low pyrolysis temperature (400 °C), and high pyrolysis temperature (450 °C). The residence times were specifically defined for each reactor type that was utilized at Mississippi State University (MSU), National Renewable Energy Laboratory (NREL) and Renewable Oil International (ROI). The pyrolysis oils (9) were produced from small-scale auger reactor (4-MSU), large-scale auger reactor (1-ROI), and entrained flow reactor (4-NREL). The three additives used were anisole (A), glycerol (G), and methanol (M) with the concentrations of 0, 5, and 10 wt.%. The monthly (25 °C) viscosity (cP) data (M0, M1, M2, M4, and M6) of the pyrolysis oils as a function of shear rate (s^{-1}) is shown in Figures 1-10 of this Appendix. The hourly (80 °C) viscosity (cP) data (H0, H24, H48, H96, and H192) of the pyrolysis oils as a function of shear rate (s^{-1}) is shown in Figures 11-18 of this Appendix.

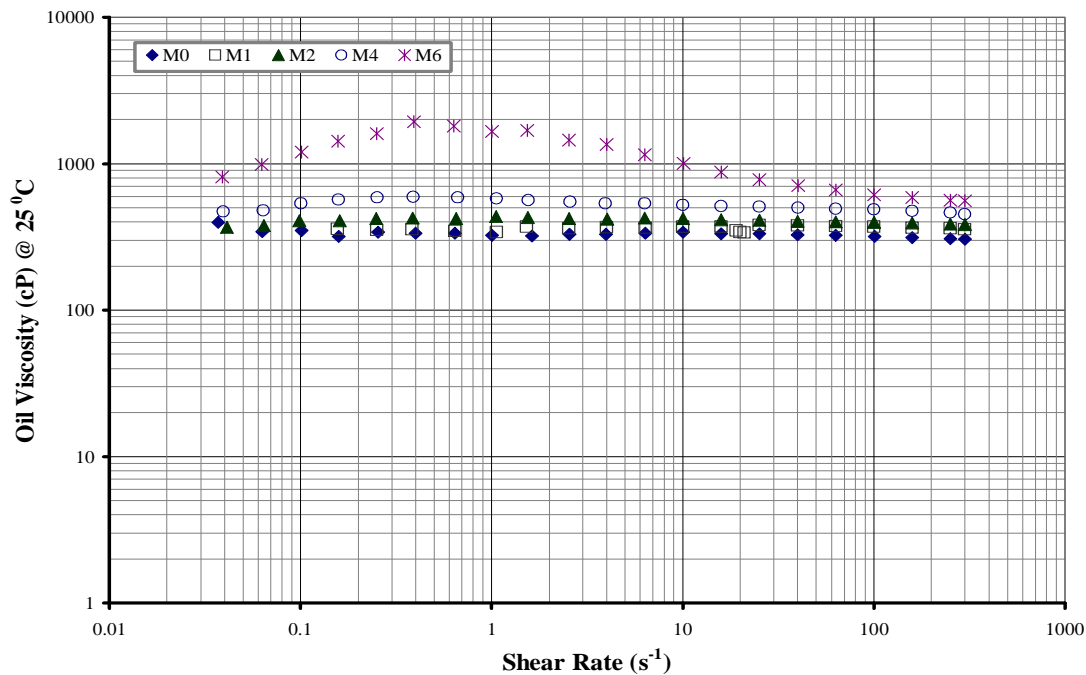


Figure E.1 Viscosity (cP) of Renewable Oil International (ROI) Pine Wood Oil Control (CTL2) as a Function of Shear Rate (s^{-1}) and Storage Time (month)

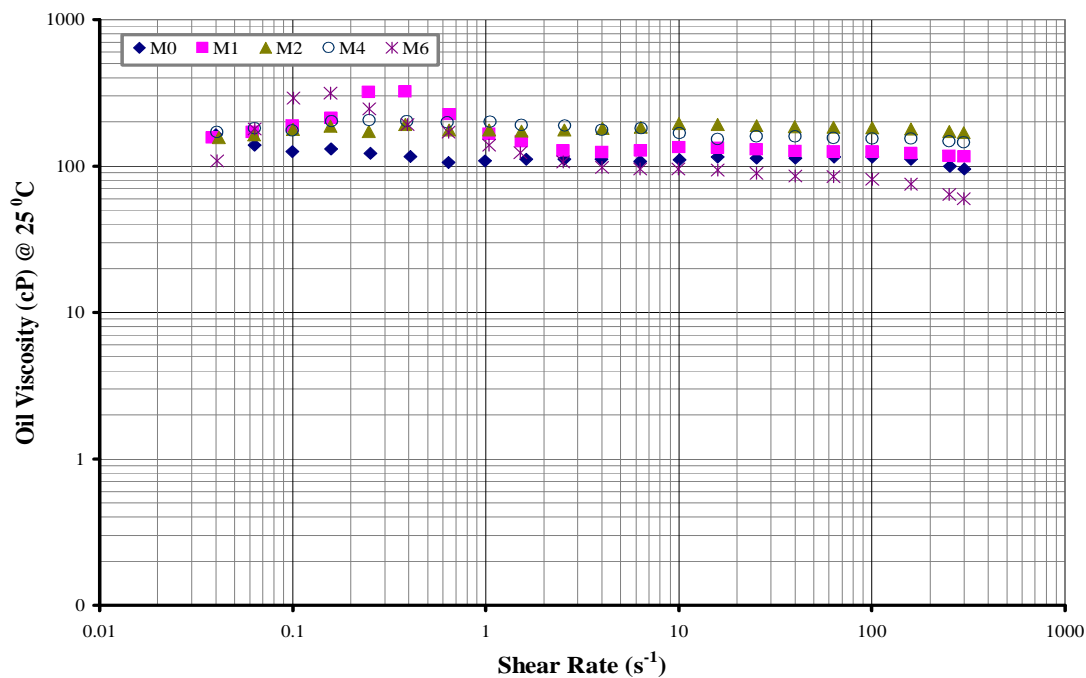


Figure E.2 Viscosity (cP) of National Renewable Energy Laboratory (NREL) Low Temperature Pine Wood Oil Control (CTL2) as a Function of Shear Rate (s^{-1}) and Storage Time (month)

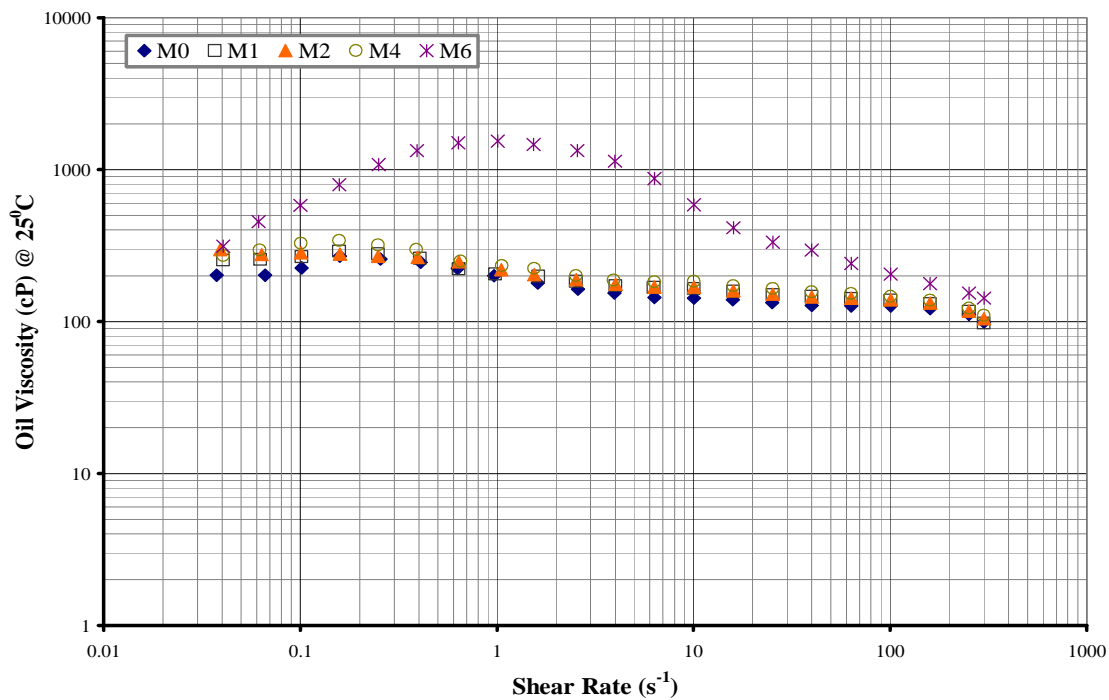


Figure E.3 Viscosity (cP) of Mississippi State University (MSU) Oak Wood Oil Control (CTL2) as a Function of Shear Rate (s^{-1}) and Storage Time (month)

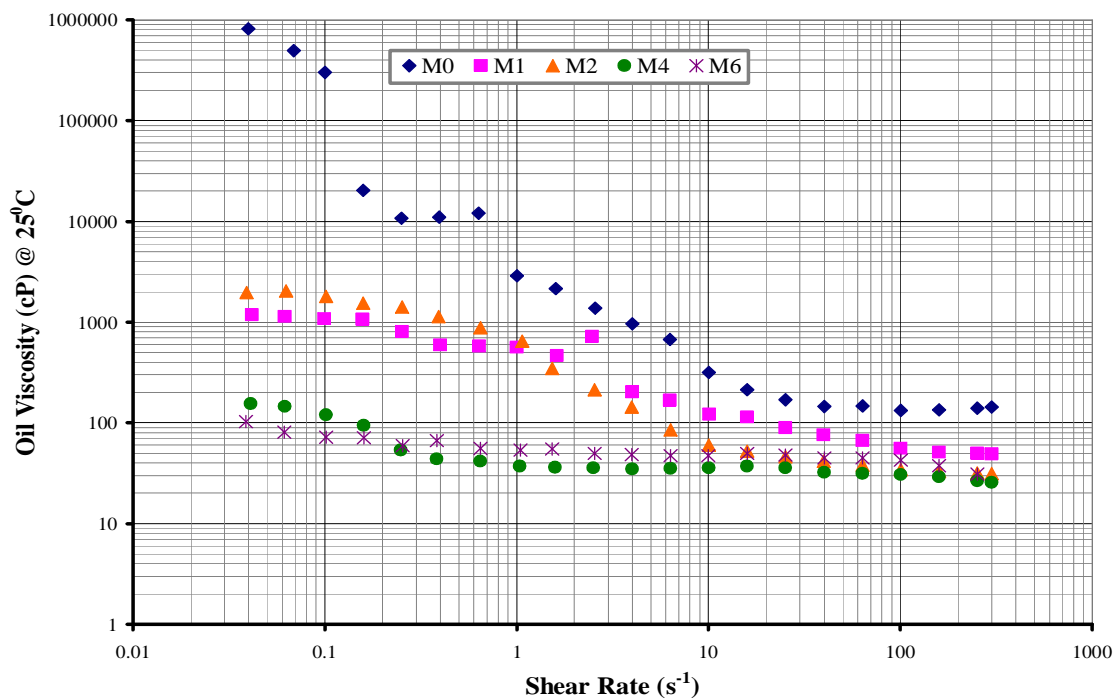


Figure E.4 Viscosity (cP) of Mississippi State University (MSU) Pine Bark Oil Control (CTL2) as a Function of Shear Rate (s^{-1}) and Storage Time (month)

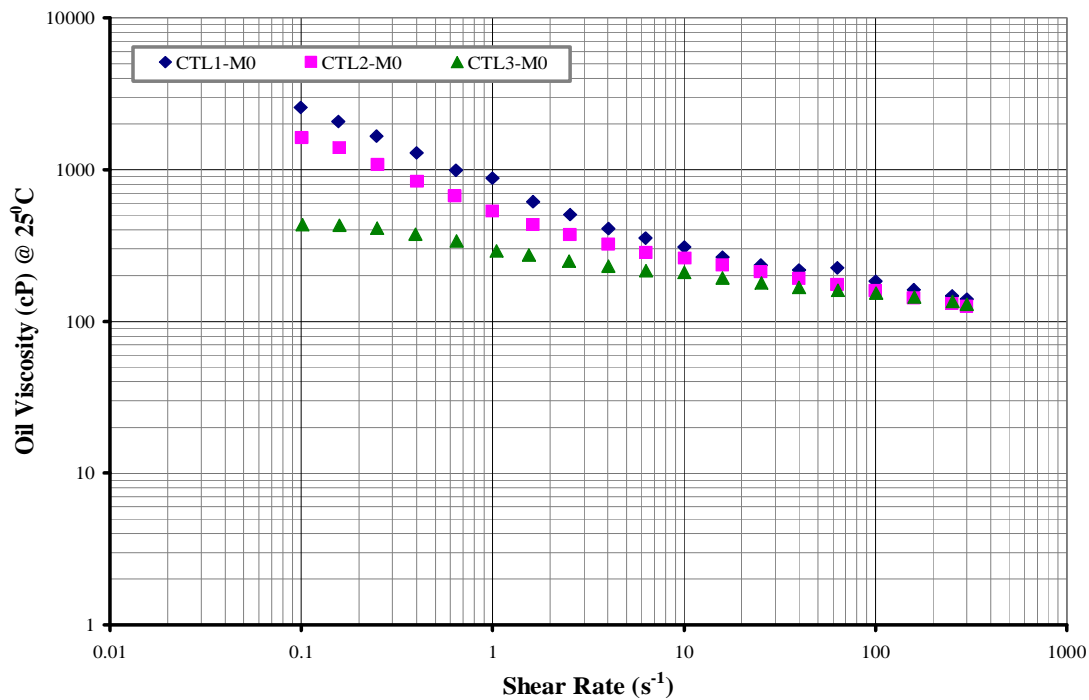


Figure E.5 Viscosity (cP) as a Function of Shear Rate (s^{-1}) of Mississippi State University (MSU) Fresh Oak Bark Oil Controls (CTL's 1-3)

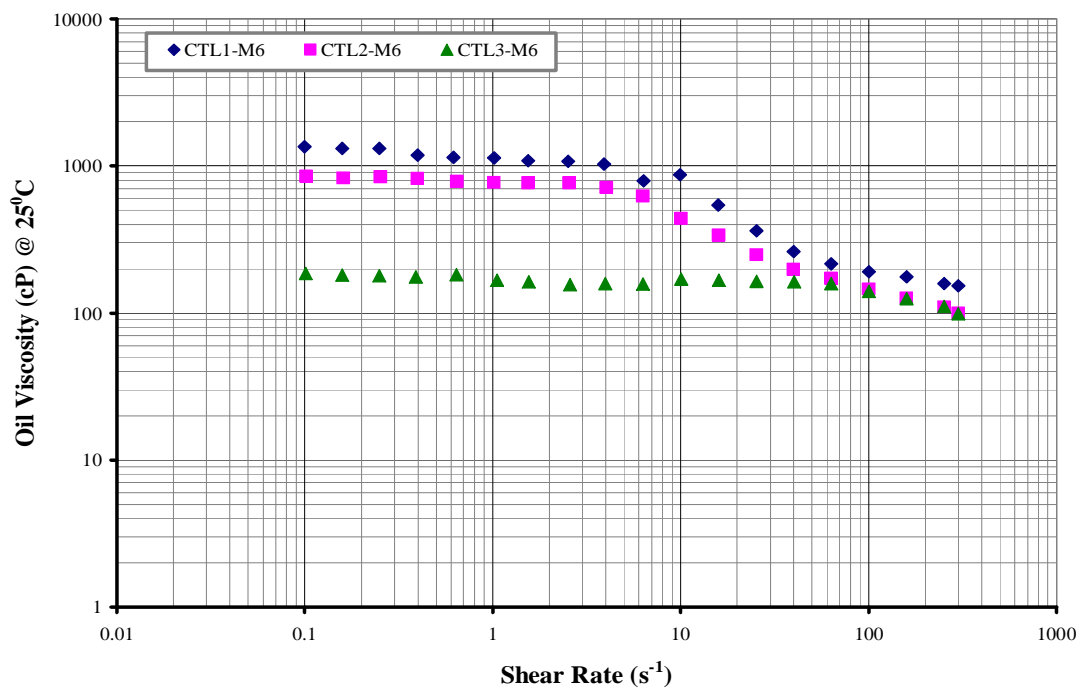


Figure E.6 Viscosity (cP) as a Function of Shear Rate (s^{-1}) of Mississippi State University (MSU) Oak Bark Oil Controls (CTL's 1-3) Aged to 180 days

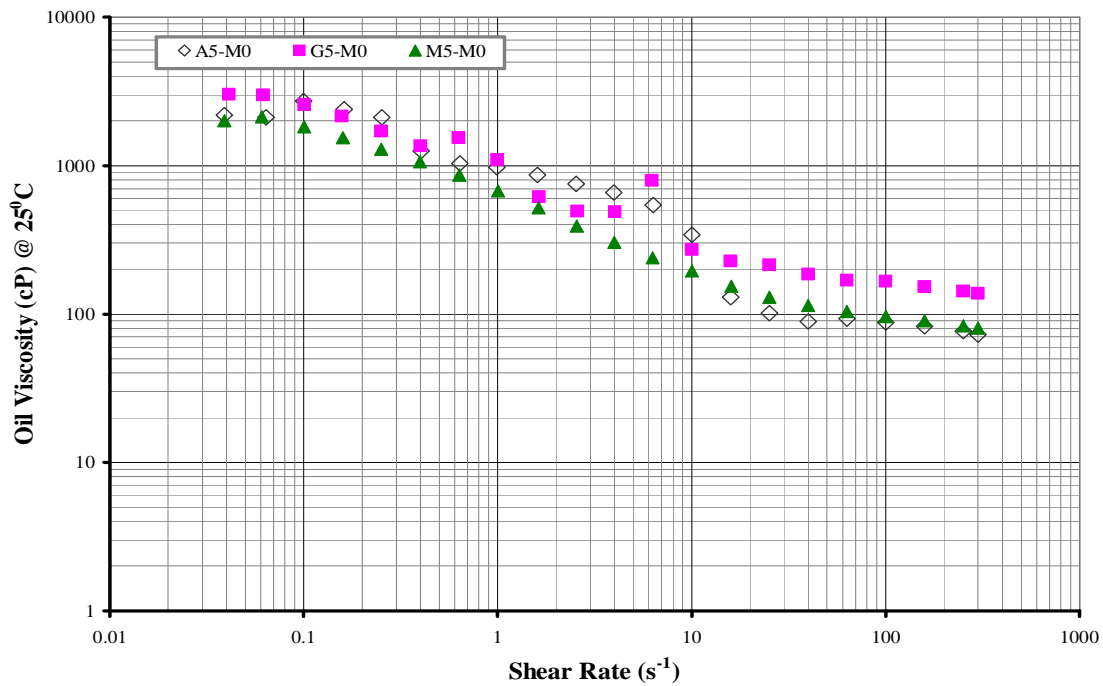


Figure E.7 Viscosity (cP) as a Function of Shear Rate (s⁻¹) of Additive Blended (5 wt.%) Mississippi State University (MSU) Fresh Oak Bark Oil

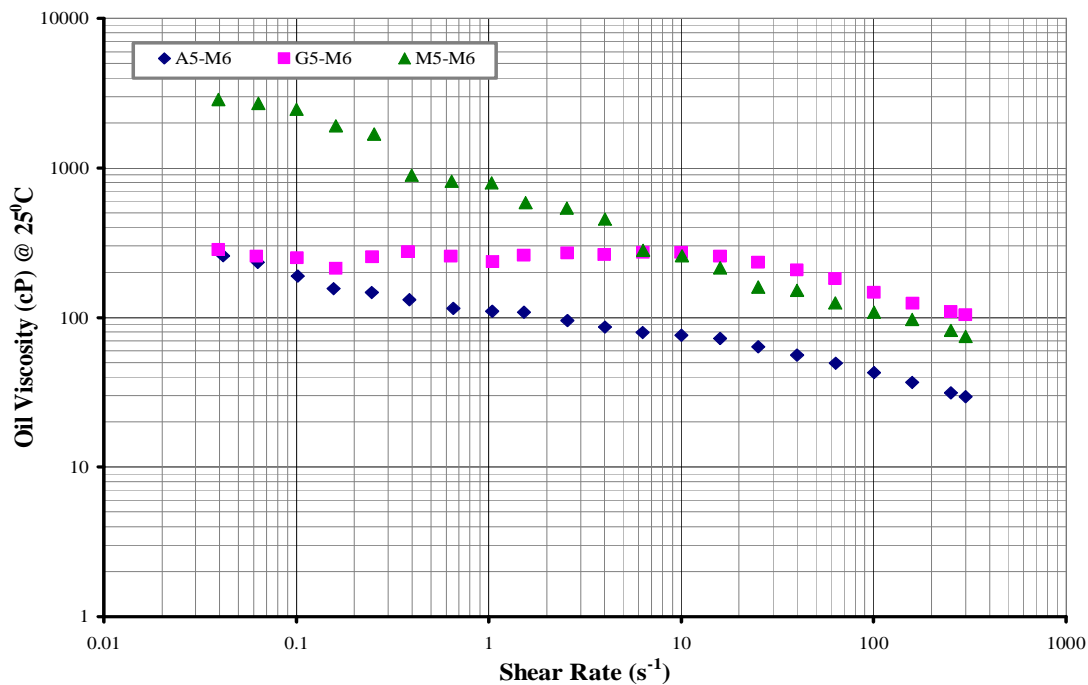


Figure E.8 Viscosity (cP) as a Function of Shear Rate (s⁻¹) of Additive Blended (5 wt.%) Mississippi State University (MSU) Oak Bark Oil Aged to 180 days

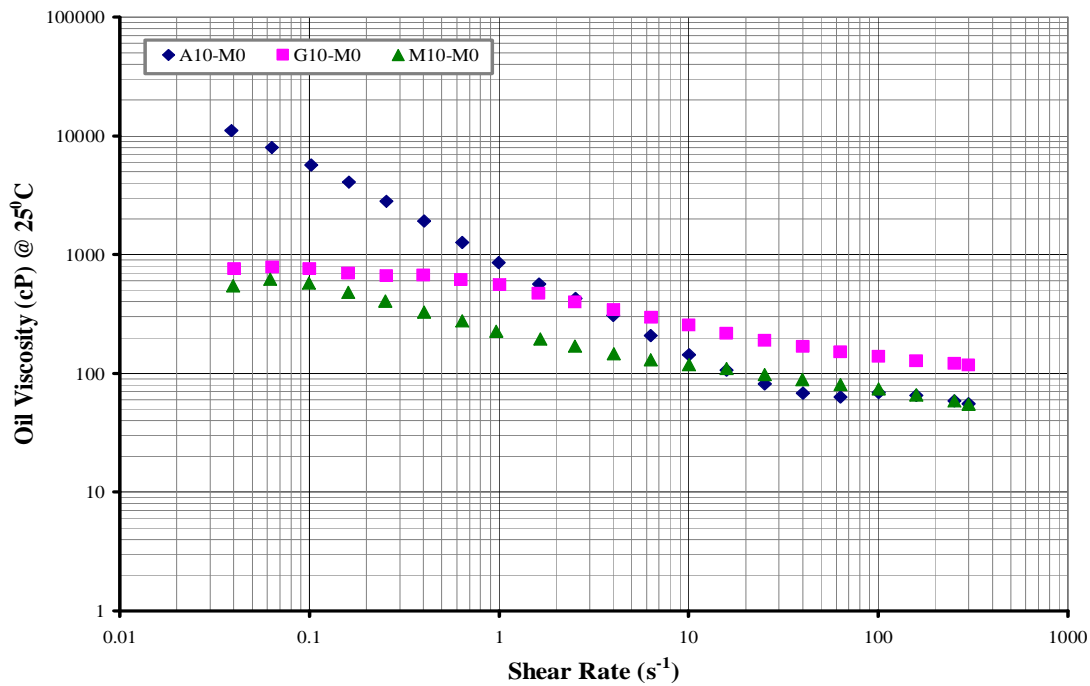


Figure E.9 Viscosity (cP) as a Function of Shear Rate (s⁻¹) of Additive Blended (10 wt.%) Mississippi State University (MSU) Fresh Oak Bark Oil

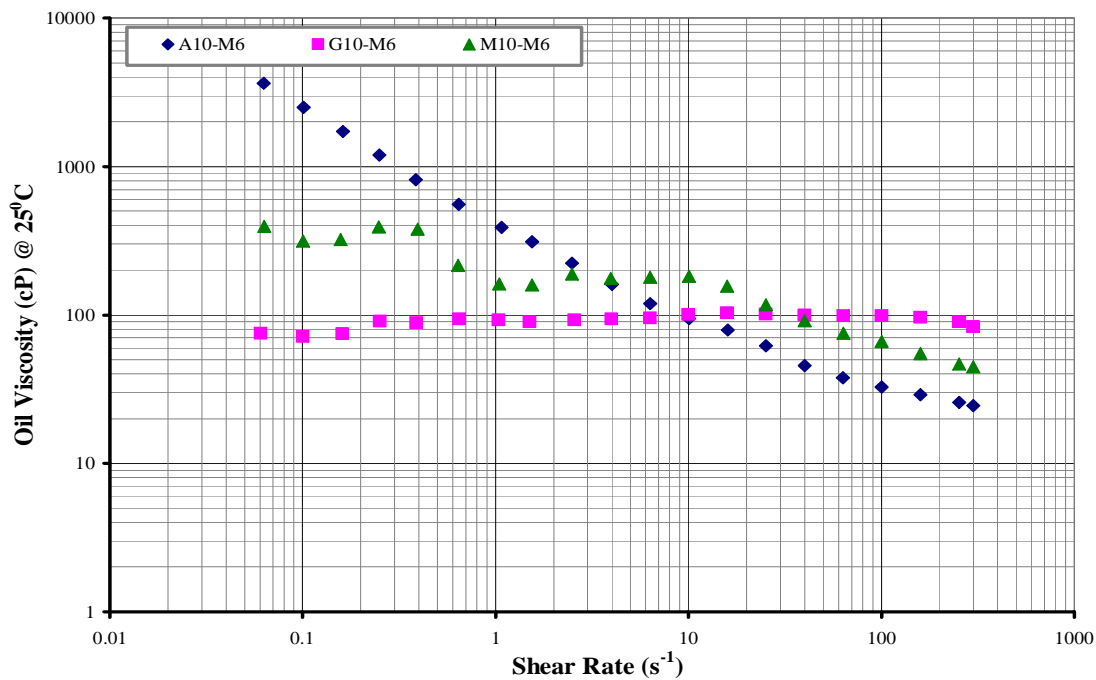


Figure E.10 Viscosity (cP) as a Function of Shear Rate (s⁻¹) of Additive Blended (10 wt.%) Mississippi State University (MSU) Oak Bark Oil Aged to 180 days

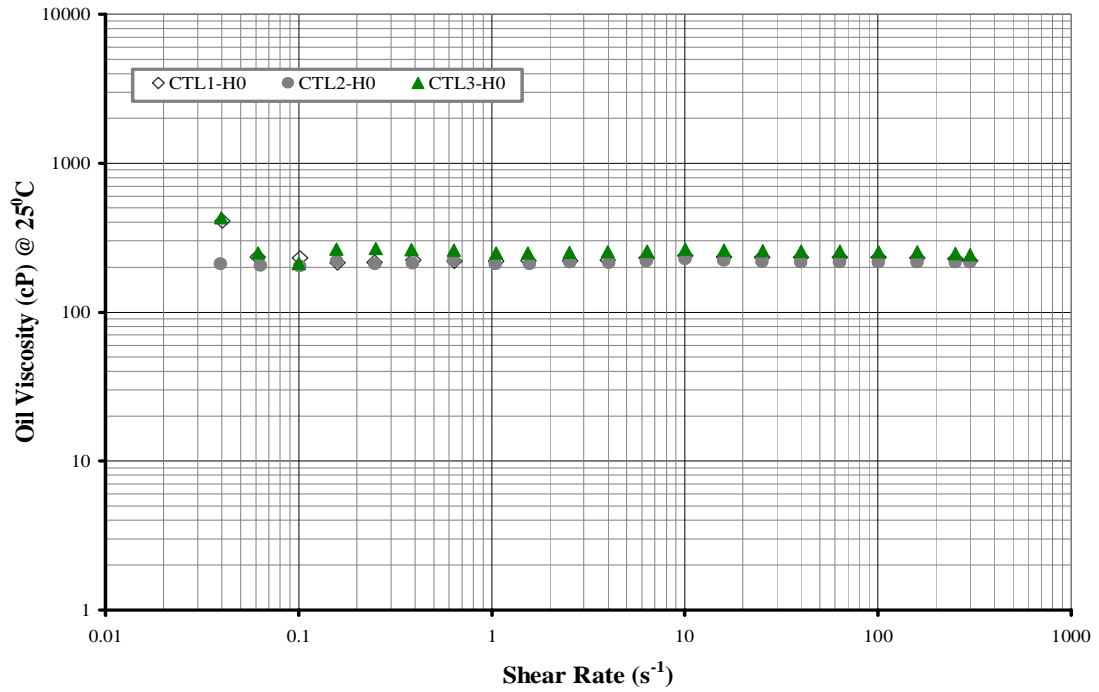


Figure E.11 Viscosity (cP) as a Function of Shear Rate (s⁻¹) of Mississippi State University (MSU) Fresh Pine Wood Oil Controls (CTL's 1-3)

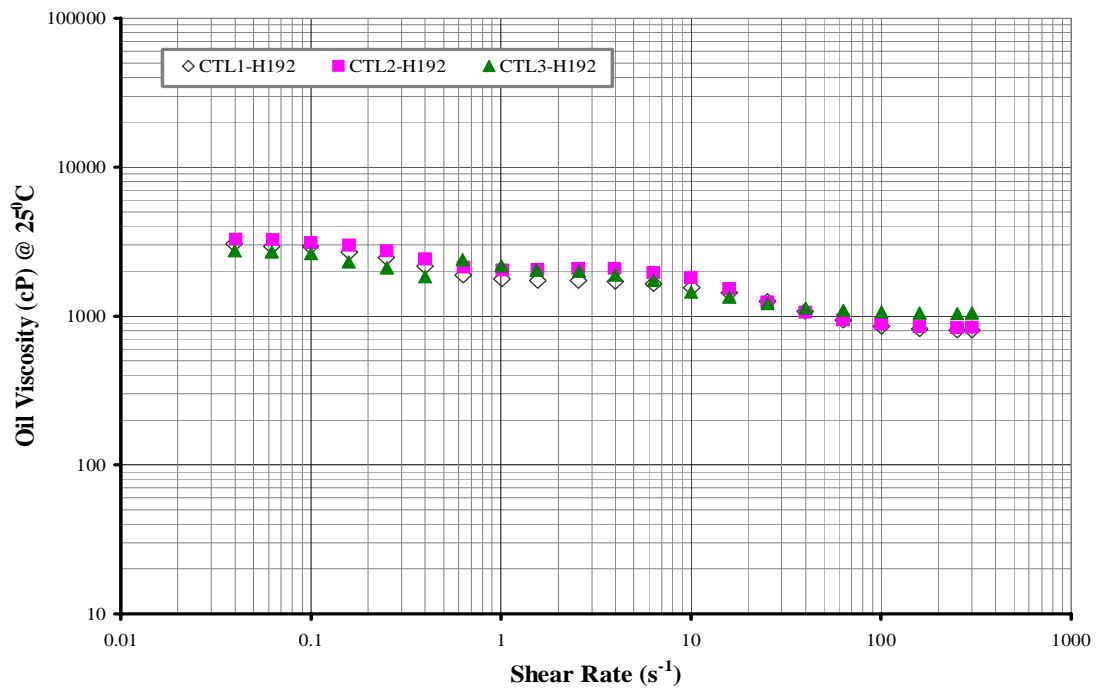


Figure E.12 Viscosity (cP) as a Function of Shear Rate (s⁻¹) of Mississippi State University (MSU) Pine Wood Oil Controls (CTL's 1-3) Aged to 192 hours

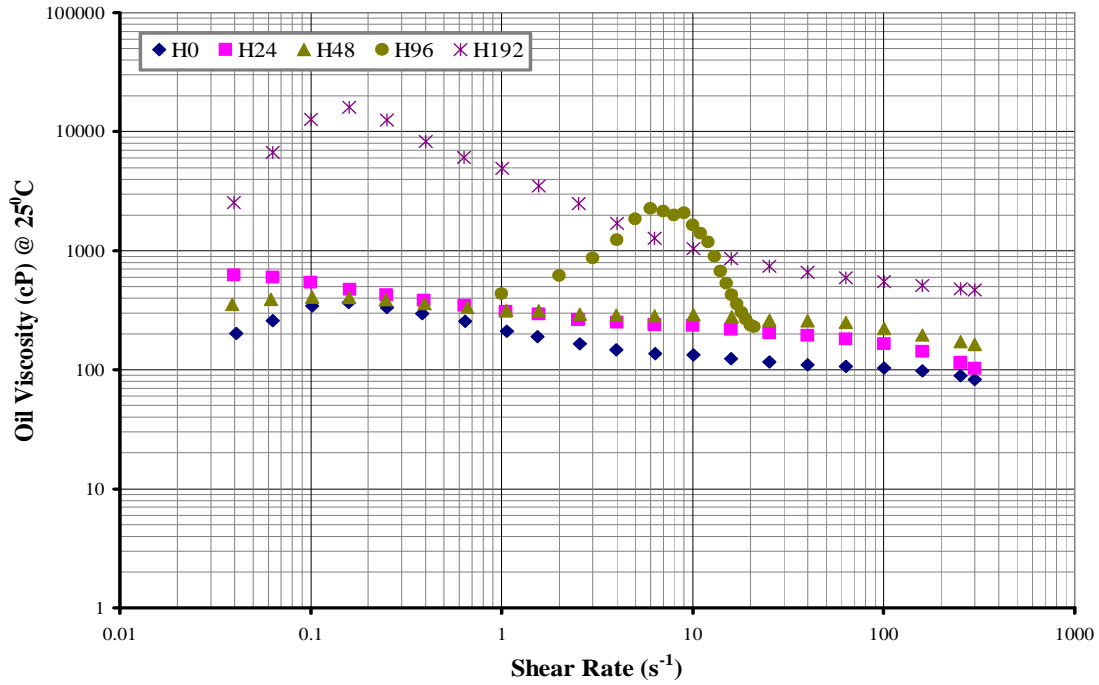


Figure E.13 Viscosity (cP) of Mississippi State University (MSU) Oak Wood Oil Control (CTL2) as a Function of Shear Rate (s⁻¹) and Storage Time (hour)

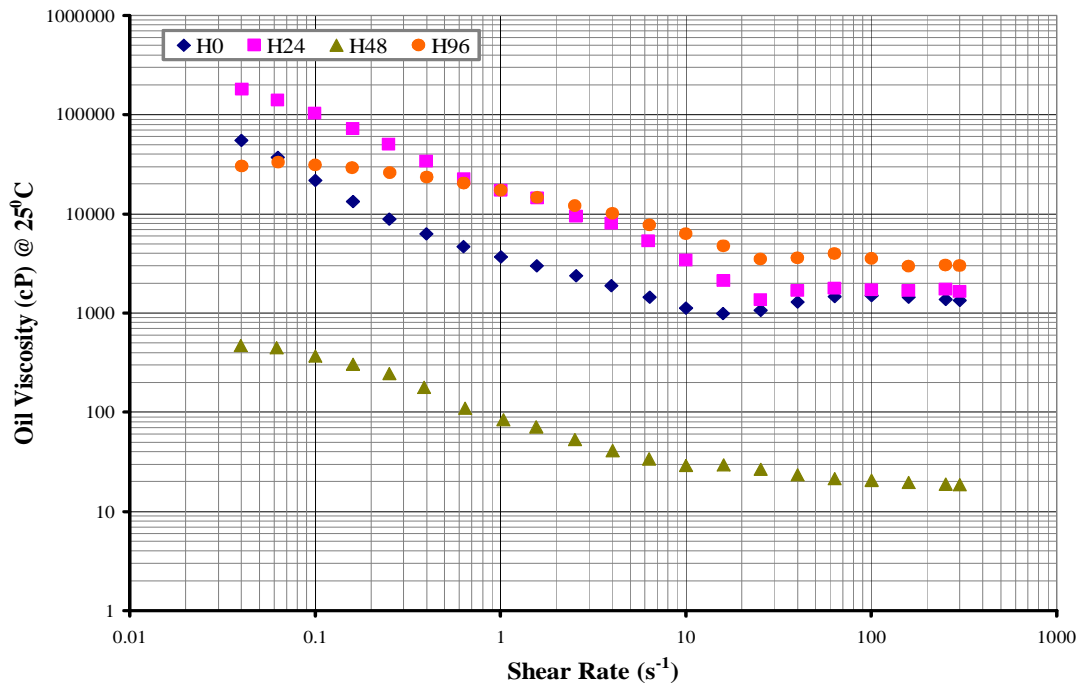


Figure E.14 Viscosity (cP) of Mississippi State University (MSU) Pine Bark Oil Control (CTL2) as a Function of Shear Rate (s⁻¹) and Storage Time (hour)

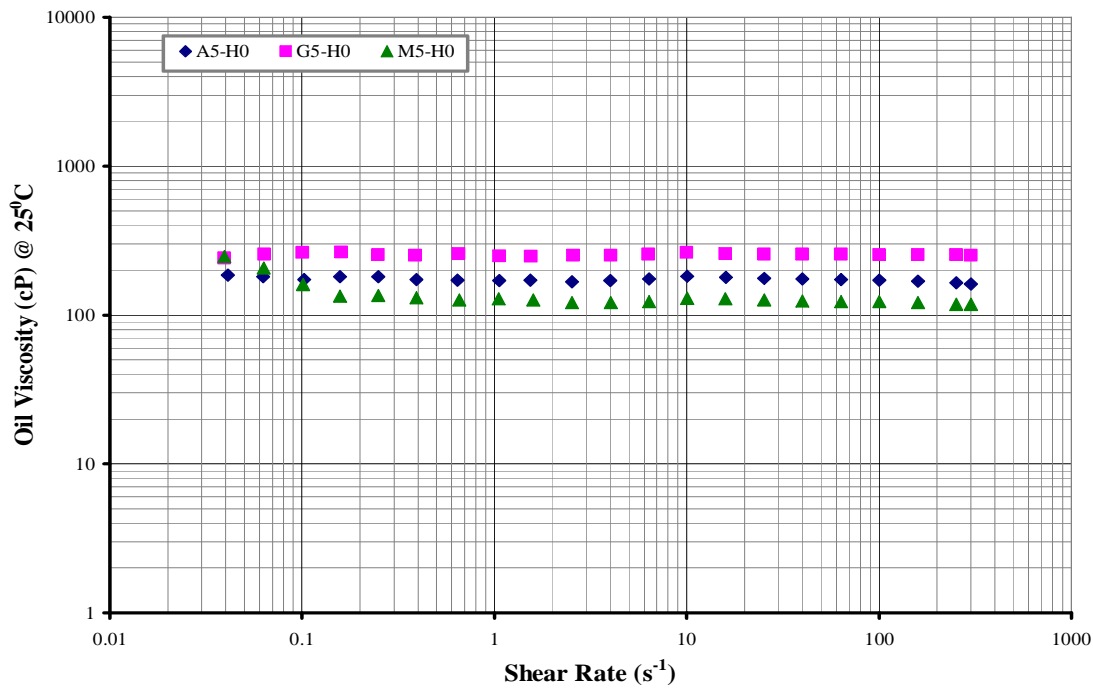


Figure E.15 Viscosity (cP) as a Function of Shear Rate (s⁻¹) of Additive Blended (5 wt.%) Mississippi State University (MSU) Fresh Pine Wood Oil

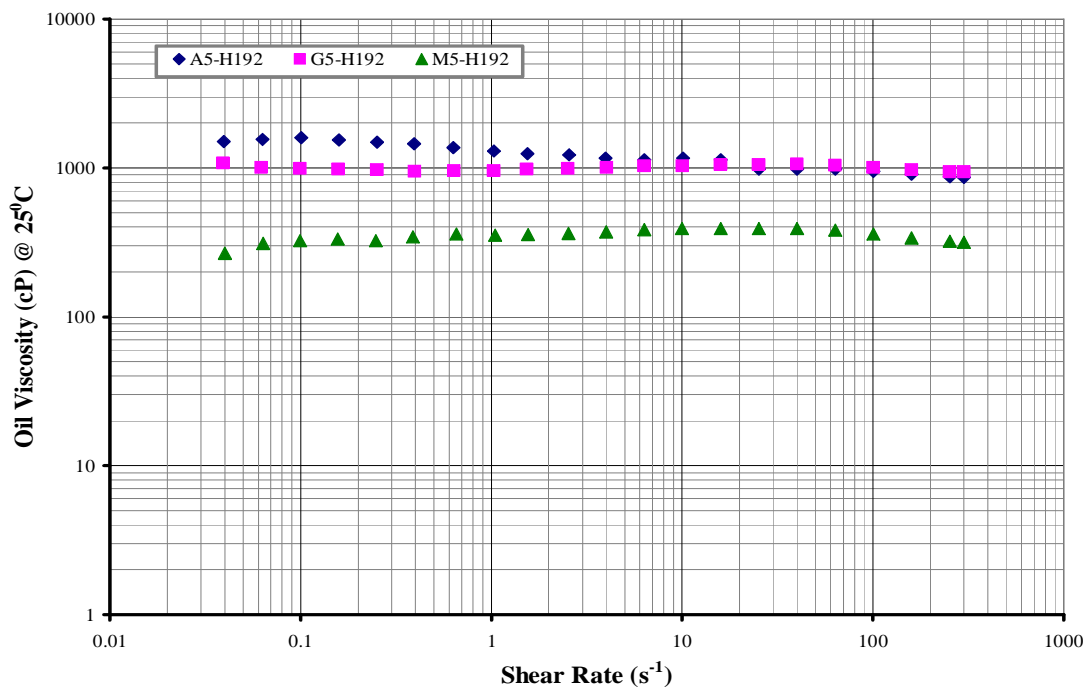


Figure E.16 Viscosity (cP) as a Function of Shear Rate (s⁻¹) of Additive Blended (5 wt.%) Mississippi State University (MSU) Pine Wood Oil Aged to 192 hours

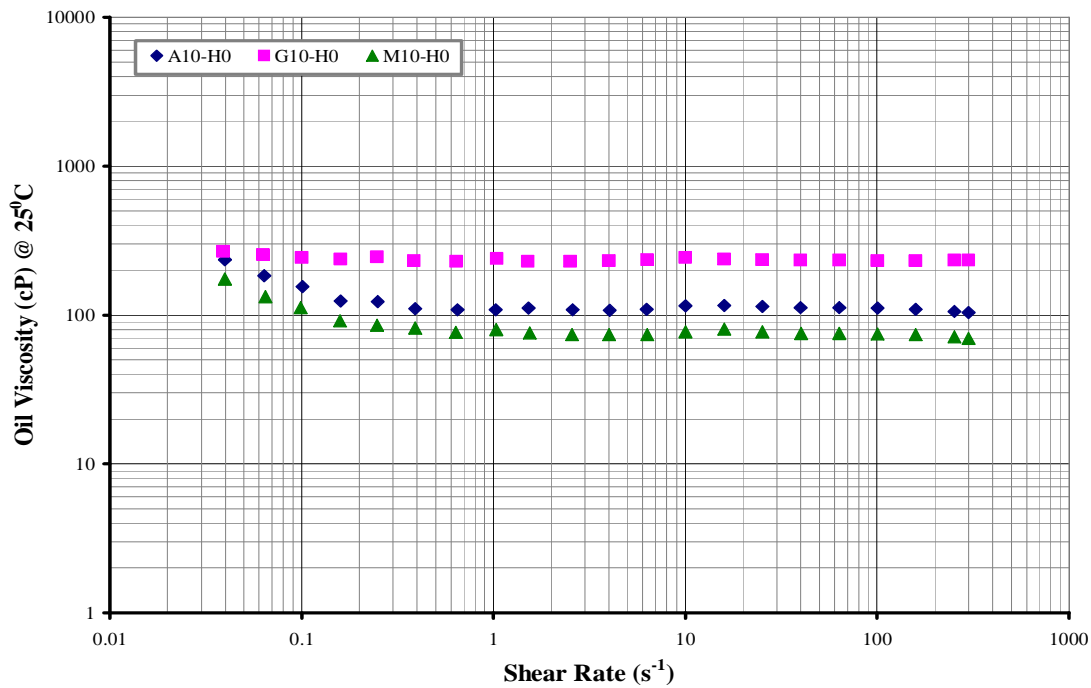


Figure E.17 Viscosity (cP) as a Function of Shear Rate (s⁻¹) of Additive Blended (10 wt.%) Mississippi State University (MSU) Fresh Pine Wood Oil

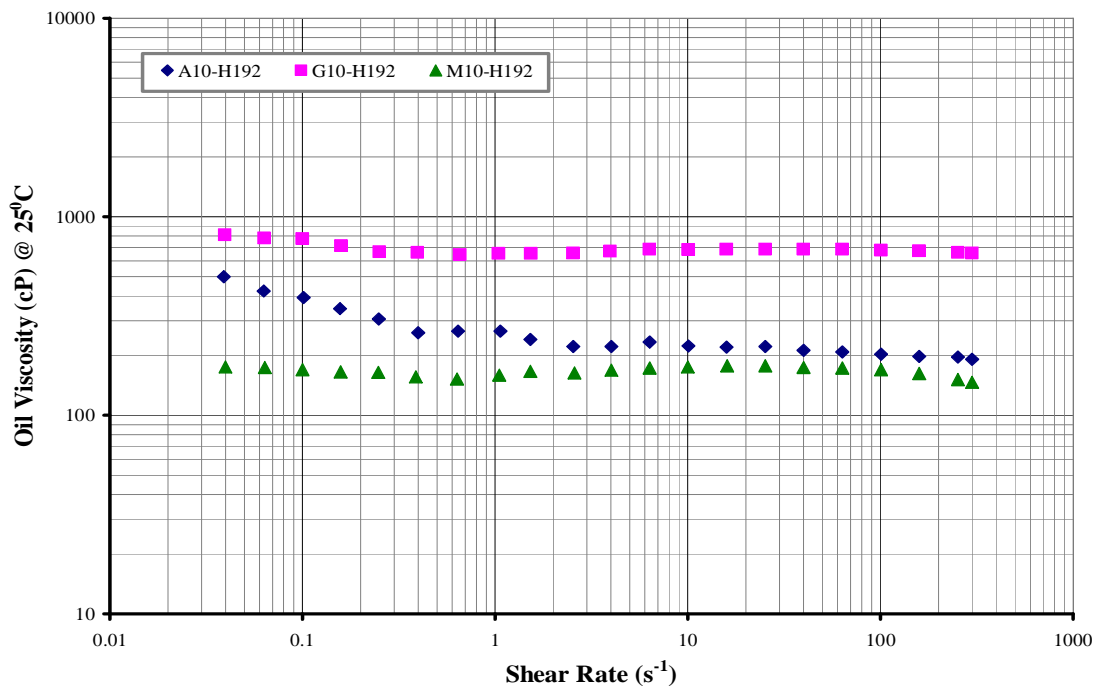


Figure E.18 Viscosity (cP) as a Function of Shear Rate (s⁻¹) of Additive Blended (10 wt.%) Mississippi State University (MSU) Pine Wood Oil Aged to 192 hours